22nd Annual Combustion Research Conference

U.S. Department of Energy
Office of Basic Energy Sciences

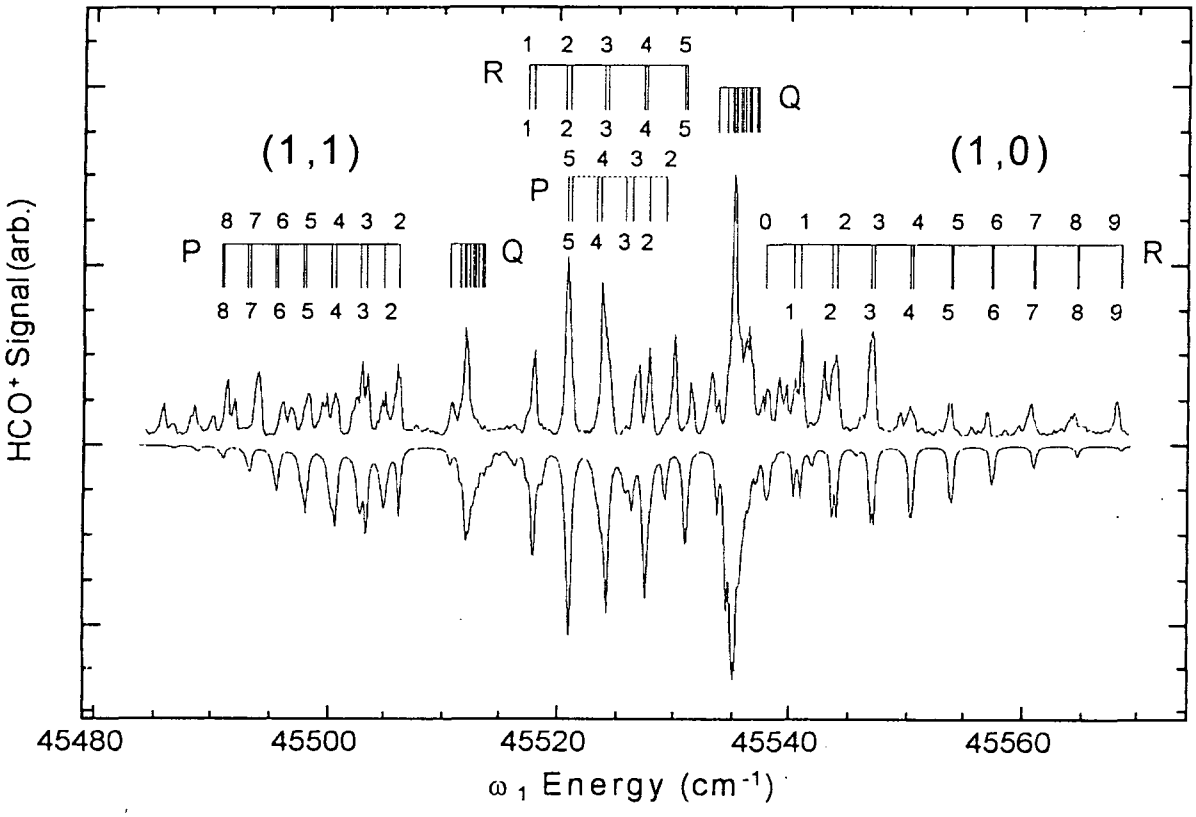

Granlibakken Conference Center
Tahoe City, California
May 29 – June 1, 2001

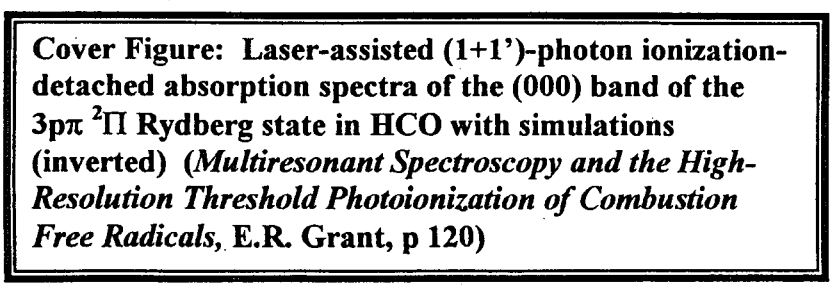

Cover Figure: Laser-assisted (1+1')-photon ionization-detached absorption spectra of the (000) band of the $3p\pi\ ^2\Pi$ Rydberg state in HCO with simulations (inverted) (*Multiresonant Spectroscopy and the High-Resolution Threshold Photoionization of Combustion Free Radicals,* E.R. Grant, p 120)

22nd Annual Combustion Research Conference

U.S. Department of Energy
Office of Basic Energy Sciences

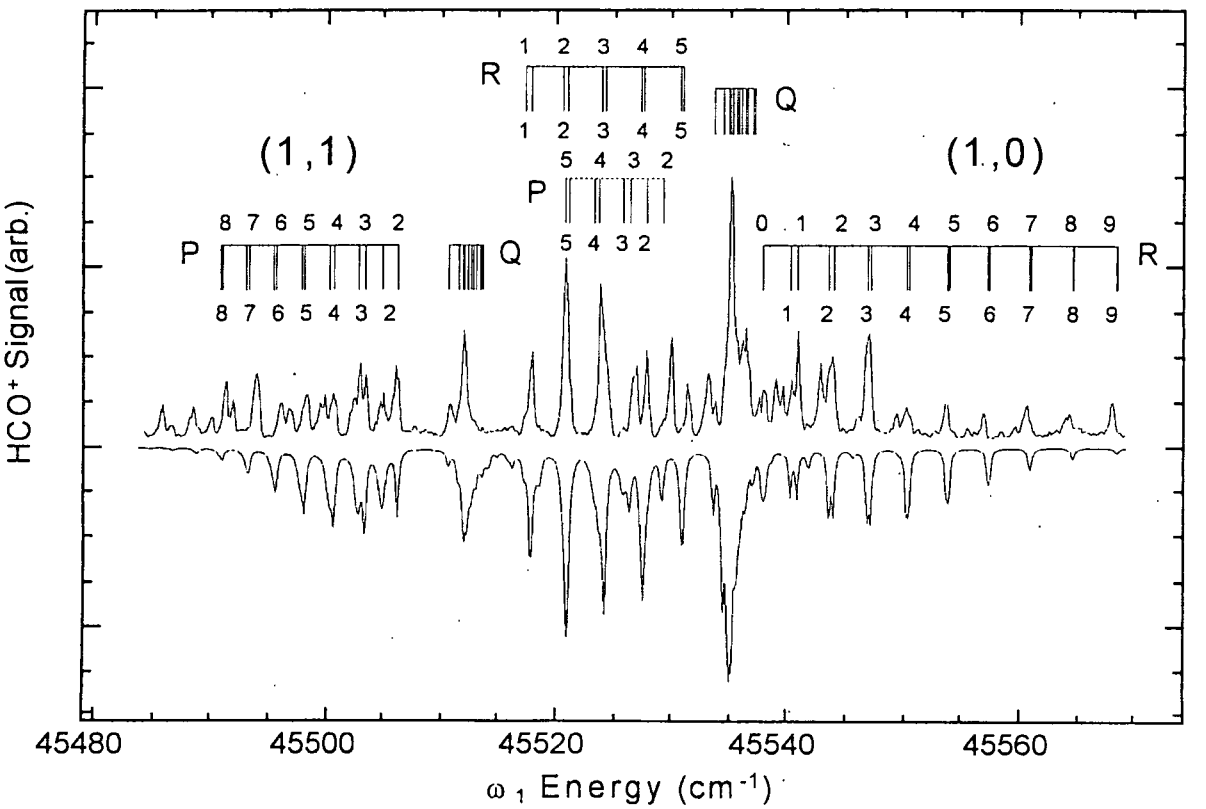

Granlibakken Conference Center
Tahoe City, California
May 29 – June 1, 2001

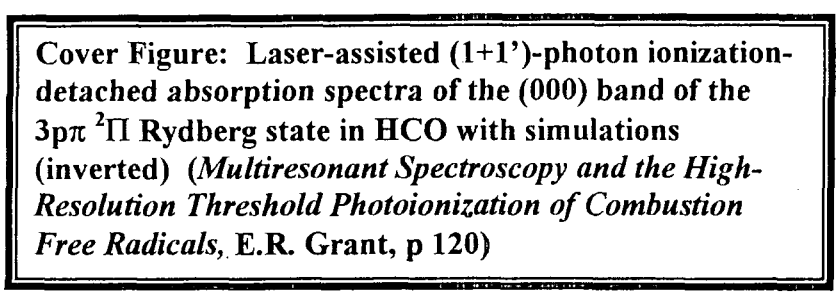

Cover Figure: Laser-assisted (1+1')-photon ionization-detached absorption spectra of the (000) band of the $3p\pi\ ^2\Pi$ Rydberg state in HCO with simulations (inverted) (*Multiresonant Spectroscopy and the High-Resolution Threshold Photoionization of Combustion Free Radicals*, E.R. Grant, p 120)

FOREWORD

The achievement of National goals for energy conservation and environmental protection will rely on technology more advanced than we have at our disposal today. Combustion at present accounts for 85% of the energy generated and used in the U.S. and is likely to remain a dominant source of energy for the coming decades. Achieving energy conservation while minimizing unwanted emissions from combustion processes could be greatly accelerated if accurate and reliable means were at hand for quantitatively predicting process performance.

The reports appearing in this volume present work in progress in basic research contributing to the development of a predictive capability for combustion processes. The work reported herein is supported by the Department of Energy's Office of Basic Energy Sciences (BES) and in large measure by the chemical physics program. The long-term objective of this effort is the provision of theories, data, and procedures to enable the development of reliable computational models of combustion processes, systems, and devices

The development of reliable models for combustion requires the accurate knowledge of chemistry, turbulent flow, and the interaction between the two at temperatures and pressures characteristic of the combustion environment. In providing this knowledge, the research supported by BES addresses a wide range of continuing scientific issues of long standing.

- For even the simplest fuels, the chemistry of combustion consists of hundreds of reactions. Key reaction mechanisms, the means for developing and testing these mechanisms and the means for determining which of the constituent reaction rates are critical for accurate characterization are all required.
- For reactions known to be important, accurate rates over wide ranges of temperature, pressure and composition are required. To assess the accuracy of measured reaction rates or predict rates that would be too difficult to measure, theories of reaction rates and means for calculating their values are needed. Of particular importance are reactions involving open shell systems such as radicals and excited electronic states.
- To assess the accuracy of methods for predicting chemical reaction rates, the detailed, state-specific dynamics of prototypical reactions must be characterized.
- Methods for observing key reaction species in combustion environments, for interpreting these observations in terms of species concentrations, and for determining which species are key are all required
- Energy flow and accounting must be accurately characterized and predicted.
- Methods for reducing the mathematical complexity inherent in hundreds of reactions, without sacrificing accuracy and reliability are required. Methods for reducing the computational complexity of computer models that attempt to address turbulence, chemistry, and their interdependence and also needed.

Although the emphasis in this list is on the development of mathematical models for simulating the gas phase reactions characteristic of combustion, ***such models, from the***

chemical dynamics of a single molecule to the performance of a combustion device, have value only when confirmed by experiment. Hence, the DOE program represented by reports in this volume supports the development and application of new experimental tools in chemical dynamics, kinetics, and spectroscopy.

The success of this research effort will be measured by the quality of the research performed, the profundity of the knowledge gained, as well as the degree to which it contributes to goals of resource conservation and environmental stewardship. In fact, without research of the highest quality, the application of the knowledge gained to practical problems will not be possible.

The emphasis on modeling and simulation as a basis for defining the objectives of this basic research program has a secondary but important benefit. Computational models of physical processes provide the most efficient means for ensuring the usefulness and use of basic theories and data. The importance of modeling and simulation remains well recognized in the Department of Energy and is receiving some support. A small initiative in computational chemistry began in FY 2001 and applications for support have been received and are under review at the time of this year's Combustion Research Conference.

During the past year, the Chemical Physics program has continued to benefit from the involvement of Dr. Eric Rohlfing, program manager for the Atomic, Molecular and Optical Physics program, Dr. Allan Laufer, team leader for the fundamental interactions programs, and more recently, Dr. Walter Stevens, program manager for Biophysics and Dr. Frank Tully, on detail from the Combustion Research Facility at Sandia National Laboratories, who will assist in the management of the Chemical Physics Program in the coming year. The efforts of Janet Kile and Julie Malicoat of the Oak Ridge Institute for Science Education and Karen Talamini of the Division of Chemical Sciences, Biosciences, and Geosciences, Office of Basic Energy Sciences in the arrangements for the meeting are also much appreciated.

It might also be appropriate at this time to add a personal note. After fourteen years serving the Chemical Physics Program, I would also like to thank all those scientists, past and present, who have participated in the program and who have contributed so much of their talents, their time, their patience, and their enthusiasm for this research endeavor. The excellence of this research program testifies to your contributions, not only of your individual research efforts, but your assistance to and collaboration with each other and your many reviews of the research proposals we receive. Keep up the good work.

William H. Kirchhoff SC-141
Division of Chemical Sciences, Biosciences, and Geosciences
Office of Basic Energy Sciences

May 29, 2001

22nd Annual Combustion Research Conference
U.S. Department of Energy
Office of Basic Energy Sciences

Agenda

Tuesday, May 29

3:00 pm	*Registration*
6:00 pm	*Dinner*
7:30 pm	*Welcoming Remarks*

7:45 pm *Invited Lecture*

Recent Advances in Molecular Beam Chemical Dynamics

Professor Yuan T. Lee
President, Academia Sinica
Nanking Taipei, Taiwan ROC

9:00 pm *Reception*

Wednesday, May 30
Morning Session

Ronald K. Hanson, Chair

Wednesday, May 30
Evening Session

F. Fleming Crim, Chair

Thursday, May 31
Morning Session

Marsha I. Lester, Chair

Thursday, May 31
Afternoon Session

David L. Osborn, Chair

Friday, June 1
Morning Session

Frank P. Tully, Chair

Table of Contents

Analysis of Turbulent Reacting Flow

William T. Ashurst and Alan R. Kerstein
Combustion Research Facility
Sandia National Laboratories
Livermore, CA 94551-0969
Email: ashurs@ca.sandia.gov

PROGRAM SCOPE

The goal of this project is to investigate the interactions among the physical and chemical processes in turbulent reacting flow by performing first-principles simulations and by developing simplified computational models of these interactions. Recent work has focused on gaining scientific understanding and developing models of the processes governing liquid-gas interactions in turbulent flow under high shear conditions. This work is intended to address phenomena such as cavitation, liquid fragmentation during sudden expansion, and shear-driven instabilities at liquid-gas interfaces. Another important focus is turbulence-chemistry interactions, both at the molecular scale and at the level of continuum modeling of couplings among multistep chemical kinetics, multicomponent transport, and local strain fluctuations caused by turbulent fluid motion.

Three methodologies are used in this work. Two of them are first-principles approaches and the other is a model.

One of the first-principles approaches is molecular dynamics (MD). Though MD simulation idealizes atomic and molecular interactions by adopting a pair-potential interaction, the equations of motion within this framework are solved exactly. This approach is essential for simulating phenomena such as cavitation onset that are governed by molecular-scale fluctuations not represented in continuum fluid dynamics.

Continuum fluid dynamics as implemented in direct numerical simulations (DNS) of the Navier-Stokes equations is nevertheless essential to capture the coupling of these localized phenomena to initial and boundary conditions and flow forcings. For this reason, DNS, a first-principles approach at the continuum level, is being used to simulate turbulent two-phase flows. This effort will focus on the overall system dynamics of liquid breakup driven by turbulence in the liquid and gas phases and shear at the liquid-gas interface.

Computational cost limits DNS of this problem to moderate turbulence intensities. Therefore DNS cannot be used over a sufficient range of turbulence intensities to determine the scaling laws that extrapolate simulated phenomena to the very high turbulence intensities of practical interest. For this purpose, large eddy simulation (LES) is commonly employed, but in its present state of maturity, it is unsuitable for application to the liquid-breakup problem because it does not resolve the fine scales at which the essential governing physics must be accurately represented. Similar concerns impede the application of LES to turbulent reacting flows, though efforts are underway to augment LES with subgrid models that provide sufficiently accurate representations of fine-scale multiphase and chemical reaction processes.

This project does not involve LES *per se*, but rather, involves a modeling approach that focuses directly on the interaction between turbulence and microscale processes. This approach, denoted One-Dimensional Turbulence (ODT), is potentially usable as a subgrid model for LES, and efforts to couple these two methodologies have been initiated. In this project, however, the focus

is on distilling the phenomenology of turbulence-microscale interactions into a reduced description within the ODT framework and then using ODT as a tool for the interpretation of measurements and the discovery of new physics.

ODT is a one-dimensional (1D) model formulated as a fully resolved unsteady simulation representing the time evolution of velocity profiles and advected fluid properties along a 1D line of sight in a turbulent flow. In this formulation, viscous momentum transport, species molecular transport, and chemical reactions evolve according to 1D equations of conventional form, as in 1D laminar strained flame computations. Turbulent eddies are represented by instantaneous rearrangements of property profiles on the 1D domain. The occurrence of these rearrangements is governed by a statistical sampling procedure in which event likelihoods depend on local turbulence production mechanisms (e.g., shear profile along the 1D domain). The rearrangement rules induce gradient amplification and fluid overturns that simulate reacting flow phenomena such as the unsteady evolution of multiple interacting flamelets.

RECENT PROGRESS

Recent applications of ODT to turbulent diffusion flames focused on extinction/reignition phenomena. Two flames studied experimentally in the Combustion Research Facility, in which the fuels were CH4 and a CO/H2 mixture, respectively, were simulated. Using a methodology developed in a prior study of H2 flames [1], the extinction/reignition characteristics of these flames were reproduced by the simulations [2,3]. This result suggests that the flame-flame interaction mechanism of reignition, which is captured by the model, is more important than the triple-flame propagation mechanism, a multidimensional process that the 1D formulation cannot emulate.

In preparation for the planned application of ODT to a variety of multiphase flow regimes, several generalizations of the model that are essential for this purpose have recently been formulated and demonstrated. First, the flow representation in ODT was generalized by incorporating a 1D profile of the full 3D velocity vector. (Previously, only one velocity component was represented.) This generalization allowed the incorporation of pressure-fluctuation effects that transfer kinetic energy between velocity components. This formulation was validated by means of comparisons to published DNS results [4]. Second, ODT was generalized to incorporate variable-density effects. A formulation limited to small density variations was shown to reproduce the spontaneous layering observed in stirred stably stratified fluids, including the parameter dependences of layer thicknesses [5]. Incorporation of a full dynamical representation of variable-density effects is in progress.

Although generalization of ODT to include two continuum phases has not yet been implemented, an initial step has been taken toward two-phase-flow representation. Droplets that are coupled to ODT gas-phase flow by means of a drag law and a vaporization law have been introduced. The key challenge in developing this formulation was to formulate a reasonable interaction mechanism between the droplets and ODT eddies, which are instantaneous. A procedure that interpolates consistently between the zero-inertia and infinite-inertia limits (for which the interaction mechanism is unambiguously defined) was developed and implemented. This formulation was used for simulation of the distribution of droplet trajectories previously measured in a pilot-scale liquid waste incinerator. The simulations demonstrated a novel capability to characterize the destruction efficiency of hazardous waste incineration processes [6].

FUTURE DIRECTIONS

The MD fragmentation studies to date achieved a homogeneous strain rate by imposing periodic boundaries that translate at a constant rate, with adjustment of the velocity of an atom crossing a boundary to account for the spatial gradient of the imposed initial velocity. Alternatively, fragmentation can be accomplished within a constant domain by incorporating a shrinking molecular diameter along with an increasing potential well depth. This system will be simulated to determine whether the droplet distribution is the same as found in the expanding system.

The near-term goal of ODT combustion studies will be to interpret and guide ongoing and planned experiments at the Combustion Research Facility. Further turbulent diffusion flame studies will be performed in coordination with new experimental capabilities that are now becoming operational in the Turbulent Combustion Laboratory at the Combustion Research Facility. Line Raman measurements will provide 1D instantaneous species concentration profiles from turbulent diffusion flames. ODT is unique among available models in its ability to predict most quantities derivable from line Raman. It therefore allows detailed comparisons between measurements and model simulations.

An important fundamental issue in turbulent combustion will be investigated that ODT is uniquely suited to address. Namely, ODT will be used to investigate whether flame dynamics become independent of turbulence intensity in the high-intensity limit. Reasoning based on the gross scaling properties of turbulence suggests that this is true, but certain theories of the fluctuation statistics of turbulent strain suggest that a weak (logarithmic) dependence on turbulence intensity may persist. ODT captures the pertinent fluctuation properties and can be implemented over a sufficient range of turbulence intensities to detect the postulated dependence if it is present.

The simulation of droplets coupled to ODT gas-phase simulation by drag and vaporization laws will be further generalized by incorporating more detailed droplet-gas interactions, including the Saffman lift force, near-wall corrections to the drag law, and thermophoretic effects in variable-temperature flow. These generalizations will allow detailed comparison to a recent DNS study that incorporated these effects, thus providing a basis for a broader study of the thermal-fluid couplings governing the performance of multiphase turbulent thermal reactors.

The nearly completed extension of ODT to flows with high density contrasts will lay the groundwork for the next planned extension to full multiphase flow dynamics. This extension will involve the introduction of phase interfaces with surface tension, enabling ODT simulations of liquid-jet breakup. For this application, the ODT domain represents a radial line of sight through the liquid column. Velocity components on this domain evolve by conventionally implemented viscous momentum transport and by rearrangement events (if the fluid is turbulent), as in other ODT formulations. A family of possible binary scission events is parameterized by the location of the scission point along the line. A time scale is assigned to each possible event based on a conventional Weber-number criterion in terms of daughter-droplet kinetic energy (were separation to occur) and the surface-tension energy of the additional surface area that would be created. This allows the formulation of a rate distribution for scission events, which is sampled in order to generate the event sequence. This is analogous to the sampling of ODT eddies. The advantage of ODT for the liquid-breakup problem derives from the fact that the model resolves the range of scales required to capture the broad size distribution of the evolved droplets, and incorporates spatial inhomogeneities, such as the difference between liquid interior and near-surface flow structure, that play an important role in the breakup process. The initial scientific focus of this effort will be an assessment of the contributions of liquid-phase turbulence, liquid-

gas interfacial shear, and surface tension to the evolution of a liquid column during the early stages of breakup. This study will be a step toward predictive modeling of atomization processes relevant to internal combustion engines.

REFERENCES

[1] T. Echekki, A. R. Kerstein, J-Y Chen, and T. D. Dreeben, Comb. Flame, in press.
[2] T. Echekki, A. R. Kerstein, and J-Y Chen, Comb. Flame, submitted for publication.
[3] J. C. Hewson and A. R. Kerstein, Comb. Theor. Model., submitted for publication.
[4] A. R. Kerstein, W. T. Ashurst, S. Wunsch, and V. Nilsen, J. Fluid Mech., in press.
[5] S. Wunsch and A. R. Kerstein, Phys. Fluids **13**, 702 (2001).
[6] J. R. Schmidt, J. O. L. Wendt, and A. R. Kerstein, Comb. Flame, submitted for publication.

PUBLICATIONS SINCE 1999

1. Wm. T. Ashurst, "Flow Frequency Effect upon Huygens Front Propagation," Comb. Theor. Model. **4**, 99 (2000).
2. Wm. T. Ashurst and B. L. Holian, "Droplet Formation by Rapid Expansion of a Liquid," Phys. Rev. E **59**, 6742 (1999).
3. Wm. T. Ashurst and B. L. Holian, "Droplet Size Dependence on Volume Expansion Rate," J. Chem. Phys. **111**, 2842 (1999).
4. Wm. T. Ashurst, H. N. Najm and P. H. Paul, "Chemical Reaction and Diffusion: a Comparison of Molecular Dynamics Simulations with Continuum Solutions," Comb. Theor. Model. **4**, 139 (2000).
5. T. D. Dreeben and A. R. Kerstein, "Simulation of Vertical Slot Convection Using One-Dimensional Turbulence," Int. J. Heat and Mass Transf. **43**, 3823 (2000).
6. T. Echekki, A. R. Kerstein, J-Y Chen, and T. D. Dreeben, "One-Dimensional Turbulence Simulation of Turbulent Jet Diffusion Flames: Model Formulation and Illustrative Applications," Combust. Flame, in press.
7. Y. Hu, R. Hurt, J. Calo, and A. R. Kerstein, "Kinetics of Orientational Order/Disorder Transitions and Their Application to Carbon Material Synthesis," Model. Sim. Mat. Sci. Eng. **7**, 275 (1999).
8. A. R. Kerstein, "One-Dimensional Turbulence: Formulation and Application to Homogeneous Turbulence, Shear Flows, and Buoyant Stratified Flows," J. Fluid Mech. **392**, 277 (1999).
9. A. R. Kerstein, "One-Dimensional Turbulence - Part 2. Staircases in Double-Diffusive Convection," Dyn. Atmos. Oceans **30**, 25 (1999).
10. A. R. Kerstein, Wm. T. Ashurst, S. Wunsch, and V. Nilsen, , "One-Dimensional Turbulence: Vector Formulation and Application to Free Shear Flows," J. Fluid Mech., in press.
11. A. R. Kerstein and T. D. Dreeben, "Prediction of Turbulent Free Shear Flow Statistics Using a Simple Stochastic Model," Phys. Fluids **12**, 418 (2000).
12. A. M. Lisewski, W. Hillebrandt, S. E. Woosley, J. C. Niemeyer, and A. R. Kerstein, "Distributed Burning in Thermonuclear Supernovae of Type IA," Astrophys. J. **537**, 405 (2000).
13. S. Wunsch, "Scaling Laws for Layer Formation in Stably Stratified Turbulent Flows," Phys. Fluids **12**, 672 (2001).
14. S. Wunsch and A. R. Kerstein, "A Model for Layer Formation in Stably Stratified Turbulence," Phys. Fluids **13**, 702 (2001).

Modeling Unimolecular Reactions Dynamics of Moderate Sized Ionic Systems

Tomas Baer (baer@unc.edu)
Department of Chemistry
University of North Carolina
Chapel Hill, NC 27599-3290

DOE Grant DE-FG02-97ER14776

Program Scope

The photoelectron photoion coincidence (PEPICO) technique is utilized to investigate the dissociation dynamics and thermochemistry of energy selected medium to large organic molecular ions. Extensive modeling of the dissociation rate constant using the RRKM theory or variational transition state theory (VTST) is used in order to determine the dissociation limits of energy selected ions. These studies are carried out with the aid of molecular orbital calculations of both ions and the transition states connecting the ion structure to their products. The results of these investigations yield accurate heats of formation of ions and free radicals. In addition, they provide information about the potential energy surface that governs the dissociation process. Isomerization reactions prior to dissociation are readily inferred from the PEPICO data.

The PEPICO Experiment

The photoelectron photoion coincidence (PEPICO) experiment in Chapel Hill is carried out with a laboratory H_2 discharge light source. Threshold electrons are collected by passing them through a set of small holes that discriminate against electrons with perpendicular velocity components. The electrons provide the start signal for measuring the ion time of flight distribution. When ions dissociate in the microsecond time scale, their TOF distributions are asymmetric. The dissociation rate constant can be extracted by modeling the asymmetric TOF distribution. A high-resolution version of this experiment is carried out at the Chemical Dynamics Beamline of the ALS, in which pulsed field ionization is used to detect the electrons with a resolution of 1 meV. When combined with coincidence ion detection, the results permit the measurement of ion dissociation limits to within 1 meV or 0.1 kJ/mol.

Recent Results

The Dissociation Dynamics and Thermochemistry of Energy Selected $CpCo(CO)_2^+$ Ions

The interest in these compounds is that they have been used extensively as catalysts for a variety of reactions important in biology and industry. Their effectiveness depends on several factors of which the availability of metal sites that can participate in the chemical reaction is of paramount importance Photoelectron photoion coincidence (PEPICO) spectroscopy has been used to investigate the dissociation dynamics of cobalt pentadienyl dicarbonyl $CpCo(CO)_2^+$. The dissociation proceeds by the sequential loss of the two CO molecules. Both reactions proceed with no reverse activation energies and are slow near their dissociation onset.

Of particular interest is the recent measurement of the ionization energy of transient species, CpCoCO, which is obtained by CO loss from the parent molecule. By heating the inlet system this transient CpCoCO can be generated and its ionization energy measured. The neutral bond energy can thus be determined by combining the following two equations.

$$CpCo(CO)_2 + h\nu \rightarrow CpCoCO^+ + CO + e^- \qquad (1) \qquad AE = 8.890 \text{ eV}$$

$$CpCoCO + h\nu \rightarrow CpCoCO^+ + e^- \qquad (2) \qquad IE = 7.01$$

$CpCo(CO)_2 \rightarrow CpCoCO + CO$ (3) BE = AE-IE=1.88 eV

This is the first neutral metal carbonyl bond energy measured through the ion cycle.

The Dissociation Dynamics and Thermochemistry of Energy Selected $CpMn(CO)_3^+$ and other Organometallic Ions

Following the $CpCo(CO)_2$ study, the loss of all three CO groups from $CpMn(CO)_3^+$ have been investigated. The analysis of these onsets is not easy because the ions are slow to dissociate due to the large density of states associated with the C_5H_5 (Cp) group. A related molecule, CpMnCp was also investigated in order to measure the loss of the first Cp unit. This produces the $CpMn^+$ ion, which is also a product of the $CpMn(CO)_3^+$ dissociation. However, the derived heats of formation were off by about 50 kJ/mol because of the uncertain heat of formation of the neutral CpMnCp and $CpMn(CO)_3$ molecules. The discrepancy is currently being worked out so that good heats of formation for the two molecules can be determined.

The data analysis is also difficult to analyze because the sequential loss of CO groups broadens the remaining energy in each subsequent ionic fragment. This is taken into account using the phase space theory (PST) for energy partitioning. In the case of the $Cp(CO)_3NO$, this broadening dominates the breakdown diagram because the diatomic groups carry away a significant fraction of the energy in the form of translational and rotational energy with each dissociation step.

Pulsed Field Ionization – Photoelectron Photoelectron Photoion Coincidence (PFI-PEPICO) Studies at the Advanced Light Source

A major advance in ion state selection was achieved at the chemical dynamics beam line of the ALS when the high-resolution capability of pulsed field ionization was coupled with ion coincidence measurements. The standard threshold photoelectron photoion coincidence (TPEPICO) technique is generally limited to 5-10 meV resolution. This resolution is only possible when using synchrotron radiation operating in the few bunch mode so that the electrons can be energy selected not only by their angular distributions, but by their time of flight as well. Because all third generation synchrotrons have great difficulty in operating in the few bunch mode because of low electron currents, 5 meV resolution cannot be practically achieved. The advance that has made possible high-resolution PEPICO studies with multi-bunch mode synchrotron radiation is based on two properties of the ALS light. First the 6.65 m monochromator can achieve the very high resolution necessary to make PFI feasible. Secondly, the pulse structure of the ring contains a 144 ns "dark" gap in which no light is generated. We have utilized this dark gap to distinguish the direct electrons from the long-lived field ionized Rydberg states. The result is a scheme that permits sub-meV resolution for ions such as CH_4.

TPEPICO studies with the 2-bunch Mode

Some experiments during the past 2-bunch mode of operation at the ALS, have shown that it is possible to select threshold electrons with a resolution of less than 10 meV. This is done by timing the electron relative to the ALS photon pulse. An added advantage is that the hot electron tail is cut off after about 20 meV. This mode of electron selection is easily coupled with ion detection for TPEPICO studies. The signal level is greater than it is for PFI-PEPICO, which makes it ideal for the study of large molecules, where the high-resolution PFI signal is quite weak.

One Year as Director of the Chemical Dynamics Beamline at the ALS

As of July 1, 2000, the PI assumed the directorship of the Chemical Dynamics Beamline at the ALS. This coincided with the departure of Arthur Suits who had been the director since its inception in 1995. The beamline is undergoing a number of changes. More long-term outside users are being brought in. Of particular note is the construction of a flame diagnostics experiment in which the products and intermediates generated in flames will be detected by photoionization. This PI source replaces the more commonly used electron ionization approach with its many attendant problems of ion fragmentation. Terry Cool, Phil Westmoreland, and Andy McIlroy are leading this effort. Another new experiment is the photoionization of liquid He droplets doped with various molecules such as Ar, NO, C_n. Finally, the high flux, 3m monochromator will finally come on line with a new grating so that radical IE's and imaging experiments can be carried out.

Future Plans

The dissociation dynamics of large ions generally involve slow dissociations. In addition, it is often difficult to produce cold beams using cw beam technology. As a result, the high resolution PFI-PEPICO approach may not be the most suitable. During the past year, experiments at the ALS have shown that the 2-bunch mode is ideal for preparing ions in selected energy states using the more standard threshold electron PEPICO (TPEPICO) experiment in which the electrons are selected by their TOF relative to the photon signal from the synchrotron. Such a set-up is currently being designed and will be utilized in July during the next 2-bunch mode of operation. This will permit the study of large ions as well as low vapor pressure samples that require a heated inlet system. It can also be used for TPEPICO studies of free radicals generated in the molecular beam. One of the molecules that we plan to study is the complete dissociative photoionization of $CpMn(CO)_3$ and CpMnCp. By determining the onset for the production of:

$$CpMn(CO)_3 + h\nu \rightarrow Cp + Mn^+ + 3\ CO$$

and

$$CpMnCp + h\nu \rightarrow 2\ Cp + Mn^+$$

it will be possible to determine the heat of formation of the starting molecules. As mentioned previously, these heats of formation are essentially not know to better than ± 40 kJ/mol. Photon energies in excess of 14 eV, available at the ALS light source, are required to dissociate these ions.

Other studies in the Chapel Hill laboratory will include further work on organo-metallic species as well as the study of acrolein. This interesting molecule does not have an experimentally determined heat of formation. However, by accurately measuring the dissociative ionization onset, it will be possible to determine its heat of formation.

Research Publications Resulting from DOE grant 1999-2000

O.A. Mazyar and T. Baer "Ethene loss kinetics of methyl 2-methyl butanoate ions studied by TPEPICO: The enol ion of methyl propionate heat of formation", *J.Am.Soc.Mass Spectrom.* **10** 200-208 (1999)

O.A. Mazyar and T. Baer "Isomerization and dissociation in competition: The two-component dissociation rates of methyl propionate ions", *J.Phys.Chem.* **103** 1221-1227 (1999)

T. Baer, R. Lafleur, and O.A. Mazyar, "The role of ion dissociation dynamics in the study of ion and neutral thermochemistry", in *Energetics of Stable Molecules and Reactive Intermediates*, M.E. Minas da Piedade (Ed) Kluwer Academic Publ. (1999)

G.K. Jarvis, K.M. Weitzel, M. Malow, T. Baer, Y. Song, and C.Y. Ng, "High resolution pulsed field ionization photoelectron-photoion coincidence spectroscopy using synchrotron radiation" *Rev. Sci. Instrum.* **70** 3892-3906 (1999)

K.M. Weitzel, M. Malow, G.K. Jarvis, T. Baer, Y. Song, and C.Y. Ng, "High-resolutioni pulsed field ionization photoelectron-photoion coincidence study of CH_4: Accurate 0K dissociation threshold for CH_3^+, *J.Chem.Phys.* **111** 8267-8270 (1999)

G.K. Jarvis, K.M. Weitzel, M. Malow, T. Baer, Y. Song, and C.Y. Ng, "High-resolution pulsed field ionization photoelectron photoion coincidence study of C_2H_2: Accurate 0K dissociation threshold of C_2H^+" *Phys.Chem.Chem.Phys.*, **1**, 5329-5332 (1999)

T. Baer, Y.Song, C.Y. Ng, J.Liu, and W. Chen, "The heat of formation of 2-$C_3H_7^+$ and proton affinity of C_3H_6 determined by pulsed field ionization - photoelectron photoion coincidence spectroscopy" *J.Phys.Chem.-A*, **104**, 1959-1964 (2000)

R.D. Lafleur, B. Sztaray, and T. Baer "A photoelectron-photoion coincidence study of the ICH2CN ion dissociation: The Thermochemistry of $^{\bullet}CH_2CN$, $^{+}CH_2CN$, and ICH_2CN" *J. Phys.Chem.* A **104**, 1450-1455 (2000)

Baer, Y.Song, J.Liu, W. Chen, and C.Y. Ng, "Pulsed field ionization - photoelectron photoion coincidence spectroscopy with synchrotron radiation: The heat of formation of the $C_2H_5^+$ ion" *Disc. Faraday Soc.* # **115** 137-145 (2000)

B. Sztaray and T. Baer, "The dissociation dynamics and thermochemistry of energy selected $CpCo(CO)_2^+$ ions" *J.Am.Chem.Soc.* **122**, 9219-9226 (2000)

T. Baer "Ion dissociation dynamics and thermochemistry by photoelectron photoion coincidence (PEPICO) spectroscopy", *In.J.Mass Spectrom.* **200** 443-457(2000)

Y.Li, B. Sztaray, and T. Baer, "The dissociation kinetics of energy selected $CpMn(CO)3^+$ ions studied by threshold photoelectron photoion coincidence spectroscopy", *J.Am.Chem.Soc.* (2001) in press

K.-M. Weitzel, G. Jarvis, M. Malow, Y. T. Baer, Song, and C. Y. Ng, "Observation of Accurate Ion Dissociation Thresholds in Pulsed Field Ionization Photoelectron Studies", *Phys. Rev. Lett.*, (2001) in press

Turbulence-Chemistry Interactions in Reacting Flows

Robert S. Barlow
Combustion Research Facility
Sandia National Laboratories, MS 9051
Livermore, California 94551
barlow@ca.sandia.gov

Program Scope

This experimental program is directed toward a more complete understanding of the coupling between turbulence and chemistry in both nonpremixed and premixed reacting flows. Simultaneous temporally and spatially resolved measurements of temperature and the concentrations of N_2, O_2, H_2, H_2O, CH_4, CO_2, CO, OH, and NO are obtained using the combination of Rayleigh scattering, spontaneous Raman scattering, and laser-induced fluorescence (LIF). The temperature and major species data are used to correct fluorescence signals for the effects of shot-to-shot variations in Boltzmann fraction and collisional quenching rate in turbulent flames. These detailed measurements of instantaneous thermochemical states in turbulent flames provide insights into the fundamental nature of turbulence-chemistry interactions. The emphasis of our recent work has been on i) the development of an internet-accessible library of data sets on turbulent nonpremixed flames that are appropriate for testing and understanding the capabilities of state-of-the-art combustion models, and ii) experimental validation of submodels for radiation, chemistry, mixing, and scalar dissipation. Experiments often involve visiting scientists, primarily from universities.

We have developed a new Turbulent Combustion Laboratory (TCL) that includes unique capabilities for single-shot, line-imaging measurements of multiple scalars, as well as state-of-the-art diagnostics for velocity measurements and combined velocity/scalar imaging. This new laboratory allows quantitative investigations of the spatial structure of turbulent flames that are being used to investigate fundamental aspects of emerging combustion technologies and to evaluate turbulent combustion models.

In addition to our experimental work, this program plays a leading role in organizing the International Workshop on Measurement and Computation of Turbulent Nonpremixed Flames (TNF), which facilitates collaboration among experimental and computational researchers working on fundamental issues of turbulence-chemistry interactions in gaseous diffusion flames and partially premixed flames. Collaborations and interactions with several combustion modeling and experimental groups are carried out in the context of the TNF Workshop.

Recent Results

Turbulent Flame Experiments

Three experimental campaigns involving multiscalar measurements in turbulent flames were conducted in the Turbulent Diffusion Flame (TDF) Laboratory during the past year. First, a series of swirl-stabilized flames of various fuels (CH_4, CH_4/air, and CH_4/H_2) was investigated in collaboration with the Peter Kalt and Assaad Masri (University of Sydney, Australia). Swirling flames are of great practical importance, and they represent a significant challenge for combustion models, due to the complexity of the fluid dynamics. Consequently, there is keen

interest within the modeling community to address current deficiencies in predictions of such flames. The objective of the present work is to develop and fully characterize a relatively simple swirl flame burner, which can serve as a benchmark for models.

The structure of turbulent lifted flames, stabilized on a vitiated-coflow burner, was investigated in collaboration with Ricardo Cabra, Bob Dibble, and J.-Y. Chen (UC Berkeley). Here, the high-temperature coflow (~1400K, generated by a large premixed flat flame) serves to promote ignition of the fuel stream and stabilization of the flame without the flow complications of recirculation or swirl. Thus, the submodels for chemistry and mixing can be tested for accuracy in predicting ignition delay in high-temperature, partially-premixed regimes analogous to those in some types of practical combustor.

In a related project, CH_4/H_2 jet flames were studied in an intermediate-temperature (~900K) coflow having varying levels of oxygen (mass fractions of 3%, 6%, and 9%). This work, which was conducted in collaboration with Bassam Dally (University of Adelaide, Australia), tests the accuracy of detailed methane mechanisms with regard to combustion at reduced flame temperatures, where NO production is very low. The measured regimes approached conditions of "flameless oxidation," in which slower reaction rates cause the reaction zone to be broadly distributed and with low luminosity. Flameless oxidation is under intense investigation in Asia for application in high-efficiency, low-emission furnaces. However, the reaction zone structure is poorly understood at the fundamental level, and chemical mechanisms are not well tested in this reduced temperature regime.

We have collaborated over the past two years with Johannes Janicka and Dirk Geyer (TU Darmstadt, Germany), Nondas Mastorakos (ICEHT, Greece), and J.-Y. Chen (UC Berkeley) on the development of an opposed-jet apparatus for fundamental studies of turbulent mixing and combustion. The Sandia copy of this burner was been assembled and operated in the TCL. We anticipate an extended collaborative experimental and modeling program based on this burner, and we expect to add turbulent opposed-jet flames to the TNF Workshop library. This geometry is of particular interest with regard to turbulent mixing, as the mixing regime is very different from that found in jet flames. Predictive models must be robust enough to handle a wide range of flow and combustion regimes.

Progress on Partially Premixed Laminar Flames

An experimental and computational study of steady, laminar, opposed-flow, partially-premixed CH_4/air flames was completed. Fuel-side equivalence ratios of ϕ=3.17 and ϕ=2.17 were considered, with the former mixture being the same used in previous work on turbulent piloted jet flames. Strain rates roughly corresponding to the modeled conditional mean scalar dissipation rate at x/d=30 in piloted flame D were applied in order to investigate discrepancies among measured and modeled results for fuel-rich conditions in the turbulent flames. Laminar flame calculations were performed by J.-Y. Chen (UC Berkeley), using a detailed mechanism from Jim Miller, as well as detailed and reduced versions of GRI 2.11 and GRI 3.0 mechanisms. An optically-thin radiation model was included in these calculations.

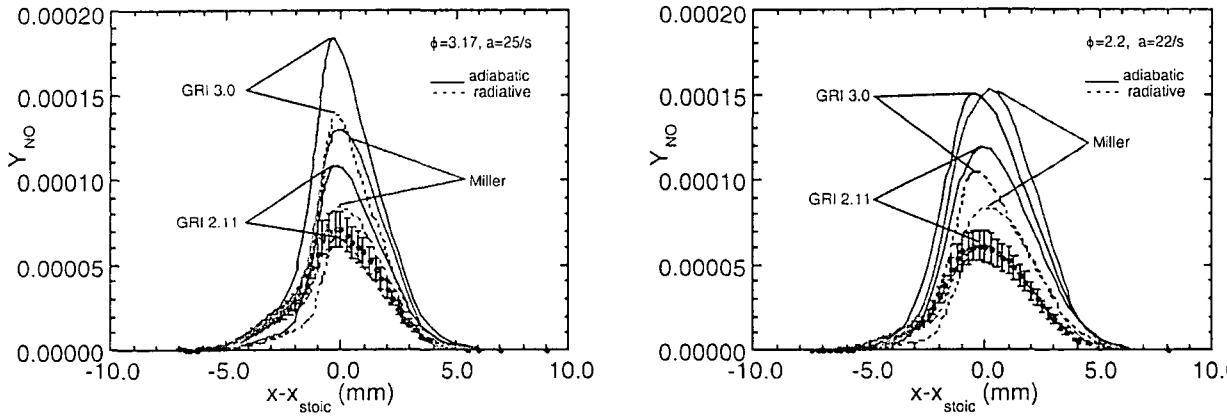

Fig. 1. Measured and calculated results for NO mass fraction in laminar, partially premixed CH_4/air flames.

Results demonstrated that measured and calculated mass fractions of the major species were in agreement, pointing to possible problems with current models for scalar dissipation in turbulent flames. Results also showed that GRI 3.0 significantly over predicts NO levels in these flames (Fig. 1), a finding that is in agreement with recent work from Purdue. Measurements in an opposed flow flame with ϕ=1.8 and in laminate jet flames with all three equivalence ratios were obtained recently and are being analyzed.

Progress in the Turbulent Combustion Laboratory

The Turbulent Combustion Laboratory includes two matched flow stations and complementary diagnostics for scalar and velocity measurements. PLIF and PIV systems are now fully operational at one of these flow stations. They have been applied by Bob Schefer (BES contributor) in studies of the structure and stability of lean premixed CH_4/air and CH_4/H_2/air flames with swirl stabilization. The other flow station is dedicated to a unique line-imaging system for multiscalar measurements that will allow single-shot measurements of scalar

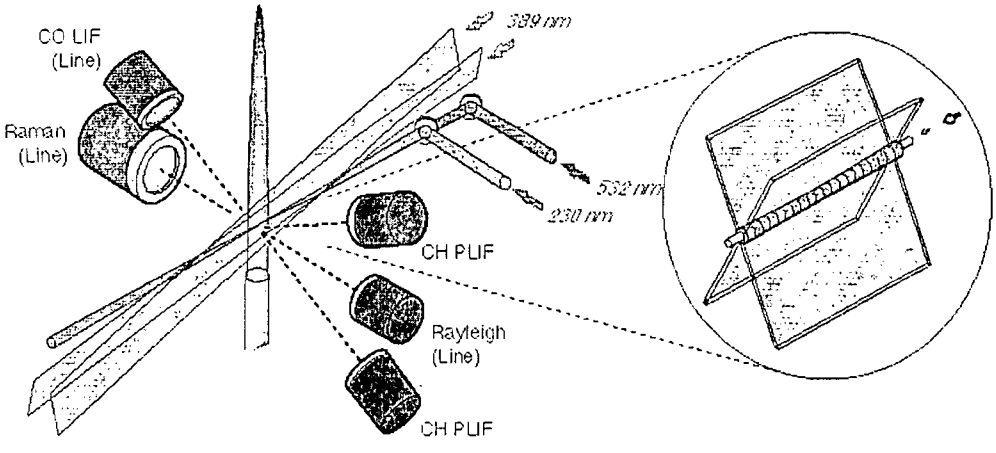

Fig. 2. Configuration for line-imaging and CH-PLIF in the TCL.

dissipation, along with species and temperature. Lasers, optics, and camera systems for line imaging of Rayleigh scattering, spontaneous Raman scattering, and two-photon LIF of CO are all in place. The Raman system makes use of four high-power Nd:YAG lasers, an optical pulse

stretcher, a custom high-speed mechanical shutter (9 μs FWHM), and an unintensified, back-illuminated CCD array detector. This combination yields unprecedented precision. The integration of all cameras, data acquisition, and experimental control systems is in progress.

Future Plans

Our first priority for scalar experiments on turbulent flames in the TCL will be to measure scalar gradients in the series of piloted CH_4/air jet flames and to extract information related to the conditional scalar dissipation. These data will help to resolved questions that have come out of model comparisons in the TNF Workshops, and they should be very useful for validation of submodels for scalar dissipation that are used in RANS and LES methods. We intend to investigate the joint statistics of mixture fraction, scalar dissipation, species mass fractions, flame curvature, and flame orientation. These statistics will be compared with results from LES and DNS calculations. Investigations of scalar structure and NO formation in laminar flame will continue with emphasis on methane diffusion flames at reduced-temperature (reduced O_2 in the oxidizer stream dilution). Ethylene flame will also be investigated, though interferences are expected to be an issue for Raman measurements.

BES Supported Publications (1999 - present)

R. S. Barlow, N. S. A. Smith, J.-Y. Chen, and R. W. Bilger, "Nitric Oxide Formation in Dilute Hydrogen Jet Flames: Isolation of the Effects of Radiation and Turbulence-Chemistry Submodels," Combust. Flame, **117**, 4-31 (1999).

R. S. Barlow and P. C. Miles, "A Shutter-Based Line-Imaging System for Single-Shot Raman Scattering Measurements of Gradients in Mixture Fraction," *Twenty-Eighth Symposium (International) on Combustion*, (Edinburgh, Scotland, July 30-August 4, 2000).

R. S. Barlow, G. J. Fiechtner, C. D. Carter, and J.-Y. Chen, "Experiments on the Structure of Turbulent $CO/H_2/N_2$ Jet Flames," Combust. Flame, **120**:549-569 (2000).

J. H. Frank, R. S. Barlow, and C. Lundquist, "Radiation and Nitric Oxide Formation in Turbulent Nonpremixed Jet Flames," *Twenty-Eighth Symposium (International) on Combustion*, (Edinburgh, Scotland, July 30-August 4, 2000).

W. Meier, R. S. Barlow, Y.-L. Chen, and J.-Y. Chen, "Raman/Rayleigh/LIF Measurements in a Turbulent $CH_4/H_2/N_2$ Jet Diffusion Flame: Experimental Techniques and Turbulence-Chemistry Interactions," Combust. Flame **123**:326-343 (2000).

P. C. Miles and R. S. Barlow, "Fast Mechanical Shutter for Spectroscopic Applications," Meas. Sci. Technol. **11**:392-397 (2000).

P. A. Nooren, M. Versiuis, T. H. van der Meer, R. S. Barlow, and J. H. Frank, "Raman-Rayleigh-LIF Measurements of Temperature and Species Concentrations in the Delft Piloted Turbulent Jet Diffusion Flame," Appl. Phys. B, **71**:95-111 (2000).

Web-Based Information

http://www.ca.sandia.gov/tdf/Workshop.html	TNF Workshop Information
http://www.ca.sandia.gov/tdf/Lab.html	Turbulent Diffusion Flame Laboratory

Energy Partitioning in Elementary Chemical Reactions

Richard Bersohn
Department of Chemistry
Columbia University
New York, NY 10027
rb18@columbia.edu

The goals of this research are 1) to measure the yields of all the important channels of the reactions of $O(^3P)$ with unsaturated hydrocarbons and radicals and 2) by measurement of state distributions to understand the detailed mechanism. i.e. the trajectories of the atoms during the reactive collision.

Vibrational distribution of vinoxy radicals

The nascent vibrational distributions of diatomic and triatomic molecule rreaction products have been extensively measured by LIF and REMPI techniques. Most larger molecules either do not fluoresce or they are not reaction products. Vinoxy, $\cdot CH_2\text{-}CH{=}O$ is a fortunate exception.. It is a product of the reaction of $O(^3P)$ atoms with terminal alkenes $RCH{=}CH_2$ as well as the photodissociation of alkyl vinyl ethers, $R\text{-}O\text{-}CH{=}CH_2$. Excitation to its vibrationless B state produces bright fluorescence. As shown by Rohlfing, the resolved fluorescence spectrum stretches over a wide energy range.[1] The relative intensities of the different emission bands from the same excited state level are equal to the relative Franck-Condon factors of the transitions. The breadth of the emission spectrum gives rise to the possibility of probing the vibrational state distribution by exciting fluorescence from hot bands. That is, transitions originating from vibrationally excited states and terminating on the vibrationless upper state will have intensities proportional to the product of the vibrational state population and the Franck-Condon factor. (Fig.1).

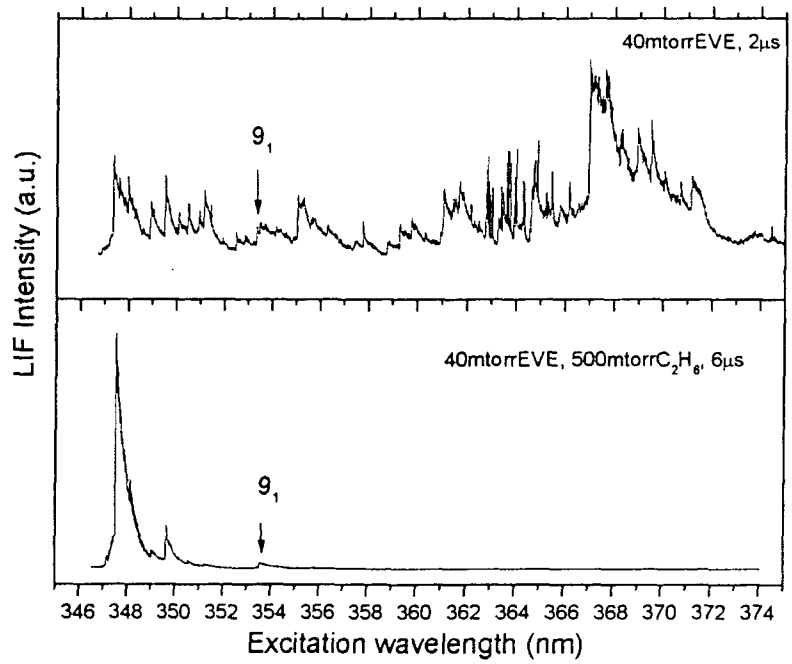

Fig.1 LIF hot band spectra of nascent and relaxed vinoxy

Vibrational relaxation of vinoxy radicals

The most evident aspect of the hot band spectrum is its breadth and complexity. Part of the complexity is due to sequence bands which are intermixed with hot bands. However, the central finding is that the nascent vinoxy is excited in many different modes and combinations of modes. The second part of Fig.1 shows the LIF excitation spectrum after vibrational relaxation. The only bands left are the strong 0_0^0 band origin and a weak 9_1^0 band due to a small fraction of the molecules which have one quantum (500 cm^{-1}) of the ν_9 mode excited. These two pictures show clearly the possibility of measuring the time dependence of the populations of individual vibrational levels. At higher energies, where numerous vibrations are simultaneously excited and assignment is difficult, at least the total energy is known.

The time dependence of the populations of a number of energy levels was measured in the presence of an excess of the following buffer gases: C_2H_6, SF_6, CH_4 , CO_2, N_2 and O_2. A common trend was found for all. The highest energy levels decay monotonically on a fast time scale. The populations of intermediate energy levels first rise and then decay on an intermediate time scale to an asymptotoic value near zero. The ground state population increases monotonically on the slowest time scale toward an asymptote For each individual relaxer, relaxation rate constants increase roughly linearly with energy reaching gas kinetic values at around 5000 cm^{-1} of internal energy. Rate constants also increase with the size of the molecule; for example, ethane is an order of magnitude more effective than oxygen. The curves shown in Fig.2 are due to relaxation caused by collisions with SF_6 but are typical. They provide a semiquantitative estimate of the maximum vibrational energy content of the radical. The populations of the highest levels can only decay because levels higher than them are sparsely populated. The intermediate level populations rise because they are being fed rapidly from above and decay on a somewhat slower time scale to lower levels. The population of the ground state, being initially

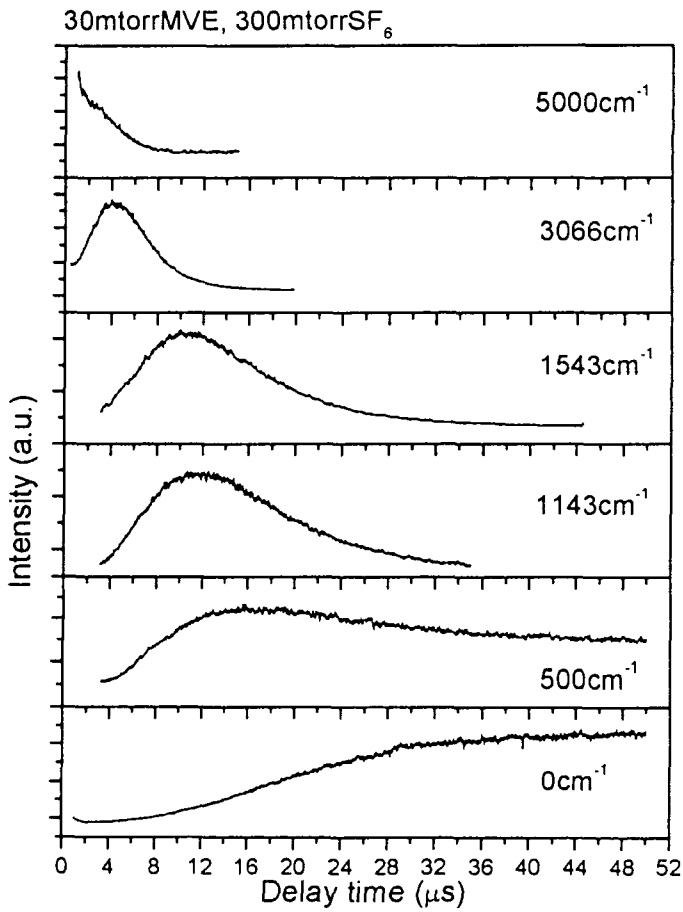

Fig.2 LIF intensity as a function of time and energy

rather small because of the photodissociation dynamics, rises monotonically; in the end most molecules are in the ground state...

O + RCH=CH$_2$ --> R· + ·CH$_2$CH=O

Fig.3 below shows the low energy part of the hot band spectra of the vinoxys from the reaction of O(^{3}P) atoms with a series of terminal alkenes. The longer the alkyl group R, the smaller is the 4_1^0 peak at the right relative to the band origin at the left. The R group acts as a bath which cools the vinoxy product. By implication the reaction complex must live long enough for internal vibrational redistribution to occur i.e. some tens of ps. This is consistent with a measurement of 217 ps for the lifetime of the ethylene- O atom reaction complex byAbou-Zied and McDonald.[2] It is inconsistent with the finding by Yuan Lee's group that the vinoxy radical is preferentially scattered backwards in the center of mass system.[3]

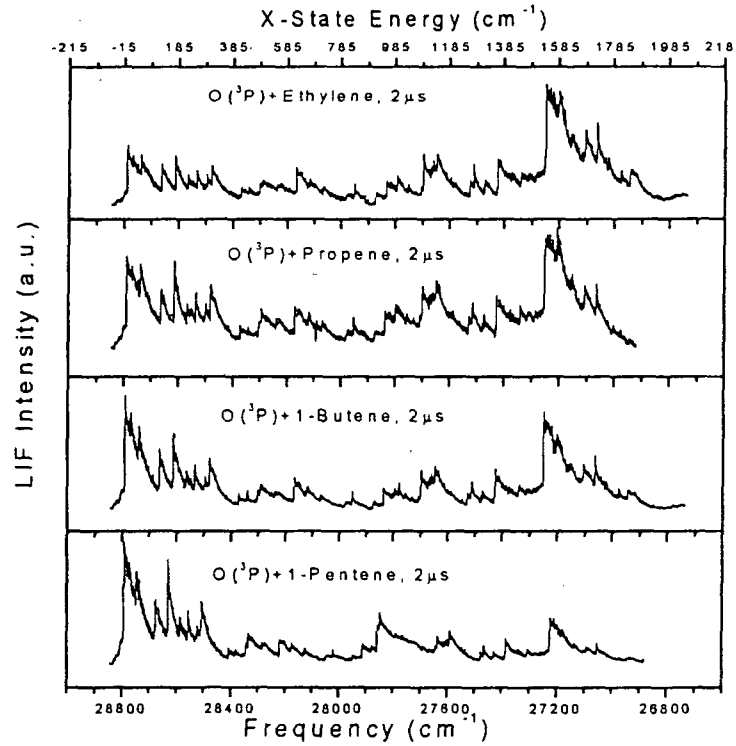

Fig.3 Hot band spectra of vinoxy product from different alkenes

Future plans

Experiments on the hot band absorptions of ketenyl similar to those decribed on vinoxy are being carried out. Partially deuterated ethylene and propene will be reacted with $O(^3P)$ to produce labelled vinoxys. The positions of the deuterons may provide information about the reactiuon mechanism. A minimolecular beam machine will be built in which two oppositely directed valves will open for 10 μs and release hydrocarbon molecules and oxygen atoms respectively. Detection of radicals will be by vuv photoionization in a TOF mass spectrometer. This will be a new version of an old experiment of D.Gutman and coworkers.[4] which will be closer to the ideal limit of single collisions.

References

1. L.R.Brock and E.A.Rohlfing, J.Chem.Phys. **106,**10048(1997)
2.O.K.Abou-Zied and J.D.McDonald, J.CHem.Phys. **109,**1293(1998)
3.A.M.Schmoltner,P.M.Chu,R.J.Brudzynski,Y.T.Lee, J.Chem.Phys. **91**,6926(1989)
4.J.R.Kanofsky,D.Lucas,F.Pruss and D.Gutman, J.Phys.Chem.**78,**311(1973)

Publications in years 1999, 2000 and 2001

1. The CO product of the reaction of $O(^3P)$ with CH_3 radicals,
   Z.Min,R.W.Quandt,T-H.Wong and R.Bersohn,
   J.Chem.Phys. **111,**7369(1999)
2. The Reactions of $O(^3P)$ with Alkenes: The Formyl Radical Channel,
   Z.Min,T-H.Wong,R.W.Quandt and R.Bersohn,
   J.Phys.Chem.A **103,**10451(1999)
3. Reaction of $O(^3P)$ with Alkenes: Side Chain vs. Double Bond Attack,
   Zhiyuan Min, Teh-Hwa Wong, Hongmei Su and Richard Bersohn,
   J.Phys.Chem.A **104,**9941(2000)
4.Photodissociation of acetaldehyde: the CO + CH_4 channel
   Benjamin Gherman, Richard Friesner, Teh-Hwa Wong, Zhiyuan Min,
   and Richard Bersohn, J.Chem.Phys. **114,**6128(2001)
5. Vibrational Distribution and Relaxation of Vinoxy Radicals,
   Hongmei Su and Richard Bersohn, J.Chem.Phys. **114,**xxxx(2001)

Theoretical Studies of Combustion Dynamics

Joel M. Bowman
Cherry L. Emerson Center for Scientific Computation and
Department of Chemistry, Emory University
Atlanta, GA 30322,
bowman@euch4e.chem.emory.edu

Program Scope

The goals of my DOE-supported research are the development and application of quantum mechanical methods to processes of importance in gas-phase combustion. The applications are generally to systems that are either of specific interest to combustion and/or to experiments that probe fundamental aspects of unimolecular and bimolecular reactions.

Recent work has focused on the quantum, state-specific unimolecular dissociation of HOCl. The rates of this dissociation have been measured in experiments by the Rizzo and Sinha groups for specific rotational states of the fifth overtone of the OH-stretch.[1,2] In these states the dissociation takes place just above the energetic threshold and, not surprisingly, the dissociation rates are very slow (i.e., of the order of 10^7/sec) and display very non-statistical behavior with the rotational quantum numbers J and K_a.

We have succeeded in calculating the rates of dissociation for these states,[3] using a very accurate *ab initio* potential energy surface.[4] In very recent work we extended our calculations to the sixth and seventh overtone states of the OH-stretch,[5] in response to very recent experiments of the Rizzo group,[6] and describe some of the results below.

In the area of bimolecular reactions, we have recently finished calculations of the $O(^3P)$+HCl and $O(^1D)$+HCl reactions.[7,8] The former reaction is a putatively simple direct reaction with a barrier and the latter one is a complex one with two reaction products, ClO+H and OH+Cl, that is governed by two wells corresponding to HOCl and HClO. Some of the highlights of this work, which involve important collaborations, are reviewed below.

Recent Progress

The widths and final state distributions of the OH product of the unimolecular dissociation of HOCl with the OH-stretch excited to the sixth and seventh overtones have been calculated. The widths of these resonances have been determined experimentally by Rizzo and co-workers to be approximately 0.01 and 1 cm^{-1}, respectively.[6] Our calculations made use of the highly accurate potential that we developed previously in collaboration with Kirk Peterson (PNNL).[4] The new calculations have been written up and are in press.[5] The calculated widths are in very good agreement with experiment. In addition the calculations predict significant vibrational excitation of the OH product from the dissociation of HOCl(v_{OH}=8).

Quantum calculations of the rate constant of the $O(^3P)$+HCl have been reported using a new *ab initio* potential energy surface of Ramachandran, *et al.* The quantum calculations were done in collaboration with Stephen Gray (ANL).[7(a)] These calculations were compared in a recent publication with rate constants from various approximate calculations.[7(b)] Those based on the widely used ICVT/μOMT method were found to be in error by a factor of 4.25 at 300 K and a factor of 3 at 400 K, even though they

fortuitously agree well with experiment. The source of the errors in this and other approximate calculations was traced to resonances in the tunneling region found in the quantum calculations. These resonances appear to be due to the presence of prominent Van der Waals minima in this potential. Further analysis of these resonances will be carried out in future work, as described below.

Reduced dimensionality (in six degrees of freedom) quantum calculations were completed for the $H+CH_4 \rightarrow H_2+CH_3$ reaction.[9] The thermal rate constant was obtained and compared with recently reported full dimensional ones of Huarte-Larrañaga and Manthe, and very good agreement was found. The original calculations of Huarte-Larrañaga and Manthe[10] were full dimensional in directly obtained the cumulative reaction probability, but used the harmonic approximation for the vibrational partition function of CH_4. The reported rate constant was found to be factors of 3 or more above those of previous reduced dimensionality quantum calculations. We pointed out that the harmonic treatment of methane vibrations is inconsistent with an exact treatment of the cumulative reaction probability. Using our code "MULTIMODE", we obtained the exact vibrational energies of full dimensional (9 degrees of freedom) CH_4, and re-computed the thermal rate constant. The use of the correct zero point energy of CH_4, which is 0.47 kcal/mol below the harmonic approximation, effectively increases the ground state adiabatic barrier height and decreases the rate constant by a factor of 2-3 in the temperature range considered by Huarte-Larrañaga and Manthe.[11]

Future Plans

New exact calculations, in collaboration with David Manolopoulos (Oxford) are underway, to characterize the eight low energy resonances in the $O(^3P)+HCl$ reaction. These calculations will be done for a large range of total angular momentum, J, to determine numerically the "J-trajectories" of these resonances. This information will help with the characterization of the resonances. We also plan to do large-scale calculations of the wave functions of these resonances, which we speculate span the region of both the Van der Waals minima and the saddle point of the reaction.

We plan to re-examine the lifetime of the important HN_2 radical. Calculations of the lifetime were reported earlier using a realistic potential energy surface.[12] These calculations were only done for zero total angular momentum, which is not appropriate for combustion temperatures. We plan to extend these calculations for rotational states that are the most populated at combustion temperatures. These calculations will make use of the efficient methods we have developed for the study of HOCl unimolecular dissociation. In addition, in collaboration with Stephan Irle of the Emerson center, we plan new *ab initio* calculations of the potential energy surface(s) for this very important unimolecular reaction, to investigate the possible role of electronically non-adiabatic effects.

References

1. G. Dutton, R. J. Barnes, and A. Sinha, J. Chem. Phys **111**, 4976 (1999).
2. A. Callegari, J. Rebstein, R. Jost, and T. R. Rizzo, J. Chem. Phys **111**, 7359 (1999).
3. (a) S. Skokov and J. M. Bowman, J. Chem. Phys. **110**, 9789 (1999); (b) S. Skokov and J. M. Bowman, J. Chem. Phys. **111**, 4933 (1999).
4. S. Skokov, K. Peterson, and J. M. Bowman, Chem. Phys. Lett **312**, 494 (1999).

5. S. Zou, S. Skokov, and Joel M. Bowman, Chem. Phys. Lett., in press (2001).
6. A. Callegari and T. R. Rizzo, Phys. Chem. Chem. Phys, (2001) in press.
7. (a) S. Skokov, T. Tsuchida, S. Nambu, J. M. Bowman, and S. Gray, J. Chem. Phys. **113**, 227 (2000); (b) S. Skokov, S. Zou, J. M. Bowman, T. C. Allison, D. G. Truhlar, Y. Lin, B. Ramachandran, B. C. Garrett, and B. J. Lynch, J. Phys. Chem. **105** 2298 (2001).
8. (a) K. Christoffel, Y. Kim, S. Skokov, J. M. Bowman and S. Gray, Chem. Phys. Lett. **315**, 275 (1999); (b) M. Bittererova, J. M. Bowman, and K. Peterson, J. Chem. Phys. **113**, 6186 (2000).
9. D. Wang and J. M. Bowman, J. Chem. Phys., submitted.
10. F. Huarte-Larrañaga and U. Manthe, **113**, 5115 (2000).
11. J. M. Bowman, Dunyou Wang, Xinchuan Huang, Fermin Huarte-Larrañaga and U. Manthe, J. Chem. Phys. in press (2001).
12. (a) H. Koizumi, G. C. Schatz, and S. P. Walch, J. Chem. Phys. **95**, 4130 (1991); (b)H. Koizumi, G. C. Schatz, and J. M. Bowman, in *Isotope Effects in Gas-Phase Chemistry,* Kaye, J. A., Ed. (American Chemical Society, Washington, D.C., 1992), Chap. 3.

PUBLICATIONS SUPPORTED BY THE DOE (1999-present)

Non-separable transition state theory for non-zero total angular momentum: Implications for J-shifting and application to the OH+H_2 reaction, J. M. Bowman and H. Shnider, J. Chem. Phys. **110**, 4428 (1999).

Calculation of resonance states of non-rotating HOCl using an accurate *ab initio* potential, S. Skokov, J. Bowman, and V. Mandelshtam, Phys. Chem. Chem. Phys. **1**, 1279 (1999).

Non-separable RRKM theory applied to unimolecular dissociation of HCO → H+CO, K. Christoffel and J. M. Bowman, J. Phys. Chem. **A103**, 3020 (1999).

Calculations of low-lying vibrational states of cis and trans-HOCO, J. M. Bowman, K. Christoffel, and G. Weinberg, J. Mol. Struct. (Theochem) **461**, 71 (1999).

Potential energy surface and vibrational eigenstates of the H_2-CN($X^2\Sigma^+$) van der Waals complex, A. L. Kaledin, M. C. Heaven, and J. M. Bowman, J. Chem. Phys. **110**, 10380 (1999).

Variation of the resonance width of HOCl($6\nu_{OH}$) with total angular momentum: Comparison between ab initio theory and experiment, S. Skokov and J. M. Bowman, J. Chem. Phys. **110**, 9789 (1999).

Variation of resonance widths of HOCl($6\nu_{OH}$) with total angular momentum: Comparison between ab initio theory and experiment, S. Skokov and J. M. Bowman, J. Chem. Phys. **111**, 4933 (1999).

Quantum and quasiclassical reactive scattering of O(^{1}D)+HCl using an *ab initio* potential, K. Christoffel, Y. Kim, S. Skokov, J. M. Bowman and S. Gray, Chem. Phys. Lett. **315**, 275 (1999).

The spin-forbidden reaction CH($^2\Pi$)+N_2 → HCN + N(^{4}S) revisited. II.-Non-adiabatic transition state theory and application, Q. Cui, K. Morokuma, J. M. Bowman, and S. J. Klippenstein, J. Chem. Phys **110**, 9469 (1999).

Wavepacket propagation for reactive scattering using real L^2 eigenfunctions with damping, S. Skokov and J.M. Bowman, Phys. Chem. Chem. Phys. **2**, 495 (2000)

Approximate time independent methods for polyatomic reactions, J. M. Bowman, in Reaction and Molecular Dynamics (Proceedings of the European School on Computational Chemistry, Perugia, Italy, July (1999)) Lagana, A., Riganelli, A., (Eds.) (Springer, 2000)

Quantum dynamics and rate constant for the $O(^3P)$+HCl reaction, S. Skokov, T. Tsuchida, S. Nambu, J. M. Bowman, and S. Gray, J. Chem. Phys.**113**, 227 (2000).

A reduced dimensionality quantum calculation of the reaction of H_2 with diamond (111) surface, S. Skokov and J. M. Bowman, J. Chem. Phys. **113**, 779 (2000)

A wavepacket calculation of the effect of reactant rotation and alignment on product branching in the $O(^1D)$+HCl $\rightarrow$ ClO+H, OH+Cl reaction, M. Bittererova and J. M. Bowman, J. Chem. Phys. **113**, 1 (2000).

Quantum scattering calculations of the $O(^1D)$+HCl reaction using a new ab initio potential and extensions of J-shifting, M. Bittererova, J. M. Bowman, and K. Peterson, J. Chem. Phys. **113**, 6186 (2000).

Quantum calculations of the effect of bend excitation in methane on the HCl rotational distribution in the reaction $CH_4 + Cl \rightarrow CH_3 + HCl$, S. Skokov and J. M.Bowman, J. Chem. Phys. **113**, 4495 (2000).

Thermal and state-selected rate coefficients for the $O(^3P)$ + HCl reaction and new calculations of the barrier height and width, S. Skokov, S. Zou, J. M. Bowman, T. C. Allison, D. G. Truhlar, Y. Lin, B. Ramachandran, B. C. Garrett, and B. J. Lynch, J. Phys. Chem. **105** 2298 (2001).

State-to state reactive scattering via real L^2 wave packet propagation for reduced dimensionality AB + CD reactions, S. Skokov and J. M. Bowman, J. Phys. Chem., in press (2001).

Ab initio calculation of the lifetimes of HOCl($7\nu_{OH}$ and $8\nu_{OH}$) and comparison with experiment, S. Zou, S. Skokov, and J. M. Bowman, Chem. Phys. Lett., in press (2001).

The importance of an accurate CH_4 vibrational partition function in full dimensionality calculations of the $H + CH_4 \rightarrow H_2 + CH_3$ reaction, J. M. Bowman, D. Wang, X. Huang, F. Huarte-Larrañaga and U. Manthe, J. Chem. Phys. in press (2001).

Very High Pressure Single Pulse Shock Tube Studies of Aromatic Species

Kenneth Brezinsky
Department of Chemical Engineering (M/C 110)
University of Illinois at Chicago
810 S. Clinton St.
Chicago, IL 60661
Kenbrez@uic.edu

PROGRAM SCOPE AND FOCUS

The Office of Basic Energy Sciences is committed to developing the fundamental understanding necessary for reduction and mitigation of the environmental impacts of energy use. Consequently, fundamental research programs have focused on the chemical reactions necessary for the quantitative, predictive modeling of the chemistry of environmentally deleterious emissions. Prediction of emissions through detailed chemical kinetic models can be accomplished through a better understanding of the elementary reaction steps of the oxidation and pyrolysis of the aromatic species benzene, toluene and related compounds which are contained in typical energy producing fuels like gasoline.

The research in this program focuses on oxidation and pyrolysis experiments of benzene and toluene in a very high pressure single pulse shock tube in order to obtain data at extremes of pressure and temperature. With these data, flaws in existing models will be addressed permitting the development of a comprehensive benzene/toluene oxidation model potentially applicable to the reduction and prevention of pollution.

The means for accomplishing the research is to shock dilute mixtures of benzene and toluene, less than 100 ppm, with and without oxygen (from fuel rich to fuel lean stoichiometries and pyrolysis) at temperatures ranging from 1000 to 1500K and pressures ranging from 300 to 1000 atmospheres. Reactions times at these conditions can be varied from as short as 250 microseconds to 2.0 milliseconds. At the completion of reaction, defined by quenching in the single pulse shock tube, gas samples are extracted from the end wall region of the shock tube for subsequent analysis by gas chromatography/mass spectrometry. The stable intermediate species identified and quantified by GC/MS are be the data used for development and validation of a comprehensive model.

RECENT PROGRESS

Shock Tube Constructed and Testing Completed:

The construction and testing of the very high pressure single pulse shock tube necessary for the examination of the oxidation reactions of aromatics has been completed. The shock tube has been designed for operation at approximately 1000 atmospheres and temperatures to 2000K. A variable length driven section permits reaction times to be varied from approximately 250 μsec to 1.5 ms. A very high-pressure profile, greater than 1000 atm, obtained from the shock tube, is shown below.

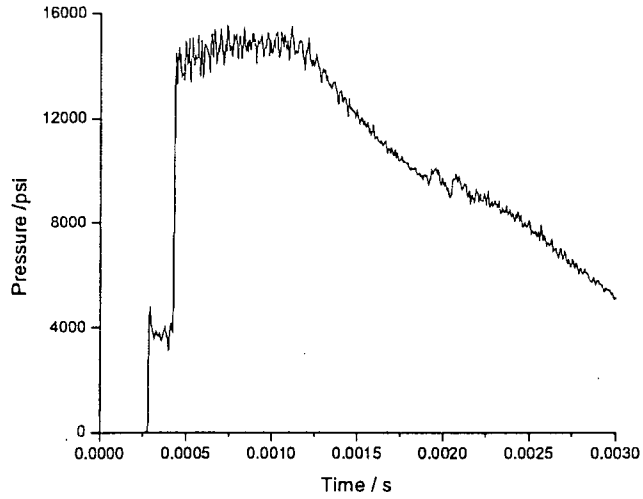

High pressure, > 1000 atm, , profile
from the single pulse shock tube.

Chemical Analysis Instrumentation Installed and Operational:

A gas chromatograph/mass spectrometer which is the heart of the gas phase chemical analysis procedure, is completely operational with analysis protocols developed for hydrocarbons ranging in size from C1 to C8. A supplemental device, a purge and trap concentrator, has been installed as an injector on the GC/MS for the analysis of very low concentration species. In addition, a supplemental high performance liquid chromatograph has been acquired and made operational if it becomes necessary to analyze high molecular weight species that are not amenable to GC/MS analysis.

Shock Tube Operation Optimized:

Extensive examinations of the effects of driver section lengths on the quality of the high pressure profiles were conducted as part of a student's Master Degree research work. Driver section lengths required to produce repeatable high quality pressure profiles have been established. Driver section length is varied by the insertion of brass plugs.

Extensive examination of the optimum brass diaphragm thickness' and scorings has been conducted. From this examination a protocol for routinely fabricating in excess of 100 scored diaphragms per day using a computer controlled milling machine has been developed.

External standard calibration of shock temperatures has been achieved. The species, 1,1,1-trifluoroethane, has been used as a "chemical thermometer" for the external calibration procedure. A representative calibration curve is shown below.

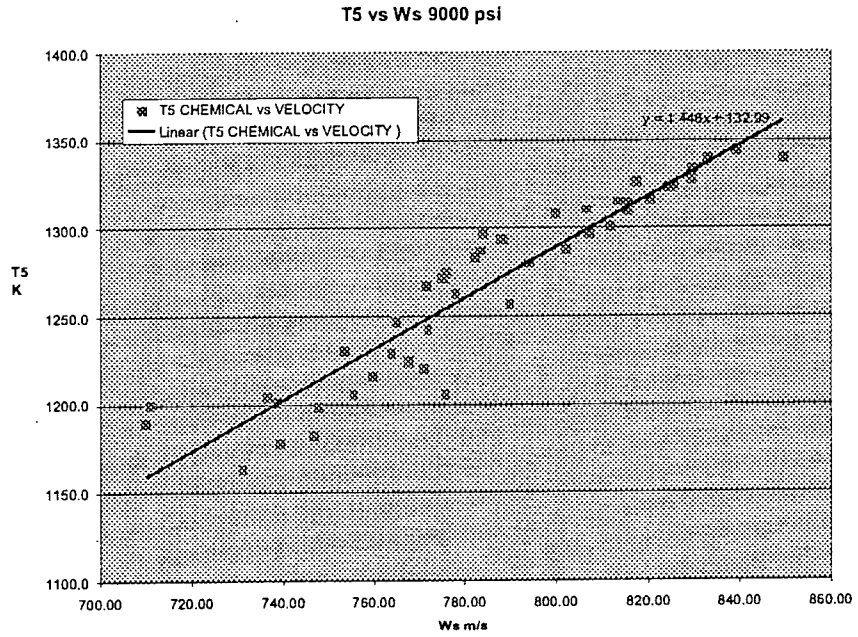

Post shock temperature calibration using
1,1,1-trifluoroethane as a "chemical thermometer".

Shock velocity measurement, which is essential to temperature calibration, has been optimized.

Optimum gas sampling times have been determined through extensive sampling of reacted gases as a function of sampling time. An optimum sampling time of 0.3 sec has been established for driven section lengths in excess of 101 inches.

Heating jackets for high temperature operation of the shock tube with aromatic species have been designed. Materials only need to be purchased for implementation.

Investigation and evaluation of a high-pressure ball valve for isolation of the sample section of the shock tube has been conducted.

Ethane and Propane Pyrolysis Studies Begun:

Extensive experimental and modeling examinations of the pyrolysis of both ethane and propane have begun in preparation for studies of aromatic species. Examination of ethane and propane has been conducted at 5000 psi (340 atm) and 9000 psi (612 atm) and species mole fractions obtained as a function of temperature have been compared with the predictions of chemical kinetic models. Shown below is the comparison between the decay of ethane, at two different initial mole fractions, as a function of temperature and GRIMECH 3.0 predictions at the same conditions.

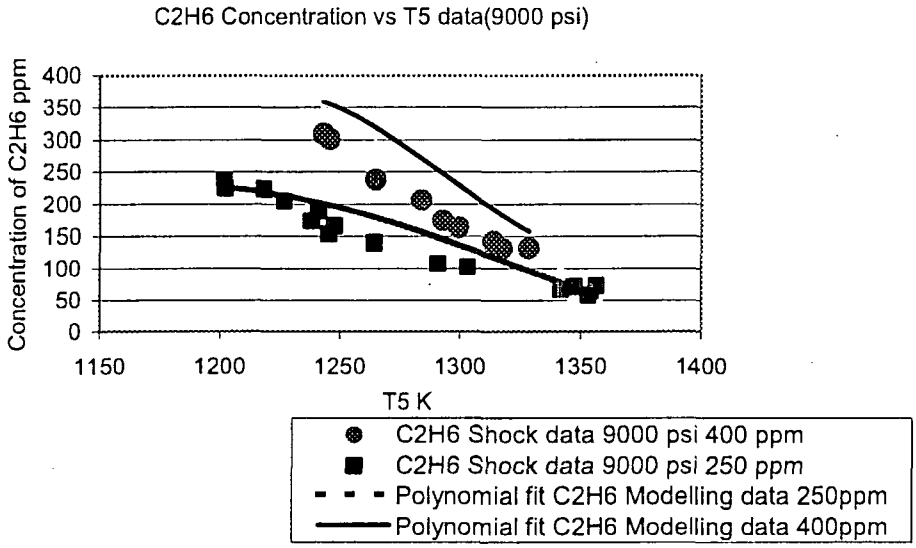

Comparison of experimental and modeling results
for ethane pyrolysis at very high pressure.

Papers and Presentations:

Our first refereed manuscript has been accepted for publication in Review of Scientific Instruments. The manuscript is entitled "Design of a High Pressure Single Pulse Shock Tube for Chemical Kinetic Investigations".

The recent work on the pyrolysis of ethane and propane was presented at the 2nd Joint Meeting of the U.S. Combustion Sections in March 2001. A Proceedings paper accompanied the presentation.

Poster presentations of shock tube work were made at both the 27th and 28th International Symposium on Combustion entitled
"A Single Pulse Shock Tube for Examination of Combustion Reactions At High Pressures",
"Temperature Calibration of a High Pressure Shock Tube"

It is expected that the ethane and propane pyrolysis work will soon lead to submission to refereed journals.

The extensive work on the use of an external calibration source for temperature evaluation at very high pressures will also lead to a submission in the near term to a refereed journal.

FUTURE WORK

Confirmation of the temperature calibrations with another chemical thermometer, cyclohexene, is planned. Also planned is the initiation of ethane and propane oxidation investigations in preparation for aromatics oxidation experiments as well as the first oxidation experiments of benzene and toluene.

COMBUSTION CHEMISTRY

Principal Investigator: Nancy J. Brown
Environmental Energy Technologies Division
Lawrence Berkeley National Laboratory
Berkeley, California, 94720
510-486-4241
NJBrown@lbl.gov

PROJECT SCOPE

Combustion processes are governed by chemical kinetics, energy transfer, transport, fluid mechanics, and their complex interactions. Understanding the fundamental chemical processes offers the possibility of optimizing combustion processes. The objective of our research is to address fundamental issues of chemical reactivity and molecular transport in combustion systems. Our long-term research objective is to contribute to the development of reliable combustion models that can be used to understand and characterize the formation and destruction of combustion-generated pollutants. We emphasize studying chemistry at both the microscopic and macroscopic levels. To contribute to the achievement of this goal, our current activities are concerned with five tasks: Task 1) developing models for representing combustion chemistry at varying levels of complexity to use with models for laminar and turbulent flow fields to describe combustion processes; Task 2) developing tools to facilitate building and validating chemical mechanisms; and Task 3) modeling combustion in multi-dimensional flow fields. A theme of our research is to bring new advances in computing and, in particular, parallel computing to the study of important, and computationally intensive combustion problems.

RECENT PROGRESS

Task 1: Developing models for representing combustion chemistry at varying levels of complexity to use with models for laminar and turbulent flow fields to describe combustion processes (with **Shaheen R. Tonse, Michael Frenklach, and Nigel W. Moriarty**)**:** Most practical combustion systems are turbulent, and the dominant computational cost in modeling turbulent combustion phenomena numerically with high fidelity chemical mechanisms is the time required to solve the ordinary differential equations associated with the chemical kinetics. To develop models that describe pollutant formation in practical fuels, the computational burden attributable to chemistry must be reduced. We have pursued an approach that can contribute to this problem, PRISM (Piecewise Reusable Implementation of Solution Mapping). PRISM has been developed as an economical strategy for implementing complex kinetics into high fidelity fluids codes. This approach to mechanism reduction draws upon factorial design, statistics and numerics, caching strategies, data structures, and long term reuse. A solution-mapping procedure is applied to parameterize the solution of the initial-value ordinary differential equation system as a set of algebraic polynomial equations. In a previous PRISM study we simulated laminar premixed and turbulent non-premixed H_2+air combustion and gained considerable speedup (for chemistry alone). Mean reuse rates of 7000-8000 per hypercube were observed, ample to recover costs, since cost-effectiveness is achieved at reuse of about 300 for the H_2+air case. Although the reuse distribution has a mean of ~7000, it is skewed with a large number of hypercubes having very low reuse (less than 10). The mean usage is raised by a small number of very highly reused hypercubes. Consequently, an *a priori* calculation of the number of expected reuses would help to identify hypercubes with insufficient reuse. It would be more efficient to call the ODE solver rather than construct polynomials for the hypercubes having insufficient reuse.

A hypercube will have high degree of reuse if it is in a portion of **C** visited by the chemical trajectories of many CFD cells, or if it is in a part of **C** where trajectories move relatively slowly, thereby taking many steps through the hypercube. We use the rates at which trajectories are moving to calculate a trajectory "velocity" using either solely chemical rate information, or including the displacement of the chemical composition vector from CFD effects such as diffusion and convection. The trajectory velocity is then combined with an estimated trajectory length to determine number of expected reuses and identify hypercubes with insufficient reuse to warrant a parametrization calculation. The four cases studied were a point reaction case with zero spatial dimensions and 3 CFD simulations: a 1D laminar premixed H_2+air flame, a 2D premixed H_2+air turbulent jet, and a 2D non-premixed H_2+air turbulent jet. We found a purely chemical trajectory to be a useful indicator for the zero-dimensional case. The usefulness decreased as we moved to the laminar flame, and then to the turbulent jet calculations. If a CFD-based trajectory velocity was used, the performance improved to the point of practical use for the laminar flame, but degraded slightly for the turbulent premixed jet. Neither method was effective for the non-premixed turbulent jet case.

Task 2: Developing tools for to facilitate building and validating chemical mechanisms (with Kenneth Revzan): Proper descriptions of transport properties are essential for combustion modeling. Recent research suggests that the treatment of transport in the CHEMKIN codes is outdated. To investigate the consequences of this for mechanism construction, we have performed sensitivity analysis of the observables: species concentrations, mass flow rate, and temperature to molecular transport coefficients. We have determined the relative importance of various transport parameters: mixture-averaged and multi-component binary diffusion coefficients, thermal conductivity, thermal diffusion ratios as well as to the fundamental parameters that underlie them, collision diameters and well depths, in the determination of chemical mechanisms. We have built codes for the evaluation of transport sensitivities (at both the macroscopic and microscopic levels) in both first and second order. Sensitivities of diffusion coefficients are largest, and their normalized sensitivities are commensurate with those associated with the most influential chemical reactions. We compared sensitivities calculated within the mixture-averaged approximation with those computed using the multicomponent approximation for diffusion. The largest sensitivities were common (18/20) to both calculations; however the rank order of the sensitivities differed, and sometimes sensitivities had different signs. Sensitivities to thermal conductivity were of the same magnitude as those for diffusion coefficients, but they were smaller. Thermal diffusion ratio sensitivities were an order of magnitude less than those associated with other transport properties. Sensitivities of observables were found to be an order-of-magnitude greater for collision diameters associated with a Lennard-Jones potential than for the corresponding well depths. These results show that we will not get the chemistry right in building chemical mechanism without an improved treatment of transport. Transport also must be dealt with at the molecular level. We are currently directing effort toward achieving an improved transport description.

Task 3: Modeling combustion in multi-dimensional flow fields (with Shaheen R. Tonse, John B. Bell, and Marcus S. Day): We have continued our efforts concerned with finding the dimensionality of chemical composition space. In our previous work, we averaged over time. Currently, we are examining specific snapshots in time. The chemical concentrations of an instantaneous snapshot of a spatially extended chemical reaction can be mapped into a multi-dimensional chemical composition space **C** to form a continuous multi-dimensional manifold **M** embedded in **C**. A manifold constructed in this manner is actually a dense set of discrete points; however, if not viewed at too small a length scale, we can make a continuum approximation and speak meaningfully of its dimensionality. In the limit of infinitely small length-scales the dimensionality **d** of **M** is limited to that of the physical space, but at larger length-scales it may appear to have a higher dimension than the theoretical bounds provided that **M** is sufficiently convoluted. Our interest in **d** is stimulated by our interest in PRISM, a piecewise reuse method. PRISM divides **C** into finite partitions, and in each replaces the chemical

kinetics equations with a computationally simpler quadratic polynomial. Its accuracy increases as partition size decreases, but this necessitates construction of more partitions in a way that depends exponentially on **d**. Determination of **d** is of importance in the design and development of PRISM or any such chemical mechanism reduction method.

The quantity, **d** is computed by repeatedly reducing the partition size and measuring the increase in number of partitions required to cover **M**. For example, for a one-dimensional **M**, halving the size will only double the number required to cover **M**, for a two-dimensional **M** the number required will quadruple. In general the number of partitions used should rise by 2^d. An independent method of estimating dimensionality was through principal component analysis (PCA), and this was also applied to the manifold of each partition. PCA is an eigenvalue problem used to determine the most significant variables (or linear combinations of variables) in a multi-variant data set. In our case, PCA returns an estimate of the dimensionality. We performed evaluations of it with Monte Carlo'ed manifolds of know dimensionality, and have determined that PCA is very accurate for determining dimensionality.

The geometric binning and PCA methodologies for determining the dimensionality of **C** were applied to the interactions of two and three dimensional premixed hydrogen flames into which a localized region of turbulence was superimposed over the cold region below the flame front. H_2+air inflow occurred at the bottom of the domain, with outflow occurring at the top. The inflow velocity was set to the laminar flame speed so that the flame was stationary in the absence of turbulence. The sides of the domain were periodic. In some cases the turbulence was present as a superimposed patch, while in others, the turbulent velocity fluctuations were fed in at the inlet boundary. The inflow velocity convected the turbulent region toward the flame front. We computed the solution with turbulent intensities in the range 0.2 m/s to 20 m/s to represent a broad range of wrinkled flame phenomena. The table below shows evolution of **d** (Dimensionality) in going from a quiescent laminar state to a turbulent one, made for a two-dimensional grid case. Corresponding results from principal component analysis (N_{PC}) are displayed alongside.

DESCRIPTION	TIME (ms)	DIMENSIONALITY	N_{PC}
Laminar undisturbed	0	1	1.1
Slightly deformed	0.05	2.2	2.1
Developing turbulence interaction	0.1	2.9	2.8
Well developed interaction	1.1	3.2	3.2

At early times before any turbulence-flame interaction, **d** =1. This is expected as the initial condition is translationally symmetric across the grid from left to right, i.e. the problem is essentially 1D. With time **d** rises from 1 to 2 as fluctuations, most likely caused by diffusion, break the symmetry, and then it rises to about 3 as the turbulence interacts with the flame. We see that **d** has a value of approximately 1 higher than the theoretical limit of 2. The PCA result shows very good agreement with the binning method. The table below shows variation of **d** for a 2-dimensional grid case with varying levels of turbulent intensity. All snapshots are taken when turbulence-flame interaction is well developed. As before, corresponding results from principal component analysis are displayed alongside.

Turbulent intensity (m/s)	d	N_{PC}
0.2	2.8	2.2
10	3.1	2.9
20	3.1	3.2

Varying turbulent intensities between the ranges 0.2 to 20 m/s does not appear to have much effect on **d**. Additionally, we have one result from a well-developed 3D grid case, in which **d** has a value of approximately 4. In conclusion, we see that the dimensionality is 0.5 to 1 above the theoretical bound of being equal to the spatial dimensionality. We also observe that independent measurements of dimensionality from the geometrical binning method and a principal component analysis (PCA) agree reasonably well. The results were presented at the Joint Symposium of the Combustion Institute at Oakland, CA in March 2001.

PUBLICATIONS

Bell, J.B., Brown, N.J., Day, M.S., Frenklach, M., Grcar, J.F., Propp, R.M., and Tonse, S.R., "Scaling and Efficiency of PRISM in Adaptive Simulations of Turbulent Premixed Flames," (2000) Proceedings of the Combustion Institute 28. (in press). Also Lawrence Berkeley National Laboratory Report No. LBNL-44732

Bell, J.B., Brown, N.J., Day, M.S., Frenklach, M., Grcar, J.F., and Tonse, S.R., "Effect of Stoichiometry on Vortex-Flame Interactions," (2000) Proceedings of the Combustion Institute 28. (in press) Also Lawrence Berkeley National Laboratory Report No. LBNL-44730

Tonse, Shaheen R. and Brown, N.J., "Emulation of Chemical ODE System by Response Surfaces in CH_4 Combustion,"Division of Fluid Dynamics, American Physical Society, Washington DC, November 2000

Tonse, Shaheen R., Bell, J.B., Brown, N.J., and Day, M.S., ."The Dimensionality of a Chemical Manifold through a Progressing Reaction, 2nd Joint Symposium of the Combustion Institute at Oakland, CA, March 2001

Brown, N. J., Revzan, K. L. and Frenklach, M.,(1998) "Detailed Kinetic Modeling of Soot Formation in Ethylene/Air Mixtures Reacting in Ethylene/Air Mixtures Reacting in a Perfectly Stirred Reactor," Proceedings of the Combustion Institute 27. pp 1573-1580

Frenklach, M.. Moriarty, N. L., and Brown, N.J., (1998) "Hydrogen Migration in Polyaromatic Growth," Proceedings of the Combustion Institute 27

Lazarides, A. A., Rabitz, H., Chang, J., and Brown, N. J., (1998), " Identifying Collective Dynamical Observables Bearing on Local Features of Potential Surfaces," J. Chem. Phys. Chem. 109, pp 2065-2070.

Tonse, S.R., Moriarty, N. L., Brown, N. J., Frenklach, M., (1999), "PRISM: Piecewise Reusable Implementation of Solution Mapping. An Economical Strategy for Chemical Kinetics," Israel Journal of Chemistry 39, pp 97-106. Invited paper for a special issue on Combustion Chemistry to commemorate the 70th birthday of Professor Assa Lifshitz. Also Lawrence Berkeley National Laboratory Report No. LBNL-42576

Moriarty, N. W., Brown, N.J., and Frenklach, Michael, (1999), "Hydrogen Migration in the Phenylethene-2-yl Radical," J.Phys. Chem. 103, pp 7127-7135. Also Lawrence Berkeley National Laboratory Report No. LBNL-43163

A co-author of the National Research Council Report of the Committee on Ozone-Forming Potential of Reformulated Gasoline, National Academy Press, (1999) Committee members: W.L. Chameides, C.A. Amann, R. Atkinson, N.J. Brown, J.G. Calvert, F.C. Fehsenfeld, J.P. Longwell, M.J., Molina, S.T. Rao, A.G. Russell, S.L. Saricks.

Dynamics of Radical Combustion Intermediates: Product Branching and Photolytic Generation

Laurie J. Butler
The University of Chicago, The James Franck Institute
5640 South Ellis Avenue, Chicago, IL 60637
LJB4@midway.uchicago.edu

I. Program Scope

We have recently begun pursuing a new direction in my laboratory, the study of the competing unimolecular dissociation, and isomerization, channels of isomerically-selected highly vibrationally excited radicals. The experiments allow us to investigate in the ground electronic state the competition between C-H and C-C bond fission product channels as a function of internal energy in the selected radical isomer. We have also continued our studies of photodissociation processes used to generate radical intermediates important in combustion and our work on generalizing a method for determining absolute branching ratios for competing radical product channels in both unimolecular and ground state bimolecular reactions in mass spectrometric experiments. We use a combination of experimental techniques including analysis of product velocity and angular distributions in a crossed laser-molecular beam apparatus and emission spectroscopy of dissociating molecules. Much of the work also serves to test and develop our fundamental understanding of chemical reaction dynamics. We focus on testing the range of applicability of two fundamental assumptions used in calculating reaction cross sections and the branching between energetically-allowed product channels: the assumption of complete intramolecular vibrational energy redistribution often used in transition state theories and the assumption of electronic adiabaticity used in defining the reaction coordinate in transition state theories and the multidimensional potential energy surface in quantum scattering calculations.

II. Recent Progress

Our work in the last year included: 1) completing and publishing[4] our crossed laser-molecular beam photofragment scattering experiment on methyl vinyl ether, a study motivated by the need to calibrate product branching in the thermal O+ ethylene reaction which also served to test propensity rules for the electronic accessibility of product channels; 2) completing a collaborative project, with Dr. Fei Qi at the Chemical Dynamics Beamline at the Advanced Light Source (ALS), that probed the primary and secondary reactions in the photodissociation of allyl chloride, including the secondary unimolecular dissociation of the allyl radical from primary C-Cl fission and of the C_3H_4 product (to propargyl + H) from primary HCl elimination; and 3) initiating the investigation of the competing unimolecular dissociation channels of several isomerically selected hydrocarbon radicals, including the allyl radical and the 1-propenyl radical.

A. The Photofragmentation Pathways of Methyl Vinyl Ether: Electronic Accessibility and Calibrating Branching Ratios between the Dominant Product Channels of O + Ethylene

These experiments first allow us to determine absolute branching ratios between energetically-allowed product channels in thermal bimolecular reactions, in this case O + ethylene, in principle without relying on unreliable semiempirical estimates for the neutral products' ionization cross-sections. The experiments use the $CH_2CH\text{-}O\text{-}CH_3 \rightarrow CH_2CHO + CH_3$ photodissociation channel

of methyl vinyl ether to calibrate the absolute branching between the two dominant pathways (Rxn.s 1 and 2 below) in the thermal $O(^3P) + C_2H_4$ reaction:

$$O(^3P) + C_2H_4 \rightarrow CH_3 + HCO \quad (1)$$
$$\rightarrow H + CH_2CHO \quad (2)$$
$$\rightarrow CH_2 + CH_2O \quad (3)$$

Experimental determinations of the product branching vary widely, ranging from Rxn. 1 contributing 71 (-9/+6) % of the products (assuming the yield of the third channel is small) to it contributing 44 (±15%) of the products. The reported experimental yield of 71 (-9/+6) % for Rxn. 1 comes from a crossed molecular beams scattering experiment in Y. T. Lee's group (Schmoltner *et al.*, J. Chem. Phys. 91, 6926 (1989)) at a 6 kcal/mol collision energy, so has the chance of being a benchmark for theoretical work on this system. However their branching ratio between Rxn.s 1 and 2 relied on estimating the ratio of the ionization cross sections of the vinoxy radicals and HCO radicals with an empirical method not tested for polyatomic radicals and on comparing signals from two scattering experiments, one with isotopically labeled reactants. The experiments we have published this year use the 1:1 production of the methyl and vinoxy radical fragments from the photodissociation of methyl vinyl ether to calibrate the mass spectrometric sensitivity to these products at the required daughter ions, allowing us to extract a more reliable branching ratio from the Lee data.

To summarize, the experiments investigated the photodissociation of methyl vinyl ether at 193 nm in a crossed laser-molecular beam apparatus. We observed two C-O bond fission channels, a minor channel producing $CH_3 + CH_2CHO$ ($\tilde{X}^2A''$) and the major channel yielding $CH_3 + CH_2CHO$ ($\tilde{A}^2A'$). Some of the neutral $\tilde{A}$ state vinoxy product undergoes secondary dissociation to produce ketene + H. Using the measured photofragment velocities and product branching we calibrate the relative sensitivity of mass spectrometric detection to the methyl and vinoxy polyatomic radical products at the m/e=15 daughter ion, taking into account the loss of neutral vinoxy to ketene + H formation. This relative mass spectrometric sensitivity calibration factor is determined to be 0.116±.022. Using this factor to extract the product branching ratio (from the m/e=15 scattering data of Y. T. Lee) between the two major competing primary product channels from the $O(^3P)$ + ethylene reaction, give a $CH_3 + HCO$ / $H + CH_2CHO$ product branching ratio of R=0.61±.11, corresponding to 38% (±5%) branching to the $CH_3 + HCO$ channel. Secondly, we use the result that the channel producing $\tilde{A}$ state vinoxy dominates over the formation of ground state vinoxy to test propensity rules being developed to help predict what product channels may be suppressed by electronically nonadiabatic effects in chemical reactions. These propensity rules discriminate between channels that are "electronically facile" and those that are "electronically difficult/prohibitive". We find that a qualitative analysis of the changes in electronic configuration from reactant to each of the available product channels for the photodissociation of methyl vinyl ether correctly predicts the dominant channel to be the production of excited state ($\tilde{A}$) vinoxy, the "electronically facile" channel.

B. Primary and Secondary Reactions in the Photodissociation of Allyl Chloride

This study, manuscript in preparation, elucidates the competing HCl elimination channels and C-Cl bond fission channels of allyl chloride photodissociated at 193 nm as well as the

secondary dissociation of both the allyl radical produced from C-Cl fission and the C_3H_4 product from HCl elimination. Prior work showed that C-Cl fission and HCl elimination occur upon $\pi\pi^*$ excitation of allyl chloride, but did not elucidate the mechanisms for the two HCl elimination processes. Tunable VUV photoionization detection of the HCl and its momentum-matched C_3H_4 product in the present work allows us to gain both a crude measure of the level of HCl vibrational excitation as well as a probe of the secondary dissociation of some of the C_3H_4 products to propargyl + H. The reaction also allows us to probe the secondary dissociation of the allyl radical from a previously undetected low kinetic energy C-Cl bond fission channel. Interestingly, the photoionization detection of HCl from allyl chloride showed the HCl to have considerably less internal vibrational energy than the HCl elimination product from 2-chloropropene. Since HCl elimination from 2-chloropropene can only proceed via four-center elimination transition states that have a long H-Cl distance compared to R_e of the HCl product, 1.8 angstroms at the transition state, one is tempted to conclude that HCl elimination in allyl chloride is a three-center, 1,1, elimination of HCl with a smaller H-Cl distance at the transition state, not a 4-center process. This may shed light on the elusive mechanism for HCl elimination from vinyl chloride as well. Blank et al. proposed a three-center mechanism with synchronous isomerization for the HCl elimination from vinyl chloride at 193 nm, but we find that the photoionization spectrum of the HCl product they measured indicates it is much more vibrationally excited than the HCl product from allyl chloride. The photoionization efficiency curve for HCl that Blank et al. measured is, however, nearly identical to that of the HCl product from 2-chloropropene, suggesting that the dominant HCl elimination mechanism in vinyl chloride is via a four-center transition state.

C. Investigating the Internal Energy Dependence of the Competing Unimolecular Dissociation Channels of Selected C_3H_5 Radical Isomers: Allyl Radical and 1-Propenyl Radical

Radical intermediates play a key role in a wide range of processes important to combustion. However, even after decades of the finest kinetics research, the competition between the ground electronic state unimolecular reactions of many key isomeric radical intermediates eludes direct experimental probes. In the past nine months we have been pursuing an exciting series of experiments with DOE support that build on a study of the unimolecular dissociation of 2-propenyl radicals that we did at the end of our NSF grant in Spring 2000. The experiments allow us to investigate the competition between unimolecular reactive channels of an important class of radical intermediates, polyatomic hydrocarbon radicals that can exist in multiple isomeric forms. Our molecular beam scattering method allows us to resolve the branching between the competing C-H and C-C bond fission channels of particular radical isomers as a function of internal energy in the selected radical. The experiments we pursue allow us to produce the selected radical isomer at energies that span the lowest dissociation and isomerization barriers, so provide data on product branching with is sensitive to the relative barrier heights of the competing reaction channels to within a couple kcal/mol. In contrast, product branching in UV photodissociation experiments on radicals, such as those pursued by Chen, Neumark, and Lee, probe the branching at much higher internal energies where the data is primarily sensitive to the ratio of A factors. One early result of interest from our study of the unimolecular dissociation channels of the allyl radical establishes that the barrier to isomerization to 2-propenyl radical is

over 60 kcal/mol, at least 14 kcal/mol higher than that derived from bulk kinetics measurements on the C_3H_5 systems. The new experimental results are consistent with ab initio calculations of the isomerization barrier published in 1998. The key feature of our method is that although photolysis of a halogenated precursor produces radicals with a wide range of recoil kinetic energies and thus internal energies, each radical's velocity is a signature of its internal energy, which is simply determined by momentum matching with the halogen atom produced in the photolytic step. This effectively disperses both the stable and unstable radicals by internal energy, allowing us to resolve the internal energy dependence of the ensuing dissociation and isomerization processes. In particular, it allows us to resolve the how the branching to each unimolecular H atom loss product channel changes as a function of internal energy in the radical since the time-of-arrival of the heavy C-H fission product from the unimolecular dissociation of the radical identifies the internal energy of the parent dissociative radical from which it came. The experiments detect the velocities of the radical's C-H bond fission products using the molecular beam apparatus with tunable VUV photoionization detection at the ALS and also resolve the C_3H_4 product isomers (allene and propyne) in each velocity subgroup with tunable photoionization. We have taken extensive data on the competing C-C and C-H bond fission channels for two C_3H_5 radical isomers with DOE support, the allyl radical (dispersed by internal energy in the scattering apparatus from the 193 nm photodissociation of allyl iodide) and the 1-propenyl radical (from 1-bromopropene). We are analyzing that data now.

III. Future Plans

The end of our current grant period is dedicated to completing the analysis of our data on the competing C-C and C-H bond fission channels for the two C_3H_5 radical isomers studied, the allyl radical and the 1-propenyl radical. Our proposed experiments for the next funding period include the application of this experimental method to resolving the competition between unimolecular dissociation channels of radicals important to soot formation. We also plan to apply our method described in Section II.A. for determining absolute branching ratios for competing radical product channels in ground state bimolecular reactions to determine the absolute branching ratio between product channels in the O + ethane reaction.

IV. Publications Acknowledging DE-FG02-92ER14305 (1999 or later)

1. Photodissociating Trimethylamine at 193 nm to Probe Electronic Nonadiabaticity at a Conical Intersection and to Calibrate Branching Ratios between Radical Products, N. R. Forde, M. L. Morton, S. L. Curry, S. Jarrett Wrenn, and L. J. Butler, J. Chem. Phys. 111, 4558-68 (1999).
2. A Combined Experimental and Theoretical Study of Resonance Emission Spectra of SO_2 ($\tilde{C}\,^1B_2$), B. Parsons, L.J. Butler, D. Xie, and H. Guo, Chem. Phys. Lett. 320, 499-506 (2000).
3. Characterization of Nitrogen-Containing Radical Products from the Photodissociation of Trimethylamine at 193 nm using Photoionization Detection, N. R. Forde, L. J. Butler, B. Ruscic, O. Sorkabi, F. Qi and A. Suits, J. Chem. Phys. 113, 3088-97 (2000).
4. Photodissociating Methyl Vinyl Ether to Calibrate O + Ethylene Product Branching and to Test Propensity Rules for Product Channel Electronic Accessibility, M. L. Morton, D. E. Szpunar, and L. J. Butler, J. Chem. Phys. 114, in press (2001).

Independent Generation and Study of Key Radicals in Hydrocarbon Combustion (DE-FG02-98ER14857).

Barry K. Carpenter
Department of Chemistry and Chemical Biology
Cornell University
Ithaca, NY 14853-1301
E-mail: bkc1@cornell.edu

1. Cyclopropyl Radical and Allyl Radical.

1.1 Calculations on the Ring Opening of Cyclopropyl Radical and Cyclopropyl Cation.[1]

As part of our combined experimental and computational investigation of the C_3H_5 potential energy surface, we have carried out a variety of *ab initio* and density functional calculations on the title reactions. The reactions provide significant tests of computational models that might be considered for mechanistic investigation of combustion processes. The small-ring reactants, the open-shell nature of the species involved (in the radical reaction), and the interconversion of σ and π electrons that occurs during the ring opening, together suggest that large basis sets and extensive treatement of both dynamic and nondynamic electron correlation may be necessary in order to describe the processes accurately. Calculations were carried out at the B3LYP/cc-pVQZ, CASPT2(3,3)/cc-pVTZ// CASSCF(3,3)/cc-pVTZ, and CCSD(T)/6-311G(2d) levels. The computational models were found to agree well with each other and, where data were available, with experiment. The barrier to ring opening of cyclopropyl radical was found to be 21 kcal/mol ($\Delta H^{\ddagger}$ at 0K), and the reaction enthalpy was calculated to be –31 kcal/mol. The cyclopropyl cation was found to be a transition state. Its barrierless ring opening was calculated to have a reaction enthalpy of –34 kcal/mol.

Although the ring opening of cyclopropyl radical involves highly asynchronous rotation of the two CH_2 groups, the process is nevertheless topologically disrotatory and hence nominally "forbidden." It is the rise in energy of the singly occupied MO during the ring opening that provides the barrier to the reaction. When this odd electron is removed, generating the cation, the barrier to ring opening is also removed.

1.2 Photolysis of Cyclopropyl Iodide.[2]

In collaboration with Paul Houston in this Department, we have studied the UV photodissociation of cyclopropyl iodide. We have shown that in solution the photolysis generates both cyclopropyl and allyl radicals. The allyl radicals almost certainly *do not* arise from ring opening of hot cyclopropyl, since collisional cooling is estimated to be at least three orders of magnitude faster than ring opening in solution. In the gas phase we have used ion and electron imaging techniques to determine the nature and translational kinetic energy distribution of the products. Iodine atoms are formed in both the spin-orbit ground state (the I channel) and excited state (the I* channel). For both I and I* channels, the translational kinetic energy of a substantial fraction of products is found to exceed the maximum possible value (i.e. the photon energy minus the C–I bond dissociation energy) by up to 30 kcal/mol. The most plausible explanation is that at least some of the photochemistry occurs by *direct* formation of allyl radical. The enthalpy difference between allyl and cyclopropyl (*vide supra*) would then account for the

translational energy anomaly. Electron imaging shows that allyl radical can be detected in the photolysis fragments.

We hypothesize that the direct formation of allyl radical from $^1(n,\sigma^*)$ cyclopropyl iodide occurs by a double surface crossing between open-shell (• •) and closed-shell (+ –) potential energy surfaces. The dissociation begins on the radical-pair surface but then encounters a crossing with the ion-pair surface. This crossing occurs because the rise in energy of the singly occupied MO of cyclopropyl, upon attempted ring opening (*vide supra*), lowers the IP of the radical enough to make electron transfer to I• favorable. Once this occurs, the resulting cyclopropyl cation can ring open without barrier. The ring opening causes the energy of the nonbonding MO to drop again, making back electron transfer favorable – i.e. a second surface crossing is encountered. Using state-averaged CASSCF(4,4) calculations we have determined the geometries of both crossing points. In summary, the crossing from (• •) to (+ –) surface and back again provides a pathway for cyclopropyl radical to ring open without having to surmount the barrier that the adiabatic reaction would face. This has potential implications for other alkyl halide photolyses, as described below.

1.3 Polarized IR Spectra of Matrix-Isolated Allyl Radicals.

(Nandi, S.; Arnold, P.A.; Carpenter, B.K.; Nimlos, M.R.; Dayton, D.R.; Ellison, G.B. *J. Phys. Chem. A*, submitted.)

In a collaboration with Barney Ellison and coworkers, we have synthesized 3-iodopropene-2-d_1 and 3-iodopropene-d_5. These have been used, along with unlabeled 3-iodopropene to generate the corresponding isotopomers of the allyl radical in an Ar matrix at 10K. Polarized IR spectra have been obtained on all three species and have been characterized with the aid of UB3LYP/6-311-G(d,p) calculations. A final set for all the vibrational frequencies for the allyl radical can be recommended as a result of this work.

2. Investigation of Surface Crossings in Alkyl Halide Photolyses.

The double surface crossing that we believe occurs in cyclopropyl iodide photolysis provides the system with a mechanism for undergoing a ring-opening reaction without surmounting the barrier that would be faced by the adiabatic process. We believe that there may be several other examples of this kind of phenomenon, and that "covert" reactions, not expected of radicals, can occur on a transiently accessed ion-pair surface. A potentially important example is the 1,2-hydrogen migration. For radicals, this is generally expected to be a reaction with a very high barrier. Indeed, the most recent calculations on the 1,2-hydrogen migration in ethyl radical suggest the transition structure located in some earlier calculations is probably an artifact of basis-set superposition error, and that in fact the lowest energy pathway for the reaction is simply to dissociate an H atom and then readd it.[3] In contrast, the intramolecular 1,2-hydrogen migration in carbocations is an essentially barrierless reaction that is a ubiquitous feature of their chemistry. The reason for this difference in behavior of the radicals and the cations is essentially identical to the reason for the difference in behavior of cyclopropyl radical and cation. That analogy leads one to wonder whether 1,2-hydrogen migrations might

not occur during alkyl halide photolysis, as a result of surface crossing to an ion-pair state. We have preliminary evidence that they can.

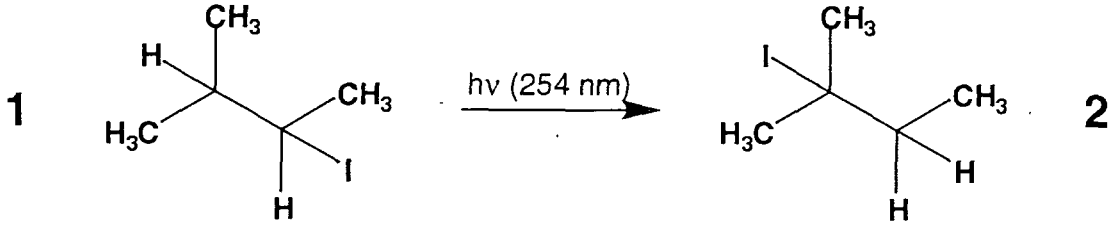

Photodissociation of 2-iodo-3-methylbutane (**1**) at 254 nm in hexane solution results in rapid isomerization to 2-iodo-2-methylbutane (**2**). One possibility is that this occurs by initial generation of a radical-pair (• •) state that crosses to an ion-pair (+ –) state. In the (+ –) state a 1,2-hydrogen migration occurs. The products either directly collapse to **2** or undergo back electron transfer to a (• •) state, which then gives **2**. However, we need to do more experiments to rule out alternative mechanistic possibilities before concluding that this is the most likely pathway. One alternative mechanism is that the electron transfer is an outer-sphere process occurring in a solvent-caged radical pair. If so, gas-phase photodissociation of **1** should not give **2**. The gas-phase photochemistry is currently under investigation. Another possibility is that the first-formed radical pair disproportionates to give HI + 2-methyl-2-butene, and that the product arises from the standard thermal reaction between these two. Investigation of that possibility requires a double-labeling crossover experiment. We are currently exploring the synthesis of the necessary isotopically labeled analog of **1**. If these alternative mechanisms can be excluded, leaving the surface-crossing mechanism as the best candidate, the consequences for the combustion program could be fairly significant, since alkyl halide photolysis is one of the most common procedures used to generate the radicals that are of interest in this field. Covert rearrangements of the radicals as a result of transient excursions onto ion-pair surfaces could compromise some of the data acquired in such studies.

3. Dioxiranylmethyl Radical

The dioxiranylmethyl radical (center of the diagram on the next page) is now believed to play a key role in the known conversion of vinylperoxy radical to CHO + CH_2O. The G2M(RCC,MP2) calculations of Mebel *et al.* on the formation and subsequent reactions of dioxiranylmethyl indicated that the rate-determining step, starting at vinylperoxy, was the conversion of dioxiranylmethyl to the oxiranyloxy radical. This reaction was found to have a barrier of 23 kcal/mol, 7.5 kcal/mol higher than the barrier for reversion of dioxiranylmethyl to vinylperoxy.[4]

We have reinvestigated this reaction at the CASPT2(23,15)/cc-pVTZ//CASSCF (23,15)/ cc-pVTZ level, and have found a rather different result.[5] While the same step was found to be rate limiting, the difference in barrier heights for the forward and backward reactions of dioxiranylmethyl was found to be only 0.6 kcal/mol, and the barrier to the forward step was found to be only 12.5 kcal/mol instead of 23. We attribute the discrepancy to the use of single-reference methods in the calculation of electron correlation by the G2M(RCC,MP2) model. As shown in the diagram on the next page,

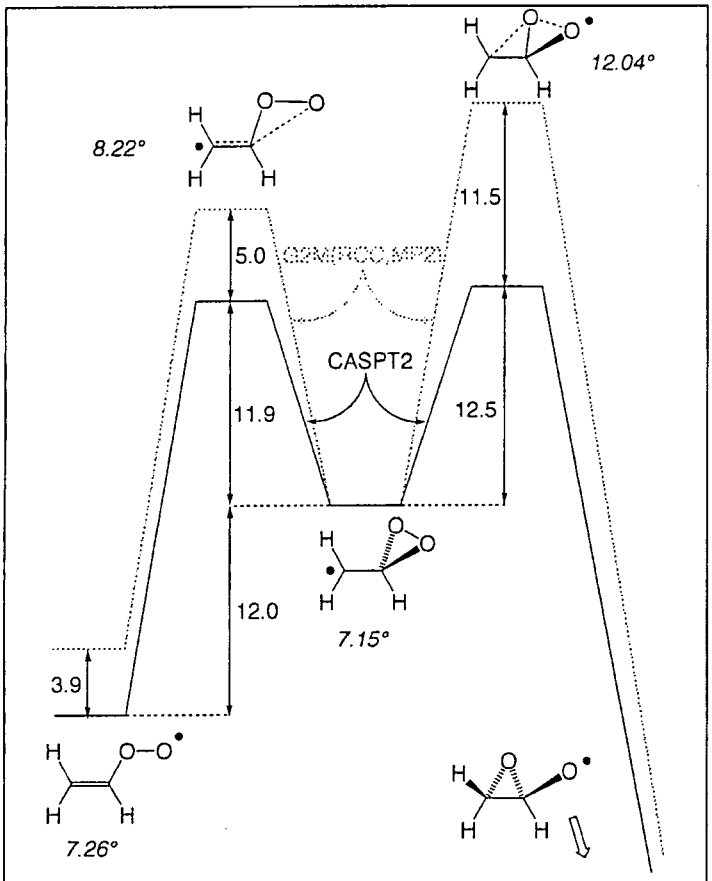

Comparison of G2M(RCC,MP2) and CASPT2 calculations. Plain numbers are energies in kcal/mol. Italicized numbers are values of θ_{pop} (see text).

the parameter θ_{pop}, calculated as indicated in the equation below, and taken as a measure of the multideterminant nature of the wavefunction, correlates with the discrepancy between the two computational models.

$$\theta_{pop} = \cos^{-1}\left(\frac{1}{45}\sum_{i=5}^{19}\rho_i^{CASSCF}\rho_i^{ROHF}\right)$$

The population vectors respectively have elements ρ_i^{CASSCF} – the population of CASSCF natural orbital i – and ρ_i^{ROHF} – the population (2, 1, or 0) of orbital i in a ROHF wavefunction.

Given the apparently inadequate treatment of nondynamic electron correlation by the G2M(RCC,MP2) model for this reaction, it is possible that it or any other single-reference method may be unreliable for certain kinds of transition structures, and that such methods should consequently be used with caution in mechanistic analyses.

Literature Citations

1. Arnold, P.A.; Carpenter, B.K. *Chem. Phys. Lett.* **2000**, *328*, 90.

2. Arnold, P.A.; Cosofret, B.R.; Dylewski, S.M.; Houston, P.L.; Carpenter, B.K. *J. Phys. Chem. A* **2001**, *105*, 1693.

3. Kobko, N.; Dannenberg, J.J. *J. Phys. Chem. A* 2001, **105**, 1944.

4. Mebel, A. M.; Diau, E. W. G.; Lin, M. C.; Morokuma, K. *J. Am. Chem. Soc.* **1996**, *118*, 9759.

5. Carpenter, B.K. *J. Phys. Chem. A* **2001**, in press.

Ion Imaging Applied to Chemical Dynamics

David W. Chandler
Combustion Research Facility, Mail Stop 9055, Sandia National Laboratories, Livermore, CA 94551-0969, chandler@ca.sandia.gov

Scope of Program

Chemical dynamics is the exacting study of individual details of chemical reactions. Chemical reactions occur on potential energy surfaces, therefore chemical dynamics studies focus on learning about and testing potential energy surfaces. My research focuses on developing and using two-dimensional imaging techniques to study all areas of chemical dynamics. These techniques allow one to measure the velocity of quantum-state-selectively photo-ionized products of unimolecular and bimolecular interactions. For a two body interaction the measurement of both the quantum state of one of the products and its velocity along with conservation of energy and momentum equations provides detailed information about the unobserved fragment. Many times the ability to ionize a molecule by a laser beam is dependent on its alignment and orientation relative to the polarization axis of the ionizing laser beam. Therefore, the alignment and orientation of a product molecule or atom can be determined by utilizing this interaction. In the last two years we have made significant improvements in these techniques with the further development of the velocity mapping technique and the completion and utilization of a crossed molecular beam apparatus for the study of bimolecular interactions.

Recent Progress

Unimolecular Photodissociation

The vibrational predissociation of van der Waals dimers produces a kinetic energy recoil. This process was studied in collaboration with Dr. John Barker of the University of Michigan. The distribution of this recoil energy has been investigated in the predissociation of triplet state mixed van der Waals dimers which contain ~2000 to ~8000 cm^{-1} of vibrational energy. One member of a dimer is an aromatic molecule, such as pyrazine or benzene, and the second is a rate gas atom, a diatomic, or a small polyatomic molecule. The recoiling aromatic member was ionized and the recoil energy distribution acquired by ion imaging. The resulting probability distributions peak near zero energy and are monotonically decreasing functions of recoil energy. Average center of mass recoil energies range from ~100 to >300 cm^{-1}. The results of pyrazine/Ar clusters have been modeled using classical trajectory calculations and the results are compared with the experiment. The V-T energy-transfer distributions obtained from this study cannot be fit to a simple exponential energy gap or a surprisal analysis model. Also the triplet state vibrational energy appears to have only a small effect on the recoil energy of aromatic/Ar clusters while the identity of the cluster partner has a large effect. Hydrogen bonded dimers Pyrazine/NH_3 and Pyrazine/H_2O have average recoil energies twice as large as Pyrazine/Ar or Pyrazine/Xe clusters.

Bimolecular Scattering

CO/Ne Scattering

State-to-state differential cross sections for rotational excitation of CO by Ne were determined at 533 cm^{-1} of collisional energy. Scattered molecules were ionized with 2+1 resonance enhanced multiphoton ionization and detected with velocity mapped ion imaging. This experiment was done in collaboration with Prof. George McBane. In figure 1 is shown the data set and simulated images for CO / Ne scattering. Cross sections were determined for

most of the energetically allowed final states of CO. The results were compared with predictions from two high quality CO/Ne *ab initio* potential energy surfaces.

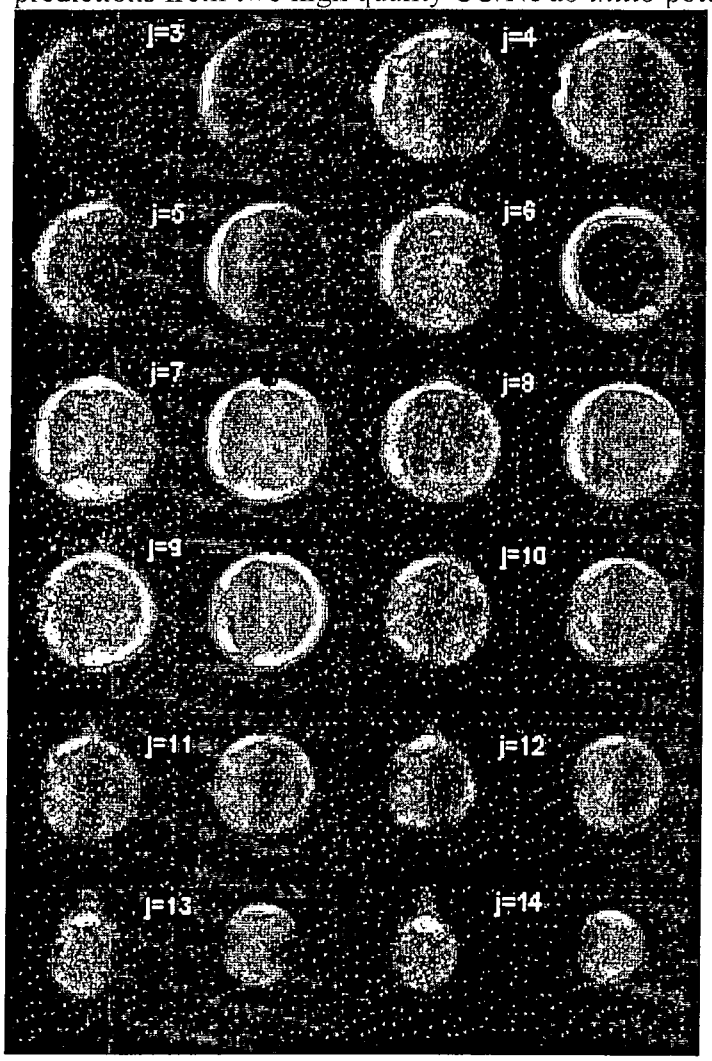

Figure 1 Data for Co scattering from Ne along with simulated images.

NO/Ar Scattering

The collision-induced rotational alignment of NO ($X^2\Pi_{1/2}$, v' = 0, j' =4.5, 8.5, 11.5, 12.5, and 15.5) has been measured for rotationally inelastic scattering of NO($X^2\Pi_{1/2}$, v" = 0, j "=0.5) with Ar at 520 ± 70 cm^{-1} of center-of-mass collision energy. The experiments were performed by velocity-mapped ion imaging with polarized 1 + 1' REMPI of the scattered NO product. Differential cross-sections, corrected for alignment effects, are also reported. While the alignment correction is important, it does not change the positions of the observed rotational rainbows. The alignment moments and differential cross-sections are compared with calculations using Alexander's CCSD(T) PES's. The theoretical and experimental DCS's show excellent agreement, but the theoretical and experimental alignment moments show relatively poor agreement. The theoretical calculations are in better agreement with experiment for low Δj collisions and for forward-scattered trajectories. The alignment moments derived from the experimental images are also compared with the predictions of the kinematic apse model of Khare. This model assumes a sudden impact. This model predicts well the shape of the distribution of angular momentum vectors observed but does not seem to do a well in predicting the orientation of that distribution relative to the recoil velocity vector.

The orientation of the angular-momentum vector of the scattered NO product, whether it is rotating clockwise or counterclockwise, has also been measured. In the absence of external influences the collision of achiral reactant species such as NO and Ar would not be expected to produce a net preferential sense of molecular rotation in the full product state distribution. However a preferred sense of rotation is possible for single NO product rotational states j' and deflection angles within that distribution. Our experiment is both quantum state and scattering angle resolved so it is possible for us to measure this quantity for the first time. We detect the NO product sense of rotation in the detector plane by comparing photoionization probability for right and left circularly polarized ionization light. This is done by subtracting two images taken with opposite polarizations and normalizing the image by the sum of the two images. The resulting image is a direct mapping of the sense of rotation as a function of scattering angle. As is evident from inspection of the images for low J states there is an oscillating pattern to the orientation. The oscillation frequency is faster for lower J states than higher J states but the magnitude of the oscillation is larger at high J.

Future Directions

Unimolecular Reactions:

One project that will be made possible by the improvements presently under way will be done in collaboration with Prof. R. Field. Dr. Field has been interested in the spectroscopy of acetylene for many years. One important question is the singlet-triplet mixing in the exited A state of acetylene. In order to determine this we will photoionize acetylene through different intermediate states. The photoelectron spectrum will reflect the nature of the intermediate state.

Bimolecular scattering and reactions:

Two extensions of our NO/Ar orientation experiment are obvious. We can use different rare gas collision partners thereby changing the kinematics of the collision. One would predict that collisions with He would be fast and the possibility of multiple interactions during a collision would be small. We would predict little orientation in this case. Collisions of NO with Xe would by nature be slower therefore leading to a higher probability of multiple interactions during a single collision resulting in a larger amount of orientation. A second extension would be to use cooled or heated molecular beams in order to change the energy of the collision. At lower collision energy the interaction would be less "repulsive" and more sensitive to the attractive nature of the potential energy surfaces.

Reactive scattering is a goal of this laboratory as well. Recently it has been shown that the product of a reactive scattering event performed in a single molecular beam between a photolytically produced radial and a reactant then using the ion imaging technique the differential cross section can be directly obtained. For instance if ICl and CH_4 are both entrained in a molecular beam of Ar and a laser photodissociates the ICl producing hot Cl atoms that react with the CH_4 producing HCl + CH_3 then the HCl or the CH_3 can be ionized and imaged. From this image and the differential cross section for the reaction is obtained. The analysis is simply the inverse Abel transform of the image. We would like to do the above mentioned experiment, Cl + CH_4, in this manner measuring both the reactivity of ground state and excited state Cl atoms with CH_4. In this way we can directly measure the adiabatic and non-adiabatic reaction probability for this reaction. Recent reports on F + H_2 and Cl + H_2 have indicated that the non-adiabatic reactive channel is more important than previously expected. In opposition to conventional wisdom, for the Cl + H_2 reaction it is claimed that the excited state Cl ($^2P_{1/2}$) is more reactive than the ground state Cl ($^2P_{3/2}$).

BES Supported Publications

1) L. M Yoder, J. R. Barker, K. T. Lorenz and D. W. Chandler, "Ion Imaging the Recoil Energy Distribution Following Vibrational Predissociation of Triplet State Pyrazine-Ar van der Waals Clusters" Chem. Phys. Lett., **302**, p. 602 (1999).

2) D. W. Neyer, A. J. R. Heck, D. W. chandler, "Photodissociation of N_2O: J-dependent anisotropy revealed in N_2 Photofragment Images", J. Chem. Phys. **110**, p. 3411 (1999).

3) D. W. Chandler and D. H. Parker, "Velocity mapping of multiphoton excited molecules" Advances in Photochemistry, Vol. 25, eds. D. C. Neckers, D. Volman, G von Bunau (John Wiley and Sons, New York, 1999) page 59.

4) Neyer DW, Heck AJR, Chandler DW, Teule JM, Janssen MHM "Speed-dependent alignment and angular distributions of $O(^1D_2)$ from the ultraviolet photodissociation of N_2O" J Phys Chem A , v. 103(#49) pp. 10388 (1999)

5) K. T. Lorenz, M. S. Westley, D. W. Chandler, "Rotational state-to-State differential Cross sections of the HCl-Ar Collision system using velocity Mapped Ion imaging" Phys. Chem. Chem. Phys. **2**, 481 (2000).

6) J. M. Teule, G. C. Groenenboom, D. W. Neyer, D. W. Chandler and M. H. M. Janssen, "State-to-state photodynamics of nitrous oxide and the effect of long-range interaction on the alignment of $O(^1D_2)$ " Chem. Phys. Lett., Volume: 320, Issue: 1-2, 177 (2000)

7) J. A. Davies, R. E. Continetti, D. W. Chandler, and C. C. Hayden "Femtosecond Time-Resolved Photoelectron Angular Distributions Probed during Photodissociation of NO_2" Phys. Rev. Lett. 84, 5983 (2000).

8) D. W. Chandler, J. R. Barker , A. J. R. Heck, M. H. M. Janssen, K. T. Lorenz, D. W. Neyer, W. Roeterdink., S. Stolte and L. M. Yoder "Ion Imaging Studies of Chemical Dynamics" Atomic and Molecular Beams:the state of the art 2000 editied by R. Campargue, Springer publishing 2000 page 519.

9) M. S. Westley , K. T. Lorenz and D. W. Chandler and P. L. Houston "Differential cross sections for rotationally inelastic scattering of NO from He and D_2" J. Chem. Phys. 114, 2669 (2001).

10) L. M. Yoder, J. R. Barker, K. T. Lorenz and D. W. Chandler "Recoil Energy Distributions in van der Waals Cluster Vibrational Predissociation" In Imaging in Chemical Dynamics ed Arthur Suits and Robert Continetti, ACS symposium series, page 151 (2001).

11) K. T. Lorenz, M. S. Westley and D. W. Chandler "Extracting Rotational State-to-State Differential Cross-Sections from Velocity–Mapped Ion Imaging Data" In Imaging in Chemical Dynamics ed Arthur Suits and Robert Continetti, ACS symposium series, page 197 (2001)

12) V. K. Nesterov, R. Hinchliffe, R. Uberna, J. I. Cline, K. T. Lorenz and D. W. Chandler " Measurement of bipolar moments for photofragment angular correlations in ion imaging experiments" submitted for publication JCP (2001)

13) J. I. Cline, K. T. Lorenz, W. A. Wade, J. W. Barr and D. W. Chandler "Ion Imaging Measurement of Collision-Induced Rotational Alignment in Ar-NO Scattering" submitted as communication to JCP (2001)

14) M. H. M. Janssen, J. M. Teule, D. W. Neyer, D. W. Chandler, G. C. Groenenboom, "Imaging of the state-to-state photodynamics of Nitrous Oxide in the 205 nm region of the stratospheric solar window, Atomic and Molecular Beams:the state of the art 2000 editied by R. Campargue, Springer publishing 2000 page 317.

Direct Numerical Simulation and Modeling of Turbulent Combustion

Jacqueline H. Chen, Tarek Echekki, and Scott Mason
Sandia National Laboratories, Mail Stop 9051
Livermore, California 94551-0969
phone: (925) 294-2586
email: jhchen@ca.sandia.gov

Program Scope

Direct numerical simulation (DNS) of turbulence-chemistry interactions has been an invaluable tool in the understanding of complex interactions between combustion chemistry, transport and unsteady flow in gas phase combustion. The scope of the present research is to use massively parallel DNS with detailed chemical mechanisms for hydrocarbon and hydrogen fuels to simulate multi-dimensional unsteady effects relevant to compression ignition, turbulent flame propagation, flame stabilization and flame structure. The physical insights gained from these fundamental studies are being used to guide and validate models of combustion and scalar transport in Reynolds-Averaged Navier-Stokes (RANS) and Large-eddy Simulation (LES) of practical combustion devices.

Recent Progress

In the past year DNS simulations have been used to investigate two fundamental combustion problems related to turbulent flame propagation and autoignition in turbulent media. These simulations were performed on massively parallel computational platforms with up to 1024 processors using MPI for scaleable parallelism. The results from these simulations are described below.

The Effect of Turbulence Intensity and Diffusive-Thermal Instability on Turbulent Burning Velocity [1]

The turbulent burning velocity, S_T, is a central quantity in the understanding and modeling of turbulent premixed combustion in the flamelet and thin-reaction zone regimes. Its parameterization in terms of intrinsic thermochemical and transport properties and external turbulent aerodynamic stretch has been the focus of numerous studies, both experimental and computational. Theoretical considerations of this subject date back to the seminal work of Damköhler in 1940. Damköhler incorporated a Huygens propagation model for thin flames whereby enhancements in the turbulent burning velocity over its laminar value were attributed to turbulent flame area generation above the laminar cross-sectional area. In this model the turbulent velocity increases linearly with turbulence intensity. Recently a new regime of combustion has been identified – the thin reaction zone regime- where small eddies are able to penetrate the preheat convective-diffusive zone, but not the thin reaction zone. Scaling arguments in this regime suggest that the turbulent burning velocity levels off as the turbulence intensity increases, hence possibly accounting for the observed "bending effect". However, there exists significant scatter in flame speed measurements, and computations thus far have not been able to resolve a wide enough range of scales to detemine the turbulent burning velocity. Hence, the parameterization of the turbulent burning velocity remains an open question.

In the present study DNS of turbulent premixed hydrogen air flames are performed over a wide range of turbulence intensities spanning the flamelet and thin-reaction zone regimes. Unlike

previous DNS, the ratio of the turbulence integral to flame thermal thickness scales varies by over an order of magnitude. As a result, the turbulence decay is minimal, even for intense turbulence rms velocity, during the time that the turbulent burning velocity reaches a stationary state. The premixture corresponds to hydrogen/air at an equivalence ratio of 0.6 at 300K and atmospheric pressure. This represents a mixture that is slightly diffusive-thermally unstable and provides for interesting coupling between the unstable mixture and unsteady aerodynamic strain. The ratio of the initial turbulence intensity to laminar flame speed, u'/S_L was varied between 3 and 30. Flame propagation statistics were monitored between 2 and 4 eddy turnover times.

Qualitative differences are observed in the flame structure as a function of the initial turbulence intensity. For low turbulence intensity, $u'/S_L = 3$, there exists the spontaneous appearance of cellular structures along cusps whose center of curvature is in the burnt gas. These cells originate at locations along the flame front where the tangential strain rate is a small positive value. The cell sizes are approximately a flame thermal thickness initially. Consistent with diffusive-thermal instability theory, the cells burn more intensely at the leading edge and are nearly extinguished in the troughs between the cells. The cells subsequently are stretched and wrinkled by the large turbulence scales. The self-turbulization of the flame front via this mechanism contributes to the generation of flame area. At higher turbulence intensities, $u'/S_L > 10$, there exists substantial mutual flame annihilation in the flame brush as the surface density increases due to the intense wrinkling of the front. In fact, a continuous front is no longer distinguishable for $u'/S_L > 15$ due to the frequency of flame-flame interactions.

The DNS data is also used to evaluate the parameterization of the turbulent burning velocity, S_T/S_L, with u'/S_L. The turbulent burning velocity increases linearly with this quantity up to $u'/S_L = 10$ and then levels off for larger values. The turbulent flame area, A_T/A_L, exhibits a similar behavior. Further, for the wide range of turbulence conditions studied, the normalized mean consumption speed remains of order unity, with variations due to strain and instability effects contributing to decreases of 25% and increases of up to 10%, respectively, from the laminar value. Therefore, the enhancement in the turbulent burning velocity is mainly due to the flame area increase. However, the surface density appears to reach a plateau for large turbulence intensities, possibly due to the frequency of flame-flame interactions as the flame area within the brush increases.

Studies of Auto-ignition Phenomena in Turbulent Non-Homogeneous Media[2]

The process of autoignition of hydrogen and hydrocarbon mixtures in a turbulent environment is a fundamental problem that is not well understood in combustion. It depends on the coupling between the relevant ignition chemistry, which is pressure dependent, and on the local mixing rates and mixture composition. Practical applications that include diesel and homogeneous charged compression ignition engine and gas turbine combustion rely on autoignition as either the primary mode of combustion or as the initial phase of combustion following spray evaporation. This process presents many challenges for its modeling and simulation. It strongly depends upon the competition between mixing and chemistry over a broad range of scales. Moreover, it is a strongly transient process in which the dominant chemistry may shift during the induction and subsequent high temperature combustion phases of the process. The induction chemistry is also pressure dependent.

The autoignition of spatially heterogeneous hydrogen-air mixtures in a 2-D random turbulence field has been studied using DNS coupled with detailed kinetics. The simulations were carried out at different pressures. By varying the pressure between 1-10 atmospheres, an array of different autoignition conditions related to the effects of pressure on autoignition chemistry and molecular

transport are reproduced. The initial conditions are based on heated air at 1200 K and cold fuel at 300K in a 50% hydrogen/50% nitrogen mixture by volume. The present calculations illustrate a number of features of relevance to autoignition modeling for non-homogeneous mixtures.

The simulations show that autoignition is initiated by radical build-up in very lean (less than 0.1 mixture fraction), relatively homogeneous mixtures. The large differences in temperatures between the fuel and oxidizer streams, to a large extent, contribute to this mode of burning. The spatial homogeneity is consistent with the relatively low rates of dissipation. While the reacting mixture displays a range of lean mixture fractions that are favorable to the onset of ignition, this preferred range evolves in time as combustion switches from the ignition kernels to propagating fronts. Accordingly, the radical pool build-up is subsequently shifted toward richer, near stoichiometric conditions in a second phase of the autoignition process. This phase is characterized by an important increase in heat release rates and the formation of lean ignition/propagation fronts that are sustained by radical concentrations. These fronts that are generated from igniting kernels propagate, at least initially, as lean premixed flames. Finally, the fronts propagate into the remaining stratified mixture.

The simulations show the presence of both ignited and partially extinguished conditions resulting from relatively high dissipation rates. The rate of burning and the induction time at the different conditions is dependent on the competition between mixing/dissipation and chemistry. While chemistry is faster at higher pressure leading to shorter induction times, mixing rates also increase with pressure due to enhanced diffusivities. As a result, the progress of reaction trend as a function of pressure is not monotonic. Indeed, a relative comparison between the simulations at different pressures shows that at 3 atmospheres, more complete burning is exhibited at comparable times. Therefore, the progress of reaction past ignition is determined by the competition between chemical and mixing time scales. Accordingly, a mixture Damköhler number governs the fate of this competition.

As the mixture evolves from the induction phase to the propagation of ignited kernels, the elementary reactions involved in the radical build-up evolve in time. The dominant chemistry involved during the autoignition process at the various pressures is identified using reaction flux analysis. To illustrate, H atom is produced, similar to homogeneous ignition, by

$$O + H_2 = H + OH \qquad \text{(R2)}$$

and

$$OH + H_2 = H + H_2O \qquad \text{(R3)}$$

H atom is consumed primarily by

$$H + O_2 = O + OH \qquad \text{(R1)}$$

at three atmospheres. The net production rate of H atom follows closely R2 at lower pressure; however, at five atmospheres it tracks more closely R3. At 5 atmospheres the contribution of reaction R9,

$$H + O_2 + M = HO_2 + M \qquad \text{(R9)}$$

becomes more important. The rate of rise of chemical reaction during ignition is largest for intermediate pressure at 3 atmospheres as also reflected in the reaction progress variable. At 5 and

10 atmospheres HO_2 concentration increases leading to the formation of H_2O_2 via R14 and R17. This leads to further chain branching in the ignition kernels via a new chemical pathway that involves the consumption of H_2O_2 in R15,

$$HO_2 + HO_2 = H_2O_2 + O_2 \qquad \text{(R14)}$$
$$HO_2 + H_2 = H_2O_2 + H \qquad \text{(R17)}$$
$$H_2O_2 + M = 2OH + M \qquad \text{(R15)}$$

Future Plans

We plan to continue our DNS studies of unsteady multi-dimensional flames with detailed hydrocarbon kinetics on massively parallel distributed memory computational platforms with a focus towards understanding and modeling inhomogeneous compression ignition, premixed flame stability in the lean flammability limit, turbulent flame propagation in stratified mixtures, and the competition between mixing and hydrocarbon autoignition chemistry at high pressures.

References

[1] J. H. Chen, "Burning Velocity Statistics in the Flamelet and Thin-Reaction Zone Regimes, " 2nd Joint Meeting of the U.S. Sections of the Combustion Institute, Oakland, CA, (2001).

[2] T. Echekki and J. H. Chen, "Direct Numerical Simulation of Autoignition in Nonhomogeneous Hydrogen-Air Mixtures, " 2nd Joint Meeting of the U.S. Sections of the Combustion Institute, Oakland, CA, (2001).

BES Publications (1999-2001)

[1] J. H. Chen and H. G. Im, "Stretch Effects on the Burning Velocity of Turbulent Premixed Hydrogen-Air Flames," *Twenty-Eighth Symposium (International) on Combustion*, (Edinburgh, Scotland, July 30-August 4, 2000), to appear.

[2] H. G. Im and J. H. Chen, "Effects of Flow Transients on the Burning Velocity of Hydrogen-Air Premixed Flames," *Twenty-Eighth Symposium (International) on Combustion*, (Edinburgh, Scotland, July 30-August 4, 2000), to appear.

[3] H. G. Im and J. H. Chen, "Structure and Propagation of Triple Flames in Partially-Premixed Hydrogen/Air Mixtures," *Combust. Flame*, **119**, 436 (1999).

[4] H. G. Im and J. H. Chen, "Effects of Flow Strain on Triple Flame Propagation", *Combust. Flame*, pending, (2001).

[5] W. Kollmann, J. H. Chen, and H. G. Im, "A Geometric Criterium for Non-equilibrium and Triple Flame Domains," *Proceedings of the Eighth European Turbulence Conference, ETC8,* (2000).

[6] T. Echekki and J. H. Chen, "Analysis and Computation of the Different Contributions to Flame Propagation in Turbulent Premixed Methane-Air Flames," *Combust. Flame*, **118**, No. 12 (1999).

[7] H. G. Im, J. H. Chen and J.-Y. Chen, "Chemical Response of Methane/Air Diffusion Flames to Unsteady Strain Rate," *Combust. Flame,* **118**, 204 (1999).

[8] J. H. Chen, T. Echekki, and W. Kollmann, "The Mechanism of Two-Dimensional Pocket Formation in Lean Premixed Methane-Air Flames with Implications to Turbulent Combustion," *Combust. Flame* **116**,15 (1999).

[9] H. G. Im, J. H. Chen, R. Subramanya and R. Reddy, "Direct Numerical Simulations of Turbulent Premixed Flame Interaction using Parallel Computing, " *1st MIT Conference on Applied Mechanics and Fluid Mechanics*, Elsevier Science, (2001).

Turbulent Combustion

Robert K. Cheng
Environmental Energy Technologies Div.
Lawrence Berkeley National Laboratory
70 –109, 1 Cyclotron Rd.
Berkeley, CA 94720

E-mail : rkcheng@lbl.gov

Larry Talbot
Dept. of Mechanical Engineering
University of California at Berkeley
6173 Etcheverry Hall
Berkeley, CA 94720-1740

E-mail : Talbot@cmsa.Berkeley

Scope

This research program focuses on lean premixed combustion which is an emerging low emission energy technology being deployed in advanced heat and power generation systems. Our objective is to investigate experimentally the fluid mechanic processes that control combustion intensity, flame stabilization, extinction and pollutant formation. The goal is to provide the scientific underpinnings for energy technologies so that it might be captured in models that will become accurate and reliable tools for predicting combustion process performance. This effort is responsive to DOE's mission to "foster a secure and reliable energy system that is environmentally and economically sustainable." Combustion processes of practical interests are turbulent and are not sufficiently well characterized and understood to guide the refinement of turbulent combustion theories and to support the development of robust numerical models. Our approach follows a theoretical concept of classifying premixed flames according to the initial turbulence conditions and chemi. To conduct a systematic exploration of the evolving flame structures at different turbulence intensities and scales, we use laser diagnostics and laboratory burners capable of operating at a wide range of fuel/air ratios and turbulence conditions. In the past, our laboratory experiments have concentrate on flames at standard temperature and pressure (i.e., typical furnace and boiler conditions). With the development of a new experimental facilities, the experimental conditions will be extended to higher flow velocities (i.e. closer simulation to conditions of large burners) and higher pressures and temperatures (i.e., closer simulation of gas turbine conditions).

Recent Progress

Our expeirmental investigations of flames in moderate and intense turbulence have shown that the Klimov-Williams criterion at unity Karlovitz number, $Ka = 1$, is too stringent. This criterion is a longstanding theoretical concept that separates two types of premixed turbulent flames. Wrinkled flames ($Ka < 1$) occur at low to moderate turbulence under which the flame front remains undisturbed by turbulence and retain most features of a wrinkled laminar flame. Flames with "distributed reaction zones" ($Ka > 1$) occur at higher turbulence levels where small intense eddies may penetrate and broaden the reaction zone. Because the operating conditions of most practical systems span this criterion, the problem is of interest to both fundamental and applied research. The main implication is that different flame models may be required.

The use of our low-swirl burner (LSB) has been crucial to this experimental investication. Fitted with a special turbulence generator, it enabled the study of flames with high intensity near-isotropic turbulence of up to 4 m/s RMS velocity. The experimental conditions we have investigated range from moderate ($u'/S_L = 3$) to intense ($u'/S_L = 19$) turbulence. At LBNL, we use a two-component laser Doppler anemometry (LDA) system to measure velocity statistics, and

laser schlieren, laser tomography and Planar Laser Induced Fluorescence for OH (OH-PLIF) to capture flame structures. We collaborate with RWTH-Aachen where an identical burner was built and studied using simultaneous OH-Laser Induced Prodissociateive Fluorescence (OH-LIPF) with either 2D Rayleigh or Particle Image Velocimetry (PIV). OH is a convenient marker of the reaction zone at the trailing edge of the flame front. 2D Rayleigh scattering maps the density distribution in the preheat zone closer to the leading edge.

The experimental results indicate that the transition from flamelet to distributed reaction zone occur at much higher Karlovitz numbers. At the highest turbulent condition investigated, the flame fronts shown on the 2D Rayleigh images are broadened and disrupted by turbulence. The corresponding OH-PLIF images remain consistently less wrinkled and do not show significant broadening. These observations provide qualitative support for a 'thin reaction zone' regime ($1 < Ka < 10$). In this new regime, the smallest turbulent eddy is smaller that the flame front thickness, d_L (about 1 mm for most atmospheric hydrocarbon flames) but is still an order of magnitude larger than the reaction zone (about 0.1 mm). The main implication to modeling is that turbulent transport become significant within the pre-heat zone of the flame front. To what extend will this affect the local reaction rate remains unknown.

To quantify the degree of pre-heat zone broadening and flame front structures of flames within the new regime, we initiated a detail analysis of simultaneous OH planar laser induced fluorescence (LIPF) and 2D Rayleigh scattering data obtained jointly with the group at Aachen. Analysis of the OH-LIPF data is relatively straight forward utilizing the image processing software developed previously to deduce local flame curvatures and wrinkle scales. Analysis of 2D-Rayleigh is more complex. To show the overall pre-heat zone broadening effect we are deducing the wrinkle scales and curvatures for different isotherms. If the thin reaction zone regime is valid, we expect that at low to moderate turbulence the wrinkle scales of the reaction zone represented by the high temperature isotherms will be consistent with those obtained from the preheat zone. With higher turbulence intensities, the wrinkle scales of the preheat zone will be smaller than those of the reaction zone due to increase turbulence transport. To quantify pre-heat zone broadening along the flame front is non-trivial. Due to the 3D nature of the turbulent flame fronts, apparent broadening associated with out-of-plane flame inclination needs to be considered. Several approaches are under consideration to develop a consistent and reproducible method.

Our BES supported basic work on turublent combustion has spun-off applied research on developing the low-swirl burners as a low emission combustion technology. Experience gained from scaling the burner to practical sizes (approaching 1 MW) have provided new insight on premixed turbulent flame properties to guide our basic research. Typcial operating velocities of practical low-swirl burner prototype are from 10 to 90 m/s. The fact that the low-swirl burner operates over such a large velocity range implies a linear relationship between the displacement flame speed and turbulence intensity. This is direct contrast with current theory that predicts a "bending effect" where the displacement flame speed correlation ceases to increase with increasing turbulence. Concentrations of unburned hydrocarbon measured in the exhaust indicate close to complete combustion. These data do not support the notion of local flame quenching due to turbulence. The fact that NO_x emission decreases with increasing burner input power also suggest complex flame-turbulence-chemistry interactions that current flame models may not be able to handle. To obtained a fundamental understanding of these interesting flame phenomena, we initiated an experiment to study flames with very high propagating speed. As the flow supply

and exhaust system in our laboratory is limited, reducing the size of the burner is the only viable approach to access high speed. We constructed a half-scale low-swirl burner (2.5 cm i.d.) that should operate up to 50 m/s. Preliminary tests are being conducted to optimize the burner and flow control hardware for experiments comencing in later part of FY01.

We also initiate a study of lean premixed turbulent flames at high initial pressures and temperatures. The motivation is to extend our capabilities to address fundamental issues relevant to gas turbine combustion. During the past decade, the gas turbine industry has adopted lean premixed combustors to help reduce NO_x emissions. However, lean premixed gas turbine has been plagued by problems with flame stabilization, combustion oscillations and blowoff. As this is a relatively new technology, it has yet to generate significant interest from the scientific community to study fundamental properties of steady lean premixed turbulent flames under gas turbine operating conditions. The experimental facility to investigate lean premixed flames under high pressures is designed to simulate idling and mid-load conditions of a small gas turbine combustor (15 atm and 200° C inlet temperature). The centerpiece is a stainless steel combustion chamber that mounts on top of a premixed burner. The chamber is fitted with four 25.4 mm thick 101.6 mm round sapphire windows to allow laser access. The burner has a 25.4 mm round exit port and can be adapted to generate different flame configurations. This facility has computer control provisions to set the fuel/air ratio, to monitor chamber pressure and surface temperatures, and to analyze combustion byproducts. The comissioning process of the facility is complete. Conditions tested thus far include conical flames with mean flow velocity of 3m/s at 5 atm.

In addition to our experimental effort, we are also pursuing a modest numerical study of the numerical simulation of turbulent open v-flames by the discrete vortex method. This 2D method is particularly well suited for investigating the dynamics of the turbulent flow and its effects on flame wrinkling. Though other more elaborate numerical approaches have been developed for premixed turbulent flames, the discrete vortex method focuses on the fluid mechanical processes and provides a better tool to resolve dynamic flame/turbulence interactions that control the development of the turbulent flame brush. A rod-stabilized v-flame was chosen because of the wealth of experimental data on the turbulent flowfield and flame wrinkle structures that have collected in our experimental database and are available for direct comparison with numerical results. Our collaborator on the numerical simulation is Prof. C. K. Chan of the Hong Kong Polytechnic University. The achievement in the past year include improvement in the simulation of the complex flame fronts by a novel numerical technique called Contour Adection with Surgery. Considerably better quantitative agreement with a limited set of our experimental data has also been obtained.

4. Summary of Planned Research

For our study of open high speed flames at atmospheric conditions, the use of LDA will determine the displacement flame speed and an explanation to why the low-swirl flame stabilization method does not exhibit non-linearity in its flame speed correlation. OH-PLIF and Rayleigh techniques (point or 2D) will be used to study the local and mean burning rates and investigate if wrinkled flame structures still exist at high speed. Other issues to be address include preheat zone broadening due to small scale turbulence, and flame quenching due to turbulence.

For our study of premixed turbulent flames at high pressures, the initial effort will be focussed on an extensive survey of the effects of high pressure on overall flame features by the use of simple

imaging methods such as schlieren. This study will involve several flame configurations. Changes in flame size with pressures will provide qualitative information on the mean combustion intensity and mean burning rate. Because the laminar flame thickness decreases with increasing pressure, the important implication is that the wrinkle flame model is valid.

As the high-pressure facility cannot afford a very long run time, our diagnostics has to be upgraded to accommodate this limitation. For velocity measurement, we plan to develop a 2D Planar Particle Velocimetry system. To validate the thin flame model through detailed measurement of turbulence flowfield and flame structure, adopting OH-PLIF and Rayleigh scattering to the high pressure facility will be a major effort.

If funding is available, we plan to use the improved discrete vortex model and extend the computations to high turbulence intensities and possible predictions of local extinction. Another extension would be to treat the problem of flame stabilization by a recirculation region behind a finite size flameholder. The model would include the effects of shear turbulence produced by the flame stabilizer and its role in the recirculation zone within the products. Formulation and exploitation of the model for the stagnation point flame configuration will also be explored. These new numerical simulation developments would represent a significant and practically important advance in the prediction of premixed flame behavior by means of vortex dynamics, and the numerical problems which would have to be overcome are far from trivial. Although additional experiments designed to validate numerical predictions would also be formulated.

Publications

1. Plessing, T., Kortschik, C., Mansour, M. S., Peters, N. and Cheng, R. K. "Measurement of the Turbulent Burning Velocity and the Structure of Premixed Flames on a Low Swirl Burner" Transaction of the Combustion Institute, *28*, 2000.
2. Shepherd, I. G., and Cheng, R. K. "The Burning Rate of Premixed Flames in Moderate and Intense Turbulence" to appear Combustion and Flame, 2001.
3. Cheng, R. K., Bedat, B., Shepherd I. G. and Talbot, L. "Premixed Turbulent Flame Structures in Moderate and Intense Isotropic Turbulence" to appear Combustion Science and Technology 2001.

Electronic Structure Studies of Geochemical and Pyrolytic Formation of Heterocyclic Compounds in Fossil Fuels

DOE Chemical Science Grant # DE–FG02–97ER14758

J. Cioslowski

Department of Chemistry and
School of Computational Science & Information Technology
Florida State University
Tallahassee, FL 32306.

jerzy@csit.fsu.edu
(850) 644–8274

and

D. Moncrieff

School of Computational Science & Information Technology
Florida State University
Tallahassee, FL 32306.

moncrieff@csit.fsu.edu
(850) 644–4885

Program Scope

This research program has as its objective uncovering of the reaction mechanisms responsible for the formation of various heteroatom-containing combustion emittants. As such, it holds the promise of guiding the practitioners of applied science and engineering in their efforts to significantly reduce the pyrolytic production of carcinogens and other hazardous substances. At the same time, it is slated to test practical limits of the predictive power of modern quantum-chemical methods and shed light on mechanisms of many reactions that are commonly employed in organic syntheses.

Our research targets a large number of reaction pathways of relevance to pyrolytic processes involving heterocyclic compounds that occur during genesis, acquisition, and combustion of fossil fuels. A broad spectrum of theoretical approaches, ranging from very accurate interpolative schemes such as G3 to the methods of density functional theory, is invoked. As the result, reliable values of thermodynamic properties become available for molecules that are not readily amenable to experimental measurements. New mechanisms of important reactions are revealed and the rules governing thermal fates of heterocyclic species are discovered.

Recent Progress

A number of research projects were completed in 2000. These projects, which yielded data of much interest to both experimental and theoretical chemists, required very substantial computer resources.

Results of B3LYP/6-311G* and MP2/6-311G* electronic structure calculations provided a definitive characterization of all the conformers of the S_5, S_6, S_7, and S_8 homocycles and elucidated their interconversions [7]. The S_5 ring was confirmed to exist exclusively in a highly fluxional C_s conformation. Two conformers of the S_6 homocycle, linked through two transition states, were identified, the D_{3d} structure corresponding to a global energy minimum and the higher-energy species possessing C_{2v} symmetry. The S_7 ring was found to adopt one of two highly fluxional C_s conformations that are separated by a substantial barrier. The complete set of the conformers of the S_8 homocycle, which consists of the C_{2v}, C_2, C_s (and possibly also C_{2h}) structures in addition to the low-energy D_{4d} species, was uncovered.

Relative energies for $C_{60}F_N$ flurofullerenes were found to be reproduced reasonably well at the B3LYP/6-311G** level of theory employed in conjunction with isodesmic transfluorination reactions, although overestimation of steric repulsions among nonbonded atoms was evident for species with larger values of N [8]. On the other hand, the MNDO method was found to be less suitable for studies of flurofullerene thermochemistry. The gas-phase standard enthalpy of formation of the $C_{60}F_{18}$ species was predicted to lie between 1500 and 1400 [kJ/mol].

For all isolated pentagon isomers of the fullerenes C_{60} C_{86} with non-zero band gap and for one non-classical C_{72} isomer (C_{2v}), endohedral chemical shifts were computed at the GIAO-SCF/3-21G level of theory using B3LYP/6-31G* optimized structures [9]. The experimental ^{3}He NMR signals were reproduced reasonably well in cases where assignments are unambiguous (*e.g.* C_{60}, C_{70} and C_{76}). On the basis of the calculated thermodynamic stability order and the comparison between the computed and experimental ^{3}He chemical shifts, the assignments of the observed ^{3}He NMR spectra were discussed for all higher fullerenes, and new assignments were proposed for on C_{82} and one C_{86} isomer (C_{82}:3 and C_{86}:17). The calculated helium chemical shifts led to reassignment of the $\delta(^3\mathrm{He})$ resonances of two C_{78} isomers.

Ring opening of the cyclic $[(Bu^tP)_3As]^-$ anion results from the reactions with electrophiles (RX = H_2O, MeI, CH_2=$CHCH_2I$, and $PhCH_2Br$), providing a simple and general approach to triphosphine ligands of the type $[(Bu^tP)(Bu^tRP)_2]$ [10]. Model electronic structure calculations, incorporating solvent effects, were used to confirm the thermodynamic stability of the triphosphine complexes.

Future Plans

In the coming year, our research will focus on the elucidation of the formation of five- and six-membered heterocycles in pyrolytic reactions. To achieve this end, we are planning to complete the following projects:

1. *Thermochemistry and electronic structures of azynes.* Standard enthalpies of formation of pyridynes (**1** **6**), diazynes (**7** **17**), and other azynes (**18** **26**) will be computed at the G3 level of theory. Both the singlet and triplet electronic states will be investigated. The general rules governing relative energies and singlet-triplet splittings in azynes will be deduced from the computed data.

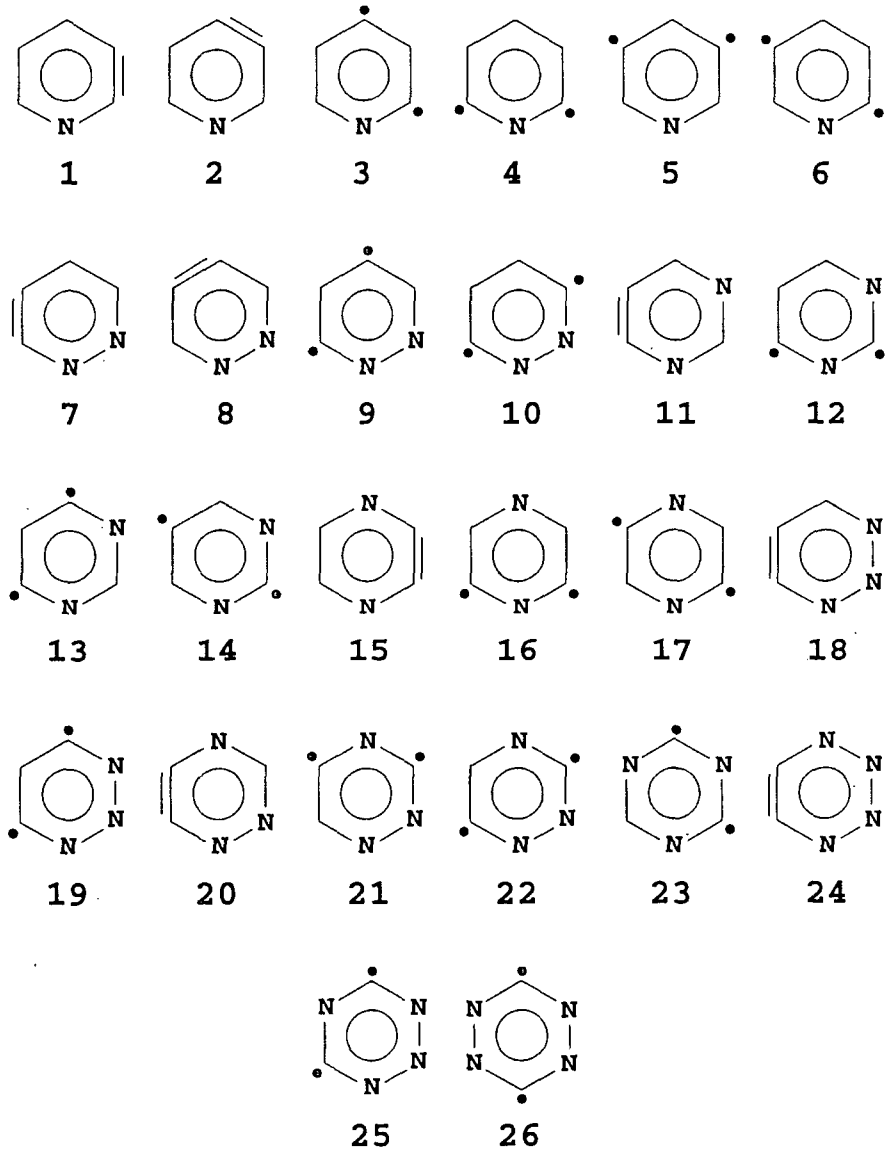

2. *Thermochemistry and electronic structures of naphthalynes, quinolynes, and isoquinolynes.* In previous studies, the energy of 1,2-didehydrogenation of naphthalene has been found to be weakly dependent on the site of hydrogen removal. In order to investigate the positional dependence of the energetics of analogous processes in annelated azines, high-level electronic structure calculations will be carried out for 1,2-naphthalyne (**27**), 2,3-naphthalyne (**28**), five quinolynes (**29**–**33**), and four isoquinolynes (**34**–**37**).

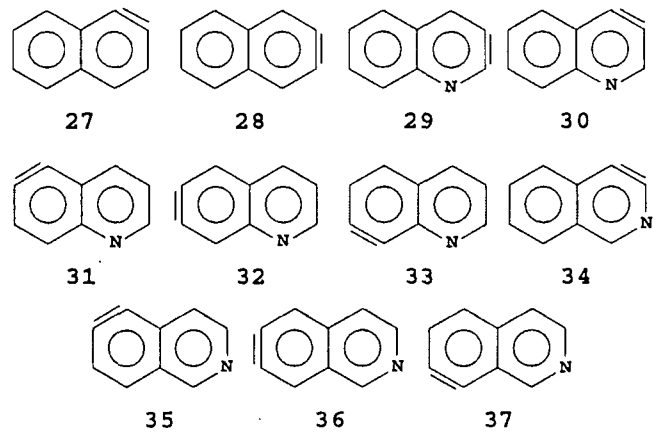

Publications Resulting from the DOE Sponsored Research (1999–2001)

1. J. Cioslowski, M. Schimeczek, P. Piskorz and D. Moncrieff: **Journal of the American Chemical Society 121 (1999) 3773.** Thermal Rearrangement of Ethynylarenes to Cyclopentafused Polycyclic Aromatic Hydrocarbons: An Electronic Structure Study.

2. J. Cioslowski, G. Liu and D. Moncrieff: **Journal of Physical Chemistry A 103 (1999) 11465.** Theoretical Thermochemistry of the 1-Buten-3yn-1-yl Radical and it's Chloro Derivatives.

3. J. Cioslowski, G. Liu and D. Moncrieff: **Chemical Physics Letters 316 (2000) 536.** The Concerted Trimerization of Ethyne to Benzene Revisted.

4. J. Cioslowski, M. Schimeczek, G. Liu and V. Stoyanov: **Journal of Chemical Physics 113 (2000) 9377.** A Set of Standard Enthalpies of Formation for Benchmarking, Calibration, and Parameterization of Electronic Structure Methods.

5. J. Cioslowski and A. Szarecka: **Journal of Computational Chemistry (in press).** First-Principles Conformational Analysis of the $C_{36}H_{36}$ Spheriphane.

6. J. Cioslowski, N. Rao and D. Moncrieff: **Journal of the American Chemical Society 122 (2000) 8265.** Standard Enthalpies of Formation of IPR Fullerenes and Their Analysis in Terms of Structural Motifs.

7. J. Cioslowski, A. Szarecka and D. Moncrieff: **Journal of Physical Chemistry A 105 (2001) 501.** Conformations and Thermodynamic Properties of Sulfur Homocycles: I. The S_5, S_6, S_7, and S_8 Molecules.

8. J. Cioslowski, N. Rao, A. Szarecka, and K. Pernal: **Molecular Physics (in press).** Theoretical Thermochemistry of the $C_{60}F_{18}$, $C_{60}F_{36}$, and $C_{60}F_{48}$, Fluorofullerenes.

9. Z. Chen, J. Cioslowski, N. Rao, D. Moncrieff, M. Buhl, A. Hirsch, and W. Thiel: **Theoretical Chemistry Accounts (submitted).** Endohedral Chemical Shifts in Higher Fullerenes with 72-86 Carbon Atoms.

10. D.R. Armstrong, N. Feeder, A.D. Hopkins, M.J. Mays, D. Moncrieff, J.A. Wood, A.D. Woods and D.S. Wright: **Journal of Chemical Society Chemical Communications (2000) 2483.** Electrophilic Ring-Opening of $[(RP)_nAs]^-$ Anions, A Simple Route to Funtionalised Neutral Phosphines of the Type $[(Bu^tP)(Bu^tRP)_2]$.

Half-Collision Dynamics of Elementary Combustion Reactions
Grant DE-FG03-98ER14879

Robert E. Continetti
Department of Chemistry and Biochemistry
University of California San Diego
9500 Gilman Drive
La Jolla, CA 92093-0340
rcontinetti@ucsd.edu
April 12, 2001

Program Scope

The focus of this research program has been the study of the dynamics of hydroxyl radical reactions. Using negative-ion photodetachment techniques, energy-selected neutral complexes are created in configurations near the transition-state for bimolecular reactions. The products and dissociation dynamics of the nascent neutral complexes on the potential energy surface controlling the neutral bimolecular reaction are then measured using translational spectroscopy. We have applied this technique to both the OH + H_2O and OH + OH reactions and are currently extending these studies to the H + CO_2 reaction system. The central goal of these experiments is to provide experimental benchmarks for the evaluation of potential energy surfaces and dynamics calculations on these important systems. To support these experimental efforts we have carried out *ab initio* and dynamics calculations.

We have also carried out studies of radicals and other transient species using new techniques in photoelectron spectroscopy. In the last year we demonstrated photodetachment imaging techniques adapted from work carried out in Carl Hayden's laboratory at Sandia National Laboratories on photoelectron-photoion coincidence imaging. We used these new techniques to study the electron affinity of CF_3 and the thermochemistry of CF_3^-, yielding improved values for these quantities.

Recent Progress

Dynamics of Elementary Combustion Reactions
$OH + H_2O \rightarrow H_2O + OH$

The hydrogen exchange reaction OH + $H_2O \rightarrow H_2O$ + OH is one of the simplest reactions of the hydroxyl radical, and thus of both practical and fundamental interest. Photoelectron spectroscopy studies by Arnold *et al.*[1] of the $H_3O_2^-$ anion showed that photodetachment can be used to probe regions near the transition-state for this reaction. We have studied the transition-state dynamics of this reaction using dissociative photodetachment of $OH^-(H_2O)$ and $OD^-(D_2O)$ at 258 nm (4.80 eV) using photoelectron-photofragment coincidence spectroscopy.[publication 1 below] The photoelectron spectra are consistent with the previous results of Neumark and co-workers,[1] and the quantum yield for dissociation of the neutral into two fragments is unity. The photoelectron-photofragment coincidence spectrum for the $OH^-(H_2O)$ anion, however, reveals considerably more information as discussed in the last progress report.

To aid in the analysis of the observed dynamics, *ab initio* calculations were performed for the anion and neutral complexes. The initial goal was to calculate the electronic structures of the stationary points in the anion and neutral consistently and find a method accurate enough for calculation of the potential energy surface for both the anion and the neutral. Owing to constraints on computer time, calculations were carried out at the (U)QCISD level of theory with the 6-311++G(d,p) basis set. The energy of the system was calculated at 60 points (120 by

symmetry) for the anion and 120 points (240 by symmetry) for the neutral, varying the bond distances between the shared H atom and the O atoms in a collinear O-H-O geometry with overall C_{2h} symmetry in the H-O-H-O-H complex. These points were fit with an analytic function, allowing two–dimensional time-dependent wavepacket dynamics simulations of the observed photoelectron spectra, extending the previous one-dimensional calculations of Arnold, *et al.*[1] The simulations showed that use of the *ab initio* surfaces for the anion and neutral lead to a significant broadening of the simulated photoelectron spectra, more consistent with the experimental result, and also providing a measure of the sensitivity of these data to the true potential energy surface governing hydroxyl radical reactions. This work is still in preparation, but we hope that our theoretical efforts and observations will encourage further high-level theoretical structure and dynamics calculations in a larger number of degrees of freedom for this benchmark reaction of hydroxyl radicals.

$OH + OH \rightarrow O(^3P) + H_2O$

The reaction between two hydroxyl radicals forming $O(^3P) + H_2O$ is an exothermic reaction that can produce H_2O in hydrocarbon flames, while the reverse reaction is a chain-branching process. On a fundamental level this reaction is one of the simpler radical-radical reactions and thus of interest as a prototype. There have been few studies of the chemical dynamics of this reaction outside of transition-state spectroscopy experiments by Arnold *et al.*[1]

We have also carried out photoelectron-photofragment coincidence studies of the OH + OH $\rightarrow O(^3P) + H_2O$ reaction by dissociative photodetachment of $O^-(H_2O)$ and $O^-(D_2O)$ at 258 nm (4.80 eV). As in the $OH+H_2O$ reaction, the data reveal vibrationally resolved product translational energy distributions for both dissociation pathways. The total translational energy distribution shows an overlapping vibrational progression indicating excitation of the antisymmetric stretch in the water product in the exit channel and OH stretch in the entrance channel. Due to the fact that dissociative photodetachment produces both OH + OH and $O + H_2O$ products, and the photofragment mass resolution in these experiments is unable to resolve these channels, the correlation spectrum $N(E_T,\text{eKE})$ has correlated signals for both channels. The photoelectron spectra have been compared to a two-dimensional time dependent wavepacket dynamics simulations based on an anharmonic potential in the anion and a model collinear potential energy surface for the neutral complex. These simulations are in qualitative accord with the experimental results, and also show the strong influence that vibrational excitation in the anion can have on the product branching ration. From the kinetic energy release data we also derived the ionic dissociation energies $D_0(H_2O_2^- \rightarrow H_2O + O^-) = 1.15 \pm 0.08$ eV and $D_0(D_2O_2^- \rightarrow D_2O + O^-) = 1.05 \pm 0.08$ eV for its deuterated analog.

Ab initio quantum chemical calculations have been performed to characterize the equilibrium structure of $O^-(H_2O)$ and the reaction coordinate on the neutral surface in a reduced dimensionality approximation. The OH + OH system is very difficult one since it involves the interaction of two free radicals – in this case, the *ab initio* calculations on the neutral surface were only used to obtain reasonable barrier heights to use in scaling semiempirical London-Eyring-Polanyi-Sato surfaces used in wavepacket propagation calculations of the photoelectron spectra.

$HCO_2^- \rightarrow H + CO_2 + e^-$

Our most recent transition-state dynamics experiments have focused on the dissociative photodetachment of HCO_2^- and DCO_2^-. These studies once again build on earlier photoelectron spectroscopy experiments by Neumark and co-workers.[2] We have found that the nascent HCO_2 and DCO_2 neutrals dissociate into $H+CO_2$ and $D+CO_2$ with a quantum yield of unity. Thus, these experiments are not likely to shed much insight into the transition-state region for the important $OH+CO \rightarrow H+CO_2$ reaction, but nonetheless should provide an important test of potential energy surfaces and dynamics calculations on this much-studied system. This marks the first time we have detected H and D atoms and the most interesting result is that the preliminary experiments indicate that we can resolve the bending excitation of the CO_2 products in the translational energy distributions.

Energetics of Free Radicals: Photodetachment Imaging of CF_3^-

Our collaboration with Dr. Carl Hayden at Sandia National Laboratories in Livermore has also led to the development of three-dimensional photodetachment imaging capabilities in our laboratory.[3] The first results from this new spectrometer were recently published, in a theoretical and experimental study of the photodetachment of CF_3^-, providing an improved experimental electron affinity of the important CF_3 radical. One important quantity, the adiabatic electron affinity (EA) of CF_3 was still in question prior to our measurements of the photoelectron spectra of trifluoromethyl anion, CF_3^-, at 355 nm and 258 nm.[publication 5 below]

Due to the large geometry change between the anion and neutral, *ab initio* calculations and Franck-Condon simulations of the photoelectron spectrum were required to extract the adiabatic electron affinity $EA[CF_3] = 1.80\ 60.05$ eV and the heat of formation for the trifluoromethyl anion derived from the adiabatic electron affinity is $\Delta H^0_{f,298}[CF_3^-] = -152.9\ 6\ 1.1$ kcal/mol. These calculations were carried out using a grant of time at the National Energy Research Supercomputer Center at Berkeley.

Future Plans

In addition to our currently ongoing studies of the $H+CO_2$ reaction, we plan to carry out PPC experiments on the OH+F reaction (isoelectronic with the OH+OH system previously studied) and the fundamental $OH+H_2$ reaction. We hope to expand our studies of the energetics and dynamics of combustion radicals (including vinylidene, allyl and cyclopentadienyl radicals) by implementing VUV photodetachment methods to reach higher excited states in an outgrowth of our collaboration with Hayden's laboratory at Sandia National Laboratory.

To support these experimental studies we also plan to continue carrying out electronic structure and dynamics calculations when possible. In addition to *ab initio* calculations to characterize the equilibrium structure of the precursor anion and the region of the neutral potential energy surface probed by photodetachment, it will be of interest to extend the wavepacket dynamics calculations to extract simulated correlated photoelectron-photofragment kinetic energy distributions, as measured in these experiments. This will require longer propagation times to reach the true asymptotic limit of the product state distributions, similar to calculations on the OH + F system by Dixon and Tachikawa.[4]

Publications: 1999 - Present

1. H.-J. Deyerl, A.K. Luong, T.G. Clements and R.E. Continetti, "Transition State Dynamics of the OH + H_2O Hydrogen Exchange Reaction Studied by Dissociative Photodetachment of $H_3O_2^-$.", Faraday Discussion **115**, 147-160 (2000).
2. L.S. Andrews, A. Rohrbacher, C.M. Laperle and R.E. Continetti, "Laser Desorption - Ionization of Transition Metal Atoms and Oxides from Solid Argon.", J. Phys. Chem. A **104**, 8173-8177 (2000).
3. R.E. Continetti, "Dissociative Photodetachment Studies of Transient Molecules by Coincidence Techniques.", in Advanced Series in Physical Chemistry: Photoionization and Photodetachment Vol. II, ed. C.Y. Ng, World Scientific, Singapore (2000), pp. 748-808 .
4. A.G. Suits and R.E. Continetti, "Imaging in Chemical Dynamics - the State of the Art.", ACS Symposium Series Vol. 770, Imaging in Chemical Dynamics, eds. A.G. Suits and R.E. Continetti, ACS , Washington DC (2000), pp. 1-18.
5. H.-J. Deyerl, L.S. Alconcel and R.E. Continetti, "Photodetachment Imaging Studies of the Electron Affinity of CF_3.", J. Phys. Chem. A **105**, 552-557 (2001).
6. A. Rohrbacher, R.E. Continetti, "A Multiple-Ion-Beam Time-of-Flight Mass Spectrometer.", Rev. Sci. Instrum. (in press, 2001).
7. R.E. Continetti, "Coincidence Spectroscopy.", Annual Reviews of Physical Chemistry, Vol. 52 (in press).

Literature Cited

1. D. W. Arnold, C. Xu and D. M. Neumark, *Spectroscopy of the transition state – elementary reactions of the hydroxyl radical studied by photoelectron spectroscopy of $O^-(H_2O)$ and $H_3O_2^-$.*, J. Chem. Phys. **102**, 6098 (1995).
2. E.H. Kim, S.E. Bradforth, D.W. Arnold, R.B. Metz and D.M. Neumark, *Study of HCO_2 and DCO_2 by negative ion photoelectron spectroscopy.*, J. Chem. Phys., **103**, 7801 (1995).
3. J.A. Davies, J.E. LeClaire, R.E. Continetti and C.C. Hayden, *Femtosecond time-resolved photoelectron-photoion coincidence imaging studies of dissociation dynamics.*, J. Chem. Phys. **111**, 1 (1999); J.A. Davies, R.E. Continetti, D.W. Chandler and C.C. Hayden, *Femtosecond time-resolved photoelectron angular distributions probed during photodissociation of NO_2.*, Phys. Rev. Lett. **84**, 5983 (2000).
4. R.N. Dixon and H. Tachikawa, *The photodetachment spectrum of OHF^-: the influence of vibration at a transition state.*, Mol. Phys. **97**, 195 (1999).

VIBRATIONAL STATE CONTROL OF PHOTODISSOCIATION

F.F. Crim
Department of Chemistry
University of Wisconsin–Madison
Madison, Wisconsin 53706
fcrim@chem.wisc.edu

Our research investigates the chemistry of vibrationally excited molecules. The properties and reactivity of vibrationally energized molecules are central to processes occurring in environments as diverse as combustion, atmospheric reactions, and plasmas and are at the heart of many chemical reactions. The goal of our work is to unravel the behavior of vibrationally excited molecules and to exploit the resulting understanding to determine molecular properties and to control chemical processes. A unifying theme is the preparation of a molecule in a specific vibrational state using one of several excitation techniques and the subsequent photodissociation of that prepared molecule. Because the initial vibrational excitation often alters the photodissociation process, we refer to our double resonance photodissociation scheme as *vibrationally mediated photodissociation.* In the first step, fundamental or overtone excitation or stimulated Raman scattering prepares a vibrationally excited molecule and a second photon, the photolysis photon, excites the molecule to an electronically excited state. Vibrationally mediated photodissociation provides new vibrational spectroscopy, measures bond strengths with high accuracy, alters dissociation dynamics, and reveals the properties of and couplings among electronically excited states. Several recent measurements illustrate the scope of the approach and point to new directions.

ONE-PHOTON DISSOCIATION

The simple, one-photon photolysis of molecules is an important reference point in our vibrationally mediated photodissociation measurements. For example, we have studied non-adiabatic processes and have explored the controlled cleavage of selected bonds by comparing product yields in the photolysis of ground state and vibrationally excited molecules.

One example of a simple photodissociation is our study of dimethyl sulfoxide ($(CH_3)_2SO$) molecules cooled in a molecular beam. We photolyze them with different wavelengths of ultraviolet light and determine the yields of the various products and the extent of secondary dissociation using laser induced fluorescence and multiphoton ionization to detect the products. Our most extensive study of one-photon dissociation has investigated isocyanic acid (HNCO), which has available two spin-allowed decomposition pathways producing either H + NCO or singlet NH + CO,

$$\mathrm{HNCO}\ (^1\mathrm{A}'') \rightarrow \mathrm{H}\ (X\,^2\Sigma) + \mathrm{NCO}\ (X\,^2\Pi)$$
$$\mathrm{HNCO}\ (^1\mathrm{A}'') \rightarrow \mathrm{NH}\ (a\,^1\Delta) + \mathrm{CO}\ (X\,^1\Sigma^+),$$

and one lower energy spin-forbidden pathway producing triplet NH + CO,

$$\mathrm{HNCO}\ (^1\mathrm{A}'') \rightarrow \mathrm{NH}\ (X\,^3\Sigma^-) + \mathrm{CO}\ (X\,^1\Sigma^+).$$

The experiments probe dissociation dynamics involving three different electronic surfaces (the ground state S_0, the singlet excited state S_1, and the first triplet state T_1). By detecting the three products, ^{1}NH, ^{3}NH, and NCO, we have measured the relative yield in each channel. The general trend is that each new dissociation path dominates the product yield as it becomes energetically accessible. The lowest energy products, ^{3}NH + CO, give way to NCO + H when the photolysis energy is large enough energy to form them, and, at still higher photolysis energies, the major products are ^{1}NH + CO. This highest energy channel accounts for about 80% of the products at the largest energies we use.

DISSOCIATION OF VIBRATIONALLY EXCITED STATES

Controlling Non-adiabatic Pathways

Dissociating vibrationally excited molecules at the same *total* energy as in the one-photon photolysis allows us to compare the effect that starting in a different vibrational state and, hence, having access to other parts of the ground and excited electronic potential energy surfaces has on the dissociation dynamics. The photolysis of vibrationally excited HNCO is one dramatic example. Preparing HNCO with three quanta of N-H stretching excitation turns the minor (20%) H + NCO channel in the one-photon photolysis into the major (60%) channel. Detailed experimental and theoretical studies of the one-photon dissociation and the vibrationally mediated photodissociation indicate that the origin of the change in the competition between formation of ^{1}NH and NCO is that initial N-H stretching vibration makes it more difficult for the system to move along the HN-CO coordinate. The longer lifetime in the excited state allows more extensive internal conversion to the ground electronic state where the decomposition to H + NCO occurs. Classical trajectory calculations by Schinke and Bittererova [Chem. Phys. Lett. **332,** 611-616 (2000)] support this simple picture.

Probing Excited States and Electronic Spectroscopy

Photodissociation of vibrationally excited states provides new information on the nature of the excited state surface. We have performed a combined experimental and theoretical study of the photolysis of vibrationally excited hydroxylamine (H_2NOH) in which we obtain vibrational overtone spectra and product yields for states with three, four, or five quanta of stretching excitation and draw inferences about barriers in the excited state.

Excitation to the electronically excited state of HNCO from vibrational states prepared with substantial bending excitation and a well-known total energy using stimulated Raman excitation locates the origin of the electronically excited state in that molecule. The key is to excite near the origin of S_1 and detect the ^{3}NH product formed following the non-adiabatic transition to and decomposition on T_1. This scheme is particularly useful for detecting molecules excited near the origin of the electronically excited state, which is not accessible from the ground vibrational state, and we have combined our results with those from Reisler and coworkers, who access higher lying levels, to map out the electronic spectroscopy over more than 5000 cm^{-1}. The well-resolved spectra show clear progressions that allow us to assign the N-C stretching vibration (ω_3=1034±11 cm^{-1}), the H-N-C bending vibration (ω_4=1192±19 cm^{-1}), and the N-C-O bending vibration (ω_5=599±7 cm^{-1}) in the excited state. Extrapolating the vibrational progressions to their origins locates the zero-point of the excited state 32,449±20 cm^{-1} above the zero-point of the ground electronic state. *Ab initio* calculations of the energy of the electronically excited state span a range from roughly 30,600 cm^{-1} to 32,970 cm^{-1}.

The experimental measurements have permitted a detailed comparison with theory and have allowed the identification of a promoting mode for internal conversion from S_1 to S_0.

Vibrational Spectroscopy

We have extended our vibrationally mediated photodissociation experiments to molecules cooled in a supersonic expansion in order to simplify the vibrational spectroscopy. The analysis of the vibrational spectroscopy of HNCO molecules cooled in a supersonic expansion, using the photodissociation solely as a detection technique, is particularly informative. We have extracted molecular constants and identified interactions among vibrations in the region of three, four, and five quanta of N-H stretching excitation. The interaction matrix elements we extract agree well with *ab initio* calculations by East, Johnson and Allen [J. Chem. Phys. **98**, 1299 (1993)]. The identification of the states that are mixed into the nominal N-H stretching vibrations is important in understanding controlled photodissociation and non-adiabatic processes in the first excited state of HNCO.

FUTURE DIRECTIONS

The ability to use REMPI detection has allowed us to detect H atoms from the photodissociation methanol (CH_3OH) cooled in an expansion and excited in the region of either three or four quanta of O-H stretching vibration. We have made our first measurements of the kinetic energy of the products. Completing and refining these measurements is the next step with similar dissociation experiments on other molecules and in clusters to follow. We have begun studying the photodissociation of ammonia and explore the influence of vibrational excitation on the non-adiabatic pathways by monitoring the product of ground and electronically excited NH_2.

PUBLICATIONS SINCE 1999 ACKNOWLEDGING DOE SUPPORT

An Experimental and Theoretical Study of the Vibrationally Mediated Photodissociation of Hydroxylamine, David Luckhaus, Jacqueline L. Scott, and F. Fleming Crim, J. Chem. Phys. **110**, 1533 (1999).

Photofragment Energy Distributions and Dissociation Pathways in Dimethyl Sulfoxide. Gail M. Thorson, Christopher M. Cheatum, Martin J. Coffey, and F. Fleming Crim, J. Chem. Phys. **110**, 10843 (1999)

Vibrational Spectroscopy and Intramolecular Energy Transfer in Isocyanic Acid (HNCO) M. J. Coffey, H.L. Berghout, E. Woods III, and F. F. Crim, J. Chem. Phys. **110**, 10850 (1999).

The Electronic Origin and Vibrational Levels of the First Excited Singlet State of Isocyanic Acid (HNCO). H. Laine Berghout, F. Fleming Crim, Mikhail Zyrianov, and Hanna Reisler, J. Chem. Phys. **112**, 6678 (2000).

Controlling the Bimolecular Reaction and Photodissociation of HNCO through Selective Excitation of Perturbed Vibrational States. Ephraim Woods III, H. Laine Berghout, Christopher M. Cheatum, and F. Fleming Crim, J. Phys. Chem. A **104**, 10356 (2000).

Relative Product Yields in the One-Photon and Vibrationally Mediated Photolysis of Isocyanic Acid (HNCO). H. Laine Berghout, Shizuka Hsieh, and F. Fleming Crim, J. Chem. Phys. (*in press*).

INFRARED ABSORPTION SPECTROSCOPY AND CHEMICAL KINETICS OF FREE RADICALS

Robert F. Curl and Graham P. Glass
Department of Chemistry and Rice Quantum Institute
Rice University, Houston, TX 77251
(713)348-4816 (713)348-3285
rfcurl@rice.edu gglass@rice.edu

PROGRAM SCOPE

This research is directed at the detection, monitoring, and study of the chemical kinetic behavior by infrared absorption spectroscopy of small free radical species thought to be important intermediates in combustion. In the last year, work on the reaction between NH_2 and NO_2 and the quantum yield for $O(^1D)$ in the photolysis of NO_2 at 193 nm has been completed and work on the reactions of $O(^1D)$ with acetaldehyde and OH with acetaldehyde has been initiated.

THE REACTION BETWEEN NH_2 AND NO_2

The reaction system produced by 193 nm flash photolysis of a mixture of NH_3 and NO_2 has been investigated experimentally and modeled. The accepted belief that only two channels are of significance for the reaction between NH_2 and NO_2 producing (a) N_2O and H_2O and (b) NH_2O and NO is confirmed by the absence of H_2O_2 absorption signals and the absence of early HNO, as H_2O_2 and HNO are produced by two of the possible five $NH_2 + NO_2$ channels. The fact that the OH concentration extrapolated to the flash is less than the initial NH_2 concentration indicates that the channel producing two OH molecules is not significant. HNO is observed to be produced on a slower time scale than that of the NH_2 + NO reaction and is believed to be formed by the reaction of OH with NH_2O (OH is formed by the reaction of NO_2 with H produced by the flash photolysis of NH_3). NH_2O does not appear to react with NO_2 at 296 on our time scale. Modeling of the reaction system gives a rate for the reaction between NH_2O + OH of $1.8(10)\times10^{-10}$ cm^3sec^{-1}. An excess continued decay of OH at long times after NH_2O has virtually disappeared can be accounted for by reaction of OH with HNO with a rate in the range $(2\text{-}8)\times10^{-11}cm^3sec^{-1}$.

$O(^1D)$ QUANTUM YIELD AT 193 NM

Infrared kinetic spectroscopy has been used to investigate the photo-dissociation of NO_2 at 193 nm. The $O(^1D)/((O(^1D) + O(^3P))$ branching ratio was measured as 0.55± 0.03 by adding a large excess of H_2 to the system, and comparing the amount of NO_2 removed during the photolysis to the amount of OH formed by the subsequent fast reaction between $O(^1D)$ and H_2. The rate constant for the reaction between $O(^1D)$ and NO_2 was measured as (1.5±0.3) x 10^{-10} $cm^{-3}s^{-1}$, and the 193 nm absorption cross section for NO_2 was estimated as (2.9±1.2) x 10^{-19} cm^2.

$O(^1D)$ REACTION WITH ACETALDEHYDE

The rate of the reaction between $O(^1D)$ and CH_3CHO has been determined by competition. N_2O is photolyzed at 193 nm to produce $O(^1D)$ which then reacts with .or is quenched by N_2O and CH_3CHO. Methyl radical is produced by one channel of the reaction with CH_3CHO and is quantitatively measured by observation of the CH stretch of CH_3. The reaction scheme can be written

$$O(^1D) + CH_3CHO \rightarrow CH_3 + X \quad (1a)$$

$$\rightarrow \text{other products} \quad (1b)$$

$$O(^1D) + N_2O \rightarrow \text{products} \quad (2)$$

These reactions are complete within a few μsec; the CH_3 signal rises rapidly within less than 30 μsec and decays quite slowly over more than 1 msec. Thus we can easily measure $[CH_3]_\infty$, the CH_3 concentration after the reactions above are complete. Analysis of the kinetic scheme above with N_2O and CH_3CHO in large excess gives

$$\frac{1}{[CH_3]_\infty} = [O(^1D)]_0\left(k_1/k_{1a} + \frac{k_2[N_2O]}{k_{1a}[CH_3CHO]}\right) \quad (3)$$

Thus plotting $1/[CH_3]_\infty$ vs $1/[CH_3CHO]$ should yield a straight line as shown in Figure 1.

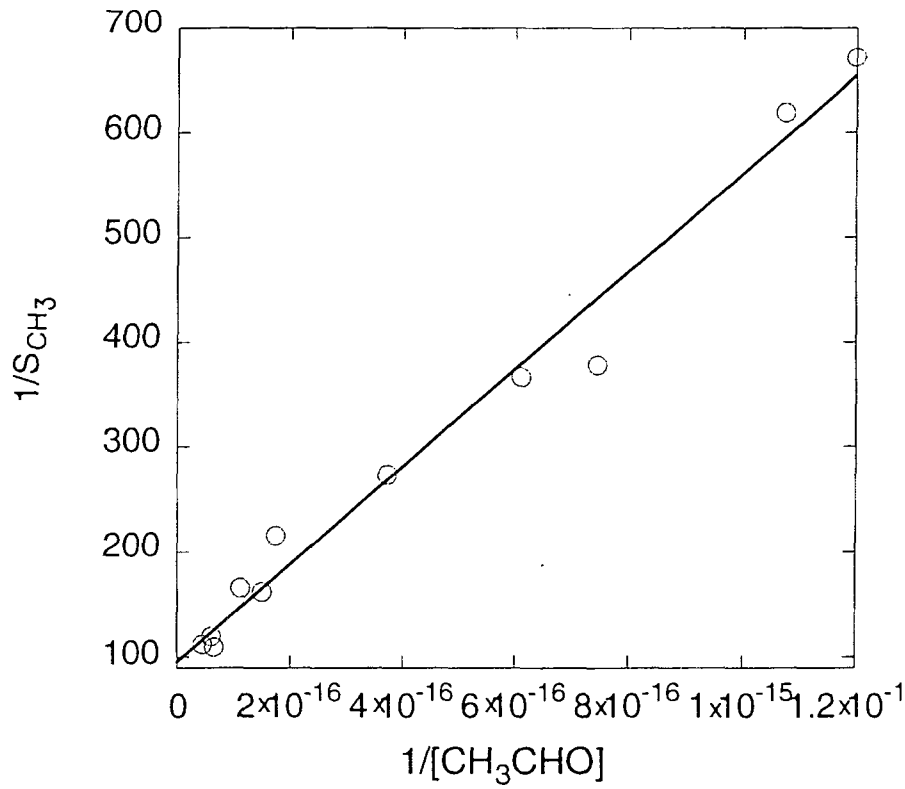

Fig. 1 Reciprocal of integrated intensity measure (peak absorbance (base e) times linewidth) of CH_3 signal at 35 μsec plotted against $1/[CH_3CHO]$.

S_{CH_3} is proportional to $[CH_3]$ ($S_{CH_3} = k[CH_3]$); we could convert S_{CH_3} into $[CH_3]$, but it is not necessary for our purposes. The slope and intercept of the fitted line above can be used to calculate k_1.

$$k_1 = k_2[N_2O]\frac{\text{intercept}}{\text{slope}} \qquad (6)$$

Using the known[1] rate constant for reaction (2) of 1.16×10^{-10} cm^3sec^{-1}, a value for k_1 of $2.1(5) \times 10^{-10}$ is obtained. The reaction between $O(^1D)$ and CH_4 produces only OH + methyl.[2] Therefore the intercept of a plot similar to Fig. 1 of $1/[CH_3]_\infty$ vs $1/[CH_4]$ at the same excimer power and $[N_2O]$ yields as its intercept $k^{-1}[O(^1D)]_0$. The branching ratio into channel (1a) can then be obtained from the ratio of intercepts.

$$k_{1a}/k_1 = \frac{\text{intercept}(CH_4)}{\text{intercept}(CH_3CHO)} = 0.49(10) \qquad (7)$$

.As a check of the procedure for determining k_1, the CH_4 rate constant was measured using the analogue of Fig. 1 giving the result 1.3×10^{-10} cm^3sec^{-1} for the CH_4 reaction with $O(^1D)$, which is in good agreement with the reported[1] value of 1.4×10^{-10} cm^3sec^{-1}.

We have also considered the other channels of the reaction (1) which have been lumped together as (1b). An obvious possibility is an H atom abstraction channel producing OH and either vinoxy or acetoxy radical. OH production is observed, but it is difficult to make a quantitative estimate of the branching ratio into this channel, because the OH signal rises over about 10 μsec and OH reacts rapidly with CH_3CHO disappearing by 20 μsec after the flash. The concentrations are such that $O(^1D)$ should disappear within about a microsecond so that OH is probably being produced either rotationally or vibrationally excited. We do not know how much excited OH has reacted so that modeling the OH signal cannot provide the branching ratio for H atom abstraction. The obvious solution is to reduce the CH_3CHO concentration lengthening the OH lifetime. However, CH_3CHO has to compete with N_2O for $O(^1D)$ and the concentration of N_2O must be kept large because its photolysis produces the $O(^1D)$ and N_2O has a small absorption cross-section at 193 nm. A way to obtain the OH branching ratio is discussed below.

We have begun to study the reaction of OH with acetaldehyde by adding H_2 in excess thereby converting $O(^1D) + H_2$ into OH + H. Very preliminary results indicate that little or no CH_3 is produced by the reaction between OH and acetaldehyde. We plan to continue this study.

FUTURE PLANS

In the short term, our work will be directed towards completing the study of the reaction of $O(^1D)$ with CH_3CHO. Specifically, we shall attempt to measure the branching ratio for production of OH. In order to do this, we intend to use an alternative source of $O(^1D)$; namely, the 248 nm photolysis of ozone. Since the absorption cross section for the photolysis of ozone at 248 nm is approximately an order of magnitude greater than that for photolysis of N_2O at 193 nm, it should be possible to monitor OH production using partial pressures of ozone as low as 10 mtorr. Then it should be possible to reduce the CH_3CHO concentration to a level

that allows the OH lifetime to be lengthened well beyond its vibrational relaxation time.

There are a several other $O(^1D)$ reactions for which we are interested in attempting to determine product branching ratios, specifically the reactions of $O(^1D)$ with formaldehyde, with ethylene, and with acetylene.

We also plan further searches for the NH stretch of NH_2O by increasing the NH_3 and NO_2 concentration levels in the NH_2+NO_2 reaction in order to raise the NH_2O concentration levels

---

[1]R. Atkinson, D. L. Baulch, D. R. A.Cox, R. F. Hampson Jr., J. A. Kerr, M. J. Rossi, J. Troe, *J. Phys. Chem. Ref. Data.* **26** 521 (1997) .

[2]P. H. Wine, A. R. Ravishankara, *Chem. Phys.* **69** 365 (1982)..

Publications

1. "Rotational Analysis of ν_{13} of Allyl Radical," J. D. DeSain and R. F. Curl, *J. Mol. Spectrosc.* **196**, 324-328 (1999).

2. "Kinetics of the Reaction of Propargyl Radical with Nitric Oxide," J. D. DeSain, P.Y. Hung, R. I. Thompson, G. P. Glass, G. Scuseria and R. F. Curl, *J. Phys. Chem. A* **104**, 3356-3363 (2000).

3. "Photolysis of ketene at 193 nm and the rate constant for H+HCCOat 297 K," G.P. Glass, S.S. Kumaran, and J.V. Michael, *J. Phys. Chem. A* **104**,:8360-8367 (2000).

4. "The Photolysis of NO_2 at 193 nm," F. Sun, G. P. Glass, and R. F. Curl, *Chem. Phys. Lett.* **337**, 72-78 (2001).

5. "The reaction of NH_2 with NO_2: the reaction of OH with NH_2O," F. Sun, J. D. DeSain, Graham Scott, P.Y. Hung, R. I. Thompson, G. P. Glass, and R. F. Curl, *J. Phys. Chem. A* (accepted).

Highly Vibrationally Excited Molecules: Energy Transfer and Transient Species Spectroscopy

Hai-Lung Dai
Department of Chemistry, University of Pennsylvania, Philadelphia, PA 19104-6323
email: dai@sas.upenn.edu

I. Program Scope

There are a variety of highly excited molecules in combustion processes. In order to be able to improve the energy efficiency of combustion, it is essential that we understand the energy transfer properties and chemical reactions of these highly excited molecules. It is important to realize that some of the excited species, because of their transient nature have not been characterized in terms of their structure and spectroscopy, which are needed as a basis for the study of their reactions. Presently, our effort concentrates on 1) characterizing the collision energy transfer dynamics of highly excited molecules in general and 2) determining the structure and spectroscopy of transient species in combustion processes.

Experimentally, nanosecond time-resolved Fourier transform emission spectroscopy has been developed and used for probing the energy content as well as the structure of the molecules excited to high internal energies with a laser pulse. In energy transfer studies, the most important discovery is that collision energy transfer from highly vibrationally excited molecules, with energies as high as 150 kcal/mol, is dominated by long range interactions through transition dipoles. Experimental evidence from time-resolved IR emission studies shows that energy loss per collision increases dramatically with the excitation energy and is proportional to the transition dipole of the excited molecule. There appear to be thresholds in the excitation energy that coincide with the origins of intramolecular vibronic coupling, which enhances the transition dipoles. The energy transfer efficiency in V-T collisions also increases with polarizability. Furthermore, relaxation cross section, measured through kinetic quantum beat spectroscopy, of highly excited molecules is found to be much larger than the Lennard-Jones cross section. The long-range interactions become important at high energies because of the relaxation of the resonance condition and the increase of transition dipole, all resulted from strong intramolecular coupling and high level density.

In our effort of characterizing transient molecules, a new approach for detecting the vibrational spectrum of transient species is developed and demonstrated on the vinyl radical, for which after decades of effort only one vibrational mode was experimentally detected previously. Using the new approach we have now detected all its nine vibrational modes. In this approach Photodissociation of carefully chosen precursors at selected photolysis wavelengths produces highly vibrationally excited radicals. IR emission from these radicals is then measured by time-resolved Fourier Transform Spectroscopy with nanosecond time resolution.

II. Transient Species Vibrational Spectroscopy through Time-Resolved Fourier Transform IR Emission

Information on vibrational modes are conventionally obtained through absorption spectroscopy but can in principle be acquired through emission spectroscopy, provided the molecules are produced with excess vibrational energy. Time-Resolved Fourier Transform Emission Spectroscopy (TR FTES) has proven to be a viable method for resolving the emission spectra in calibrated absolute frequencies over a wide frequency range with sufficient frequency and time resolution. We have demonstrated an approach which applies TR FTES to disperse the IR emission of radicals produced in their electronic ground state but with vibrational excitation. This approach is particularly useful for detecting previously unknown vibrational modes of a radical.

The radical species is generated through photodissociation of selected precursor molecules. The precursor and photolysis wavelengths are chosen such that, due to the exothermicity of the reaction, the radical is produced with excess vibrational energy. Time resolution (as fast as 10 ns) allows observation of the nascent emission, as well as evolution of the emission features in time to ensure the assignment of the spectral features to the radical species. A non-reactive quenching gas is used at a pressure much higher than the precursor to promote collision induced vibrational relaxation so the transition frequencies and intensities of the radical can eventually be observed as close as possible to the fundamental transitions. The spectral resolution is expected to be limited by the rotational bandwidth of the molecules, as the molecules have a room temperature rotational state distribution. The resultant spectrum using this approach should reveal all of the IR active modes and serve as a guide for high resolution studies.

This strategy is demonstrated first on the vinyl radical (C_2H_3). Vinyl has been the subject of numerous experimental and theoretical studies. Yet, despite the effort so far, only one electronic ground state vibrational mode has been optically detected while spectroscopy of excited electronic states has been more successful. This may be a result of the dissociative behavior of the first electronic excited state which hindered vibrational spectroscopy through electronic transitions. The only definite identification of a ground state level was performed by Kanamori, Endo and Hirota using an IR diode laser absorption measurement in the region of 820 - 960 cm^{-1} of vinyl produced by photodissociation of vinyl halides.

In our experiments, the vinyl radical was produced by 193 nm photolysis of several precursor molecules which give the common product of vinyl as well as various additional products. The precursor molecules selected were vinyl bromide (VBr), vinyl chloride (VCl), methyl vinyl ketone (MVK) and butadiene (BD). The dissociation reactions of all these precursors are sufficiently exothermic to produce vinyl radical with excess internal energy. Furthermore, at low pressures, the 193 nm dissociation quantum yield for all of the precursor molecules is expected to be close to unity and would not produce excited precursor molecules which may contribute to the emission spectra.Infrared emission spectra from the photodissociation products of the four precursors were detected. To confirm which emission peaks are from vinyl we compare spectra from photodissociation products generated from different precursors. The peaks which are common to each of these spectra are assigned to vinyl. This data represents the first experimental report of the entire set of 9 vibrational mode frequencies and relative intensities, shown in Table 1.

Even without a definite assignment of the observed peaks, comparison with the theoretical calculations summarized in Table 1 generates several noteworthy observations. The most striking

observation is that experimentally the strongest band is the one at 1280 cm^{-1}, with the CH stretching modes at 3000 cm^{-1} only slightly weaker. This is in dire contrast with the theoretical prediction that the higher frequency out-of-plane bend around 900 - 950 cm^{-1} is the strongest by more than one order of magnitude than the rest of the modes. The theoretical calculations put the barrier of the double minimum along the CCH rock coordinate to be between 4.4 and 8.9 kcal/mole. With the internal degrees of freedom excited, the vinyl radical following the dissociation samples the entire energetically accessible coordinate and therefore should have an effective C_{2v} structure. The theoretical estimates reported in Table 1 were, however, calculated for the C_s structure and may not be suitable to compare directly with the experimental observation. Indeed a preliminary *ab initio* calculation shows that when the structure is constrained so that the CCH axis is linear, the higher frequency out-of-plane mode no longer has the strongest intensity while the CH stretching modes are becoming comparable in strength. Moreover, this restriction does not much change the frequencies of the modes. Whether this speculation is correct or not remains to be seen. It is also known that ab initio calculations of open shell systems like radicals still need to be perfected. From the discrepancies found in the observed and calculated frequencies and intensities, it is apparent that more theoretical investigations for radicals, particularly concerning the relationship between the vibrational modes and the rigidity of the structure, are called for.

Table 1

Experimental and theoretical vibrational frequencies (in cm^{-1}) and relative intensities (with the strongest peak set to 100) of the ground electronic state of the vinyl radical (C_2H_3). The experimental intensities shown have been converted from the detected emission intensities in the longer time spectra to the integrated absorption intensities. Uncertainties in the fundamental frequencies are determined by calculating the half width at half maximum of each feature which was fit to a Gaussian function. Assignment of the theoretically calculated normal mode frequencies is noted in the table, however, specific assignment of experimentally observed features remains uncertain.

Experimental		*Calculated (DuPuis et al, '84)*			*Calculated (Mebel et al, '97)*	
ν (cm⁻¹)	*Intensity*			*Normal Mode*	*ν (cm⁻¹)*	*Intensity*
3235 ± 12	7	3265	3.6	αCH stretch	3215	1.4
3164 ± 20	11	3192	23.3	CH_2 asym. stretch	3156	1.4
3103 ± 11	0.5	3116	13.1	CH_2 sym. stretch	3049	1.3
1700 ± 35	0.1	1670	0.6	CC stretch	1609	4.3
1277 ± 20	100	1444	5.4	CH_2 sym. bend	1411	8.5
1099 ± 16	43	1185	11.3	CH_2 asym. + αCH bend	1098	8.9
955 ± 7	32	918	100	CH_2 + CH oop bend	944	100
895 ± 9	11	827	17.1	CH_2 asym. + αCH bend	830	12.9
758 ± 5	93	783	0.9	CH_2 + CH oop bend	764	23.0

III. Future Work

A. The Cyanovinyl and Other Radicals

Knowing the structure and vibrational frequencies of the cyano radicals is essential for a quantitative analysis of the reactivity of the hydrocarbons with nitrogen containing molecules. Because these radicals are difficult to produce in a laboratory setting there have been few experimental studies performed to uncover the structural information. Larger cyano radicals have been even less well studied. Only an ESR study was done on cyanovinyl which suggested that the

structure of the radical changes with increased temperature to the linear CCCN configuration. On the other hand, several theoretical studies have been performed to determine the electronic structure and the minimum energy structure of the cyanovinyl radical. In the experiments proposed here, the cyanovinyl radical will be produced by acrylonitrile photodissociation. The primary dissociation channel is the H elimination, resulting in cyanovinyl. This channel leaves 40 kcal/mole excess energy in the products. Thus, it is highly likely that IR emission of cyanovinyl can be detected.

Other radicals we propose to study include OCCN, difluorovinylidene and vinylidene.

B. Collision Energy Transfer

We will continue to characterize the contribution of long range interactions in the V-T collision energy transfer from highly excited molecules, using the time-resolved FT emission spectroscopy technique. The collision relaxation cross section of a few highly excited molecules over a wide temperature range will be measured by the kinetic quantum beat spectroscopy technique.

IV. Publications from DOE Sponsored Research since 1999

L. Letendre, H.L. Dai, I.A. McLaren, and T.J. Johnson, "Interfacing a Transient Digitizer to a Fourier Transform Spectrometer for Nanosecond Time-Resolved Spectroscopy" *Rev. Sci. Inst.*, 70, 18-22 (1999)

L. Letendre, D.K. Liu, C.D. Pibel, J.B. Halpern, and H.L. Dai, "Structure and Dynamics of Highly Excited Molecules from Time-Resolved FTIR Emission Spectroscopy" *Proceedings of the 12th International Conference on FT Spectroscopy*, eds. K. Itoh and M. Tasumi (Waseda University Press, Tokyo, Japan, 1999), p. 115-8

L. Letendre, D.K. Liu, C.D. Pibel, J.B. Halpern and H.L. Dai, "Vibrational Spectroscopy of a Transient Species through Time-Resolved Fourier Transform Emission Spectroscopy: The Vinyl Radical" *J. Chem. Phys.*, 112, 9209-12 (2000)

D. Qin, G.V. Hartland and H.L. Dai, "V-V Energy Transfer from Highly Vibrationally Excited Molecules through Transition Dipole Coupling: A QuantitativeTest on Energy Transfer from SO_2 to $SF_6(3_1)$" *J. Phys. Chem. A*, 104, 10460-3 (2000)

D. Qin, G.V. Hartland, C.L. Chen and H.L. Dai, "Collisional Deactivation of Highly Vibrationally Excited SO_2 : A Time Resolved Fourier Transform Emission Spectroscopy Study" *Z. Phys. Chem.*, 214, 1501-19 (2000)

D.K. Liu, L. Letendre and H.L. Dai, "193 nm Photolysis of Vinyl Bromide: Nascent Product Disribution of the $C_2H_3Br \rightarrow C_2H_2$ (vinylidene) + HBr Channel" *J. Chem. Phys.*, submitted.

Bimolecular Dynamics of Combustion Reactions

H. Floyd Davis
Department of Chemistry and Chemical Biology
Baker Laboratory, Cornell University, Ithaca, NY 14853-1301
HFD1@Cornell.edu

I. Program Scope:

The aim of this project is to better understand the mechanisms and product energy disposal in bimolecular reactions fundamental to combustion chemistry. Using the crossed molecular beams method, a molecular beam containing highly reactive free radicals is crossed at right angles with a second molecular beam. The angular and velocity distributions of the products from single reactive collisions are measured.

II. Recent Progress:

a. $OH + D_2 \rightarrow HOD + D$ at E_{coll} = 6.6 kcal/mol (Publication 1).

Over the past twenty years, the most detailed studies of chemical reactions have focused on systems containing three atoms such as $D + H_2$ and $F + H_2$.[1] Four-atom reactions present new challenges to experiment and theory, with the dimensionality increasing from three to six. In four-atom reactions, the triatomic reactant or product (if nonlinear) has three independent vibrational degrees of freedom. When a triatomic molecule is produced in a four-atom reaction, it becomes possible to ask not only how much energy is deposited into product vibration, but also how energy is distributed among the product vibrational modes.

The $OH + H_2 \rightarrow H_2O + H$ reaction is of great practical importance because it is the primary source of water in hydrogen combustion. This reaction has become the most important benchmark in the study of four-atom reactions.[1] We have recently carried out an experimental study of the reaction, $OH + D_2 \rightarrow HOD + D$. Comparison is made to three scattering calculations on progressively-newer potential energy surfaces.[2,3,4] OH radicals were produced in their ground vibrational state (v=0) by 193 nm photolysis of HNO_3. Pulsed lasers were used to excite the D atom products to high-lying Rydberg states (n = 40) which evolved spatially through a distance of 29.2 cm to a detector where they were field ionized and collected.[5]

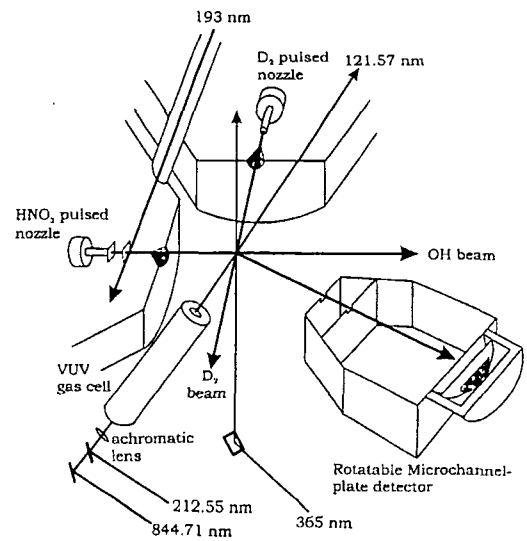

Fig. 1: Experimental Apparatus

As shown in Fig. 2, it was possible to resolve HOD vibrational structure in the D atom time-of-flight (TOF) spectra. From conservation of energy and momentum, the faster and slower peaks correspond to

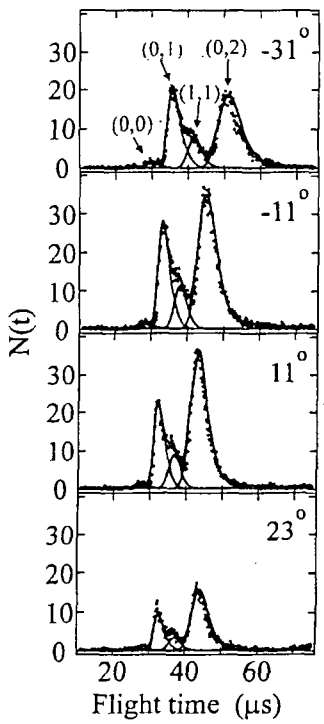

Fig. 2. D atom product time-of-flight spectra at four selected laboratory angles relative to the OH initial velocity vector.

one and two quanta of excitation in the OD local stretching mode, respectively [(0,1) and (0,2)] in HOD. A smaller feature appearing between these peaks corresponds to one quantum of OD stretching and one quantum of HOD bend (1,1). A very small fast contribution indicates a small yield of vibrationless HOD (0,0). This reaction thus exhibits mode-specific behavior in which the newly-formed OD bond is preferentially vibrationally excited. This is consistent with theoretical calculations that indicate that the OD bond is significantly longer in the transition state (1.36 Å) than in the HOD product (0.957Å).[3,4] Relatively little excitation of the bending mode is observed since the transition state HOD angle (97.1°) is only slightly smaller than that of the product (104.5°).

The upper vibrational distribution in Fig. 3 was calculated using the first analytical OH + H_2 potential energy surface by Schatz and Elgersma (SE), published in 1980.[2] The second distribution was from a more recent potential energy surface calculated by Kliesch, Werner, and Clary (KWC).[3] The third calculated vibrational energy distribution was obtained from recent quantum scattering calculations on a new potential energy surface by Ochoa de Aspuru and Clary (OC), generated from a full six-dimensional fit to the same *ab initio* data used for the KWC potential.[4] The good agreement with our experimental measurements demonstrates that quantum theoretical calculations have progressed to the point where it is now possible to accurately predict energy disposal in 4-atom reactions involving six dimensions.

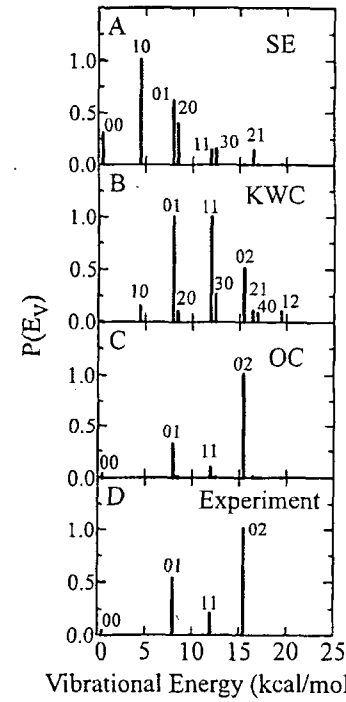

Fig. 3. Comparison of three different theoretical predictions to experimental measurements.

b. Inelastic Scattering of Rydberg H Atoms (Publication 2).

The Rydberg tagging method appeared to be a particularly powerful approach for studying the inelastic scattering of ground state H atoms from small molecules like O_2. Although the reaction H + O_2 → OH + O is generally considered to be *the* most important reaction in combustion chemistry, many features of the reaction remain poorly understood. Since the reaction involves a substantial potential energy barrier, and may proceed via a long-lived HO_2 complex, we expected that nonreactive scattering studies would provide important new insight into the reaction dynamics.

We investigated the inelastic scattering of H + O_2 (and, for comparison, H + N_2) at a collision energy of 1.84 eV. The degree of vibrational inelasticity in the case of O_2 was found to be extraordinarily large. Further tests indicated that we were in fact observing two independent processes: 1) inelastic scattering of ground state H atoms from the target molecules (the process that we intended to study), as well as 2) scattering of high-n Rydberg H atoms from the target

molecules in which the Rydberg atoms remained in high-n states after the collision. By realigning the Rydberg excitation lasers upstream of the collision zone, we were able to study the latter process separately.

In collisions of high-n Rydberg atoms with nonpolar diatomic molecules such as N_2 or O_2, the dominant forces are of relatively short-range, and only become appreciable at distances two orders of magnitude smaller than the H (n = 40) Bohr radius of 848 Å. Since the velocity of a Rydberg H atom with ~2 eV kinetic energy is only a factor of three smaller than the average orbital velocity of the Rydberg electron, the Born-Oppenheimer approximation, which assumes that electrons move rapidly relative to nuclei, does not hold. Consequently, the dynamics of Rydberg atom collisions with atoms and molecules are qualitatively different from those involving ground state or low-lying excited state species. Scattering events involving Rydberg atoms have been described using the free electron model in which electron- target and ion core-target scattering events are treated independently.[6,7] To date, few experiments have focussed on the interactions of the target with the ion core of the Rydberg atom.

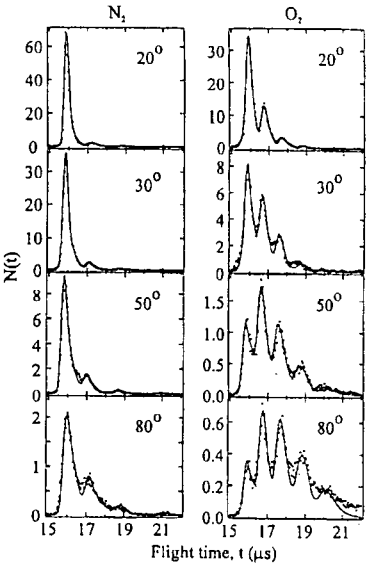

Fig. 4: Rydberg H atom time-of-flight spectra at indicated laboratory angles for N_2 and O_2 collisions at 1.84 eV.

A fast monoenergetic H atom beam was produced by photolysis of hydrogen iodide (HI) at 248 nm. The H atom velocity was either 19,130 m/s or 13,870 m/s; either could be selected by appropriate delay between the photolysis and Rydberg tagging lasers. The H atoms were excited to Rydberg states *before* entering the collision region. Inelastically scattered Rydberg atoms were detected by field ionization as previously described.

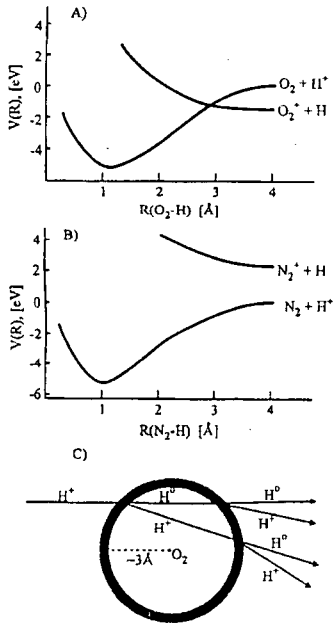

Fig. 5: a) Potential energy curves for HO_2^+. b) Potential energy curves for HN_2^+. c) Four possible trajectories for H^+ scattering from O_2.

Representative TOF spectra are shown in Fig. 4 for N_2 and O_2 scattering at 1.84 eV. In both cases, individual peaks are resolved corresponding to excitation to different vibrational levels in the target molecule. From momentum conservation, the large-angle Rydberg atom deflection observed in this experiment must be due to core-target scattering. The most striking observation is the factor of 4 times more vibrational excitation in O_2 than in N_2. This same trend was seen in experiments by Gianturco *et al.* on the high energy collisions of protons with diatomic molecules and explained by a double charge transfer mechanism.[8,9] In the collision involving O_2, the $H^+ + O_2$ and $H + O_2^+$ crossing region near 3Å is passed twice, each time with the possibility of adiabatic charge transfer, leading to four possible scattering processes. For vibrationally inelastic scattering, charge transfer occurs at *both* crossings. The equilibrium internuclear distance of O_2^+ (1.12Å) is considerably shorter than that of O_2 (1.21Å). Therefore, by accessing the $H + O_2^+$ surface briefly during the collision, a considerable amount of vibrational excitation results. A much smaller amount of vibrational excitation is seen in $H^+ + N_2$ scattering because charge transfer is highly endothermic and cannot occur.

The similarity to proton scattering is further evidence that the free electron model applies to collisions involving the ionic core of a Rydberg atom. For $H^* + O_2$, the H^+ core undergoes two charge transfer events while the Rydberg electron remains a spectator, even when the core has transferred a considerable amount of momentum to O_2 vibrational energy.

III. Future Work:

We have recently reconfigured the apparatus in order to study the reaction $OH + D_2 (v=1) \rightarrow HOD + D$. The D_2 is pumped to a single rotational level of $v = 1$ using stimulated Raman pumping. We will study the reaction at collision energies below the potential energy barrier for the reaction of D_2 ($v = 0$).

In the near future, we also plan to study insertion reactions of singlet methylene ($^1CH_2$) generated by photodissociation of ketene at 308 nm. At Cornell, we will use the Rydberg D atom tagging method to study the simplest 5-atom insertion reaction $^1CH_2 + D_2 \rightarrow CH_2D_2 \rightarrow CH_2D + D$. At endstation 1 at the Advanced Light Source (LBNL), we will use the photolytic $^1CH_2$ source to study the competing pathways from reactions such as $^1CH_2 + H_2O$, which proceed through formation of highly vibrationally excited CH_3OH.

IV. References:

1. P. Casavecchia, *Reports on Progress in Physics.* **63**, 355 (2000).
2. G. C. Schatz, H. Elgersma, *Chem. Phys. Lett.* **73**, 21 (1980).
3. M. Alagia, P. Casavecchia *et al.*, *Chemical Physics* **207**, 389 (1996).
4. a) G. Ochoa de Aspuru, D. C. Clary, *J. Phys. Chem. A* **102**, 9631 (1998).

   b) S. K. Pogrebnya, J. Palma, D. C. Clary, J. Echave, *Phys. Chem. Chem. Phys.* **2**, 693 (2000).
5. a) L. Schnieder *et al.*, *Science* **269**, 207 (1995).

   b) L. Schnieder *et al. J. Chem. Phys.* **107**, 6175 (1997).
6. M. Matsuzawa, in *Rydberg States of Atoms and Molecules*, R. F. Stebbings and F. B. Dunning Eds. (Cambridge University Press, New York, 1983).
7. T.F. Gallagher, *Rydberg Atoms* (Cambridge University Press, Cambridge, 1994).
8. F. A. Gianturco, U. Gierz, and J. P. Toennies, J. Phys B: At. Mol. Phys. **14**, 667 (1981).
9. M. Noll and J. P. Toennies, *J. Chem. Phys.* **85**, 3313 (1986).

V. Publications since 1999:

1. Mode Specific Energy Disposal in the 4-atom reaction $OH + D_2 \rightarrow HOD + D$. B. Strazisar, C. Lin and H.F. Davis, *Science* **290**, 958 (2000).
2. Vibrationally Inelastic Scattering of High-n Rydberg H atoms from N_2 and O_2. B. Strazisar, C. Lin and H.F. Davis, *Physical Review Letters*, in press, April 2001.

Multiple–time–scale kinetics

Michael J. Davis

Chemistry Division
Argonne National Laboratory
Argonne, IL 60439
Email: davis@tcg.anl.gov

Research in this program focuses on three interconnected areas. The first involves the study of intramolecular dynamics, particularly of highly excited systems. The second area involves the use of nonlinear dynamics as a tool for the study of molecular dynamics and complex kinetics. The third area is the study of the classical/quantum correspondence for highly excited systems, particularly systems exhibiting classical chaos.

Recent Progress

Several projects involving nonlinear kinetics were continued or undertaken in the last year. The study of a small master equation describing vibration-to-vibration relaxation was completed and a paper was published in collaboration with Skodje (Boulder). A low–dimensional manifold was uncovered and the asymptotic dynamics was explained in terms of the manifold. The general study of low-dimensional manifolds was also continued in collaboration with Skodje. The existence of low-dimensional manifolds in complex kinetics systems was described in more mathematical terms and a new method for generating low-dimensional manifolds was developed.

This new method is useful because it provides an operational definition for low-dimensional manifolds and it is faster than many other methods we have developed. It is particularly useful because it has a convergence procedure, based on a propagation time. For zero-time propagation it gives the Maas-Pope approximation to manifolds. At long time propagation it converges to the exact manifold. The top panel of the figure demonstrates this. The solid line shows the exact manifold for a simple model system. The model systems is not very stiff and is chosen to accentuate the breakdown of the Maas-Pope approximation, which is generally very good. The highest, dotted line shows the Maas-Pope approximation for the manifold. Three sets of curves show results for our new method. The asterisks which lie on top of the Maas-Pope curve show zero-time propagation. The dashed curve shows short-time propagation and the solid dots on top of the exact manifold show longer time propagation. This final time propagation is much shorter than the long-time motion on the manifold.

The study of the geometry of association-dissociation kinetics was continued in collaboration with Klippenstein (Sandia). The project involves two parts. A detailed study of the association/dissociation kinetics of $CH_3 + CH_3 \leftrightarrow C_2H_6$ described by the phenomenological rate law and Lindemann mechanisms and a less detailed investigation of a full master equation describing the reaction. The second part also involves a new method to extract rate constants from matrix diagonalization in association/dissociation kinetics. A paper has been completed on the first part of the project. Results for this are

shown in the middle two panels of the figure. These panels are for a Lindemann mechanism derived from the master equation results and the conditions of the system are such that the final equilibrium, shown as a large dot on both panels, has a mixture of methyl and ethane. The y-axis describes the fraction of density in methyl and the x-axis the fraction of unexcited ethane. Trajectories (dashed lines) on the left middle panel approach a one-dimensional manifold (solid line) which is nearly linear. The large arrows indicate the direction of the flow into the manifold and the smaller arrows on the manifold describe approach to equilibrium on the manifold. The left middle panel indicates that some trajectories approach equilibrium from the associative side of the manifold and others from the dissociative end. This process can be described by studying the phase space structure of the system, as is done in the middle right panel. The infinite phase space is projected onto a circle and part of the phase space is the basin for the equilibrium point: all trajectories started inside it reach the equilibrium point. This basin, described by the outer curve, can be divided by the dotted line into regions which approach equilibrium along the slow manifold (solid line with arrows) from the associative or associative end.

The nonlinear master equation work has been extended to the study of vibrational relaxation in shock tubes, in collaboration with Kiefer (Illinois, Chicago). Several experiments performed in his laboratory over the years showed evidence for nonlinear relaxation over a few microseconds. Earlier simulations by his group indicated that relaxation appearing to be nonlinear could be observed from a linear master equation with an energy-dependent ΔE_{down}, but good fits to the experiments were not obtained. We have undertaken master equation simulations which have gone beyond their earlier simulations in two important ways. The effect of self-collisions have been included and the temperature dependence of the bath has also been included. Good fits have been obtained for a set of experiments describing the vibrational relaxation of oxirane. Results for experiments on 2%, 3.92%, and pure oxirane have been fit. In the 2% and 3.92% cases ΔE_{down} was assumed to increase linearly with energy. In the pure case, which equilibrates at a much lower temperature, the assumption needed to fit experiments was that ΔE_{down} decreases with temperature exponentially. Results for one of the 3.92% cases are demonstrated in the panel on the lower left. The dots show experimental results and the solid line the master equation simulation. Our results demonstrate that for the more dilute cases, where Kr-oxirane collisions are much more common than oxirane-oxirane collisions, the effect of the self-collisons is much greater. ΔE_{down} in these cases is much larger and there are resonance effects. The asymptotic behavior has been studied and typical trajectories (dashed curves) rapidly reach a one-dimensional manifold (solid curve), as shown in the panel on the bottom right. The experimental initial conditions are shown as a solid dot and the panel indicates that nearly all of the experiment is run on the one-dimensional manifold, that is under quasi-steady state conditions. Further analysis of the conditions are indicated by the dotted curve, which shows the results of a vibrational equilibrium with changing vibrational temperature. This indicates that though the motion on the one-dimensional manifold is close to vibrational equilibrium, it is significantly removed from it.

Future Plans

The low-dimensional manifold work will continue. An increased effort to understand low-dimensional manifold in partial differential equations will be undertaken. The work on association/dissociation kinetics will be completed, as will the study of vibrational relaxation for nonlinear master equations. It is expected that a realistic system combining the elements of the two nonlinear master equation studies will be undertaken. It is also expected that the geometry of the phase space of the chemical species in reactive flows will be studied under realistic conditions.

Publications

C. C. Martens, M. J. Davis, and G. S. Ezra, "Comment on 'Local frequency analysis and the structure of classical phase space of LiNC/LiCN' [J. Chem. Phys. **108**, 63 (1998)].", J. Chem. Phys. **109**, 6507 (1998).

M. J. Davis and R. T. Skodje, "Geometric investigation of low-dimensional manifolds in systems approaching equilibrium", J. Chem. Phys. **111**, 859 (1999).

M. J. Davis and R. T. Skodje, "Geometric approach to multiple-time-scale kinetics: A nonlinear master equation describing vibration-to-vibration relaxation", Z. Phys. Chem. **215**, 233 (2001).

R. T. Skodje and M. J. Davis, "Geometrical simplification of complex kinetic systems", J. Phys. Chem. A. (submitted).

M. J. Davis and S. J. Klippenstein, "Geometric investigation of association/dissociation kinetics", to be submitted

M. J. Davis, "Assignment of highly excited vibrational eigenstates", to be submitted.

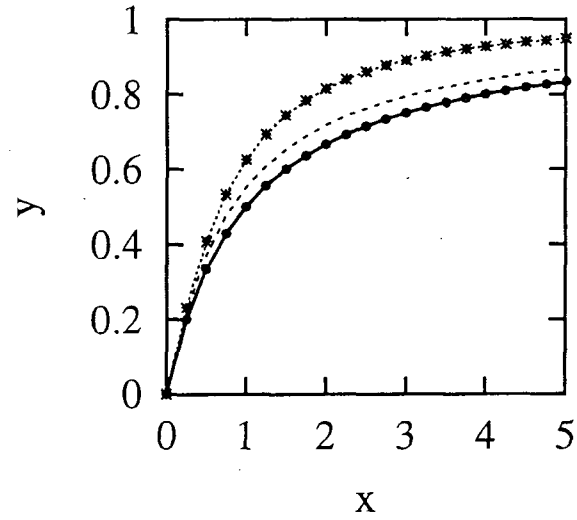

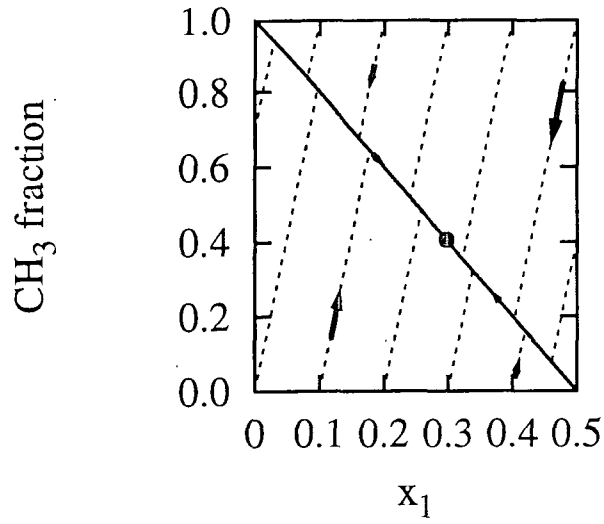

Basin for equilibrium point

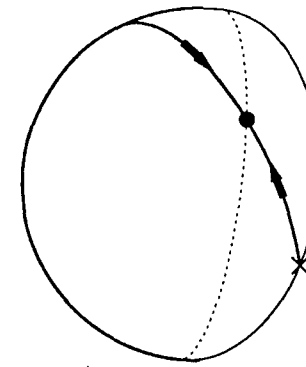

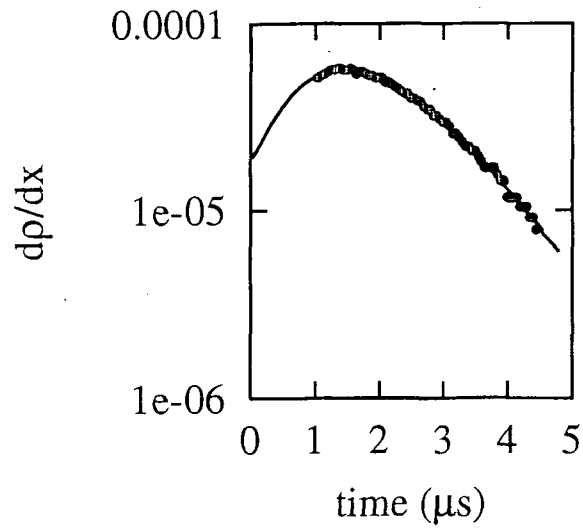

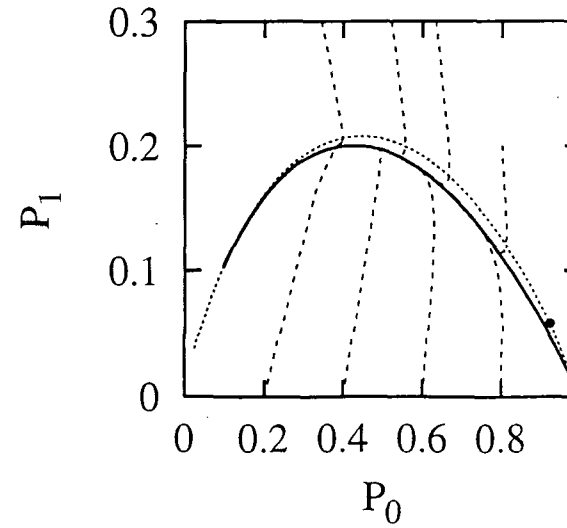

COMPREHENSIVE MECHANISMS FOR COMBUSTION CHEMISTRY: EXPERIMENT, MODELING, AND SENSITIVITY ANALYSIS

Frederick L. Dryer
Department of Mechanical and Aerospace Engineering
Princeton University, Princeton, New Jersey 08544-5263
fldryer@princeton.edu

Grant No. DE-FG02-86ER-13503

Program Scope

The experimental aspects of our work are conducted in a10 cm-diameter flow reactor, at pressures from 0.3 to 20 atm, temperatures from 500 K to 1200 K, and with observed reaction times from 0.5 x 10^{-2} to 2 seconds. Measurements of stable reactant, intermediate, and product species provide a significantly constrained set of kinetic data for elucidating mechanistic behavior, validating detailed kinetic mechanisms, and extracting specific rate constant information. Continuing efforts of this program are: (1) utilizing the perturbations of the H_2/O_2 and CO/H_2O/Oxidant reaction systems by the addition of small amounts of other species to further clarify elementary reaction properties; (2) further elucidating the reaction mechanisms for the pyrolysis and oxidation of small hydrocarbons (alkanes, olefins) and oxygenates (aldehydes, alcohols, and ethers).

Recent Progress

Recent progress, including selected summaries of published works, those in press, those in review for publication and some of the efforts currently underway, are presented below.

1. **J.J. Scire, Jr., F.L. Dryer, and R.A. Yetter, "Comparison of Global and Local Sensitivity Techniques for Rate Constants Determined Using Complex Reaction Mechanisms", Int. J. Chem. Kin., April 2001. (Submitted)**

Last year, we reported new rate constant measurements on three methyl radical reactions,

$$CH_3+HO_2 \rightarrow CH_3O+OH \quad (1)$$
$$CH_3+HO_2 \rightarrow CH_4+O_2 \quad (2)$$
$$CH_3+O_2 \rightarrow CH_2O+OH \quad (3)$$

determined by fitting high-pressure flow reactor experiments on methane-perturbed carbon monoxide oxidation near 1000 K (Scire, et al., Int. J. Chem. Kin., 33:75-100, 2001). A local, first-order sensitivity analysis of the fitted rate constants was used to examine the mechanistic dependence of the results and to determine uncertainty factors from the literature uncertainty factors for the other rate constants in the model. We also briefly described analogous global calculations of sensitivities and error limits that were obtained by importance-sampled Monte Carlo integration. The latter procedure enables efficient determination of rigorous error limits, taking into account the fit quality over the range of unfitted parameter uncertainties. The paper noted above further elaborates on the procedures and, based upon additional analyses, revises the earlier reported results. New results are summarized in Table 1, along with the original fit results and the results of the local analysis. The global analyses result in rigorous error bounds for reaction (3) that are significantly narrower than those estimated by the local method. All three reactions also show significant asymmetry in their error bounds, indicating the importance of higher order sensitivities over the range of parameter uncertainties. In the submitted paper, the global method was also applied to our earlier determination of the low-pressure rate constant for

$$H+O_2 (+N_2) \rightarrow HO_2 (+N_2). \quad (4)$$

(Mueller, et al., Proc. Combust. Instit. 27:177-184, 1998). Subsequent to this publication, Mueller (Mueller, Ph.D. Thesis, Princeton University, 2000) reported minor revisions that include additional rate constant values at seven different temperatures between 817 and 882 K derived from single experiments on hydrogen oxidation perturbed with nitric oxide. Mueller et al. performed a brute force uncertainty analysis on their fit results, varying the locally sensitive reactions over their uncertainty ranges. The uncertainty analysis was recently criticized by Ashman (Ph.D. Thesis, University of Sydney, 1999), who suggested that much larger uncertainties existed. Local and global analyses of Mueller's results give a second example of the global methods described in this paper.

Ashman and Haynes (Proc. Combust. Instit. 27:185-191, 1998) evaluated the low-pressure rate constant for reaction (4) using the same centering factor and high-pressure limit as Mueller, over a range of temperatures from 750 to 900 K. Their data are compared with that of Mueller in Fig. 1. Mueller's points are shown with the error bars calculated using the global method. On average, the points of Ashman and Haynes fall a factor of 1.5 times higher than those of Mueller. Ashman (1999) reports an uncertainty factor of 1.34 for the Ashman and Haynes evaluations. There is sufficient overlap of the error bars such that the two sets of data agree within the combined uncertainties. However, Ashman notes that significantly better agreement is expected because both groups used the same rate constant (the primary source of uncertainty) for the reaction $NO_2+H \rightarrow NO+OH$ in evaluating their measured rates for $H+O_2(+N_2) \rightarrow HO_2(+N_2)$. Ashman dismisses the discrepancies, based upon of his own uncertainty analysis of the Mueller et al. data, concluding that the uncertainties are much higher (~ 1.6) than originally reported. However, the present Monte Carlo calculations further support and rigorously quantify the uncertainty assessments originally reported by Mueller. Further scrutiny of Ashman's uncertainty analysis reveals several flaws. Thus, the discrepancies between the two sets of data for Reaction 4 remain unresolved. In addition to developing rigorous error bounds for Mueller's results, the Monte Carlo calculations also reveal large lower

uncertainty factors for two of Mueller's points. This behavior was traced to strong higher order behavior in the rate constant fits when initial NO levels surpassed the threshold value associated with H atom consumption routes in this system.

2. **J.J. Scire, Jr., S.D. Klotz, F. L. Dryer, "Initial Observations of Ketene in Flow Reactor Kinetic Studies", International Journal of Research in Physical Chemistry and Chemical Physics, August, 2000. (In Press)**

Variable Pressure Flow Reactor (VPFR) experiments were conducted for ethene/methane mixtures utilizing both FTIR analyses of extracted gas samples and *in situ* line-of-sight far-UV absorption measurements. *In situ* observations of ketene prompted the re-evaluation of the presence of ketene in previous acetaldehyde oxidation and pyrolysis experiments in the VPFR. In earlier experiments, only extractive sampling (with FTIR analysis) had been used, and ketene had not been observed. In reconsidering the previously obtained FTIR spectra, ketene is found present in levels on the order of other important acetaldehyde reaction intermediates, such as CH_2O, H_2, and C_2H_4. Through a comparison of the results of the *in situ* and extractive ketene diagnostics, it has been shown that significant losses of ketene can occur in sample handling and that the principal ketene-loss mechanism is surface-dominated. It is likely that this difficulty in ketene sampling, common to many experimental systems, has led to the omission of important ketene pathways in many kinetic models.

3. **J.S. Lee, R.A. Yetter, F.L. Dryer, A.G. Tomboulides, and S.A. Orszag, "Simulation and Analysis of Laminar Flow Reactors", Combust. Sci. Tech. 159:199-212 (2001).**

Laminar flow reactors are frequently used to experimentally study isolated elementary reaction steps or chemical kinetic mechanisms involving many coupled reactions. This classical method is effective in measuring kinetic rate parameters when the effects of mass diffusion and wall surface reactions can be neglected or accurately assessed. We perform a series of two-dimensional direct numerical simulations to investigate issues related to the operation of this classical apparatus. By utilizing a well-established gas-phase kinetic mechanism for moist CO oxidation and a commonly used sub-model for multi-component diffusive transport, we investigate a virtual elementary kinetic experiment. In particular, we extract data from the simulations and evaluate the rate parameters of the reaction $CO+OH \rightarrow CO_2+H$ as one would in an actual experiment. We show that under appropriate operating conditions, the desired elementary reaction rate parameters can be recovered accurately with minimal efforts in analyzing the experimental data. We also demonstrate that two-dimensional simulations can be useful in refining the operating conditions of an experiment to minimize uncertainties in the determined rate parameters. Numerical results confirm that operating conditions that differ from the classical "plug flow" condition yield more accurate results. Finally, we investigate laminar reactor operating conditions typical of those used in the literature to study reacting systems of many coupled elementary reactions. Using the same CO oxidation mechanism as an example, we show that for oxidation experiments conducted at 1atm pressure, the coupling between transport and chemical kinetics results in a highly two-dimensional reacting flow field. Interpreting these results on a one-dimensional basis can lead to significant inaccuracies in the evaluated rate parameters.

4. **H.J. Curran, S.L. Fischer, and F.L. Dryer, "A Flow Reactor Study of Dimethyl Ether. I: High Temperature Pyrolysis and Oxidation", Int. J. Chem. Kin. 32: 713-740 (2000).**

Dimethyl ether pyrolysis was studied in a variable-pressure flow reactor at 2.5 atmospheres and 1118 K. A second, near-pyrolysis experiment was performed in an atmospheric-pressure flow reactor, at 1060 K. In addition, the atmospheric-pressure flow reactor was used to study the oxidation of dimethyl ether at an average temperature of 1086 K, with the equivalence ratio (ϕ) varying from $0.32 < \phi < 3.4$. All experiments were performed with approximately 98 % nitrogen dilution. On-line extraction sampling in conjunction with Fourier Transform Infra-Red, Non-Dispersive Infra-Red (for CO and CO_2), and electrochemical (for O_2) analyses were performed to quantify species at specific locations along the axis of the turbulent flow reactors. Species concentrations were correlated against residence time in the reactor and these species evolution profiles were compared to the predictions of a previously published detailed kinetic mechanism. Some minor changes were made to the model in order to simulate the present experimental data. In addition, this model is able to reproduce the high temperature kinetic data obtained in a jet-stirred reactor (JSR).

5. **H.J. Curran, S.L. Fischer, and F.L. Dryer, "A Flow Reactor Study of Dimethyl Ether. II: Low Temperature Oxidation", Int. J. Chem. Kin. 32:741-759 (2000).**

Dimethyl ether oxidation has been studied in a variable pressure flow reactor over an initial reactor temperature range of 550 to 850 K, in the pressure range 12 to 18 atm, at equivalence ratios of $0.7 < \phi < 4.2$ with nitrogen diluent of approximately 98.5 %. On-line extraction sampling in conjunction with FTIR, NDIR for CO and CO_2, and electrochemical (for O_2) analyses were performed to quantify species at specific locations along the axis of the turbulent flow reactor. Product species concentrations were correlated against residence time (at constant inlet temperature) and against temperature (at fixed mean residence time) in the reactor. Formic acid was observed as a major intermediate of dimethyl ether oxidation at low temperatures. The experimental species evolution profiles were compared to the predictions of a previously published detailed kinetic mechanism (Curran et al., Int. J. Chem. Kin. 30:229-241, 1998). This mechanism did not predict the formation of formic acid. In the current study we have included chemistry leading to formic acid formation (and oxidation). This new chemistry is discussed and is able to reproduce the experimental observations with good accuracy. In addition, this model is

able to reproduce low temperature kinetic data obtained in a jet-stirred reactor (Dagaut et al., Proc. Combust. Instit. 27:361-369, 1998) and the shock tube results of Pfahl et al. (Proc. Combust. Instit. 26:781-789, 1997).

6. Other Recent Work

In addition to the above papers that are in review or have been published, we have made significant progress on several other topics, briefly summarized below.

- **Oxidation and Pyrolysis Study of Ethanol**

New ethanol oxidation and pyrolysis experiments have been performed in both an atmospheric pressure flow reactor (APFR) and a variable pressure flow reactor (VPFR). Prior to this study, literature data on the oxidation of ethanol were mainly restricted to observations near atmospheric pressure. Furthermore, data on the pyrolysis of ethanol at temperatures accessible to flow reactors were not available. Our earlier studies of ethanol oxidation (Norton and Dryer, Int. J. Chem. Kin. 24:319-344, 1992) were performed using gas chromatography to quantify intermediate species profiles. As a result, CH_2O and H_2O, important ethanol oxidation intermediates, were not measured. Additional studies have been performed in the APFR utilized by Norton and Dryer, now using on-line chemical analysis based upon Fourier Transform Infrared (FTIR) detection. The obtained ethanol oxidation data are in good agreement with earlier measurements. However, due to the improvements in the analytical techniques, the present results are more accurate. Additional extensive oxidation and pyrolysis experiments over a range of pressures (3–12 atm), temperatures (800–950 K), and equivalence ratios (0.6–1.4) have also been performed in the VPFR.

Recent modeling efforts reported by Marinov (Int. J. Chem. Kin. 31:183-220, 1999) suggest that ethanol decomposition contributes significantly to the destruction of ethanol, even under oxidative conditions, at the temperatures relevant to the present studies. For a case of ethanol oxidative pyrolysis at 1089 K and 1 atm, Marinov's model predicts the ethanol destruction rate and species profiles for CO, H_2O, CH_4, and CH_2O reasonably well. However, the model poorly predicts the evolution of C_2H_4 and CH_3CHO. More detailed pathway analysis shows that trace oxygen is consumed rapidly within the first 30 ms, and oxygen background does not significantly affect the subsequent pyrolysis of the remaining ethanol. Furthermore, the model predicts that the principle source of C_2H_4 and H_2O during the pyrolysis stage is the molecular decomposition channel, $C_2H_5OH \rightarrow C_2H_4 + H_2O$. Therefore, nearly equal amounts of C_2H_4 and H_2O are expected to be produced during the pyrolysis stage (Fig. 2). The experimental results, on the other hand, show much less than one/one yield of C_2H_4/H_2O. Consequently, mechanism revisions to reproduce the pyrolysis data require investigation of both decomposition and abstraction channels (including branching ratios). New ethanol decomposition kinetic data have emerged recently (Park, Chen, Chen, and Lin, 16th Int. Symp. Gas Kinetics, Cambridge, UK, 2000; Tsang, 2nd Joint Meeting the Combust. Inst., Oakland, CA, 2001), and we are presently developing a new reaction mechanism for ethanol pyrolysis and oxidation.

- **High Pressure Studies on Formaldehyde Oxidation**

Experiments on the high-pressure oxidation of formaldehyde are ongoing. Experimentally, formaldehyde is generated through the decomposition of the formaldehyde trimer, 1,3,5-trioxane. The trioxane is delivered in solution with water. This allows for formaldehyde mole fractions up to 400 ppm and temperatures from 800-1000 K. The lowest temperature is limited by the decomposition rate of the trioxane. Experiments have been conducted at 6 atm and 850 K, in order to isolate the rate constant of

$$CH_2O+HO_2 \rightarrow HCO+H_2O_2. \qquad (5)$$

The importance of reducing the uncertainty in this rate constant was demonstrated in our earlier methyl radical oxidation study (Scire et al., Int. J. Chem. Kin. 33:75-100, 2001).

- **Oxidation Studies on Propene**

Initial studies on the oxidation of propene have been performed in the VPFR. Species profiles were obtained at a temperature of 1040 K and a pressure of 3 atm for lean (φ = 0.7) and stoichiometric conditions. Carbon monoxide, ethene, methane, formaldehyde, acetylene, allene, and methylacetylene were quantitatively detected by FTIR spectrometry. In contrast to previously published work (Davis, et al., Combust. Flame 119:375-399, 1999), on-line continuous sampling enabled FTIR quantification of formaldehyde. The comparison of the new data and the predictions of the most recent model of propene oxidation (Davis et al.) indicates that the overall reaction time predicted by the model is much shorter than the experimental reaction time. Nevertheless, the profiles of major species mole fractions versus the reacted fuel percentage agree reasonably well, with the exception of those for formaldehyde. The minor species profiles, on the other hand, were not well reproduced. Further studies are currently in progress to gather additional data necessary to improve our understanding of propene oxidation kinetics over a wide range of conditions.

Plans

Reaction systems of present interest over the coming year, in addition to those discussed above, include the pyrolyses and oxidations of acetaldehyde, methyl formate, dimethoxy methane, and ethylene.

Publications, 1999 - Present

1. J.J. Scire, Jr., F.L. Dryer, and R.A. Yetter, "Comparison of Global and Local Sensitivity Techniques for Rate Constants Determined Using Complex Reaction Mechanisms", Int. J. Chem. Kin., April 2001 (Submitted).

2. J.J. Scire, Jr., S. D. Klotz, and F.L. Dryer, "Initial Observations of Ketene in Flow Reactor Kinetic Studies", International Journal of Research in Physical Chemistry and Chemical Physics, August 2000, In Press.
3. J.C. Lee, R.A. Yetter, F.L. Dryer, A.G. Tomboulides, and S.A. Orszag, "Simulation and Analysis of Laminar Flow Reactors", Combust. Sci and Tech. 159:199-212 (2000).
4. J.J. Scire, Jr., R.A. Yetter, and F.L. Dryer, "Flow Reactor Studies of Methyl Radical Oxidation Reactions in Methane Perturbed Moist Carbon Monoxide Oxidation at High Pressure with Model Sensitivity Analysis", Int. J. Chem. Kin. 33:75-100 (2000).
5. H.J. Curran, S.L. Fischer, and F.L. Dryer, "A Flow Reactor Study of Dimethyl Ether. I: High Temperature Pyrolysis and Oxidation", Int. J. Chem. Kin. 32:713-740 (2000).
6. H.J. Curran, S.L. Fischer, and F.L. Dryer, "A Flow Reactor Study of Dimethyl Ether. II: Low Temperature Oxidation", Int. J. Chem. Kin. 32:741- 759 (2000).

Presentations

1. T. Carriere, P.R. Westmoreland, A. Kazakov, Y.S. Stein, F.L. Dryer, "Modeling Ethylene Combustion From Low To High Pressure", 2nd Joint Meeting of The U.S. Sections of the Combustion Institute, Oakland, Ca – March 25-28, 2001. Paper No. 89.
2. J. Li, S.D. Klotz, A. Kazakov and F.L. Dryer, "Oxidation and Pyrolysis Experiments of Ethanol in an Atmospheric Pressure Flow Reactor", 28th Symposium (Int.) on Combustion, Edinburgh, Scotland, July 30- August 4, 2000. Work in Progress Poster No. 4-D15, Abstracts of Work in Progress Poster Presentations, The Combustion Institute, Pittsburgh, PA. p.327.
3. Z. Zhao, S.D. Klotz, A. Kazakov, and F.L. Dryer, "Laminar Flame Speed Study of Dimethylether", 28th Symposium (Int.) on Combustion, Edinburgh, Scotland, July 30- August 4, 2000. Work in Progress Poster No. 5-A06, Abtracts of Work in Progress Poster Presentations, The Combustion Institute, Pittsburgh, PA. p.435.

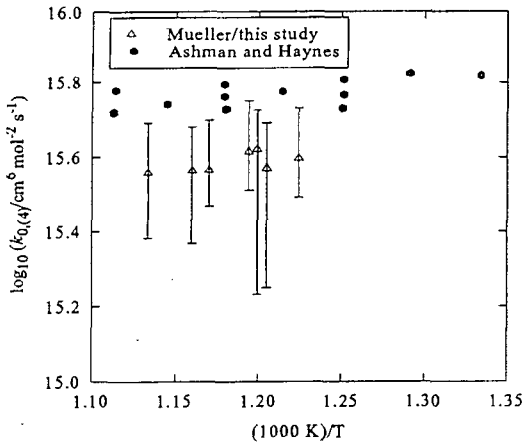

Figure 1 - Arrhenius plot of the Mueller (2000) data for $H+O_2(+N_2)\rightarrow HO_2(+N_2)$ showing the 95% confidence intervals established by Monte Carlo integration. The error bars also include experimental error. Also shown are the data of Ashman and Haynes (Proc. Combust. Instit. 27:185-191, 1998).

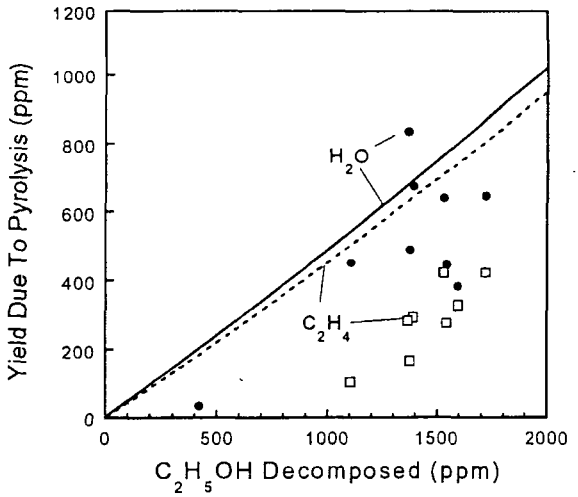

Figure 2 – Production of C_2H_4 and water during pyrolysis of C_2H_5OH (oxidative pyrolysis conditions: T_i = 1089 K, P = 1 atm, and $C_2H_5OH_i$ = 0.545%, background O_2 = 300 ppm). Symbols – experimental data, lines – predictions of Marinov's mechanism.

Table 1 - Comparison of rate constant uncertainty factor estimates for local and Monte Carlo techniques applied to the methyl radical reactions. Numbers in parentheses give 95% confidence intervals for the Monte Carlo results and the bias to sampling error ratio. Best fit rate constants are also given.

Reaction	k (fit) ($cm^3mol^{-1}s^{-1}$)	Uncertainty Factor and Sampling Errors		
		Local	Global Lower (error, bias/error)	Global Upper (error, bias/error)
(1)	$1.48(10)^{13}$	2.24	2.03 (1.08, 0.00)	1.61 (1.08, 0.00)
(2)	$3.16(10)^{12}$	2.89	2.61 (1.16, 0.00)	2.71 (1.09, 0.02)
(3)	$2.36(10)^{8}$	4.23	2.97 (1.13, 0.00)	2.16 (1.09, 0.05)

LASER PHOTOELECTRON SPECTROSCOPY OF IONS

G. Barney Ellison
Department of Chemistry & Biochemistry
University of Colorado
Boulder, CO 80309-0215
Email: **barney@JILA.colorado.edu**

1. Phenyl Radical, C_6H_5

In collaboration with our friends at NREL, we have established an experimental vibrational force field for the Phenyl Radical, C_6H_5 [*J. Am. Chem. Soc.*, **123**, 1977-1988 (2001)]. We measured the infrared absorption spectrum of C_6H_5, $\tilde{X}\ ^2A_1$, in an Ar matrix at 10 K. The experimental frequencies (cm^{-1}) and polarizations follow. a_1 modes: 3086, 3072, 3037, 1581, 1441, 1154, 1027, 997, 976, 605; b_1 modes: 972, 874, 706, 657, 416; b_2 modes: 3071, 3060, 1624, 1432, 1321, 1283, 1159, 1063, and 587. Three different methods have been used for the production of the phenyl radicals. Infrared absorption spectra of five deuterated isotopomers, C_6D_5, *p*-C_6H_4D, *p*-C_6HD_4, *o*-C_6H_4D, and *m*-C_6H_4D, were recorded in order to compare experimental frequency shifts with calculated (UB3LYP/cc-pVDZ) harmonic frequency shifts. The use of CO_2 or NO as internal standards enabled the experimental determination of absolute infrared intensities. The linear dichroism was measured with photooriented samples in order to establish experimental polarizations of each vibrational band. True gas-phase vibrational frequencies were estimated by considering the gas-to-matrix shifts and matrix inhomogeneous line broadening. The phenyl radical matrix frequencies listed above are within ± 1% of the gas phase vibrational frequencies.

2. Allyl Radical, CH_2CHCH_2

With the help of Prof. Barry Carpenter (Cornell) and our friends at NREL, we have established an experimental force field for the allyl radical, CH_2CHCH_2. The manuscript, "Polarized Infrared Absorption Spectrum of Matrix-Isolated Allyl Radicals," was submitted to *J. Phys. Chem. A* by Sreela Nandi Pamela A. Arnold, Barry K. Carpenter, Mark R. Nimlos, David R. Dayton, G. Barney Ellison. We have measured the polarized infrared absorption spectrum of the allyl radical, CH_2CHCH_2 $\tilde{X}\ ^2A_2$, in an argon

matrix at 10 K. The experimental CH_2CHCH_2 frequencies (cm^{-1}) and polarizations follow: a_1 modes — 3109, 3052, 3027, 1478, 1242; b_1 modes — 983, 801, 510; b_2 modes — 3107, 3020, 1464, 1390, and 1182. Two modes (ν_6 and ν_{18}) are very weak and could not be detected; the lowest frequency a_1 mode (the CH_2-CH-CH_2 bending mode, ν_7) is estimated to be beyond the wavelength range of our MCT infrared detector. Infrared absorption spectra of two deuterated isotopomers, CH_2CDCH_2 and CD_2CDCD_2, were recorded in order to compare experimental frequency shifts with calculated [UB3LYP/6-311-G(d,p)] harmonic frequencies. Linear dichroism spectra were measured with photo-oriented samples in order to establish experimental polarizations of most vibrational bands. True gas-phase vibrational frequencies were estimated by considering the gas-to-matrix shifts and matrix inhomogeneous line broadening. The allyl radical matrix frequencies listed above are within ± 1% of the gas phase vibrational frequencies. A final experimental set of all the vibrational frequencies for the allyl radical are recommended.

3. Alkylperoxyl Radicals, CH_3OO and CH_3CH_2OO

In collaboration with Prof. Mitchio Okumura (Caltech) and our friends in Boulder, we have studied the photodetachment spectroscopy and gas phase ion chemistry of the two simplest alkylperoxyl radicals. The manuscript, "Negative Ion Photoelectron Spectroscopy, Gas Phase Acidity, and Thermochemistry of the Peroxyl Radicals CH_3OO and CH_3CH_2OO," was submitted to *J. Am. Chem. Soc.* by Tanya M. Ramond, Stephen J. Blanksby, Gustavo E. Davico, Mark R. Nimlos, Shuji Kato, Veronica M. Bierbaum, W. Carl Lineberger, G. Barney Ellison, and Mitchio Okumura. Methyl, d_3-methyl and ethyl hydroperoxide anions (CH_3OO^-, CD_3OO^- and $CH_3CH_2OO^-$) have been prepared by deprotonation of their respective hydroperoxides in a stream of helium buffer gas. Photodetachment by a 364 nm Ar III (3.408 eV) laser was used to measure the adiabatic electron affinities; $EA[CH_3OO, \tilde{X}\,^2A"] = 1.161 \pm 0.005$ eV, $EA[CD_3OO, \tilde{X}\,^2A"] = 1.154 \pm 0.004$ eV and $EA[CH_3CH_2OO, \tilde{X}\,^2A"] = 1.186 \pm 0.004$ eV. The photoelectron spectra yield values for the term energies: $\Delta E(\tilde{X}\,^2A"\text{-}\tilde{A}\,^2A')[CH_3OO] = 0.914 \pm 0.005$ eV, $\Delta E(\tilde{X}\,^2A"\text{-}\tilde{A}\,^2A')[CD_3OO] = 0.913 \pm 0.004$ eV and $\Delta E\,(^2A"\text{-}\tilde{A}\,^2A')[CH_3CH_2OO] = 0.938 \pm 0.004$ eV. A localized O-O stretching mode was observed at around 1100 cm^{-1} for the

ground state of all three radicals and smaller bending modes are also reported. Proton transfer kinetics of the hydroperoxides have been measured in a tandem flowing afterglow-selected ion flow tube (FA-SIFT) to determine the gas phase acidity of the parent hydroperoxides: $\Delta_{acid}G_{298}(CH_3OOH)$ = 367.8 ± 0.4 kcal mol^{-1}, $\Delta_{acid}G_{298}(CD_3OOH)$ = 368.3 ± 0.4 kcal mol^{-1} and $\Delta_{acid}G_{298}(CH_3CH_2OOH)$ = 363.9 ± 2.0 kcal mol^{-1}. From these acidities we have derived the enthalpies of deprotonation: $\Delta_{acid}H_{298}(CH_3OOH)$ = 374.8 ± 0.5 kcal mol^{-1}, $\Delta_{acid}H_{298}(CD_3OOH)$ = 375.3 ± 0.5 kcal mol^{-1}, and $\Delta_{acid}H_{298}(CH_3CH_2OOH)$ = 371.0 ± 2.1 kcal mol^{-1}. Use of the negative ion acidity/EA cycle provides the ROO-H bond enthalpies, $DH_{298}(CH_3OO\text{-}H)$ = 87.9 ± 0.6 kcal mol^{-1}, $DH_{298}(CD_3OO\text{-}H)$ = 88.3 ± 0.6 kcal mol^{-1} and $DH_{298}(CH_3CH_2OO\text{-}H)$ = 84.8 ± 2.1 kcal mol^{-1}. We review the thermochemistry of the peroxyl radicals, CH_3OO and CH_3CH_2OO. Using experimental bond enthalpies, DH_{298}(ROO-H), and CBS/APNO/CI *ab initio* electronic structure calculations for the energies of the corresponding hydroperoxides, we derive the heats of formation of the peroxyl radicals. The "Electron Affinity/Acidity/CBS" cycle yields $\Delta_fH_{298}[CH_3OO]$ = 4.9 ± 0.9 kcal mol^{-1} and $\Delta_fH_{298}[CH_3CH_2OO]$ = -6.8 ± 2.2 kcal mol^{-1}.

In addition to the ion studies above, we have studied the matrix infrared spectroscopy of the methylperoxyl radical. We have used a tandem pair of supersonic nozzles to produce clean samples of CH_3OO radicals in cryogenic matrices. One hyperthermal nozzle decomposes CH_3NNCH_3 to generate intense pulses of CH_3 radicals while the second nozzle alternately fires a burst of O_2/Ar at the 20 K matrix. The CH_3/O_2 radical sandwich reacts to produce target methylperoxyl radicals. The absorption spectra of the radicals are monitored with a Fourier Transform infrared spectrometer. We report 10 of the 12 infrared bands of the methylperoxyl radical CH_3OO, $\tilde{X}\ ^2A''$, in an argon matrix at 20 K. The experimental frequencies (cm^{-1}) and polarizations follow. The a′ modes: 3032, 2957, 1448, 1410, 1180, 1109, 902, 492 and a″ modes: 3024 and 1434. We do not detect the asymmetric CH_3 rocking mode, ν_{11}, nor the torsion, ν_{12}. The infrared spectra of $CH_3{}^{18}O^{18}O$, $^{13}CH_3OO$, and CD_3OO have been measured as well in order to determine the isotopic shifts. The experimental frequencies, $\{\nu\}_i$, for the methylperoxyl radicals are compared to harmonic frequencies, $\{\omega\}_i$, resulting from an *ab initio* electronic

structure calculation [UB3LYP/6-311G(d,p)]. Linear dichroism spectra were measured with photo-oriented radical samples in order to establish the experimental polarizations of most vibrational bands. True gas-phase vibrational frequencies of the methylperoxyl radicals were estimated by considering the gas-to-matrix shifts and matrix inhomogeneous line broadening. The methylperoxyl radical matrix frequencies listed above are within ± 1% of the gas phase vibrational frequencies.

Publications

- G. Barney Ellison, Adrian F. Tuck, and Veronica Vaida, "Atmospheric Processing of Organic Aerosols," J. Geophys. Res., **104**, 11633-11643 (1999).
- Michael J. Travers, Daniel C. Cowles, Eileen P. Clifford, G. Barney Ellison and Paul C. Engelking, "Photoelectron Spectroscopy of the CH_3N^- Ion," J. Chem. Phys. **111**, 5349-5360 (1999).
- Gregory J. Frost, G. Barney Ellison, and Veronica Vaida, "Organic peroxyl radical photolysis in the near-infrared: Effects on tropospheric chemistry," J. Phys. Chem. A, **103**, 10169-10178 (1999).
- Carl R. Kemnitz, G. Barney Ellison, William L. Karney, and Weston Thatcher Borden, "CASSCF and CASPT2 *Ab Initio* Electronic Structure Calculations Find Singlet Methylnitrene Is an Energy Minimum", J. Am. Chem. Soc. **122**, 1098-1101 (2000).
- Jonathan C. Rienstra-Kiracofe, G. Barney Ellison, Brian C. Hoffman, and Henry F. Schaefer III, "The Electron Affinities of C_3O and C_4O," J. Phys. Chem. A **104**, 2273-2280 (2000).
- A. V. Friderichsen, J. G. Radziszewski, M. R. Nimlos, P. R. Winter, D. C. Dayton, D. E. David and G. B. Ellison, "The Infrared Spectrum of the Matrix-Isolated Phenyl Radical", J. Am. Chem. Soc., **123**, 1977-1988 (2001).

Thermochemistry of Hydrocarbon Radicals: Guided Ion Beam Studies

Kent M. Ervin
Department of Chemistry/216
University of Nevada, Reno
Reno, Nevada 89557
Telephone: 775-784-6676
E-mail: ervin@chem.unr.edu

Project Scope

Gas phase negative ion chemistry methods are employed to determine enthalpies of formation of hydrocarbon radicals that are important in combustion processes. Using guided ion beam tandem mass spectrometry, we measure collisional threshold energies of endoergic proton transfer and hydrogen atom transfer reactions of hydrocarbon molecules with negative reagent ions. The measured reaction threshold energies for proton transfer yield the relative gas phase acidities. In an alternative methodology, competitive collision-induced dissociation of proton-bound ion–molecule complexes provides accurate gas phase acidities relative to a reference acid. Combined with the electron affinity of the R· radical, the gas phase acidity yields the RH bond dissociation energy of the corresponding neutral molecule, or equivalently the enthalpy of formation of the R· organic radical. The threshold energy for hydrogen abstraction from a hydrocarbon molecule yields its hydrogen atom affinity relative to the reagent anion, providing the RH bond dissociation energy directly. Electronic structure calculations are used to evaluate the possibility of potential energy barriers or dynamical constrictions along the reaction path, and as input for RRKM model calculations.

Recent Progress

During the past year of the project, our work on the dynamics of proton transfer reactions of anions has continued.[1,2] Using both bimolecular proton transfer reactions and collision-induced dissociation experiments,[3] we completed experimental measurements of the bond dissociation energies of the polyynes, C_nH_2 (n = 4, 6, 8) and have pursued experiments on polyynyl radicals, C_nH. Extending our work to larger polyatomic systems, we have begun work on polycyclic aromatic hydrocarbons.[4] We also published a major review on experimental techniques in gas phase ion thermochemistry.[5]

Bimolecular endoergic proton transfer. In our previous work translational activation of bimolecular endoergic proton transfer reactions of F^- with H_2O and small alcohols,[6] we found that the vibrational internal energy of the reactants was available to promote reaction, but questioned the role of rotational energy. In work on a more complete set of 17 proton transfer reactions on systems with established gas phase acidities,[2] we have confirmed that rotational

energy is not generally available, possibly due to a dynamic mismatch between slow rotational periods and short collisional interaction times for the reactions with threshold energies greater than 0.5 eV. Also, we observed isolated systems that exhibit high threshold energies, in excess of the reaction endoergicity, despite the absence of an actual potential energy barrier along the reaction path. These effective barriers are attributed to systems that do not form strongly hydrogen-bonded complexes, leading to dynamic constrictions hindering proton transfer between the reactant and product ions. Using these results, we were also able to obtain a refined value for the OH bond dissociation energy of phenol.[2,7]

The applicability of the bimolecular proton transfer method may also be influenced by the presence of competitive reactions. In studies[1,8] on the reaction of $F^- + CH_3Cl$ and the reverse reaction of $Cl^- + CH_3F$, we found different results for proton transfer. In the first system, the proton transfer channel rises at its thermochemical threshold energy despite competition from the fast, exothermic S_N2 reaction. In the reverse reaction, both proton transfer and S_N2 have translational activation energies in excess of their thermochemical endoergicities. We employed ab initio calculations of the multidimensional potential to gain an understanding of these effects. We propose that the fundamental difference is that in the first reaction the two transition states are independent, but in the second reaction the system must pass over the common, restricted S_N2 transition state, followed by competitive dissociation into proton transfer or S_N2 products.

Bond dissociation energies of polyynes. We produce carbon cluster ions, C_n^- and C_nH^- (n = 3–8), which are believed to be linear chains in this size range, with a high voltage dc discharge using a graphite cathode, with hydrogen added in the discharge to make the C_nH^- ions, or with a microwave discharge with acetylene precursor gas. The ions are thermalized in our flow tube reactor source by about 10^5 collisions with the helium and argon buffer gas mixture.

We used the competitive TCID method to measure the gas phase acidities of the polyynes, $C_{2n}H_2$, relative to the known acids, CH_3CHO and H_2S. The proton-bound complex of $C_{2n}H^-$ with acetaldehyde or hydrogen sulfide was prepared in the flow tube ion source. This complex undergoes collision-induced dissociation with xenon target gas to give the two possible proton-transfer products:

$$[HC_{2n}\cdot\cdot H\cdot\cdot X]^- + Xe \rightarrow HC_4^- + HX + Xe$$
$$\rightarrow HC_4H + {}^-X + Xe$$

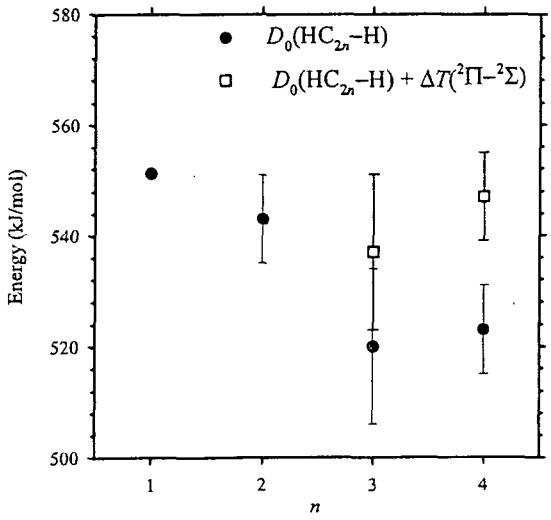

We model the reaction cross sections in the threshold energy region using RRKM theory, which gives the product branching ratio as a function of available energy. Ab initio calculations are used to determine the transition state parameters for the two channels. The experiments yield the gas phase acidities of the polyynes, which can be combined with the electron affinities of the radicals measured by Neumark and coworkers[9] to obtain the preliminary bond

dissociation energies shown in the figure. These values represent the first experimental determinations of the CH bond dissociation energies for diacetylene and longer polyynes.[3,10] Contrary to the assumption of bond additivity rules,[11] HC_6H and HC_8H have CH dissociation energies that are smaller than the known value for aceytlene.[12] This can be attributed to electronic stabilization of the larger radicals, which are known[9] to have $^2\Pi$ ground states rather than the $^2\Sigma$ ground states for C_2H and C_4H.

Energetics of polycyclic aromatic hydrocarbons. Our ion chemistry methods can also examine gas phase acidities of PAHs, but the electron affinities of the corresponding radicals are not generally known. In collaboration with the Lineberger group at the University of Colorado,[4] we have conducted negative ion photoelectron spectroscopy experiments on the naphthyl anion, $C_{10}H_7^-$. Detailed Franck-Condon simulations identify the anion as the isomer resulting from deprotonation of naphthalene at the α site rather than the β site. We obtain $EA_0(\alpha\text{-}C_{10}H_7)$ = 1.403±0.015 eV. Combined with previous measurements of the gas phase acidity of naphthalene, we have obtained a new estimate of the bond dissociation energy, $D_{298}(\alpha\text{-}C_{10}H_7\text{–H})$ = 472±14 kJ/mol. We plan to refine the gas phase acidity with our own experiments, and to extend these experiments to larger PAHs. We also obtained a photoelectron spectrum of coronene anion, $C_{12}H_{24}^-$, with partially resolved vibronic bands.

Future Plans

We will continued pushing our bond energy measurements toward larger polyatomic systems with our work on polyynes and polycyclic aromatic hydrocarbons. In our effort to obtain more precise measurements of the reaction energetics, we are also pursuing measurements of the kinetic energy release of products in proton transfer and hydrogen atom transfer reactions. These experiments will be conducted both on our existing guided ion beam tandem mass spectrometer and using a new quadrupole ion trap/reflectron TOF mass spectrometer that is under construction.

References

(1) Angel, L. A.; Ervin, K. M. *J. Phys. Chem. A* **2001**, (in press).
(2) DeTuri, V. F.; Ervin, K. M. *J. Phys. Chem. A* (submitted for publication).
(3) Shi, Y.; Ervin, K. M. (work in progress).
(4) Ervin, K. M.; Davico, G. E.; Ramond, T. M.; Schwartz, R. L.; Casey, S. M.; Lineberger, W. C. **2001**, (manuscript in preparation).
(5) Ervin, K. M. *Chem. Rev.* **2001**, *101*, 391-444.
(6) DeTuri, V. F.; Su, M. A.; Ervin, K. M. *J. Phys. Chem. A* **1999**, *103*, 1468-1479.
(7) DeTuri, V. F.; Ervin, K. M. *Int. J. Mass Spectrom.* **1998**, *175*, 123-132.
(8) Angel, L. A.; Garcia, S. P.; Ervin, K. M. *J. Phys. Chem. A* **2001**, (manuscript in preparation).
(9) Taylor, T. R.; Xu, C.; Neumark, D. M. *J. Chem. Phys.* **1998**, *108*, 10018-10026.
(10) Shi, Y.; Ervin, K. M. *Chem. Phys. Lett.* **2000**, *318*, 149-154.
(11) Kiefer, J. H.; Sidhu, S. S.; Kern, R. D.; Xie, K.; Chen, H.; Harding, L. B. *Combust. Sci. Tech.* **1992**, *82*, 101-130.
(12) Mordaunt, D. H.; Ashfold, M. N. *J. Chem. Phys.* **1994**, *101*, 2630-2631.

Publications, 1999–present

"Dynamics of endoergic bimolecular proton transfer reactions. F^- + ROH → HF + RO^- ® = H, CH_3, CH_3CH_2, $(CH_3)_2CH$, and $(CH_3)_3C$)", V. F. DeTuri, M. A. Su, and K. M. Ervin, *J. Phys. Chem. A.* **103,** 1468-1479 (1999).

"Orientational effects in the direct Cl^- + CH_3Cl S_N2 reaction at elevated collision energies: Hard-ovoid line-of-centers collision model", K. M. Ervin, *Int. J. Mass Spectrom.* **185/186/187,** 343-350 (1999).

"Gas-phase acidities of alcohols: bimolecular endoergic proton transfer versus CID of proton-bound complexes", V. F. DeTuri and K. M. Ervin, Proceedings of the 47th ASMS Conference on Mass Spectrometry and Allied Topics, Dallas, TX, June 13-17, 1999.

"Competitive threshold collision-induced dissociation: Gas phase acidities and bond dissociation energies for a series of alcohols", V. F. DeTuri and K. M. Ervin, *J. Phys. Chem. A* **103**, 6911-6920 (1999).

"Microcanonical analysis of the kinetic method. The meaning of the 'effective temperature'", K. M. Ervin, *Int. J. Mass Spectrom.* **195/196**, 271-284 (2000).

"Gas phase acidity and C–H bond energy of diacetylene", Y. Shi and K. M. Ervin, *Chem. Phys. Lett.* **318**, 149-154 (2000).

"Collisional activation of the endoergic hydrogen atom transfer reaction $S^-(^2P)$ + H_2 → SH^- + H", K. Rempala and K. M. Ervin, *J. Chem. Phys.* **112**, 4579-4590 (2000).

"Experimental techniques in gas phase ion thermochemistry", K. M. Ervin, *Chem. Rev.* **101**, 391-444 (2001).

"Dynamics of the gas-phase reactions of fluoride ions with chloromethane", L. A. Angel and K. M. Ervin, *J. Phys. Chem. A*, (in press, released on web 4/3/2001)

Low Energy Ion-Molecule Reactions: Gases and Interfaces

James M. Farrar
Department of Chemistry
University of Rochester
Rochester, NY 14627
E-mail: farrar@chem.rochester.edu

Program Scope

This objective of this project is to study the dynamics of the interactions of low energy ions important in combustion with small molecules and with liquid hydrocarbon surfaces. Our program has focused on extending and developing methods and concepts originally advanced to describe very simple atom-diatom reactions to more complex gas phase systems. For gas phase investigations, we have employed crossed molecular beam methods under single collision conditions at collision energies from below one eV to several eV, to probe potential surfaces over a range of distances and interaction energies. The data from such experiments test dynamical models describing chemical reactivity and extend their predictive capabilities in realistic systems, including combustion. We infer intimate details about the nature of collisions leading to chemical reaction by measuring the angular and energy distributions of the reaction products with vibrational state resolution. The project provides detailed information on such concepts as the utilization of specific forms of incident energy, the role of preferred reagent geometries, and the disposal of total reaction energy into product degrees of freedom. With a reasonable level of understanding of the key features that govern simple gas phase systems at low energies, we are now attempting to use these concepts to understand what happens at a gas-liquid interface. In the past two years, we have made a significant transition in the nature of this program as we have begun to apply both the methods and concepts of gas phase dynamics to the study of interactions of low energy ions with liquid hydrocarbon surfaces.

Recent Progress

The primary focus of our program, using the experimental methods developed in our laboratory for crossed beam studies of gas phase reactions, is the very interesting, but relatively unexplored problem of gas-liquid surface interactions and dynamical processes occurring at such interfaces. These processes are important in understanding the degradation of lubricants under harsh conditions, evaporation of multicomponent mixtures such as diesel fuels, the stability of polymers and other hydrocarbon-based materials in adverse environments, and also the heating and fuel evaporation stages of droplet combustion. Conventional wisdom on the subject of fuel droplet combustion[1] suggests that the actual combustion process is homogeneous, occurring in the gas phase. The collisional processes that lead to fuel heating and evaporation at interfaces are poorly known. The most straightforward approach to probing these issues is to direct projectiles at the surface of a hydrocarbon liquid having a very low vapor pressure, such that all collisions are those occurring at the gas-liquid interface. To meet this objective, we have built a rotating disk source modeled on the work of Nathanson

and collaborators[2], in which a polished wheel rotates through a reservoir of the liquid of interest, allowing a film of thickness 100 μ to form. The surface is scraped mechanically just prior to interaction with the ion beam to remove surface contaminants.

Our initial experiments have been conducted with the long chain hydrocarbon squalane, $C_{30}H_{62}$. With a vapor pressure below 10^{-8} torr at room temperature, this liquid surface can be probed without interfering collisions from vapor phase molecules. Ions colliding with the surface have included both anionic species such as O^- and the cations He^+, Ne^+, C^+, CH_3^+, and CF_3^+. We have discovered that at collision energies below 10 eV, a significant fraction of the incident ions undergo "soft landing" and measurable surface charge builds up. Although this phenomenon is potentially quite important because of the possibility of surface modification, we have had to focus attention first on how such interactions shift the electrostatic potential that governs kinetic energy disposal in nonreactive collisions. We have done several experiments as a function of ion deposition rate to understand the evolution of surface charge. The initial experiments, performed at an angle of incidence of 45° with respect to the surface normal, involve measurements of nonreactive scattering distributions. The measurements allow us to assess accommodation of kinetic energy at the droplet surface and probe the nature of direct collisions with surface molecules. Under the ion deposition rates and estimated sticking coefficients of these experiments, surface potentials rise by a maximum of only 0.1 volt during the residence time of ions on the freshly scraped surface. The scattering data show two components: the first consists of a sharp, quasielastic, near-specular feature with an angular width that provides information about thermal roughening. We hope to be able to interpret these data in terms of capillary waves. A lower energy feature with a much weaker angular dependence provides information about the trapping and ultimate desorption of ions that accompanies surface charge buildup. By measuring energy distributions as function of angle, a simple kinematic analysis[3] allows us to calculate the "effective surface" mass. For the system O^- with squalane, this rudimentary calculation yields an effective mass of approximately 40 mass units, suggesting that the incoming ion interacts with the three methyl groups that orient themselves at the surface of the liquid. Such a kinematic analysis is necessary in order to calculate energy transfer in appropriate center of mass coordinates.

Future Plans

We plan to continue these experiments and to supplement their interpretation with molecular dynamics simulations of ion sticking coefficients, and energy and angular distributions of scattered products. We have also begun a series of experiments at collision energies between 50 and 100 eV, with the objective of examining collisional activation of polyatomic ions, expecting to gain insight into specific details of surface energy transfer that leads to dissociation.

Publications, 1999-2001

Susan Troutman Lee and James M. Farrar, "Vibrational State-Resolved Study of the O^- + H_2 Reaction: Isotope Effects on the Product Energy Partitioning", *J. Chem. Phys.* **111**, 7348 (1999).

Susan Troutman Lee, Elizabeth Richards O'Grady, Michael A. Carpenter, and James M. Farrar, "Dynamics of the Reaction of O^- with D_2 at Low Collision Energies: Reagent Rotational Energy Effects", *Phys. Chem. Chem. Phys.*, **2**, 679 (2000).

Susan Troutman Lee and James M. Farrar, "Dynamics of the OH^- + D_2 Isotope Exchange Reaction: Reactive and Nonreactive Decay of the Collision Complex", *J. Chem. Phys.* **1123**, 581 (2000).

References

1. J. Warnatz, U. Maas, and R. W. Dibble, *Combustion* (Springer, Berlin, 1996), pp. 205-09

2. See, for example, M. E. Saecker, S. T. Govoni, D. V. Kowalski, M. E. King, and G. M. Nathanson, *Science*, **252**, 1421 (1991).

3. T. K. Minton, private communication

Picosecond Nonlinear Optical Diagnostics

R.L. Farrow, T.A. Settersten, T.A. Reichardt, and F. Di Teodoro*
Combustion Research Facility, P.O. Box 969, MS 9055
Sandia National Laboratories
Livermore, CA 94551-0969
Telephone: (925)294-3259, email: farrow@ca.sandia.gov

Program Scope

Optical spectroscopic techniques are widely applied as chemically specific probes of gases in combustion and chemical physics research, environmental monitoring, and a variety of other applications. Techniques that provide chemical and thermodynamic information from gaseous flows are often based on molecular spectroscopy, and quantitative interpretation of the data can require a detailed understanding of collisional energy transfer. Energy transfer processes can occur at rates of 10^9 s^{-1} or faster, as in the cases of rotational energy transfer and collisional electronic quenching at atmospheric pressure. We have established a new laboratory equipped with subnanosecond lasers and fast (>1 GHz) detectors to allow direct measurements of these and other fast processes affecting optical diagnostics. Because laser sources with the requisite combination of spectral and temporal characteristics are not available commercially, we have developed tunable visible/uv lasers with 60-100 ps pulse durations and transform-limited linewidths. Two widely tunable, synchronized laser systems are planned for this facility, which is open to visiting researchers. The first experiments in the new laboratory have investigated rotational energy transfer of OH in collisions with Ar, N_2, O_2, and H_2O and electronic quenching of CO in a variety of bath gases at room temperature. Recently we extended the CO quenching studies to higher temperatures (see abstract by Settersten *et al.* in this volume). As summarized below, we have recently investigated the use of picosecond pulses for minimizing the effects of molecular collisions in nonlinear spectroscopic techniques.

Recent Progress

While nanosecond lasers have been used often for nonlinear diagnostic measurements of flame composition, picosecond lasers offer considerable advantages for such techniques. A picosecond laser produces significantly greater peak power for the same pulse energy, potentially improving the signal strength of multiphoton techniques such as degenerate four-wave mixing (DFWM) and polarization spectroscopy (PS). The spectral bandwidth of a transform-limited, 50-150-psec pulsewidth laser is sufficiently narrow to couple effectively with molecular transitions, yet the pulses can resolve most collisional decay times in an atmospheric combustion environments. Excitation with such lasers can be relatively insensitive to the collisional environment because the excitation rate far exceeds the relaxation rates induced by collisions.[1]

Polarization spectroscopy has received attention for measurements of temperature[2] and species concentrations[3] in flames. We have conducted experimental and theoretical investigations to assess the collision-rate dependence of the PS signal generated with picosecond pulses. In the experiments, we probed the $A^2\Sigma^+$-$X^2\Pi$ (0,0) $P_1(2)$ transition of OH in a flow cell with a buffer gas of argon, and monitored the PS signal strength as a function of buffer gas pressure (collision rate). For the theoretical study, we used a perturbative approach to examine the effects of pulse length and Doppler broadening on the collision-rate dependence of the PS signal. Direct numerical integration (DNI) was also used to model strongly saturated signal dependences.

---

*Current address: Division of Optical Sciences, Naval Research Labs, 4555 Overlook Ave. SW, Washington, DC 20375

In the PS experiment, a pump beam and a lower-power probe beam are crossed at the measurement location. The probe beam is passed through two orthogonally oriented linear polarizers positioned on opposite sides of the measurement location. The pump beam is either circularly polarized or linearly polarized 45° with respect to the polarization of the probe beam. When the pump beam is tuned to a resonance of the interaction medium, it induces an optical birefringence, causing the polarization of the probe beam to rotate as it passes through the medium. The PS signal is observed as leakage of the probe beam through the second polarizer.

Figure 1 displays saturation curves acquired by recording single-pulse laser-induced fluorescence (LIF) and PS signal strengths, for various pump energies with the laser tuned to line center. At low pulse energies the LIF and PS signals increase with increasing laser irradiance until the laser radiation significantly populates the upper energy level of the transition, decreasing the efficiency of the signal generation. The LIF and PS signals experience saturation at a pump beam energy of ~1 μJ. At higher energies the LIF signal becomes nearly independent of laser power. However, the PS signal exhibits a plateau between 1 and 3 μJ pump energy, then increases again until finally rolling over near 10 μJ. Similar saturation effects seen in theoretical studies of DFWM using short-pulse lasers were attributed to Rabi beating.[1]

To study the effect of varying collision rates on the PS signal, we tuned the laser through resonance with the isolated OH transition and spectrally integrated the resulting profiles. Fig. 2 shows the integrated signal magnitudes obtained as a function of total gas pressure, for saturating (open circles) and nonsaturating (closed circles) pump pulse energies. The collisional dependence of the former is seen to be significantly lower than the latter; such behavior has also been observed in DFWM of small diatomics.[4] For a variation of a factor of 50 in collision rate, both curves exhibit sublinear dependences, with the saturated PS signals varying only by a factor of 3 and the nonsaturated signals varying by a factor of 18. As shown by the solid curve, a weak-field calculation based on perturbation theory[5] agrees well with the dependence of the nonsaturated measurements. *Most significantly, the theory predicts a much stronger dependence for a 10-ns pulse width,* as shown by the chain-dashed curve. Similarly strong collision-rate dependences have been observed in DFWM with non-saturating, 8-ns laser pulses,[5] where a signal reduction of more than 3 orders of magnitude was observed in NO measurements under similar conditions. These results show that significant reductions in four-wave mixing signal dependences on collision rates are possible using picosecond excitation.

Future Plans

Many species of interest in combustion are not easily detected using LIF or other sensitive, emission-based techniques. Measurements of polyatomic radicals such as CH_3, HO_2, and HCO are of great interest in combustion science, but must usually be performed using line-of-sight absorption methods, restricting studies to two-dimensional flames. In addition, absorption techniques may suffer from poor selectivity, either because of spectral congestion (e.g, in IR spectroscopy) or excessively broad absorption features (UV spectroscopy). We will evaluate the technique of two-color four-wave mixing (FWM) using IR and UV wavelengths. Two intense, pulsed IR beams from a coherent source will be crossed to form a volume intensity grating. When tuned to a molecular absorption line, a corresponding population-difference grating will be generated. This grating will be probed by a UV laser tuned to an electronic transition originating from one of the levels coupled by the IR excitation. The probe beam will resonantly diffract from the associated population grating and will be detected using a photomultiplier tube. This method is attractive for the following reasons:

- the double-resonance condition provides selectivity and spectral simplification even when several species absorb at the IR wavelength, since only one is likely to also absorb at the UV wavelength,
- compared to one-color IR FWM, detection will take advantage of faster, more sensitive UV photodetectors, and
- broad applicability is anticipated from one IR source since many combustion species can be excited in the CH- or OH-stretch region (2.8 – 3.3 μm).

We will also investigate the use of PS to detect the IR-pumped populations. Optical birefringence produced by the IR-pumped states will produce a rotation of the UV probe polarization, resulting in partial transmission of the probe light. Recently we obtained large double resonance signals from OH in a flame using both of these detection methods.

DFWM using picosecond pulses will be investigated for obtaining increased sensitivity in hydrocarbon flames in comparison with nanosecond-pulse DFWM. Evidence indicates that interfering signals from hydrocarbon intermediates originate from thermal-grating scattering, which has a build-up time of several nanoseconds. However, from measurements of DFWM signal decays in flames, we found that (non-thermal-grating) signal generation is complete within 500 ps when excited by <100-ps pulses. We will investigate the use of such pulses at 225 nm to perform DFWM of NO in flames and will compare to our results with nanosecond lasers. If successful, the method will be applied to detection of CH_3 by DFWM, which also suffers from similar interferences in hydrocarbon flames.

References

1. T.A. Reichardt and R.P. Lucht, J. Opt. Soc. Am. B **13**, 2807 (1996).
2. K. Nyholm, Opt. Commun. **111**, 66 (1994).
3. K. Nyholm, R. Maier, C.G. Aminoff, and M. Kaivola, Appl. Opt. **39**, 919 (1993).
4. R.L. Farrow and D.J. Rakestraw, Science **257**, 1894 (1992).
5. Ref. 6 below.

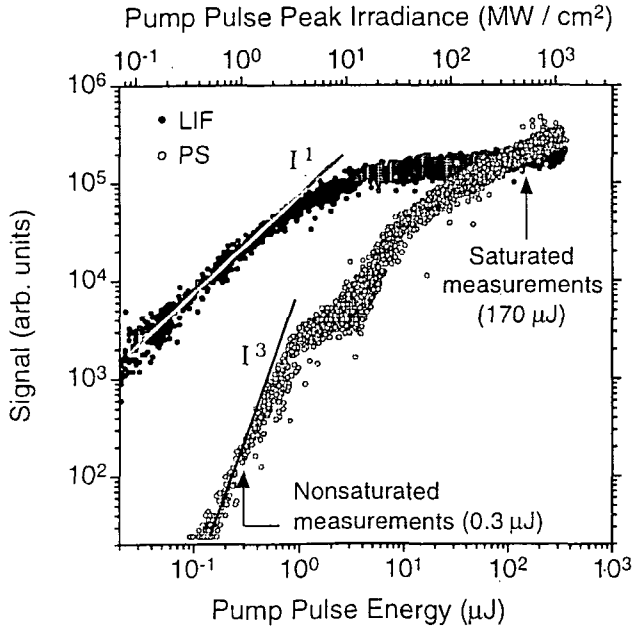

Fig. 1. LIF (closed circles) and PS (open circles) saturation curves of the $P_1(2)$ transition of OH. OH was produced from photolysis of H_2O_2/H_2O vapors. The cell pressure was 103 torr Ar, with 2.6 torr H_2O_2/H_2O. Straight lines indicate expected pulse-irradiance dependences for LIF (I^1) and PS (I^3) in the weak-field limit. Arrows indicate the pump laser energy maintained for the measurements displayed in Fig. 2.

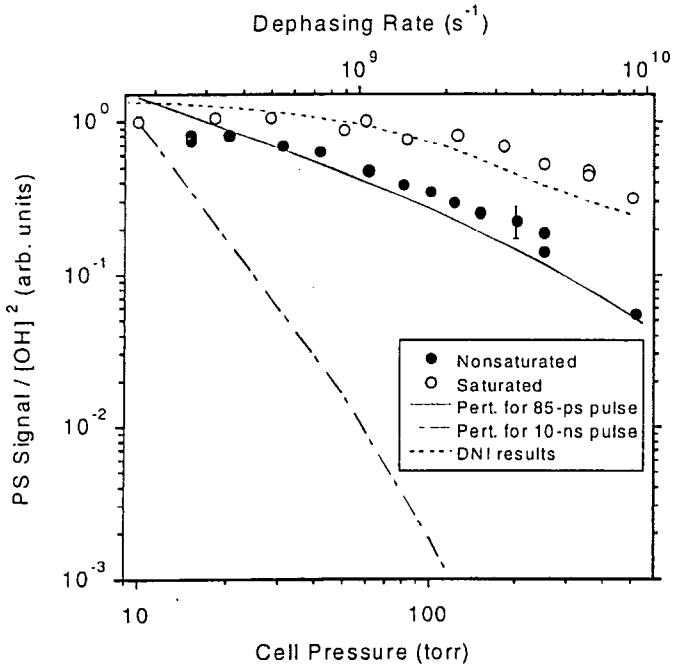

Fig. 2. Spectrally integrated PS signal (normalized by the square of the OH concentration) as a function of cell pressure. Results are shown for both a nonsaturating pump beam and a saturating pump beam. Also included are the results of the theoretical weak-field analysis for an 85-psec pulse and a 10-nsec pulse as well as a DNI simulation[5] including the effects of saturation.

BES-Sponsored Publications, 1999-present

1. D.A.V. Kliner and R.L. Farrow, "Measurements of Ground-State OH Rotational Energy-Transfer Rates," J. Chem. Phys. **110**, 412-422 (1999).
2. R.L. Farrow and D.J. Rakestraw, "Analysis of Degenerate Four-Wave Mixing Spectra of NO in a $CH_4/N_2/O_2$ Flame," Appl. Phys. B, **68**, 741-747 (1999).
3. M.D.Di Rosa and R.L. Farrow, "Cross Sections of Photoionization and Ac Stark Shift Measured from Doppler-free B←X (0,0) Excitation Spectra of CO," J. Opt. Soc. Am. B. **16**, 861-870 (1999).
4. M.D.Di Rosa and R.L. Farrow, "Two-Photon Excitation Cross section of the B←X (0,0) Band of CO Measured by Direct Absorption," J. Opt. Soc. Am. B. **16**, 1988-1994 (1999).
5. P.P. Yaney, D.A.V. Kliner, P.E. Schrader, and R.L. Farrow, "Distributed-Feedback Dye Laser for Picosecond UV and Visible Spectroscopy," Rev. Sci. Instr. **71**, 1296-1305 (2000).
6. T.A. Reichardt, F. Di Teodoro, R.L. Farrow, S. Roy, and R.P. Lucht, "Collisional Dependence of Polarization Spectroscopy with a Picosecond Laser," J. Chem. Phys. **113**, 2263-2269 (2000).
7. F. Di Teodoro, J.E. Rehm, R.L. Farrow, and P.H. Paul, "Collisional Quenching of CO $B\ ^1\Sigma^+$ (v'=0) Probed by Two-photon Laser-induced Fluorescence using a Picosecond Laser," J. Chem. Phys. **113**, 3046-3054 (2000).
8. F. Di Teodoro and R. L. Farrow, "CO^+ $B\ ^2\Sigma^+$ (v=0) Emission Induced by Laser Excitation of Neutral CO at 230 nm," J. Chem. Phys. **114**, 3421-3428, (2001).
9. M. D. Di Rosa and R. L. Farrow, "Temperature-Dependent Collisional Broadening and Shift of Q-branch Transitions in the B←X (0,0) Band of CO Perturbed by N_2, CO_2, and CO," J. Quant. Spectrosc. Radiat. Transfer **68**, 363-375 (2001).
10. T. A. Reichardt, P. E. Schrader, and R. L. Farrow, "Comparison of Gas Temperatures Measured by Coherent anti-Stokes Raman Spectroscopy (CARS) of O_2 and N_2," Appl. Opt. **40**, 741-747, (2001).

Nonlinear Raman spectroscopy of jet-cooled organic radicals and radical complexes

Peter M. Felker
Box 951569, Department of Chemistry, University of California
Los Angeles, CA 90095-1569

Program Scope:

The DoE-sponsored project in this laboratory involves (a) the development of nonlinear spectroscopic methods for use in characterizing the geometries, level structures and dynamics of species in sparse, gaseous samples and (b) the application of such techniques to the study of species, particularly organic free radicals and radical complexes, in cold, molecular beams.

Recent Progress:

In the past year we have advanced in three areas: (1) We have made some progress in the application of mass-selective, ionization-detected stimulated Raman spectroscopy (IDSRS) to the study of organic free radicals. (2) We have continued our development of computational methods aimed toward the dynamically exact calculation of rovibrational level structures in species with large-amplitude motions. (3) We have continued the development of variants of rotational coherence spectroscopy (RCS) that might be put to service in characterizing the geometries of large radicals and radical-containing complexes.

1. Nonlinear Raman spectroscopy of organic free radicals

For numerous years we have been using mass-selective IDSRS to make species-selective measurements of the Raman spectra of molecules and molecular clusters at 0.03 cm^{-1} resolution (e.g., Refs. 1–4). The primary focus of the present DoE project is to extend such measurements to organic radicals and complexes thereof. In this regard we have made some progress, though there is considerably more to do.

First, we have successfully generated cold molecular beams of benzyl radicals by discharge-induced electrolysis of toluene or benzyl chloride in the throat of a pulsed valve. We have detected the radicals by both fluorescence-excitation spectroscopy and mass-selective, resonantly-enhanced two-photon ionization (R2PI) spectroscopy in the vibronic band system of the species near 22,000 cm^{-1}.[5,6] At this stage it appears that this electrolysis mode of radical generation will be suitable for the production of the stable molecular-beam samples required for the application of IDSRS. We are currently experimenting with electrode design and discharge parameters with the aim of achieving this end.

Second, we have made progress in developing IDSRS methods involving two-color R2PI probing. In all of our prior application of IDSRS to closed-shell species the relevant

vibronic level structures allowed for single-color R2PI probing. In the case of benzyl (and many other radicals) such probing is not possible through the lowest-energy accessible vibronic band system, since the relevant single-photon energies are less than half-way to the ionization threshold. In consequence, two-color R2PI probing is required. Unfortunately, the additional probe field complicates the implementation of IDSRS. In order to develop the expertise required to deal with this complication, we have performed IDSRS experiments with two-color probing on closed-shell species such as benzene dimer. The results show that the two-color probe scheme can be just as effective as the single-color one in the measurement of nonlinear Raman spectra.

2. Calculations of rovibrational level structures

In a prior DoE funding period progress was made in this laboratory toward the dynamically exact calculation of intermolecular level structures in weakly bound molecular complexes.[7] Since that work, we have developed computer code applicable to a variety of types of species (atom-molecule, linear molecule-nonlinear molecule, etc.) and to the calculation of other properties (transition moments and rotational energy levels), as well.[8] Calculations employing such code will be relevant to the interpretation of the experimental results that we anticipate obtaining on radical-containing complexes.

3. Rotational coherence spectroscopy

Structural studies of large gaseous species can be difficult or impossible by conventional rotational spectroscopies. However, by measuring the manifestations of free rotational motion in the time domain via rotational coherence spectroscopy (RCS),[9] high resolution rotational information can be obtained on species whose study by frequency-domain rotational methods is not feasible. In the past, the RCS apparatus used in this laboratory, by virtue of the relatively low power output and high repetition rate of the laser system employed, limited the application of RCS to species that could be readily entrained in continuous supersonic beams and that had large vibronic transition dipoles. In an effort to overcome these limitations so that, for example, the geometries of large radical-containing complexes might be studied by RCS, we have been involved in implementing ionization- and fluorescence-detected RCS schemes with a relatively high-power, 20 Hz laser system. Owing in part to the need to construct part of this laser system, its utility thus far has been rather limited.[10] Nevertheless, with the recent acquisition of a wavemeter applicable to pulsed light sources we have largely sorted out the problems that limited that utility. We expect now to be able to apply RCS routinely in structural studies of large radicals and complexes thereof.

Future Work:

Our future work under the auspices of the DoE will be aimed largely toward measuring the ground-state vibrational spectra of organic free radicals involved in combustion systems and of complexes and clusters containing such radicals. These studies in part will involve

pulsed-discharge generation of radicals in supersonic expansions. In addition, we very soon shall set up a thermolysis source of jet-cooled radicals, like the ones employed by the groups of Chen[11] and Ellison,[12] for example. Pending the availability of supplemental funding for an excimer laser, we would also like to set up a photolysis-based radical-beam source. We will focus initial attention on benzyl radical and complexes containing that species. We intend to try first to implement IDSRS with two-color R2PI probing, the first color being tuned to a band in the 22,000 cm^{-1} vibronic system of the species and the second at 266 nm (quadrupled Nd:YAG). Depending on the success, or lack thereof, of these experiments, we may also go to single-color R2PI probing through the vibronic band system near 305 nm. Species targeted for subsequent Raman studies include the allyl,[13] C_4H,[14] and C_6H radicals.[15] The interest will be to characterize the vibrational level structures of these species in spectral regions difficult to access by other means. In regard to the experiments on complexes we hope to help in the effort to characterize the interactions between open-shell species and other molecules via intermolecular vibrational spectroscopy.

In addition to vibrational spectroscopic studies of organic radicals, we also anticipate that RCS experiments on the species, particularly complexes involving aromatic radicals, may well prove useful in characterizing the structures of the species. Such experiments will be undertaken, again with benzyl-containing species likely being the first to be studied. Also in regard to the radical-containing species, we anticipate that dynamically exact intermolecular level-structure calculations will be essential in any attempt to interpret fully experimental results, particularly ones relating to intermolecular Raman transitions and vibrationally averaged geometries. Such calculations will be carried out as the need arises.

References

1. P. M. Felker, P. M. Maxton, and M. W. Schaeffer, Chem. Rev. **94**, 1787 (1994).
2. W. Kim and P. M. Felker, J. Chem. Phys. **107**, 2193 (1997).
3. W. Kim and P. M. Felker, J. Chem. Phys. **108**, 6763 (1998).
4. W. Kim, M. W. Schaeffer, S. Lee, J. S. Chung, and P. M. Felker, J. Chem. Phys. **110**, 11264 (1999).
5. For example, G. C. Eiden and J. C. Weisshaar, J. Chem. Phys. **95**, 6194 (1991).
6. R. Disselkamp and E. R. Bernstein, J. Chem. Phys. **98**, 4339 (1993).
7. W. Kim, D. Neuhauser, M. R. Wall, and P. M. Felker, J. Chem. Phys. **110**, 8461 (1999).
8. For example, P. M. Felker, D. Neuhauser, and W. Kim, J. Chem. Phys. **114**, 1233 (2001). P. M. Felker, J. Chem. Phys. **114**, xxx (2001).
9. For example, P. M. Felker, J. Phys. Chem. **96**, 7845 (1992).
10. P. Benharash, M. J. Gleason, and P. M. Felker, J. Phys. Chem. A **103**, 1442 (1999).
11. D. W. Kohn, H. Clauberg, and P. Chen, Rev. Sci. Instrum. **63**, 4003 (1992).
12. A. V. Friderichsen, J. G. Radziszewski, M. R. Nimlos, P. R. Winter, D. C. Dayton, D. E. David, and G. B. Ellison, J. Am. Chem. Soc. **123**, 1977 (2001).
13. For example, A. D. Sappey and J. C. Weisshaar, J. Phys. Chem. **91**, 3731 (1987).

14. K. Hoshina, H. Kohguchi, Y. Ohshima, and Y. Endo, J. Chem. Phys. **108**, 3465 (1998).
15. M. Kotterer and J. P. Maier, Chem. Phys. Lett. **266**, 342 (1997).

DoE Publications 1999-2001

1. P. Benharash, M. J. Gleason, and P. M. Felker:
"Rotational coherence spectroscopy and structure of naphthalene trimer,"
J. Phys. Chem. A **103**, 1442-1446 (1999).

2. W. Kim, D. Neuhauser, M. R. Wall, and P. M. Felker:
"Six-dimensional calculation of intermolecular states in molecule-large molecule complexes by filter diagonalization: Benzene-H_2O,"
J. Chem. Phys. **110**, 8461-8475 (1999).

3. W. Kim, M. W. Schaeffer, S. Lee, J. S. Chung, and P. M. Felker:
"The intermolecular vibrations of naphthalene trimer by ionization-detected stimulated Raman spectroscopy,"
J. Chem. Phys. **110**, 11264-11276 (1999).

Spectroscopic and Dynamical Studies of Highly Energized Small Polyatomic Molecules

Robert W. Field and Robert J. Silbey
Massachusetts Institute of Technology
Cambridge, MA 02139

Program Definition: Our research program is centered on the development and application of experimental and theoretical methods for studying the dynamics (Intramolecular Vibrational Redistribution and Isomerization) and kinetics of combustion species. Our primary focus is the dynamics of acetylene at internal energies above which acetylene-vinylidene isomerization becomes feasible.

Recent Progress

At MIT we have recorded and analyzed Dispersed Fluorescence (DF) Spectra of $^{12}C_2H_2$, $^{13}C_2H_2$, and $^{12}C_2HD$ isotopomers at $\sim$7 and $\sim$15 cm^{-1} resolution, which corresponds to sampling the dynamics on the S_0 potential energy surface during the first $\sim$ 1ps after a Franck–Condon (FC) pluck of the molecule at $t = 0$. We have also collaborated with Professor Kaoru Yamanouchi's group at the University of Tokyo, where IR–UV double resonance DF spectra of $^{12}C_2H_2$ at $\sim$4 cm^{-1} resolution were recorded. Those spectra sample the slightly longer–time dynamics ($\sim 2ps$) subsequent to different classes of FC plucks on the S_0 surface. The MIT $^{12}C_2H_2$ and $^{13}C_2H_2$ data sets sample exclusively *gerade* levels illuminated by CC stretch and *trans*–bend plucks, whereas the Tokyo data set samples exclusively *ungerade* levels illuminated by FC plucks augmented by excitation of 1 quantum of the FC inactive *cis*–bend (ν_5'') or antisymmetric stretch (ν_3'') vibrational modes. An internally consistent, global analysis has emerged of the *early time* dynamics initiated by large amplitude plucks of the FC active modes.

We have also collaborated with the research group of Professors Kevin Lehmann and Giacinto Scoles at Princeton. Much higher resolution (6×10^{-4} cm^{-1}) IR–Visible double resonance spectra of $^{12}C_2H_2$ and $^{13}C_2H_2$ sample the dynamics of a profoundly different class of initial pluck (mostly CH stretch) for a vastly longer time ($\sim$10 ns). On this longer time scale, the polyad quantum numbers, observed to be conserved on the $\sim$1ps time scale, are completely broken, but two crucial dynamical constraints revealed by the lower resolution DF data sets were shown to survive on the $\sim$10ns time scale: the extreme stability of the local bender motions and the exclusive access of large amplitude local bender plucks to the acetylene$\leftrightarrow$vinylidene transition state. Although the Princeton experiments demonstrate that anharmonic interactions serve to illuminate nearly every symmetry–accessible vibrational state, the small subset of eigenstates with significant amplitude in the vinylidene region of configuration space remain unobservable on the 10ns timescale via the so–far exploited IR–visible–DR plucks. Access to the vinylidene region would have been manifest as permutation splittings in the spectra of $^{13}C_2H_2$.

In order to shed spectroscopic light onto the acetylene$\leftrightarrow$vinylidene transition state, we have been exploiting two complementary approaches to the essential large amplitude local bend initial pluck of the dynamics on the S_0 surface. These two approaches are: (i) careful analysis of anharmonic perturbations in the acetylene S_1 state of the form $3\nu_3'$ (*trans*–bend)$\sim 4\nu_{bend}'$ (torsion and antisymmetric in–plane bend); (ii) the DF spectrum of $^{12}C_2HD$, an inherently local–bender isotopomer. The $4\nu_{bend}'$ perturber has a half–linear structure at its turning points, which closely resemble the turning points for large amplitude local bender motions along the S_0 minimum energy isomerization path. DF spectra of $^{13}C_2H_2$, recorded from an appropriately selected $4\nu_b'$ perturber, will directly illuminate the acetylene$\leftrightarrow$vinylidene transition state. The DF spectra of $^{12}C_2HD$ have been recorded and partially analyzed. The DF spectra of this asymmetric isotopomer cannot be organized using the polyad quantum numbers that were key to the analysis of $^{12}C_2H_2$ and $^{13}C_2H_2$ DF spectra.

Accurate Franck–Condon factor calculations hold the key to extracting useful information from both the $\tilde{A}$–state perturbation–based local–bender DF spectra of $^{13}C_2H_2$ and the extremely complicated and congested DF spectra of $^{12}C_2HD$. (i) $4\nu_b'$–facilitated transition–state spectroscopy. Spectra originating from the $4\nu_b'$ perturber will provide a local–bend–like initial pluck of the dynamics on the S_0 surface. Pure bend polyads will have the form $(n_{left}, n_{right} = N_{bend} - n_{left})$ for the left and right local–benders. The polyad component that best samples the transition state is $(N_{bend}, 0)$ and this component should exhibit the largest permutation splitting. FC calculations will provide relative intensities of the $(N_{bend}, 0), (N_{bend} - 2, 2), (N_{bend} - 4, 4), \ldots$ components. The FC calculations will tell us the spectral signature of the extreme local–bender components of pure bender polyads. This will tell us exactly where to look, with the highest sensitivity and resolution available to us (SEP spectra), for conclusively assignable permutation doublets which in turn will determine the location and energy of the vinylidene zero–point vibrational level. (ii) $^{12}C_2HD$ DF spectroscopy. Both CCH and CCD local bending modes are expected to be FC bright in DF spectra from $^{12}C_2HD$. We see long progressions in the CCD bender but

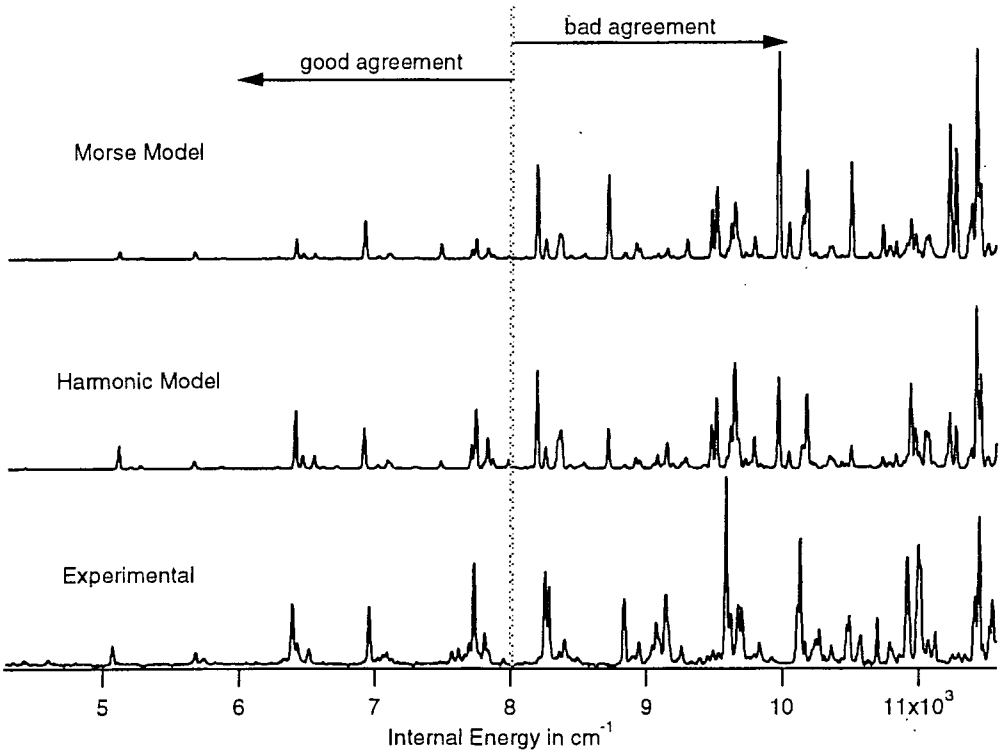

Figure 1: A comparison between predicted and observed Dispersed Fluorescence spectra of $^{12}C_2H_2$. The two different models, Harmonic and Morse, differ in their perspective basis set that is adopted to describe the CC stretching wavefunctions.

hardly any activity in the CCH bender. This implies that the CCH bender is profoundly more IVR active than the CCD bender. Quantitative FC calculations are useful to distinguish between alternative vibrational assignments and to quantify the intensity lost from sharp, regular vibrational progressions owing to rapid IVR.

As Figure 1 describes, our current Franck-Condon calculation has good agreement with the experiment up to around 8000 cm^{-1}. This algorithm uses the local mode basis; and as a first order approximation, we assume a constant transition moment across the entire spectra. The advantage of using the local mode basis for FC calculations is that the local modes in the upper and lower states are only related by an offset: the local-stretching modes are connected by equilibrium bond length differences, and for the local-bending modes, the equilibrium bond angle differences. The disagreement above 8000 cm^{-1} is due to either one of the following reasons:

1. The calculation is wrong.

2. The model is insufficient in that it didn't include the cross anharmonicities or a suitable dependence of the electronic transition moment on the bending coordinate.

3. The fact that the experimental intensity is significantly lower than what is predicted by the FC factors, indicates the possibility of strong IVR above 8000 cm^{-1}.

One major goal is to observe tunnelling splittings in the spectra of $^{13}C_2H_2$ which are indicative of acetylene-vinylidene isomerization. In $^{12}C_2H_2$ one member of each tunnelling doublet has zero statistical weight and consequently will not be present in the spectra. A wealth of information can be gained through the observation of these splittings such as the height and shape of the acetylene $\leftrightarrow$ vinylidene barrier and as well as the locations of vinylidene vibrational levels. DF and LIF spectra of $^{13}C_2H_2$ have been recorded and we are currently analyzing this data set in order to identify ideal pump and probe transitions for planned SEP experiments. Upon comparing the DF spectra of $^{13}C_2H_2$ and $^{12}C_2H_2$ the dynamics in $^{13}C_2H_2$ are noticeably simpler than the dynamics in $^{12}C_2H_2$. At low energy, the DF spectrum of $^{13}C_2H_2$ appears similar to that of $^{12}C_2H_2$. Surprisingly, the DF spectra of $^{13}C_2H_2$ at high energy are simpler than the DF of its counterpart, $^{12}C_2H_2$, implying much simpler dynamics. This simplicity can be qualitatively explained due to a detuning of the 3,245 resonance. There is nearly complete absence of energy flow from the bend modes of $^{13}C_2H_2$ to the stretch modes. The stretch-bend interactions in $^{13}C_2H_2$ are "turned off" because

the anharmonic interaction that is responsible for these interactions in $^{12}C_2H_2$ is detuned from resonance in $^{13}C_2H_2$. The relative simplicity of the dynamics in $^{13}C_2H_2$ is particularly noticeable above 15,000 cm^{-1}. This is beneficial for observing the qualitative changes in the unimolecular dynamics that we expect will be related to isomerization. In $^{12}C_2H_2$, $\omega_3 - (\omega_2 + \omega_4 + \omega_5) \approx 2$ cm^{-1}, which makes the resonance strong and pervasive; in $^{13}C_2H_2$, the energy gap is ≈ 60 cm^{-1}. Consequently, it is reasonable to expect that this resonance has little impact on the short-time dynamics. Thus the detuning of this resonance accounts for part of the simplicity of the $^{13}C_2H_2$ DF spectrum relative to $^{12}C_2H_2$. It is important to note that this does not imply that these resonances cannot play a major role in the dynamics at high energy. It is quite possible that bend-stretch resonances may "tune in" at higher energy. One way to qualitatively check this is to look at how the effective mode frequencies change as v_4 increases. This can be done semi-classically where the classical zero-order frequencies are calculated from our effective Hamiltonian as the partial derivatives of the zero-order energies with respect to each of the quantum numbers. In Figure 2 $\omega_3 - (\omega_2 + \omega_4 + \omega_5)$ is plotted versus quanta of *trans*–bend for a particular polyad. It is evident that the resonance plays a role in $^{12}C_2H_2$ and never really turns on in $^{13}C_2H_2$.

In order to proceed further with SEP experiments to investigate acetylene-vinylidene isomerization, it is necessary to identify "ideal" launch/intermediate states that will have the appropriate local bender character which will result in high Franck -Condon overlap with levels near the transition state in the ground state potential. To this end, we have begun to analyze perturbations evident in the DF and LIF spectra of $4\nu_3'$ in $^{13}C_2H_2$ that may be of use in SEP experiments. In the DF spectra recorded via the $4\nu_3'$ level, the intensity alterations of eigenstates within a fractionation pattern are not identical to that of the fractionation patterns extracted from the spectra of $2\nu_3', \nu_2' + \nu_3', \nu_2' + 2\nu_3'$. As a result, we conclude that the $4\nu_3'$ level must be perturbed and these perturbations give rise to a second class of bright states in our DF spectrum. Typically in our DF experiments the bright state is (0,v_2,0,0,v_4,0) but we postulate that (0,$\bar{v}_2$,0,0,v_4-2,2) levels have their own intrinsic intensity. This is possible if the $4\nu_3'$ level interacts with either ν_4' (cis bend) or ν_6' (torsion) which correlate to the ν_5'' cis bend mode in the ground state. Furthermore by investigating DF spectra originating from several rotational lines of $4\nu_3'$ we can examine how the perturbations evolve with J. DF spectra recorded via Q(0), Q(1), Q(2), Q(2), Q(4), R(0), R(1), R(2), R(3), R(4), exhibit similar fractionation patterns indicating that the perturbation is remote and anharmonic. Anharmonic perturbations of the type described above have been identified in $3\nu_3'$ and it is well established that $3\nu_3'$ interacts with $4\nu_{bend}'$ where $4\nu_{bend}' = 4\nu_4', 2\nu_4' + 2\nu_6', 4\nu_6', 3\nu_4' + 1\nu_6'$, and $1\nu_4' + 3\nu_6'$. Moreover, LIF experiments reveal further evidence of perturbations. For J=8-12 perturbations are obvious in the P and R branches and not in the Q branch. We are currently in the middle of deperturbing and fitting the entire LIF spectrum of the $4\nu_3'$ level.

We have initiated a collaboration with Professor William H. Green (MIT, Dept. of Chemical Engineering) with the goal of investigating some reactions of free radicals involved in combustion chemistry. The radicals are generated by flash photolysis and monitored using ultra-sensitive absorption-based techniques. Many of the spectra of these radicals have been poorly characterized, and some have never been observed in the gas phase. Initial survey scans and kinetic measurements are performed in liquid phase using a commercial kinetic spectrometer (Applied Photophysics) and in gas phase using a Herriott cell apparatus built in the Field group lab. In liquid phase we have recorded absorption spectra of cyclohexadienyl ($C_6H_7^{\bullet}$), which plays a central role in the oxidative and pyrolytic chemistry of aromatics, and figures prominently in many kinetic models of combustion. We have also measured the rate constants of cyclohexadienyl's self-reaction and oxidation. Attempts are now in progress to observed cyclohexadienyl signal in the gas phase apparatus.

Future Directions

Once the analysis of the $^{13}C_2H_2$ LIF spectra and the FC calculations are complete, we will be able to identify ideal candidates for the pump step in SEP experiments such that a local bender "pluck" of S_0 acetylene will induce large amplitude motions directly along the minimum energy isomerization path and directly sample the isomerization transition state. A global H_{eff}, which takes into account all DF data obtained for $^{13}C_2H_2$, will be developed to complement the H_{eff} modeling of the pure-bending polyads completed last year. A new collaboration with Soji Tsuchiya at Japan Women's University will focus on the barrier to linearity and to *cis-trans* isomerization in the S_1 state of acetylene. This collaboration aims to further understanding of IVR in the S_1 state of acetylene through investigating Renner-Teller, Coriolis and anharmonic interactions.

Recent DOE-Supported Publications (Since 1999)

1. M.P. Jacobson, R.J. Silbey, and R.W. Field, "Local Mode Behavior in the Acetylene Bending System," J. Chem. Phys. 110, 845 - 859 (1999).

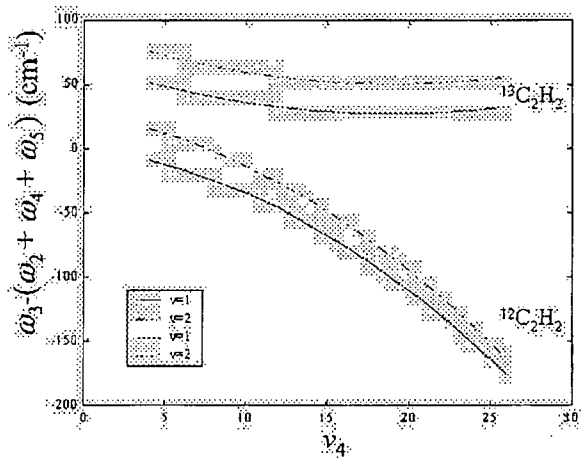

Figure 2: Classical zero-order frequency detuning for the (3,245) resonance in $^{13}C_2H_2$ and $^{12}C_2H_2$ calculated from our effective Hamiltonian model. This figure shows that $^{12}C_2H_2$ should be much more strongly influenced by the (3,245) resonance than $^{13}C_2H_2$.

2. M.P. Jacobson, C. Jung, H.S. Taylor, and R.W. Field, "State-by-State Assignment of the Bending Spectrum of Acetylene at 15,000 cm^{-1}: A Case Study of Quantum-Classical Correspondence," J. Chem. Phys. 111, 600-618 (1999).

3. D.B. Moss, Z. Duan, M.P. Jacobson, J.P. O'Brien, and R.W. Field, "Observation of Coriolis Coupling Between $\nu_2 + 4\nu_4$ and $7\nu_4$ in C_2H_2 by Stimulated Emission Pumping Spectroscopy," J. Mol. Spectrosc. 199, 265-274 (1999).

4. M.P. Jacobson and R.W. Field, "Acetylene at the Threshold of Isomerization," J. Phys. Chem. 104, 3073-3086 (2000).

5. M.P. Jacobson and R.W. Field, "Visualizing IVR: Expectation Values of Resonance Operators," Chem. Phys. Lett. 000, 0000-0000 (2000).

6. H. K. Srivastava, A. Conjusteau, H. Mabuchi, A. Callegari, K.K. Lehmann, G. Scoles, M. L. Silva, and R. W. Field, "Rovibrational spectroscopy of the v=6 manifold in $^{12}C_2H_2$ and $^{13}C_2H_2$," J. C.Phys. 113, 7376-7383 (2000).

7. M.L. Silva, M. P. Jacobson, Z. Duan, and R.W. Field, "Anomalous Simplicity of the Dispersed Fluorescence Spectrum of $^{13}C_2H_2$," J. Mol. Struc. 000, 0000-0000 (2001).

8. M.L. Silva, R. Jongma, R.W. Field, A.M. Wodtke, "The Dynamics of 'Stretched Molecules': Experimental Studies of Highly Vibrationally Excited Molecules with Stimulated Emission Pumping", Annu. Rev. Phys. Chem. 52, 0000-0000 (2001).

9. K.Hoshina, A. Iwasaki, K Yamanouchi, M.P. Jacobson and R.W. Field, "The infrared-ultraviolet dispersed fluorescence spectrum of acetylene: New classes of bright states," J. Phys. Chem. 000, 0000-0000 (2001).

Laser Studies of Chemical Reaction and Collision Processes

George Flynn, Department of Chemistry, Columbia University
Mail Stop 3109, 3000 Broadway, New York, New York 10027
flynn@chem.columbia.edu

Introduction and Overview

Our work involves the study of energy transfer during collisions between molecules. We have focussed our attention on what we believe is the most important energy transfer problem in current studies of chemical and collision dynamics: the collisional cooling of molecules with "chemically significant" amounts of vibrational energy. A molecule with "chemically significant" energy is one that is sufficiently energetic to undergo chemical reaction or bond rupture. Our efforts are aimed at determining both a qualitative and quantitative picture of these collision processes. The qualitative picture constitutes the "mechanism" that controls relaxation for these high energy collision events. By mechanism we mean the quantum state resolved picture of the quenching process, which in turn provides insight into the relative effectiveness of short and long range forces in mediating the energy transfer. The quantitative measure of these collision events is contained in the energy transfer probability distribution function, P(E,E'), which gives the probability for transferring an amount of donor internal energy □E=E-E' during a collision.[1-16] A key result of our efforts over the past few years has been the development of a method to invert our data and obtain directly significant portions of this distribution function. P(E,E') is the *sine qua non* for meaningful comparisons between experimental data and theoretical calculations. Despite its close connection to theoretical descriptions of energy transfer processes, this function is also of enormous practical significance since kinetic models of unimolecular reactions employing master equation techniques require P(E,E') as input. We have had some notable successes in determining both the qualitative, mechanistic energy transfer picture for these high energy collision events and the quantitative shape and magnitude of P(E,E'). These results have left a number of well posed, unanswered questions about energy transfer for molecules with chemically significant amounts of energy that we plan to investigate over the next year. We hope through these experiments to improve our basic understanding of photochemical and photophysical phenomena and to provide dynamical and mechanistic data of fundamental interest for combustion and atmospheric reaction processes.

Our effort to understand and develop a quantum state resolved picture of the quenching of unimolecular reactions is one aspect of the more general field of vibrational energy transfer, the process by which molecules transfer their internal vibrational energy during collisions. The high energy of the quenched species distinguishes the present experimental studies from those vibrationally quantum state resolved investigations involving donors with only a few quanta of internal vibrational energy, carried out in the 1960's and 1970's at the dawn of the laser/energy transfer era. Similarly, the truly remarkable spectral resolution of the present experiments, providing as it does deep physical insight into the quenching process for these high energy molecules, distinguishes these investigations from most of the unimolecular reaction quenching studies carried out from roughly 1925 through 1990.

Experimental Approach

Our success in obtaining new levels of understanding about these high energy collision events has been based on the use of infrared diode lasers to probe the post collision quantum state population distributions of one of the collision partners.[1,12-16] The application of infrared diode lasers to study time-dependent dynamic events was developed in our laboratory under D.O.E. sponsorship. The technique as applied to studies of dynamic molecular processes in our laboratory is by now well established. In brief, in the experimental approach that we are using to study these energy transfer processes, substrates (S) of essentially arbitrary complexity are produced with high energy by laser pumping methods. The collision processes that relax these highly excited S*

molecules are investigated by probing the quantum states of the bath molecules B' produced by the interaction between S* and B. By using relatively simple bath molecules and sophisticated laser probe methods to follow the quantum states of B', the nature of the mechanism for energy loss by S* can be "seen" through the behavior of the (small) energy acceptor molecule, B. To fully analyze the deactivation process for such highly vibrationally excited molecules as S*, however, the level of excitation, rotational profiles and translational recoils of *different* vibrational modes of the bath acceptor B' are required. Furthermore, the amount of energy transferred to the rotational and translational degrees of freedom of the *ground* (vibrationless) state of the bath molecules is also of interest. Our technique is capable of supplying all of this extremely valuable information.

Results

The present molecular system that we are studying consists of highly excited pyrazine donor molecules, which have about 5 eV of internal vibrational energy, colliding with cold (room temperaure) CO molecules. In these kinds of experiments, CO is a particularly appealing bath acceptor for a number of reasons. First, the relatively large rotational constant (B=1.92 cm^{-1}) causes the rotational state population distribution to be localized in a relatively small number of low J states. (The peak of the rotational distribution occurs in J=7 at room temperature and few molecules are found in J states above 20.) This reduces the uncertainty in measured values of the angular momentum change, □J, due to collisions, since the initial rotational state angular momentum of the CO is better defined than in a thermal sample of heavier molecules. Second, the relatively short bond length of the CO allows us to test a number of issues concerning the influence of molecular shape and dimension on the energy transfer process. Third, the transition moment for the CO (v=0→1) vibrational transition is relatively small, especially compared to the CO_2 molecule, a bath species that we have studied extensively. This transition moment is likely to be the controlling factor determining the energy transfer efficiency between highly excited donors such as pyrazine and room temperature CO for those collisions that produce vibrationally excited CO (v=1) in a vibration-vibration energy transfer process such as:

$$C_4N_2H_4^{(E)} + CO\ (v=0;\ J') \rightarrow C_4N_2H_4^{(E-\square E)} + CO\ (v=1;J)\ [V\text{-}V\ Transfer]\ [1]$$

Probing Angular Momentum Constraints

There are two kinds of angular momentum constraints for which we have clear evidence in our experiments to date. These include constraints for both impulsive collisions and constraints for soft collisions mediated by long range forces.

For processes such as [1] above, which produce vibrationally excited CO (v=1), we find that the dominant channels are those with J'-J=□J=±1, reminiscent of energy transfer by a long range, soft collision mechanism, mediated by the CO (v=0→1) transition moment. Qualitatively, the probability for excitation of the v=1 vibrationally excited state is much lower than the probability for excitation of the analogous state in CO_2 ($00^0 1$) in collisions with highly excited pyrazine. While further experiments are under way to quantify the CO (v=1) excitation probability, the qualitative results so far are consistent with the fact that the transition moment for the CO_2 ($00^0 0 \rightarrow 00^0 1$) transition is 10 times larger than that for CO (v=0→1).

The picture for collisions that leave CO in the v=0 state but cause a change in angular momentum J is completely different. This process can be described by the equation:

$$C_4N_2H_4^{(E)} + CO\ (v=0;\ J',V') \rightarrow C_4N_2H_4^{(E-\square E)} + CO\ (v=0;J,V)\ [Quench]\ [2]$$

V is CO velocity. Here J'-J = □J>>±1, and the line width for transitions such as CO (v=0;J→v=1;J±1) is found to be well above room temperature, indicating that the CO (v=0;J,V) produced by equation [2] is

translationally hot. These are characteristics of hard, impulsive collisions in which the CO directly strikes one of the vibrating atoms on the highly excited pyrazine. In these impulsive collisions we find a direct, linear correlation between the velocity recoil of a CO bath molecule and its rotational angular momentum quantum number. The maximum final J state observed in these experiments is roughly 40. In contrast for similar experiments involving CO_2 as a bath acceptor molecule, the maximum final J is roughly 80! Part of this difference is due to the larger mean initial (thermal) J for the CO_2, but the lion's share of the difference is actually due to the fact that CO is only about half as long as CO_2.

P(E,E') Distributions

We have also obtained a preliminary P(E,E') energy transfer distribution function for hot pyrazine/CO collisions. When compared to similar distributions for hot pyrazine/CO_2 encounters at the same collision energy, the value of P(E,E') at large □E=E-E' is smaller for the CO partner than for CO_2. In both cases P(E,E') can be fit reasonably well by a double exponential function of the form:

P(E,E')/N=(1-f)exp[-□E/□$_1$] + (f)exp[-□E/□$_□$], with f<<1 and □$_□$>>□$_1$. The second exponential is generally referred to as the "supercollision" tail of P(E,E').

Present and Future Experimental Program

We plan to continue to use the high resolution, high speed infrared diode laser probe technique to determine final vibrational, rotational, and translational energy distributions for bath product species formed as the result of a collision event. In particular quantum state and velocity distributions will be determined for acetylene and for hydrogen halide molecules recoiling from high energy donor molecules such as 1-phenylpyrrole and pyrazine containing chemically significant amounts of vibrational energy (4-6 eV). 1-phenylpyrrole is a particularly appealing donor molecule because its broad absorption bands throughout the near ultraviolet spectral region provide an opportunity to study collision events with very different initial energies, thereby obtaining P(E,E') distributions for different initial donor energies, E. Model trajectory calculations have been started and already have produced preliminary, interesting results. These will be continued in order to determine the dependence of the shape and magnitude of the energy transfer distribution function, P(E,E'), on initial collision excitation energy, E, on angular momentum, and on the initial quantum state of the bath molecule.

References

1. C. A. Michaels and G. W. Flynn, J. Chem. Phys. 106, 3558 (1997)
2. I. Oref and D.C. Tardy, Chem. Rev. 90, 1407 (1990)
3. J. R. Barker, J. D. Brenner, and B. M. Toselli, Advances in Chemical Kinetics and Dynamics, 2B, 393-425 (1995); John Barker, Ed.; JAI Press Inc., Greenwich, CT
4. I. Oref, Advances in Chemical Kinetics and Dynamics, 2B, 285-298 (1995); John Barker, Ed.; JAI Press Inc., Greenwich, CT
5. F. A. Lindemann, *Trans. Faraday Soc.*, 1922, 17, 598.
6. D. C. Tardy and B. S. Rabinovitch , Chem. Rev. 77, 369(1977)
7. J. Troe, J. Chem. Phys. 66, 4745 (1977).
8. T. Lenzer, K. Luther, J. Troe, R. G. Gilbert, and K. F. Lim, J. Chem. Phys. 103, 626 (1995).
9. J. Troe, J. Chem. Phys. 97, 288 (1992).
10. V. Bernshtein and I. Oref, J. Phys. Chem. 97, 12811 (1993).
11. J. R. Barker, J. Phys. Chem., 96, 7361(1992); J. D. Brenner, J. P. Erinjeri, and J. R. Barker, Chem. Phys. 175, 99 (1993).
12. Chris A. Michaels, Amy S. Mullin, Jeunghee Park, James Z. Chou, and George W. Flynn, J. Chem. Phys., 108, 2744-2755 (1998)

13. C. A. Michaels, Z. Lin, A. S. Mullin, H. C. Tapalian, and G. W. Flynn, J. Chem. Phys., 106, 7055-7071 (1997)
14. G. W. Flynn, C. A. Michaels, H. C. Tapalian, Z. Lin, E. Sevy, and M. A. Muyskens in *Highly Excited Molecules: Relaxation, Reaction, and Structure*, ACS Symposium Series, 678, pp134-149, Eds. Amy Mullin and George Schatz, American Chemical Society, Washington, DC, 1997
15. E.T. Sevy, C. A. Michaels, H. C. Tapalian, and G.W. Flynn, "Competition Between Photochemistry and Energy Transfer in UV-excited Diazabenzenes: II. Identifying the Dominant Energy Donor for 'Supercollisions'", J. Chem. Phys., 112, 5844-51 (2000)
16. E. T. Sevy, Seth Rubin, Z. Lin, and G. W. Flynn, "Translational and Rotational Excitation of the $CO_2(00^00)$ Vibrationless State in the Collisional quenching of Highly Vibrationally Excited 2-Methylpyrazine: Kinetics and Dynamics of Large Energy Transfers", J. Chem. Phys., 113, 4912-4932 (2000)

DOE Publications:

(1999-2001)

1. E.T. Sevy, M.A. Muyskens, S.M. Rubin, and G.W. Flynn, "Competition Between Photochemistry and Energy Transfer in UV-excited Diazabenzenes: I. Photofragmentation Studies of Pyrazine at 248 nm and 266 nm", J. Chem. Phys.,112, 5829-43 (2000)
2. E.T. Sevy, C. A. Michaels, H. C. Tapalian, and G.W. Flynn, "Competition Between Photochemistry and Energy Transfer in UV-excited Diazabenzenes: II. Identifying the Dominant Energy Donor for 'Supercollisions'", J. Chem. Phys., 112, 5844-51 (2000)
3. Jack M. Preses, Christopher Fockenberg, and George Flynn, "A Measurement of the Yield of Carbon Monoxide from the Reaction of Methyl Radicals and Oxygen Atoms", J. Phys. Chem., 104, 6758-6763 (2000)
4. E. T. Sevy, S. M. Rubin, Z. Lin, and G. W. Flynn, "Translational and Rotational Excitation of the $CO_2(00^00)$ Vibrationless State in the Collisional quenching of Highly Vibrationally Excited 2-Methylpyrazine: Kinetics and Dynamics of Large Energy Transfers", J. Chem. Phys., 113, 4912-4932 (2000)
5. E. T. Sevy, M. A. Muyskens, Z. Lin, and G. W. Flynn, "Competition Between Photochemistry and Energy Transfer in UV-excited Diazabenzenes: III. Photofragmentation and Collisional Quenching in Mixtures of 2-Methylpyrazine and Carbon Dioxide", J. Phys. Chem. A, 104, 10538-10544 (2000)
6. George W. Flynn, "Energy Transfer in Gases", Encyclopedia of Chemical Physics and Physical Chemistry, in press
7. Cortney Higgins, Quan Ju, Natalie Seiser, George Flynn and Sally Chapman, "Classical Trajectory Study of Energy Transfer in Pyrazine-CO Collisions", J. Phys. Chem., accepted
8. Natalie Seiser, Quan Ju, Eric Sevy, and George Flynn, "Quenching of Pyrazine by CO: Angular Momentum Constraints for Impulsive Encounters", in preparation
9. Natalie Seiser, K. Kavita, and George Flynn, "Long Range Energy Transfer in Pyrazine-CO Collisions: Excitation of CO (v=1)", in preparation

GAS-PHASE MOLECULAR DYNAMICS: CHEMICAL KINETICS AND THEORY

Christopher Fockenberg (fknberg@bnl.gov), James T. Muckerman (muckerma@bnl.gov)
and Jack M. Preses (preses@bnl.gov)
Chemistry Department, Brookhaven National Laboratory, Upton, NY 11973-5000

Program Scope

This research is carried out as part of the Gas-Phase Molecular Dynamics group program in the Chemistry Department at Brookhaven National Laboratory. The goal is a fundamental understanding of the kinetics of elementary reactions related to combustion processes, and the theoretical description of the spectroscopy of radical species and the energetics and dynamics of elementary chemical reactions in which they are involved.

Recent Progress

The reaction of triplet methylene, $CH_2(\tilde{X}\ ^3B_1)$, with methyl radicals:

$$^3CH_2 + CH_3 \rightarrow C_2H_4 + H\ , \qquad (1)$$

and in parallel the recombination reaction of two methyl radicals:

$$CH_3 + CH_3 \rightarrow C_2H_6 \qquad (2)$$

have been investigated as part of an ongoing study on the kinetics and product distributions of the reaction between methyl and hydroxyl radicals, which has two major competing product channels leading either to methanol or to singlet methylene, $CH_2(\tilde{a}\ ^1A_1)$, and water. Subsequent reactions of $^1CH_2$ can be safely neglected for our experiment because most of the methylene radicals generated in excited electronic states are rapidly deactivated to $^3CH_2$ by collisions with bath gas atoms under our experimental conditions.

Methyl radicals were generated by the 193 nm laser photolysis of acetone:

$$CH_3C(O)CH_3 + h\nu_{193nm} \rightarrow 2CH_3 + CO\ . \qquad (3)$$

A fraction, typically 2 to 5 percent depending on the laser intensity, of the methyl radicals created by (3) was subsequently photolyzed by the same pulse producing methylene (CH_2) radicals:

$$CH_3 + h\nu_{193nm} \rightarrow CH_2 + H\ . \qquad (4)$$

Using time-resolved time-of-flight mass spectrometry, the temporal evolution of the concentration of reactants as well as products could be observed simultaneously. Rate coefficients at $T = (300 \pm 3)$ K and $P = 1$ Torr (He) have been determined to be: $k_1 = (2.1 \pm 0.7) \times 10^{-10}$ cm^3 molecule^{-1} s^{-1} for $^3CH_2 + CH_3$ and $k_2 = (4.6 \pm 1.0) \times 10^{-11}$ cm^3 molecule^{-1} s^{-1} for $CH_3 + CH_3$. The rate constant for the $^3CH_2 + CH_3$ reaction found here is about three times as high as the one used in most combustion-simulation-related reaction mechanisms suggesting that the value for k_1 should be reconsidered for these calculations.

To include reactions of methylene radicals into our portfolio, we added a separate parallel production line to our gas supply system generating ketene by the pyrolysis of acetic anhydride. Helium is bubbled through acetic anhydride, which then passes through an externally heated quartz reactor filled with small quartz pieces. Water and unreacted acetic anhydride are frozen out in a cold trap at dry-ice temperature before the ketene/He flow is mixed into the main flow. The drop in the acetic anhydride signal after the oven is turned on indicates that more than 90% of the precursor can be converted into ketene with acetone and propanol as additional, minor byproducts. Methylene radicals can then be generated by the photolysis of ketene at 193 nm.

Previous studies of reactions of methyl radicals using diode-laser absorption needed to be performed using deuterated methyl-radical precursors because diode lasers were not available in the 3000 cm^{-1} C-H stretching region. We have investigated two paths around the limitations necessitated by deuteration: diode laser absorption in the 1440 cm^{-1} C-H bending region and the use of newly available diodes that provide emission in the 3000 cm^{-1} region.

The locations of methyl (and ethyl) radical C-H bending absorption lines (in matrices) are available in the literature and can be used as guides for finding gas-phase absorptions. The intensities of C-H bending

vibrations are inherently weaker than C-H stretching vibrations and make detection of species at C-H bending wavelengths challenging. While diode intensity near 1440 cm^{-1} was satisfactory and tuning to the necessary wavelengths was achieved, signals were too small to be useful. However, addition of two-tone frequency-modulation techniques (see below) ought to make these experiments feasible and improve the signal-to-noise ratio of other experiments.

Calibration of a 3050 cm^{-1} laser diode is complete and the search for C-H stretching signals from ethyl and methyl radicals has begun. Initial work involves demonstrating detection of C_2H_5 radicals from known sources such as diethyl ketone (DEK). Dilute mixtures of DEK in rare gas are irradiated with 193-nm radiation and the decay of C_2H_5 radicals by recombination and other processes is detected. See below for planned experiments.

Experimental work on HCBr in our program is complemented by extensive *ab initio* calculations of the electronic potential energy surfaces combined with dynamical solution of the vibrational problem to estimate anharmonic frequencies and vibronic transition moments as an aid to understanding the observed spectra. Calculations were performed using the MOLPRO 2000 program package.[1] The potential energy surfaces for the three electronic states of HCBr were obtained by performing a CASSCF calculation involving the twelve valence electrons and nine valence orbitals followed by an IC-MRCI calculation[2] of the three target states at each point of a direct-product discrete-variable representation (DVR) grid in CH–Br Jacobi coordinates. The resulting two singlet surfaces yielded stretching frequencies that were slightly (*ca.* 6.5%) lower than those observed experimentally (2768 *vs.* 2948 cm^{-1} for CH and 643 *vs.* 681 cm^{-1} for CBr in the ground singlet state). The CH and CBr distances were therefore scaled by a common linear scaling factor on all three surfaces according to the relation[3] $R'_{cx} = R'_{cx} + \alpha_{cx}(R_{cx} - R'_{cx})$, where X is H or Br and the prime indicates the scaled coordinate, to achieve better agreement with the experimental stretching frequencies. This scaling preserves the global features of the potential energy surfaces such as the degeneracy of the two singlet surfaces for all linear HCBr geometries. The three surfaces are shown in Fig. 1 along a cut at constant R_{CH} = 1.111225 Å, the calculated equilibrium value in the $\tilde{X}\ ^1A'$ state. The T_{00} value for the singlet-to-singlet transition is calculated to be 12451 cm^{-1}; the experimental value is 11972.8 cm^{-1}. Making this shift, along with a similar one for the triplet state, and including spin-orbit coupling, the calculations make testable predictions of the position of the triplet and singlet state vibronic levels.

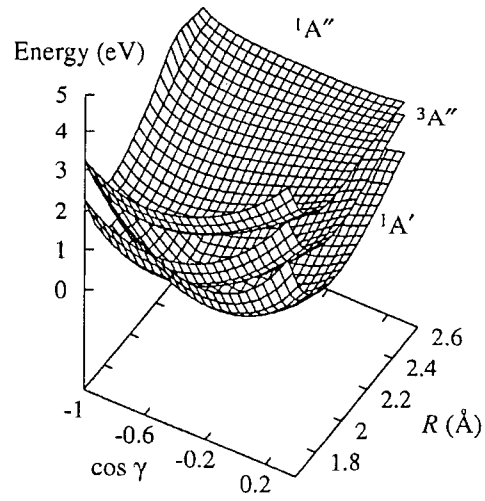

Fig. 1. Potential energy surfaces for the three lowest-lying electronic states of HCBr from the scaled *ab initio* MRCI calculation with the cc-pVTZ basis described in the text. Here R is the distance from the center of mass of the CH moiety to the Br atom, and γ is the angle between **R** and the **r**, the C-to-H distance. Note the intersection of the $X\ ^1A'$ and $a\ ^3A''$ surfaces at intermediate values of cos γ, and the degeneracy of the two singlet surfaces at all linear configurations (cos $\gamma = -1$) as the two components of a $^1\Delta$ state.

Future Plans

The next step in the investigation of the CH_3 + OH reaction is the development of an *in situ* production method for hydroxyl radicals. We are focusing our attention on the photolysis of nitrous oxide, N_2O, in the presence of water, hydrogen, or methane. The respective concentrations would be chosen in such a way that the generated $O(^1D)$ atoms would exclusively react with these hydrogen containing compounds producing hydroxyl radicals. In the case of methane as a reaction partner aside from the major channel giving CH_3 and OH, two additional channels have been observed leading to formaldehyde and methanol, respectively. However, the product distribution is not well characterized warranting separate experiments to quantify the product yields.

In parallel to the photolysis experiments on nitrous oxide, we plan to study the photolysis, *i.e.*, products and their quantum yields, of propargyl chloride (C_3H_3Cl) and allene (C_3H_4). These initial experiments will determine the suitability of both precursors to produce propargyl radicals, C_3H_3. The focus with respect to the propargyl chemistry will be the reaction of C_3H_3 with hydrogen atoms, which would help attempts to theoretically model the reaction of the predominant production route for propargyl radicals in combustion system: $^1CH_2 + C_2H_2$.

Building on our previous work studying reactions of CH_3 radicals *via* TOFMS and transient Tunable-Diode Laser Absorption (TDLAS)[4,5], we will undertake a series of experiments to measure rates of radical-radical reactions monitoring decay of C_2H_5 (or with substitution of appropriate precursors, CH_3) concentration using transient diode laser C-H stretching absorptions of ethyl (or analogously, methyl) radicals:

$$C_2H_5COC_2H_5 + h\nu_{193nm} \rightarrow 2\mathbf{C_2H_5} + CO \quad (5a)$$

$$SO_2 + h\nu_{193nm} \rightarrow SO + \mathbf{O} \quad (5b)$$

$$\mathbf{C_2H_5} + \mathbf{O} \rightarrow \text{products} \quad (5c)$$

and the similar reactions with the important OH radical:

$$C_2H_5COC_2H_5 + h\nu_{193nm} \rightarrow 2\mathbf{C_2H_5} + CO \quad (6a)$$

$$N_2O + h\nu_{193nm} \rightarrow NO + O(^1D) \quad (6b)$$

$$O(^1D) + H_2O \rightarrow 2\mathbf{OH} \quad (6c)$$

$$\mathbf{C_2H_5} + \mathbf{OH} \rightarrow \text{products} . \quad (6d)$$

The CH_3 reactions analogous to reactions (5) have already been studied by TOFMS and TDLAS and time-dependent FTIR.[6] Reactions (5) themselves have also been studied using time-dependent FTIR.[7] Direct detection of CH_3 disappearance *via* TDLAS will confirm the measured reaction rates, and the measurement of the C_2H_5 reactions rates will help to refine the various values in the literature. Experiments using both TOFMS and TDLAS may also clarify identification of products in (5c) and (6d).

The sensitivity of near-IR detection of spectroscopy and kinetics of radicals has benefited greatly from the use of frequency-modulation techniques to improve signal-to-noise ratios. Such methods cannot directly be applied to the mid-IR due to the lack of sufficiently fast detectors to permit RF-modulation. However, so-called two-tone FM methods[8] may permit application of this powerful approach to the mid-IR using relatively fast HgCdTe detectors. We intend to investigate using two-tone frequency modulation to extend our ability to detect small radical concentrations and/or weak absorptions.

Future theoretical studies will focus on the further development and application of a *K*-dependent adiabatic approximation to the Renner-Teller effect for triatomic molecules such as HCBr and HCCl, the calculation of the vibronic spectra of metal-containing radicals such as TiO, TiC, TiCH, TiC_2, ZrC and MoC for comparison with experimental spectra obtained in our program, and the quantum dynamics of the OH-overtone-induced predissociation of *trans*-HOCO using a many-body potential energy surface calibrated against new *ab initio* calculations. We have already characterized the critical points on the HOCO potential energy surface to a very high accuracy, and the quantum dynamical calculations will guide spectroscopic studies of the predissociation process.

References

1. MOLPRO is a package of *ab initio* programs written by H.-J. Werner and P. J. Knowles, with contributions from R. D. Amos, A. Bernhardsson, A. Berning, P. Celani, D.L. Cooper, J. J. O. Deegan, A. J. Dobbyn, F. Eckert, C. Hampel, G. Hetzer, T. Korona, R. Lindh, A. W. Lloyd, S. J. McNicholas, F. R. Manby, W. Meyer, M. E. Mura, A. Nicklass, P. Palmieri, R. Pitzer, G. Rauhut, M. Schütz, H. Stoll, A. J. Stone, R. Tarroni, and T. Thorsteinsson.
2. R. Lindh, U. Ryu, and B. Liu, *J. Chem. Phys.* **95**, 5889 (1991); H.-J. Werner and P. J. Knowles, *J. Chem. Phys.* **82**, 5053 (1985); P. J. Knowles and H.-J. Werner, *Chem. Phys. Lett.* **115**, 259 (1985); H.-J. Werner and P. J. Knowles, *J. Chem. Phys.* **89**, 5803 (1988); P. J. Knowles and H.-J. Werner, *Chem. Phys. Lett.* **145**, 514 (1988); P. J. Knowles and H.-J. Werner, *Theor. Chim. Acta* **84**, 95 (1992).
3. J. M. Bowman and B. Gazdy, *J. Chem. Phys.* **94**, 816 (1990); *J. Chem. Phys.* **95**, 6309 (1991).
4. *Kinetics and Product Study of the Reaction of CH_3 Radicals with $O(^3P)$ Atoms using Time Resolved Time-of-Flight Spectrometry*, C. Fockenberg, G. E. Hall, J. M. Preses, T. J. Sears and J. T. Muckerman, *J. Phys. Chem.* A **103**, 5722-5731 (1999).
5. *A Measurement of the Yield of Carbon Monoxide from the Reaction of Methyl Radicals and Oxygen Atoms*, J. M. Preses and C. Fockenberg, *J. Phys. Chem. A* **104**, 6758-6763 (2000).
6. See 1 and 2 and references therein.
7. *The Direct Production of $CO(v = 1–9)$ in the Reaction of $O(^3P)$ with the Ethyl Radical,* J. P. Reid, T. P. Marcy, S. Kuehn, and S. R. Leone, *J. Chem. Phys.* **113** 4572-4580 (2000).
8. For a review of FM methods see *Transient Laser Frequency Modulation Spectroscopy,* G. E. Hall and S. W. North, *Annu. Rev. Phys. Chem.* 51 243-74 (2000) and references therein.

Publications since 1999

Repetitively Sampled Time-of-Flight Mass Spectrometry for Gas-Phase Kinetics Studies, C. Fockenberg, H. J. Bernstein, G. E. Hall, J. T. Muckerman, J. M. Preses, T. J. Sears and R. E. Weston, Jr., *Rev. Sci. Instrum.* **70**, 3259-3264 (1999).

Kinetics and Product Study of the Reaction of CH_3 Radicals with $O(^3P)$ Atoms using Time Resolved Time-of-Flight Spectrometry, C. Fockenberg, G. E. Hall, J. M. Preses, T. J. Sears and J. T. Muckerman, *J. Phys. Chem. A* **103**, 5722-5731 (1999).

Ion Yields for Tetramethylgermane Exposed to X-Rays near the Ge K-Edge, R. A. Holroyd, J. M. Preses and T. K. Sham, *J. Phys. Chem. A* **104**, 2859-2864 (2000).

A Measurement of the Yield of Carbon Monoxide from the Reaction of Methyl Radicals and Oxygen Atoms, J. M. Preses, C. Fockenberg, and G. W. Flynn, *J. Phys. Chem. A* **104**, 6758-6763 (2000).

Radiation Chemical Effects of X-rays on Liquids, R. A. Holroyd and J. M. Preses in *Chemical Applications of Synchrotron Radiation*, Sham, T. K., ed.; World Scientific Publishing, in press.

A Direct Measurement of the Rate Constant for the $CH_2(\tilde{X}\ ^3B_1) + CH_3$ Reaction at 300 K, Baoshan Wang and Christopher Fockenberg, submitted to *J. Phys. Chem. A*

Strong-Field Optical Control of Vibrational Dynamics: Vibrational Stark Effect in Planar Acetylene, L. Liu and J. T. Muckerman, *J. Chem. Phys.* **110**, 2446-2451 (1999).

Competition Between Photochemistry and Energy Transfer in UV-Excited Diazabenzenes: I. Photofragmentation Studies of Pyrazine at 248 nm and 266 nm, E. T. Sevy, M. A. Muyskens, S. M. Rubin, G. W. Flynn and J. T. Muckerman, *J. Chem. Phys.* **112**, 5829-5843 (2000).

Experimental and Theoretical Studies of the Near-IR Spectrum of Bromomethylene, H.-G. Yu, T. Gonzalez-Lezana, A. J. Marr, J. T. Muckerman and T. J. Sears, *J. Chem. Phys.*, submitted (2001).

The E-X Spectrum of Jet-Cooled TiO Observed in Absorption, K. Kobayashi, G. E. Hall, J. T. Muckerman, T. J. Sears and A. J. Merer, *J. Chem. Phys.*, submitted (2001).

A K-dependent adiabatic approximation to the Renner-Teller effect for triatomic molecules, H.-G. Yu, J. T. Muckerman and T. J. Sears, *J. Chem. Phys.*, submitted (2001).

Acknowledgment

Work at Brookhaven National Laboratory was carried out under Contract No. DE-AC02-98CH10886 with the U.S. Department of Energy and is support by its Division of Chemical Sciences, Office of Science.

Quantitative Imaging Diagnostics for Reacting Flows

Jonathan H. Frank
Combustion Research Facility
Sandia National Laboratories, MS 9051
Livermore, CA 94551
jhfrank@ca.sandia.gov

Program Scope

The primary objective of this project is the development and application of laser-based imaging diagnostics for studying reacting flows. Imaging diagnostics provide temporally and spatially resolved measurements of species, temperature, and velocity distributions over a wide range of length scales. Multi-dimensional measurements are necessary to determine spatial correlations, scalar and velocity gradients, flame orientation, curvature, and connectivity. Our current efforts focus on planar laser-induced fluorescence (PLIF) techniques for probing the detailed structure of isolated flow-flame interactions. These basic interactions are of fundamental importance in understanding the coupling between turbulence and chemistry in turbulent flames. These studies require the development of a new suite of imaging diagnostics to measure key species in the hydrocarbon-chemistry mechanism as well as to image rates of reaction.

Recent Progress

Recent research has continued to emphasize the development and application of novel PLIF diagnostics for probing the detailed structure of reaction zones during flow-flame interactions. The coupling of measurements with simulations remains an essential element of this program. Research activities have included the following: i) Investigation of temporal evolution of reaction-rate in a flame-vortex interaction using simultaneous OH/CO PLIF. ii) An initial study of a new diagnostic for C_2 species to provide insight into C_2 reaction pathways in hydrocarbon oxidation. iii) Feasibility study of single-shot CO PLIF imaging for rich premixed and nonpremixed flames. iv) Examination of OH levels in flame-vortex interaction with improved temporal resolution.

Reaction-rate Imaging We have investigated CO/OH PLIF reaction-rate imaging for studying the flow transient response of premixed CH_4/air flames. The diagnostic technique uses simultaneous CO and OH PLIF to derive an image of the forward rate of the reaction CO + OH $\Rightarrow$ CO_2 + H. This reaction represents the primary pathway for the formation of CO_2 in a methane-air flame. The basic concept of the diagnostic involves using the product of simultaneous OH and CO PLIF measurements to obtain a signal that is proportional to the reaction rate. Measurements were performed in the V-flame/line-vortex interaction flow facility. Preliminary analysis of the results indicates that a depression in the CO levels coincides with the previously measured burst in OH levels. The CO+OH reaction does not appear to extinguish during the vortex-flame interaction. Improvements in the quantitative nature of the CO/OH reaction rate technique are ongoing with the main focus on the interpretation of the CO PLIF signal.

Development of C_2-Species Imaging Diagnostic Current chemical reaction mechanisms for hydrocarbon combustion have significant uncertainties with regard to C_2 chemistry. Consequently, computations of the effects of flow-flame interactions on C_2 reactions have considerable limitations, and experimental measurements are needed. However, there is a lack of diagnostic techniques for imaging C_2 species. To this end, we have conducted an initial investigation into a new diagnostic tool for probing C_2 chemical reaction pathways in premixed flames. Swan-band emission from laser-generated C_2* was measured in premixed methane-air flames with sufficient signals for imaging. To identify the source of this signal, we performed measurements of laser-generated C_2* emission spectra in a low-pressure cell from a variety of species including C_2H_2, C_2H_3, C_2H_4, C_2H_6, C_3H_6, C_4H_6, and CH_4. The most challenging of these measurements was the C_2H_3, which was produced by photolysis of methyl vinyl ketone (CH_3-C_2H_3-CO). The products of photofragmentation were CH_3, C_2H_3, and CO in equal proportions. We investigated the utility of two-photon CO LIF as a means to quantify the relationship between C_2* emission and the concentration of C_2H_3 in the probe volume. Our experimental results coupled with an inspection of the photolysis energetics indicate that the possible sources of laser-generated C_2* are acetylene (C_2H_2) and vinyl (C_2H_3). However, our measurements show that photolysis of C_2H_3 is significantly more efficient at generating C_2* emission than is photolysis of C_2H_2. This suggests that we may have a diagnostic technique for 2D measurements of C_2H_3 in flames. Further analysis and comparisons between C_2* emission spectra in the cell and in premixed flames is required. Experiments were performed in collaboration with D. Osborn.

CO PLIF Imaging We demonstrated two-photon CO PLIF imaging in rich premixed and nonpremixed flames with minimal C_2* interference. Swan-band emission from laser-created C_2* is a significant fluorescence interference and presents a limitation to the use of CO PLIF in rich premixed flames and nonpremixed flames. The C_2* emission increases with equivalence ratio and occurs over a broad spectral range, which overlaps fluorescence emission from the $B^1\Sigma^+ \rightarrow A^1\Pi$ band of CO. This significantly complicates the use of a broadband detection scheme for CO PLIF. In our approach, we have spectrally isolated the strongest transition of the $B^1\Sigma^+ \rightarrow A^1\Pi$ band using a custom high-transmission optical interference filter that blocks the C_2* emission. In order to attain adequate signal for imaging, we combined the laser beams from two Nd:YAG-pumped optical parametric oscillators (OPO) to form a single intense laser sheet for excitation of CO PLIF. Both OPO's were operated at 230.1 nm to pump several overlapping transitions of the $B^1\Sigma^+ \leftarrow\leftarrow X^1\Sigma^+$ band of CO. Using this pump-detection configuration, we have demonstrated the feasibility of single-shot CO PLIF imaging with minimal C_2* interference in both rich premixed flames and a diffusion flame with partial premixing (CH_4/air = 1/3 by volume). This demonstration lays the groundwork for instantaneous CO PLIF imaging in turbulent rich premixed and nonpremixed flames.

Study of OH in Flame-Vortex Interaction We performed OH PLIF measurements in the V-flame/line-vortex interaction with 100μs-time-steps during the phase of the interaction when the OH levels dramatically increase. All previous measurements had coarser temporal resolution (1ms-time-steps). The flame considered was a fuel rich CH_4/air flame (ϕ=1.2) with 30% N_2 dilution. The recent results showed the initiation of the OH burst occurring in the upstream region of the vortex pair. The OH burst in this region progressed in stages, with the first stage lasting approximately 300μs. Subsequently, the OH burst spread in the downstream direction

along the vortex-flame interface. This pattern of a localized OH burst with subsequent spreading along the vortex may vary with vortex strength and translational velocity, and further measurements are needed. We have also measured the OH PLIF in richer flames (ϕ>1.2) with less N_2 dilution (<30%). We found that the relative increase in OH levels during the flame-vortex interaction was enhanced dramatically when the equivalence ratio was increased. Detailed analysis of this data and comparisons with computations are ongoing.

Future Plans

In the near term, we will continue to expand our suite of novel laser-based imaging diagnostics and apply these techniques to the study of flow-flame interactions in highly reproducible, building-block flames. We will investigate the extension of diagnostics to single-shot measurements in turbulent flames. This represents a first step towards our long-term goal of using imaging diagnostics to apply our understanding of building-block flames to turbulent flow-flame interactions. In all of these endeavors, we will strive to couple our experimental measurements with simulation and modeling efforts.

Reaction Rate & Heat-release Rate We plan to continue the development of diagnostics that provide imaging measurements of reaction-rates and heat-release rates. Further studies using HCO, CH_2O/OH, and CO/OH measurements are planned. In the near future, our primary emphasis will be further developing the simultaneous CO/OH measurement technique to obtain the spatial distribution of the forward reaction rate of the CO + OH $\Rightarrow$ CO_2 + H reaction in both reproducible flow-flame interactions and turbulent flames. One of our goals is to obtain reaction-rate imaging measurements in the series of CH_4 jet flames being used for model validation in the Turbulent Nonpremixed Flame (TNF) Workshop.

Mixture Fraction Ultimately, we plan to couple the reaction-rate diagnostics with mixture fraction imaging in the turbulent nonpremixed flames of the TNF Workshop. The development of mixture fraction imaging techniques is a multi-year collaborative effort between Yale University, The University of Sydney, and Sandia. The primary motivation for developing such a diagnostic is to provide information on flame structure and scalar dissipation, which is determined from the gradient of the mixture fraction. While considerable progress has been made in developing schemes for obtaining images of mixture fraction in both H_2 and CH_4 flames, there remain challenges that need to be addressed for further use of these techniques. We plan to continue pursuing a mixture fraction imaging technique that can be verified with the line Raman/Rayleigh/LIF measurements performed with R. Barlow in Sandia's Turbulent Combustion Laboratory. Simultaneous measurements of mixture fraction and reaction-rate could provide insight into correlations between scalar dissipation rates and reaction rates. These measurements will be compared with results from current models of turbulent nonpremixed flames. Experiments will be performed in collaboration with M. Long of Yale University.

C_2-Species Diagnostic We will continue our development of a new diagnostic tool for probing C_2 chemical reaction pathways in premixed flames. We will perform detailed measurements of C_2* spectra in a variety of premixed flames for comparison with spectra obtained in the low-pressure cell. Further low-pressure cell measurements will investigate alternative methods for producing vinyl (C_2H_3), such as photolysis of vinyl chloride (C_2H_3Cl) or vinyl bromide (C_2H_3Br). These

low-pressure cell experiments will be used to evaluate the dependence of laser-generated C_2* emission on the production method of C_2H_3.

CO PLIF The interpretation of CO PLIF measurements remains semi-quantitative because of the lack of information on the complex photophysics of CO. To improve the quantitative nature of CO PLIF, we will perform a detailed analysis using measurements of CO PLIF signal levels, laminar flame calculations, and recent results of the species-specific temperature dependence of CO quenching by T. Settersten and R. Farrow. This analysis will provide a map to the accuracy of planar CO concentration measurements as a function of equivalence ratio.

Flame-Vortex Interactions Further studies on flame-vortex interactions will continue to examine the effects of N_2 dilution levels and stoichiometry. Experiments will be coupled with new computations by H. Najm. Additional measurements will include joint CO/OH PLIF imaging, and particle-imaging velocimetry. Particle image velocimetry (PIV) measurements will be performed to quantify the velocity field and better match the computations of Najm with the experiments.

Effects of Transient Strain The combined effect of unsteady strain and curvature complicates our efforts to resolve discrepancies between computations and experiments of flame-vortex interactions. To isolate the effect of transient strain, we plan to perform a series of measurements in a pulsed opposed flow burner.

DOE Supported Publications

J. H. Frank, R. S. Barlow, and C. Lundquist, "Radiation and nitric oxide formation in turbulent nonpremixed jet flames," *Proc. Combust. Inst.* 28, in press.

R. S. Barlow, J. H. Frank, and J.-Y. Chen, "Scalar profiles and NO formation in laminar opposed-flow partially-premixed methane/air flames," *Combust. Flame* submitted (2001).

P. A. Nooren, M. Versluis, T. H. van der Meer, R. S. Barlow, and J. H. Frank, "Raman-Rayleigh-LIF measurements of temperature and species concentrations in the Delft piloted turbulent jet diffusion flame," *Applied Phys. B* 71:95-117 (2000).

MECHANISM AND DETAILED MODELING OF SOOT FORMATION

Principal Investigator:Michael Frenklach

Department of Mechanical Engineering
The University of California
Berkeley, CA 94720-1740

Phone: (510) 643-1676; E-mail: myf@me.berkeley.edu

Project Scope: Soot formation is one of the key environmental problems associated with operation of practical combustion devices. Mechanistic understanding of the phenomenon has significantly advanced in recent years, shifting the focus of discussion from conceptual possibilities to specifics of reaction kinetics. However, along with the success of initial models comes realization of their shortcomings. The project focuses on fundamental aspects of physical and chemical phenomena critical to the development of predictive models of soot formation in combustion of hydrocarbon fuels, as well as on the computational techniques for development of predictive reaction models and their economical application to CFD simulations. The work includes theoretical and numerical studies of gas-phase chemistry of gaseous soot particle precursors, soot particle surface processes, particle aggregation into fractal objects, and development of economical numerical approaches to reaction kinetics.

Recent Progress:

Formation of Cyclopentadienyl from Addition of Acetylene to Propargyl (with N. W. Moriarty, X. Krokidis, and W A. Lester, Jr.)

The addition of acetylene and propargyl forming a cyclopentadienyl radical was investigated using highly accurate theoretical methods. The energetics of chemical species were calculated with the quantum Monte-Carlo method in the diffusion Monte Carlo (DMC) variant and several density-functional-theory (DFT) methods. Geometry optimizations were performed at all stationary points on the potential energy surface for the reaction system, and each point geometry was characterized by a frequency calculation to confirm its status as either a minimum or a transition state. The kinetics of the reaction system were examined employing the recently-updated MutiWell code for time-dependent solution of energy-transfer master equations. Numerical simulations were performed for a range of temperatures and pressures and were run to chemical equilibrium.

Diffusion Monte-Carlo calculations led to predictions in good accord with available experimental data for this reaction system, namely for the heat of formation of cyclopentadienyl and the rate of its thermal decomposition. The most reliable DMC predictions were those obtained from the formation and atomization reaction calculations, resulting, respectively, in 62.6±0.4 and 63.7±0.4 kcal/mol, for the cyclopentadienyl heat of formation at 298 K. It is important to note that DMC is not only a highly accurate quantum-mechanical method, but is also, and most importantly for establishing reliable thermochemical database, a method that provides good estimates of prediction uncertainty.

The DMC-based theoretical predictions of the thermodynamics and kinetics for the formation of the cyclopentadienyl radical from the addition of acetylene to propargyl both favor this reaction path. The equilibrium constants of reaction

$$C_3H_3 + C_2H_2 \rightarrow c\text{-}C_5H_5 \qquad (3\text{-}2)$$

at 1000 and 1500 K are 1×10^8 and 2.5×10^2 atm^{-1}, respectively. These results indicate that for an atmospheric flame and an acetylene mole fraction of 0.1, the equilibrium of this reaction is shifted toward cyclopentadienyl at temperatures below 1700 K, thus implying the formation direction within the temperature window of aromatics inception. The predicted for these conditions (pressure 1 atm and temperature 1500 K) rate coefficient of $k_{3\text{-}2} \sim 1\times10^{11}$ cm^3 mol^{-1} s^{-1} indicates that the kinetics of this reaction is also favorable. Indeed, let us compare the rate of reaction (3-2) to that of reaction (3-3),

$$C_3H_3 + C_3H_3 \rightarrow \text{benzene or phenyl} + H \qquad (3\text{-}3)$$

The literature value of $k_{3\text{-}3}$ is on the order of $1\text{–}5\times10^{12}$ cm^3 mol^{-1} s^{-1}, which is 10 to 50 times larger than $k_{3\text{-}2}$. However, the C_3H_3 flame concentration is roughly $10^2\text{–}10^4$ lower than the C_2H_2 concentration, and hence the reactant concentration product $[C_3H_3][C_3H_3]$ of reaction (3-3) is lower than the reactant concentration product $[C_3H_3][C_2H_2]$ of reaction (3-2) by the same factor. Combining the two factors, the rate coefficient and the reactant concentration product, favors the rate of reaction (3-2) over that of (3-3) by a factor of 2 to 10^3. In other words, reaction (3-2) is predicted to be not just fast enough to make a difference, but probably to play a dominant role in the formation of the first aromatic ring.

Carlo Simulation of Soot Particle Aggregation with Simultaneous Surface Growth (with P. Mitchell)

Mature soot particles appear as fractal-like aggregates randomly formed by branched chains of nearly spherical primary particles. Soot particle formation is initiated with homogeneous nucleation of precursors in the gas phase. The condensed phase material coalesces, leading to the formation of the first recognizable primary particles. The earliest visible particles are typically on order of 1–2 nm. After this initial stage, there is a transition from purely coalescent growth to aggregation. Aggregation is the process whereby emerging particles floc together forming the larger, more complex particle agglomerates. Particles also grow due to surface deposition. Gas-phase species, such as acetylene, "attach" themselves to the surface of the growing particles during both the coalescent and aggregation stages of coagulation. Surface growth adds a layer of mass on the soot particle surface thereby generating most of the solid-phase material. This growth mechanism encourages a rounder, more uniform shape, countering a portion of the geometric randomness added by aggregation, and in the extreme forming perfectly spheroidal particles. Formation of primary particles precedes that of aggregates. However, the transition between the two modes of growth is not well understood.

We investigated this transition using dynamic Monte-Carlo simulations. The simulations construct soot particles via ensemble-averaged collisions between small, geometrically perfect spheres. Simultaneously with the collisions, the particle sphere surfaces grow with a prescribed rate. The result is a union of overlapping spheres. A point sampling algorithm was implemented

to compute particle center of mass, volume, surface area, fractal dimension, and radius of gyration.

During the past year we developed of a method for quantitative characterization of particle geometry. Our simulated particles are constructed from a union of mathematically perfect balls. Therefore, we introduced shape descriptors to measure the amount of intersection between the balls comprising the particle. These descriptors are able to differentiate between chain-like and spheroidal particles. The two shape descriptors we use are related to what are referred to in the literature as *rugosity* and *globularity* and are derived from the particle volume and surface area. With a method to quantify geometry we have gained the ability to detect when the particles shift from one geometric regime to another. That is to say, the shape descriptors allow a method to detect the transition between the coalescent and fractal regimes of particle formation.

Using the shape descriptors, we have investigated the cause of the spheroidal shape of primary particles. We attribute this to regions in the flame where surface growth is intense and collisions occur between small, densely populated soot particles. In the inception zone of laminar premixed flames, surface growth rate is fast and the average particle radius remains relatively small due to the large nucleation rate. If we look at the total particle number density we see that early on nucleation is incredibly fast. In this window of time, if we look at size density as a function of size class, we see that the particle ensemble is dominated by small, newly emerging particles. Therefore, in this region collisions occur most often between small soot particles. Small particles that collide and stick to each other quickly turn spheroidal due to surface deposition. The smaller the particles the easier they are buried under layers of mass due to surface deposition. The transition occurs when nucleation has subsided and the number of small, newly incepted particles decreases. The average size of soot particles increases and surface deposition rate declines. This corresponds to cessation of surface growth and a region in the flame where the collector particle collides more often with larger candidate particles. As a result the collector transitions away from the coalescent regime towards the fractal limit.

Increasing Efficiency of PRISM: Use of Reaction Trajectory (with S. R. Tonse, N. J. Brown, and N. W. Moriarty)

We continue to explore the PRISM methodology. In PRISM we describe the thermochemical state of a reacting fluid as a point in the chemical composition space. A solution mapping technique is used to parameterize the results of time-integration of the chemical rate equations by algebraic polynomial response surfaces over hypercubes of the chemical composition space. The parameterization is done piecewise with a distinct parameterization for each hypercube, developed on the fly, as needed. The numerical efficiency of PRISM relies on the high degree of hypercube reuse.

As a means to ascertain a priori whether a hypercube will have sufficient usage to warrant its construction, we have investigated the use of trajectory velocity—a measure of how fast the reaction trajectory is moving in the chemical composition space. We have studied three cases: a point reaction case with zero spatial dimensions and two CFD simulations, a one-dimensional laminar premixed hydrogen-air flame and two-dimensional non-premixed hydrogen-air turbulent jet. We found the trajectory velocity to be a useful indicator for the zero-dimensional case, to a lesser extent for the laminar flame, and essentially ineffective for the turbulent jet case.

Future Plans

1. *Soot Chemistry*: To continue ab initio quantum-chemical analysis of reactions critical to the development of kinetic models of aromatic growth. As the propargyl + acetylene → cyclopentadiene is near completion, we will focus on the next step of this reaction pathway: cyclopentadiene + acetylene system. (In collaboration with Lester).
2. *Particle Aggregation*: To complete parameterization of particle formation. The parameterization will use the geometric shape descriptors reported above. Using the developed parameterization, we will perform self-contained numerical calculations of particle formation, simulating the transition between the coalescent limit and fractal aggregation.
3. *Numerical Approaches to Reaction Kinetics*: Further investigation of approaches to increase the economy of the PRISM method: (a) Selection of the hypercube size based on the topology of the chemical composition space, such as species sensitivities; and (b) Reduction of the number of dimensions in the factorial design, e.g., by combining PRISM with other techniques of mechanism reduction.

Publications

1. "PRISM: Piecewise Reusable Implementation of Solution Mapping. An Economical Strategy for Chemical Kinetics," S.R. Tonse, N.W. Moriarty, N.J. Brown and M. Frenklach, *Israel Journal of Chemistry* **39**, 97–106 (1999).
2. "Hydrogen Migration in the Phenylethen-2-yl Radical," N. W. Moriarty, N. J. Brown, and M. Frenklach, *J. Phys. Chem. A* **103**, 7127–7135 (1999).
3. "Propargyl Radical: An Electron Localization Function Study," X. Krokidis, N. W. Moriarty, W. A. Lester, Jr., and M. Frenklach, *Chem. Phys. Lett.* **314**, 534–542 (1999).
4. "Kinetic Modeling of Soot Formation with Detailed Chemistry and Physics: Laminar Premixed Flames of C_2 Hydrocarbons," J. Appel, H. Bockhorn, and M. Frenklach, *Combust. Flame* 121, 122–136 (2000).
5. "On Unimolecular Decomposition of Phenyl Radical," H. Wang, A. Laskin, N. W. Moriarty, and M. Frenklach, *Proc. Combust. Inst.* **28**, in press.
6. "The Dependence of Chemistry on the Fuel Inlet Equivalence Ratio in Vortex-Flame Interactions," J. B. Bell, N. J. Brown, M. S. Day, M. Frenklach, J. F. Grcar, and S. R. Tonse, *Proc. Combust. Inst.* **28**, in press.
7. "Ab Initio Study Of Naphthalene Formation By Addition Of Vinylacetylene To Phenyl," N. W. Moriarty and M. Frenklach, *Proc. Combust. Inst.* **28**, in press.
8. "Scaling and Efficiency of PRISM in Adaptive Simulations of Turbulent Premixed Flames," J. B. Bell, N. J. Brown, M. S. Day, M. Frenklach, J. F. Grcar, R. M. Propp, and S. R. Tonse, *Proc. Combust. Inst.* **28**, in press.
9. "Solution Mapping Approach to Modeling Combustion," M. Frenklach, *First MIT Conference on Computational Solid and Fluid Mechanics,* Elsevier, in press.

Multiresonant Spectroscopy and the High-Resolution Threshold Photoionization of Combustion Free Radicals

Edward R. Grant
Department of Chemistry
Purdue University
West Lafayette, IN 47907
edgrant@purdue.edu

Program Definition/Scope

In this research we apply methods of multiresonant spectroscopy and rotationally resolved threshold photoionization to characterize the structure, thermochemistry and intramolecular dynamics of excited neutrals and cations derived from combustion free radicals. The objectives of this work are: (1) To measure ionization potentials with wavenumber accuracy for a broad set of polyatomic molecules of relevance to combustion and combustion modeling; (2) To determine vibrational structure for cations as yet uncharacterized by ion absorption and fluorescence spectroscopy, including the study of anharmonic coupling and intramolecular vibrational relaxation at energies approaching thresholds for isomerization; (3) By threshold photoionization scans, referenced in double resonance to specific cation rovibrational states, to obtain information on originating-state level structure useful for the development of neutral-species diagnostics; (4) To measure rotationally detailed state-to-state photoionization cross sections for comparison with theory; and (5) To spectroscopically study near-threshold electron-cation scattering dynamics of relevance, for example, to plasma processes such as dissociative recombination, by acquiring and analyzing rotationally resolved high-Rydberg spectra.

Recent Progress

Laser-assisted (1+1')-photon resonant ionization-detected absorption spectroscopy of the $3p\pi\ ^2\Pi$ state of HCO and DCO

We have found that a high-power visible laser, used as an ionization field, significantly enhances the sensitivity of ionization-detected absorption as a means to locate transition energies in the $3p\pi\ ^2\Pi \leftarrow X\ ^2A'$ system of HCO and DCO. For example, it is only with difficulty that conventional ultraviolet (1+1)-photon ionization spectroscopy resolves the Franck-Condon unfavorable $3p\pi\ ^2\Pi$ (000) $\leftarrow X\ ^2A'$ (000) origin for HCO. This transition is not seen at all for DCO. Using a visible laser to drive the ionization step, origin band systems emerge clearly for both systems, as shown below in Figure 1.

We have recorded (1+1')-photon resonant-ionization spectra of higher vibrationally excited states in the $3p\pi\ ^2\Pi$ systems of HCO and DCO. Visible laser assistance reveals numerous transitions to higher vibronic angular momentum components in Renner-Teller split bending progressions. Analysis of this structure enables an unambiguous assignment of the

(001) fundamental and a clear measure of the effect of (040) – (100) bend-stretch Fermi resonance on Renner-Teller coupling in this state.

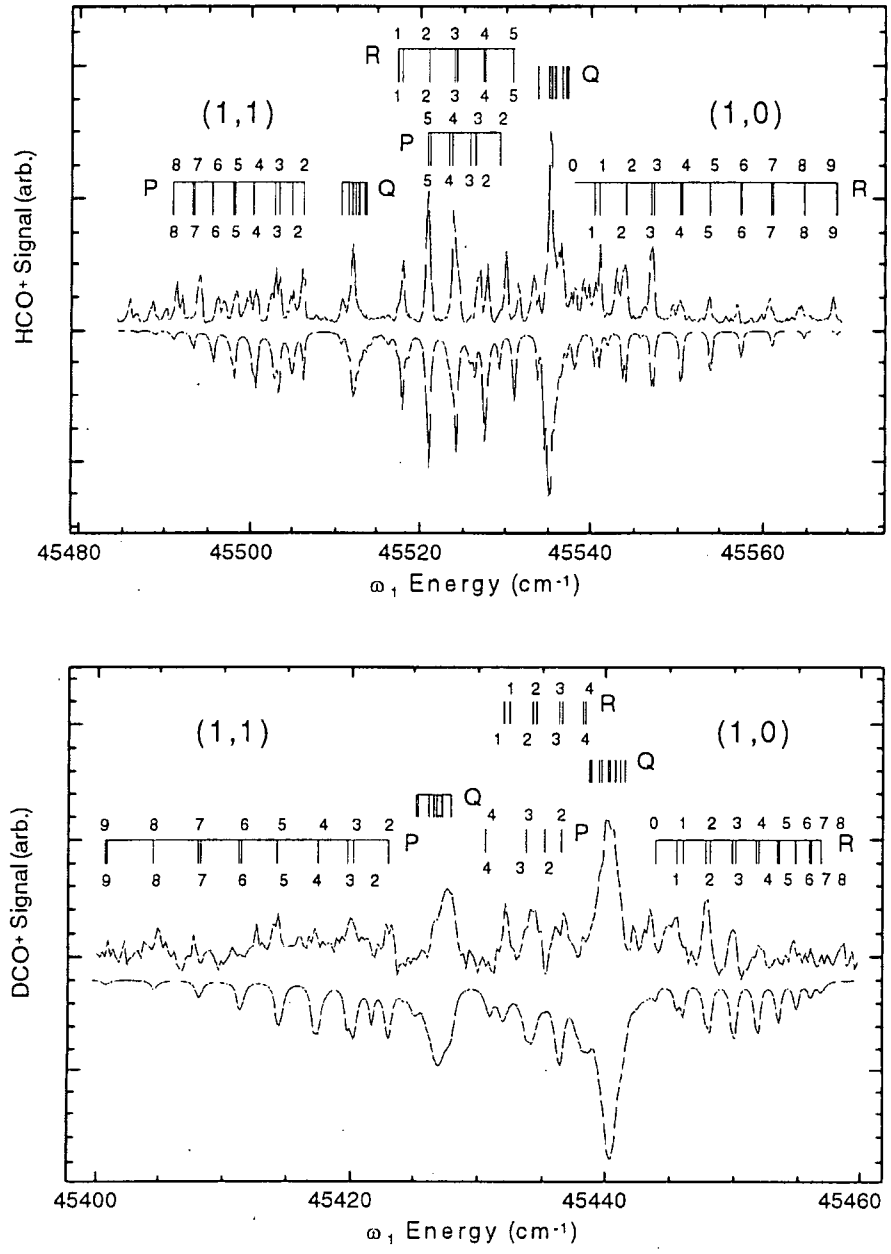

Figure 1. Laser-assisted (1+1')-photon ionization-detected absorption spectra of the (000) band of the 3pπ $^2\Pi$ Rydberg state in HCO (top) and DCO (bottom) with simulations (inverted). Parenthetical quantum numbers are (K',K'), referring to the principal axis projections of the excited and ground-state total angular momentum.

Double-resonant photoionization efficiency (DR/PIE) spectroscopy: A precise determination of the adiabatic ionization potential of DCO

We have made the first high-resolution measurement of the adiabatic ionization potential of DCO and the fundamental bending frequency of DCO^+. Fixing a first-laser frequency on

selected ultraviolet transitions to individual rotational levels in the (000) band of the 3pπ $^2\Pi$ intermediate Rydberg state of DCO, we have scanned a second visible laser over the range from 20000 to 20300 cm^{-1} to record double-resonance photoionization efficiency (DR/PIE) spectra. Intermediate resonance with this Rydberg state facilitates transitions to the threshold for producing ground-state cations by bridging the Franck-Condon gap between the bent neutral radical and linear cation. By selecting a single rotational state for ionization, double-resonant excitation eliminates thermal congestion. Spectroscopic features for first-photon resonance are identified by reference to a complete assignment of the 3pπ $^2\Pi$ (000) – X ^{2}A' (000) band system of DCO. By calibration with HCO, for which the adiabatic ionization threshold is accurately known, we have established an instrument function for this experiment that accounts for collisional effects on the shape of the photoionization efficiency spectrum near threshold. Analysis of the DR/PIE threshold for DCO yields an adiabatic ionization threshold of 65616 ± 3 cm^{-1}.

By extrapolation of vibrationally autoionizing Rydberg series reached in double-resonant transitions from the Σ^+ component of the 3pπ $^2\Pi$ (010) intermediate state, we have determined an accurate rotationally state-resolved threshold for producing DCO^+ (010). This energy, together with the threshold determined for the vibrational ground state of the cation provides a first estimate of the bending frequency for DCO^+ as 666 ± 3 cm^{-1}. Assignment of the (010) autoionization spectrum further yields a measurement of an energy of 4.83 ± 0.01 cm^{-1} for the (2-1) rotational transition in the $^1\Sigma^+$ (01^10) state of DCO^+. Figure 1 shows an ionization-detected absorption spectrum of Rydberg states built on the fundamental bending excited state of DCO^+, selected in transitions from 3pπ $^2\Pi$ (010) Σ^+ N' = 0. The simulation identifies resonances converging to robvibrational thresholds N^+ = 1, 2 and 3 in $^1\Sigma^+$ (010) DCO^+.

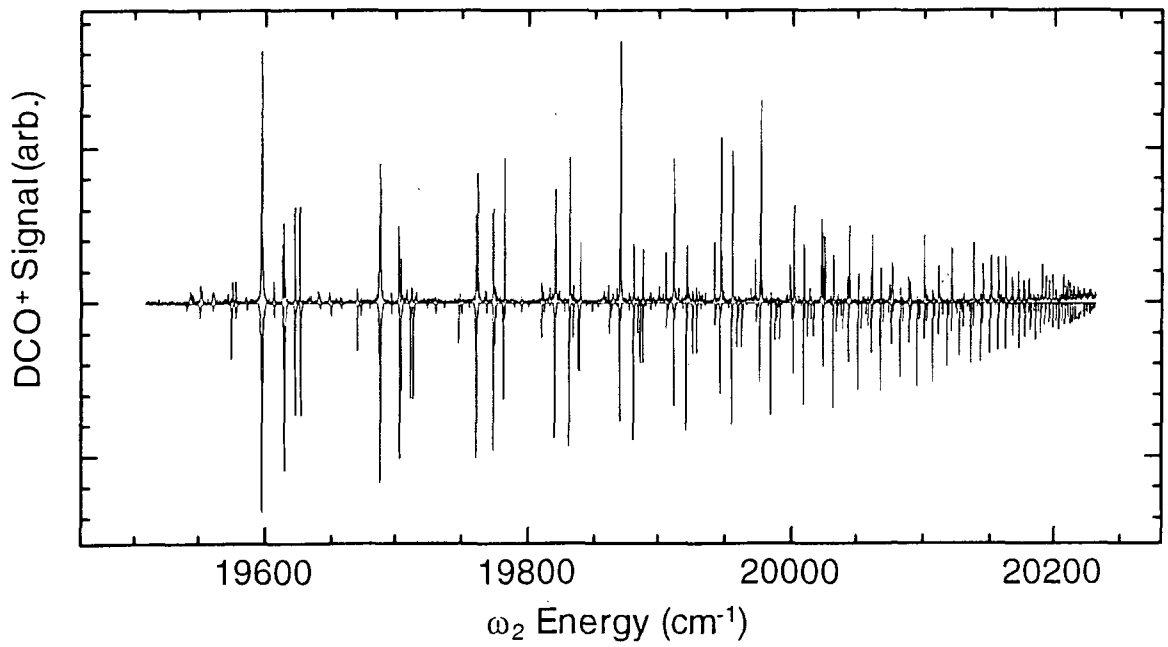

Figure 2. Scan of ω_2 from the adiabatic ionization threshold to the vertical limit for producing DCO^+ (010) originating from the 3pπ $^2\Pi$ (010) Σ^+ N' = 0 intermediate state. Inverted simulation based on Rydberg parameters

for series of constant quantum defect converging to rotational levels N^+ = 1, 2 and 3 in the (010) vibrational state of DCO^+..

An experimental measure of anharmonicity in the bending of DCO^+

Extrapolating rovibrationally isolated Rydberg series of DCO to higher vibrationally excited states of DCO^+, we have produced a map, with sub-wavenumber accuracy, of individual rotational level positions in the bending fundamental and first overtone of DCO^+. By analysis of this structure, we have determined fundamental frequencies, rotational constants and low-order anharmonicities associated with the bending mode of the cation. Rotational properties of excited DCO^+ found by Rydberg extrapolation are observed to agree well with quantities measured by microwave spectroscopy. The CASSCF-MRCI potential energy surface of Puzzarini and coworkers, which yields fundamental frequencies that agree with experiment for HCO^+, is shown to conform well with these first measurements of the bending frequencies of DCO^+.

References to publications of DOE sponsored research (1999-2001)

A characterization of vibrationally excited NO_2^+ by ZEKE high-resolution threshold photoionization spectroscopy, G. K. Jarvis, Y. Song, C. Y. Ng and E. R. Grant, *Advanced Light Source Compendium 1998* (Lawrence Berkeley Laboratory, Berkeley, CA, 1999).

A characterization of vibrationally and electronically excited NO_2^+ by high-resolution threshold photoionization spectroscopy, G. K. Jarvis, Y. Song, C. Y. Ng and E. R. Grant, *J. Chem. Phys.* **111**, 9568 (1999).

Experimental Characterization of the Higher Vibrationally Excited States of HCO^+: Determination of ω_2, x_{22}, g_{22} and $B_{[030]}$, R. J. Foltynowicz, J. D. Robinson, E. J. Zückerman, H. G. Hedderich and E. R. Grant, *J. Mol. Spectrosc.* **199**, 147-157 (2000).

Double-resonant photoionization efficiency spectroscopy: A precise determination of the adiabatic ionization potential of DCO, R. J. Foltynowicz, J. D. Robinson and E. R. Grant, *J. Chem. Phys.* **114**, 5224 (2001).

An experimental measure of anharmonicity in the bending of DCO^+, J. D. Robinson, R. J. Foltynowicz and E. R. Grant, *J. Chem. Phys.* **114**, xxxx (2001).

The A $^1\Pi$ -- X $^1\Sigma^+$ (2,0) Transition in ^{11}BH and ^{10}BH Observed by (1+2)-Photon Resonance-Enhanced Multiphoton Ionization Spectroscopy, J. Clark, M. Konopka, L.-M. Zhang and E. R. Grant, *Chem. Phys. Lett.*, in press.

CHEMICAL DYNAMICS IN THE GAS PHASE: QUANTUM MECHANICS OF CHEMICAL REACTIONS

Stephen K. Gray
Chemistry Division
Argonne National Laboratory
Argonne, IL 60439

E-mail: gray@tcg.anl.gov

PROGRAM SCOPE

This work concerns mostly the development and application of accurate quantum methods to describe gas phase chemical reactions and highly excited molecules. Classical molecular dynamics calculations of larger systems are also pursued. Much of the quantum work involves time-dependent or iterative quantum approaches that, in addition to computational simplifications, yield mechanistic insights. Applications to systems of current experimental and theoretical interest, and relevance to combustion, are emphasized. The results of these calculations also allow one to gauge the quality of the underlying potential energy surfaces and the reliability of more approximate theoretical approaches such as classical trajectories, transition state and statistical theories.

RECENT PROGRESS

The previously developed real wave packet (RWP) approach [1] for reactive scattering was applied to the $O(^1D) + H_2$ (v=0,j) $\rightarrow$ OH + H reaction in three dimensions, including many total angular momenta (within a helicity decoupled approximation) *and* allowing for the effect of excited electronic states and non-adiabatic dynamics (Gray, Balint-Kurti, Schatz, and co-workers, 2000). These challenging and extensive calculations led to energy-resolved differential cross sections. A crossed molecular beam study at one collision energy, motivated by our theoretical work, led to a ratio of differential cross sections from rotationally excited (j=1) to cold (j=0) reactants that was in quantitative agreement with theory. It had previously been suggested that this ratio should exhibit interesting behavior as a function of collision energy [2], serving as an indicator for when the excited state and non-adiabatic dynamics becomes more important. The new theoretical results, however, while including all relevant non-adiabatic effects, do not show such a strong variation in the ratio. However, it remains to be seen if the good agreement between theory and experiment and one collision energy will be extended to a wider range of energies.

Other interesting features of the $O(^1D) + H_2 \rightarrow$ OH + H reaction, and isotopic analogs, were also explored with the RWP methodology. The OH vibrational and rotational product state distributions were determined (Hankel, Balint-Kurti and Gray, 2000) and contrasted with available experimental data. Interesting discrepancies between theory and experiment, particularly for high OH vibrational states, were noted and need to be addressed with both better theory and experiment. A study of ground and first excited state dynamics of the isotopic analog reaction $O(^1D) + HD \rightarrow$ OH(OD) + D(H) was

also carried out (Hankel, Balint-Kurti, and Gray, 2001). Vibrational product state distributions and also OD/OH branching ratios were determined and compared to classical trajectory results and experiment. The OD/OH branching ratio appears to be somewhat higher than available experimental results, a trend also present in the trajectory results.

The $O(^3P) + HCl \rightarrow OH + Cl$ reaction was studied on a new *ab initio* potential surface, using both the "standard" RWP approach [1] and a transition state -RWP (TS-RWP) approach (Forsythe and Gray, 2000) to the cumulative reaction probability in collaborative work with Bowman's group (Skokov et al., 2000). Previous theoretical results on earlier potential surfaces led to significantly higher rate constants than experiment and it had been expected that the new surface, which had a higher barrier, would lead to results in better accord with experiment. The remarkable result was that the new theoretical rate constant turned out to be slightly larger than the old one, i.e., definitely not an improvement in the level of theoretical/experimental agreement. Other features of the transition state (e.g., frequencies normal to the transition state and the barrier thickness) must come into play, as well as perhaps more interesting resonance features at low energy.

The *ab initio* dynamics of singlet ketene dissociation, $CH_2CO \rightarrow CH_2 + CO$, was investigated in collaboration with Klippenstein and Hall [3]. The original aim of this work was to attempt to explain some fascinating non-statistical product rotational state distributions observed in Hall's laboratory [4]. These experiments showed that low CO rotational states, with CH_2 also in a low rotational state, were less probable than expected on the basis of statistical, phase space theory (PST). Very extensive dynamics calculations were carried out employing forces generated at a reasonable level of electronic structure theory. We were able to demonstrate that exit channel effects are responsible for certain deviations of the *uncorrelated* CO and CH_2 rotational distributions from PST. The theoretical dynamics based correlated distributions, however, did not agree as well with experiment and were in fact closer to PST. Our calculations assumed a sampling of phase points at a transition state, and it is possible that more subtle dynamical effects occur in the strong interaction region

FUTURE PLANS

The RWP [1] and TS-RWP (Forsythe and Gray, 2000) methodology will be extended to four-atom dynamics problems. A variety of methodological issues will be investigated regarding the development of an efficient, four-atom quantum dynamics code, including new methods for the evaluation of the kinetic energy operator, a significant computational bottleneck in many calculations.

Strong motivation for this extension comes from recent experimental work of Lester and co-workers [5] on the combustion important OH + CO system. In particular, there are fascinating questions regarding the role of entrance channel complexes in this reaction, and coupled with high level ab initio potential surface results from Harding at Argonne, it should be possible to probe many spectroscopic and dynamics aspects of this system with the RWP and related methodologies. (It has already proved possible to develop an iterative code for the determination of quasibound states in the OH-CO system, and reasonable agreement with experiment has been found.)

Reduced dimension models of $CH_2CO \rightarrow CH_2 + CO$ will be developed, with the hope of ultimately explaining the correlated distribution results from Hall's laboratory [4]. In order to complement our

previous classical molecular dynamics work [3], it may prove useful to consider the quantum (wave packet) dynamics of such models.

---

[1] S. K. Gray and G. G. Balint-Kurti, J. Chem. Phys. **108**, 950 (1998).
[2] S.-H. Lee and K. Liu, J. Chem. Phys. **111**, 4351 (1999).
[3] K. M. Forsythe, S. K. Gray, S. J. Klippenstein and G. E. Hall, J. Chem. Phys., submitted (2001).
[4] M. L. Costen, H. Katayanagi, and G. E. Hall, J. Phys. Chem. A **104**, 10247 (2000).
[5] M. I. Lester, B. V. Pond, D. T. Anderson, L. B. Harding, and A. F. Wagner, J. Chem. Phys. **113**, 9889 (2000).

PUBLICATIONS, S. K. Gray (1999-2001)

1. S. K. Gray, E.M. Goldfield, G.C. Schatz, and G.G. Balint-Kurti, Helicity decoupled quantum dynamics and capture model cross sections and rate constants for $O(^1D) + H_2 \rightarrow OH + H$, Phys. Chem. Chem. Phys. **1**, 1141 (1999).

2. S. K. Gray, C. Petrongolo, K. Drukker and G. C. Schatz, Quantum wave packet study of nonadiabatic effects in $O(^1D)+H_2 \rightarrow OH + H$, J. Phys. Chem. A **103**, 9448-9459(1999).

3. K. M. Christoffel, Y. Kim, S. Skokov, J. M. Bowman and S. K. Gray, Quantum and quasiclassical reactive scattering of $O(^1D)$ + HCl using an *ab initio* potential, Chem. Phys. Lett. **315**, 275-281(1999).

4. K. M. Forsythe and S. K. Gray , A transition state real wavepacket approach for obtaining the cumulative reaction probability, J. Chem. Phys. **112**, 2623 -2633 (2000).

5. S. Nanbu, S. K. Gray, T. Kinoshita and M. Aoyagi, Theoretical study of the potential energy surfaces and bound states of HCP, J. Chem. Phys., **112**, 5866-5876 (2000).

6. S. Skokov, T. Tsuchida, S. Nanbu , J. M. Bowman, and S. K. Gray, A comparative study of the quantum dynamics and rate constants of the $O(^3P)$ + HCl reaction described by two potential surfaces, J. Chem. Phys. **113**, 227- 236 (2000).

7. S. K. Gray, G. G. Balint-Kurti, G.C. Schatz, J. J. Lin, X. Liu, S. Harich, and X. Yang, Probing the effect of H_2 rotational state in $O(^1D) + H_2 \rightarrow OH + H$: Theoretical dynamics including nonadiabatic effects and a crossed molecular beam study, J. Chem. Phys. **113**, 7330-7344 (2000).

8. M. Hankel, G. G. Balint-Kurti, and S. K. Gray, Quantum mechanical calculation of product state distributions for the $O(^1D) + H_2 \rightarrow OH + H$ reaction on the ground electronic state surface,

J. Chem. Phys. **113**, 9658-9667(2000).

9. S. K. Gray, B. G. Sumpter, D. W. Noid, and M. D. Barnes, Quantum mechanical model of localized electrons on the surface of polymer nanospheres, Chem. Phys. Lett. **333**, 308-313 (2001).

10. M. Hankel, G.G. Balint-Kurti, and S. K. Gray , Quantum mechanical calculation of reaction probabilities and branching ratios for the O(1D) + HD $\rightarrow$ OH(OD) + D(H) reaction on the 1A' and 1A" adiabatic potential energy surfaces, J. Phys. Chem. A. in press (2001).

11. S. K. Gray and E. M. Goldfield, Highly excited bound and low-lying resonance states of H_2O, J. Phys. Chem. A, in press (2001).

Computer-Aided Construction of Chemical Kinetic Models

William H. Green, Jr., MIT Department of Chemical Engineering,
77 Massachusetts Ave., Cambridge, MA 02139. email: whgreen@mit.edu

Industrial Collaborators: A.M. Dean* & J.M. Grenda, ExxonMobil Res. & Eng. Co.
* present address: Dept. of Chemical Engineering, Colorado School of Mines

Project Scope

The combustion chemistry of even simple fuels can be extremely complex, involving hundreds or thousands of kinetically significant species. The most reasonable way to deal with this complexity is to use a computer not only to numerically solve the kinetic model, but also to construct the kinetic model in the first place. We previously developed [8] an effective algorithm for constructing kinetic models appropriate to the reaction conditions, presuming one could estimate the rates and that one could solve the models numerically. However, this algorithm (and all existing computer-construction approaches) have several deficiencies, e.g. they are unable to compute k(T,P) or even enumerate the chemically-activated product channels. Also, it is very difficult to solve flame simulations using these large chemistry models. We are developing the methods needed to make computer-construction of combustion models practical and accurate.

Our work during this grant period has focused on: 1) development of improved reaction rate estimates suitable for systems involving many large molecules, with a special focus on k(T,P) calculations and 2) development of a new "Adaptive Chemistry" method for coupling complex chemical kinetics into flame simulations.

Recent Progress

I. Reaction Rate Estimation

A. Pressure Dependent Rate Calculations

To assess the accuracy of various approaches, we performed k(T,P) calculations using different approximations for the various inputs: microcanonical rate constants k(E), densities of states ρ(E), and the collisional energy transfer model. We also compared master equation solutions with Troe's strong-collision approximation. Our study [1] of $OH+NO_2$ indicated that the HOONO channel significantly affected high-pressure experimental measurements, a prediction recently confirmed by Hippler & Golden.

Our k(T,P) calculations [3] on $C_6H_5+C_2H_2$ and $C_{10}H_9+C_2H_2$ indicate that even reactions involving large (C_{12}) molecules at high pressure can be far from the high-pressure-limit at combustion temperatures, something which has been neglected in virtually all existing combustion models. In each of our published cases, the *a priori* predictions are within about a factor of 5 of the experimental k(T,P) over the whole range of conditions where experimental data are available; this is accurate enough for determining whether the reactions can be neglected.

We also developed, in collaboration with Dean and Grenda, a general algorithm for constructing the multiwell unimolecular reaction network required for a fall-off or chemical-activation calculation of k(T,P). We were able to prove rigorous bounds on the error introduced by neglecting the less important pathways and wells (isomers) in our "ASA" method.[5] For large molecules it is important to avoid detailed computations

along these negligible pathways, since the number of isomers grows exponentially with molecular size. For example, there are more than 200 C_8H_{15} isomers energetically accessible after addition of an unsaturated C4 radical to a C4 alkene. It is critical to prune the resulting intramolecular reaction network as it is constructed (by using ASA), to keep the pressure-dependence calculation manageable.

We are currently testing predictions made using ASA against experimental data. The complete program uses modules from the model-generation software suite to construct all the non-negligible activated complexes and the network of reaction pathways that connects these isomers with each other and with the bimolecular product channels. After solving the system it constructed, the program returns k(T,P) for each non-negligible product channel. For solving the system, we are currently using the best publicly available multi-well pressure-dependence solvers.[9,10] In the near future we plan to develop an even more flexible solver for complex multiwell chemically-activated reactions, utilizing the most efficient techniques possible to achieve user-specified precision tolerances.

B. Group Additivity for Transition States

Often the accuracy of the simulation is constrained primarily by the accuracy of the high-pressure-limit rate parameters employed. It is unlikely that either experiment or high-quality quantum calculations will be able to provide the very large number of rate constants needed. Instead, we are generalizing from a limited number of quantum calculations and experimental data, using the idea of functional groups. Benson's group additivity scheme very accurately describes thermochemical properties for stable species; we are extending this approach to predict the transition state properties (e.g. the free-energy of activation, needed to compute reaction rates). Our group additivity predictions are within 40% of the dozens of individual quantum (CBS-Q, canonical TST, Wigner tunneling) rates we have tested over the whole T range. One advantage of our approach over the more conventional linear free-energy relationship (LFER) approach is that group-additivity naturally predicts Arrhenius plot curvature. Our quantum-based group additivity estimates for H-abstraction reactions are generally within a factor of 5 of the best literature rates above 500 K.

Our TS group additivity work [6,7] has focused on bimolecular H-abstraction reactions, where there are numerous excellent experimental data for validation and there is no significant pressure dependence. Having demonstrated the reliability of the method, we will now address more difficult types of reactions, where much less is known and the need for *a priori* rate estimates is correspondingly greater.

C. Hindered Internal Rotors

When computing molecular entropies, heat capacities, and rate constants, a very significant uncertainty (up to a factor of 10 in rates) is introduced by the treatment of "floppy" large amplitude motions. The most common type of large amplitude motion in hydrocarbon chemistry is hindered internal rotation. Methods for computing rotor partition functions have not advanced very much since the classic work of Pitzer. To tighten the uncertainties in our rate predictions, we recently performed the first calculations which take the couplings between the large-amplitude rotation and the other modes into account, to see how much they affect kinetic and thermodynamic properties. We constructed [11] a Hamiltonian that picks up the dominant kinetic energy and potential energy couplings between this mode and the stiff small-amplitude vibrations.

We were able to convert this into an effective Hamiltonian for the internal rotation that can be solved numerically.

The couplings between the internal rotation and the other modes are found to have big effects on the energy spectrum, though most of these effects average out when one computes the thermal partition function. Larger effects are seen on some reaction rates, where certain internal rotations change dramatically as the reaction proceeds, and so are strongly coupled with the reaction coordinate. This new approach gives excellent predictions for the experimental heat capacities of methanol and propene, and more reliable predictions for reaction rates such as $CH_3 + CH_3OH$. The next step is to integrate these calculations into the automated rate-estimation software.

II. Progress in "Adaptive Chemistry" Reacting Flow Simulations

Reacting flow simulations are most valuable for reactors/combustors with large concentration or temperature gradients, where one expects the chemistry to be dramatically different in different spatial regions (or at different times in a dynamic simulation). However, most reacting flow simulations are performed using the same chemistry model at all mesh positions and at all times. These calculations typically require a very large amount of CPU time and computer memory, limiting most reacting-flow simulations of hydrocarbon combustion to oversimplified chemical kinetic models.

Computational efficiency without sacrificing accuracy is possible by 'adapting' the chemistry model to the local reaction conditions in much the same way that modern simulations use adaptive time-steps and adaptive mesh refinement. The idea in all three cases is to use a lot of detail when it is necessary, but to use a less-detailed description whenever possible without sacrificing accuracy. Our Adaptive Chemistry approach of ignoring chemical species where they are insignificant is very advantageous, since the best available methods for solving the kinetic equations and for computing the multicomponent diffusion coefficients both scale super-linearly with the number of chemical species considered.

We have implemented Adaptive Chemistry [12] into a CFD code for 2-d steady laminar or turbulent (RANS) reacting flows. At each macro-iteration the computer selects the chemistry model appropriate for each finite volume based on the current estimate of the local state variables (concentrations, temperature, etc.). The CFD code then advances by one or more time-steps Δt_{flow} (converging to a steady-state solution at long times). The chemistry model is solved over each period Δt_{flow} using a stiff ODE solver, while the flow equations are solved using a preconditioned diagonalized ADI approach [13]. Our operator-splitting strategy is particularly effective for finding accurate steady-state solutions when the chemical kinetic equations are stiff. After reaching convergence with the given chemistry models, the appropriateness of each kinetic model for the local reaction conditions is checked, and if inappropriate they are replaced and the next macro-iteration begins.

As an example, we have simulated a methane burner flame using a 217 reaction mechanism. The Adaptive Chemistry calculation is more than a factor of 6 faster than the conventional full-chemistry simulation (which took a week of CPU time), and requires only 1/8 as much memory. Better speed-ups are certainly achievable with more refined reduced kinetic models. We have recently developed an effective algorithm for generating the required reduced models based on global optimization theory.[14]

Future Plans

We will proceed along 3 research directions. First, we will continue to develop improved rate estimates for computer-construction of combustion models, in the context of our TS Group Additivity approach, with close coupling to our ASA method of computing k(T,P) and our new method for accurately handling internal rotations. Second, in collaboration with R.W. Field, we will experimentally test the rate predictions for relatively several unsaturated free radicals, taking advantage of their strong absorption spectra, which we have recently observed. Finally, we will continue to develop the "Adaptive Chemistry" technique in collaboration with established CFD groups, using our new methods for 'optimal' model reduction to construct the required reduced models. We expect this "Adaptive Chemistry" work will be funded by SciDAC and non-BES sources.

Publications Resulting from DOE Sponsorship (Since 1999)

1. D.M. Matheu & W.H. Green, "*A priori* Falloff Analysis for OH + NO_2", *Int. J. Chem. Kinetics* **32**, 245-262 (2000).
2. H. Richter, T.G. Benish, O.A. Mazyar, W.H. Green, & J.B. Howard, "Formation of Polycyclic Aromatic Hydrocarbons and their Radicals in a Nearly Sooting Premixed Benzene Flame", *Proc. Combust. Inst.* (2000).
3. H. Richter, O.A. Mazyar, R. Sumathi, W.H. Green, J.B. Howard, & J.W. Bozzelli, "Detailed Kinetic Study of the Growth of Small Polycyclic Aromatic Hydrocarbons. I. 1-Naphthyl + Ethyne", *J. Phys. Chem. A* (2001).
4. W.H. Green, P.I. Barton, B. Bhattacharjee, D.M. Matheu, D.A. Schwer, J. Song, R. Sumathi, H.H. Carstensen, A.M. Dean, & J.M. Grenda, "Computer-Construction of Detailed Models for Gas-Phase Reactors", *Ind. & Eng. Chem. Res.* (2001).
5. D.M. Matheu, T.A. Lada, W.H. Green, A.M. Dean, & J.M. Grenda, "Rate-Based Screening of Pressure-Dependent Reaction Networks", *Comp. Phys. Commun.* (2001).
6. R. Sumathi, H.H. Carstensen, & W.H. Green, "Reaction Rate Prediction via Group Additivity, Part 1: H Abstraction from Alkanes by H and CH_3", *J. Phys. Chem. A* (submitted).
7. R. Sumathi, H.H. Carstensen, & W.H. Green, "Reaction Rate Prediction via Group Additivity, Part 2: H Abstraction from Alkenes, Alkynes, Alcohols, Aldehydes and Acids by H atoms", *J. Phys. Chem. A* (submitted).

Other Literature Cited

8. R.G. Susnow, A.M. Dean, W.H. Green, P. Peczak, & L.J. Broadbelt, *J. Phys. Chem. A* **101** (1997) 3731-3740.
9. A.Y. Chang, J.W. Bozzelli, & A.M. Dean, *Z. Phys. Chem.* **214** (2000) 1533-68.
10. J.R. Barker, *Int. J. Chem. Kinet.* 33 (2001) 246-251.
11. M.J. Bramley, W.H. Green, & N.C. Handy, *Mol. Phys.* **73** (1991) 1183.
12. W.H. Green & D.A. Schwer, "Adaptive Chemistry", *Proc. First MIT Conference on Fluid & Solid Mechanics* (2001).
13. D.A. Schwer & W.H. Green, "Split-Operator Methods for Computing Steady-State Reacting Flow-fields", *Proc. 15th AIAA Computational Fluid Dynamics Conference*, Anaheim, CA (2001).
14. B. Bhattacharjee, W.H. Green, P.I. Barton, "Globally Optimal Model Reduction", AIChE National Meeting, Los Angeles, CA (2000).

HIGH-RESOLUTION SPECTROSCOPIC PROBES OF CHEMICAL DYNAMICS*

Gregory E. Hall (gehall@bnl.gov)
Chemistry Department, Brookhaven National Laboratory, Upton, NY 11973-5000

PROGRAM SCOPE

This research is carried out as part of the Gas Phase Molecular Dynamics group program in the Chemistry Department at Brookhaven National Laboratory. High resolution spectroscopic tools are developed and applied to problems in chemical dynamics. Recent topics have included the dynamics of barrierless unimolecular reactions, unimolecular rate theory, multiple surface branching reactions and coherent effects in direct multi-surface dissociations, kinetics, and the spectroscopy of transient species.

RECENT PROGRESS

A. Experimental and Theoretical Studies of Dynamical Effects on Barrierless Unimolecular Reactions

The photoinitiated dissociation of ketene to singlet CH_2 and CO has already provided one of the most rigorous and complete benchmarks for the validation of variational RRKM theory for computation of microcanonical rates in a barrierless polyatomic dissociation. The energy dependence of the product distributions shows a pattern of deviations from the phase space theory (PST) limit, that have not been specifically addressed by more advanced theory. State-resolved fragment velocity distributions are directly related to the coincident internal energy distribution of the undetected co-fragment. A series of such measurements can be used to construct the two-dimensional joint product distribution, row by row, or column by column, depending on which fragment is detected. The way in which the product distribution begins to deviate from the phase space theory (PST) limit as the excess energy is increased can be used to test our understanding of the variational transition state and the orientational couplings and energy transfer between fragments beyond the transition state.

We have measured nascent photofragment Doppler absorption spectra of CH_2 using transient FM Doppler spectroscopy in a pulsed slit jet expansion. Supersonic expansion cooling provides an essential sharpening of the internal energy distribution of the precursor molecules and improves the velocity resolution of the fragment Doppler spectra by cooling the transverse velocity distribution of the parent molecules. Building on extensive previous spectroscopic studies of singlet methylene in our group, we have measured velocity distributions of selected rotational states of CH_2 in its vibrational ground state, following optical excitation about 2350 cm^{-1} above the threshold for dissociation to CO and singlet CH_2. These velocity distributions can be directly related to the energy distributions of CO produced in coincidence with the selected CH_2 states. The correlated state distributions offer a penetrating look at the dynamical effects influencing the deviations from statistical product distributions. It has been known that at total energies 2000-3000 cm^{-1} above the singlet CH_2 threshold, the rotational distribution of vibrationless CH_2 is colder than statistical, while the CO produced in the vibrationless channel is slightly hotter than statistical. The correlated state measurements provide a more distinctive data set, from which we attempt to understand this pattern in terms of energy dependent variational transition states, energy transfer between CO and CH_2 in the exit channel, or possible non-statistical effects at the transition state.

In collaboration with S. Gray (ANL) and S. Klippenstein (Sandia CRF), direct *ab initio* dynamics calculations have been performed to investigate the effects of orientational couplings between CH_2 + CO beyond the variational transition state, and to search for explanations for the patterns in the product state distributions. The suppression of high rotational states of CH_2 among the reaction products, compared to

*This work was performed at Brookhaven National Laboratory under Contract No. DE-AC02-98CH10886 with the U.S. Department of Energy and supported by its Division of Chemical Sciences.

a statistical product distribution, is reproduced in the exit channel dynamics calculations. The relative deficiency of low internal energy fragment pairs, compared to the statistical product distribution, is not reproduced in the calculations.

B. Adiabatic/Nonadiabatic Branching and Coherent Effects on Multiple Potential Energy Surfaces

We have completed an extensive experimental study of the near UV photodissociation of ICN, a prototype system displaying direct dissociation on multiple, coupled surfaces. The technique of transient FM Doppler spectroscopy is ideally suited for the investigation of the highly polarized CN photofragments produced in this dissociation. The studies entailed a substantial amount of development of both instrumental and mathematical analysis tools to identify, optimize and extract the dynamical content of the FM Doppler lineshape measurements. In addition to the advances made in probing the multiple surface dynamics of ICN dissociation, the development of transient FM Doppler spectroscopy as a quantitative tool for polarized photofragment analysis has been a major recent accomplishment.

New insights gained from recent ICN experiments are relevant to the axial recoil limit of direct photodissociation, in which the radial separation of fragments is rapid compared to the tangential motion of the rotating precursor molecule. Parallel and perpendicular transitions are simultaneously allowed at the same wavelength, and may lead to the same fragment states via adiabatic and nonadiabatic paths. In the axial recoil limit, these paths are distinguishable by means of their angular distribution, which acts as a polarization label. All of the high-*j* photofragment properties observable with linearly polarized one-photon absorption spectroscopy: branching ratios, velocity anisotropy, and rotational alignment are insensitive to phase differences between the two paths. With circularly polarized photolysis and probe light, two additional photofragment properties are observable: a coherent and an incoherent orientation. These two orientation mechanisms are distinguishable by the velocity dependence of the circular dichroism. The experiments are easier than the analysis and interpretation.

FUTURE WORK

A. Rotational polarization as a probe of multiple surface dynamics

In ICN, we are continuing the analysis and interpretation of circularly polarized transient FM Doppler spectroscopy. In an absorption experiment, it is only with circularly polarized light that the multiple path interference effects in this system can be detected. Experimental results show a previously unobserved velocity dependence to the CN orientation. The variation of the circular dichroism with Doppler shift shows the predicted signature of a coherent mechanism for fragment orientation. The coherence is between parallel and perpendicular transitions from the same initial state, resulting in the same fragment state. This coherent orientation has been recorded as a function of CN rotational state and coincident I spin-orbit state at 248 nm and 266 nm. We can confirm previous speculation, based on lower resolution LIF experiments, that many CN rotational states have opposite space-fixed orientations for fast and slow components, coincident with $I(^2P_{3/2})$ and $I(^2P_{1/2})$. The fragment orientation displays variations with rotational state and photolysis energy as well as the coincident iodine channel.

Low rotational states of CN produced by circularly polarized photodissociation light can theoretically display an additional, different type of velocity-dependent circular dichroism, arising from an incoherent orientation. This effect arises from a pure perpendicular transition, excited by circularly polarized light, in which the photofragment expresses the excess single quantum of angular momentum in the same direction as the photon. The effect becomes negligible at high rotational levels, but has a predictable magnitude and sign for low-*j* fragments. Remarkably, the predicted signature of this incoherent orientation is completely absent from the low-*j* CN fragments, which continue to show only coherent orientation. We speculate that the symmetry of the surface couplings is responsible for this loss of incoherent orientation. Low rotational levels of CN are only produced in the excited, $I(^2P_{1/2})$ channel, which is produced only on surfaces of A′ symmetry.

The incoherent orientation is characterized by selective optical excitation to $\Omega = +1$ or -1 components of the $^1\Pi_1$ excited state, depending on the space-fixed direction of the body axis. Propagation on the coupled surfaces resolves pure Ω states into mixtures of A′ and A″, which diverge into different product channels. The low-*j* states are only produced along A′ symmetry paths, destroying the incoherent orientation in a way we suspect is analogous to the action of a linear polarizer on a circularly polarized beam of light.

In order to measure the quantitative polarization properties of the low-*j* CN fragments crucial for this analysis of coherent and incoherent orientation effects, we need to address questions of depolarization due to spectator electron and nuclear spins. Some initially surprising quantum beat patterns have been observed in the polarization properties of low-*j* CN states. The depolarization due to electron spin (***N*** precessing around ***J***=***N***+***S***) is completely avoided by spectroscopic resolution of the fine structure states (***J***=***N***+½ and ***N***-½). The hyperfine depolarization (***J*** precessing around ***F***=***J***+***I***) is fully time resolved with periods of 20-100 ns. Observing the time-dependent alignment and orientation allows us to estimate the "intrinsic" alignment and orientation (of ***J***, not ***N***) that characterize the dissociation prior to depolarization.

B. Barrierless unimolecular dynamics

New experiments are in progress to measure correlated state distributions for the ketene dissociation at available energies closer to threshold. These measurements should be able to characterize the onset of the non-statistical effects at lower energies. The first excited bending state (010) of CH_2 is produced at 308 nm with an excess energy of about 1000 cm^{-1}. We hope to measure coincident CO rotational distributions for selected rotational states of $CH_2(010)$ using hot band transitions that were inaccessible with the laser system used in the earlier experiments.

DOE SPONSORED PUBLICATIONS SINCE 1999

The E-X spectrum of jet-cooled TiO observed in absorption, K. Kobayashi, G. E. Hall, J. T. Muckerman, T. J. Sears, and A. J. Merer, (submitted 2001)

An ab initio molecular dynamics study of S_0 ketene fragmentation, K. M. Forsythe, S. K. Gray, S. J. Klippenstein and G. E. Hall, (submitted 2001)

State correlations in the unimolecular dissociation of ketene, M. L. Costen, H. Katayanagi and G. E. Hall, *J. Phys. Chem. A.* **104**, 10247-10258 (2000)

Near infrared spectroscopy of bromomethylene in a slit jet expansion, B.-C. Chang, M. L. Costen, A. J. Marr, G. Ritchie, G. E. Hall and T.J. Sears, *J. Molec. Spectrosc.* **202**, 131-43 (2000)

Transient frequency modulation absorption spectroscopy of molecules produced in a laser ablation supersonic expansion source, T. C. Steimle, M. L. Costen, G. E. Hall, and T. J. Sears, *Chem. Phys. Lett.* **319**, 363-67 (2000)

Transient Laser Frequency Modulation Spectroscopy, G. E. Hall and S. W. North, *Annu. Rev. Phys. Chem.* **51**, 243-74 (2000)

Relationship between bipolar moments and molecule-frame polarization parameters in Doppler photofragment spectroscopy, T. Peter Rakitzis, G. E. Hall, M. L. Costen and R. N. Zare, *J. Chem. Phys.* **111**, 8751-54 (1999).

Vector Signatures of Adiabatic and Diabatic Dynamics in the Photodissociation of ICN, M. L. Costen, S. W. North and G. E. Hall, *J. Chem. Phys.* **111**, 6735-49 (1999).

A Kinetics and Product Study of the Reaction of CH_3 Radicals with $O(^3P)$ Atoms using Time Resolved Time-of-Flight Spectrometry, C. Fockenberg, G. E. Hall, J. M. Preses, and J. T. Muckerman, *J. Phys. Chem. A.* **103**, 5722-31 (1999).

Repetitively Sampled Time-of-Flight Mass Spectrometry for Gas-Phase Kinetics Studies, C. Fockenberg, H. J. Bernstein, G. E. Hall, J. T. Muckerman, J. M. Preses, T. J. Sears, and R. E. Weston, Jr., *Rev. Sci. Instr.* **70**, 3259 (1999).

SPECTROSCOPY AND KINETICS OF COMBUSTION GASES AT HIGH TEMPERATURES

Ronald K. Hanson and Craig T. Bowman
Department of Mechanical Engineering
Stanford University, Stanford, CA 94305-3032
hanson@me.stanford.edu, bowman@navier.stanford.edu

Program Scope

This program involves two complementary activities: (1) development and application of cw laser absorption methods for the measurement of species concentrations and fundamental spectroscopic parameters of species of interest in combustion; and (2) shock tube studies of reaction kinetics relevant to combustion. Species investigated in the spectroscopic portion of the research include: NO_2, using fixed-frequency UV diode laser absorption; H_2O, using tunable near-IR diode laser absorption; OH and CH_3, using narrow-linewidth UV ring dye laser absorption; and NH_2 and OH, using frequency-modulation laser absorption methods. Reactions of interest in the shock tube kinetics research include: $NH_2 + NO \rightarrow$ Products; $H + O_2 + M \rightarrow HO_2 + M$, with M = Ar, N_2, H_2O; $C_2H_6 \rightarrow CH_3 + CH_3$; and $CH_3 + O_2 \rightarrow$ Products.

Recent Progress

Shock Tube Chemical Kinetics

We have completed investigation of the pressure-dependent reaction

$$H + O_2 + M \rightarrow HO_2 + M, \quad \text{with M = Ar, } N_2\text{, and } H_2O, \qquad (1)$$

using a high-pressure shock tube facility. This reaction plays a significant role in the ignition process and in the noncatalytic process for NO-removal (SNCR) from combustion products. Reaction (1) was kinetically isolated by monitoring NO_2 concentrations in relatively low temperature (1050 - 1250 K), but high pressure (7 - 152 atm) $NO/H_2/O_2/Ar$ shock tube experiments. Values of k_1 were inferred from comparisons of measured NO_2 concentration profiles, whose plateau values show a strong sensitivity to this rate coefficient, with profiles modeled using the GRI-Mech mechanism. Errors attributable to the calibration were reduced by a careful study of the temperature and pressure dependence of the absorption coefficient of NO_2 at the Ar^+ laser wavelength 472.7 nm. To measure the reaction rate for M=N_2 or H_2O, some of the argon was replaced by N_2 or H_2O. The present results for k_1 exhibit significantly reduced scatter compared with previous literature values. A simple modified hindered-Gorin model of the transition state was used in an RRKM analysis of the results to facilitate comparisons of this work with measurements from other researchers at lower pressures. Measured values of the reaction rate for M = Ar in the highest pressure experiments fall below both simple RRKM analysis and the more sophisticated treatment of Troe using an *ab initio* potential energy surface. Collision efficiencies of N_2 and H_2O relative to Ar at 1200 K are 3.3 and 20 respectively.

We have used a low-pressure shock tube facility to investigate the two primary channels of the reaction of NH_2 and NO,

$$NH_2 + NO \rightarrow OH + NNH \quad (2a)$$
$$NH_2 + NO \rightarrow N_2 + H_2O \quad (2b)$$

The branching ratio, $\alpha = k_{2a}/(k_{2a}+k_{2b})$, of these two primary channels is an important parameter in the modeling of NO_X reduction by the Thermal $DeNO_X$ process. Our approach is to take advantage of the very high sensitivity of NH_2 detection available with frequency-modulation (FM) spectroscopy methods to establish accurate high-temperature values of both the overall rate and the branching ratio. In particular, using low (ppm level) concentrations of NH_2 generated by excimer laser photolysis of NH_3/NO/Ar mixtures, it is possible at certain conditions to measure α with minimum dependence on the overall rate coefficient. This results in a very accurate determination of the branching ratio near $\alpha = 0.5$. The best-fit curve of selected recent determinations over the temperature range 300 –2000 K is given by $\alpha = 0.057 + 7.01 \times 10^{-6} \times (T/K)^{1.503}$.

The overall rate coefficient of the reaction $NH_2 + NO \rightarrow$ products is also being determined in shock tube experiments using FM detection of NH_2. The source of the NH_2 radicals in the experiments is the thermal decomposition of CH_3NH_2, monomethylamine, or $C_6H_5CH_2NH_2$, benzylamine. To determine k_{2a+2b}, a perturbation strategy is employed that is based on changes in the NH_2 profiles when NO is added to the precursor/Ar mixtures. Sensitivity analysis shows that NH_2 profiles in the precursor/NO/Ar mixtures are sensitive primarily to the overall rate, with low sensitivity to the branching ratio and other NH_2 reactions, when low concentrations of NH_2 are utilized. The measured NH_2 profiles are interpreted by detailed kinetic modeling to obtain k_{2a+2b} values in the temperature range 1262-1726 K using benzylamine, and 1716-2507 K using monomethylamine, the lower temperature experiments overlapping with the Thermal DeNOx window; see Fig. 1.

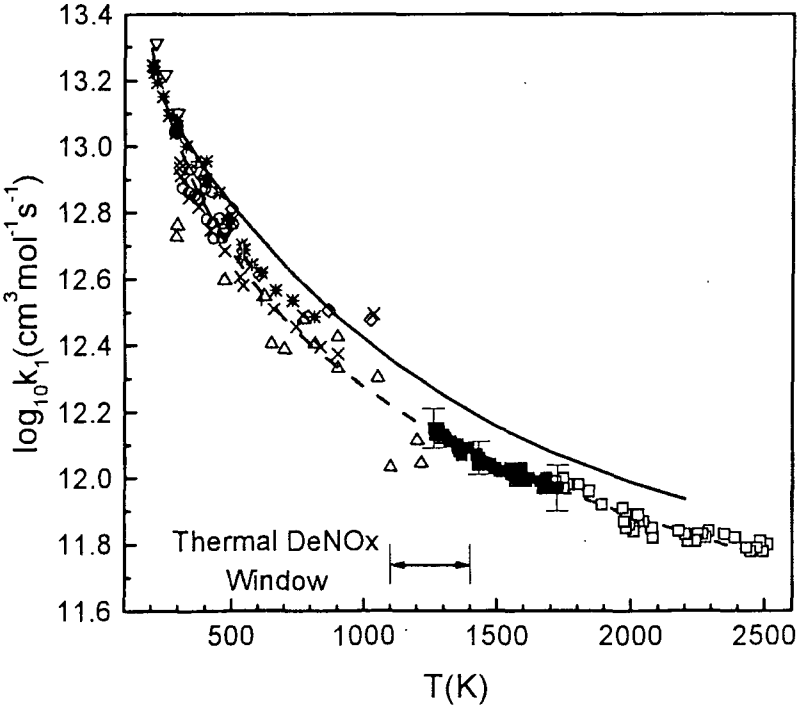

Fig. 1. Summary of k_1: ■ Data from benzylamine experiments; □ data from monomethylamine experiments; ○ Lesclaux et al. (1975); △ Silver and Kolb (1982); ▽ Stief et al. (1982); ◇ Atakan et al. (1989); + Wolf et al. (1994); × Park and Lin (1997); ✳ Wolf et al. (1997); — Miller and Klippenstein (2000); - - - best fit. The vertical bars represent the combined fitting errors and uncertainties associated with secondary reactions.

The present k_{2a+2b}-values are consistent with recent theoretical results of Miller and co-workers. There is no evidence for a positive activation energy for this reaction at elevated temperatures as reported in several other high-temperature experimental studies. Combining the present high-temperature data with lower temperature determinations yields the following simple expression for the overall reaction rate, $k_{2a+2b} = 6.83 \times 10^{15} T^{-1.20} \exp(106/T)$ [cm^3/mol/s] for the temperature range 300-2500K.

Absorption Diagnostics and Spectroscopy

We are continuing to apply FM absorption spectroscopy methods to NH_2 detection at 597 nm. This method, similar to that used by Sears and colleagues at Brookhaven, allows direct cancellation of the noise caused by the interaction of the laser beam and the shock-induced flow. Using this method we have achieved a minimum detectable absorption of 0.01% in a single-pass configuration, which represents a factor of 10-20 improvement in detection sensitivity over conventional laser absorption. New work is aimed at extending FM spectroscopy to ultra-sensitive detection of OH.

In a new effort, we are investigating the collision-width and -shift parameters of several rotational lines in the OH A-X(0,0) band using our novel rapid-tuning ring dye laser. This work should improve understanding of the collision parameters for OH and their dependences on rotational quantum number J", rotational branch, and temperature. Correct understanding of lineshape parameters are critical to the accuracy of the OH laser absorption diagnostic in shock tube work. The shift measurements are being performed using a shock tube and an atmospheric flame, along with a low pressure reference cell. We have continued to improve the signal-to-noise ratio of these laser absorption measurements through installation of a low-noise, solid-state cw pump laser; the use of frequency modulation for signal noise reduction; and large area detectors to permit operation at high pressures where beam steering effects are greatest.

An improved diagnostic for monitoring NO_2 over the temperature range 300 to 2000 K has been developed utilizing a tunable diode laser at 390.130 nm. This improvement is possible because of the higher absorption coefficient at this wavelength compared to that previously used (472.7 nm generated with an Ar+ laser), and the low noise properties of the grating-stabilized external cavity diode laser. When this diagnostic was used to investigate the decomposition reaction: $NO_2 + Ar = NO + O + Ar$, good agreement between modeling and experiment was achieved if we used the recent rate coefficient measurement by Rohrig et al. (1997) in our laboratory.

Measurement of the rate coefficient for $H+O_2+H_2O$ requires accurate measurements of water concentration in the shock tube. Determination of pre-shock water vapor concentration is performed using semiconductor diode laser absorption at wavelengths near 1405 nm. Very little experimental collision-broadening data exists in the literature on these transitions, and hence we have conducted a series of tests over an extended range of temperature (300-2000 K) to acquire these data. We have also measured the pressure-shift of these transitions using shock waves to generate step changes in pressure.

Improvements have recently been made to the BBO frequency-doubling ring dye system that is used to generate radiation in the 212 to 230 nm range. More stable operation and higher powers have been achieved with the use of a high-performance external doubling cavity.

Future Plans

A. Shock Tube Kinetics

Work will proceed on several fronts. 1) Complete studies of the reaction NO + NH_2 → products, including determination of the overall reaction rate and branching ratio. 2) Investigate the chemistry of benzylamine, C_6H_5-CH_2-NH_2, which was used as a precursor for NH_2 radicals. 3) Complete RRKM studies of the reaction H + O_2 + M → HO_2 + M with M = H_2O, N_2, and Ar. 4) Initiate studies of the reaction CH_3 + O_2 → products, using high-sensitivity FM laser absorption methods.

B. Fundamental Spectroscopy and Laser Diagnostics Development

Work will proceed on several fronts. 1) Develop second-generation improvements to the frequency modulation absorption diagnostic used in the NH_2 studies at 597 nm. 2) Extend the frequency modulation laser absorption technique to the detection of OH at 306 nm. 3) Develop techniques to measure CH_3 quantitatively at high pressures using laser absorption at 216 nm. 4) Continue modeling and measurement of collision-broadening and -shift parameters of OH near 306 nm at low and high pressures.

Publications of DOE Sponsored Research (1999-2001)

1. J. T. C. Liu, R. K. Hanson and J. B. Jeffries, "High-Sensitivity Absorption Diagnostic for NO2 Using a Blue Diode Laser," accepted for publication, J. Quant. Spectrosc. Radiat. Transfer (2001).

2. R. W. Bates, D. M. Golden, R. K. Hanson, and C. T. Bowman, "Experimental Study and Modeling of the Reaction H + O_2 + M = HO_2 + M (M = Ar, N_2, H_2O) at Elevated Pressures and Temperatures between 1050 and 1250 K," Phys. Chem. Chem. Phys. 3, advance article (2001).

3. J. T. Herbon and R. K. Hanson, "Measurements of Collision-Shift in Absorption Transitions of the OH A-X (0,0) Band using a Shock Tube," accepted for publication in the proceedings of the 23rd International Symposium on Shock Waves (2001).

4. D. F. Davidson and R. K. Hanson, "Spectroscopic Diagnostics," Chapter 5.2 in *Handbook of Shock Waves*, G. Ben-Dor, O. Igra, and T. Elperin eds. Academic Press, San Diego, 2001.

5. S. Song, R. K. Hanson, C. T. Bowman, and D. M. Golden, "Shock Tube Determination of the Overall Rate of NH_2+NO → Products at High Temperatures," accepted for publication in the Proceedings of the Twenty-eighth Symposium (International) on Combustion (2000).

6. E. L. Petersen and R. K. Hanson, "Non-Ideal Effects Behind Reflected Shock Waves in a High-Pressure Shock Tube," Shock Waves 10, 405-420 (2000).

7. V. Nagali, D. F. Davidson and R. K. Hanson, "Measurements of Temperature-Dependent Argon-Broadened Half-Widths of H_2O Transitions in the 7117 cm-1 region," J. Quant. Spectrosc. Radiat. Transfer 64, 651-655 (2000).

8. M. Votsmeier, S. Song D. F. Davidson and R. K. Hanson, " A Shock Tube Study of Monomethylamine Thermal Decomposition and NH_2 High Temperature Absorption Coefficient," Int. J. Chem. Kinet. 31, 323-330 (1999).

9. M. Votsmeier, S. Song, D. F. Davidson and R. K. Hanson, "Sensitive Detection of NH_2 in Shock Tube Experiments using Frequency Modulation Spectroscopy," Int. J. Chem. Kinet. 31, 445-453 (1999).

10. M. Votsmeier, S. Song, R. K. Hanson and C. T. Bowman, "A Shock Tube Study of the Product Branching Ratio for the Reaction NH_2+NO using Frequency-Modulation Detection of NH_2," J. Phys. Chem. A 103, 1566-1571 (1999).

Theoretical Studies of Potential Energy Surfaces*

Lawrence B. Harding
Chemistry Division
Argonne National Laboratory
Argonne, IL 60439
harding@anl.gov

Program Scope

The goal of this program is to calculate accurate potential energy surfaces for both reactive and non-reactive systems. Our approach is to use state-of-the-art electronic structure methods (MR-CI, CCSD(T), etc.) to characterize multi-dimensional potential energy surfaces. Depending on the nature of the problem, the calculations may focus on local regions of a potential surface (for example, the vicinity of a minimum or transition state), or may cover the surface globally. A second aspect of this program is the development of techniques to fit multi-dimensional potential surfaces to convenient, global, analytic functions that can then be used in dynamics calculations. Finally a third part of this program involves the use of direct dynamics for high dimensional problems to by-pass the need for surface fitting.

Recent Results

Potential Surfaces: A feature of this program is the development of analytic potential surfaces that can be used in subsequent dynamical studies. This year a three dimensional surface characterizing the long-range interaction between OH and CO was completed using CCSD(T)/aug-cc-pvdz calcualtions. The calculations show that the long-range potential is dominated by the electrostatic interaction between the quadrupole of CO and the dipole of OH. This leads to two collinear minima , OH-CO and OH-OC, of which, the OH-CO minimum is predicted to be more stable. Planar minimum energy paths were followed to shorter distances. These calculations show that the more stable collinear minimum correlates directly to the transition state leading to the covalently bound HOCO intermediate. The 3D analytic surface is now being used in quantum dynamics calculations by Gray with the goal of aiding in the assignment of the IR action spectrum observed by Lester and co workers.

Also completed this year were studies of the HO_2 potential surface from both the $H+O_2$ and OH+O directions. This work was done in collaboration with Jürgen Troe.

CH_3+O→ products: Most combustion models assume the reaction of CH_3 with O atoms occurs as follows,

$$CH_3+O\rightarrow CH_3O\rightarrow H+H_2CO.$$

In 1992, Seakins and Leone[1] reported the observation of CO as a direct product in this reaction. This result has now been confirmed by three, more recent experiments[2-4]. However, calculations by the author have failed to find any accessible reaction paths leading to the observed CO product. This year we have completed a higher level, CCSD(T)/aug-cc-pvtz, re-investigation of this surface. The new study confirms our earlier finding that there are no accessible reaction paths connecting the reactants, CH_3+O, with the observed CO product. We have also completed (in collaboration with Stephen Klippenstein) a direct dynamics, classical trajectory, simulation of this reaction, using a B3LYP/6-31G* surface. The simulation predicts a CO yield of ~15%, in excellent agreement with the Brookhaven[3,4] experiments. Analysis of the trajectories shows that the CO is produced in a step-wise process,

$$CH_3+O\rightarrow CH_3O\rightarrow H_2+HCO\rightarrow H+H_2+CO$$

where the second step (elimination of H_2 from CH_3O) occurs over a barrier but not through a saddle point. Due to the large amount of excess energy available to the chemically activated methoxy radicals, some trajectories cross into the H_2+HCO valley even though the only accessible saddle points for decomposition of methoxy lead to H+H_2CO. One trajectory showing a typical path for this second step is shown below:

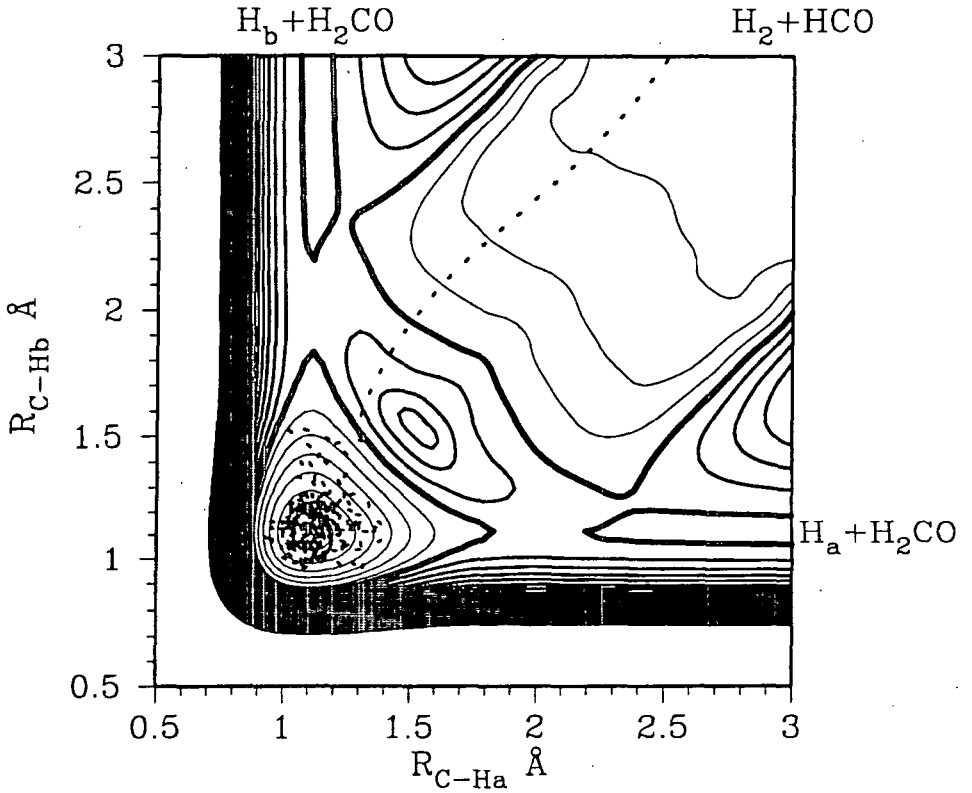

Our calculations also predict the branching ratio to CO in the CD_3+O reaction is significantly smaller than in CH_3+O. The calculated isotope effect on the branching ratio is in quantitative agreement with a recent measurement by Leone and coworkers.

Heat of formation of OH: The currently accepted heat of formation of OH is based on Birge-Sponer extrapolations of the vibrational levels of the A state of OH. This year we completed a simulation of the extrapolation using a CAS+1+2/aug-cc-pV5Z potential curve. The conclusion from this work is that although the experimental extrapolation is very short, (only one bound vibrational level was not observed) the resulting bond energy is liable too high by ~0.5 kcal/mole. This conclusion is in agreement with new positive ion cycle measurements by Ruscic and a direct, high level, ab initio calculation of the heat of formation by Feller and coworkers.

Future Plans

We have now used direct transition state theory coupled with multi-reference CI calculations to predict recombination rates for CH_3+CH_3, CH_3+OH (in progress) and OH+N_2H. We plan to extend these studies to several O atom recombination reactions, including O+CH_3, O+C_2H_5 and O+HCO. We also plan to use this technique to study some more complicated radical-radical recombinations involving hydrocarbon radicals such as CH_3+C_2H_3 and C_2H_3+C_2H_3. The direct dynamics/classical trajectory study we completed this year on O+CH_3 demonstrates the

feasibility of using this approach to address questions concerning product branching ratios in radical-radical recombination reactions. We now plan to use this technique on several more complicated reactions such as $O+C_2H_5$ and $CH_3+C_2H_3$.

Acknowledgement: This work was performed under the auspices of the Office of Basic Energy Sciences, Division of Chemical Sciences, U.S. Department of Energy, under Contract W-31-109-Eng-38.

References:

(1) P.W. Seakins and S.R. Leone, *J. Phys. Chem.* **96**, 4478 (1992).
(2) Z. Min, R.W. Quandt, T.-H. Wong and R. Bersohn, *J. Chem. Phys.* **111**,7369(1999).
(3) C. Fockenberg, G.E. Hall, J.M. Preses, T.J. Sears, and J.T. Muckerman, *J. Phys. Chem. A,* **103**,5722(1999).
(4) J.M. Preses, C. Fockenberg, and G.W. Flynn, *J. Phys. Chem. A*, **104**, 6758 (2000).

PUBLICATIONS (1999 - Present):

New Studies of the Unimolecular Reaction $NO_2 \rightarrow O+NO$. II. Relation between High Pressure Rate Constants and Potential Parameters, L. B. Harding, H. Stark, J. Troe, and V.G. Ushakov *Phys. Chem. Chem. Phys.* **1**, 63-72 (1999)

A Theoretical Study of the Kinetics of C_2H_3+H, S.J. Klippenstein and L.B. Harding *Phys. Chem. Chem. Phys.* **1**, 989-997 (1999)

Exploring the Reactions Dynamics of Nitrogen Atoms: A combined Crossed Beam and Theoretical Study of $N(^2D)+D_2 \rightarrow ND+H$, M. Alagia, N. Balucani, L. Cartechini, P. Cassavecchia, G.G. Volpi, L.A. Pederson, G.C. Schatz, G. Lendvy, L.B. Harding, T. Hollebeek, T.-S. Ho and H. Rabitz, *J. Chem. Phys.* **110**, 8857-8860 (1999)

Reaction of H with Vibrationally Excited Water: Activated or Not ?, G.C. Schatz, G. Wu, G. Lendvay, D.-C. Fang, L.B. Harding, *Faraday Discussions* **113**, 151-165 (1999)

A Direct Transition State Theory Based Study of Methyl Radical Recombination Kinetics S.J. Klippenstein and L.B. Harding, *J. Phys. Chem.* **103**, 9388-9398 (1999)

An Empirical Potential Surface for the Ne-OH/D Complexes, H.-S. Lee, A.B. McCoy, L.B. Harding, C.C. Carter and T.A. Miller, *J. Chem. Phys.* **111**, 10053-10060 (1999)

Potential Energy Surface and Quasiclassical Trajectory Studies of the $N(^2D)+H_2$ Reaction L.A. Pederson, G.C. Schatz, T.-S. Ho,T. Hollebeek, H. Rabitz, L.B. Harding and G. Lendvay *J. Chem. Phys.* **110**, 9091-9100 (1999)

Classical Trajectory Calculations of the High Pressure Limiting Rate Constants and of Specific Rate Constants for the Reaction $H+O_2 \rightarrow HO_2$: Dynamic Isotope Effects Between Tritium+O_2 and Muonium+O_2, L.B. Harding, J. Troe, and V.G. Ushakov, *Phys. Chem. Chem. Phys.* **2**, 631-642 (2000)

Potential Energy Surface of the A State of NH_2 and the role of Excited States in the $N(^2D)+H_2$ Reaction, L.A. Pederson, G.C. Schatz, T. Hollebeek, T.-S. Ho, H. Rabitz and L.B. Harding, *J. Phys. Chem.* **104**,2301-2307 (2000)

A Summary of "A Direct Transition State Theory Based Study of Methyl Radical Recombination Kinetics", S.J. Klippenstein and L.B. Harding, *J. Phys. Chem.* **104**,2351-2354 (2000)

Barrier to Methyl Internal Rotation of 1-Methylvinoxy Radical in the X(^{2}A") and B(^{2}A") States: Experiment and Theory, S. Williams, L.B. Harding, J.F. Stanton, and J.C. Weisshaar, *J. Phys. Chem. A* **104**,10131-10138(2000)

A New Potential Surface and Quasiclassical Trajectory Study of $H+H_2O \rightarrow OH+H_2$, G.-S. Wu, G.C. Schatz, G. Lendvay, D.-C. Fang, L.B. Harding, *J. Chem. Phys.* **113**, 3150-3161 (2000)

Exploring the OH+CO Reaction Coordinate via Infrared Spectroscopy of OH-CO Reactant Complexes, M. I. Lester, B. V. Pond, D. T. Anderson, L. B. Harding, A. F. Wagner *J. Chem. Phys.* **113**, 9889-9892 (2000)

Statistical Rate Theory for the $HO + O \leftrightarrow HO_2 \leftrightarrow H + O_2$ Reaction System: SACM/CT Calculations between 0 and 5000 K, L.B. Harding, A. I. Maergoiz, J. Troe, and V.G. Ushakov *J. Chem. Phys.* **113**, 11019-11034 (2000)

Is There Evidence for a Lower Enthalpy of Formation of Hydroxyl Radical and a Lower Gas Phase Bond Dissociation Energy of Water, B. Ruscic, D. Feller, D. A. Dixon, K. A. Peterson, L. B. Harding, R. A. Asher, and A. F. Wagner. *J. Phys. Chem. A* **105**, 1-4 (2001)

Construction of reproducing kernel Hilbert space potential energy surfaces for the 1A" and 1A' states of the reaction $N(^2D)+H_2$,
T. Hollebeek, T.-S. Ho, H. Rabitz and L.B. Harding, *J. Chem. Phys.* **114**, 3945-3948 (2001)

Barrier to Methyl Internal Rotation of Cis and Trans 2-Methylvinoxy Radical in the X(^{2}A") and B(^{2}A") States: Experiment and Theory, S. Williams, L.B. Harding, J.F. Stanton, and J.C. Weisshaar, *J. Phys. Chem. A,* (in press)

Initiation in H_2/O_2: Rate Constants for $H_2+O_2 \rightarrow H+HO_2$ at High Temperature,
J.V. Michael, J.W. Sutherland, L.B. Harding, and A.F. Wagner,
28th Symposium (International) on Combustion, (in press)

Theoretical Kinetic Estimates for the Recombination of Hydrogen Atoms with Propargyl and Allyl Radicals,
L.B. Harding and S.J. Klippenstein, *28th Symposium (International) on Combustion,* (in press)

Mapping the $OH+CO \rightarrow HOCO$ reaction pathway through infrared spectroscopy of the OH-CO reactant complex, M. I. Lester, B. V. Pond, M.D. Marshall, D. T. Anderson, L. B. Harding, A. F. Wagner, *Faraday Discussions*, **118** (in press)

Comment on "On the High Pressure Rate Constants for the H/Mu + O_2 Addition Reactions",
L.B. Harding, J. Troe, and V.G. Ushakov, *Phys. Chem. Chem. Phys.* (in press)

A Direct Transition State Theory Based Analysis of the Branching in NH_2+NO, De-Cai Fang, L.B. Harding, S.J. Klippenstein and J.A. Miller,, *Farady Discussions*, **119** (submitted)

Theoretical and Experimental Investigation of the Dynamics of the Production of CO from the CH_3+O and CD_3+O Reactions, T.P. Marcy, R. R. Diaz, D. Heard, S.R. Leone, L.B. Harding and S.J. Klippenstein, *J. Phys. Chem.* (submitted)

Femtosecond Laser Studies of Ultrafast Intramolecular Processes

Carl Hayden
Combustion Research Facility, MS9055
Sandia National Laboratories
Livermore, CA 94551-0969
CCHAYDE@SANDIA.GOV

Program Scope

The purpose of this research program is to characterize important fundamental chemical processes by probing them directly in time. In this work femtosecond laser pulses are used to initiate chemical processes and follow their progress. The development of new techniques that take advantage of the time resolution provided by femtosecond lasers for studies of chemical processes is an integral part of this research.

Our research focuses on studies of ultrafast energy relaxation and unimolecular reaction processes in very highly excited molecules. The goal of these studies is to provide measurements of the time scales for elementary chemical processes that play critical roles in the reaction mechanisms of highly excited reaction intermediates. Over the past several years we have developed femtosecond time-resolved photoelectron spectroscopy as a method for studying ultrafast energy relaxation processes. To extend these studies to processes involving dissociation we recently developed the time-resolved photoelectron-photoion coincidence imaging technique. The apparatus we have constructed for this work can simultaneously measure fragment recoil velocities and photoelectron velocities. This approach provides many new capabilities for femtosecond time-resolved experiments. Of primary interest to us is the ability to study the time evolution of hot radical fragments generated by photolysis of appropriate precursors. Realization of this capability requires the characterization of femtosecond photolysis processes and the development of femtosecond time-resolved ionization probes suitable for hot molecules and also sensitive to the processes, such as isomerization, that are of interest in hot radicals.

Recent Progress:

Measurements of femtosecond time-resolved photoelectron angular distributions

Photoelectron angular distributions (PADs) are potentially very useful probes of dynamics in molecules. PADs are sensitive to the nature of the molecular orbital that is ionized, the geometry and orientation of the molecule as the electron departs, and the dynamics of the photoionization process. Unfortunately, much of the information is lost when the PAD is measured from a randomly oriented sample of molecules and hence PADs have not been extensively studied. In femtosecond time-resolved experiments the time scale of the experiment is often short compared to molecular rotation times so it is possible to measure PADs from aligned or oriented molecules. Several recent theoretical studies have suggested the possibility of using femtosecond time-resolved PADs to probe ultrafast dynamics.[1,2,3]

For our initial study of this type, done in collaboration with Dr. Julia Davies and Dr. Katharine Reid at Univ. of Nottingham, England, we have chosen to study the internal conversion in triethylenediamine, commonly known as DABCO. This molecule has an optically allowed transition to the $^1E'(S_2)$ state at 251 nm that rapidly internally converts to a $^1A_1'$ (S_1) state 4000 cm^{-1} lower in energy.[4,5] In these experiments the molecule is ionized with a 390 nm pulse at a variable time delay after excitation of the S_2 state, and full three-dimensional images of the ejected photoelectrons are collected. After sorting the electrons by energy, PADs can be

constructed corresponding to ionization of the individual molecular electronic states. Results of spherical harmonic fits to the data are shown in Fig. 1 for ionization at very short time delays after excitation and for different combinations of pump and probe polarizations. The PADs are quite distinctive for the two different electronic states, illustrating the potential of PADs for probing electronic structure. A simple physical explanation for the results seen in Fig. 1 is that the S_1 state is an s-type Rydberg state, which is spherically symmetric and hence insensitive to the relative orientation of the pump and probe polarizations. The S_2 state is a p-type Rydberg state and upon ionization dipole selection rules allow s and d electron partial waves. The production of different d-wave components for the different polarization orientations give rise to the shapes observed for the PADs. The PADs for crossed polarizations are not cylindrically symmetric about any axis so the three-dimensional imaging capability of our apparatus is critical for their reconstruction.

We have also measured the state resolved PADs as a function of time delay and the results are shown for crossed polarizations in Fig. 2. This figure shows the alignment sensitivity of the PADs. As the initial alignment decays due to molecular rotation the PAD structure simplifies, becoming cylindrically symmetric about the ionization laser polarization at long time delays when the sample has become essentially randomly oriented. The longest delay time data also shows the results that would be observed in experiments without femtosecond time resolution. These results demonstrate the potential for PADs to probe the time-resolved electronic configuration and alignment of molecules.

Time-resolved studies of NO dimer photodissociation

In collaboration with Dr. James Shaffer and Dr. Albert Stolow at the Steacie Institute, NRC, Canada we have studied the UV photodissociation of NO dimers at 210 nm. This system has been extensively studied in the past,[6,7] but the mechanism for the dissociation has not been determined. In our experiments the NO dimer is excited at 210 nm then probed with time delayed ionization in our coincidence imaging apparatus. The experiments demonstrate that the dissociation is not direct because no correlation is measured between the photofragment and photoelectron energies. The broad photoelectron energy spectrum shows that the dimer undergoes a very rapid geometry change upon excitation, and the new geometry preferentially ionizes to an excited state of the ion. The total kinetic energy distributions determined from coincident fragment and electron energies suggest a vibrational predissociation mechanism for the dissociation. These studies are ongoing.

Time-resolved studies of CF_3I dissociative ionization

In collaboration with Anouk Rijs and Dr. Maurice Janssen at Vrije University, Amsterdam, The Netherlands we have performed extensive measurements on the dissociative multiphoton ionization of CF_3I using coincidence imaging. In these studies the molecule is multiphoton excited with a 260 nm pulse then probed by time delayed ionization with a 390 nm pulse. The dissociation exhibits very interesting behavior with the fragment recoil energy distribution oscillating rapidly in time. Using our coincidence imaging capabilities with crossed excitation and probe laser polarizations we have determined that the fragments recoil preferentially along the excitation laser polarization while the photoelectrons recoil along the probe laser polarization. This provides us with information on which step in the multiphoton excitation produces dissociation and what mechanism leads to the ionization. Data from these experiments are still in early stages of analysis.

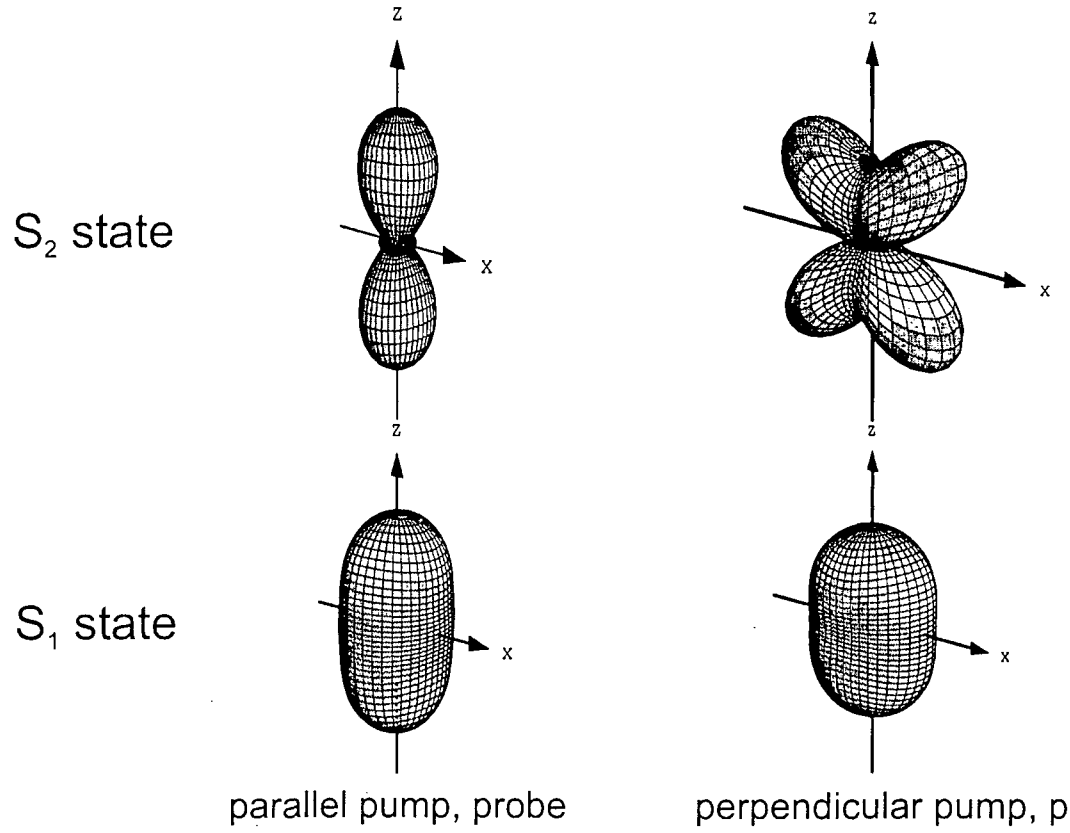

Figure 1. Photoelectron angular distributions from DABCO at 200 fs pump-probe delay

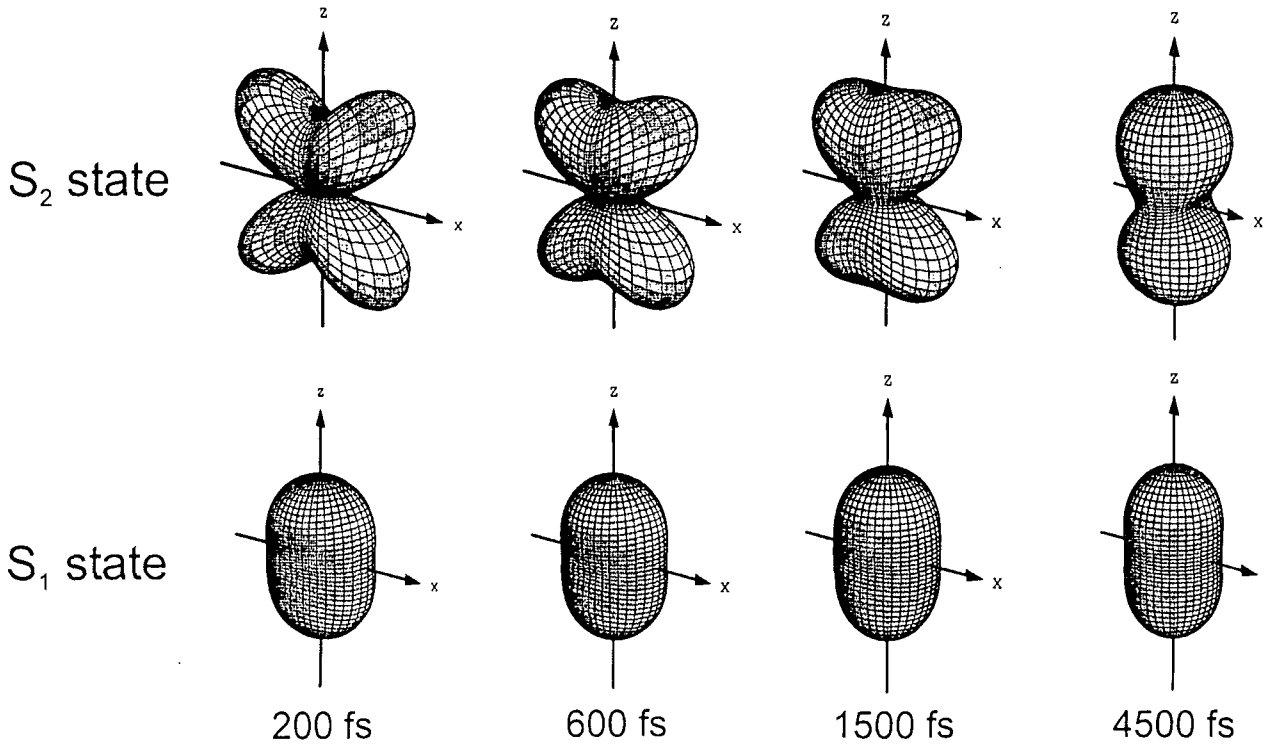

Figure 2. Time-resolved photoelectron angular distributions from DABCO for perpendicular pump-probe polarization

Future Plans

One of the main purposes for developing the coincidence imaging technique is to study unimolecular processes in hot radicals. Photolysis of precursor molecules can produce hot radicals, but with a wide distribution of internal energies. However, if the radical fragment is photoionized then we can determine the fragment recoil energy, and hence internal excitation, for individual radicals using our arrival-time and position-sensitive ion imaging technique. The electron produced in the photoionization probe step is collected in coincidence and its energy determined. Thus, collection of many coincident ions and electrons provides time-resolved photoelectron spectra over a range of radical internal energies. Coincident ion and electron images taken at a range of time delays between generation of the radicals by photolysis and their detection by photoionization, provide a means to follow processes such as isomerization in hot radicals as a function of time and internal energy.

Femtosecond pulses in the vacuum ultraviolet(VUV) are very attractive as ionization probes for radicals. VUV ionization is general and easily applied to new radicals of interest while multiphoton ionization schemes must be tailored to individual radicals. For all these reasons we have worked extensively on the development of femtosecond VUV pulses. In collaboration with Prof. Robert Continetti at Univ. of California, San Diego, we have built a high repetition rate, pulsed, high-temperature pyrolysis source[8] that makes it possible to generate many different radical species. We have taken VUV photoelectron spectra of many radicals from this source, including allyl and propargyl. The photoelectron spectra show that the radicals are quite hot, providing data on the nature of the spectra of hot radicals, and verifying that femtosecond VUV ionization of hot radicals should be effective for detecting them. The next step in this work is assembling the apparatus needed to introduce both the femtosecond VUV and UV photolysis pulses into the detection chamber with necessary baffling so that experiments using VUV ionization of radical products from photolysis will be possible.

References

1. Y. Arasaki, K. Takatsuka, K. Wang, and V. McKoy, Chem. Phys. Lett. **302**, 363 (1999).
2. S. C. Althorpe and T. Seideman, J. Chem. Phys. **110**, 147 (1999).
3. T. Zuo, A. D. Bandrauk, and P. B. Corkum, Chem. Phys. Lett. **259**, 313 (1996).
4. A. M. Halpern, J. L. Roebber, and K. Weiss, *J. Chem. Phys.* **49**, 1348 (1968).
5. D. H. Parker, and P. Avouris, *J. Chem. Phys.* **71**, 1241 (1979).
6. Y. Naitoh, Y. Fujimura, K. Honma, O. Kajimoto, J. Phys. Chem., **99**, 13652 (1995).
7. V. Blanchet, A. Stolow, J. Chem. Phys., **108**, 4371 (1998).
8. D. W. Kohn, H. Clauberg, and P. Chen, Rev. Sci. Instrum. **63**, 4003 (1992).

Publications: 1999-Present

C. C. Hayden and A. Stolow, "Non-Adiabatic Dynamics Studied by Femtosecond Time-Resolved Photoelectron Spectroscopy", in *Adv. Ser. in Phys. Chem., Vol. 10: Photoionization and Photodetachment*, edited by C. Y. Ng, (World Scientific, Singapore, 2000).

J. A. Davies, J. E. LeClaire, R. E. Continetti, and C. C. Hayden, "Femtosecond Time-Resolved Photoelectron-Photoion Coincidence Imaging Studies of Dissociation Dynamics", J. Chem. Phys. **111**, 1 (1999).

J. A. Davies, R. E. Continetti, D. W. Chandler, and C. C. Hayden, "Femtosecond Time-Resolved Photoelectron Angular Distributions Probed During Photodissociation of NO_2", Phys. Rev. Lett., **84**, 5983 (2000).

CHEMICAL ACCURACY FROM AB INITIO MOLECULAR ORBITAL CALCULATIONS

Martin Head-Gordon
Department of Chemistry, University of California, Berkeley, and,
Chemical Sciences Division, Lawrence Berkeley National Laboratory,
Berkeley, CA 94720.
mhg@cchem.berkeley.edu

1. Scope of Project.

Short-lived reactive radicals and intermediate reaction complexes are believed to play central roles in combustion, interstellar and atmospheric chemistry. Due to their transient nature, such molecules are challenging to study experimentally, and our knowledge of their structure, properties and reactivity is consequently quite limited. To expand this knowledge, we develop new theoretical methods for reliable computer-based prediction of the properties of such species. We apply our methods, as well as existing theoretical approaches, to study prototype radical reactions, often in collaboration with experimental efforts. These studies help to deepen understanding of the role of reactive intermediates in diverse areas of chemistry. At the same time, these challenging problems sometimes reveal frontiers where new theoretical developments are needed in order to permit better calculations in the future.

2. Summary of Recent Major Accomplishments.

2.1 Density functional theory for ground and excited states of radicals.

Density functional theory is a simple and effective computational tool for computational studies of the ground and excited states of radicals. For excited states, time-dependent density functional theory (TDDFT) provides a formally exact framework for the calculation of excitation energies. In practice, however, approximate functionals are employed and the adiabatic approximation is invoked. We have shown [8,11,12,13] that low-lying excited states of radicals can usually be adequately described using TDDFT with existing functionals. This is a particularly exciting result because such states often involve substantial double excitation character that is tremendously difficult to describe within wavefunction-based approaches. The positive results of these investigations significantly expand the range of radicals that are amenable to simulation by electronic structure methods.

Over the past year, we have completed two applications of TDDFT, with a third study in progress. Very encouraging results for the low-lying A_g (dark) excited states of polyene oligomers were obtained [18], which were previously beyond the reach of simple ab initio excited state methods. Additionally pilot calculations were performed on the excited states of closed shell polycyclic aromatic hydrocarbon (PAH) cations which are known to be intermediates in sooting flames. They may also be of relevance in the interstellar medium, and our initial study of their electronic spectra suggests that experimental efforts to obtain laboratory spectra are worthwhile. We are also completing

a study of excited states of the phenyl peroxy radical. Experiments in solution by the Ingold group (NRC), and in the gas phase by Lim (Emory) showed that it has an absorption in the visible. This is in contrast to the vinyl peroxy radical which only absorbs in the UV, based on experiments by Fahr and Lauffer. TDDFT is able to correctly predict the substituent effects on peroxy excitation energies, which is encouraging. Furthermore, based on examination of the calculations, we are able to extract a simple and satisfying qualitative picture of the origin of the substituent effects.

2.2 High accuracy electronic structure calculations.

While density functional calculations are extremely valuable, the highest levels of accuracy currently possible come from wavefunction-based electronic structure calculations (which are also dramatically more expensive). Along these lines, we have performed highly accurate calculations [14] on low-lying triplet excited states of the acetylene molecule to permit direct comparison with the recent experiments of Suits et al (LBNL/Brookhaven). While we have made exhaustive efforts to ensure that the theoretical calculations are converged, they remain in disagreement with experiment for the adiabatic excitation energy from the ground state to the triplet.

Calculations such as acetylene that are on closed shell molecules are normally very satisfactory using standard high-accuracy wavefunction methods, such as coupled cluster theory. The same cannot always be said for radicals. We have performed systematic benchmarks of the performance of existing electronic structure methods for structure and vibrational frequency prediction for radicals. Advanced coupled cluster methods performed significantly less well than for closed shell molecules, with the widely used CCSD(T) method offering no net improvement over CCSD itself. This appears to be largely due to problems with the use of the underlying Hartree-Fock orbitals in (T).

To overcome the deficiencies of (T) corrections for radicals and for the related problem of bond-dissociation to radical fragments, we have developed a new correction to singles and doubles coupled cluster methods [13,15]. This new method is a true second order correction to a coupled cluster reference, and therefore we denote the correction as (2). The physics of this correction, when applied to a singles and doubles coupled cluster reference, is that it accounts for the leading 3 and 4-electron correlations between electrons. The reference itself only accounts for pair correlations. We demonstrated great improvement relative to (T) corrections for the important problem of single bond dissociations [13].

3. Summary of Research Plans.

3.1 Density functional theory for excited states of radicals.

We are planning further development and application of the time-dependent density functional (TDDFT) approach to excited states of large molecules, particularly radicals. We shall complete our study of the phenyl peroxy radical, with examination of other radicals isoelectronic to the phenyl peroxy species (eg. Ph-C_2H_3, etc). We intend to study excited states of large unsaturated hydrocarbon cations which are current laboratory interest. At present we are beginning work on excited states of $C_{13}H_9^+$, for which some

experimental data is available, and also a series of larger cations ($C_{30}H_{16}^+$ and $C_{40}H_{20}^+$) that are analogs of the perylene cation. A collaboration with the Fleming group (Berkeley) is also underway to apply TDDFT to study low-lying excited states in the carotenoids involved in photosynthetic energy transfer. This builds upon our recent study of polyenes discussed above [18]. We are beginning work on extensions of TDDFT to explore excited potential energy surfaces via gradient and possibly hessian evaluation, extending the techniques we have successfully developed for CIS [8]. We also plan to implement and study improved functionals, to better describe charge transfer and Rydberg excited states for which current functionals perform poorly.

3.2 Radical reaction chemistry.

We have two projects that are in progress concerning radical reaction chemistry. The first concerns the C + acetylene reaction, which has been the object of a number of experimental and theoretical studies over the past several years. We are performing high level calculations of the barriers and stationary points for the C_3H_2 complex to probe the isomerization dynamics. Additionally we are performing ab initio "on-the-fly" quasiclassical trajectories to directly observe the dynamics. The second effort is a preliminary examination of the intermolecular interaction energies of medium to large unsaturated hydrocarbon molecules (for example, initially naphthalene and perylene). It is possible that physical aggregation plays a significant role in the build-up of soot particles, and calculations of the interaction energies will help to clarify this possibility, as well as to provide input for refinement of force fields for simulation.

3.3 Accurate electronic structure methods.

The development of a highly accurate new method for electronic structure calculations, based on second order (2) corrections to coupled cluster theory is under way in our group, as described above. Further work will be performed on the development and application of the (2) corrections. The initial implementation will be extended from optimized orbital coupled cluster doubles (OD(2)), to the full singles and doubles coupled cluster method, CCSD(2). The code will be made more efficient and tests for reaction barriers, accurate thermochemistry and spectroscopic constants of small radicals will be performed. Additional theoretical advances will be sought that improve the ability to describe bond-breaking in the reference function (which presently at the OD or CCSD level is really only adequate for single bond-breaking).

4. Publications from DOE Sponsored Work, 1999-present.

[1] "Crossed-beam Reaction of Carbon Atoms with Sulfur Containing Molecules I: Chemical Dynamics of Thioformyl (HCS; X^2A') Formation From Reaction of C (^3P_j) with Hydrogen Sulfide, H_2S (X^1A_1)", R.I.Kaiser, C.Ochsenfeld, M.Head-Gordon and Y.T.Lee, J. Chem. Phys. 110, 2391-2403 (1999).

[2] "Quasidegenerate Second Order Perturbation Corrections to Single Excitation Configuration Interaction for Excitation Energies", M.Head-Gordon, M.Oumi, and D.Maurice, Mol. Phys. 96, 593-602 (1999)

[3] "Ab Initio Molecular Orbital Calculations of the Excited States of Chalcone", M.Oumi, D.Maurice and M.Head-Gordon, Spectrochim. Acta 55A, 525-537 (1999).
[4] "Accurate Calculations on Excited States: New Theories Applied to the –OX –XO, and –XO2 (X=Cl and Br) Chromophores and Implications for Stratospheric Bromine Chemistry", T.J.Lee, S.Parthiban and M.Head-Gordon, Spectrochim. Acta 55A, 561-574 (1999).
[5] "Neutral-Neutral Reactions in the Interstellar Medium. II. Isotope Effects in the Formation of Linear and Cyclic C3H and C3D radicals in Interstellar Environments", R.I.Kaiser, C.Ochsenfeld, M.Head-Gordon, and Y.T.Lee, Astrophys. J. 510, 784-788 (1999).
[6] "On the Performance of Density Functional Theory for Symmetry Breaking Problems", C.D.Sherrill, M.S.Lee and M.Head-Gordon, Chem. Phys. Lett. 302, 425-430 (1999).
[7] "Time-dependent Density Functional Theory for Radicals: An Improved Description of Excited States with Substantial Double Excitation Character", S.Hirata and M.Head-Gordon, Chem. Phys. Lett. 302, 375-382 (1999).
[8] "Analytical Second Derivatives for Electronic Excited States using the Single Excitation Configuration Interaction Method: Theory and Application to Benzo[a]pyrene and Chalcone", D.Maurice and M.Head-Gordon, Mol. Phys. 96, 1533-1541 (1999).
[9] "A Coupled Cluster Ab Initio Investigation of Singlet/triplet CH2S Isomers, and the Reaction of Atomic Carbon with Hydrogen Sulfide to HCS/HSC", C.Ochsenfeld, R.I.Kaiser, Y.T.Lee, and M.Head-Gordon, J. Chem. Phys. 110, 9982-9988 (1999).
[10] "Time-dependent Density Functional Study of the Electronic Excitation Energies of Polycyclic Aromatic Hydrocarbon Radical Cations of Napthalene, Anthracene, Pyrene and Perylene", S.Hirata, T.J.Lee, and M.Head-Gordon, J. Chem. Phys. 111, 8904-8912 (1999).
[11] "Time-dependent Density Functional Theory within the Tamm-Dancoff Approximation", S.Hirata and M.Head-Gordon, Chem. Phys. Lett. 314, 291-299 (1999)
[12] "Configuration Interaction Singles, Time-dependent Hartree-Fock, and Time-dependent Density Functional Theory for the Electronic Excited States of Extended Systems", S.Hirata, M.Head-Gordon and R.J.Bartlett, J. Chem. Phys. 111, 10774-10786 (1999).
[13] "A Second Order Correction to Singles and Doubles Coupled Cluster Methods Based on a Perturbative Expansion of a Similarity-Transformed Hamiltonian", S.R.Gwaltney and M.Head-Gordon, Chem. Phys. Lett. 323, 21-28 (2000).
[14] "Complete Basis Set Extrapolations for Low-lying Triplet Electronic States of Acetylene and Vinylidene", C.D.Sherrill, E.F.C.Byrd, and M.Head-Gordon, J. Chem. Phys. 113, 1447-1454 (2000).
[15] "Second Order Perturbation Corrections to Singles and Doubles Coupled Cluster Methods: General Theory and Application to the Valence Optimized Doubles Model", S.R.Gwaltney, C.D.Sherrill, M.Head-Gordon, and A.I.Krylov, J. Chem. Phys. 113, 3548-3560 (2000).
[16] "Excited States Theory for Optimized Orbitals and Valence Optimized Orbitals Coupled-Cluster Doubles Models", A.I.Krylov, C.D.Sherrill, and M.Head-Gordon, J. Chem. Phys. 113, 6509-6527 (2000).
[17] "Q-Chem 2.0: A High Performance Ab Initio Electronic Structure Program Package", J.Kong, C.A.White, A.I.Krylov, C.D.Sherrill, R.D.Adamson, T.R.Furlani, M.S.Lee, A.M.Lee, S.R.Gwaltney, T.R.Adams, C.Ochsenfeld, A.T.B.Gilbert, G.S.Kedziora, V.A.Rassolov, D.R.Maurice, N.Nair, Y.Shao, N.A.Besley, P.E.Maslen, J.P.Dombroski, H.Daschel, W.Zhang, P.P.Korambath, J.Baker, E.F.C.Byrd, T.Van Voorhis, M.Oumi, S.Hirata, C.-P.Hsu, N.Ishikawa, J.Florian, A.Warshel, B.G.Johnson, P.M.W.Gill, M.Head-Gordon, J.A.Pople, J. Comput. Chem. 21, 1532-1548 (2000).
[18] "Excitation Energies from Time-Dependent Density Functional Theory for Linear Polyene Oligomers: Butadiene to Decapentaene", C.-P.Hsu, S.Hirata and M.Head-Gordon, J. Phys. Chem. A 105, 451-458 (2001).

Infrared Laser Studies of the Combustion Chemistry of Nitrogen

John F. Hershberger

Department of Chemistry
North Dakota State University
Fargo, ND 58105
John_Hershberger@ndsu.nodak.edu

Time-resolved infrared diode laser spectroscopy is used in our laboratory to study the kinetics and product channel dynamics of several chemical reactions of importance in the gas-phase combustion chemistry of nitrogen-containing radicals. This program is aimed at improving the kinetic database of reactions crucial to the modeling of NO_x control strategies such as Thermal de-NO_x, RAPRENO$_x$, and NO-reburning. The data obtained is also useful in the modeling of propellant chemistry. The emphasis in our study is the quantitative measurement of product branching ratios. For example, in recent years we have quantitatively measured the branching ratios of the CN+NO_2, NCO+NO, NCO+NO_2, CD+NO and several other reactions

HCCl + NO_x Reactions

We have investigated reactions of the HCCl radical using both laser-induced fluorescence and infrared absorption techniques. This radical is of interest in modeling the combustion of chlorinated hydrocarbons. We form HCCl from 193-nm photolysis of $HCClBr_2$, and detect it by LIF spectroscopy at 602.53 nm. We have measured rate constants for HCCl + NO and HCCl + NO_2 over the temperature ranges 298-572 and 298-476 K, respectively. Using LIF detected of HCCl and standard pseudofirst order kinetics, we obtain a total rate constant of $(2.75\pm0.2)\times10^{-11}$ cm^3 molecule^{-1} s^{-1} at 296 K for HCCl+NO, which is somewhat higher than the one previous report of $(1.5\pm0.5)\times10^{-11}$ of H. Gg. Wagner et al.[1] For the HCCl + NO_2 reaction, we obtain $k=(1.10\pm0.02)\times10^{-10}$ cm^3 molecule^{-1} s^{-1} at 296. This is the first reported kinetic study of this reaction. These reactions have only a very slight temperature range, negative for NO, positive for NO_2:

$k=(2.225\pm0.05)\times10^{-11}\exp[(62.05\pm6.9)/T]$ (HCCl+NO)

$k=(1.775\pm0.27)\times10^{-9}\exp[(-869.11\pm57.3)/T]$ (HCCl+NO_2)

For HCCl+NO, several product channels are possible:

HCCl + NO $\rightarrow$ HCNO + Cl (a) $\Delta H_r^0 = -129.6$ kJ/mole
$\rightarrow$ HNCO + Cl (b) $\Delta H_r^0 = -405.7$ kJ/mole

$\rightarrow$ NCO + HCl (c) $\Delta H_r^0 = -386.2$ kJ/mole
$\rightarrow$ HCN + ClO (d) $\Delta H_r^0 = -188.9$ kJ/mole
$\rightarrow$ CN + HOCl (e) $\Delta H_r^0 = -64.7$ kJ/mole

Using infrared diode absorption spectroscopy, we have detected HCNO, N_2O, and CO_2 product molecules upon photolysis of $CHClBr_2/NO/SF_6$ mixtures. We attribute the formation of N_2O and CO_2 to the following secondary reaction:

$$NCO + NO \rightarrow N_2O + CO$$
$$\rightarrow CO_2 + N_2$$

Previous experiments in several laboratories including our own have shown that this reaction is fast and produces N_2O and CO_2 in roughly equal yields. Our best numbers are ϕ_a=0.44 and ϕ_b=0.56, independent of temperature over the range 296-500 K.[2]

Calibration of N_2O and CO_2 signals is straightforward using published linestrengths. Our results show that the relative yields of these molecules is consistent with the statement that they originated entirely from the NCO+NO reaction. By measuring the 193-nm absorption coefficient of $HCClBr_2$ and assuming a quantum yield for HCCl production of unity, we obtain a branching ratio of 0.24±0.04 into the NCO + HCl channel.

HCNO (fulminic acid) is the major product of this reaction. Calibration of these signals is more difficult. We have used ketene (CH_2CO) photolysis followed by reaction with NO to calibrate these signals:

$$CH_2CO + h\nu(193\text{ nm}) \rightarrow CH_2 + CO$$
$$\rightarrow HCCO + H$$

Both CH_2 and HCCO react with NO, forming (approximately) known and nearly equal yields of HCNO.[3-5] Using this information, we were able to calibrate our HCNO signals from the HCCl+NO reaction. We obtain $\phi_a = 0.68\pm0.06$ at 296 K. Since $\phi_a+\phi_c$ is close to unity, we conclude that our assumptions about unity photolysis quantum yields are correct, and that no other channel makes a major contribution.

Current and future work

We are currently investigating reactions of CCO radicals with NO_x. We have detected infrared absorption signals near 1970 cm^{-1} assignable to CCO[6] upon photolysis of carbon suboxide (C_3O_2). The transients have rather long risetimes of ~50 μsec, possibly because CCO is initially formed in an exited singlet electronic state. Other workers report that 248 nm photolysis produces mostly ground state CCO, which may more amenable for kinetic studies.

We have an ongoing interest in the ketenyl radical, HCCO. The reaction of this species with NO is a crucial step in the NO-reburning process. Two major product channels are likely:

$$HCCO + NO \rightarrow HCN + CO_2$$
$$\rightarrow HCNO + CO$$

Although the products are readily detected by infrared spectroscopy, this reaction is a difficult problem because of the lack of clean photolytic sources of the HCCO radical. In earlier work, we formed HCCO from a minor channel of the 193-nm photolysis of ketene, CH_2CO.[3] By knowing the behavior of the methylene radicals that are formed in the dominant photolysis channel, we were able to obtain an estimate of the branching ratio. The number of unwanted background reactions in this approach was uncomfortably high, however. Another approach we have tried including using a reaction like $CN+CH_2CO$ to make HCCO. This did not work, however, because the major product of $CN+CH_2CO$ was $CH_2CN + CO$.[7] An approach that we plan to try in the near future is the reaction $H+C_3O_2$ (carbon suboxide) $\rightarrow$ HCCO + CO. Although this reaction rate constant has a substantial activation barrier and is quite slow at 296 K[8], this reaction may occur efficiently if using translational hot hydrogen atoms, such as those formed from H_2S or HI photolysis. If this works, we may be able to study HCCO reactions with less interference from secondary chemistry.

References

1. R. Wagener and H.Gg. Wagner, Z. Phys. Chem. **175**, 9 (1992).
2. W.F. Cooper, J. Park, and J.F. Hershberger, J. Phys. Chem. **97**, 3283 (1993).
3. K.T. Rim and J.F. Hershberger, J. Phys. Chem. A **104**, 293 (2000).
4. U. Eickhoff and F. Temps, Phys. Chem. Chem. Phys. **1**, 243 (1999).
5. J. Grussdorf, F. Temps, and H. Gg. Wagner, Ber. Bunsenges. Phys. Chem. **101**, 134 (1997).
6. C. Yamada, H. Kanamori, H. Horiguchi, S. Tsuchiya, and E. Hirota, J. Chem. Phys. **84**, 2573 (1986).
7. M.A. Edwards and J.F. Hershberger, Chem. Phys. **234**, 231 (1998).
8. P. Van de Ven and J. Peeters, Bull. Soc. Chim. Belg. **99**, 509 (1990)

Publications acknowledging DOE support (1999-present)

"Temperature Dependence of the Product Branching Ratio of the $CN+O_2$ Reaction", K.T. Rim and J.F. Hershberger, J. Phys. Chem. A **103**, 3721 (1999).

"Kinetics of the NCS Radical", R.E. Baren and J.F. Hershberger, J. Phys. Chem. A **103**, 11340 (1999).

"Product Branching Ratio of the HCCO+NO Reaction", K.T. Rim and J.F. Hershberger, J. Phys. Chem. A **104**, 293 (2000).

"Recent Progress in Infrared Absorption techniques for Elementary Gas Phase Reaction Kinitics", C. Taatjes and J.F. Hershberger, Ann. Rev. Phys. Chem., in press.

Kinetics of HCCl + NO_X Reactions", R.E. Baren, M. Erickson, and J.F. Hershberger, Int. J. Chem. Kinet., submitted.

Small-Angle X-ray Scattering Studies of Soot Inception and Growth

Jan P. Hessler

Chemistry Division, Argonne National Laboratory
9700 South Cass Avenue, Argonne, Illinois 60439-4831
E-mail: hessler@anl.gov

1. Scope

Under fuel-rich conditions hydrocarbon fuels produce soot, which appear as an ensemble of ultra-fine particles in the size range up to a few hundred nanometers. A comprehensive theory or model that is capable of predicting the inception and growth of soot over a wide range of chemical and physical conditions is just beginning to emerge. Such a model is needed to help reduce the health hazards associated with soot production, improve the radiative transfer of energy in industrial applications, and devise efficient production process that use soot in various applications. The high spectral intensity of x-rays produced by the undulator at the Basic Energy Sciences Synchrotron Radiation Center of Argonne's Advanced Photon Source has allowed us to perform small-angle x-ray scattering (SAXS) studies of the initial distribution of soot particles formed by various fuels. SAXS provides an *in situ* probe of the morphology of soot in the region between 1 and 100 nm and complements the *ex situ* technique of electron microscopy.

Both *ex situ* and *in situ* techniques have been used to study soot formation. Optical techniques such as absorption[1], induced luminescence[2], and wide-angle elastic scattering[3] are examples of *in situ* techniques. More precisely[4], elastic Lorenz-Mie scattering provides information on the morphology of particles that range in size from 100 to 5000 nm while lower-resolution quasi-elastic scattering, which can not provide information on morphology, can be used for particles from 1 nm to 10 μm. Laser-induced incandescence has been used to detect mean particle radii between 1.8 and 10 nm[5]. Cavity ring-down spectrometry has been used to detect soot precursors such as the phenyl radical[6]. The formation of larger precursor species have been studied in low-pressure flames by photoionization mass spectrometry[7] and gas-chromatography/mass spectrometry[8]. From these results we note that it is difficult to use *in situ* techniques and extract information on the structure of particles in the 1 to 100 nm. Electron microscopy has bridged this gap, but it is an *ex situ* technique and kinetic information is difficult to obtain. Small-angle x-ray scattering (SAXS) is ideally suited to provide *in*

situ measurements of the morphology of soot formation in this important region.

2. Recent Progress

2.1. Extension to larger scattering angles

Last year we discussed our preliminary measurements of soot formed by the complex fuel toluene. A flat-flame burner that supports a CH_4/H_2/air or CO/H_2/air diffusion flame stabilized by N_2 coflow produces a nearly constant temperature region above the flame where the pyrolysis and combustion of the fuel occurs. Kinetic information is obtained by performing measurements of the scattered intensity profile as a function of the magnitude of the scattering vector, $q = (4\pi/\lambda)\sin(\theta/2)$ where θ is the scattering angle, for various heights above the burner. These profiles were studied in the region $0.07 \leq \mathrm{q(nm^{-1})} \leq 0.4$ and were reduced to give the mean radius and dispersion of a distribution of spherical particles. Mean radii between 0.8 and 18 nm were observed. This year we extended our measurement on toluene, methylcyclohexane, heptane, and biphenyl in heptane to the higher q-region. The size of the particles that dominate in a give region scale as $1/q$, therefore, higher q implies small particles and, we feel, a region where chemistry will play a more important role. In addition, we have also studied the less complex fuels acetylene, ethylene, and propylene by removing the methane and carbon monoxide from the system to produce a diffusion flame. In the low-q region, $q \leq 0.7$ nm^{-1}, all of profiles approach a slope of -1.8, which is expected for fractal aggregrates. This behavior is consistent with the observations of Sornsen, Oh, Schmidt, and Rieker[9] who observe similar behavior in the region $0.1 \leq q(nm^{-1}) \leq 1$. The most striking feature of these profiles in the region $\mathrm{q(nm^{-1})} \geq 0.7$ is the fact that some of them approach zero. Initially, we thought this behavior indicated the existence of a significant amount of soot that had the same size. However, as we discuss below, this may not be the case.

2.2. Abel inversion and the negative scattering intensity

All of the optical and x-ray techniques used to study soot are basically line-of-sight measurements. Therefore, they integrate over the path length of the observation. In situations where the flame has cylindrical symmetry information about the radial dependence of the observations may be obtained by the inverse Abel transform. During March of this year, we performed measurements that provide the data needed to perform this inversion. An example of the transformed scattering intensity at 0.4 nm^{-1} is shown in figure 2. The solid line represents scattering from the acetylene diffusion flame and the dashed from the toluene system. As in all SAXS experiments the scattering intensity is

relative to the intensity of the background scattering, which in our case is taken as 6 mm from the center of the flame. Clearly, acetylene displays a negative scattering intensity. This observation may be explained in terms of a reduced density of background scattering centers near the flame. This lower density is due to the constant pressure nature of the experiment and the temperature gradient near the flame. This gradient is not present in the toluene system.

3. Future Plans

The prototype of the annular detector that we have designed to have a temporal resolution that will match the revolution time of an electron bunch at the APS, 3.68 μs will be tested later this summer. With this detector we will be able to monitor the formation of soot in a shock tube in the critical period that is not accessible to elastic scattering in the optical region. We now feel that we have developed enough experience in SAXS that we can obtain scattering information in both real and recriprocal space that can be used to test models of soot formation. We plan to perform experiments that are designed to test crucial aspects of these models.

Work performed under the auspices of the U.S. Department of Energy, Office of Basic Energy Sciences, Division of Chemical Sciences, under Contract No. W-31-109-ENG-38.

References

[1] J. Zhu and M. Y. Choi, *Int. J. Heat Transfer*, 2000, **43**, 3299-3302.

[2] M. Y. Choi and K, A, Jensen, *Combust. Flame*, 1998, **112**, 485-491.

[3] S. di Stasio, P. Massoli, and M. Lazzaro, *J. Aerol. Sci.*, 1996, **27**, 897-913.

[4] O. Glatter, in *Modern Aspects of Small-Angle Scattering*, (H. Brumberger, ed.) Kluwer Academic Publishers, Dordrecht, Boston, & London, 1995, pp. 107-180.

[5] D. Woiki, A. Giesen, and P. Roth, *Proc. Combust. Inst.,* 2000, **28**, in press.

[6] Y. M. Choi, W. S. Xia, J. Park, and M. C. Lin, *J. Phys. Chem. A*, 2000, **104**, 7030-7035.

[7] A. Bhargava and P. R. Westmoreland, *Combust. Flame,* 1998, **113**, 333-347.

[8] H. Richter, W. J. Grieco, and J. B. Howard, *Combust. Flame, 1999,* **119**, 1-22.

[9] C. M. Sornsen, C. Oh, P. W. Schmidt, and T. P. Rieker, *Phys. Rev. E*, 1998, **58**, 4666-4672.

Publications Supported by this Program 1998-present

Calculation of Reactive Cross Sections and Microcanonical Rates from Kinetic and Thermochemical Data
J. P. Hessler, *J. Phys. Chem.*, **102**, 4517-4526 (1998).

New empirical rate expression for reactions without a barrier: Analysis of the reaction of CN with O_2
J. P. Hessler, *J. Chem. Phys.*, **111**, 4068-4076 (1999).

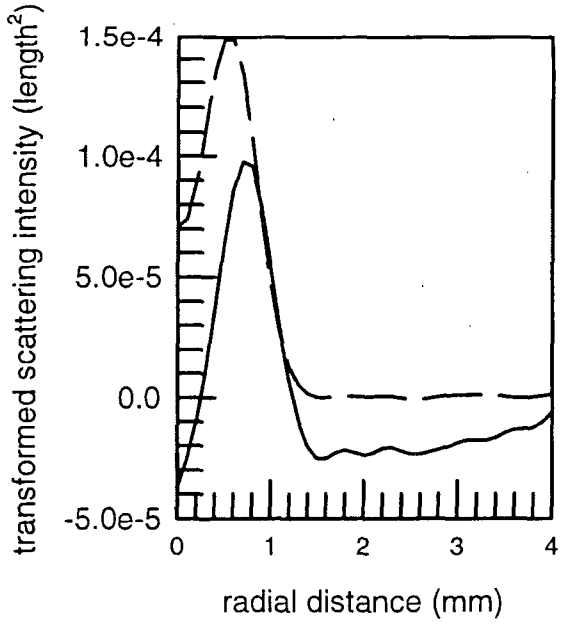

Figure 3.1: Transformed scattering intensity at 0.4 nm^{-1} for an acetylene diffusion flame, solid line, and toluene pyrolysis, dashed line.

DOE/ER/13934-1

PRODUCT IMAGING OF COMBUSTION DYNAMICS

P. L. Houston
Department of Chemistry
Cornell University
Ithaca, NY 14853-1301
plh2@cornell.edu

Program Scope

The technique of product imaging is being used to investigate several processes important to a fundamental understanding of combustion. The imaging technique produces a "snapshot" of the three-dimensional velocity distribution of a state-selected reaction product. Research in three main areas is planned. First, the imaging technique will be used to measure rotationally inelastic energy transfer on collision of closed-shell species with several important combustion radicals. Such measurements improve our knowledge of intramolecular potentials and provide important tests of *ab initio* calculations. Second, product imaging will be used to investigate the reactive scattering of radicals or atoms with species important in combustion. These experiments, while more difficult than studies of inelastic scattering, are now becoming feasible. They provide both product distributions of important processes as well as angular information important to the interpretation of reaction mechanisms. Finally, experiments using product imaging at the Advanced Light Source will explore the vacuum ultraviolet photodissociation of CO_2 and other important species. Little is known about the highly excited electronic states of these molecules and, in particular, how they dissociate. These studies will provide product vibrational energy distributions as well as angular information that can aid in understanding the symmetry and crossings among the excited electronic states.

Recent Progress

a. Differential Cross Sections for Rotationally Inelastic Scattering of NO($X^2\Pi_{1/2}$,v=0,J=0.5,1.5) from He or D_2 to NO($X^2\Pi_{1/2}$,J=2.5-12.5)

State selective differential cross sections for rotationally inelastic scattering of NO (J_i = 0.5, 1.5, $F_1 \rightarrow J_f$ = 2.5–12.5, F_1 and J_f=1.5-9.5, F_2) from He and D_2 measured by crossed molecular beam product imaging are reported. The differential cross sections were extracted from the data images using a new basis image iterative fitting technique. The images typically exhibit a single broad rotational rainbow maximum that shifts from the forward to the backward scattering direction with increasing ΔJ. The angle of the rainbow maximum was lower at a given ΔJ for D_2 than for He as a collision partner. At a collision energy of ~500 cm^{-1}, primarily the repulsive part of the potential surface is probed, which can be modeled with a 2-D hard ellipse potential. This model for rotationally inelastic scattering is shown to

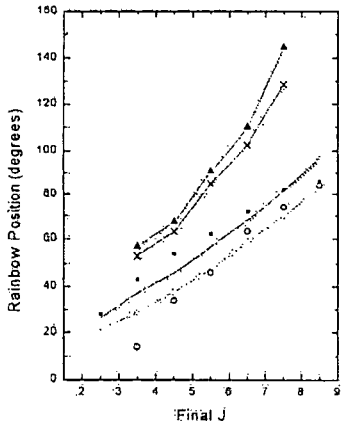

Plot of rainbow maxima versus J_f for data, the Yang-Alexander PES, and the hard ellipse models. Closed circles are data for D_2/NO; open squares are data for He/NO; solid and dashed lines are fits to a hard-ellipse model for the D_2 and He data, respectively; triangles and crosses are HIBRIDON predictions for He/NO at collision energies of 491 and 545 cm^{-1}, respectively.

qualitatively match the experimental differential cross sections. A more advanced correlated electron pair approximation potential energy surface for NO+He does not give substantially better agreement with the experiment, as shown in the figure on the preceding page. The differences between scattering of He and D_2 are partially attributed to their differing structure and partially to a small difference in collision energy used in the two experiments.

b. Evidence of a Double Surface Crossing Between Open and Closed Shell Surfaces in the Photodissociation of Cyclopropyl Iodide

Gas-phase photodissociations of cyclopropyl iodide were conducted at 266 nm and 279.7 nm, and the radical products were probed by multiphoton ionization, with imaging of the resulting ions and their corresponding electrons. Solution-phase photodissociations of cyclopropyl iodide were also conducted with TEMPO-trapping of the radical dissociation products. In both gas and solution phases, allyl radical was found to be a direct product of the cyclopropyl iodide photodissociation. CASSCF calculations indicate that the allyl radical could be formed directly from photoexcited cyclopropyl iodide by way of two surface crossings between open- and closed-shell potential energy surfaces. Each surface crossing represents a point of potential bifurcation in the reaction dynamics. Thus, cyclopropyl iodide that is excited to a $^1(n,\sigma^*)$ state can remain on an open-shell surface and generate the cyclopropyl radical and an iodine atom or can cross to a closed-shell (ion-pair) surface. The cyclopropyl cation that results from the surface crossing can undergo barrierless ring opening to the allyl cation before crossing back to an open-shell surface to generate allyl radical and an iodine atom. In this manner, both cyclopropyl radical and allyl radical can be formed as direct products of cyclopropyl iodide photodissociation.

d. Rotational Differential Cross Sections for Vibrational Excited States

Differential cross sections for the Ar + NO(v=5,J=0) ➔ Ar + NO(v=5,J) have been obtained for three different final J states, and these have been compared to the corresponding cross sections for the similar processes in v = 0. The figure at the right, for example, compares the DCS for J= 20.5 in v=0 and v=5. The differences are small, as might be expected from the small change in equilibrium bond length for the two vibrational levels. Similar data has been obtained for J = 6.5 and J = 16.5. Analysis of these data are currently underway.

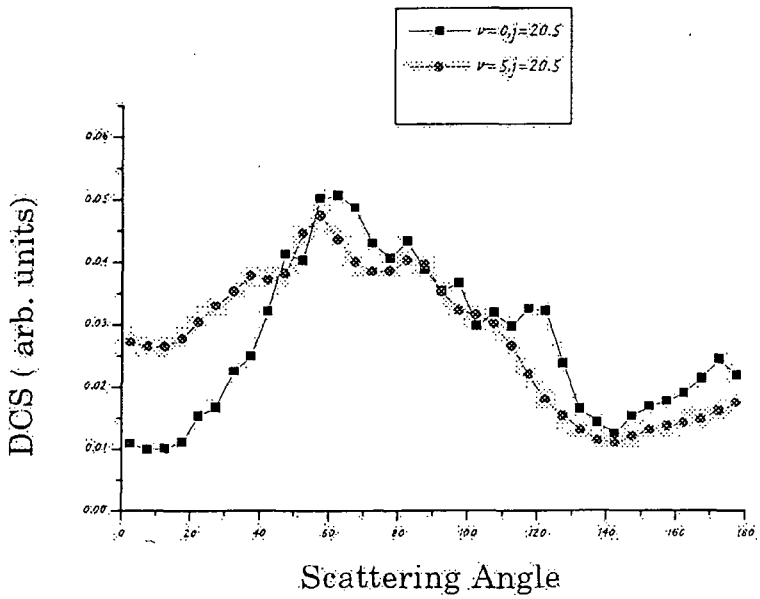

Future Directions

Our success in measuring differential cross sections for rare gas collisions with the densities of NO(v,J) that we can produce in our photolysis source gives us confidence that we can use the capabilities of our source to study differential cross sections for collisions of rare gas atoms with various radical species. Members of our group (as well as others) have extensive experience in creating radicals by photolysis, and many of these can be ionized by simple REMPI schemes. For example, for comparison to the work of Bowman and co-workers, we could create HCO from 308 nm photolysis of acetaldehyde and detect the product rotational states by ionization. Other systems amenable to study by this technique include collisions of rare gases or small molecules with the following radicals: SO, SH, PO, NH, CH_3 and CH_3O.

We also plan to investigate differential cross sections for reactive collisions. A start has been made on the $O(^1D)$ + N_2O system and the OH + CO system, but improvements to the apparatus will be required to make these practical.

A third area of future investigation is determination of vibrational distributions following VUV photodissociation of small molecules. Despite the large absorption coefficients of small molecules in the vacuum ultraviolet region of the spectrum, little is known either about their excited states or about the products they dissociate to. The availability of a beam line at the Advanced Light Source now makes it possible to investigate the dynamics of energy release for small molecules following absorption of a VUV photon. Typical absorption cross sections in the region from 110-140 nm are on the order of 1×10^{-16} cm^2. For triatomics, multi-photon ionization of the atomic photodissociation fragment can be performed with very high efficiency. It should thus be possible using the product imaging facilities of End Station Three at the ALS to image the atomic fragment, thereby determining the vibrational distribution of the sibling diatomic fragment. Such information should help in understanding what bonds in addition to the dissociative one either lengthen or bend during the dissociation process. Angular distributions of products also provide information about the symmetry of the excited state and the time scale for dissociation.

Publications Prepared with DOE Support 2000-2001

P. J. Pisano, M. S. Westley and P. L. Houston, "The NO vibrational state distribution in the reaction $O(^1D) + N_2O \rightarrow 2\ NO$," *Chem. Phys. Lett.* **318**, 385-392 (2000).

K. T. Lorenz, M. S. Westley, and D. W. Chandler, "Rotational State-to-state Differential Cross Section for the HCl-Ar Collisional System Using Velocity-Mapped Ion Imaging," *PCCP* **2,** 481-494 (2000).

M. S. Westley, K. T. Lorenz, D. W. Chandler, and P. L. Houston, "Differential Cross Sections for Rotationally Inelastic Scattering of $NO(X^2\Pi_{1/2}, v=0, J=0.5, 1.5)$ from He or D_2 to $NO(X^2\Pi_{1/2}, J=2.5\text{-}12.5)$," *J. Chem. Phys.* **114**, 2669-2680 (2001).

P. A. Arnold, B. R. Cosofret, S. M. Dylewski, P. L. Houston, and B. K. Carpenter, "Evidence of a Double Surface Crossing Between Open and Closed Shell Surfaces in the Photodissociation of Cyclopropyl Iodide," *J. Phys. Chem. A*, **105,** 1693-1701 (2001).

P. L. Houston, B. R. Cosofret, A. Dixit, S. M. Dylewski, J. D. Geiser, J. A. Mueller, R. J. Wilson, P. J. Pisano, M. S. Westley, K. T. Lorenz, and D. W. Chandler, "Product Imaging Studies of Photodissociation and Bimolecular Reaction Dynamics," *J. Chinese Chem. Soc,* accepted.

AROMATICS OXIDATION AND SOOT FORMATION IN FLAMES

J. B. Howard and H. Richter
MIT Department of Chemical Engineering
77 Massachusetts Avenue
Cambridge, MA 02139-4307
Email: jbhoward@mit.edu

Scope

This project is concerned with the kinetics and mechanisms of aromatics oxidation and soot and fullerenes formation inflames. The overall objective of the aromatics oxidation work is to extend the study of benzene oxidation by measuring concentration profiles for important benzene decomposition intermediates such as phenyl and phenoxy radicals which could not be adequately measured with molecular-beam mass spectrometry to permit definitive testing of benzene oxidation mechanisms. The focus includes polycyclic aromatic hydrocarbons (PAH) radicals which are of major importance under fuel-rich conditions although their concentrations are in many cases too low to permit measurement with conventional molecular beam mass spectrometry. The radical species measurements are used in critical testing and improvement of benzene oxidation and PAH growth mechanisms. The overall objective of the research on soot formation is to extend the measurement of radicals into the overlapping region of large molecular radicals and small soot particles with radical sites. The ultimate goal is to understand how nascent soot particles are formed from high molecular weight compounds, including the roles of planar and curved PAH and the relationships between soot and fullerenes. The specific aims are to characterize both the high molecular weight compounds involved in the nucleation of soot particles and the structure of soot including internal nanoscale features indicative of contributions of planar and/or curved PAH to particle inception.

Recent Progress

The development of a kinetic model describing the growth of polycyclic aromatic hydrocarbons (PAH) was continued and its predictive capability was tested for different fuel types and equivalence ratios. The model consists currently of 234 species and 963 reactions. Thermodynamic property data were updated using the recent literature and new computations. The geometries of more then 100 stable and radical species were optimized by means of density functional theory calculations allowing for the determination of entropies and heat capacities after vibrational analysis. Heats of formation were deduced via isodesmic reactions. An analysis of the potential energy surface of the reactions phenyl + acetylene and 1-naphthyl + acetylene including transition states as well as various four- and five-membered ring species, was conducted using density functional theory. High-pressure rate constants were deduced by means of transition state theory and used as input for subsequent QRRK analysis. Rate constants describing the formation of all major products such as phenylvinyl, 1-vinyl-2-phenyl, phenylacetylene and 1-naphthylvinyl, 1-vinyl-8-naphthyl, 1-naphthylvinyl, acenaphthylene, 1-acenaphthenyl were determined at 20 and 40 torr as well as 1 and 10 atm covering a temperature range from 300 to 2100 K [1]. The assessment of the competition between different product channels, in particular between the formation of acetylene-substituted and cyclopentaPAH, by means of the QRRK technique using an improved modifed strong collision approach [2] was extended to larger PAH up to pyrene and the resulting rate constants were included in the kinetic model. QRRK computations were also conducted to determine rate constants of other chemically activated reactions present in the model. In addition to the kinetic model for low-pressure conditions, an atmospheric pressure version has been developed. Its predictive capability has been tested with encouraging results against experimental data available for fuel-rich ethylene and benzene combustion in a coupled well-stirred reactor/plug-flow reactor [3] as well as in premixed flames [4,5].

An investigation of the reaction pathways responsible for the growth of PAH has been conducted in low-pressure premixed flames for which extensive experimental data are available. A low pressure

benzene flame (equivalence ratio ϕ= 1.8, 30% argon, cold gas velocity v= 50 cm s^{-1}, pressure= 2.67 kPa) investigated by means of molecular beam sampling coupled to mass spectrometry [6] and nozzle-beam sampling followed by radical scavenging with dimethyl disulfide (DMDS) and subsequent analysis by gas chromatography (GC-MS) [7] was used for the comparison of model predictions for stable species as well as radical intermediates with experimental concentration profiles. Standards were used for the GC analysis of many scavenging products allowing for the individual quantification of radical isomers such as 1-, 2-naphthyl and 1-,2-,4-pyrenyl. The model showed at least satisfactory predictive capabilities for all major combustion products and stable as well as radical intermediates measured by MBMS, i. e., C_0 to C_8 species, and was therefore found to be suitable for the further investigation of PAH formation and consumption. In addition, the applicability of the model was extended to acetylene and ethylene low-pressure combustion. The completed model was applied to fuel-rich premixed acetylene/oxygen (ϕ= 2.4, 5% argon, v= 50 cm s^{-1}, 2.67 kPa) [8,9], ethylene/oxygen (ϕ= 1.9, 50% argon, v= 62.5 cm s^{-1}, pressure= 2.67 kPa) [10] low pressure flames as well as a lean ethylene/oxygen flame (ϕ= 0.75, 56.91% argon, v= 62.5 cm s^{-1}, 4.00 kPa) [11] for which experimental temperature profiles and flame structure data measured by means of MBMS were available. At least satisfactory, and often good or excellent, agreement with experimental concentration profiles was observed for all measured major stable and radical species. Therefore the kinetic model appears to describe the flame chemistry appropriately for different aromatic and aliphatic fuels and equivalence ratios. Rates of production of species of interest were determined in order to assess the relative contributions of individual reaction pathways to their formation or consumption.

Consumption of benzene and its degradation to cyclopentadienyl, a key intermediate of subsequent naphthalene formation, were investigated in some details in the premixed benzene flame [6,7]. Hydrogen abstraction reactions, mainly by OH but also by H and O, to form phenyl and to some extent phenoxy and phenol were major pathways. Unimolecular decomposition of phenoxy and phenol to cyclopentadienyl and cyclopentadiene are included in the model. Rate constants for the oxidation of phenyl by molecular oxygen to phenoxy were determined by means of a QRRK computation based on the work of DiNaro et al. [12]. Oxidation of phenyl to benzoquinones [13] was identified to be a potentially important pathway with the ortho-isomer, a major product which rapidly decays. Kinetic data available in the literature, based on the detailed computational study of potential energy surfaces and treatment of pressure effects, were included in the model for the description of cylcopentadienyl oxidation [14] and its unimolecular decay [15].

The analysis of napththalene formation and consumption was completed. In the premixed benzene flame [6,7], napththalene is mainly formed by resonantly stabilized self-combination of cyclopentadienyl and hydogen-abstraction to 1- and 2-naphthyl are the major consumption pathways. The contribution of OH to naphthalene consumption was found to be higher than that of hydrogen radicals. The impact of thermodynamics on PAH formation and consumption was shown to be significant due to often tightly balanced reactions. For instance, the reaction of the phenylacetylene radical with acetylene to 1-naphthyl was shown to be the major 1-naphthyl consumption pathway at heights above the burner of more than 0.7 cm while a small contribution of this reaction to 1-naphthyl formation was observed close to the burner. Similarly, the reaction of 1-naphthyl with acetylene to acenaphthylene + H, commonly considered to be a major acenaphthylene formation pathway, contributed to the formation of 1-naphthyl beyond a height above the burner of about 0.6 cm. The latter observation is closely related to the presence in the model of another dominant acenaphthylene formation pathway, i. e., the formation of biphenylene by benzyne self-combination followed by hydrogen addition, isomerization and final hydrogen loss. Evidence of the importance of this pathway was provided by at least satisfactory agreements of model predictions for acenaphthylene, benzyne and biphenylene with experimental data.

Both naphthylacetylene isomers could be identified unambiguously by GC-MS after nozzle-beam sampling and collection in dimethyl disulfide (DMDS) [7]. They are formed by acetylene addition to 1- and 2-naphthyl using rate constants determined by means of transition state theory followed by QRRK analysis. The competition with ring closure to acenaphthylene was taken into account in the case of 1-naphthyl [1]. Consumption by hydrogen abstraction followed by acetylene addition leading to

phenanthrene and anthracene radicals was included in the model for both naphthalene radicals. Comparison of the profiles predicted for 1- and 2-naphthylacetylene with experimental data showed satisfactory agreement in the reaction zone but insufficient depletion in the postflame zone indicating the existence of additional consumption pathways.

Future Plans

The research on aromatic compounds in flames will involve the continued application of the radical scavenging method and use of the experimentally measured concentration profiles to test and improve critical submechanisms in the overall model of aromatic oxidation and PAH and fullerenes formation. Specific objectives are to resolve differences between radical concentration measurements in this project and previous measurements; to extend the measurement of radicals concentration profiles to larger PAH radicals than have been measured previously and to additional radicals of interest in studies of PAH growth mechanisms but whose identities could not be confirmed to date in this project; to measure concentration profiles of oxygen-containing PAH pertinent to the modeling of aromatic

References

1. Richter, H., Mazyar, O., Sumathi, R., Green, W. H. and Howard, J. B. Detailed Kinetic Study of the Growth of Small Polycyclic Aromatic Hydrocarbons I. 1-Naphthyl + Ethyne. J. Phys. Chem. A. **105**, 1561-1573 (2001).

2. Chang, A. Y., Bozzelli, J. W. and Dean, A. M. Kinetic Analysis of Complex Chemical Activation and Unimolecular Dissociation Reactions Using QRRK Theory and the Modified Strong Collision Approximation. Z. Phys. Chem. **214**, 1533-1568 (2000).

3. Marr, J. A. PAH Chemistry in a Jet-Stirred/Plug-Flow Reactor System. Ph.D. thesis, Massachusetts Institute of Technology, Cambridge, MA 1993.

4. Castaldi, M. J., Marinov, N. M., Melius, C. F., Huang, J., Senkan, S. M., Pitz, W. J. and Westbrook, C. K. Experimental and Modeling Investigation of Aromatic and Polycyclic Aromatic Hydrocarbon Formation in a Premixed Ethylene Flame. Proc. Combust. Inst. **26**, 693-702 (1996).

5. Tregrossi, A., Ciajolo, A. and R. Barbella The Combustion of Benzene in Rich Premixed Flames at Atmospheric Pressure. Combust. Flame **117**, 553-561 (1999).

6. Bittner, J. D. and Howard, J. B. Composition Profiles and Reaction Mechanisms in a Near-Sooting Premixed Benzene/Oxygen/Argon flame. Proc. Combust. Inst. **18**, 1105-1116 (1981).

7. Benish, T. G. PAH Radical Scavenging in Fuel-Rich Premixed Benzene Flames. Ph.D. thesis, Massachusetts Institute of Technology, Cambridge, MA 1999.

8. Westmoreland, P. R., Howard, J. B. and Longwell, J. B. Tests of Published Mechanisms by Comparison with Measured Laminar Flame Structure in Fuel-Rich Acetylene Combustion. Proc. Combust. Inst. **21**, 773-782 (1986).

9. Westmoreland. P. R. Experimental and Theoretical Analysis of Oxidation and Growth Chemistry in a Fuel-Rich Acetylene Flame. Ph.D. thesis, Massachusetts Institute of Technology, Cambridge, MA 1986.

10. Bhargava, A. and Westmoreland, P. R. Measured Flame Structure of Kinetics in a Fuel Rich Ethylene Flame. Combust. Flame **113**, 333-347 (1998).

11. Bhargava, A. and Westmoreland, P. R. MBMS Analysis of a Fuel-Lean Ethylene Flame. Combust. Flame **115**, 456-467 (1998).

12. DiNaro, J. L., Howard, J. B., Green, W. H., Tester, J. W., Bozzelli, J. W. Elementary Reaction Mechanism for Benzene Oxidation in Supercritical Water. J. Phys. Chem. A, **104**, 10576-10586 (2000).

13. Alzueta, M. U., Glarborg, P. and Dam-Johansen, K. Experimental and Kinetic Modeling Study of the Oxidation of Benzene. Int. J. Chem. Kinet. **32**, 498-522 (2000).

14. Wang, H. and Brezinsky, K. Computational Study on the Thermochemistry of Cyclopentadiene Derivatives and Kinetics of Cyclopentadienone Thermal Decomposition. J. Phys. Chem. A **102**, 1530-1541 (1998).

15. Moskaleva, L. V. and Lin, M. C. Unimolecular Isomerization/Decomposition of Cyclopentadienyl and Related Bimolecular Reverse Process: *Ab Initio* MO/Statistical Theory Study. J. Comput. Chem. **21**, 415-425 (2000).

Publications of DOE Sponsored Research, 1999-2001

1. Pope, C.J., Shandross, R.A. and Howard, J.B.: "Variation of Equivalence Ratio and Element Ratios with Distance from Burner in Premixed One-Dimensional Flames," *Combust. Flame*, **116**, 605-614, *1999*.

2. Richter, H., Grieco, W.J. and Howard, J.B.: "Formation Mechanism of Polycyclic Aromatic Hydrocarbons and Fullerenes in Premixed Benzene Flames," *Combust. Flame* **119**, 1-22, 1999.

3. Swallow, K.C., Howard, J.B., Grieco, W., Benish, T., Taghizadeh, K., Plummer, E.F. and Lafleur, A.L.: "Correlation of PAH Structure and Fullerenes Formation in Premixed Flames," *Polycyclic Aromatic Compounds*,**14** and **15**, 201-208(1999).

4. Richter, H. Benish, T.G., Ayala, F. and Howard, J.B.: "Kinetic Modeling of the Formation of Polycyclic Aromatic Hydrocarbons," *A.C.S. Fuel Chem. Div. Preprints* **45(2)**, 273-277, 2000.

5. Grieco, W.J., Howard, J.B., Rainey, L.C. and Vander Sande, J.B.: "Fullerenic Carbon in Combustion-Generated Soot," *Carbon* **38**, 597-614, 2000.

6. Richter, H., Benish, T.G., Mazyar, O.A, Green, W.H. and Howard, J.B.: "Formation of Polycyclic Aromatic Hydrocarbons and Their Radicals in a Nearly Sooting Premixed Benzene Flame," *Proc. Combust. Inst.*, **28** (in press).

7. Richter, H. and Howard, J.B.: "Formation of Polycyclic Aromatic Hydrocarbons and their Growth to Soot – A Review of Chemical Reaction Pathways," *Prog. Energy and Combust. Sci.* **26**, 367-380 , 2000.

8. Richter, H., Mazyar, O.A., Green, W.H., Howard, J.B. and Bozzelli, J.W.: "A Detailed Kinetic Study of the Growth of Small Polycyclic Aromatic Hydrocarbons," *J.Phys Chem. A*, **105**, 1561-1573, 2001.

IONIZATION PROBES OF MOLECULAR STRUCTURE AND CHEMISTRY

Philip M. Johnson
Department of Chemistry
State University of New York, Stony Brook, NY 11794
Philip.Johnson@sunysb.edu

PROGRAM SCOPE

Photoionization processes provide very sensitive probes for the detection and understanding of molecules and chemical pathways relevant to combustion processes. Laser based ionization processes can be species-selective by using resonances in the excitation of the neutral molecule under study or by exploiting the fact that different molecules have different sets of ionization potentials. Therefore the structure and dynamics of individual molecules can be studied, or species monitored, even in a mixed sample. We are continuing to develop methods for the selective spectroscopic detection of molecules by ionization, to use these spectra for the greater understanding of molecular structure, and to use these methods for the study of some molecules of interest to combustion science.

RECENT PROGRESS

The exploitation of Rydberg molecules has enabled orders-of-magnitude increases in the resolution available for recording the spectra of molecular ions. These spectra provide information equivalent to photoelectron spectra, but contain much more information by virtue of that resolution and the versatility of laser preparation of the states involved.

We have developed techniques called mass analyzed threshold ionization spectroscopy (MATI) and photoinduced Rydberg ionization spectroscopy (PIRI) to provide high resolution access to the spectroscopy of the electronic states of ions. To accomplish this we create high Rydbergs state just below an ionic threshold. A small field is used to separate the prompt ions from the Rydberg molecules and then after a delay of a few microseconds either a small electrical pulse field ionizes the Rydbergs (MATI) or a tunable laser beam is sent through the Rydberg molecules (PIRI). In the latter, if this laser is resonant with a transition of the ionic core, core-excited Rydberg molecules are created which promptly autoionize. These ions are again separated from the remaining Rydbergs and after a further few microseconds the various ion packets are sent into a TOF mass spectrometer, where they arrive as a distinct groups whose intensity can be recorded as the either the Rydberg preparation laser or the final laser is scanned. The resonant nature of MATI and PIRI are of great use in sorting out the vibrational structure of some ionic states.

I. The effects of symmetry on the Jahn-Teller effect in benzene

The ground state and first excited state of benzene cation both exhibit substantial perturbations on the vibrational structure due to the Jahn-Teller effect. MATI and PIRI provide the means to study both of these states with the advantage that the multiple-resonant nature of the spectroscopy enables the absolute symmetry assignments of many of the vibrational transitions.

These two states, while both of necessity doubly degenerate, have different symmetries, E_{1g} and E_{2g}. Fundamental considerations from the model used to construct Jahn-Teller theory predict that first order coupling should be strong in the former and weak in the latter. These considerations

have been somewhat ignored in the recent literature, and have never been tested experimentally.

While the treatment of the Jahn-Teller coupling in the cation E_{1g} ground state is relatively straightforward, the excited state structure that we record in PIRI spectra is complicated by the fact that the electronic transition from the cation ground state is optically forbidden, and that the upper state is subject to a strong pseudo-Jahn-Teller effect, as well a quadratic coupling in several vibrations. For this reason, it has defied our analysis beyond a few lower fundamental vibrations. In the past year, improvements in our computer program have enabled the analysis to proceed. We are now able to include linear, quadratic, and pseudo-Jahn-Teller couplings in the same multi-mode calculation, and to make a least squares fit of the coupling parameters and vibrational frequencies to the experimental lines.

In the $^2E_{2g}$ state, there is relatively strong quadratic or pseudo- coupling in every degenerate vibration that is identifiable. However, for mode 6, which should be the major vibration to exhibit a linear coupling, this drops from 0.4 in the ground state to 0.005 in the $^2E_{2g}$ state. For this mode, the quadratic effect is much larger than the linear one. This result establishes the general principle that only states that have a wavefunction with a single nodal plane through the principle axis (and therefore one quantum of pseudo-angular momentum) have a strong linear coupling. The ground state fulfills this condition and has a strong linear coupling, while the $^2E_{2g}$ state has two nodes and the coupling is weak. This principle should extended other molecules.

II. Methyl torsional motions in cations

The torsional analysis of polyatomic cations is a field still in its infancy, with the first papers dating to 1992. In order to better understand how the molecular geometry changes from the neutral molecule to the cation, and how these changes affect the normal modes and torsional barriers, one needs high resolution spectroscopic data from the cation. The reason for the interest in this field spans many areas of chemistry and physics, from the understanding of thermodynamic cycles, to obtaining more accurate values of dissociation energies, and understanding molecular conformational changes.

The MATI spectra of trans-2-butene and propene have been obtained using single-step VUV excitation. The ionization potential for trans-2-butene is 73605±4 cm^{-1}, while for propene it is 78587±4 cm^{-1}. Both species have progressions of the low frequency, torsional, normal modes. Using the torsional normal mode and first overtone from trans-2-butene cation the torsional barrier is determined to be approximately 453cm^{-1}, assuming a sinusoidal potential. Normal mode analysis indicates that all low frequency normal modes of the propene cation involve substantial internal motion of the vinyl component, and the spectrum shows a very anharmonic torsional mode progression. These factors complicate direct torsional barrier analysis from the experimental lines, but through the use of various *ab-initio* methods the propene torsional barrier is determined to be approximately 429cm^{-1}. Due to the anharmonicity found in propene, the correlation corrected Vibrational Self-Consistent Field (cc-VSCF) method in GAMESS was used to verify the assignments of the experimental lines. The torsional barriers for both cations are found to lie approximately 275-300 cm^{-1} below the barrier heights of the neutral species.

III. The ionization potential of dioxane

In a situation that is unfortunately fairly common, the ionization potential of the common solvent dioxane has been reported from to be 9.13 eV to 9.43 eV. Using MATI spectroscopy, the correct IP is 73062 +/- 4 cm^{-1} (9.058 eV), roughly 575 cm^{-1} lower than the best previously reported

value. The cation spectrum of this molecule is very regular, agreeing remarkably well with calculations in both its vibrational frequencies and intensities.

FUTURE PLANS

We are currently working on a new method of PIRI detection that involves collecting electrons instead of ions. This would enable the extension of this method to many molecules that have short Rydberg lifetimes and are now difficult to do. It will also allow the use of continuous Rydberg excitation sources (such as synchrotron light) and CW PIRI lasers. The goal is to develop a general method for cation electronic spectroscopy with orders of magnitude higher optical resolution than current techniques.

DOE PUBLICATIONS

"Photoinduced Rydberg Ionization (PIRI) Spectroscopy of the B-state of Fluorobenzene Cation," Richa Anand, Jeffrey E. LeClaire, and Philip Johnson, J. Phys. Chem.A, **103**, 2618 (1999).

"Assignment Of The $\tilde{B}^+$ State Of The Chlorobenzene Cation: Photoinduced Rydberg Ionization (PIRI) Spectroscopy", Richa Anand, J. D. Hofstein, Jeffrey E. LeClaire, Philip Johnson, and Claudina Cossart-Magos, J. Phys. Chem. A, **103**, 8927-8934 (1999).

"Infrared spectrum of the -CH_2 out of plane fundamental of C_2H_5," Trevor J. Sears, Philip M. Johnson and Joanne BeeBe-Wang, J. Chem. Phys., **111**, 9213-9221 (1999).

"Vibrational effects on the torsional motion of ethyl radical," Philip M. Johnson and Trevor J. Sears, J. Chem. Phys., **111**, 9222-9226 (1999).

"Reassessing the orbitals of pi systems using photoinduced Rydberg ionization spectroscopy," Philip Johnson, Richa Anand, Jason Hofstein and Jeffrey LeClaire, J. Electron Spect. and Related Phenom., **108**, 177-187 (2000).

"Mass-analyzed cation spectroscopy using Rydberg states: MATI and PIRI", Philip M. Johnson, Adv. Ser. in Phys. Chem.,Vol. 10A, *Photoionization and Photodetachment*, edited by C. Y. Ng (World Scientific, Singapore, 2000).

"Torsional analyses of trans-2-butene and propene cations: A comparative investigation of two prototypical ions with different degrees of symmetry", Andrew Burrill and Philip Johnson, Journal of Chemical Physics, *in press*.

DYNAMICAL ANALYSIS OF HIGHLY EXCITED MOLECULAR SPECTRA

Michael E. Kellman
Department of Chemistry, University of Oregon, Eugene, OR 97403

kellman@oregon.uoregon.edu

PROGRAM SCOPE:

The objective of our program is to develop new theoretical tools to unlock knowledge of intramolecular dynamics encoded in highly excited experimental spectra.
Spectra of highly excited molecules are essential to understanding intramolecular processes of fundamental importance for combustion. Because of the breakdown of the standard normal modes picture in highly excited vibrational states, new theoretical tools are needed to interpret the information about ultrafast internal molecular motion contained in high energy spectra.

The departure from ordinary normal mode behavior in highly excited states is due to the combination of strong anharmonicity and multiple Fermi resonance couplings. This gives rise to new dynamical behavior, including the birth in bifurcations of new anharmonic modes, and the onset of widespread chaotic classical dynamics. In a bifurcation, a normal mode changes character, with an abrupt change in the natural motions of the molecule. This involves a branching, or bifurcation, into new types of anharmonic motion.

Our current goal is to handle dynamics of increasing complexity in larger systems, including spectra of isomerizing systems up to and above the isomerization barrier. Acetylene appears to be the system where there is greatest likelihood that experimental access will become possible to all the dynamical problems of interest to us. Other systems include water, substituted formaldehyde, and methanol.

RECENT PROGRESS:

Isomerization spectroscopy: Reaction modes born in bifurcations. Isomerizing species are of crucial importance in understanding combustion processes, and their spectroscopic observation has been a long-standing goal for a variety of systems. Spectroscopy experiments and theory have had isomerization of HCN and its analog HCP as targets of interest. Experimental "isomerization spectra" of HCP have been observed by Ishikawa and coworkers. Analysis indicates a bifurcation to an "isomerization mode", signaled by the observation of a spectral pattern originally predicted by our group, as described next.

Predictions confirmed: Spectral patterns of bifurcating normal modes.
When a bifurcation of normal modes into new types of anharmonic motion takes place, a key problem is identifying spectral patterns associated with this change. Several years ago, we predicted (Svitak et al., J. Chem. Phys. 1995) distinct hallmark patterns associated with different types of bifurcation. The simplest such pattern was predicted to be a minimum in the spacing of adjacent levels assigned with sequential quantum numbers, using the new assignment procedures developed in our work for systems with Fermi resonance. Exactly this pattern, connected to the onset of the "isomerization mode", was observed by Ishikawa and coworkers in analysis of experimental spectra of isomerizing HCP. The data of Ishikawa were not complete, however. We therefore analyzed a complete set of vibrational levels for the system calculated from a molecular potential surface by Schinke and coworkers, who noted odd patterns in the spectrum. With coworkers, we identified these as a second type of pattern, of a kind which we had also predicted earlier. All the evidence now fits together and points to the conclusion of an abrupt birth in a bifurcation of an "isomerization mode". This shows the potential of bifurcation methods to make connections with notions of reaction pathways. A recent publication [2] describes the five-way collaboration of groups from MIT (R. Field), Tokyo (H. Ishikawa), Gottingen (R. Schinke), Grenoble (M. Joyeux), and my student V. Tyng and myself.

Spectral patterns of chaotic acetylene: Assigning spectra with diabatic correlation diagrams. It is now very clear that one can obtain important dynamical information about both polyad constants and bifurcations from analysis of the spectroscopic Hamiltonian. The natural question is then how far one can go in making a direct link between *observed* features of spectra of complex systems, and interpretation with dynamical analysis. We would like to detect directly in spectra the effects of bifurcations and resulting birth of new anharmonic modes. As discussed above, we have learned how to do this for relatively simple systems with a single resonance, identifying spectral patterns characteristic of distinct kinds of bifurcations. But are analogous patterns and their detection possible in chaotic systems involving many modes and multiple resonances? This question becomes important for systems of increasing complexity like acetylene, precisely those in which the chaotic, many-mode dynamics made the polyad detection itself a challenging problem.

There is no a priori justification to search for such patterns at the subpolyad level in chaotic systems, since there are no rigorous quantum numbers known that would be related to such patterns, even at the level of approximation inherent in the polyad structure of the spectroscopic Hamiltonian.

Nonetheless, in an early test case we succeeded in identifying approximate subpolyad patterns in H_2O, using a diabatic correlation diagram technique (Rose and Kellman, J. Chem. Phys. 1996). The basic idea is simple: the couplings of a spectroscopic Hamiltonian are gradually turned on, and the diabatic energy level curves of the correlation diagram are followed across avoided crossings. The result is the assignment to each level of a set of approximate "dynamical" quantum numbers. These assignments give a grouping of the levels into sets labeled by effective quantum numbers. In many

respects, these groupings are analogous to the progressions and sequences assigned with normal mode quantum numbers at lower energy. At the same time, their energy and intensity patterns are markedly different, showing the influence of bifurcations.

We have now applied this diabatic correlation procedure to acetylene spectra, and have again succeeded in identifying novel energy and intensity patterns. [4,5]

Visualization of complex molecular dynamics. One of the most important goals of current and proposed research is to convert the fairly abstract dynamical knowledge of the bifurcation analysis into a directly visualizable representation. For this, we are now using computer animation techniques to make movies of the anharmonic modes born in bifurcations. Examples of our animations can be found on a website at http://darkwing.uoregon.edu/~meklab/ , which the reader is urged to access.

FUTURE PLANS: COMPLEXITY AND REACTIVE DYNAMICS IN LARGER SYSTEMS.

The biggest questions for the future are whether earlier successes can be extended to larger systems of greater complexity, and to the realm of reactive phenomena such as unimolecular rearrangements involving a potential barrier. The key challenges: (1) are current methods practical for larger, more complex systems, with more degrees of freedom, and if so, making the results intelligibly understood and utilized; and (2) the very difficult problem of extending the spectroscopic Hamiltonian to handle qualitatively new physical situations, in particular, motion in multiple potential wells, and very large-amplitude motion above two or more wells.

The polyad number and analytical bifurcation analysis. In H_2O and now in acetylene, we have taken a particular approach to the bifurcation analysis, which we believe is the key to making the analysis of larger systems tractable. This involves the polyad, or total vibrational quantum number in a key role. The presence of the polyad number in the spectroscopic Hamiltonian is of enormous value in bifurcation analysis, because it makes solution for the bifurcations of the normal modes essentially analytic - avoiding the alternative of numerical searching of computational solutions of Hamilton's equations. This is true even for many degrees of freedom with multiple resonances couplings and chaos. The bifurcation problem thereby is reduced from numerical searching to the much simpler task of finding the solutions of analytical (polynomial) equations.

First steps: pure bending spectra of acetylene. As a first step, we have been performing the bifurcation analysis, using the polyad approximation, for the acetylene bends system. We have successfully reproduced the numerical results of Jacobson and coworkers (M.P. Jacobson, C. Jung, H.S. Taylor, and R.W. Field, J. Chem. Phys. 111, 66 (1999)). The bifurcation diagram, along with the animations animations mentioned above, are conveniently available at http://darkwing.uoregon.edu/~meklab/ .

Isomerization dynamics: Full stretch-bend complexity, above-barrier motion. Developing methods to uncover the molecular motion involved in the acetylene-vinylidene isomerization is the central goal of research in the foreseeable future. It leads us to explore three distinct, but related sets of problems. (1) What is the fate of the pure local bending mode, the supposed isomerization mode, as the barrier is approached and surmounted? (2) Is the isomerization process one that really involves only the bending modes? Is it necessary to include the stretches to achieve isomerization? If so, what does the bifurcation analysis say about the fate of known modes (e.g. in the movies at the above web site) as they turn into the real isomerization modes? (3) Finally, suppose spectroscopy does access the isomerization. This will involve vibrations of acetylene below the top of the barrier; motion on the other side of the barrier in the small vinylidene well; and motion above the barrier that samples both the acetylene and vinylidene regions. Can one build a spectroscopic Hamiltonian to accommodate all of these phenomena? This has not previously been done; if feasible, it will involve a significant extension of the use of effective spectroscopic Hamiltonians. Then, what will be the signatures in the vibrational spectrum of the isomerization process?

Recent publications related to DOE supported research:

1. M.E. Kellman, article on "Correlation", McGraw-Hill 1999 Yearbook of Science and Technology (McGraw-Hill, New York, 1999).
2. M. Joyeux, D. Sugny, V. Tyng, M.E. Kellman, H. Ishikawa, and R.W. Field, "Semiclassical Study of the Isomerization States of HCP", J. Chem. Phys. 112, 4162 (1999).
3. S. Yang and M.E. Kellman, "Direct Trajectory Method for Semiclassical Wavefunctions", Phys Rev A 62, 022105 (2000).
4. J.P. Rose and M.E. Kellman, "Spectral Patterns of Chaotic Acetylene", J. Phys. Chem. A. 104, 10471 (2000).
5. M.E. Kellman, J.P. Rose, and Vivian Tyng, "Spectral Patterns and Dynamics of Planar Acetylene", in press, European Physical Journal D : Atoms, Molecules and Clusters.
6. M.E. Kellman, "Internal Molecular Motion", in press, Encyclopedia of Chemical Physics and Physical Chemistry, J.H. Moore, Ed. (Institute of Physics, London).
7. M.E. Kellman and M.W. Dow, "Dressed Basis for Highly Excited Molecular Vibrations", submitted to J. Chem. Phys.
8. M.E. Kellman, "Dances With Molecules", submitted, Accounts of Chemical Research.

KINETICS OF COMBUSTION-RELATED PROCESSES AT HIGH TEMPERATURES

J. H. Kiefer and R.S. Tranter
Department of Chemical Engineering
University of Illinois at Chicago
Chicago, IL 60607
(kiefer@uic.edu)

Program Scope

This program involves the use of the shock tube with laser-schlieren, laser-flash absorption, and dump-tank GC/MS analysis diagnostics to explore reactions and energy transfer processes over an extremely wide range of temperatures and pressures. We also report some recent theoretical efforts motivated by the experiments. Over the last two years, our work has greatly benefited from collaboration with A. F. Wagner and L. B. Harding at Argonne, H. Wang at the University of Delaware (Mechanical Engineering), and R. D. Kern at UNO.

Recent progress

The study of early precursors to soot formation: the pyrolysis of propargyl iodide.

It is widely believed that aromatic rings are essential for efficient soot formation. The path or paths to aromatics in aliphatic pyrolysis or oxidation has consequently been a subject of much study over the past few years. At present the most popular [1] route is through recombination of propargyl (C_3H_3) radicals generating benzene and/or phenyl and H-atom. In a recent paper, Scherer, Just and Frank (SJF) [2] reported H-atom and I-atom ARAS and product analyses from C_3H_3I in shock waves using $C_3H_3I \rightarrow C_3H_3 + I$ as a pyrolytic source of propargyl radical over 1.5-2.2 bar, and 1100-2100K. They found the only dissociation channel is the C-I fission. The H-atom concentrations from C_3H_3 dimerization are very low suggesting a small contribution from phenyl formation; observed products were primarily benzene and other C_6H_6 isomers.

The experiments of SJF strongly suggest a laser-schlieren investigation. If stabilized benzene is indeed formed, an initial positive gradient from the iodide dissociation should be followed by a negative gradient from the large (~ 145kcal/mole) exothermicity of benzene formation. It should then be possible to determine the rate to benzene over an extremely wide range of conditions as well as derive a rate for the C_3H_3I dissociation.

We have now performed some 60 low-pressure (80 - 150 torr) experiments in 2% C_3H_3I/Kr covering 800 - 1500K. Typical results are shown in the attached figure. For low temperatures the gradients are initially positive, as expected, and then turn negative at later time or higher temperature. At still lower temperatures the gradient is positive throughout the observation time. An important observation, common to all the experiments, is that the gradient accurately returns to zero late in the process.

Understanding and modeling of the experiments is complicated by the number of possible C_6H_6 isomers that can be formed by propargyl dimerization. The possible products of this combination were fully enumerated in the theoretical work of ref. 1, where they include ($\Delta_fH^\circ_{298}$): 1,5-hexadiyne (99), and the other two direct addition products 1,2,4,5-

hexatetraene (98), and 1,2- hexadien-5-yne (99); the H-atom shift isomer 1,3-hexadien-5-yne (87); and the cyclics 3,4-dimethylenecyclobut-1-ene (80), fulvene (52) and benzene (20).

The possible reactions in this system reduce to the simple scheme:

$$C_3H_3I \rightarrow C_3H_3 + I$$
$$2C_3H_3 \rightarrow C_6H_6\,(?)$$

Where the C_6H_6 may be any combination of the above isomers. The list of these may be reduced by recognizing that any version of the above two reactions that produces an observable gradient from the second reaction creates a steady state in the C_3H_3 by the onset of negative values. Because this needs two C_3H_3I dissociations for each C_6H_6 formed, and this dissociation is ~45kcal/mol endothermic, generation of a negative gradient requires a negative ΔH for the combination in excess of 90kcal/mol. The latest value for the propargyl $\Delta_fH^\circ_{298}$ is 82.5kcal/mol, so negative gradients require a product whose heat of formation is less than 75kcal/mol. Thus fulvene and/or benzene must be formed and stabilized at very low pressures and for temperatures as high as 1500K(C_6H_5 + H channel is also endothermic in steady state).

We have modeled the experiments in the figure with a three-step mechanism having C_3H_3I dissociation and propargyl combination to just 1,5-hexadiyne and benzene. Rate constants for the latter pair of reactions were: $\log_{10}k(cm^3/mol\text{-}s)$ = 13.6 and 13.2 respectively. The rate constant for the C_3H_3I dissociation had and Ea of 30 kcal/mol in the experiments below 1100K, but had to be reduced by up to a factor two at the highest temperatures. Of course this behavior is consistent with strong falloff of this fast reaction. As can be seen the results are more than adequate. The gradient returns to zero here because of depletion of the C_3H_3 by both dimerizations. Without the weakly endothermic hexadiyne formation, depletion is not sufficient. Of course any combination of the possible thermoneutral or slightly endothermic products can substitute for this reaction.

Pyrolysis of 1,1,1-trifluoroethane.

The molecular dissociation of $CF_3CH_3 \rightarrow HF + CF_2{=}CH_2$ is a popular "chemical thermometer" for single pulse studies; it is currently being used by the K. Brezinsky group to calibrate their high-pressure tube. Although the reaction has been studied a number of times [3], there is no record of falloff having been seen. We thus carried out a series of laser-schlieren measurements on this process. These experiments used 5% CF_3CH_3 /Kr mixtures, and covered P = 77 - 574 torr, 1570-2230K. As expected for a process with only one reaction (dissociation of the product ethene is negligible for T < 2200K and t <5μs), the fit of the profiles is virtually quantitative. the reaction shows the expected (RRKM) falloff reduction in E_a from the previous k_∞ = (74kcal/mol) [3] to an average 43kcal/mol, but there is little sign of pressure dependence in the rates. This anomaly is not understood. The construction of a RRKM model was facilitated by L. B. Harding, who provided transition state properties. The only modification needed to accurately match the available high-pressure, low-temperature rate data [3] with this model was a reduction of the 71kcal/mol barrier by 0.5kcal/mol.

Thermodynamic properties of cyclopentadienyl radical.

In collaboration with A. F. Wagner and H. Wang, we have now calculated new thermodynamic functions for this Jahn-Teller distorted radical. These calculations used

high-level *ab initio* methods for the PE surface and an accurate solution of the wave equation for nuclear motion on that surface. We again find the increase in entropy from the pseudorotation is actually rather small, and the equilibrium constants for the important reactions

$$C_5H_6 \rightarrow C_5H_5 + H$$
$$C_5H_5 \rightarrow C_3H_3 + C_2H_2$$

are not much affected. This appears to be the only example of a complete and quantitative calculation of properties for a Jahn-Teller species. This work is described more fully in the abstract of A. F. Wagner.

Future Plans

We plan to continue and extend our efforts on the propargyl reactions with low-temperature experiments at higher pressures, and high-temperature, very low pressure shocks to see is we can block stabilization of the initial chemically activated benzene. An interesting possibility is the addition of excess C_2H_2, looking for C_5H_5 formation. We still plan to continue our earlier efforts on the c-C5 compounds with dimethylcyclopentadiene decomposition. Here the conversion to benzene should occur at even lower temperatures, and we may nowbe able to identify fulvene in the products.

References (Further sources may be found in the cited examples)

1) C. F. Melius, J. A. Miller, and E. M. Eveleth, Proc. Combust Inst. **24**: 621 (1993).

2) S. Scherer, Th. Just, and P. Frank, Proc. Combust. Inst. **28**: (2000), in press.

3) Tsang, W. and Lifshitz, A., Int. J. Chem. Kinet. **30**, 621 (1998).

Publications of DOE Sponsored Research During 1999-2001.

"The Pyrolysis of Methylcyclopentadiene: Isomerization and Formation of Aromatics", E. Ikeda, R.S. Tranter, J.H. Kiefer, R.D. Kern, H.J. Singh, and Q. Zhang, Proc. Combust. Inst. **28** (2000) in press.

"Observation and Analysis of Nonlinear Vibrational Relaxation of Large Molecules in Shock Waves", J.H. Kiefer, L.L. Buzyna, A. Dibb, and S. Sundaram, J. Chem. Phys. **113**: 48 (1999).

"Thermolysis of Cyclopentadiene in the Presence of Excess Acetylene or Hydrogen", R.D. Kern, H.J. Singh, Q. Zhang, B.S. Jursic, J.H. Kiefer, R.S. Tranter, E. Ikeda, and A.F. Wagner, 22nd International Symposium on Shock Waves (1999).

"The Application of Densitometric Methods to the Measurement of Rate Processes in Shock Waves", J. H. Kiefer, in "Handbook of Shock Waves" Chapter 16.2, Academic Press, New York; p. 29 - 76 (2001).

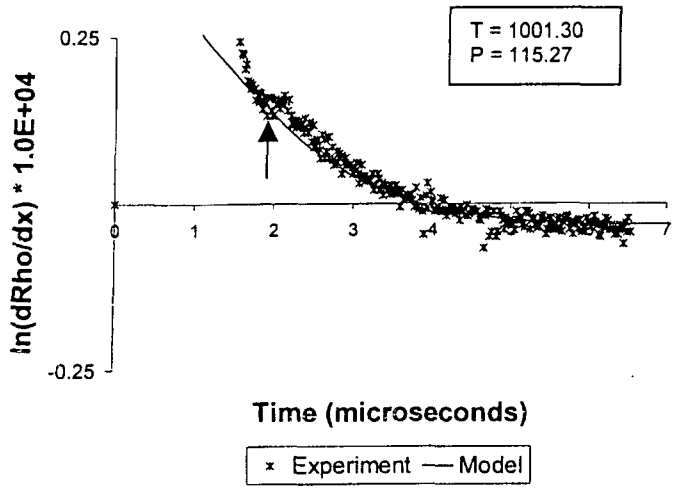

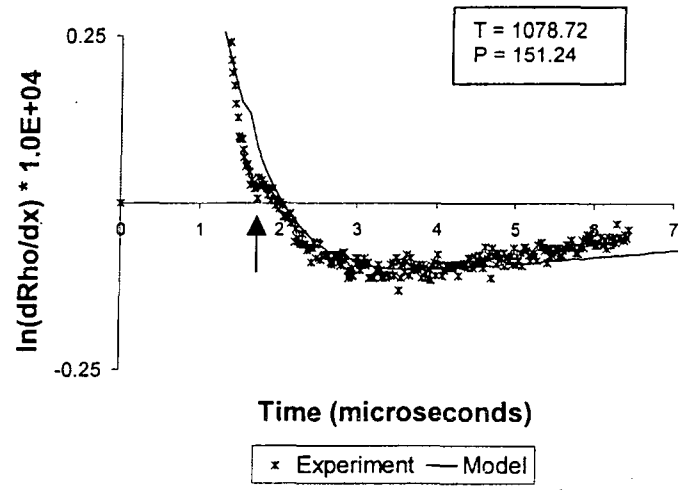

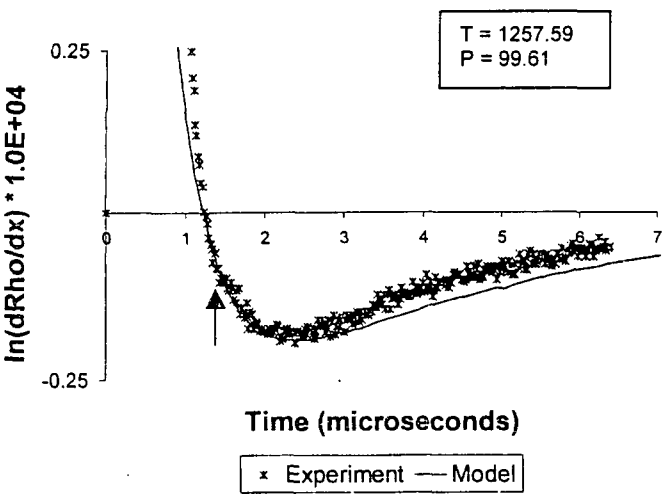

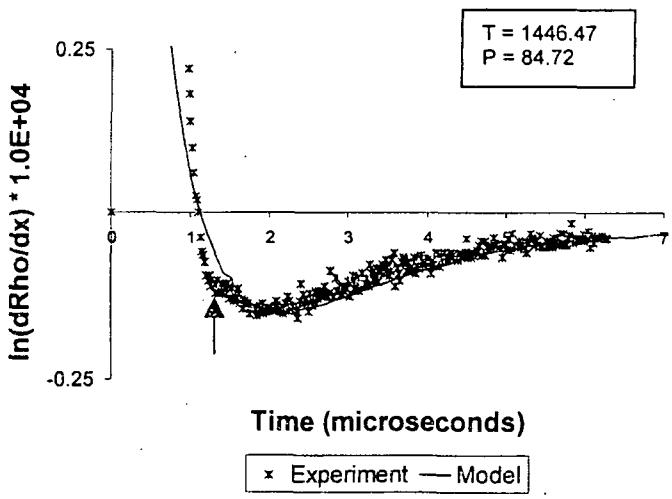

Linear plots of density gradients from low-pressure laser-schlieren experiments in 2% C_3H_3I/Kr. The steeply falling early measured values are a consequence of shock-front diffraction/refraction and are ignored; in each case this interference is over at the vertical arrows.

THEORETICAL CHEMICAL KINETICS

Stephen J. Klippenstein
Combustion Research Facility
Sandia National Laboratories
Livermore, CA, 94551-0969
E-mail: sjklipp@sandia.gov

Program Scope

The focus of this program is the theoretical estimation of the kinetics of elementary reaction steps of importance in combustion chemistry. The research involves a combination of *ab initio* quantum chemistry, variational transition state theory, and master equation simulations. The emphasis of our current applications is on (i) reactions of importance in soot formation, and (ii) radical oxidation reactions. We are also interested in a detailed understanding of the limits of validity of and, where feasible, improvements in the accuracy of transition state theory. As such, the research includes the development of novel implementations of transition state theory, and of the procedures for coupling such simulations with quantum chemical evaluations. Detailed comparisons with experiments are used to explore and improve the predictive properties of the theoretical models. Direct dynamics simulations are also being performed as a means for testing the statistical assumptions, for exploring reaction mechanisms, and for generating theoretical estimates where statistical predictions are inadequate.

Recent Progress

Master Equation Analyses

We have recently completed master equation based analyses of two key reactions of propargyl radical: $C_3H_3 + C_3H_3$ and $C_3H_3 + O_2$.[1,2] In both cases, quantum chemical estimates for the properties of the relevant stationary points were employed in obtaining transition state theory estimates for the underlying channel specific rate constants. These two studies, were performed in collaboration with Jim Miller, and a summary of the propargyl plus propargyl reaction is provided in his abstract.

Our analysis of the $C_3H_3 + O_2$ reaction began with a density functional theory based exploration of the potential energy surface. A combination of QCISD(T)/6-311++G*(d,p)* and MP2/6-311++G*(3df,2pd)* evaluations at the B3LYP/6-311+G*(d,p)* geometries provided higher level energy estimates. In many respects, the potential energy surface is at least qualitatively analogous to those for $C_2H_3 + O_2$ and for $HCC + O_2$.[3-5] However, among other things, the resonance stabilization of the radical leads to important quantitative differences.

At low temperatures the reaction is dominated by addition to the CH_2 side of the propargyl radical followed by stabilization. Addition to the CH side, which is followed by one of various possible internal rearrangements, becomes the dominant process at higher temperatures. These internal rearrangements involve a splitting of the O-O bond via the formation of 3-, 4-, or 5-membered rings, with the apparent products being $CH_2CO + HCO$. Rearrangement via the 3-membered ring is predicted to dominate the kinetics, but the saddlepoints for the 4- and 5-membered rings lie only a few kcal/mol higher. Rearrangement

from the CH_2 addition product, via a 4-membered ring, would yield H_2CO + HCCO, but the barrier to this rearrangement is too high to be kinetically significant. Other possible products require H transfers and as result appear to be kinetically irrelevant.

Modest variations in the energies of a few key stationary points (most notably the entrance barrier heights), yields kinetic results that are in good agreement with the available experimental results.[6,7] The small values for the master equation predictions of the $C_3H_3 + O_2$ rate coefficient ($<10^{-13}$ cm^3 s^{-1} for temperatures of 2000 K or lower) provide an explanation for the enhanced concentrations of resonantly stabilized free radicals in the combustion environment. The smallness of the rate coefficients is the direct result of various effects arising from the resonance stabilization of the propargyl radical. Firstly, the addition to either side is predicted to have a significant saddlepoint arising from the need to break the resonance during the addition process. In contrast, related calculations for a variety of other alkyl radicals provide no indication of a saddlepoint along the addition path. The resonance stabilization also results in a sharp reduction in the well depth for the addition products, from 30-50 kcal/mol for related radicals[6-9] to <20 kcal/mol for propargyl and allyl radicals. This reduction in the well depths correlates with increased barrier heights (relative to reactants) for the internal rearrangements required for bimolecular product formation. These internal rearrangement barriers provide the dominant bottleneck to reaction at higher temperatures.

We have also recently examined a variety of radical oxidation reactions including ethyl, propyl, and butyl plus O_2 reactions. Our detailed analysis of the $C_2H_5 + O_2$ reaction is also summarized in Jim Miller's abstract. For the propyl and butyl radical oxidation reactions, we generated analogous ab initio based mechanisms for each of the isomers of the two radicals. The detailed experimental results of Taatjes for the time dependent HO_2 and OH yields provide important tests for our master equation simulations.[10,11] For the propyl reaction minor modifications of the calculated energies (by ~1-2 kcal/mol) allows for a quantitative reproduction of the experimental observations.

One interesting finding from the ab initio studies is that the hydroperoxy species (generally labeled QOOH and formed via the internal transfer of an H atom) have high barriers to bimolecular product formation when they are formed via transition states with 6-membered rings or smaller. Only one of the QOOH species in n-butyl, formed via a 7-membered ring transition state, is expected to yield a significant increase in the OH yield. Apparently, the product cyclic ethers must have a ring size of 5 or greater in order to minimize the ring strain in the transition state for the OH producing channel.

Direct Dynamics

The reaction of methyl radicals with oxygen atoms is an important pathway for the removal of methyl radicals, particularly under lean fuel conditions.[12] While H + H_2CO is the dominant product, recent experimental studies have indicated that H_2 + HCO is a significant secondary product.[13-15] The initial stage in the reaction is expected to involve the formation of a CH_3O complex. However, attempts to locate a saddlepoint for the $CH_3O \rightarrow H_2 + HCO$ process have been unsuccessful. As a result, it is difficult to develop meaningful statistical models for the branching. Instead, in collaboration with Larry Harding at Argonne, we have studied the branching with a direct dynamics approach, using the B3LYP density functional, with CCSD(T) evaluations at the stationary points demonstrating the apparent validity of the B3LYP functional

for this reaction.[16] The large exothermicities for the relevant processes validates the use of classical dynamics in the propagation of the nuclear coordinates.

Attempts to use various configurations along the trajectories as starting points for locating the saddlepoint for $CH_3O \rightarrow H_2 + HCO$ were unsuccessful. An H atom abstraction saddlepoint connecting $H + H_2CO$ with $H_2 + HCO$ does exist. However, in many instances, the dynamics avoids this saddlepoint region, instead simply passing over the ridge that separates CH_3O from $H_2 + HCO$. This dynamics is reminiscent of that in the isoelectronic $H_2 + CN$ system, as studied by Schatz and coworkers.[17] The estimated branching fraction of 0.15 ± 0.03 is in good agreement with the experimental observations,[13-15] and is essentially temperature independent. This branching fraction is predicted to decrease by a factor of 0.61 upon deuteration of methyl in agreement with the experimental observations of our collaborator Stephen Leone.

We have also performed ab initio molecular dynamics simulations of the unimolecular dissociation of ketene.[18] Here we were interested in the deviations of the product rotational distributions from phase space theory (PST) predictions. The average rotational energy in both the CO and the $^1CH_2$ fragments were found to decrease during the propagation from the inner (variational) transition state onto the separated fragments. Asymptotically, the propagated CO distribution remains slightly hotter than PST, whereas that for $^1CH_2$ ends up significantly colder than PST, with both results being in good agreement with experiment.[19-22] Our calculations did not, however, reproduce the experimentally observed correlations between $^1CH_2$ and CO rotational states, in which the simultaneous formation of low rotational levels of each fragment is suppressed relative to PST.[23]

Future Directions

A key area of emphasis for our application studies will be on the reactions of importance in the formation of the first aromatic ring. Our study of the $C_3H_3 + C_3H_3$ reaction[1] will be extended to include an analysis of the thermal dissociation of various isomers. Comparison with experimental studies of such dissociation processes[24] should allow for refinements of the modeling and may well suggest appropriate areas for further quantum chemical analysis. This analysis will require some revisions of the VARIFLEX software package[25] since it is currently setup to handle multiwell problems only when chemically activated. We will also extend our study of the $H + C_3H_3$ reaction[26] to include an analysis of the temperature and pressure dependence of the reaction, including the bimolecular channel to form $C_3H_2 + H_2$. The bimolecular reaction may be the key mechanism for removal of C_3H_3.

The addition of acetylene to C_4H_3 and/or C_4H_5 have also been postulated to be key steps in the formation of aromatic ring compounds.[27] We will investigate each of these reactions, considering both the *n* and *i* isomers for each one, since they are effectively separate species with quite different kinetic properties. This study will build on the earlier quantum chemical work of Walch,[28] but will include a more wide-ranging analysis of the reaction pathways. The temperature and pressure dependence of the rate constant will again be estimated via master equation analyses. We have recently presented a related calculation for the $C_2H_3 + C_2H_2$ reaction.[29]

References

1. J. A. Miller and S. J. Klippenstein, *J. Phys. Chem. A*, submitted, (2001).
2. D. K. Hahn, S. J. Klippenstein, and J. A. Miller, *Faraday Disc. Chem. Soc.* **119**, submitted (2001).
3. B. K. Carpenter, *J. Phys. Chem.* **99**, 9801 (1995).
4. A. M. Mebel, E. W. G. Diau, M. C. Lin, and K. Morokuma, *J. Am. Chem. Soc.*, **118**, 9759 (1996).
5. R. Sumathi, J. Peeters, and M. T. Nguyen, *Chem. Phys. Letts.*, **287**, 109 (1998).
6. I.R. Slagle, D. Gutman, *Proc. Combust. Inst.* **21**, 875 (1996).
7. D. B. Atkinson and J. W. Hudgens, *J. Phys. Chem. A*, **103**, 4242 (1999).
8. J. A. Miller, S. J. Klippenstein, and S. H. Robertson, *Proc. Combust. Inst.*, **28**, in press, (2000).
9. S. P. Walch, Chem. Phys. Letts., **215**, 81 (1993).
10. J. D. DeSain, E. P. Clifford, and C. A. Taatjes, *J. Phys. Chem. A*, in press (2001).
11. J. D. DeSain, C. A. Taatjes, D. K. Hahn, J. A. Miller, and S. J. Klippenstein, Faraday Disc. Chem. Soc. **119**, submitted (2001); and private communication.
12. J. Warnatz, in *Combustion Chemistry*; Ed. by J. C. Gardiner, (Springer-Verlag, New York, 1983)
13. P. W. Seakins and S. R. Leone, *J. Phys. Chem.*, **96**, 4478 (1992).
14. C. Fockenberg, G. E. Hall, J. M. Preses, T. J. Sears, J. T. Muckerman, *J. Phys. Chem. A*, **103**, 5722 (1999).
15. J. M. Preses, C. Fockenberg, G. W. Flynn, *J. Phys. Chem. A*, **104**, 6758 (2000).
16. T. P. Marcy, R. R. Diaz, D. Heard, S. R. Leone, L. B. Harding, and S. J. Klippenstein, in preparation.
17. M. A. ter Horst, G. C. Schatz, and L. B. Harding, *J. Chem. Phys.*, **105**, 558 (1996).
18. K. M. Forsythe, S. K. Gray, S. J. Klippenstein, and G. E. Hall, *J. Chem. Phys.*, submitted (2001).
19. I. Garcia-Moreno, E. R. Lovejoy, and C. B. Moore, *J. Chem. Phys.*, **100**, 8890, 8902 (1994).
20. E. A. Wade, H. Clauberg, S. K. Kim, A. Mellinger, and C. B. Moore, *J. Phys. Chem. A*, **101**, 732 (1997).
21. M. Drabbels, C. G. Morgan, D. S. McGuire, and A. M. Wodtke, *J. Chem. Phys.* **102**, 611 (1995).
22. C. G. Morgan, M. Drabbels, and A. M. Wodtke, *J. Chem. Phys.*, **104**, 7460 (1996).
23. M. L. Costen, H. Katayanagi, and G. E. Hall, *J. Phys. Chem. A*, **104**, 10247 (2000).
24. U. Alkemade and K. H. Homann, *Z. Phys. Chem. (Neue Folge)*, **161**, 19 (1989).
25. S. J. Klippenstein, A. F. Wagner, R. C. Dunbar, D. M. Wardlaw, S. H. Robertson, J. A. Miller, VARIFLEX Version 1.07mt, December 24, 1999.
26. S. J. Klippenstein and L. B. Harding, *Proc. Comb. Inst.*, **28**, in press, (2000).
27. H. Wang and M. Frenklach, *J. Phys. Chem.* **98**, 11465 (1994).
28. S. P. Walch, *J. Chem. Phys.* **103**, 8544 (1995).
29. J. A. Miller and S. J. Klippenstein, *J. Phys. Chem. A*, **104**, 7525, (2000).

DOE Supported Publications, 1999-Present

1. Stephen J. Klippenstein and Lawrence B. Harding, *A Theoretical Study of the Kinetics of C_2H_3 + H,* Physical Chemistry-Chemical Physics, **1**, 989 (1999).
2. Qiang Cui, Keiji Morokuma, Joel M. Bowman, and Stephen J. Klippenstein, *The Spin-Forbidden Reaction $CH(^2\Pi) + N_2 \rightarrow HCN + N(^4S)$ Revisited. II. Non-Adiabatic Transition State Theory and Applications*, J. Chem. Phys., **110**, 9469 (1999).
3. James A. Miller and Stephen J. Klippenstein, *Angular Momentum Conservation in the $O + OH \leftrightarrow H + O_2$ Reaction*, Int. J. Chem. Kinet., **31**, 753 (1999).
4. Stephen J. Klippenstein and Lawrence B. Harding, *A Direct Transition State Theory Based Study of Methyl Radical Recombination Kinetics*, J. Phys. Chem. A, **103**, 9388 (1999).
5. James A. Miller and Stephen J. Klippenstein, *Theoretical Considerations in the NH_2 + NO Reaction,* J. Phys. Chem A, **104**, 2061 (2000).
6. Stephen J. Klippenstein and Lawrence B. Harding, *A Summary of "A Direct Transition State Theory Based Study of Methyl Radical Recombination Kinetics",* J. Phys. Chem. A, **104**, 2351, (2000).
7. James A. Miller and Stephen J. Klippenstein, *A Theoretical Analysis of the Reaction Between Vinyl and Acetylene: Quantum Chemistry and Solution of the Master Equation*, J. Phys. Chem. A, **104**, 7525, (2000).
8. James A. Miller, Stephen J. Klippenstein, and Struan H. Robertson, *A Theoretical Analysis of the Reaction Between Ethyl and Oxygen*, Proc. Comb. Inst., **28**, *in press*, (2000).
9. Stephen J. Klippenstein, and Lawrence B. Harding, *Theoretical Kinetic Estimates for the Recombination of Hydrogen Atoms with Propargyl and Allyl Radicals*, Proc. Comb. Inst., **28**, *in press*, (2000).
10. Holger Thiesemann, Eileen P. Clifford, Craig A. Taatjes and Stephen J. Klippenstein, *Temperature Dependence and Deuterium Kinetic Isotope Effects in the CH(CD) + $C_2H_4(C_2D_4)$ Reaction Between 295 and 726 K* , J. Phys. Chem. A, *in press* (2001).

TIME-RESOLVED FTIR EMISSION STUDIES OF LASER PHOTOFRAGMENTATION AND RADICAL REACTIONS

Stephen R. Leone
JILA and Department of Chemistry and Biochemistry
University of Colorado
Boulder, Colorado 80309-0440
(303) 492-5128 srl@jila.colorado.edu

Scope of the Project

This project involves the study of laser-initiated radical reactions, photofragmentation, and energy transfer processes related to problems in combustion dynamics. The vibrationally excited species generated in such processes are probed by time-resolved Fourier transform infrared (FTIR) emission spectroscopy. Dynamics is accomplished by acquiring time-resolved signals from a high repetition rate pulsed excimer laser at each mirror position of the spectrometer. This is a relatively unique facility, applicable to the study of diatomic and polyatomic species that are the products of photofragmentation and radical reactions. The current research involves several major thrusts. One is to develop methods for studying radical reactions to determine the nascent product species and states formed in a variety of important radical-radical and radical-molecule processes. The other thrust is to develop studies of collisional energy transfer and photofragmentation involving polyatomic molecules and radical species with nascent vibrational and rotational state detail.

Spectroscopic Pattern Recognition of Product State Distributions of Photofragmentation

A large block of recent published work involved the development of new tools for spectroscopic pattern recognition and the use of these tools to study complex photodissociation pathways in ammonia and deuterated ammonia molecules. The method of time-resolved FTIR spectroscopy permits the experimentalist to study the progress of many simultaneous reaction pathways, monitoring the infrared-emitting product state distributions and branching ratios of different reaction channels. While this is a fundamental advantage of the technique, detailed analyses of the spectroscopic data obtained, and their variation with reaction conditions, are a necessary prerequisite to the interpretation of the chemical system under study. In some cases, the parallel reaction pathways under study can become so convoluted and the spectroscopy so complex that it may be difficult to readily gain any clear understanding from the analysis.

The spectral pattern recognition technique developed by Field and coworkers for the systematic study of equilibrium states has been extended to the realm of reactive product state distributions. The simplest reaction to consider is a photodissociation in which branching ratios of vibrational and rotational states for different bond cleavages are of key importance. The method was applied to a study of ammonia and deuterated ammonia species. In the case considered here, not only was the competition for products from different parent molecules investigated (e.g. ND_2 from ND_3 or from ND_2H), but the technique was applied to separate out the product state distributions arising from all four deuterated parent molecules undergoing simultaneous dissociation to give up to six different final state distributions. This is the first application of the spectral pattern deconvolution procedure to dynamical product state distributions.

The photodissociation dynamics of ammonia was explored in detail by the study of the mixed deuterated species NH_3, NH_2D, ND_2H and ND_3. The factors governing the fragmentation process are highlighted by studying these mixed species for which the dynamics vary dramatically. Excitation of the parent molecule, using 193 nm light from an ArF excimer laser, prepares the parent molecule in its first ($\tilde{A}$) excited electronic state with simultaneous excitation of the umbrella bending vibration. It was previously established that the NH_2 ($\tilde{A}$) fragment is produced with a highly selective rotational alignment around the K_a axis, with levels occupied up to the energetic limit. A new bimodal distribution of rotational states about the K_a axis of rotation was determined, which can be attributed to dissociation from planar and bent geometries. In addition, the rotation about the b/c axes was quantified further, resulting in a significant parent-molecule zero-point motion effect in the distribution of energy about the b/c axes of rotation.

Rapid H/D-atom exchange between the deuterated ammonia species does not allow the mixed deuterated species to be chemically isolated and studied individually. Instead, the dissociation dynamics of these molecules must be investigated with four species simultaneously. By performing the dissociation experiments with many different equilibrium mixtures of varying composition of the four parent species, and by subsequently implementing the spectral pattern recognition technique, product state distributions for each of the possible fragmentation pathways from all of the parent species were extracted.

Differences in the product state distributions of NH_2 and ND_2 from the dissociation of NH_3 and ND_3, respectively, can be mainly attributed to the competition of direct dissociation at planar geometries and dissociation by tunneling at non-planar geometries where the barrier to dissociation is higher in energy. The ND_2 fragment is born with less rotational excitation about its principal K_a axis than NH_2, reflecting less D-atom tunneling compared to H-atom tunneling and hence the preference for ND_3 to undergo direct dissociation at geometries closer to the planar configuration. H/D-atoms which break the D_{3h} symmetry of the parent molecule as they dissociate, due to zero-point energy in an in-plane vibrational mode, yield rotational excitation about the minor-rotational axes. This zero-point motion is smaller in amplitude for the ND_3 case than for NH_3 and consequently the impact of this symmetry breaking motion is less severe, with less energy being transformed into rotation about these axes in the former case.

The dissociation of NH_2D and ND_2H show that the competing nature of the adiabatic and non-adiabatic processes influences the dissociation dynamics. Quantum yields calculated from the pattern recognition technique suggest that the yield of the ND_2 ($\tilde{A}$) fragment, produced from the dissociation of ND_2H, is much higher than that from ND_3, with a large enhancement by a factor of approximately 6 ± 1 in the bending excitation of the product $ND_2(v=1)$. The large increase in the ND_2 quantum yield on comparing ND_2H and ND_3 may be due to the increased tunneling probability with the breaking of an N-H bond as opposed to an N-D bond. Some $ND_2(v=2)$ is also observed, reflecting the available energy, since the N-H bond is the weakest and the bending frequency of ND_2 the lowest. The rotational distributions of the products from the dissociation of NH_2D and ND_2H have also been obtained. Surprisingly, little NHD product emission is observed from the dissociation of either NH_2D or ND_2H, although the lack of transition moments for NHD prohibits the calculation of an accurate branching ratio.

Ethyl + O and CD_3/CH_3 + O Radical-Radical Reactions

The ethyl + O radical-radical reaction has been conclusively shown to yield a CO(v) product. Previous results had only reported the OH + C_2H_4, CH_3 + H_2CO, and CH_3CHO + H channels. The results of this detailed study required a large number of kinetic tests to eliminate the possibility that methyl + O or other processes might be the source of the observed vibrationally excited CO. The vibrational distribution of the CO(v=1-9) product was obtained and an estimate of the yield of CO(v) for ethyl + O, which is 0.9 of that from CH_3 + O, was obtained. The mechanism of this reaction could be to form either CO + CH_4 + H or CO + CH_3 + H_2. Both are exothermic pathways. Although nothing is known about the products that accompany the CO channel, from the theoretical mechanistic studies by Harding and Klippenstein described next, it is possible that the CO + CH_3 + H_2 channel may be favored.

In a joint experimental and theoretical work, together with Larry Harding and Stephen Klippenstein, the relative production of CO in the reactions of CD_3/CH_3 + O was investigated. The yield of CO(v=1) from the deuterated methyl + O reaction is measured to be 69±10% of the yield of CO(v=1) from the hydrogenated methyl + O reaction. Classical trajectory studies confirm the CO producing channel, arising from the sequence CH_3O _ HCO + H_2 _ CO(v) + H + H_2. The calculations also indicate the experimentally observed lower yield of CO in the deuterated reaction. Finally, the calculations show the importance of the reaction mechanism. This reaction, which proceeds through methoxy, CH_3O, has no transition state in the potential surface for the production of H_2 from the methoxy intermediate. Instead, the calculations show that the H_2 product is formed by passing over a high energy ridge in the potential, rather than via a minimum energy path. This surprising result explains the controversy over the CO producing channel in the methyl + O reaction. The results also mean that such new types of reactive mechanisms must be considered for other highly energized systems, which may not proceed through saddle point transition states. By analogy to this mechanism, a possible speculation for the ethyl + O case is that the primary product corresponding to the CO forming channel may be H_2 rather than CH_4.

Novel Addition-Insertion-Elimination Product of the CF_3CH_2I + O Reaction

In exploring various 5-member ring transition states, such as occur in the reaction of ethyl iodide with O atoms to form HOI + ethylene, we discovered a new reaction involving O atoms with alkyl iodides that produces an unexpected HF(v) product. Such reactions involve a common structural group such as CF_3CH_2I. The mechanism is thought to involve the addition of O atoms at the iodine site, to form CF_3CH_2IO. Then the O atom can exchange places with the iodide to form CF_3CH_2OI. This releases a substantial amount of energy, activating the complex, whereupon the HF(v) product can be eliminated. In recent studies, we proved kinetically that this reaction occurs in a simple bimolecular combination of O atoms with CF_3CH_2I and related precursors, and we obtained results for the monotonically decreasing vibrational distributions of the HF(v). The reaction also occurs by elimination of HCl(v) when Cl is substituted in the appropriate position for F atoms. If Br is substituted for I, the addition-insertion-elimination reaction to form HF(v) does occur, but with only 2% of the probability.

Future Plans

New studies of radical reactions and photofragmentation will be pursued, including: O atom reactions with longer chain alkyl radicals, to investigate the possibility of formation of CO(v) products, studies of NH_2 + NO, to address the product state distributions of the water vapor product and other transformations that may occur, and photofragmentation studies using jet cooled precursors, to obtain vibrational distributions of radical products.

Recent Publications

Richard A. Loomis, Jonathan P. Reid, and Stephen R. Leone, "Photofragmentation of ammonia at 193.3 nm: Bimodal rotational distributions and vibrational excitation of $NH_2(\tilde{A})$," J. Chem. Phys. **112**, 658 (2000).

Jonathan P. Reid, Richard A. Loomis and Stephen R. Leone, "Characterization of dynamical product-state distributions by spectral extended cross-correlation: Vibrational dynamics in the photofragmentation of NH_2D and ND_2H," J. Chem. Phys.,**112**, 3181 (2000).

Jonathan P. Reid, Timothy P. Marcy, Seppe Kuehn and Stephen R. Leone, "The Direct Production of CO(v=1-9) in the Reaction of $O(^3P)$ with the Ethyl Radical," J. Chem. Phys. **113**, 4572 (2000).

Jonathan P. Reid, Richard A. Loomis and Stephen R. Leone, "The effect of parent zero-point motion on the $ND_2(\tilde{A})$ rotational state distribution in the 193.3 nm photolysis of ND_3, Chem Phys Lett, **324**, 240 (2000).

Jonathan P. Reid, Richard A. Loomis and Stephen R. Leone, "Competition Between N-H and N-D Bond Cleavage in the Photodissociation of NH_2D and ND_2H," J. Phys Chem. **104**, 10139 (2000).

Jonathan P. Reid, Charles X.W. Qian and Stephen R. Leone, "Probing the cyclic transition state in the reaction $O(^3P)$ + alkyl iodides to form HOI: Electronic, steric and thermodynamic factors influencing the reaction pathway," Phys. Chem. Chem. Phys., **2**, 853 (2000).

Timothy P. Marcy, Jonathan P. Reid, Charles X. W. Qian, and Stephen R. Leone, "Addition-insertion-elimination reactions of $O(^3P)$ with halogenated iodoalkanes producing HF(v) and HCl(v)," J. Chem. Phys. **114**, 2251 (2001).

Timothy P. Marcy, Robert Richard Díaz, Dwayne Heard, Stephen R. Leone, Lawrence B. Harding, and Stephen J. Klippenstein, "CO(v) produced from CH_3 or CD_3 + O," J. Phys, Chem. (submitted).

INTERMOLECULAR INTERACTIONS OF HYDROXYL RADICALS AND OXYGEN ATOMS ON REACTIVE POTENTIAL ENERGY SURFACES

Marsha I. Lester
Department of Chemistry
University of Pennsylvania
Philadelphia, PA 19104-6323
milester@sas.upenn.edu

PROGRAM SCOPE

A primary objective of the DOE supported work in this laboratory is to examine the interaction potential and reaction dynamics of the CH_4 + OH system, one of the key initiation steps in the combustion of methane. The goal of this study is to map out the reaction pathway from the entrance valley through the transition state via spectroscopic and dynamical studies of CH_4-OH entrance channel complexes. Our approach is to stabilize the CH_4 + OH reactants in a weakly bound complex in the entrance channel to reaction and then to use stimulated Raman, infrared, and/or electronic excitation for spectroscopic characterization of the system. Vibrational or electronic excitation of one of the reactants induces a reactive and/or inelastic scattering process that starts from a well-defined initial state under the restricted geometric conditions imposed by the complex. We explore these dynamical processes through the lifetime of the vibrationally activated complexes and the quantum state distribution of the products. The results of these experiments, particularly when coupled with theoretical calculations of the experimental observables, yield a wealth of new information on the $CH_4 + OH \rightarrow CH_3 + H_2O$ potential energy surface. Finally, pre-reactive complexes of OH radicals (and O atoms) with other molecular partners of combustion importance are being investigated.

VIBRATIONAL SPECTROSCOPY OF CH_4-OH

Infrared action spectroscopy has been utilized to examine the structure and vibrational decay dynamics of CH_4-OH complexes that have been stabilized in the entrance channel to the CH_4 + OH hydrogen abstraction reaction. Infrared spectra have been obtained in the OH fundamental (ν_{OH}) and overtone ($2\nu_{OH}$) regions[1] as well as the CH_4 symmetric (ν_1) and asymmetric (ν_3) stretching regions.[2,3] The pure OH stretching bands of CH_4-OH are shifted 5.02 and 9.36 cm^{-1} to lower energy of the corresponding transitions in free OH. The rotational band structure has been analyzed in terms of a parallel pseudo-diatomic transition (P=3/2←3/2) with essentially no change in the rotor constant (B = 0.15 cm^{-1}) upon OH vibrational excitation. The experimental observations are consistent with a minimum energy structure in which the H-end of OH points toward CH_4, and has since been confirmed by *ab initio* theory.[1]

The pure OH stretching bands have homogeneous linewidths of 0.14 and 0.21 cm^{-1} in the ν_{OH} and $2\nu_{OH}$ regions, corresponding to 38 and 25 ps lifetimes for the vibrationally activated complexes.[1] The lifetimes are surprisingly short and may suggest that both inelastic and reactive channels contribute to the rapid decay, as found in a recent collision study of OH (v=1, 2) + CH_4.[4] The nascent distribution of the OH products from vibrational predissociation has also been evaluated by laser-induced fluorescence (LIF) measurements. The dominant inelastic

decay channel involves the transfer of one quantum of OH stretch to the pentad of CH_4 vibrational states near 3000 cm^{-1}.

More recent studies have focused on the vibrational spectroscopy and decay dynamics of CH_4-OH reactant complexes in the CH_4 symmetric and antisymmetric stretching regions (ν_1 and ν_3).[2,3] The vibrational spectra have been obtained using both infrared and stimulated Raman excitation with ultraviolet probe LIF detection. Stimulated Raman excitation of CH_4-OH in the symmetric stretching region reveals two blended Q branch features at 2912.5 cm^{-1} and 2911.8 cm^{-1}. An extremely weak infrared spectrum is also seen in the CH_4 symmetric stretching region, which is induced by the presence of the nearby OH partner. Infrared activation of the ν_3 mode gives rise to an intense, yet enormously broad spectrum extending over 40 cm^{-1}. The appearance of the spectra in the ν_1 and ν_3 regions has been explained in terms of a model in which the CH_4 unit is freely rotating within the CH_4-OH complex,[5,6] as found for other CH_4 complexes.[7-9] The ν_1 features are attributed to transitions involving two different nuclear spin states of CH_4. In the ν_3 region, the CH_4-OH complex can undergo a multitude of possible transitions, each associated with a rovibrational transition of free methane, which give rise to the enormous span of the CH_4-OH spectrum. The spectra also exhibit extensive homogeneous broadening ($\geq$ 1 cm^{-1}) arising from the rapid decay of vibrationally activated CH_4-OH complexes due to vibrational predissociation and/or reaction. This would be consistent with quantum reactive scattering calculations that predict a large enhancement in the CH_4 + OH reaction rate upon vibrational activation of the C-H stretching mode.[10] The OH fragments are produced with minimal rotational excitation, indicating that the dominant inelastic decay channel involves near-resonant vibrational energy transfer within the CH_4 unit from the initially prepared CH stretch to an overtone bend ($2\nu_4$) state.

Infrared Spectroscopy of OH-CO

Utilizing major resources from DOE, yet funded principally through NSF, we have also been mapping the OH + CO $\rightarrow$ HOCO reaction pathway through IR spectroscopy of the OH-CO reactant complex. We have identified a hydrogen-bonded complex composed of the OH and CO reactants, as well as the reaction pathway that connects the OH-CO complex directly to the transition state (TS1) for HOCO formation.[11,12] Using infrared action spectroscopy, we have observed the pure OH overtone transition of OH-CO (6941.7 cm^{-1}) and combination bands involving OH stretch excitation in combination with intermolecular bend and/or spin orbit excitation that lie 50 to 250 cm^{-1} above the ground intermolecular level. Complementary electronic structure calculations by Harding and Wagner have shown that the intermolecular bending modes of the OH-CO complex evolve directly into the HOCO reaction intermediate, and thereby reveal the sensitivity of the spectroscopic observables to the reaction pathway and barrier at TS1.

Future Plans

During the coming year, we plan to continue our in depth investigation of fundamental hydrogen abstraction reactions of combustion relevance. Specifically, we will continue mapping the CH_4 + OH/D potential energy surface through infrared excitation of the CH_4-OD entrance channel complexes in the OD overtone region ($2\nu_{OD}$) at 1.9 μm. The significantly lower

vibrational frequency of OD should cause a qualitative change in the inelastic scattering dynamics. We anticipate that the rate of vibrational predissociation will be dramatically slowed by the closing of a near-resonant V→V channel from OH to CH_4, and thereby impact the branching between inelastic and reactive decay channels. If vibrational predissociation is significantly slower in CH_4-OD ($2\nu_{OD}$) than CH_4-OH ($2\nu_{OH}$) and the rate of reaction is essentially unchanged upon isotopic substitution, as found in full collision experiments,[13] then the decay of CH_4-OD ($2\nu_{OD}$) may be primarily determined by chemical reaction. We will also be evaluating the rates and product state distributions for inelastic scattering and chemical reaction following infrared, stimulated Raman, and electronic excitation of CH_4-OH and H_2-OH reactant complexes. Our longer-term goal is to probe the products of these chemical reactions directly. Finally, we will begin exploring the potential energy surface for the CH_4 + O system via similar methodologies. This includes the stabilization and spectroscopic characterization of CH_4-O reactant complexes.

REFERENCES

1. M. D. Wheeler, M. Tsiouris, M. I. Lester, and G. Lendvay, *J. Chem. Phys.* **112,** 6590 (2000).
2. M. Tsiouris, M. D. Wheeler, and M. I. Lester, *Chem. Phys. Lett.* **302,** 192 (1999).
3. M. Tsiouris, M. D. Wheeler, and M. I. Lester, *J. Chem. Phys.* **114,** 187 (2001).
4. K. Yamasaki, A. Watanabe, T. Kakuda, N. Ichikawa, and I. Tokue, *J. Phys. Chem. A* **103,** 451 (1999).
5. J. M. Hutson and A. E. Thornley, *J. Chem. Phys.* **100,** 2505 (1994).
6. R. W. Randall, J. B. Ibbotson, and B. J. Howard, *J. Chem. Phys.* **100,** 7051 (1994).
7. Y. Ohshima and Y. Endo, *J. Chem. Phys.* **93,** 6256 (1990).
8. T. G. A. Heijmen, P. E. S. Wormer, A. van der Avoird, R. E. Miller, and R. Moszynski, *J. Chem. Phys.* **110,** 5639 (1999).
9. R. E. Miller, T. G. A. Heijmen, P. E. S. Wormer, A. van der Avoird, and R. Moszynski, *J. Chem. Phys.* **110,** 5651 (1999).
10. G. Nyman and D. C. Clary, *J. Chem. Phys.* **101,** 5756 (1994).
11. M. I. Lester, B. V. Pond, D. T. Anderson, L. B. Harding, and A. F. Wagner, *J. Chem. Phys.* **113,** 9889 (2000).
12. M. I. Lester, B. V. Pond, M. D. Marshall, D. T. Anderson, L. B. Harding, and A. F. Wagner, *Faraday Discuss. Chem. Soc.* **118,** in press (2001).
13. T. Gierczak, R. K. Talukdar, S. Herndon, G. L. Vaghjiani, and A. R. Ravishankara, *J. Phys. Chem. A* **101,** 3125 (1997).

DOE SUPPORTED PUBLICATIONS
1999-2001

1. M. D. Wheeler, M. W. Todd, D. T. Anderson, and M. I. Lester, "Stimulated Raman Excitation of the *ortho*-H_2-OH Entrance Channel Complex", *J. Chem. Phys.* **110**, 6732-6742 (1999).

2. M. D. Wheeler, D. T. Anderson, M. W. Todd, M. I. Lester, P. J. Krause, and D. C. Clary, "Mode-Selective Decay Dynamics of the *ortho*-H_2-OH Complex: Experiment and Theory", *Mol. Phys.* **97**, 151-158 (1999).

3. M. Tsiouris, M. D. Wheeler, and M. I. Lester, "Stimulated Raman and Electronic Excitation of CH_4-OH Reactant Complexes", *Chem. Phys. Lett.* **302**, 192-198 (1999).

4. D. T. Anderson, M. W. Todd, and M. I. Lester, "Reactive Quenching of Electronically Excited OH Radicals in Collisions with Molecular Hydrogen", *J. Chem. Phys.* **110**, 11117-11120 (1999).

5. M. D. Wheeler, M. Tsiouris, M. I. Lester, and G. Lendvay, "OH Vibrational Activation and Decay Dynamics of CH_4-OH Entrance Channel Complexes", *J. Chem. Phys.* **112**, 6590-6602 (2000).

6. M. W. Todd, D. T. Anderson, and M. I. Lester, "Infrared Spectroscopy and Inelastic Recoil Dynamics of OH Radicals in Complexes with *ortho*- and *para*-D_2", *J. Phys. Chem. A* **104**, 6532-6544 (2000).

7. M. D. Wheeler, D. T. Anderson, and M. I. Lester, "Probing Reactive Potential Energy Surfaces by Vibrational Activation of H_2-OH Entrance Channel Complexes", *Int. Rev. Phys. Chem.* **19**, 501-529 (2000).

8. M. Tsiouris, M. D. Wheeler, and M. I. Lester, "Activation of CH Stretching Vibrations in CH_4–OH Entrance Channel Complexes: Spectroscopy and Dynamics", *J. Chem. Phys.* **114**, 187-197 (2001).

Theoretical Studies of Molecular Systems

William A. Lester, Jr.
Chemical Sciences Division, Ernest Orlando Lawrence
Berkeley National Laboratory and Chemistry Department
University of California, Berkeley
Berkeley, California 94720-1460
walester@lbl.gov

Program Scope

This research program is directed at extending fundamental knowledge of atoms and molecules. The approach combines the use of ab initio basis set methods and the quantum Monte Carlo (QMC) method to describe the electronic structure, energetics, and reaction pathways of systems of primarily combustion interest.

Recent Progress

Formation of Cyclopentadienyl Radical from Addition of Acetylene to Propargyl Radical (with N. W. Moriarty, X. Krokidis, and M. Frenklach)

The addition of acetylene and propargyl radical to form cyclopentadienyl radical was studied using highly accurate theoretical methods. The energetics of the chemical systems were calculated using the quantum Monte Carlo (QMC) method in the diffusion Monte Carlo (DMC) variant and several generalized gradient approximation density functional theory (GGA-DFT) methods. Geometry optimizations were performed at all stationary points on the potential energy surface for the reaction system, and each such geometry was characterized by a frequency calculation to confirm whether the geometry is a minimum or transition state. The kinetics of the reaction system were examined using the recently updated MultiWell code for the time-dependent solution of master equations. Numerical simulations were performed for a range of temperatures and pressures and were run to chemical equilibrium.

The DMC calculations lead to predictions in good accord with available experimental data for the heat of formation of cyclopentadienyl radical at 298K and for the rate of decomposition of this species. The most reliable DMC predictions were those obtained from the formation and atomization reaction modes of calculation, resulting, respectively in 62.6 (0.4) and 63.7 (0.4) kcal/mol; the parenthetical number is the computed statistical uncertainty.

The DMC-based theoretical predictions of the thermodynamics and kinetics for the formation of cyclopentadienyl radical described both favor this reaction path over other mechanisms that have been proposed. The equilibrium constant for the reaction

$$C_3H_3 + C_2H_2 \rightarrow c\text{-}C_5H_5 \qquad (\alpha)$$

at 1000 and at 1500 K is 1×10^{8} and 2.5×10^{2} atm^{-1}, respectively. These results indicate that for an atmospheric flame and an acetylene mole fraction of 0.1, the equilibrium of this reaction is shifted toward cyclopentadienyl radical at temperatures below 1700K, implying the formation direction within the temperature window of aromatic inception. The predicted rate coefficient for these conditions (pressure of 1 atm and temperature of 1500K) of $k_\alpha \sim 1\times10^{11}$ cm^3 mol^{-1} s^{-1} indicates that the kinetics of this reaction is favorable.

It is useful to compare the rate of reaction α with that of

$$C_3H_3 + C_3H_3 \rightarrow \text{benzene of phenyl} + H \qquad (\beta)$$

The literature value of k_β is on the order of $1\text{-}5\times10^{12}$ cm^3 mol^{-1} s^{-1}, which is 10 to 50 times larger than k_α. The C_3H_3 flame concentration is, however, roughly 10^2-10^4 lower than the C_2H_2 concentration, and therefore the concentration product $[C_3H_3][C_3H_3]$ of reaction β is lower than the concentration product $[C_3H_3]$ $[C_2H_2]$ of reaction α by the same factor. Combining the two factors, the rate coefficient and reactant concentration product, favors the rate of reaction α over that of β by a factor of 2 to 10^3. In other words, reaction α is predicted to be not simply fast enough to make a difference, but likely to play a dominant role in the formation of the first aromatic ring.

Trial Function Optimization in Quantum Monte Carlo (with A. Aspuru-Guzik, O. Couronne, and I. Ovacharenko)

We have developed a new method for optimization of parameters that enter the QMC trial function. The approach can be viewed simply as the absolute value of the energies that enter variance minimization except that in the latter approach these energies enter quadratically. Testing has established that the procedure is more robust than variance minimization being able to handle successfully cases that are problematic for the latter approach.

Soft Pseudopotentials for Efficient Quantum Monte Carlo Calculations: From Be to Ne and Al to Ar (with I. Ovcharenko and A. Aspuru-Guzik)

We have developed "soft" ab initio Hartree Fock pseudopotentials for Be-Ne and Al-Ar that avoid singularities at the electron-nucleus cusp. The absence of these singularities is a desired feature for QMC calculations because it considerably reduces local energy fluctuations when sampling the QMC trial function. A modified procedure for obtaining soft pseudopotentials was developed in this work. Stability of QMC calculations with these pseudopotentials was demonstrated by the ability to use larger time-steps for comparable accuracy relative to previously available pseudopotentials.

Future Plans

Future work will continue primarily in the direction of establishing fundamental understanding of mechanisms leading to soot formation as well as other molecular species of combustion interest. The next step planned, as resources permit, is the addition of acetylene to cyclopentadienyl radical. In addition, there will be an enhanced effort to develop an efficient

scheme for the calculation of first and second derivatives with respect to position within the DMC method.

DOE Supported Publications 1999-2001

1. C. Pavão, T. C. F. Guimaraes, S. K. Lie, C. A. Taft, and W. A. Lester, Jr., "Modeling the Adsorption and Dissociation of CO on Transition Metal Surfaces," J. Mol. Struct. (Theochem) **458**, 99 (1999).
2. A. L. Almeida, J. B. L. Martins, C. A. Taft, E. Longo, and W. A. Lester, Jr., "Theoretical Study of Water Coverage on MgO Surfaces," Int. J. Quantum Chem. 71, 153 (1999).
3. J. C. Grossman, W. A. Lester, Jr., and S. G. Louie, "Cyclopentadiene Stability: Quantum Monte Carlo, Coupled Cluster, and Density Functional Theory Determinations," Mol. Phys. **96**, 629 (1999).
4. C. A. Taft, T. C. Guimarães, A. C. Pavão, and W. A. Lester, Jr., "Adsorption and Dissociation of Diatomic Molecules on Transition Metal Surfaces," Int. Rev. Phys. Chem. **18**, 163 (1999).
5. T. C. Guimarães, A. C. Pavão, C. A. Taft, and W. A. Lester, Jr., "Dissociation of N_2 on Chromium Alloys: A General Mechanism for Dissociation of Diatomic Molecules, Phys. Rev. **B60**, 11789 (1999).
6. X. Krokidis, N. W. Moriarty, W. A. Lester, Jr., and M. Frenklach, "Propargyl Radical: An Electron Localization Function Study," Chem. Phys. Letters **314**, 541 (1999).
7. J. C. Grossman, W. A. Lester, Jr., and S. G. Louie, "Quantum Monte Carlo and Density Functional Theory Characterization of 2-Cyclopentenone and 3-Cyclopentenone Formation from $O(^3P)$ + Cyclopentadiene, J. Am. Chem. Soc. **122**, 705 (2000).
8. J. A. W. Harkless and W. A. Lester, Jr., "Quantum Monte Carlo for Atoms and Molecules, "Proceedings of the Workshop on Contemporary Problems in Mathematical Physics, World Scientific Publishing (Singapore), p. 153, 2000.
9. J. A. W. Harkless and W. A. Lester, Jr., "Quantum Monte Carlo Determination of the Atomization Energy and Heat of Formation of Propargyl Radical," J. Chem. Phys. 113, 2680 (2000).
10. R. N. Barnett, Z. Sun, and W. A. Lester, Jr., "Improved Trial Wave Functions in Quantum Monte Carlo: Application to Acetylene and Its Dissociation Fragments," J. Chem. Phys. 114, 2013 (2001).
11. A. C. Pavão, C. A Taft, T. C. F. Guimarães, M. B. C. Leão, J. R. Mohallem, and W. A. Lester, Jr. "Interdisciplinary Applications of Pauling's Metallic Orbital and Unsynchronized Resonance to Problems of Modern Physical Chemistry: Conductivity, Magnetism, Molecular Stability, Superconductivity, Catalysis, Photoconductivity and Chemical Reaction," (feature article), J. Phys. Chem. 105, 5 (2001).
12. I. Ovcharenko, A. Aspuru-Guzik, and W. A. Lester, Jr., "Soft Pseudopotentials for Efficient Quantum Monte Carlo Calculations: From Be to Ne and Al to Ar," accepted by J. Chem. Phys.

Quantum Dynamics of Fast Chemical Reactions

DE-FG02-87ER13679

April 2001

John C. Light

The James Franck Institute and Department of Chemistry

The University of Chicago,Chicago,Illinois 60637

j-light@uchicago.edu

Scope:

The aims of this research and are to develop theoretical infrastructure and computational methods and to apply these methods to determine theoretically reaction rates and other dynamical quantities of interest for chemical reactions.

During the past year we have focused on three areas: development of better representations for dynamical calculations on larger systems; applications to understand the vibration/rotation structure of molecules of interest in combustion problems such as acetylene (HCCH) and protonated acetylene ($HHCCH^+$); and development of improved semi-classical approaches to dynamics.

Basis Representations:

For the large amplitude dynamics of molecular systems the size of standard quantum representations (essentially basis sets) such as DVR's[1] scale with number of particles, n, as N^{3n-6} where N, the number of basis functions per degree of freedom is usually $\geq$ 10. Thus the utility of these direct product approaches is limited to systems with fewer than six or seven large amplitude motions. Improvements in extracting eigenvalues and eigenfunctions such as filter diagonalization[2, 3] and other iterative methods[4] are very important but do not change the basic scaling problem - addition of a "floppy" atom to a "floppy" molecule increases the size of a direct product basis by roughly a factor of 10^2 to 10^3. Current alternatives either limit the large amplitude motions (e.g. normal modes or adiabatic separations) or use self consistant vibrational field approaches.

Another possible alternative to direct product bases is to use highly correlated bases such as distributed Gaussians[5]. In order to be effective the basis must be both concentrated in the appropriate region of physical space (where the wave functions are) and support wavefunctions of sufficiently oscillatory character to cover the region of momentum space desired. Thus it is important, but difficult, to distribute the basis functions to cover the appropriate region of phase space relatively uniformly in multidimensional systems[6–8]. This is a characteristic of the exact "uniformly mixed ensemble" of the phase space representation of the density matrix of the lowest N exact eigenstates and must be "mimicked" by the basis.

Although the phase space optimized direct product basis[6, 8] is more efficient than standard direct product bases, it still will suffer the scaling problem. The corrlated

basis alternative looks promising. We have developed a method to make a "quasi-random" distributed Gaussian basis which yields an appropriate phase space density. This results in a very efficient basis[9] since, in fact, the basis is properly correlated on average. This was used for the Ar_3 cluster using non-orthogonal bond coordinates and it was demonstrated that the 3D basis could be reduced in size by about a factor of 6 over a truncated direct product Gaussian basis.

Theoretial Spectroscopy: C_2H_2

Above about 15000 cm^{-1} the acetylene molecule become floppy, with energetic access to the H_2CC isomer. Although certain motions of this molecule remain regular to higher energy, it is of interest to describe the onset of very large amplitude motions. We developed a novel coordinate system to look at the full dynamics of this molecule: Radau coordinates for the hydrogens mated to a diatomic molecule (C_2) Using these coordinates the 6-D problem with three angles (in an angular momentum basis) and three distances (DVR's) could be solved just to the onset of isomerization. This work is now being prepared for publication[10].

Reaction Dynamics:

The work on reaction dynamics over the last year was very interesting. Almost all reactive scattering at thermal energies is assumed to occur on the lowest adiabatic Born-Oppenheimer potential energy surface, although studies of non-adiabatic collisions are now underway in a number of groups. However, the question of the effect of non-Born-Oppenheimer correction terms on reactions on the ground adiabatic surface has not been addressed (Kolos and Wolnewicz have, of course, done such studies on the vibrational states of H_2.) In collaboration with a quantum chemist we determined the non-Born-Oppenheimer diagonal corrections to the reactivity of a model H + H_2 system. As expected the energetic changes are small, $O(10^2\ cm^{-1})$, but this is largely due to cancellation of energy shifts between the transition state and the asymptotic states[11].

We made significant progress in two other studies on semi-classical propagation of reactive systems[12, 13]. There has been much work recently by Miller's group and others on the "initial value representation" of Herman and Kluk and on "forward-backward" propagation to cancel some of the oscillatory nature of the phase in integrals required for the correlation functions. We demonstrated two important improvements in these procedures. First, if one starts from the exact Moeller wave operators for reactive scattering and uses the Herman-Kluk semi-classical propagators, the forward-backward partial cancellation of the oscillatory phases occurs naturally, i.e. it is not related to further approximations (such as linear expansions of the action)[12].

The second result concerns the normalization factor which occurs in all initial value semi-classical calculations. This factor accounts for the divergence of quantum wave packets or of classical trajectories and is notoriously difficult to calculate (it usually diverges at long times). However, the factor is determined by the "monodromy matrix" which relates derivatives of initial and final momenta and positions and the monodromy matrix itself is nominally unitary in semi-classical calculations. We developed a *simple and stable* means of evaluating the monodromy matrix for a classical trajectory[13]. These two very recent developments should improve the accuracy and simplicity of semi-classical reactive scattering calculations noticeably. (I should note, however, that I remain somewhat of a skeptic on semi-classical methods. They require extremely large trajectory samples for convergence, even with improvements such as forward-backward partial cancellation of phases, and remain of limited accuracy.)

Ongoing Projects:

We will continue studies on improved representations as well as dynamical calculations on interesting systems.

Representations:

Ideally we would like an efficient algorithm to increase the size and efficiency of a distributed Gaussian basis in many dimensions. In particular we would like to add correlated basis functions to a representation with some idea of the improvement in accuracy which will result from the addition. That is, if one had a method of comparing, even qualitatively, the relative improvement of which two possible additions would make, then one could rapidly converge to a very efficient and accurate basis. There are two difficulties with the simple implementation of this for a basis of multidimensional Gaussians: the evaluation of the relative improvement due to the addition of basis functions must be easy, i.e. one cannot evaluate the exact results of adding a trial basis function since then the scaling is terrible. The second difficulty, perhaps exacerbated by Gaussian bases, is the non-orthogonality of the basis. This makes perturbative methods of evaluation of the improvements much more difficult. We will continue to think about this problem from a phase space ensemble point of view and hope to make progress.

The extension of the Gaussian basis approach to angular coordinates is possible but with substantial complication (error function integrals proliferate!). However, beyond 3 or maybe 4 atoms, all useful internal coordinate systems contain angles, and the extension of the localized correlated bases to these coordinates is highly desirable.

Theoretical Spectroscopy:

We have just begun work on the protonated acetylene molecule which is of astrophysical interest also. With five atoms there are 9 degrees of freedom for $J = 0$, five angles and four distances in the modified Radau coordinates of choice. Preliminary spectra have indicated that the molecule is planar at low energy with the proton being bound to the C=C double bond. At relatively low energies the molecule can tunnel between equivalent configurations with the planar transition state probably at the $H_2C{=}CH^+$ configuration. Although we have shown that Gaussian bases can be used for both localized and delocalized motions in angles, we have not yet determined the best basis. This is an ongoing project.

REFERENCES

[1] J. C. Light and T. Carrington, Jr. Discrete variable representations and their utilization. *Adv. Chem. Phys.*, 114:263, 2000.

[2] M. R. Wall and D. Neuhauser. Extraction, through filter-diagonalization, of general quantum eigenvalues or classical normal-mode frequencies from a small number of residues or a short-time segment of a signal .1. theory and application to a quantum-dynamics model. *J. Chem. Phys.*, 102:8011–8022, 1995.

[3] V. A. Mandelshtam and H. S. Taylor. *J. Chem. Phys.*, 106:5085, 1997.

[4] Shi-Wei Huang and T. Carrington, Jr. A new iterative method for calculating energy levels and wave functions. *J. Chem. Phys.*, 112:8765, 2000.

[5] I. P. Hamilton and J. C. Light. On distributed gaussian bases for simple model multidimensional vibrational problems. *J. Chem. Phys.*, 84:306, 1986.

[6] Bill Poirier and J. C. Light. Phase space optimization of quantum representations: Direct product basis sets. *J. Chem. Phys.*, 111:4869, 1999.

[7] B. Poirier. Algegbraically self-consistant semi-classical quantization on phase space. *Found. Phys.*, 30, 2000.

[8] B. Poirier and J. C. Light. Phase space optimization of quantum representations: Three-body systems and the bound states of HCO. *J. Chem. Phys.*, (In Press).
[9] Sophya Garashchuk and J. C. Light. Quasi-random distributed Gaussian bases for bound problems. *J. Chem. Phys.*, 114:3929–3939, 2001.
[10] Hua Chen. *Theoretical Spectra of Floppy Molecules.* PhD thesis, University of Chicago, Chicago, IL, 60637, 2000.
[11] S. Garashchuk, J. C. Light, and V. A. Rassolov. The diagonal Born-Oppenheimer correction to molecular dynamical processes. *Chem. Phys. Lett.*, 333:459–464, (2001).
[12] Sophya Garashchuk and J. C. Light. Semiclassical application of the Moeller operators in reactive scattering. *J. Chem. Phys.*, 114:1060, 2001.
[13] Sophya Garashchuk and J. C. Light. Simplified calculation of the stability matrix for semiclassical propagation. *J. Chem. Phys.*, 113:9390, 2000.

DOE supported publications, 2000-2001:

See above References # 8, 9, 10, 11, 12, 13

Kinetics of Elementary Processes Relevant to Incipient Soot Formation

M. C. Lin
Department of Chemistry
Emory University
Atlanta, GA 30322
chemmcl@emory.edu

I. Program Scope

Soot formation and abatement processes are some of the most important and challenging problems in hydrocarbon combustion. The key reactions involved in the formation of polycyclic aromatic hydrocarbons (PAH's), the precursors to soot, remain elusive. Small aromatic species such as C_5H_5, C_6H_6 and their derivatives are believed to play a pivotal role in incipient soot formation.

The goal of this project is to establish a kinetic database for elementary reactions relevant to soot formation in its incipient stages. In the past year, our major focus has been placed on the experimental studies on several reactions of C_6H_5 with alkenes and small aromatic hydrocarbons and computational studies on the reaction of CH_3 with O_2 and of C_6H_5 with C_2H_2 at the G2M level of theory.[1] These results are briefly summarized below.

II. Recent Progress

A. Experimental studies

We have developed three complementary methods for determination of the kinetics and mechanisms for C_6H_5 reactions with combustion species, including small alkenes and small aromatics. Combination of these methods: CRDS, P/FTIR and PLP/MS, allows us to cover a broad temperature range, 300 - 1000 K. The results of our studies on the reactions of C_6H_5 with C_3H_6 (propene), $C_6H_5C_2H$ (phenyl acetylene) and $C_6H_5C_2H_3$ (styrene) are briefly summarized below.

1. $C_6H_5 + C_3H_6$

The kinetics for the $C_6H_5 + C_3H_6$ reaction has been measured by CRDS in the temperature range $296 < T < 496$ K. The results can be represented by $k\ (C_3H_6) = 10^{11.90}\ exp\ (-646/T)$ $cm^3.mole^{-1}s^{-1}$. The reaction may occur by both addition to the C=C double bond and abstraction from the weak C-H bond in the methyl group. Product branching ratio will be determined by PLP/MS and by *ab initio* MO calculations to be carried out in the near future.

2. $C_6H_5 + C_6H_5C_2H$

The kinetics for the $C_6H_5 + C_6H_5C_2H$ reaction has been measured by CRDS in the temperature range $297 < T < 409$ K. The results can be represented by $k\ (C_6H_5C_2H) = 10^{13.30}\ exp\ (-532/T)$ $cm^3.mole^{-1}s^{-1}$. The reaction occurs by addition to the C≡C triple bond, primarily at the terminal position, according to the result of a hybrid density functional theory calculation. The adduct can undergo several rearrangement reactions producing cyclic products. The mechanism of this complex reaction will be elucidated with the help of DFT mapping of the potential energy surface involved.

3. $C_6H_5 + C_6H_5C_2H_3$

The kinetics for the $C_6H_5 + C_6H_5C_2H_3$ reaction has been measured by CRDS in the temperature range 297 < T <396 K. The results can be represented by $k\ (C_6H_5C_2H_3) = 10^{13.30}\ exp\ (-575/T)\ cm^3\ mole^{-1}\ s^{-1}$. The reaction occurs by addition to the C=C double bond, primarily at the terminal position, according to the result of a hybrid density functional theory calculation. The adduct can undergo several isomerization reactions producing cyclic products. A detailed DFT calculation to map out the PES is underway.

B. Computational Studies

1. $CH_3 + O_2 \rightarrow CH_3O_2$, $CH_2O + OH$, and $CH_3O + O$

Under combustion conditions, reactions of CH_3 radicals give rise to a variety of products, including C_2H_2, C_2H_3, CH_3C_2H, CH_2CCH_2 and C_3H_3, among others, which ultimately form PAH's and soot. Understanding the mechanism for the CH_3 removing process and the key chain branching reaction in hydrocarbon combustion processes, $CH_3 + O_2$, is therefore essential and pivotal to our ability to predict soot formation and its abatement. In a study carried out in conjunction with the combustion of a propellant-binder system,[2] we have examined the reaction in great detail at the G2M level of theory with the prediction of its product formation by variational RRKM theory calculations using the VARIFLEX program of Klippenstein et al.[3] The detailed PES, including the crossing seams between the PES, located by means of the intrinsic reaction coordinate (IRC) approach has been obtained. The rate constants for the association and product formation channels have been calculated and compared with the experimental data. Under the atmospheric pressure condition, the association reaction (a) producing CH_3O_2 dominates reaction below 1500 K. The branching probabilities for channels (b) and (c) producing $CH_2O + OH$ and $CH_3O + O$, respectively, have been calculated and compared; channel (b) is predicted to be dominant below 2000 K with the rate constant $k_b = 1.14\times10^{-22}T^{2.86}$ exp (-5120/T) $cm^3molecule^{-1}s^{-1}$. Over 2000 K, channel (c) becomes competitive; its rate constant could be represented by $k_c = 1.01\times10^{-16}T^{1.54}$exp(-13280/T) $cm^3molecule^{-1}s^{-1}$ in the temperature range of 1000~3000 K. In addition, the most exothermic products, $CHO + H_2O$, were found to be kinetically inaccessible because of the large barrier, 47.4 kcal/mol above the reactants. The predicted rate constants for the two product channels agree reasonably with most recent shock tube measurements employing more direct product diagmnostics.[4-7]

2. $C_6H_5 + C_2H_2$

The $C_6H_5 + C_2H_2$ reaction is critical to the formation of PAH's and soot. Its kinetics had been studied by CRDS several years ago by Yu, Lin and Melius,[8] whose result could be correlated with those reported earlier by Fahr et al.[9,10] acquired under very low pressure conditions, using the approximate PES obtained by BAC-MP4 calculations.[8] The mechanism employed in our interpretation of the kinetic data included the addition followed by either stabilization or decomposition producing $C_6H_5C_2H + H$. This mechanism, as shown in the attached PES computed by the G2M method, is only a small part of the overall, very complex process. As illustrated in the figure, the $C_6H_5C_2H_2$ radical adduct can undergo numerous isomerization and decomposition reactions forming very stable double ring compounds which may be accessible at high temperatures. Some of the cyclization steps have also been reported by Moriaty et al.[11] during the course of our long calculations at the G2M level of theory. It is worthnoting that our predicted addition barrier, 3.5 kcal/mol, agreed closely with our CRDS kinetic result, 3.1 ± 0.5 kcal/mol.[8]

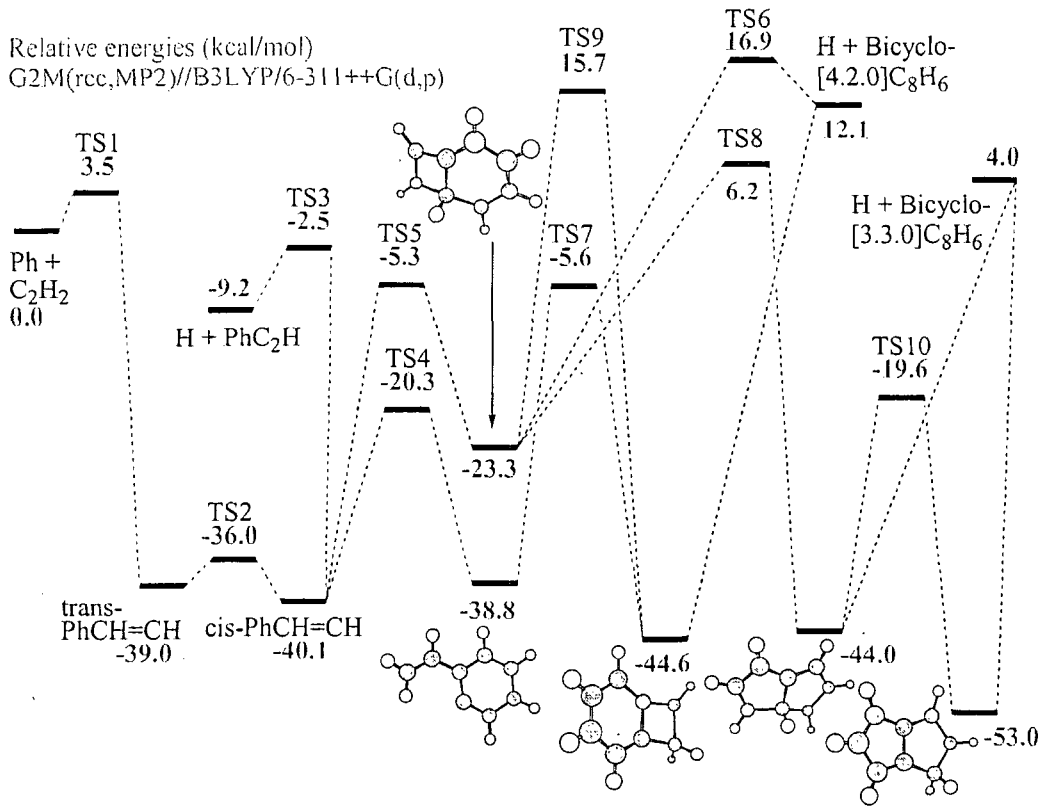

PES of the C_6H_5 + C_2H_2 system (Ref. 12)

3. H-for-X substitution in the H+C_6H_5X (X=D,CH_3) Reactions

The addition of H atoms to benzene and toluene and subsequent transformations were investigated using high level ab initio and density functional theory methods. Molecular structures and vibrational frequencies calculated at the B3LYP/6-311++G(d,p) level of theory were used in combination with adjusted G2M energetic parameters for RRKM rate constant calculations. Standard heats of formation for cyclohexadienyl and cyclohexadienyl, 6-methyl radicals calculated through isodesmic reactions amounted to 49.5 ± 2 kcal/mol and 42.9 ± 3 kcal/mol, respectively. Rate constants for various elementary reactions involved in the H-for-X exchange (X = D, CH_3) were calculated and closely correlated with the available experimental kinetic data.[13]

III. Future Plans

In the next year, we will continue the acquisition of kinetic data for C_6H_5 reactions by CRDS and PLP/MS techniques to determine the reactivity of the phenyl toward s-CH bonds and the determination of total rate constants and product branching probabilities in the C_6H_5 reactions with CH_2CO, CH_3CHO and C_3H_6. Computationally, we will carry out high-level *ab initio* MO calculations to improve our predictive capability for the rate constants and product branching ratios of C_6H_5 reactions with C_2H_4 and O_2. We also plan to extend the calculations to include the reactions of C_6H_5 radical with H_2O at the G2M level of theory.

IV. References (DOE publications, 1999-present, denoted by #)

1. A. M. Mebel, K. Morokuma and M. C. Lin, J. Chem. Phys.,103, 7414 (1995).2
#2. R. S. Zhu and M. C. Lin, "Ab Initio Study of the $CH_3 + O_2$ Reaction: Kinetics, Mechanism and Product Branching Probabilities", J. Chem. Phys., in press.
3. S. J. Klippenstein, A. F. Wagner, R. C. Dunbar, D. M. Wardlaw, and S. H. Robertson, VARIFLEX: VERSION **1.00**, 1999.
4. C. L. Yu, C. Wang, and M. Frenklach, J. Phys. Chem. 99, 14377 (1995).
5. J. V. Michael, S. S. Kumaran, and M. C. Su., J. Phys. Chem. A 103, 5942 (1999).
6. S. M. Hwang, S.-O Ryu, and K. J. De. Witt, M. J. Rabinowitz, J. Phys. Chem. A, 103, 5949 (1999).
7. M. Braun-Unkhoff, C. Naumann, P. Frank, In Shock Waves; Brun, Raymond, Cumitrescu, Lucien, Eds.; Nineteenth International Symposium on Shock Waves; Springer: Berlin, Germany, 2, 203 (1995).
8. T. Yu, M. C. Lin, and C.F. Melius, Int. J. Chem. Kinet., **26**, 1095 (1994).
9. A. Fahr, W. G. Mallard, S. E. Stein, 21st Symp. (Int.) on Combust., The Combustion Institute, 1986, p. 825.
10. A. Fahr and S. E. Stein, 22nd Symp. (Int.) on Combust., The Combust. Institute, 1988, 1023.
11. N. W. Moriaty, N. J. Brown and M. Frenklach, J. Pys. Chem. A. 103, 7127 (1999).
#12. I. V. Tokmakov and M. C. Lin, "Ab Initio MO/RRKM calculations for the $C_6H_5 + C_2H_2$ reaction", to be published.
#13. I. V. Tokmakov and M. C. Lin, "Kinetics and mechanism for the H-for-X exchange process in the $H + C_6H_5X$ (X=D, CH_3) reactions: A computational study", Int. J. Chem. Kinet., submitted.

Other DOE Publications Not Cited in the Text:

1. I. V. Tokmakov, J. Park, S. Gheyas and M. C. Lin, *J. Phys. Chem. A* **103,** 3636 (1999).
2. J. Park, S. I. Gheyas and M. C. Lin, *Int. J. Chem. Kinet.* **31**, 645 (1999).
3. J. Park, S. Burova, A. S. Rodgers and M. C. Lin, *J. Phys. A,* **103**, 9036 (1999).
4. A. M. Mebel, L. V. Moskaleva and M. C. Lin, *J. Mol. Struct.* (THEOCHEM), **461/462**, 223 (1999).
5. A. M. Mebel and M. C. Lin, *J. Phys. Chem. A* **103,** 2088 (1999).
6. L. V. Moskaleva and M. C. Lin, *PCCP*, **1**, 3967 (1999).
7. J. Park and M. C. Lin "Kinetic Studies of Aromatic Radical Reactions by Cavity Ringdown Spectrometry" *in Cavity-Ring-Down Spectrometry-A New Technique for Trace Absorption Measurements*, ACS Publication Series **720**, Chap. 13, 196 (1999).
8. M. D. Brioukov, J. Park and M. C. Lin, *Int. J. Chem. Kinet.* **31**, 577 (1999)
9. J. Park, D. Chakraborty, D. M. Bhusari and M. C. Lin, *J. Phys. Chem. A.* **103,** 4002 (1999).
10. Gi-Jung Nam, W. Xia, J. Park and M. C. Lin, *J. Phys. Chem.* A, **104**, 1233 (2000).
11. Y. M. Choi, Wensheng Xia, J. Park and M. C. Lin, J. Phys. Chem. A. 104, 7030 (2000).
12. L. V. Moskaleva and M. C. Lin, *J. Comput. Chem.* **21**, 415 (2000).
13. L. V. Moskaleva, W. S. Xia and M. C. Lin, Chem. Phys. Lett., **331**, 269 (2000).
14. L. V. Moskaleve and M. C. Lin, "The $CH + N_2$ Association Reaction at Low Temperatures: Ab Initio MO/VRRKM-Theory Analysis of Temperature and Pressure Effects", Z. Phys. Chem., in press.
15. A. M. Mebel, M. C. Lin, D. Chakraborty, J. Park, S. H. Lin and Y. T. Lee, "Ab Initio and RRKM Study of Multichannel Rate Constants for the $H + C_6H_5$ Reaction and the Unimolecular Decomposition of Benzene," *J. Chem. Phys.* in press.
16. L. V. Moskaleva and M. C. Lin, "The Spin-Conserved Reaction $CH + N_2 \rightarrow H + NCN$: A Major Pathway to Prompt NO Studied by Quantum/Statistical Theory Calculations and Kinetic Modeling of Rate Constant". Proc. Combust. Inst., in press.

INVESTIGATION OF POLARIZATION SPECTROSCOPY AND DEGENERATE FOUR-WAVE MIXING FOR QUANTITATIVE CONCENTRATION MEASUREMENTS

Principal Investigator: Robert P. Lucht
Graduate Students Supported: Sherif F. Hanna and Sukesh Roy
Department of Mechanical Engineering, Texas A&M University, Mail Stop 3123, College Station, TX 77843-3123 (rlucht@tamu.edu)

I. PROGRAM SCOPE

Polarization spectroscopy (PS) and degenerate four-wave mixing (DFWM) are techniques that show great promise for sensitive measurements of transient gas-phase species, and diagnostic applications of these techniques are being pursued actively at laboratories throughout the world. However, significant questions remain regarding strategies for quantitative concentration measurements using polarization spectroscopy and DFWM. The objective of this research program is to develop and test strategies for quantitative concentration measurements in flames and plasmas. We are investigating the physics of these processes by direct numerical integration (DNI) of the time-dependent density matrix equations that describe the resonant interaction. Significantly fewer restrictive assumptions are required using this DNI approach compared with the assumptions required to obtain analytical solutions. Inclusion of the Zeeman state structure of degenerate levels has enabled us to investigate the physics of polarization spectroscopy and of polarization effects in DFWM. Recently, we have begun to study the effects of hyperfine structure on PS signal generation. In addition, we have now successfully incorporated the multi-axial-mode laser structure that is characteristic of commercial dye lasers into our polarization spectroscopy calculations. Experimental measurements are performed in well-characterized flames, gas cells, or nonreacting flows for comparison with our theoretical calculations.

II. RECENT PROGRESS

A. Theoretical Analysis of Short-Pulse Polarization Spectroscopy

The potential advantages of short-pulse laser excitation for reducing or eliminating the effects of collisions in laser diagnostic measurements in combustion have long been recognized. A laser with a nominal pulse length of 10-100 psec is ideal for diagnostics of atmospheric pressure flames because the laser pulse length is shorter than the characteristic collisional times in the medium. In addition, the nominal laser bandwidth (Fourier transform limit) of 1.5 to 0.15 cm^{-1} is low enough that the laser radiation can couple efficiently with molecular resonances. Recently a tunable distributed-feedback dye laser (DFDL) system with pulse lengths on the order of 100 psec and a near-Fourier transform-limited bandwidth has been developed at Sandia National Laboratories.[1] The tuning of the DFDL laser is computer-controlled and the wavelength of the laser is feedback-stabilized to within 0.02 cm^{-1}, allowing the laser wavelength to be scanned over resonance lines or placed accurately at line center. Experimental measurements of OH concentrations using picosecond PS were performed in a room-temperature H_2O_2 photolysis cell[2] at room temperature for pressures ranging from 10 to 500 Torr using this laser system.[3] The results confirmed that the dependence of the PS signal intensity on the collision rate was reduced drastically compared to nanosecond PS.

Over the last year we have performed an extensive theoretical study of short-pulse PS. The direct numerical integration (DNI) method that we have developed over the last few years is particularly well-

suited for the investigation of the physics of this technique. The Zeeman-state structure of degenerate-level resonances has been incorporated in our numerical codes. The time-dependent density matrix equations for these levels are integrated numerically and the PS signal is calculated from the time-dependent third-order polarization induced in the medium by the interaction of the pump and probe beams. The results of DNI calculations of the PS signal for counterpropagating pump and probe beams, for a resonance with a Doppler width of 0.1 cm^{-1}, and for a laser pulse length of 100 psec are shown in Fig. 1. For a pump laser intensity of $1x10^{11}$ W/m^2 the PS signal decreases by only a factor of two while the pressure increases by a factor of 50. This is a very significant reduction in the sensitivity of the PS signal to the collision rate and saturated short-pulse PS seems to be a very promising technique for quantitative concentration measurements of minor species in flames.

We have investigated the laser excitation dynamics in detail by examining the temporal dependence of the Zeeman populations and the induced coherences for the allowed Zeeman transitions.
As an example of detailed information that can be obtained from the DNI analysis, the PS signal pulses for resonances with a collisional dephasing rate of 10^9 sec^{-1} and Doppler widths of 0, 0.1 and 0.3 cm^{-1}. Note the persistence of the signal generation long after the 100-psec pump and probe pulses have passed through the probe volume for the resonances with Doppler widths of 0 and 0.1 cm^{-1}, and the Rabi beating that is noticeable for each resonance.

B. Effects of Hyperfine Structure on PS Signal Intensities

We have begun to study the effects of the hyperfine structure of molecules such as OH on the generation and interpretation of PS signals. The hyperfine structure of the $Q_1(5)$ resonance of the OH (0,0) band in the $A^2\Sigma^+$-$X^2\Pi$ electronic transition is shown in Fig. 3. The $\Delta F = \Delta J$ hyperfine components have a Q-branch character, while the $\Delta F \neq \Delta J$ hyperfine components have P- or R-branch character. In general, for high-J lines, the PS signals from Q-branch lines will be strong for a linearly polarized pump and weak for a circularly polarized pump, while the opposite is the case for R- and P-branch lines. Consequently, although in general it is very difficult to resolve the hyperfine structure, the relative strengths of the $\Delta F = \Delta J$ and $\Delta F \neq \Delta J$ hyperfine components will affect significantly the relative intensities of lines with different values of J, and the dependence of the PS signal level on the pump polarization. We are presently performing experiments on OH polarization spectroscopy in flames in which we have inserted a 1/4-waveplate in the pump beam path to change the polarization of the pump beam from circular to linear in a smooth fashion. The results of DNI calculations for the $Q_1(1)$ line of OH are shown in Fig. 4. For the calculations we assumed that the spontaneous emission coefficients for the $\Delta F \neq \Delta J$ hyperfine components were a factor of five less than for the $\Delta F = \Delta J$ hyperfine components. By comparing our calculations with experiment we may be able to determine the relative strengths of the $\Delta F = \Delta J$ and $\Delta F \neq \Delta J$ hyperfine components for a wide range of OH lines.

C. Infrared Polarization Spectroscopy Measurements of the CO_2 Molecule

We have detected infrared polarization spectroscopy signals from the CO_2 molecule in experiments performed in Dr. Andrew McIlroy's laboratory at the Combustion Research Facility at Sandia National Laboratories. The experiments were performed using a Continuum Mirage 3000 optical parametric generator to produce single-mode laser radiation at 2700 nm. A PS spectrum from a jet of CO_2 at room temperature and pressure is shown in Fig. 5. Infrared polarization spectroscopy is a promising technique for detecting infrared-active species that do not fluoresce.

III. FUTURE WORK

Our investigation of the physics of picosecond PS will continue; the reduced dependence of the picosecond PS signal on collision rate for both low and high laser intensities is very encouraging. We will investigate both theoretically and experimentally the effects of hyperfine structure on the generation of PS signals for molecules. Further infrared PS experiments in collaboration with Dr. McIlroy at Sandia are planned. Theoretical work on the effect of multi-axial-mode structure on PS signal generation will also continue.[4] We are collaborating with a group at Lund University on modeling their PS data collected from a low-pressure flame using a multi-mode optical parametric generator. We will perform PS measurements in low-pressure flames for comparison with our multi-mode calculations and investigate the potential of two-color PS for sensitive concentration measurements. The DNI code will be modified for modeling two-color PS. The generation of DFWM signals from molecules with anisotropic Zeeman state distributions[5] will be investigated theoretically.

IV. REFERENCES

1. P. P. Yaney, D. A. V. Kliner, and R. L. Farrow, Rev. Sci. Instr. **71**, 1296-1305 (2000).
2. D. A. V. Kliner and R. L. Farrow, J. Chem. Phys. **110**, 412-422 (1999).
3. T. A. Reichardt, F. Di Teodoro, R. L. Farrow, S. Roy, and R. P. Lucht, J. of Chem. Phys. **113**, 2263-2269 (2000).
4. W. C. Giancola, T. A. Reichardt, and R. P. Lucht, J. Opt. Soc. Am. B **17**, 1781-1794 (2000).
5. T. Müller, T. A. W. Wasserman, P. H. Vaccaro, and B. R. Johnson **108**, 7713-7738 (1998).

V. BES-SUPPORTED PUBLICATIONS 1999-2001

1. T. A. Reichardt and R. P. Lucht, "Resonant Degenerate Four-Wave Mixing Spectroscopy of Transitions with Degenerate Energy Levels: Saturation and Polarization Effects," Journal of Chemical Physics **111**, 10008-10020 (1999).
2. T. A. Reichardt, W. C. Giancola, C. M. Shappert, and R. P. Lucht, "Experimental Investigation of Saturated Degenerate Four-Wave Mixing for Quantitative Concentration Measurements," Applied Optics **38**, 6951-6961 (1999).
3. T. A. Reichardt, W. C. Giancola, and R. P. Lucht, "Experimental Investigation of Saturated Polarization Spectroscopy for Quantitative Concentration Measurements," Applied Optics **39**, 2002-2008 (2000).
4. W. C. Giancola, T. A. Reichardt, and R. P. Lucht, "Multi-Axial-Mode Laser Effects in Polarization Spectroscopy," Journal of the Optical Society of America B **17**, 1781-1794 (2000).
5. T. A. Reichardt, F. Di Teodoro, R. L. Farrow, S. Roy, and R. P. Lucht, "Collisional Dependence of Polarization Spectroscopy with a Picosecond Laser," Journal of Chemical Physics **113**, 2263-2269 (2000).
6. R. P. Lucht and T. A. Reichardt, "Calculation of Radiative Transition Rates for Electric-Dipole Resonances with Degenerate Energy Levels," Applied Optics, submitted for publication (2001).

VI. GRADUATE DISSERTATIONS RESULTING FROM DOE/BES SUPPORT 1999-2001

1. Thomas A. Reichardt, "Investigation of Degenerate Four-Wave Mixing and Polarization Spectroscopy for Quantitative Measurements in Combustion Environments," Ph.D. Thesis, University of Illinois at Urbana/Champaign (1999).
2. William C. Giancola, "Theoretical Investigation of Polarization Spectroscopy in Multi-Axial-Mode Fields," M.S. Thesis, University of Illinois at Urbana/Champaign (1999).

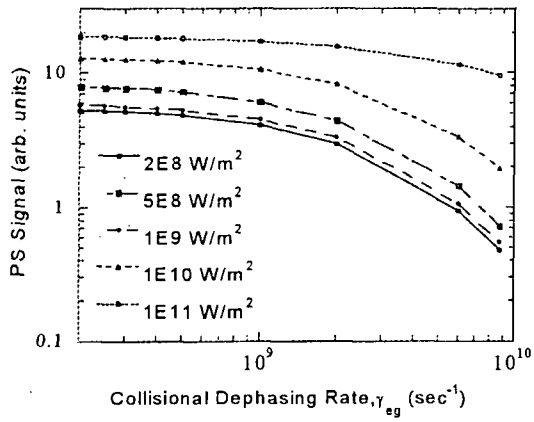

Fig. 1. Dependence of the polarization spectroscopy signal on collisional dephasing rate for different pump laser powers. The pump and probe pulses are 100 psec long (FWHM). The Doppler width (FWHM) of the $P_1(2)$ resonance is 0.1 cm^{-1} and the spontaneous emission coefficient is 10^6 sec^{-1}.

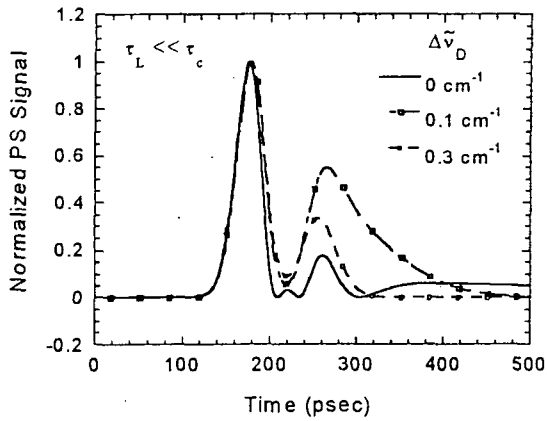

Fig. 2. Calculated temporal dependence of the polarization spectroscopy signal for a $P_1(2)$ resonance for Doppler widths of 0, 0.1, and 0.3 cm^{-1}, a collisional dephasing rate of 10^9 sec^{-1}, a pump laser power of 10^{11} W/m^2 and a spontaneous emission coefficient of 10^6 sec^{-1} for the resonance.

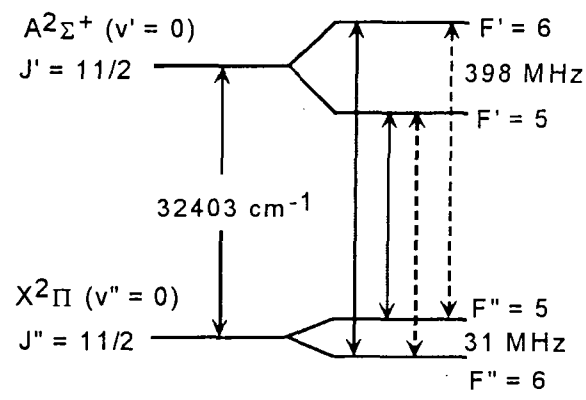

Fig. 3. Hyperfine structure of the OH $Q_1(5)$ line.

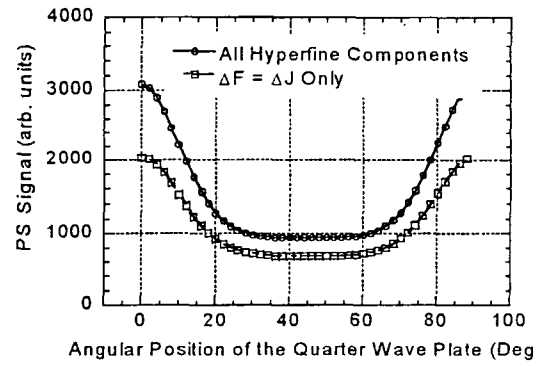

Fig. 4. Calculated PS signals as a function of the angle of a ¼-wave plate in the pump beam path considering all hyperfine components and then only those components for which $\Delta F = \Delta J$. The resonance is a $Q_1(1)$ transition.

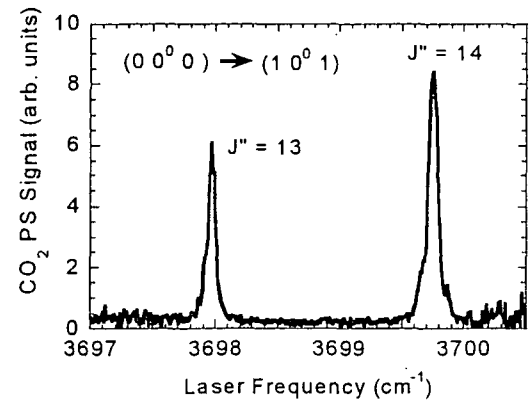

Fig. 5. Infrared PS scan for the CO_2 molecule.

Time-Resolved Infrared Absorption Studies of the Dynamics of Radical Reactions

R. G. Macdonald
Chemistry Division
Argonne National Laboratory
Argonne, IL 60439
Email: macdonald@anlchm.chm.anl.gov

Background

There is very little information available about the dynamics of radical-radical interactions. These processes are important in combustion being chain termination steps as well as generating new molecular species. To study these processes, a new experimental apparatus has been constructed to investigate radical-radical dynamics. The first radical or atomic species is produced with a known concentration in a microwave discharge flow system. The second is produced by pulsed laser photolysis of a suitable photolyte. The time dependence of individual rovibrational states of the product is followed by absorption of a continuous infrared laser. This approach will allow the reaction of interest to be differentiated from other radical reactions occurring simultaneously. The experimental approach is highly versatile, being able to detect a number of molecular species of particular interest to combustion processes such as water, methane, acetylene etc. at the state specific level. State specific infrared absorption coefficients of radicals can be measured in situ allowing for the determination of the absolute concentrations, and hence branching ratios for reactions having multiple reaction pathways.

Recent Results

The difficulty in studying radical-radical reactions is the necessity to know the time dependence of the absolute concentration of two transient species. In some cases, it may be possible to make measurements in environments where the concentration of one species is in great excess over the other, and its absolute concentration established. These circumstances result in pseudo first-order conditions, and only the time dependence of the radical with the smaller concentration need be determined, not its absolute concentration. However, such conditions are difficult to generate in practice because of the reactive nature of radicals and self-radical-radical recombination.

In the current work, the above difficulty was eliminated by simultaneously monitoring the time dependence of the absolute concentration of two radical species using state-specific time-resolved absorption spectroscopy. These experiments also illustrate the utility of the time-resolved absorption technique, and the power of infrared spectroscopy to probe a variety of molecular and/or transient species at the individual ro-vibration state level of detail.

The system being investigated is the radical-radical reaction $CN(^2\Sigma^+) + OH(^2\Pi)$. This reaction represents one of the least complex radical-radical reactions involving diatomic species. In C_s geometry, there are only two electronic surfaces that correlate with the reactants in each of the singlet and triplet manifolds, i.e. $^1A'$ and $^1A''$ and $^3A'$ and

$^3A''$. Neglecting stabilization products, there are five possible exothermic product channels, in increasing exothermisity:

$$\begin{aligned} CN\ (^2\Sigma^+) + OH(^2\Pi) &\rightarrow HNC(X^1\Sigma) + O(^3P) && (a)\\ &\rightarrow NH(a^1\Delta) + CO(X^1\Sigma) && (b)\\ &\rightarrow HCN(X^1\Sigma) + O(^3P) && (c)\\ &\rightarrow NCO(X^2\Pi) + H(^2S) && (d)\\ &\rightarrow NH(X^3\Sigma^-) + CO(X^1\Sigma) && (e) \end{aligned}$$

Some of these product channels involve either the singlet ((b) and (d)), triplet ((a), (c), (d)and (e)) or both (d) manifolds. There has been no previous direct measurement of the thermal rate constant or a determination of the product branching ratios.

Time-resolved absorption spectroscopy was used to monitor both the reactants, CN and OH as well as a transient species from each of the possible product channels. The CN radical was monitored in the CN "Red" system using the $CN(A^2\Pi \leftarrow X^2\Sigma)$ (2,0) band at 790 nm, while the other species OH, HNC, NH, HCN, and NCO were monitored in the infrared. using a tunable infrared laser. The CN radical was generated by the excimer laser photolysis of $(CN)_2$ at 193 nm and the OH radical from the reaction of O^1D with either H_2 or H_2O. The latter source of the OH radical has several advantages: there is very little generation of HCN from the slow CN + H_2O reaction and there is much less vibrational excitation in the OH reactant. Initial radical concentrations were in the range $3x10^{12}$ to $2x10^{13}$ molecules $cm.^{-3}$ The experiments were carried out at a total pressure of 3 – 6 Torr.

Although most of the chemistry occurring in this system is dominated by a few reactions, the secondary chemistry does become complicated, and detailed modeling of the compete reaction system is necessary to derive accurate measurements of the branching ratios. The total CN + OH rate constant was found to be $1.8x10^{-10}$ $cm^3molecules^{-1}s^{-1}$ independent of the experimental conditions. However an accurate determination of the branching ratios has been more difficult to obtain, and is currently under investigation.

In order to ensure that an accurate determination of the branching ratios were being made it was clear that the modeling of the chemistry in the system should predict the time dependence of the largest product channel, namely reaction (d). Unfortunately, the $NCO(X^2\Pi)$ radical has no fundamental absorption features in the 2.6-3.4 micron region, and there are no measurements of the transition moments for the fundamental vibrations. However, the $NCO(10^01) \leftarrow (00^00)$ combination band is predicted to be near 3.16 microns, and the corresponding transition in CO_2 is relatively strong. The infrared absorption spectra of this NCO band has been recorded and is being analyzed to determine the appropriate spectroscopic constants. Interestingly, although the NCO molecule has received a great deal of attention from spectroscopists, primarily because of the Renner-Teller effect, there have been only a few studies of this molecule in the infrared spectral region. The infrared study will provide much more detail about the Λ-doubling parameters then previously available. As well, the transition moment is being determined. Unlike CO_2, the transition is relatively weak as expected for a combination band, but nevertheless of sufficient strength so that the absolute concentration of NCO can be monitored following the CN + OH reaction.

Future Work

As noted in the previous paragraphs, the study of the CN + OH radical-radical reaction is proceeding on several fronts. The determination of the NCO ($10^0 1$) ← ($00^0 0$) transition moment will be of primary importance, in order to monitor all 5 possible product channels. As in previous measurements of transition moments of transient species, the concentration of NCO will be inferred from the measurement of the concentration of a species whose stoichiometry is related to the production of the NCO radical. The simplest system is the generation of NCO from the CN + O_2 reaction. The branching ratio into the NCO + O atom channel for this reaction has been carefully measured.[1] The CN radical will be generated from the photodissociation of $(CN)_2$, and the transition moment for the CN A ←X (2-0) band has been measured. Another method will be to use ClCN as the CN radical source and add a small amount of CH_4 to the reaction system to titrate the Cl atoms as HCl. The CN + CH_4 reaction is much slower than the CN + O_2 reaction and the small fraction of CN radicals that do react can be determined by measuring the HCN concentration. These experiments are currently under investigation.

Once the room temperature branching ratio measurements are complete, the measurement of the temperature dependence of the branching ratios will be undertaken. The topology of the CNOH potential energy surfaces in both the singlet and triplet manifolds is complex,[2] and how thermal energy influences the out come of an reactive encounter will be an interesting question.

References

1) K. T. Rim and J. F. Hershberger, J. Phys. Chem. 103, 3721 (1999).
2) A. M. Mebel, A. Luna, M. C. Lin, and K. Morokuma, J. Chem. Phys. 105, 6439 (1996).

Publications 1999-2001.

Experimental and theoretical determination of the magnetic dipole transition moment for Br($4p^5$) ($^2P_{1/2}$ ← $^2P_{3/2}$) fine-structure transition and the quantum yield of Br($^2P_{1/2}$) from the 193 nm photolysis of BrCN.
-G. He, M. Seth, I. Tokue, and R. G. Macdonald
J. Chem. Phys. 110, 7821-7831 (1999).

Rotational and translational energy distributions of CN(v=0,J) from the hot atom reactions: H + XCN → HX + CN(v=0,J), where X = Br, Cl. And CN.
-G. He, I. Tokue, and R. G. Macdonald
J. Chem. Phys. *110*, 7821-7831 (1999).

Rotational and vibrational state distribution of HNC(0 v_2^l 0) from the hot H atom reaction: H + $(CN)_2$ → HNC + CN.
-R. G. Macdonald
J. Phys. Chem. 104A, 10202-10211 (2000)

Determination of the branching ratios for the reaction of hot H atoms with BrCN and ClCN.

-B. K. Decker, G. He, I. Tokue, and R. G. Macdonald
J. Phys. Chem. 105A, accepted.

Channeling of products in the hot atom reaction: H + $(CN)_2$ → HCN/HNC + CN, and the reaction of CN with CH_3SH.
-B. K. Decker and R. G. Macdonald
J. Phys. Chem. Submitted.

Flame Chemistry and Diagnostics

Andrew McIlroy
Combustion Research Facility
Sandia National Laboratories, MS 9055
Livermore, CA 94551-0969
Phone: (925) 294-3054
Email: amcilr@sandia.gov

Program Scope

The goal of this program is to elucidate the chemical mechanisms of combustion through a combination of experiments based on state-of-the-art diagnostics and detailed chemical kinetic modeling. The experimental program concentrates on the development and application of combustion diagnostics for the measurement of key chemical species concentrations. Although much work has been done to develop diagnostics for combustion species, many common radicals such as CH_3 and CH_2 remain challenging to study on a routine basis and many larger radicals remain difficult to detect at all. Comparison of experimental data to models employing detailed chemical kinetics allows us to determine the important chemical kinetic pathways for combustion, to test the accuracy of published models, and to develop new models. For the development and validation of chemical kinetic models, low pressure, one-dimensional laminar flames are studied. Transport issues are minimized in this configuration and well-developed models including detailed chemical kinetics, such as the Sandia PREMIX code, are available. As turbulent combustion models become increasingly sophisticated, accurate chemical kinetic mechanisms will play a larger role in computations of realistic combustion systems. Validated and well-characterized models will be required as inputs to these reactive flow codes. Only after rigorous comparisons of calculated and experimental results for a given chemical kinetic flame model over a wide range of steady conditions can these models be used with any confidence in turbulent codes. Recent studies of transiently strained flame structure indicate that even this stringent level of validation may be insufficient[1,2].

Recent Progress

Recently, we have carried out work in three general areas: the measurement of spectroscopic data needed for new flame diagnostics, the development and application of new laser and mass spectrometer diagnostics, and the testing of chemical kinetic models of combustion by careful measurements of stable species and radical intermediates. This work is briefly summarized below.

In order to increase the sensitivity and utility of our photoionization mass spectrometer (PIMS) system for probing the chemistry of low-pressure, laminar flames, we have undertaken several hardware development projects. A combination of software and hardware upgrades, including the addition of a second broadly tunable OPO system, has given us the ability to produce significant fluxes of narrow-band, broadly tunable vacuum ultraviolet (VUV) light (100 Hz pulses of ~0.1 μj, tunable from 6.5 to 1.5 eV with 0.5 meV resolution). This system will allow us to sensitively detect radical intermediates and identify species based their ionization potentials. These capabilities are demonstrated in our dimethyl ether flame studies described

below. We have also constructed a liquid fuel delivery system for our low-pressure flame systems based on a continuous flow syringe pump system and a fuel vaporizer. In collaboration with Prof. Terry Cool of Cornel University and Prof. Phil Westmoreland of the University of Massachusetts, we are building a low-pressure flame, molecular beam sampling mass spectrometer system at the Lawrence Berkeley National Laboratory Advanced Light Source (ALS) Chemical Dynamics Beamline. The new instrument will take advantage of the high VUV photon flux available at the ALS to extend PIMS methods developed at Cornel and the CRF. The new instrument has been designed and the parts currently being fabricated.

New studies of dimethyl ether combustion chemistry, using our molecular beam mass spectrometer and laser diagnostics, have produced new data on several key intermediates. We have measured HCO concentration profiles by both PIMS and cavity ringdown spectroscopy (CRDS) methods. Good agreement is found between these two methods, validating the use of our sampling probe for detecting radical intermediates. Singlet methylene and OH have also been profiled with CRDS. The chemical kinetic model of Curran and coworkers[3,4] over predicts the concentrations HCO and $^1CH_2$ by a factor of three to four. We have also identified ketene in PIMS studies and shown that the current model under predicts the concentration of this species by a factor of five and predicts a qualitatively incorrect double peaked profile. Comparison with our previous measurements of stable species profiles shows that the under prediction of ketene is likely correlated to the under prediction of acetylene, a major ketene precursor. This work has been performed in collaboration with Prof. Jay Thoman and his student Adam Steeves of Williams College.

While the propargyl radical recombination reaction has been identified as the primary pathway to benzene from C1-C3 fuels[5], the reaction pathways of larger fuels remain unclear. In particular, the importance of benzene formation from acetylene addition to C4 radicals is uncertain. We have begun a study of 1,3-butadiene combustion in doped $H_2/O_2/Ar$ flames with the goal of understanding the mechanism of benzene ring formation from this prototype C4 fuel. To date, electron impact mass spectrometer and PIMS data have been collected for two candidate flames. Benzene and toluene formation has been observed in both flames. In addition, signals have been tentatively identified for several C3 and C4 radicals. More detailed studies are required to unravel the details of these flames and make meaningful comparisons to detailed chemical kinetic models of molecular weight growth in flames also being developed by Miller and coworkers at Sandia.

Our CRDS studies of radical intermediates in combustion have been quite successful, but the future development of this technique is hampered by several factors. Most significantly, the current sensitivity is limited by the presence of uncorrelated baseline noise, which is believed to be due to scattering in the flame. An additional problem is the limited dynamic range when using medium resolution pulsed dye lasers due to multi-exponential decays present on strong transition, such as those of OH and CH. We have undertaken a program to develop new combustion diagnostics utilizing recently developed cw laser-based, high sensitivity direct absorption methods. We have begun development of a prototype system to implement the NICE-OHMS and AC cavity ringdown methods developed at JILA by Hall, Ye and coworkers[6,7]. Both these methods are high resolution, frequency modulated, intracavity

absorption techniques that make true differential absorption measurements, directly addressing the weaknesses of pulsed laser CRDS.

We have undertaken a study of the application of infrared (IR) polarization spectroscopy (PS) to combustion diagnostics. Previous laser diagnostic efforts in the IR[8] have suffered from spectral congestion due to overlapping bands from the many species present in flames. Polarization spectroscopy has the potential to select for study individual branches of a given spectrum, thus reducing spectral congestion[9-11]. Although polarization spectroscopy has been widely applied in the visible and ultraviolet regions of the spectrum, there have been no previous studies of its utility in the IR. Using cells and cold jets of CO_2, we have begun to assess the performance of IR-PS with the eventual goal of extending this work into a combustion environment. This work is performed with Prof. Bob Lucht and his student Sukesh Roy of Texas A&M University.

Future Plans

The flame sampling PIMS system is ideal for studying the formation of soot precursors such as polycyclicaromatic hydrocarbons (PAH), which are easily fragmented by other ionization techniques. After our dimethyl ether studies, we will move on to more complex fuels of current scientific and practical interest. In order to investigate the formation of the first aromatic ring in rich combustion, we will use several simple unsaturated fuels. Acetylene, ethylene, allene and 1,3-butadiene all provide excellent opportunities to investigate the initial stages of molecular weight growth. Our initial focus will be on 1,3-butadiene flames. Benzene, a component of gasoline, is a fuel that readily produces high concentrations of PAHs and soot. It has been used in a number of studies by Howard's group[12-17] and others[18,19] to investigate the mechanism of formation of PAHs and fullerenes. These fuels have been investigated by traditional sampling EI-Q-MS and in optical studies, however, our new photoionization instrument will be better able to detect many of the low concentration, larger molecular weight species that are not well quantified in these previous studies.

Unlike our commonly employed lab flames, many practical combustion devices do not use premixed fuel and oxidizer, but rather employ diffusion flames. In such devices, a much wider range of stoichiometries is present and with different temperature profiles than in premixed combustion. Thus mechanisms developed with reference solely to premixed data may fail for diffusion flames. To investigate these effects, a counterflow diffusion burner will be constructed in collaboration with Roger Farrow (Sandia). Initially, this system will rely on non-intrusive laser diagnostics. Studies will investigate the kinetics of methanol and dimethylether flames. Both of these oxygenated fuels are considered as direct-injection diesel fuels. In such engines, mixing is relatively poor and diffusion flames play an important role.

Recent BES Publications

C. D. Pibel, A. McIlroy, C. A. Taatjes, S. Alfred, K. Patrick, and J. B. Halpern, "The vinyl radical ($\tilde{A}^2A'' \leftarrow \tilde{X}^2A'$) spectrum between 530 and 415 nm measured by cavity ring-down spectroscopy, " *Journal of Chemical Physics* **110**, 1841 (1999).

A. McIlroy, "Laser studies of small radicals in rich methane flames: OH, HCO and $^1CH_2$," *Israel Journal of Chemistry* **39**, 55 (1999).

J. W. Thoman, Jr., A. McIlroy, "Absolute CH concentrations in rich low-pressure methane-oxygen-argon flames via cavity ringdown spectroscopy of the $A^2\Delta$-$X^2\Pi$ transition," *Journal of Physical Chemistry A* **104**, 4953 (2000).

A. McIlroy, T. D. Hain, H. A. Michelsen, T. A. Cool, "A laser and molecular beam mass spectrometer study of low-pressure dimethyl ether flames," 28th *International Symposium on Combustion*, 2000, in press.

H. N. Najm, P. H. Paul, O. M. Knio, A. McIlroy, "A numerical and experimental investigation of premixed methane-air flame transient response," *Combustion and Flame*, 2001, in press.

A. McIlroy and J. B. Jeffries, "Cavity ring-down spectroscopy for concentration measurements," in *Applied Combustion Diagnostic*, Eds. K. Kohse-Hoeinghaus and J. B. Jeffries, Taylor and Francis: London, accepted.

Cited References

(1) Najm, H. N.; Knio, O. M.; Paul, P. H.; Wyckoff, P. S. *Combustion Theory and Modelling* **1999**, *3*, 709-725.
(2) Najm, H. N.; Paul, P. H.; Knio, O. M.; McIlroy, A. *Combustion and Flame* **2001**, *in press*.
(3) Curran, H. J.; Pitz, W. J.; Westbrook, C. K.; Dagaut, P.; Boettner, J. C.; Cathonnet, M. *International Journal Of Chemical Kinetics* **1998**, *30*, 229-241.
(4) Curran, H. J.; Fischer, S. L.; Dryer, F. L. *International Journal of Chemical Kinetics* **2000**, *32*, 741-759.
(5) Pope, C. J.; Miller, J. A. *Proceedings of the Combustion Institute* **2000**, *28*.
(6) Ye, J.; Ma, L. S.; Hall, J. L. *Journal Of The Optical Society Of America B-Optical Physics* **1998**, *15*, 6-15.
(7) Gianfrani, L.; Fox, R. W.; Hollberg, L. *Journal of The Optical Society of America B-Optical Physics* **1999**, *16*, 2247-2254.
(8) Scherer, J. J.; Aniolek, K. W.; Cernansky, N. P.; Rakestraw, D. J. *Journal of Chemical Physics* **1997**, *107*, 6196-6203.
(9) Reichardt, T. A.; DiTeodoro, F.; Farrow, R. L.; Roy, S.; Lucht, R. P. *Journal of Chemical Physics* **2000**, *113*, 2263-2269.
(10) Reichardt, T. A.; Giancola, W. C.; Lucht, R. P. *Applied Optics* **2000**, *39*, 2002-2008.
(11) Giancola, W. C.; Reichardt, T. A.; Lucht, R. P. *Journal of the Optical Society of America B-Optical Physics* **2000**, *17*, 1781-1794.
(12) Howard, J. B.; McKinnon, J. T.; Johnson, M. E.; Makarovsky, Y.; Lafleur, A. L. *Journal of Physical Chemistry* **1992**, *96*, 6657-6662.
(13) Howard, J. B. *Proceedings of the Combustion Institute* **1992**, *24*, 933-946.
(14) Pope, C. J.; Howard, J. B. *Proceedings of the Combustion Institute* **1994**, *25*, 671-678.
(15) Richter, H.; Taghizadeh, K.; Grieco, W. J.; Lafleur, A. L.; Howard, J. B. *Journal of Physical Chemistry* **1996**, *100*, 19603-19610.
(16) McKinnon, J. T.; Howard, J. B. *Proceedings of the Combustion Institute* **1992**, *24*, 965-971.
(17) Vaughn, C. B.; Howard, J. B.; Longwell, J. P. *Combustion and Flame* **1991**, *87*, 278-288.
(18) Bachman, M.; Wiese, W.; Homann, K.-H. *Combustion and Flame* **1995**, *101*, 548-550.
(19) Smith, R. D.; Johnson, A. L. *Combustion and Flame* **1983**, *51*, 1-22.

This work was supported by the U. S. Department of Energy, Office of Basic Energy Sciences, Division of Chemical Sciences, under Contract No. W-31-109-ENG-38.

FLASH PHOTOLYSIS-SHOCK TUBE STUDIES

Joe V. Michael

Gas Phase Chemical Dynamics Group, Chemistry Division
Argonne National Laboratory, Argonne, IL 60439
e-mail: michael@anlchm.chm.anl.gov

During the past year, rate studies on one termolecular, two bimolecular, and one unimolecular reaction have been completed. In these studies, the atomic resonance absorption spectroscopic (ARAS) method was used for atom detection in reflected shock waves experiments.

The third-order reaction, H + O_2 + M, has been directly studied in reflected shock waves with N_2 and Ar bath gases between ~450-700 K using the Laser Photolysis-Shock Tube (LP-ST) technique, and the results were reported in last year's contractors meeting. In these experiments, H atom depletion was observed with H-atom ARAS.[1] This study was extended to include a room temperature determination for H + O_2 + H_2O and a temperature dependent determination for H + O_2 + O_2.[2] The measured room temperature rate constants for bath gases, H_2O, N_2, O_2, Ar, Kr, Ne, and He, are (50 ± 3), (4.32 ± 0.28), (3.13 ± 0.06), (2.16 ± 0.14), (2.10 ± 0.10), (1.40 ± 0.04), and (1.80 ± 0.07), all with 2σ errors and in units of 10^{-32} cm^6 $molecule^{-2}$ sec^{-1}, respectively. The room temperature values were combined with the T-dependent values for N_2, Ar, and O_2 yielding,

$$k_{ter}^{N_2}(T) = (4.82 \pm 1.03) \times 10^{-29}\, T^{-1.232\pm0.036}\ cm^6\ molecule^{-2}\ s^{-1}, \quad (1)$$

$$k_{ter}^{Ar}(T) = (1.26 \pm 0.27) \times 10^{-29}\, T^{-1.120\pm0.035}\ cm^6\ molecule^{-2}\ s^{-1}, \quad (2)$$

and,

$$k_{ter}^{O_2}(T) = (1.57 \pm 0.38) \times 10^{-29}\, T^{-1.094\pm0.040}\ cm^6\ molecule^{-2}\ s^{-1}, \quad (3)$$

in substantial agreement with Mueller, Yetter, and Dryer[3] and also with Bates, Hanson, Bowman, and Golden.[4] During the past year, we have attempted to explain these data, and data with other third bodies, using a consistent theoretical model. The most difficult result to explain is that with H_2O as third body. Hsu et al.[5] and Durant and Kaufman[6] have noted this difficulty before. In order to obtain a better representation of collisional deactivation, we have used the methods of Bzowski et al.,[7] as adopted by Paul[8] and Paul and Warnatz,[9] to obtain transport property force constant and size parameters (i. e., ε_{12} and σ_{12} values). These can then be used to calculate collision rates for deactivation of

HO_2^* provided collisional integrals are known. The appropriate collision integral, $\Omega(2,2)^*$ can also be evaluated as shown by Bzowski et al.[7] and repeated by Paul[8] (note that there are some typographical errors for the collision integrals in this latter paper). When this procedure is used, the difference in reactivity between the rare gases (ro-vibrational energy transfer to translation) is entirely due to the differences in sampling rate as evidenced by the the fact that a common value for $-\Delta E_{all}$ can be used for all rare gases. When a diatomic or polyatomic collider is used there is enhancement and larger values for the energy transfer parameters are needed. The largest is for H_2O followed in order by CH_4, N_2, O_2, and H_2.

The 193 nm photolysis of ketene was studied[10] by measuring the amount of atomic hydrogen produced when very dilute ketene/Ar and ketene/H_2 mixtures were irradiated by a single pulse from an ArF excimer laser. Absolute concentrations of atomic hydrogen were monitored over a time interval of 0-2.5 ms by using Lyman-α atomic resonance absorption spectroscopy (ARAS).

Four different photo-dissociation channels of ketene were identified,

$$H_2CCO + h\nu \rightarrow CH_2(^3B_1) + CO \quad (4a)$$

$$\rightarrow CH_2(^1A_1) + CO \quad (4b)$$

$$\rightarrow HCCO + H \quad (4c)$$

$$\rightarrow C_2O(b^1\Sigma^+) + H_2, \quad (4d)$$

and the quantum yields for each channel were measured as $\phi_a = 0.628$, $\phi_b = 0.193$, $\phi_c = 0.107$, and $\phi_d = 0.072$, respectively.

In order to explore the secondary chemistry that occurred when using higher pressure H_2CCO/Ar mixtures, a mechanism was constructed that used well documented reactions, and for most processes, rate constants that had already been accurately determined. Modeling studies using this mechanism showed the [H] profile to be determined largely by the rate of the reaction of HCCO with H,

$$H + HCCO \rightarrow CH_2 + CO. \quad (5)$$

An excellent fit to all of the experimental data was obtained when $k_5 = (1.7 \pm 0.3) \times 10^{-10}$ cm^3 $molecule^{-1}$ s^{-1}.

The Laser Photolysis-Shock Tube (LP-ST) technique coupled with H-atom atomic resonance absorption spectrometry (ARAS) has been used to study the reaction, $H + CH_4$ " $CH_3 + H_2$, over the temperature range, 928–1697 K.[11] Shock tube studies on the reverse of this reaction, $CH_3 + H_2$ " $H + CH_4$, using CH_3I dissociation in the presence of H_2 yielded H-atom formation rates and rate constants for the reverse process over the temperature range, 1269-1806 K. These results were transformed (using well-established equilibrium constants) to the forward direction. The combined results for $H + CH_4$ can be represented by an experimental three parameter expression, $k = 6.78 \times 10^{-21}$ $T^{3.156}$ $\exp(-4406\ K/T)$ cm^3 $molecule^{-1}$ s^{-1} (348-1950 K) that was evaluated from the present work and seven previous studies. Using this evaluation, disagreements between

previously reported values for the dissociation of CH_4 could be reconciled. The thermal decomposition of CH_4 was then studied in Kr bath gas. The dissociation results agreed with the earlier studies and were theoretically modeled with the Troe formalism. The energy transfer parameter necessary to explain both the present results and those of Kiefer and Kumaran[12] is, $-\langle\Delta E\rangle_{all}/cm^{-1} = 0.3323\ T^{0.7}$. The low temperature data on the reverse reaction, $H + CH_3$ (in He) from Brouard et al.,[13] were also modeled with the Troe formalism. Lastly, the rate constant for $H + CH_4$ was theoretically calculated using conventional transition state theory with Eckart tunneling corrections (CTST-E). The potential energy surface used was from Kraka et al.,[14] and the derived T-dependence with this method agreed almost perfectly with the experimental evaluation.

Additional atom and radical with molecule reaction studies (e. g. Cl + hydrocarbons, OH + hydrocarbons, $CF_2 + O_2$, etc.) and, also, thermal decomposition investigations (e. g. C_2H_5, C_2H_3, etc.) are in the planning stage at the present time. These reaction studies are of theoretical interest to chemical kinetics and of practical interest in hydrocarbon combustion or waste incineration.

This work was supported by the U. S. Department of Energy, Office of Basic Energy Sciences, Division of Chemical Sciences, under Contract No. W-31-109-ENG-38.

References

1. K. P. Lim and J. V. Michael, Proc. Combust. Inst. **25**, 713 (1994).
2. J. V. Michael, J. J. Carroll, J. W. Sutherland, M.-C. Su, and A. F. Wagner, in preparation.
3. M. A. Mueller, R. A. Yetter, and F. L. Dryer, Proc. Combust. Inst. **27**, 177 (1998).
4. R. W. Bates, R. K. Hanson, C. T. Bowman, and D. M. Golden, Paper 159, First Joint Meeting of the U. S. Sections of the Combustion Institute, March 14-17, 1999, Washington, D. C.
5. K.-J. Hsu, J. L. Durant, and F. Kaufman, J. Phys. Chem. **91**, 1895 (1987).
6. J. L. Durant and F. Kaufman, Chem. Phys. Lett. **142**, 246 (1987).
7. J. Bzowski, J. Kestin, E. A. Mason, and F. J. Uribe, J. Phys. Chem. Ref. Data **19**, 1179 (1990).
8. P. H. Paul, DRFM: A New Package for the Evaluation of Gas-Phase-Transport Properties, Sandia Report, SAND98-8203, November, 1997.
9. P. Paul and J. Warnatz, Proc. Combust. Inst. **27**, 495 (1998).
10. G. P. Glass, S. S. Kumaran, and J. V. Michael, J. Phys. Chem. A **104**, 8360 (2000).
11. J. W. Sutherland, M.-C. Su, and J. V. Michael, Int. J. Chem. Kinet., submitted.
12. J. H. Kiefer and S. S. Kumaran, J. Phys. Chem. **97**, 414 (1993).
13. M. Brouard, M. T. Macpherson, and M. J. Pilling, J. Phys. Chem. **93**, 4047 (1989).
14. E. Kraka, J. Gauss, and D. Cremer, J. Chem. Phys. **99**, 5306 (1993); Z. Konkoli, E. Kraka, and D. Cremer, J. Phys. Chem. A **101**, 1742 (1997).

PUBLICATIONS FROM DOE SPONSORED WORK FROM 1999-2001

■ *Rate Constants for $CH_3 + O_2$ " $CH_3O + O$ at High Temperature and Evidence for $H_2CO + O_2$ " $HCO + HO_2$*, J. V. Michael, S. S. Kumaran, and M.-C. Su, J. Phys. Chem. A **103**, 5942 (1999).

■ *Thermal Rate Constants over Thirty Orders of Magnitude for the $I + H_2$ Reaction*, J. V. Michael, S. S. Kumaran, M.-C. Su, and K. P. Lim, Chem. Phys. Lett. **319**, 99 (2000).

■ *Photolysis of Ketene at 193 nm and the Rate Constant for H + HCCO at 297 K*, G. P. Glass, S. S. Kumaran, and J. V. Michael, J. Phys. Chem. A **104**, 8360 (2000).

■ *Reply to comment on " Rate Constants for $CH_3 + O_2$ " $CH_3O + O$ at High Temperature and Evidence for $H_2CO + O_2$ " $HCO + HO_2$"*, J. V. Michael, S. S. Kumaran, and M.-C. Su, J. Phys. Chem. **104**, 9800 (2000).

■ *Initiation in H_2/O_2: Rate Constants for $H_2 + O_2$ " $H + HO_2$ at High Temperature*, J. V. Michael, J. W. Sutherland, L. B. Harding, and A. F. Wagner, Proc. Combust. Inst. **28**, 1471 (2000).

■ *Atomic Resonance Absorption Spectroscopy with Flash or Laser Photolysis in Shock Waves Experiments*, J. V. Michael and Assa Lifshitz, in *Handbook of Shock Waves, Vol. 3* ; G. Ben-Dor, O. Igra, T. Elperin, and A. Lifshitz, Eds., Academic Press, New York, 2001, pp. 77-105.

Chemical Kinetics and Combustion Modeling

James A. Miller
Combustion Research Facility
Sandia National Laboratories
Livermore, CA 94551-0969
E:mail: jamille@ca.sandia.gov

Program Scope

The goal of this program is to gain qualitative insight into how pollutants are formed in combustion systems and to develop quantitative mathematical models to predict their formation rates. The approach is an integrated one, combining low-pressure flame experiments, chemical kinetics modeling, reaction rate theory, and kinetics experiments (microscopic and macroscopic) to gain as clear a picture as possible of the processes in question. My efforts and those of my collaborators are focused on problems involved with the nitrogen chemistry of combustion systems and the formation of soot and PAH in flames, as well as on general problems in hydrocarbon combustion.

Recent Results

The Reaction Between Ethyl and Molecular Oxygen II: Further Analysis, (with Stephen J. Klippenstein)

This investigation is a rather substantial extension and elaboration of our previous work on the same reaction. In this article we accomplish three primary objectives:

1. We show quantitatively how sensitive the high-temperature rate coefficient k(T) is to E_{02}, the threshold energy of the transition state for direct molecular elimination of HO_2 from $C_2H_5O_2$ (ethylperoxy radical), deducing a value of E_{02} = -3.0 kcal/mole (measured from reactants).

2. We derive the result that $k_0(T) \approx k'_\infty(T)$ in the high-temperature regime, where $k_0(T)$ is the zero-pressure rate coefficient, and $k'_\infty(T)$ is the infinite-pressure rate coefficient for the bimolecular channel.

3. Most importantly, we discuss the three different regimes of the reaction (low-temperature, transition, and high temperature) in terms of the eigenvectors and eigenvalues of G, the transition matrix of the master equation. The transition regime is shown to be a region of avoided crossing between the two chemically significant eigenvalue curves in which the thermal rate coefficient k(T,p) jumps from one iegenvalue to the other. This jump is accompanied by a "mixing" of the corresponding eigenvectors, through which both eigenvectors deplete the reactant. The onset of the high-temperature regime is triggered by reaching the "stabilization limit" of the ethylperoxy adduct. Our identification of the prompt and secondary HO_2 formed by the reaction with these eigenvalue/eigenvector pairs leads to good agreement between theory and the experiments of Clifford, et al. [J. Phys. Chem. A 2000, 104, 11549-11560].

The Recombination of Propargyl Radicals: Solving the Master Equation, (with Stephen J. Klippenstein)

We have investigated theoretically the recombination reaction between two propargyl (C_3H_3) radicals using previously published BAC-MP4 calculations (supplemented by DFT-B3LYP results) to

characterize the potential energy surface, RRKM theory to compute microcanonical rate coefficients, and solutions to the time-dependent, multiple-well master equation to predict thermal rate coefficients and product distributions as a function of temperature and pressure. The thermal rate coefficient k(T,p) drops off precipitously at high temperature regardless of the pressure. Below 500 K, $k(T,p) \approx k_\infty(T)$, the high-pressure limit rate coefficient for initial complex formation, independent of p. For 500 K < T < 2000 K, the rate coefficient increases with increasing pressure, as one would normally expect. At 2000 K, the "coalescence temperature" for this reaction, $k(T,p) = k_0(T)$, the zero-pressure rate coefficient, and only bimolecular products (phenyl + H) are predicted, *no matter how high we make the pressure.* The latter effect is a consequence of all the intermediate complexes reaching their "stabilization limits," a concept discussed extensively in the paper. Below 800 K, many C_6H_6 isomers are formed as products, and the pressure and temperature dependence of the branching fractions is easily understood from conventional reasoning. Above 800 K, the product distributions begin to be dominated by isomers reaching their stabilization limits and disappearing as important products. Above 1200 K, the only significant products are fulvene, benzene, and phenyl + H. Beyond 1700 K fulvene disappears, and for T > 2000 K the only products are phenyl + H.

We have analyzed our results in terms of the eigenvalues and eigenvectors of G, the transition matrix of the master equation. A "good" rate coefficient exists only when the rate is controlled by a single eigenvalue of G. A jump of the k(T,p) curve for any pressure from one eigenvalue to another is triggered by the reaching of critical stabilization limits, producing "avoided crossings" of the eigenvalue curves. It is at such avoided crossings that biexponential reactant decays occur.

A Direct Transition State Theory Based Analysis of the Branching in NH_2+NO, (with De-Cai Fang and Larry Harding, Argonne National Laboratories, and Stephen J. Klippenstein, Sandia National Laboratories)

A combination of high level quantum chemical simulations and sophisticated transition state theory analyses are employed in a study of the temperature dependence of the $N_2H + OH \rightarrow HNNOH$ recombination reaction. The implications for the branching between $N_2H + OH$ and $N_2 + H_2O$ in the $NH_2 + NO$ reaction are also explored. The transition state partition function for the $N_2H + OH$ recombination reaction is evaluated with a direct implementation of variable reaction coordinate (VRC) transition state theory (TST). The orientation dependent interaction energies are directly determined at the CAS+1+2/cc-pvdz level. Corrections for basis set limitation are obtained via calculations along the cis and trans minimum energy paths employing an ~aug-pvtz basis set. The calculated rate constant for the $N_2H + OH \rightarrow HNNOH$ recombination is found to decrease significantly with increasing temperature, in agreement with the predictions of our earlier theoretical study. Conventional transition state theory analyses, employing new coupled cluster estimates for the vibrational frequencies and energies at the saddlepoints along the $NH_2 + NO$ reaction pathway, are coupled with the VRC-TST analyses for the $N_2H + OH$ channels to provide estimates for the branching in the $NH_2 + NO$ reaction. Modest variations in the exothermicity of the reaction (1-2 kcal/mol), and in a few of the saddlepoint energies (2-4 kcal/mol), yield TST based predictions for the branching fraction that are in satisfactory agreement with related experimental results. The unmodified results are in reasonable agreement for higher temperatures, but predict too low a branching ratio near room temperature, as well as too steep an initial rise.

Variation of Equivalence Ratio and Element Ratios in Low-Pressure Premixed Flames of Aliphatic Fuels (with Christopher J. Pope)

In previously published work it was found that the element ratios (such as C/O, H/O, H/C) and the equivalence ratio all varied in the flame zone of a low-pressure premixed fuel-rich benzene/oxygen/argon laminar flat flame. These variations were seen from analyses of both the data and detailed kinetic modeling. In the present work, seven additional flames were analyzed in the same manner, including five flames with a single hydrocarbon fuel (methane, acetylene, ethylene, allene, and propene) and two flames with a mixture of fuels (acetylene/allene, hydrogen/allene). All the flames had argon as the diluent, with pressures between 20 and 37.5 Torr, equivalence ratios between 1.6 and 2.5, cold gas velocities between 42 and 126 cm/sec.

All of these flames showed variations in the element ratios and equivalence ratios. Furthermore, these variations changed in a consistent pattern with respect to the molecular weight of the fuel. In the flame zone, the percent change in the H/O, C/O and equivalence ratios increased with increasing molecular weight of the fuel, except for the hydrogen/allene flame in which the C/O ratio first increases, then decreases in the flame zone. Also, unlike all the other hydrocarbon flames, the C/O ratio decreases below its inlet value for the methane flame. The H/O and equivalence ratios decrease below their inlet values for the hydrogen/allene flame. These results are explained in terms of differential diffusion effects between the products and the reactants, which increase as the fuel becomes increasingly heavier than the major carbon- and hydrogen-containing products.

Future Directions

Our work in the next year will largely focus on the cyclization and pre-cyclization chemistry of flames fueled (or partially fueled) by 1, 3 butadiene. This work will involve both theory and modeling and will proceed in parallel with the experiments in Andy McIlroy's lab at Sandia, where he is measuring the structure of a $H_2/O_2/Ar\text{-}C_4H_6$ flame.

We shall also investigate theoretically other possible paths for the $C_3H_3+C_3H_3$ reaction paths that can produce benzene without passing through the fulvene well. Particular issues concerning the nitrogen chemistry of combustion are also of interest, especially those that impact the modeling of NO_x control techniques such as Thermal De-NO_x, RAPRENO$_x$, and reburning.

Publications of James A. Miller
1999-Present

J.A. Miller and S.J. Klippenstein, "The Recombination of Propargyl Radicals: Solving the Master Equation," *J. Phys. Chem. A*, accepted (2000)

J.A. Miller and S. J. Klippenstein, "The Reaction Between Ethyl and Molecular Oxygen II: Further Analysis," *International Journal of Chemical Kinetics*, submitted (2000).

D.K. Hahn, S.J. Klippenstein, and J.A. Miller, "A Theoretical Analysis of the Reaction Between Propargyl and Molecular Oxygen," *Faraday Discussions of the Royal Society of Chemistry* **119** (2001), submitted.

D.–C. Feng, L.B. Harding, S.J. Klippenstein, and J.A. Miller, "A Direct Transition State Theory Analysis of the HNN + OH Reaction and its Implications for the Branching in NH_2 + NO," *Faraday Discussions of the Royal Society of Chemistry* **119** (2001), submitted.

J.A. Miller, S.J. Klippenstein, and S. H. Robertson, "A Theoretical Analysis of the Reaction Between Ethyl and Molecular Oxygen," *Proceedings of the Combustion Institute* **28** (2000), in press.

J.A. Miller, S.J. Klippenstein, and S.H. Robertson, "A Theoretical Analysis of the Reaction Between Vinyl and Acetylene: Quantum Chemistry and Solution of the Master Equation," *J. Phys. Chem. A* **104**, 7525-7536 (2000), see also *J. Phys. Chem. A* **104**, 9806 (2000).

C.J. Pope and J.A. Miller, "Exploring Old and New Benzene Formation Pathways in Low-Pressure Premixed Flames of Aliphatic Fuels," *Proceedings of the Combustion Institute* **28** (2000), in press.

C.J. Pope and J.A. Miller, "Variation of Equivalence Ratio and Element Ratios in Low-Pressure Premixed Flames of Aliphatic Fuels," *Combustion and Flame,* accepted (2000).

J.A. Miller and S.J. Klippenstein, "Theoretical Considerations in the NH_2 + NO Reaction" *J. Phys. Chem A* **104**, 2061-2069 (2000).

J.A. Miller and P. Glarborg, "Modeling the Thermal De-NO_x Process: Closing in on a Final Solution," *International Journal of Chemical Kinetics* **31** 757-765 (1999).

J. A. Miller and S. J. Klippenstein, "Angular Momentum Conservation in the O + OH $\leftrightarrow$ O_2 + H Reaction," *International Journal of Chemical Kinetics* **31**, 753-756 (1999).

J.D. DeSain, C.A. Taatjes, D.K. Hahn, J.A. Miller, and S.J. Klippenstein, "Infrared Frequency-Modulation Probing of Product Formation in Alkyl + O_2 Reactions: IV Reactions of Propyl and Butyl Radicals with O_2 between 295 and 750K" *Faraday Discussions of the Royal Society of Chemistry* **119** (2001) , submitted.

P. Glarborg, A.B. Bendtsen, and J. A. Miller, "Nitromethane Dissociation: Implications for the CH_3 + NO_2 Reaction", *International Journal of Chemical Kinetics* **31,** 591-602 (1999).

Reaction Dynamics in Polyatomic Molecular Systems

William H. Miller

Department of Chemistry, University of California, and
Chemical Sciences Division, Lawrence Berkeley National Laboratory
Berkeley, California 94720-1460
miller@neon.cchem.berkeley.edu

Program Scope or Definition

The goal of this program is the development of theoretical methods and models for describing the dynamics of chemical reactions, with specific interest for application to polyatomic molecular systems of special interest and relevance. There is interest in developing the most rigorous possible theoretical approaches and also in more approximate treatments that are more readily applicable to complex systems.

Recent Progress

Classical molecular dynamics (CMD) simulations (≡ classical trajectory calculations) are widely used to describe a variety of dynamical processes in complex molecular systems, e.g., chemical reactions rates involving polyatomic molecules. Classical mechanics, of course, cannot describe quantum mechanical effects such as coherence/interference, tunneling, zero-point energy constraints, etc., features that sometimes make significant contributions to the process of interest. The current focus of our research efforts is to develop practical ways for adding quantum effects to CMD by using the initial value representation (IVR) of semiclassical (SC) theory. Ref. 19 gives a comprehensive summary of the theoretical development and surveys numerous recent SC-IVR applications.

For complex molecular systems, the dynamical quantity of interest is typically expressed in terms of a time correlation function of the form

$$C_{AB}(t) = \mathrm{tr}\left[\hat{A}\, e^{i\hat{H}t/\hbar}\ \hat{B}\, e^{-i\hat{H}t/\hbar}\right], \tag{1}$$

where $\hat{A}$ and $\hat{B}$ are hermitian operators depending on the property of interest, and $\hat{H}$ is the Hamiltonian of the system. E.g., the reaction rate for a chemical reaction is the $t \to \infty$ limit of Eq. (1), where $\hat{A}$ is the Boltmannized-flux operator and $\hat{B}$ a Heaviside function that is 1 (0) on the product reactant side of a dividing surface in configuration space. If, as is often the case, $\hat{B}$ is a local function of the form B[s(q)], then the 'forward-backward' (FB) version of SC-IVR theory (refs. 5,12,19) gives the correlation function of Eq. (1) as

$$C_{AB}(t) = (2\pi\hbar)^{-F} \int d\mathbf{p}_0 \int d\mathbf{q}_0 \int dp_s\, \tilde{B}(p_s) \langle \mathbf{p}_0,\mathbf{q}_0|\hat{A}|\mathbf{p}_0',\mathbf{q}_0'\rangle\, C_0(\mathbf{p}_0,\mathbf{q}_0;p_s)\, e^{iS_0(\mathbf{p}_0,\mathbf{q}_0;p_s)/\hbar}, \tag{2}$$

where $(\mathbf{p}_0,\mathbf{q}_0)$ are the initial conditions for classical trajectories that arrive at phase point $(\mathbf{p}_t,\mathbf{q}_t)$ at time t; at time t there is a momentum 'jump',

$$\mathbf{p}_t \to \mathbf{p}_t + p_s \frac{\partial s(\mathbf{q}_t)}{\partial \mathbf{q}_t}, \tag{3}$$

and the trajectory is then evolved backward in time to t = 0; $(\mathbf{p}_0',\mathbf{q}_0')$ is the final phase point, S_0 the action integral along this FB trajectory, and C_0 a factor involving the derivatives of final values $(\mathbf{p}_0',\mathbf{q}_0')$ with respect to initial ones $(\mathbf{p}_0,\mathbf{q}_0)$. $\tilde{B}(p_s)$ is the Fourier transform of the function B(s), and $|\mathbf{p}_0,\mathbf{q}_0\rangle$ and $|\mathbf{p}_0',\mathbf{q}_0'\rangle$ are coherent states.

A dramatic illustration of the ability of the FB-IVR to describe quantum effects is provided by barrier transmission through a double-slit potential. Fig. 1 shows a contour sketch of the potential and the incident state, and the angular distribution of the transmitted particle (which can be expressed in terms of a

correlation function such as Eq. (1)) is shown in Fig. 2.

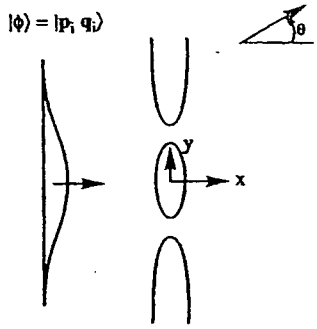

Figure 1. Contour sketch of the two-slit potential energy surface, V(x,y), with the initial state |φ> depicted; from ref. 18.

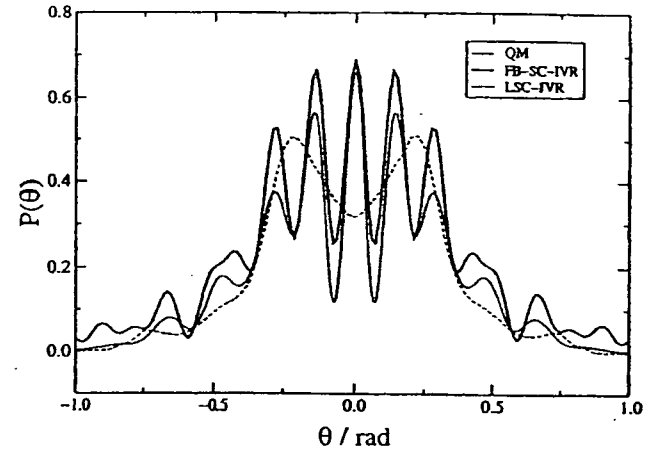

Figure 2. Angular distributions of a particle transmitted through the two-slit potential, as given by the exact quantum calculation (QM), the forward-backward IVR (FB-SC-IVR), and the linearized/classical Wigner model (LSC-IVR); from ref. 18.

One sees that the FB-IVR describes the coherence (i.e., diffraction) effects in the transmission probability quite well, while a linearized approximation to the SC-IVR (which is equivalent to a classical calculation with a Wigner distribution of initial conditions) cannot do so. Even more interesting are the results shown in Fig. 3, which is a similar calculation but with a set of 100 to 200 vibrational degrees of freedom coupled to the 2-slit potential (e.g., the phonons of the atoms making up the diffraction grating).

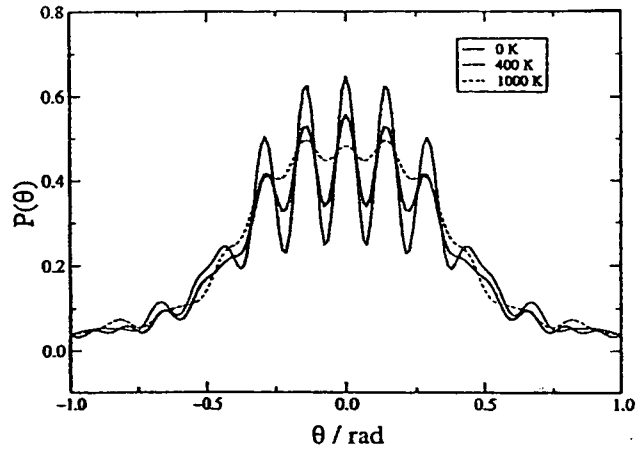

Figure 3. Same as Fig. 2, but with the addition of a bath of harmonic oscillators coupled to the two-split potential; the different curves are for different temperatures for the harmonic bath; from ref. 18.

As the temperature of this 'bath' of vibrational modes is increased, the coherence features are progressively quenched, just as one expects. The important point of this example is the demonstration that the FB-IVR approach can indeed describe quantum effects in CMD simulations for systems with hundreds of degrees of freedom. Furthermore, there is no requirement that the vibrational modes be harmonic (as those in this example were taken to be) or on the form of the coupling.

Future Plans

Future efforts will focus on the applications of these approaches to calculate thermal rate constants, k(T), for a variety of medium-size polyatomic reaction systems (OH + CH_4, for example). The goal is to make these SC-IVR approaches practical enough that, with only a modest additional effort, one will be able to apply them to any system for which a classical trajectory simulation is possible.

1999 - 2001 (to date) DOE Publications

1. D. Skinner and W. H. Miller, Application of the Semiclassical Initial Value Representation and Its Linearized Approximation to Inelastic Scattering," Chem. Phys. Lett. **300**, 20 (1999); LBNL-42302.

2. V. S. Batista, M. T. Zanni, B. J. Greenblatt, D. M. Neumark, and W. H. Miller, Femtosecond Photoelectron Spectroscopy of the I_2^- Anion: A Semiclassical Molecular Dynamics Simulation Method, J. Chem. Phys. **110**, 3736 (1999); LBNL-42303.

3. M. T. Zanni, V. S. Batista, B. J. Greenblatt, W. H. Miller, and D. M. Neumark, Femtosecond Photoelectron Spectroscopy of the I_2^- Anion: Characterization of the $\tilde{A}'\,^2\Pi_{g,1/2}$ Excited State, J. Chem. Phys. **110**, 3748 (1999); LBNL-42304.

4. H. Wang, X. Song, D. Chandler and W. H. Miller, Semiclassical Study of Electronically Nonadiabatic Dynamics in the Condensed-Phase: Spin-Boson Problem with Debye Spectral Density, J. Chem. Phys. **110**, 4828 (1999); LBNL-42176.

5. X. Sun and W. H. Miller, Forward-Backward Initial Value Representation for Semiclassical Time Correlation Functions, J. Chem. Phys. **110**, 6635 (1999); LBNL-42426.

6. V. Guallar, V. S. Batista and W. H. Miller, Semiclassical Molecular Dynamics Simulations of Excited State Double-Proton Transfer in 7-Azaindole Dimers, J. Chem. Phys. **110**, 9922 (1999); LBNL-42679.

7. H. Wang and W. H. Miller, Analytic Continuation of Real-Time Correlation Functions to Obtain Thermal Rate Constants for Chemical Reaction, Chem. Phys. Lett. **307**, 463 (1999); LBNL-42906.

8. W. H. Miller, Generalization of the Linearized Approximation to the Semiclassical Initial Value Representation for Reactive Flux Correlation Functions, J. Phys. Chem. **103**, 9384 (1999); LBNL-43208.

9. Y. Guo, D. L. Thompson and W. H. Miller, Thermal and Microcanonical Rates of Unimolecular Reactions from an Energy Diffusion Theory Approach, J. Phys. Chem. **103**, 10308 (1999); LBNL-43207.

10. D. E. Skinner and W. H. Miller, Application of the Forward-Backward Initial Value Representation to Molecular Energy Transfer," J. Chem. Phys. **111**, 10787 (1999); LBNL-44187.

11. W. H. Miller, Using Mechanics in a Quantum Framework: Perspective on "Semiclassical Description of Scattering", Theo. Chem. Accts. **103**, 236 (2000); LBNL-42905.

12. H. Wang, M. Thoss, and W. H. Miller, Forward-Backward Initial Value Representation for the Calculation of Thermal Rate Constants for Reactions in Complex Molecular Systems, J. Chem. Phys. **112**, 47 (2000); LBNL-44637.

13. E. A. Coronado, Victor S. Batista, and W. H. Miller, Nonadiabatic Photodissociation Dynamics of *ICN* in the $\tilde{A}$ Continuum: A Semiclassical Initial Value Representation Study, J. Chem. Phys. 112, 5566 (2000); LBNL-44723.

14. M. Thoss, W. H. Miller and G. Stock, Semiclassical Description of Nonadiabatic Quantum Dynamics: Application to the S_1-S_2 Conical Intersection in Pyrazine, J. Chem. Phys. 112, 10282 (2000); LBNL-44877.

15. R. Gelabert, X. Gimenez, M. Thoss, H. Wang and W. H. Miller, A Log-Derivative Formulation of the Prefactor for the Semiclassical Herman-Kluk Propagator, J. Phys. Chem. **104**, 10321 (2000); LBNL-45437.

16. V. Guallar, V. S. Batista and W. H. Miller, Semiclassical Molecular Dynamics Simulations of Intramolecular Proton Transfer in Photo-Excited 2-(2'-hydroxyphenyl-oxazole, J. Chem. Phys. **113**, 9510 (2000); LBNL-46405.

17. H. Wang, M. Thoss, K. Sorge, R. Gelabert, X. Gimenez and W. H. Miller, Semiclassical Description of Quantum Coherence Effects and Their Quenching: A Forward-Backward Initial Value Representation Study, J. Chem. Phys. **114**, 2562 (2001); LBNL-46836.

18. R. Gelabert, X. Gimenez, M. Thoss, H. Wang and W. H. Miller, Semiclassical Description of Diffraction and Its Quenching by the Forward-Backward Version of the Initial Value Representation, J. Chem. Phys. **114**, 2572 (2001); LBNL-46837.

19. W. H. Miller, The Semiclassical Initial Value Representation: A Potentially Practical Way for Adding Quantum Effects to Classical Molecular Dynamics Simulations, J. Phys. Chem. **105**, 2942 (2001); LBNL-46935.

20. M. Thoss, H. Wang and W. H. Miller, Generalized Forward-Backward Initial Value Representation for the Calculation of Correlation Functions in Complex Systems, J. Chem. Phys. (accepted); LBNL-47268.

21. V. Guallar, D. Harris, V. S. Batista, G. Loew and W. H. Miller, A Proton Transfer Mechanism for Activation of Cytochrome P450eryf, J. Am. Chem. Soc. (submitted); LBNL-46748.

22. J. Xing, E. A. Coronado and W. H. Miller, Some New Classical and Semiclassical Models for Describing Tunneling Processes with Real-Valued Classical Trajectories, J. Phys. Chem. (submitted); LBNL-47269.

23. H. Wang, M. Thoss and W. H. Miller, Systematic Convergence in the Dynamical Hybrid Approach for Complex Systems: A Numerically Exact Methodology, J. Chem. Phys. (submitted); LBNL-47557.

24. M. Thoss, H. Wang and W. H. Miller, Self-Consistent Hybrid Approach for Complex Systems: Application to the Spin-Boson Model with Debye Spectral Density, J. Chem. Phys. (submitted); LBNL-47558.

Reacting Flow Modeling with Detailed Chemical Kinetics

Habib N. Najm

Combustion Research Facility
Sandia National Laboratories, MS 9051
Livermore, CA 94551
hnnajm@ca.sandia.gov

1. Program Scope

This project focuses on the study of unsteady flame-flow interaction in multi-dimensional reacting flow using numerical modeling with detailed chemical kinetics and transport. The objectives are to provide improved understanding of the interaction between flames and turbulent flow, and to generate information leading to the development of predictive turbulent combustion models. The scope of the work covers a range of topics including development of time integration and adaptive mesh refinement numerical methods for efficient reacting flow computations, implementation of these developments in parallel computational tools, and utilization of these tools for studying detailed structure and dynamics of laboratory-scale hydrocarbon flames in vortical flow. We focus on collaborative studies with experimentalists at the CRF working on the same flame geometry and conditions for the purpose of validation of computational models. We also work on development and implementation of dynamical systems analysis tools geared towards enhancing physical insight gained from computational results and enabling effective use of experimental comparisons towards improvements in flame models.

2. Recent Progress

Recent progress is outlined below as pertaining to both numerical methods development and reacting flow studies.

2.1 Numerical Methods

We have continued developments towards more efficient operator-split implementations for reacting flow with detailed kinetics and transport, in collaboration with Prof. O. Knio of Johns Hopkins University. Recent advances include the development, implementation, and demonstration of : (1) Runge-Kutta-Chebyshev (RKC) extended-stability explicit time integration for diffusive transport terms, allowing the choice of time step based on accuracy rather than stability. (2) Coarse-jacobian utilization, whereby the evaluation of Jacobians, necessary for implicit time integration of stiff chemical source terms, is done on an effectively adaptive mesh, reverting to a coarse mesh away from the flame, thereby introducing savings on expensive Jacobian evaluations. (3) Extrapolation of transport properties internal to a time step, whereby expensive evaluations of mixture-averaged transport properties are done once at the beginning of a time step, and subsequently extrapolated for the internal RKC stages. In this manner, the increased cost of computations with mixture-averaged transport properties, versus only temperature-dependent transport properties, is reduced from a factor of 6 down to 1.4. The present construction is highly efficient, allowing utilization of large time steps, and computations of flame-flow interactions at laboratory length and time scales and with both detailed chemistry and transport.

2.2 Transient Premixed Flame Response

We have used a C_1C_2 subset of J.Miller's hydrocarbon kinetics mechanism to study the transient response of premixed methane-air flames during interactions with vortex-pairs. These computations were done at time scales commensurate with earlier experimental measurements by P.Paul, such that experimental and numerical time evolution profiles were superposable. Comparisons were done at stoichiometric and rich conditions where experimental data was available. No improvement was evident in the predicted OH and CH evolution, as compared with our earlier predictions with GRImech1.2. Comparisons with HCO revealed reasonable agreement on the time scale of decay rate of HCO signal/concentration. Experimental methoxy data was available at steady-state, and revealed a qualitative disagreement with the numerical results in that the predicted two-peaked CH_3O structure was not evident in the measurements. Variations in CH_3O-relevant reaction rate constants within their uncertainty bands were indeed found to lead to a predicted single-peak. They also lead to an increase in predicted CH_3O concentration up to levels which are more commensurate with experimental observations, as compared to those predicted with the original mechanism. Specifically, we found that a factor of 10 increase in the pre-exponential factor of the reaction $CH_3+HO_2 \rightarrow CH_3O+OH$, a variation that is within the expected uncertainty in this rate constant, may provide a more realistic model of methoxy chemistry in this flame. No validation of the predicted transient response of methoxy was possible due to the inavailability of transient flame experimental data. Additional data both on the above rate constant and on transient methoxy response will be useful for improving our confidence in the predicted structure and evolution of methoxy in this flame.

We have also evaluated the use of more accurate mixture-averaged transport properties in studies of transient flame-flow interaction, versus our earlier implementation where only temperature-dependence of transport properties was accounted for. This was done with the above indicated subset of Miller's mechanism, using the Dipole Reduced Formalism (DRFM) transport package developed by P.Paul, for the same vortex-pair-flame interaction at stoichiometric and rich conditions where experimental data is available. Results were found to exhibit some differences in steady-state flame structure and in the transient evolution of the flame. Most significant changes were observed in the transient accumulation observed for species on the reactant side of the flame, given the coupling of transport and chemistry driving these transients. On the other hand, no qualitative differences were observed in general flame response. Accordingly, the disagreements with CH and OH experimental measurements are not resolved. This suggests that these disagreements are due more to the chemical model than transport.

We have also continued the development and implementation of Computational Singular Perturbation (CSP) analysis tools for studies of multidimensional flame data sets. This work is in collaboration with Profs. M.Valorani of U.Rome and D.Goussis of ICEHT-Greece. Using coupled CSP time-scale analysis of both transport and chemistry terms, we have identified local low-dimensional manifolds where they exist in computed flame-vortex flowfields. These results were used to provide automatic simplification of the chemical kinetic mechanism away from the flame. Our results clearly indicate the need for the full mechanism in the primary flame, where identification of a lower-dimensional manifold was not possible. More specifically, CSP analysis of GRImech1.2 premixed methane-air flame-vortex results were used to identify reactions with highest importance indices relevant to the transient evolution of CH and OH. We find that the transient evolution of OH in the primary flame is determined

largely by the reactions: $OH+H_2 \Longleftrightarrow H+H_2O$ and $2OH \Longleftrightarrow O+H_2O$. As for CH, its evolution is determined primarily by the reactions: $CH+H_2 \Leftarrow H+CH_2$, $CH+H_2O \Rightarrow H+CH_2O$, and $CH+O_2 \Rightarrow O+HCO$. Except for the $2OH \Longleftrightarrow O+H_2O$ reaction, these are all dominant production/consumption channels of OH and CH at steady-state in this 20% N_2-diluted stoichiometric flame. These reactions are prime candidates for parameteric studies with variations in selected rate constants in future work.

2.3 Lifted Non-Premixed Jet Flame

We have investigated the ignition and stabilization of lifted non-premixed jet flames using an Adaptive Mesh Refinement (AMR) code with detailed C_1C_2 methane-air chemistry. This work is in collaboration with J.Ray of Sandia. After ignition with a modeled heat source, premixed flame fronts were observed to propagate into the jet mixing layers, leading to the formation of bifurcating edge flames propagating along the stoichiometric mixture fraction lines. The structure and evolution of the resulting edge flames were studied. As the edge flame propagating towards the jet inlet stabilizes against the incoming flow, its structure approaches a steady state of interest. Overall, we find this structure to be independent of whether the jet is faster than the coflow or vice-versa. In both cases, we observe an unsymmetric edge/triple flame structure. Comparisons with lifted flame-base CO data from P.Paul reveal agreement on the CO structure in the vicinity of the flame edge. Additional studies are planned with potentially interesting comparisons with laser-ignited laboratory jet flames.

3. Future Plans

Future plans are outlined in the following three relevant areas.

3.1 Numerical Methods

We have now achieved a roughly optimal time integration procedure for second order time integration of stiff multidimensional chemical systems on uniform meshes. Further work is planned in the selective use of explicit and implicit schemes, and in the utilization of CSP analysis for identification and utilization of automatically reduced chemical kinetics per specified error thresholds. Other planned work pertains to methods for second-order time integration with AMR, involving efficient and accurate projection method implementations for low Mach number flow, the utilization of RKC integration of transport terms where appropriate, and the extrapolation of transport properties. Further, we will leverage our ongoing Uncertainty Quantification (UQ) work in other projects to build UQ analysis tools for reacting flow.

3.2 Computational Implementation

A key issue with parallel implementations of AMR reacting flow computations is dynamic load balancing, which is becoming increasingly important as massively parallel hardware becomes more available. In recent years, efficient and robust AMR frameworks with built-in dynamic load balancing have become available. One such framework, GrACE, developed by Prof. M.Parashar of Rutgers U., has been implemented on large numbers of processors at the Caltech ASCI center. Our initial small scale tests with GrACE have demonstrated very efficient computations with relatively little overhead due to the underlying C++ mesh code. Working with J.Ray, we plan to proceed with migration of our AMR reacting-flow solver modules towards an object-oriented component-based implementation with GrACE.

3.3 Flame Studies

With more recent CO and PIV data being acquired by J.Frank in the V-flame experiment at the CRF, we plan further detailed comparisons between experimental and numerical flame-vortex-pair interactions. Specifically, with PIV data, we will have a much improved characterization of the shape of the vorticity field of the vortex pair and of the strain-rate field in the vicinity of the flame. This will allow computations with an improved approximation of the experimental flowfield. At the same time, we plan to selectively modify the above-reported OH and CH reactions, and to examine more recent methane-flame kinetic mechanisms, all in an effort to improve our prediction and understanding of transient hydrocarbon flame response in vortical flow.

We will also study the structure of the flame edge at the base of the lifted non-premixed jet flame using detailed kinetics. Of interest is the internal structure of the edge flame with different fuels and flow conditions, and its stabilization against incoming vortex structures. Access to massively parallel hardware will enable these AMR computations to span experimentaly relevant time scales of flame and flow evolution on laboratory-scale jet flame length scales.

DOE Supported Publications

1. Najm, H.N., Paul, P.H., Knio, O.M., and McIlroy, A., "A Numerical and Experimental Investigation of Premixed Methane-Air Flame Transient Response", *Combustion and Flame*, 125/1-2, pp. 879-892, 2001.
2. Knio, O.M. and Najm, H.N., "Effect of Stoichiometry and Strain-Rate on Transient Flame Response", *Proc. Comb. Inst.*, 28, 2000.
3. Ray, J., Najm, H.N., Milne, R.B., Devine, K.D., Kempka, S.N., "Triple Flame Structure and Dynamics at the Stabilization Point of an Unsteady Lifted Jet Diffusion Flame", *Proc. Comb. Inst.*, 28, 2000.
4. Marzouk, Y.M., Ghoniem, A.F., and Najm, H.N., "Dynamic Response of Strained Premixed Flames to Equivalence Ratio Gradients", *Proc. Comb. Inst.*, 28, 2000.
5. Ashurst, Wm.T., Najm, H.N., and Paul, P.H., "Chemical Reaction and Diffusion: a Comparison of Molecular Dynamics Simulations with Continuum Solutions", *Combustion Theory and Modeling*, 4, pp. 139-157, (2000).
6. Najm, H.N., Knio, O.M., Paul, P.H., and Wyckoff, P.S., "Response of Stoichiometric and Rich Methane-Air Flames to Unsteady Strain-Rate and Curvature", *Combustion Theory and Modelling*, 3, no. 4, pp. 709-726, (1999).
7. Knio, O.M., Najm, H.N., and Wyckoff, P.S., "A Semi-Implicit Numerical Scheme for Reacting Flow. II. Stiff Operator-Split Formulation", *J. Comput. Phys.*, 154, pp. 428-467, (1999).
8. Najm, H.N., Azoury, P.H., and Piasecki, M., "Hydraulic Ram Analysis: A New Look at an Old Problem". *J. Power and Energy, Proc. Inst. Mech. Eng. A*, 213(A2), pp. 127-141, (1999).
9. Najm, H.N., Milne, R.B., Devine, K.D., and Kempka, S.N., "A Coupled Lagrangian-Eulerian Scheme for Reacting Flow Modeling", ESAIM Proc., 7, pp. 304-313, (1999).

Free Radical Chemistry and Photochemistry

Daniel M. Neumark
Chemical Sciences Division
Lawrence Berkeley National Laboratory
Berkeley, CA 94720

This research program is aimed at elucidating the photodissociation dynamics and bimolecular chemistry of free radicals and hydrocarbons. Particular emphasis is placed on radicals that play a role in combustion chemistry. Our experiments yield primary chemistry and photochemistry, bond dissociation energies, heats of formation, and excited state dynamics.

Although much time and effort has been invested in modeling combustion chemistry, many of the primary processes involved in combustion are poorly understood. As a result, one has a situation where sophisticated kinetics models stand on a weak foundation, because the primary chemistry of the reactions in the models and the thermochemistry of the species involved in these reactions are not known. Examples include the reactions leading to soot formation in flames, and reactions in which NO is produced as a by-product of combustion. Our program is focused on fundamental studies of species and reactions relevant to combustion chemistry. We have developed a state-of-the-art instrument for studying the photodissociation dynamics of free radicals. In addition, a crossed molecular/laser beam instrument is used to investigate the primary chemistry and photochemistry of both closed-shell hydrocarbons and hydrocarbon radicals.

Three instruments are used in these studies: a fast radical beam photofragment translational spectrometer, in which radicals are generated by photodetachment of mass-selected negative ions, and two neutral beam instruments, one with electron impact ionization of products and the other (at the Advanced Light Source) with tunable vacuum ultraviolet.

Key results obtained last year are summarized below:

Photodissociation of linear carbon clusters: The photodissociation of mass-selected linear carbon clusters (C_n, n = 4 – 6) was studied using fast beam photofragment translational spectroscopy. The photofragment yield (PFY) spectra consist of several continua spanning the whole visible and ultraviolet region. The product mass distributions for dissociation of C_n clusters are dominated by C_3 and its partner fragment C_{n-3}, although some minor channels are also identified for dissociation of C_4 and C_5 clusters. Translational energy $P(E_T)$ distributions for the $C_3 + C_{n-3}$ channel were measured at several photolysis energies. The PFY spectra and $P(E_T)$ distributions indicate that multi-photon dissociation occurs at photon energies below the dissociation threshold, and that both single- and multi-photon dissociation occur above the threshold. The one-photon components of the $P(E_T)$ distributions can be modeled by phase space theory (PST), suggesting that photoexcitation is followed by internal conversion to the ground state. The PST analysis yields dissociation energies for $C_n \rightarrow C_n + C_{n-3}$ in reasonable agreement with recent Knudsen effusion mass spectrometry measurements.

Photodissociation Dynamics of the Ethoxy Radical (C_2H_5O): Photodissociation of the ethoxy (C_2H_5O) radical was investigated using photofragment translational spectroscopy. The ethoxy radical is generated by photodetachment of $C_2H_5O^-$ and subsequently

dissociated by photon absorption in the range of 270-220 nm; no dissociation is seen at higher wavelengths. The photofragment yield (PFY) spectrum is structureless, but exhibits abrupt increases in intensity at 260 and 225 nm. The product mass distribution shows that C_2H_5O dissociates into vinyl radical (C_2H_3) and H_2O throughout the entire absorption band. We propose that these products are formed by isomerization and dissociation on electronically excited surfaces rather than by internal conversion to the ground state. The translational energy $P(E_T)$ distributions for this channel are largely insensitive to photon energy. However, at the two highest photon energies (5.51 and 5.96eV), a new feature appears at $E_T \leq 0.3$eV which is assigned as production of an excited state of C_2H_3.

Photodissociation dynamics of the CNN free radical: The spectroscopy and photodissociation dynamics of the $\tilde{A}\,^3\Pi$ and $\tilde{B}\,^3\Sigma^-$ states of the CNN radical were investigated by fast beam photofragment translational spectroscopy. Vibronic transitions located more than 1000 cm^{-1} above the $\tilde{A}\,^3\Pi \leftarrow \tilde{X}\,^3\Sigma^-$ origin were found to predissociate. Photofragment yield spectra for the $\tilde{B}\,^3\Sigma^- \leftarrow \tilde{X}\,^3\Sigma^-$ band between 40800 and 45460 cm^{-1} display resolved vibrational progressions with peak spacing of $\approx$ 1000 cm^{-1} corresponding to symmetric stretch 1_0^n and combination band $1_0^n 3_0^1$ progressions. Ground state products $C(^3P) + N_2$ were found to be the major photodissociation channel for both the $\tilde{A}\,^3\Pi$ and $\tilde{B}\,^3\Sigma^-$ states. The translational energy distributions for the $\tilde{A}\,^3\Pi$ state are bimodal with high and low translational energy components. The distributions for the $\tilde{B}\,^3\Sigma^-$ state reveal partially resolved vibrational structure for the N_2 photofragment and indicate extensive vibrational and rotational excitation of this fragment. These results suggest that bent geometries are involved in the dissociation mechanism and provide more accurate values: $\Delta_f H_0(CNN) = 6.16 \pm 0.05$ eV and $\Delta_f H_{298}(CNN) = 6.15 \pm 0.05$ eV.

Photoisomerization and photodissociation pathways of the HNCN free radical: The photodissociation spectroscopy and dynamics of the HNCN free radical have been investigated by fast beam photofragment translational spectroscopy. Predissociative transitions for both the $\tilde{B}^2A' \leftarrow \tilde{X}^2A''$ band and a higher energy band system assigned to the $\tilde{C}^2A'' \leftarrow \tilde{X}^2A''$ band were observed. Photofragment mass distributions indicate that N_2 loss is the primary dissociation pathway. Translational energy distributions reveal resolved vibrational structure of the N_2 fragment, suggesting that the HNCN radical first isomerizes to a cyclic-HCN_2 intermediate. A dissociation mechanism is proposed in which electronically excited HNCN undergoes internal conversion to the ground state, followed by isomerization to cyclic HCN_2 and dissociation through a tight three-center transition state. The HNCN bond dissociation energy D_0 and heat of formation $\Delta_f H_0(HNCN)$ were determined to be 2.80 ± 0.03 eV and 3.35 ± 0.03 eV respectively. Our results imply that the HNCN radical is accessed in the $CH + N_2$ reaction and support a recent proposal that this reaction does not lead the $N(^4S) + HCN$ production, as had previously been assumed in models of prompt NO formation (through oxidation of $N(^4S)$) in combustion.

State-resolved translation energy distributions for NCO photodissociation: The photodissociation dynamics of NCO have been examined using fast beam photofragment translational spectroscopy. Excitation of the 1_0^2, 3_0^1, and $1_0^2 3_0^2$ transitions of the $\tilde{B}\,^2\Pi \leftarrow \tilde{X}\,^2\Pi$ band produces $N(^4S) + CO$ photofragments exclusively, while excitation of the $1_0^3 3_0^3$ transition yields primarily $N(^2D) + CO$ photoproducts. The translational energy

($P(E_T)$) distributions yield D_0(N-CO) = 2.34±0.03 eV, and $\Delta H^0_{f,0}$(NCO) = 1.36±0.03 eV. The $P(E_T)$ distributions exhibit vibrationally resolved structure reflecting the vibrational and rotational distributions of the CO product. The $N(^2D)$ + CO distribution can be fit by phase space theory (PST), while the higher degree of CO rotational excitation for $N(^4S)$ + CO products implies that NCO passes through a bent geometry upon dissociation. The $P(E_T)$ distributions suggest that when the $\tilde{B}\ ^2\Pi \leftarrow \tilde{X}\ ^2\Pi$ band is excited, NCO undergoes internal conversion to its ground electronic state prior to dissociation. Excitation of NCO at 193 nm clearly leads to the production of $N(^2D)$ + CO fragments. While conclusive evidence for the higher energy $O(^3P)$ + $CN(X\,^2\Sigma^+)$ channel was not observed, the presence of this dissociation pathway could not be excluded.

Photodissociation of C_4H_6 isomers: The photodissociation dynamics of 1,3-butadiene, 1,2-butadiene, and 2-butyne at 193 nm have been investigated on two instruments: endstation 1 at the Advanced Light Source, where scattered photoproducts are detected via vacuum ultraviolet (VUV) ionization, and a more traditional crossed beams instrument employing electron impact ionization. These experiments have yielded information on the primary dissociation products and pathways. Five dissociation channels from 1,3-butadiene are seen: H + C_4H_5, H_2 + C_4H_4, CH_3 + C_3H_3, C_2H_2 + C_2H_4, and C_2H_3 + C_2H_3. Translational energy $P(E_T)$ distributions indicate exit barriers for those channels in which closed-shell molecular products are formed, and no barriers for channels in which two radicals are formed. These results suggest that dissociation occurs on the ground state potential energy surface rather than on one or more excited states. The photochemistry of 1,2-butadiene and 2-butyne is considerably simpler, with only H and CH_3 elimination observed. The $P(E_T)$ distributions are again consistent with ground state dissociation.

Future plans:

Our previous studies of the NCN, CNN, and HNCN radicals were motivated by their possible role in the cleavage of N_2 to form N atoms through reactions such as

$$CH + N_2 \rightarrow HCN + N(^4S).$$

Reactions of this type have been assumed to play a role in prompt NO formation in combustions, because the N atoms are readily oxidized by O_2 to form NO + O. However, recent theoretical evidence and our own work on HNCN photodissociation suggests that N + HCN is not a major product of the above reaction, and that the mechanism for prompt NO formation may need revisiting. We plan to attack this problem on two fronts. First, photodissociation experiments on another isomer, HCNN, will be carried out on the fast radical beam instrument. This can be generated selectively by photodetachment of the $HCNN^-$ anion, just as HNCN can be generated by photodetachment of $HNCN^-$. The proposed experiments will probe a region of the CH + N_2 potential energy surface not accessible by photoexcitation of HNCN. If electronically excited HCNN undergoes internal conversion to the ground state before any dissociation or isomerization occurs, one would expect barrierless dissociation to CH + N_2, and our experiment will test if this mechanism or more complex dynamics actually occurs.

A major overhaul of the detection scheme on the fast radical instrument is planned. The current detector based on a dual wedge-and-strip anode provides time- and position-sensitive measurements for two photofragments. It cannot, however, be used if three fragments are produced from either a single or multiple photodissociation events, and its collection efficiency is low for slow photofragments. These problems will be

solved with a new design, in which a CCD camera is used to record the positions of all photofragments with high precision, and a photomultiplier tube with a segmented anode records their arrival times. By correlating the two measurements after each laser shot one obtains position and time information for all photofragments. This detector concept has been developed and used on several ion storage ring experiments in Europe and holds considerable promise for our radical photodissociation experiment.

The radical photodissociation work on the fast radical instrument will be complemented by photodissociation and crossed beam studies of radicals on the neutral molecular instruments in our laboratory and at the ALS. We have constructed a pyrolysis source for free radicals and intend to use it to generate hydrocarbon species such as phenyl and vinyl radicals for initial experiments. Plans for a photolysis source are also underway. We are particularly interested in generating the CH radical, possibly by photolysis of $CHBr_2Cl$ at 248 nm, so that we can study the bimolecular reactions of CH and directly ascertain the identity of the products.

R. T. Bise, H. Choi, H. B. Pedersen, D. H. Mordaunt and D. M. Neumark, "Photodissociation spectroscopy and dynamics of the methylthio radical (CH_3S)," J. Chem Phys. 110, 805, (1999).

W. Sun, K. Yokoyama, J. Robinson, A. Suits and D. M. Neumark, "Discrimination of product isomers in the photodissociation of propyne and allene at 193mm," J. Chem. Phys. 110, 4363, (1999).

R. T. Bise, H. S. Choi, and D. M. Neumark, "Photodissociation dynamics of singlet and triplet states of the NCN radical," J. Chem. Phys. 111, 4923, (1999).

H. Choi, R. T. Bise, A. A. Hoops, D. H. Mordaunt, D. M. Neumark, "Photodissociation of Linear Carbon Clusters C_n (n=4-6)," J. Phys. Chem. A 104, 2025, (2000).

H. Choi, R. T. Bise, A. A. Hoops, D. M. Neumark, "Photodissociation dynamics of the triiodide anion (I_3^-)". J. Chem. Phys. 113, 2255, (2000).

R.T. Bise, A. A. Hoops, H. Choi, D. M. Neumark, "Photodissociation dynamics of the CNN free radical". J. Chem. Phys. 113, 4179, (2000).

H. Choi, T. R. Taylor, R. T. Bise, A. A. Hoops, D. M. Neumark, "Excited states and photodissociation dynamics of the triiodine radical (I_3)". J. Chem. Phys. 113, 8606, (2000).

H. Choi, R. T. Bise, D. M. Neumark, "Photodissociation dynamics of the ethoxy radical (C_2H_5O)". J. Phys. Chem. A 104, 10112, (2000).

R. T. Bise, A. A. Hoops, H. Choi, D. M. Neumark, "Photoisomerization and photodissociation dynamics of the NCN, CNN and HNCN free radicals". ACS Symposium Series 770 296, (2001).

R. T. Bise, A. A. Hoops, D.M. Neumark, "Photodissociation and photoisomerization pathways of the HNCN free radical" (In press, J. Chem. Phys.)

A. A. Hoops, R. T. Bise, J. R. Gascooke, D. M. Neumark, "State-resolved translation energy distributions for NCO photodissociation" (In press, J. Chem. Phys.)

Dissociation Dynamics of High-n (n≥100) Rydberg Molecules near Their Dissociation Thresholds

C. Y. Ng

Ames Laboratory, USDOE and Department of Chemistry
Iowa State University, Ames, Iowa 50011

The recent successful implementation of pulsed field ionization (PFI) schemes[1-3] using the high-resolution vacuum ultraviolet (VUV) synchrotron radiation at the Chemical Dynamics Beamline of the Advanced Light Source has made possible the routine examination of molecular dissociative photoionization processes employing the PFI-photoelectron (PFI-PE)-photoion coincidence (PFI-PEPICO)[3] technique. Using this method, we have accurately determined the 0 K dissociation threshold or appearance energy (AE) for CH_3^+ (C_2H^+) from CH_4 (C_2H_2). Recently, we have discovered a sharp step-like feature at the 0 K AE in the PFI-PE spectrum for CH_4 (C_2H_2).[4] This observation suggests that the formation of CH_3^+ (C_2H^+) from CH_4 (C_2H_2) in PFI proceeds via processes 1(a), 1(b), and 1(d) at energies slightly above the AE, while CH_4^+ ($C_2H_2^+$) ions are produced by processes 1(a) and 1(c) below the AE.

$$\begin{array}{lcccc} & \overset{(a)}{} & & \overset{(b)}{} & \\ CH_4\,(C_2H_2) + h\nu & \longrightarrow & CH_4^*\,(C_2H_2^*) & \longrightarrow & CH_3^*\,(C_2H^*) + H \\ & & \downarrow\ (c) & & \downarrow\ (d) \\ & & CH_4^{+}{}^*\,(C_2H_2^{+}{}^*) + e^- & & CH_3^+\,(C_2H^+) + e^- \end{array} \qquad (1)$$

Here, CH_4^* ($C_2H_2^*$) and CH_3^* (C_2H^*) represent excited CH_4 (C_2H_2) and CH_3 (C_2H), respectively, in long-lived high-n (n≥100) Rydberg states and $CH_4^{+}{}^*$ ($C_2H_2^{+}{}^*$) stands for excited CH_4^+ ($C_2H_2^+$). Processes 1(c) and 1(d) are PFI processes. This mechanism indicates that CH_4^* ($C_2H_2^*$) fragments into CH_3^* + H (C_2H^* + H) at energies above the AE prior to PFI.

The dominant decay channels for CH_4^* ($C_2H_2^*$) formed by the VUV excitation process 1(a) are autoionization and fragmentation. At energies below the AE for CH_3^+ (C_2H^+), the PFI-PE signal is due to process 1(c) and is proportional to the concentration of CH_4^* ($C_2H_2^*$) species that have survived the decay for a time longer than the delay (Δt) of the PFI pulse relative to the excitation light pulse, which is estimated to be in the range of 20-552 ns. The CH_3^* (C_2H^*) species formed at the AE are expected to be in high-n Rydberg levels converging to the ground state of CH_3^+ (C_2H^+), i.e., below the IE of CH_3 (C_2H). Consequently, autoionization is not accessible to these CH_3^* (C_2H^*) fragments. The CH_3^* (C_2H^*) fragments produced at energies slightly above the AE can only autoionize by rotational autoionization. The latter process is expected to be slower than vibrational and electronic autoionization for the case of CH_4^* ($C_2H_2^*$), which lies well above the IE of CH_4 (C_2H_2). Assuming that the decay rates via fragmentation for CH_4^* ($C_2H_2^*$) and CH_3^* (C_2H^*) are similar, we expect that a larger fraction of CH_3^* (C_2H^*) survives the decay than that of CH_4^* ($C_2H_2^*$). Thus, the PFI-PE signal derived from process 1(d) slightly above the AE is higher than that obtained from process 1(c) below the AE. The step marking the 0 K AE in the PFI-PE spectrum can thus be attributed to the *lifetime switching* effect at the AE, where CH_4^* ($C_2H_2^*$) species with shorter lifetimes are converted into CH_3^* (C_2H^*) fragments with longer lifetimes. The observation of the sharp steplike feature in the PFI-PE spectrum is consistent with the conclusion that the conversion from CH_4^* ($C_2H_2^*$) to CH_3^* (C_2H^*) is complete prior to process 1(d) and that the dissociation process has a rate constant >> $1/\Delta t$ ($\approx 10^7$ s^{-1}). The observation of a sharp step at the 0 K AE in the PFI-PE spectrum is a sufficient condition for observing sharp breakdown curves.

For a slow dissociation reaction that the dissociation lifetimes for excited high-n Rydberg species for parent species are longer than Δt, the PFI-PE signal should originate entirely from PFI of excited parent species at energies both below and above the AE. Hence, the PFI-PE spectrum should be smooth across the AE. However, if excited parent ions thus formed completely dissociate within the time scale of the PFI-PEPICO experiment ($\approx 10^{-5}$ s), we still expect to observe complete dissociation at the AE, such that the disappearance energy of the parent ion can still be used to identify of the 0 K AE. This can be considered as an intermediate case, in which the 0 K AE can be determined in a PFI-PEPICO experiment, but not in a PFI-PE study.

According to a previous coincidence study, the reaction $C_2H_4 + h\nu \rightarrow C_2H_2^+ + H_2 + e^-$ has dissociation rates of 10^3-10^5 s^{-1} near its 0 K AE (13.135 eV). Thus, the dissociation lifetime of excited $C_2H_4^{+*}$ formed at the AE should be significantly longer than the time scale of the PFI-PEPICO experiment. As expected, slow varying breakdown curves were observed for $C_2H_4^+$ and $C_2H_2^+$, which are consistent with a metastable decay for parent $C_2H_4^{+*}$ ions. Furthermore, the PFI-PE spectrum for C_2H_4 is found to be smooth across the 0 K AE for $C_2H_2^+$.

For diatomic and triatomic species that have a lower density of states, a discrete peak instead of a step should be discernible at the 0 K AE in the PFI-PE spectrum. The step observed in PFI-PE measurements, together with the breakdown curves obtained in PFI-PEPICO studies, can provide unambiguous 0 K AE values for the dissociation reactions involved, which in turn can yield highly accurate energetic information for simple neutrals and cations.

References:

1. C.-W. Hsu, M. Evans, C. Y. Ng, and P. Heimann, *Rev. Sci. Instrum.* **68**, 1694 (1997).
2. G. K. Jarvis, Y. Song, and C. Y. Ng, *Rev. Sci. Instrum.***70**, 2615 (1999).
3. G. K. Jarvis, K.-M. Weitzel, M. Malow, T. Baer, Y. Song, and C. Y. Ng, *Rev. Sci. Instrum.* **70**, 3892-3906 (1999).
4. K.-M. Weitzel, G. Jarvis, M. Malow, Y. T. Baer, Song, and C. Y. Ng, *Phys. Rev. Lett.* **86**, 3526 (2001).

Publications of DOE sponsored research (1999-present)

1. Y.-S. Cheung and C. Y. Ng, "Vacuum Ultraviolet Single-Photon and Ultraviolet Non-Resonant Two-Photon Pulsed Field Ionization Photoelectron Study of CH_3SCH_3", (invited article) *Int. J. Mass Spectrom Ion Proc.* **185/186/187**, 533 (1999).
2. M. Evans, S. Stimson, C. Y. Ng, C.-W. Hsu, and G. K. Jarvis, "Rotationally Resolved Photoelectron study of $O_2^+(B^2\Sigma_g^-, {}^2\Sigma_u^-; v^+=0\text{-}7)$ at 20.2-21.3 eV", *J. Chem. Phys.***110**, 315 (1999).
3. S.-W. Chiu, Y.-S. Cheung, N. L. Ma, W.-K. Li, and C. Y. Ng, "A Gaussian-2 *ab initio* study of $[C_2H_5S]^+$ ions: II. Fragmentation pathways of $CH_3SCH_2^+$ and $CH_2CHSH_2^+$ revisited", *J. Mol. Struct. (TheoChem.)* **468**, 21-37 (1999).
4. R. C. Shiell, M. Evans, S. Stimson, C.-W. Hsu, C. Y. Ng, and J. W. Hepburn, "Characterization of Correlation Satellites Below 25 eV in Xenon Probed by Pulsed Field Ionization Photoelectron Spectroscopy", *Phys. Rev. A.***59**, 2903 (1999).
5. L.-S. Sheng, S.-Q. Yu, and C. Y. Ng, "Recent Advances in High Resolution Photoelectron Studies Using Synchrotron Radiation and Lasers", *Progress in Chemistry"* (A Review Journal in Chinese), **11**, 153 (1999).
6. K.-C. Lau, W.-K. Li, C. Y. Ng, and S. W. Chiu, "A Gaussian-2 Study of Isomeric $C_2H_2N/C_2H_2N^+$", *J. Phys. Chem.* **103**, 3330 (1999).
7. G. K. Jarvis, Y. Song, and C. Y. Ng, "High resolution pulsed field ionization photoelectron spectroscopy using multi-bunch synchrotron radiation: time-of-flight selection scheme", *Rev. Sci. Instrum.***70**, 2615 (1999).

8. G. K. Jarvis, Y. Song, and C. Y. Ng, "Rotational-Resolved Pulsed Field Ionization Photoelectron Study of $NO^+(a^3\Sigma^+, v^+ = 0\text{-}16)$ in the energy range of 15.6-18.2 eV", *J. Chem. Phys.* **111**, 1937 (1999).
9. Y. Song, M. Evans, C. Y. Ng, C.-W. Hsu, and G. K. Jarvis, "Pulsed Field Ionization Photoelectron Spectroscopy: Rotationally Resolved Photoelectron Bands for $O_2^+(X^2\Pi_{3/2,1/2}, v^+=0\text{-}38)$, *J. Chem. Phys.* **111**, 1905 (1999).
10. G. K. Jarvis, M. Evans, C. Y. Ng, and K Mitsuke, "Rotational-Resolved Pulsed Field Ionization Photoelectron Study of $NO^+(X^1\Sigma^+, v^+ = 0\text{-}32)$ in the energy range of 9.24-16.80 eV", *J. Chem. Phys.***111**, 3058 (1999).
11. G. K. Jarvis, K.-M. Weitzel, M. Malow, T. Baer, Y. Song, and C. Y. Ng, "High Resolution Pulsed Field Ionization Photoelectron-Photoion Coincidence Spectroscopy Using Synchrotron Radiation", *Rev. Sci. Instrum.* **70**, 3892-3906 (1999).
12. D. Fedorov, M. Evans, Y. Song, M. Gordon, and C. Y. Ng, "An Experimental and Theoretical Study of the Spin-Orbit Interaction for $CO^+(A^2\Pi_{3/2,1/2}, v^+=0\text{-}41)$ and $O_2^+(X^2\Pi_{3/2,1/2g}, v^+=0\text{-}38)$", *J. Chem. Phys.* **111**, 6413-6421 (1999).
13. S.-W. Chiu, Kai-Chung Lau, W.-K. Li, N. L. Ma, Y.-S. Cheung, and C. Y. Ng, "A Gaussian-2 *ab initio* study of $[C_2H_5S]^+$ ions: III. H_2 and CH_4 Eliminations from $CH_3SCH_2^+$ and $CH_2CHSH_2^+$", *J. Mol. Struct. (TheoChem.)*, **490**, 109-124 (1999).
14. D. S. Peterka, M. Ahmed, C. Y. Ng, and A. G. Suits, "Dissociative Ionization by Ion Imaging with Undulator Synchrotron Radiation: Dissociation Dynamics of SF_6^+", *Chem. Phys. Lett.* **312**, 108 (1999).
15. S.-H. Chien, K.-C. Lau, W.-K. Li and C.Y. Ng, "Energetics and Structure of the Carbonyl Chloride Radical and Oxalyl Chloride", *J. Phys. Chem.* **103**, 7913-7922 (1999).
16. C. Y. Ng, "Advances in Photoionization and Photoelectron Studies Using Third Generation Synchrotron Radiation", Proceedings for the IV International Meeting in Dissociative Recombination", June 15-20, Stockholm, Sweden (World Scientific, Singapore, 1999).
17. K.-M. Weitzel, M. Malow, G. K. Jarvis, T. Baer, Y. Song, and C. Y. Ng, "High-Resolution Pulsed Field Ionization Photoelectron Photoion Coincidence Study of CH_4: Accurate 0 K Dissociation Threshold for CH_3^+ ", *J. Chem. Phys. (Communication)* **111**, 8267-8270 (1999).
18. M. Evans and C. Y. Ng, "Rotational-Resolved Pulsed Field Ionization Photoelectron Bands for $CO^+(X, v^+=0\text{-}42)$", *J. Chem. Phys.* **111**, 8879-8892 (1999).
19. G. K. Jarvis, Y. Song, C. Y. Ng, and E. R. Grant, "A Characterization of Vibrationally Excited NO_2^+ by High-Resolution Threshold Photoionization Spectroscopy", *J. Chem. Phys.***111**, 9568-9573 (1999).
20. R. C. Shiell, M. Evans, C. Y. Ng, and J. W. Hepburn, "A High Resolution Study of the $D^2\Pi$ and $3^2\Sigma^+$ Satellite States of CO^+", *Chem. Phys. Lett.* **315**, 390-396 (1999).
21. G. K. Jarvis, K.-M. Weitzel, M. Malow, T. Baer, Y. Song, and C. Y. Ng, "High-Resolution Pulsed Field Ionization Photoelectron Photoion Coincidence Study of C_2H_2: Accurate 0 K Dissociation Threshold for C_2H^+", *Phys. Chem. Chem. Phys. (Communication),* **1**, 5259 (1999).
22. C. Y. Ng, "Advances in photoionization and photoelectron studies using third generation synchrotron radiation and UV/VUV lasers", in "Photoionization, and Photodetachment", edited by C. Y. Ng (World Scientific, Singapore, 2000), *Adv. Ser Phys. Chem.* **10A**, Chapter 9, p.394-538.
23. C. Y. Ng, editor, "Photoionization and Photodetachment I" (World Scientific, Singapore, 2000), *Adv. Ser Phys. Chem.*, Vol. **10A**, 713 pages.
24. C. Y. Ng, editor "Photoionization and Photodetachment II" (World Scientific, Singapore, 2000), *Adv. Ser Phys. Chem.*, Vol. **10B**, 664 pages.
25. Y. Song, M. Evans, C. Y. Ng, C.-W. Hsu, and G. K. Jarvis, "Rotational-Resolved Pulsed Field Ionization Photoelectron Study of $O_2^+(A^2\Pi_u, v^+=0\text{-}12)$ in the Energy Range of 17.0-18.2 eV, *J. Chem. Phys.* **112**, 1271-1278 (2000).

26. Y. Song, M. Evans, C. Y. Ng, C.-W. Hsu, and G. K. Jarvis, "Rotationally Resolved Pulsed Field Ionization Photoelectron Study of $O_2^+(a^4\Pi_u, v^+=0\text{-}18)$ in the Energy Range of 16.0-18.0 eV, *J. Chem. Phys.* **112**, 1306-1315 (2000).
27. T. Baer, Y. Song, C. Y. Ng, J. Liu, and W. Chen, "High-Resolution PFI-PEPICO Studies of Ionic Dissociation at the Advanced Light Source", *Faraday Discussion* **115**, 137-145 (2000).
28. A. Yencha, M. C. A. Lopes, G. C. King, M. Hochlaf, Y. Song, and C. Y. Ng, "Ion-Pair Formation Observed in a Pulsed-Field Ionization Photoelectron Spectroscopic Study of HF", *Faraday Discussion* **115**, 355-362 (2000).
29. G. K. Jarvis, R. C. Shiell, J. Hepburn, Y. Song, and C. Y. Ng, "Pulsed Field Ionization-Photoion Spectroscopy Using two-bunch Synchrotron Radiation: Time-of-Flight Selection Scheme", *Rev. Sci. Instrum.***71**, 1325 (2000).
30. C. Y. Ng, "Advances in Photoionization and Photoelectron Studies Using Third Generation Synchrotron Radiation", *J. Electron Spectroscopy & Related Phenomena*, **108**, 41-45 (2000).
31. T. Baer, Y. Song, C. Y. Ng, W. Chen, and J. Liu, "The Heat of Formation of $C_3H_7^+$ and Proton Affinity of C_3H_6 Determined by Pulsed Field Ionization-Photoelectron Photoion Coincidence Spectroscopy", *J. Phys. Chem.* **104**, 1959 (2000).
32. K.-C. Lau, W.-K. Li, C. Y. Ng, H. Baumgärtel, and K.-M. Weitzel, "Gaussian-2 and Gaussian-3 Study of the Energetics and Structure of Cl_2O_n and $Cl_2O_n^+$, n=1-7", *J. Phys Chem.* **104**, 3197 (2000).
33. Jianbo Lau, Wenwu Chen, C.-W. Hsu, M. Hochlaf, M. Evans, S. Stimson, and C. Y. Ng, "High-Resolution Pulsed Field Ionization-Photoelectron Study of $CO_2^+(X^2\Pi_g)$ in the energy range of 13.6-14.7 eV", *J. Chem. Phys.***112**, 10767 (2000).
34. H. Lefebvre-Brion and C. Y. Ng, "Pulsed Field Ionization Photoelectron Spectrum for $CO^+(A^2\Pi_u, v^+=1)$", *Chem. Phys. Lett.* **327**, 404-408 (2000).
35. C. Y. Ng, "Pulsed Field Ionization Photoelectron-Photoion Spectroscopy: Determination of Accurate Bond Dissociation Energies for Neutrals and Cations", *J. Electron Spectroscopy & Related Phenomena* (invited article), **112**, 31-46 2000).
36. Jianbo Liu, M. Hochlaf, and C. Y. Ng, "Pulsed Field Ionization-Photoelectron Bands of $CO_2^+(A^2\Pi_u$ and $B^2\Sigma_u^+)$: An Experimental and Theoretical Study", *J. Chem. Phys.* **113**, 7988 (2000).
37. C. Y. Ng, "Vacuum Ultraviolet Photoionization and Photoelectron Studies in the New Millennium: Recent Developments and Applications", *Int. J. Mass Spectrometry*, special issue for year 2000 (invited article), **200**, 357-386 (2000).
38. Jianbo Liu, M. Hochlaf, G. Chambaud, P. Rosmus, and C. Y. Ng, "High Resolution Pulsed Field Ionization-Photoelectron Bands for $CS_2^+(A^2\Pi_u)$: An Experimental and Theoretical Study", *J. Phys. Chem.*, in press.
39. K.-M. Weitzel, G. Jarvis, M. Malow, Y. T. Baer, Song, and C. Y. Ng, "Observation of Accurate Ion Dissociation Thresholds in Pulsed Field Ionization Photoelectron Studies", *Phys. Rev. Lett.* **86**, 3526 (2001).

KINETICS AND DYNAMICS OF COMBUSTION CHEMISTRY

David L. Osborn
Combustion Research Facility, Mail Stop 9055
Sandia National Laboratories
Livermore, CA 94551-0969
Telephone: (925) 294-4622
Email: dlosbor@sandia.gov

Program Scope

The goal of this program is to elucidate mechanisms of elementary combustion reactions through the use of absorption and emission-based spectroscopy. The main technique employed is time-resolved Fourier transform spectroscopy (TR-FTS) to probe multiple reactants and products with broad spectral coverage (> 1000 cm^{-1}), moderate spectral resolution (0.1 cm^{-1}) and a wide range of temporal resolution (ns – ms). In addition to the measurement of thermal rate coefficients as a function of temperature and pressure, the inherently multiplexed nature of TR-FTS makes is possible to simultaneously measure product branching ratios, internal energy distributions, energy transfer, and spectroscopy of radical intermediates. Together with total rate coefficients, this additional information provides further constraints upon and insights into the potential energy surfaces that control chemical reactivity.

For reactions producing vibrationally or electronically excited molecules, emission-based TR-FTS may be used to study product state distributions, energy transfer kinetics, and product branching ratios. While several groups have made great progress in gas phase emission-based TR-FTS,[1-7] there is little work in absorption.[8] Absorption techniques are also being pursued in this program because they are more general than emission methods, and are not complicated by fluorescence lifetime effects or predissociation. Another thrust of this program is toward kinetic measurements of larger molecules. The development of absorption-based TR-FTS in the mid-infrared "fingerprint" region will enable reactivity studies of larger hydrocarbons (C3 – C6) found in practical fuels. Fourier transform spectroscopy offers well-known throughput and multiplex advantages over dispersive instruments when used in the infrared. Finally, the broad-band spectral detection offered by FTS can allow the identification of unexpected product channels that might go unnoticed by narrow-band detection techniques.

Recent Progress

During the last year, several improvements were made to the time-resolved Fourier transform spectrometer. The addition of multipass optics has increased sensitivity of emission collection by more than an order of magnitude. A high-repetition rate excimer laser was added to increase data collection rates, and vibration isolation has been improved to reduce technical noise in both absorption and emission experiments.

C_3H_5—cyclopropyl and allyl radicals

Isomerization is critically important in combustion chemistry. The height of isomerization barriers and the relative reactivity of different isomers are important parameters in combustion models. For example, the cyclopropyl radical (c-C_3H_5) can ring open to the allyl radical (CH_2CHCH_2) over a (calculated) 23 kcal/mol barrier, with an exothermicity of 31 kcal/mol. Due to resonance stabilization, the allyl radical reacts very slowly with O_2 and closed-

shell species, while the cyclopropyl radical is expected to react with O_2 at a rate similar to other alkyl radicals.

Spectroscopic measurements of c-C_3H_5 are scarce.[9,10] At the Combustion Research Facility, photoelectron spectra were acquired in a femtosecond pump-probe arrangement, in which the pump pulse dissociates allyl iodide or cyclopropyl iodide, while the probe pulse ejects an electron that is energy analyzed.[11] While the allyl photoelectron spectrum (from allyl iodide) is consistent with the literature, no spectrum from the dissociated precursor was observed when c-C_3H_5I was used. Arnold and Carpenter[12] predict that ring opening occurs in a concerted process with C-I bond fission in the photodissociation of c-C_3H_5I, such that c-C_3H_5 will not be produced from photolysis of cyclopropyl halides. To find an alternative photolytic source of c-C_3H_5 for both kinetics and dynamics experiments, we have investigated the photodissociation of dicyclopropyl ketone.

Dicyclopropyl ketone ($C_3H_5COC_3H_5$, or DCPK) is a symmetric ketone analogous to acetone and diethyl ketone. When excited to the S_2 state at 193 nm, acetone undergoes ISC to the T_1 surface followed by dissociation over a barrier to produce CH_3 + CH_3CO.[13] Internal conversion to S_0 is not believed to be important. Secondary dissociation of CH_3CO to CH_3 + CO also occurs over a barrier, with a total quantum yield for CH_3 $\phi > 1.9$.[14] The total energy available to the products (CH_3 + CH_3 + CO) is 53 kcal/mol. The translational energy in both bond-breaking events peaks away from $E_T = 0$, consistent with dissociation over a potential energy barrier. The CO vibrational and rotational distributions are hotter than predicted by statistical models.[15,16]

For the case of DCPK, we have performed B3LYP DFT calculations to characterize stationary points on the PES, benchmarking against acetone calculations at the same level of theory. The calculations demonstrate several differences between acetone and DCPK. In DCPK, photodissociation at 193 nm to CO + 2(c-C_3H_5) leaves only 35 kcal/mol available energy (much less than in acetone). Substantial electron delocalization in the π-orbitals of the cyclopropyl ring creates conjugation with the carbonyl π-orbital, leading to this exceptionally strong c-C_3H_5—CO bond. In contrast, photodissociation to the ring-opened products, CO + 2(allyl), yields 97 kcal/mol. Furthermore, a transition state to ring opening in the parent molecule exists on the ground state surface. Therefore the amount of energy remaining in the photofragments should offer clues to the dissociation mechanism and the isomerization of C_3H_5.

We have investigated the 193 nm photodissociation of DCPK using time-resolved FT emission spectroscopy from 800 – 4000 cm^{-1}. Following photolysis, prompt emission is seen from diatomic CO, implying that the dissociation products are CO + $2C_3H_5$. Prompt emission is also seen in the C-H stretching region, and in the IR fingerprint region from 800 – 1600 cm^{-1}, both of which are assigned to C_3H_5. The C-H emission decays within ~25 μs, confirming a radical species as its source. At later times additional features appear, which can be definitively assigned to emission from DCPK. The temporal profile of decreasing emission from C_3H_5 and increasing emission from DCPK is consistent with energy transfer from the hot radicals to the cold parent molecules. The main question is whether the nascent hydrocarbon emission is due to cyclopropyl, allyl, or a mixture of the two radicals.

By examining the time-resolved CO emission with 0.1 cm^{-1} resolution, we can obtain the nascent vibrational distribution, and extrapolate to the nascent rotational distribution. The nascent CO vibrational distribution is fairly well described by a temperature of 3000 K, or $\langle E_{vib} \rangle$ = 3.1 kcal/mol. Similarly, we can place a lower bound on $\langle E_{rot} \rangle$(CO) > ~4 kcal/mol. This CO vibrational distribution is *hotter* than that observed from acetone or diethyl ketone, even though

the total number of parent vibrational modes is greater. While we haven't measured the translational energy release, if the dissociation mechanism involves $S_2 \rightarrow T_1$ intersystem crossing in DCPK, (analogous to acetone), we predict that 24 kcal/mol is available to the two C_3H_5 fragments. In this case, most of the radicals will survive as cyclopropyl. However, it's difficult to explain why DCPK, with twice the number of vibrational modes as acetone, and with less available energy for product excitation, should have a CO distribution hotter than in acetone.

The most reasonable explanation is that, in contrast to acetone, dissociation of DCPK occurs on S_0,. In this case, the lowest energy transition state leads to ring opening of both cyclopropyl ligands, and a much higher energy available to products (97 kcal/mol). In addition, there is an exit barrier to C-C bond fission from the allyl-CO radical of about 10 kcal/mol, which is consistent with the excited rotational and vibrational excitation of the CO fragment.

The calculated vibrational frequencies of allyl and cyclopropyl radicals are remarkably similar, which has hampered efforts to distinguish the two radicals based on spectroscopy alone. Very recently we have performed radical trapping experiments by photolyzing DCPK in the presence of excess Br_2. Using continuous FTIR we can distinguish between allyl bromide and cyclopropyl bromide, two possible trapped radical products. These experiments show evidence of allyl bromide formation, but no detectable amount of cyclopropyl bromide. Together with the time-resolved FTIR data, the trapping experiments support the following dissociation mechanism for DCPK at 193 nm. Internal conversion to the ground electronic state is followed by ring-opening isomerizations of both the cyclopropyl ligands. Dissociation occurs by sequential loss of two allyl radicals. The dissociation $C_3H_5CO \rightarrow C_3H_5 + CO$ occurs over a potential energy barrier, accounting for CO internal state distributions that are hotter than statistical distributions.

Multiphoton dissociation of C_2H_3 – a possible LIF diagnostic in methane flames

The vinyl radical is an important intermediate in the chain of C2 species in methane/air flames. Unfortunately, direct detection of vinyl using LIF is not possible due to strong predissociation. However, PLIF imaging experiments of rich methane-air flames in the Advanced Imaging Lab at the CRF show strong C_2 ($d\ ^3\Pi_g \rightarrow a\ ^3\Pi_u$) Swan band emission that is laser-prompt with 230 nm excitation of the flame. This excitation could provide a possibility to study the C_2 chemistry branch in methane flames if the parent molecule(s) responsible for Swan band emission can be identified. The narrow spatial distribution (500 μm FWHM) of C_2 emission along the flame propagation direction implies that the parent molecule is a short-lived species. The vinyl radical (C_2H_3) and acetylene (C_2H_2) are the most chemically reasonable choices for the parent molecule.

We have conducted low-pressure cell experiments to measure the efficiency, photon energy dependence, and product state distribution of C_2 Swan band emission from 230 nm multiphoton excitation of CH_4, C_2H_2, C_2H_3, C_2H_4, C_2H_6, C_3H_6, and C_4H_6. The vinyl radical was generated by photolysis of methyl vinyl ketone (MVK) at 193 nm, and emission from C_2 was collected using a gated, image-intensified CCD monochromator. The yield of vinyl radicals is calibrated by simultaneous collection of 2 photon LIF from the CO that is produced in equal numbers via photolysis of MVK. The only molecules that create significant Swan band emission are C_2H_2, C_2H_3, and C_4H_6. Both C_2H_2 and C_2H_3 require 3 photons for spin-allowed photodissociation. Our preliminary result shows that Swan band emission from the C_2H_3 radical is 2 to 3 orders of magnitude more efficient than from C_2H_2. This photodissociation process may therefore be promising as a specific diagnostic for vinyl radicals in methane flames.

Future Plans

Instrumental development will continue towards time-resolved FT absorption spectroscopy. One of the first targets will be acquisition of complete infrared spectra of cyclopropyl and allyl radicals in absorption. Fully thermalized radicals at room temperature or in a cooled cell should facilitate spectroscopic assignments, while providing a complimentary examination of the photodissociation dynamics of DCPK. Kinetics measurements of cyclopropyl reactions are also planned.

Another area of interest is chemical reactions that may not occur solely on the ground state potential energy surface, but produce radical products in low-lying electronically excited states. For example, in $C_2H_5 + O_2 \rightarrow C_2H_4 + HO_2$, production of HO_2 in its excited $\tilde{A}$ (^{2}A′) state is energetically allowed, and is a possible explanation for inconsistencies in data comparing the forward and reverse reactions. Detection of this species by TR-FTS via the $\tilde{A}$ (^{2}A′) $\rightarrow$ $\tilde{X}$ (^{2}A″) electronic emission would provide clear evidence that multiple electronic surfaces participate in this reaction.

Finally, high spectral brightness broadband sources for use in absorption-based FT spectroscopy will be investigated. Two avenues are being pursued. Self-phase modulation in dispersion-tuned microstructured fibers has recently been used to create quasi-cw ultra-broadband radiation. We will explore the use of these fibers in FT absorption spectroscopy. A second approach centers on optical parametric generation in quasi phase-matched nonlinear materials. A brighter, more collimated source of IR radiation would increase the detection sensitivity of FT absorption spectroscopy.

References

[1] R. E. Murphy and H. Sakai, in *Proceedings of the Aspen International Conference on Fourier Transform Spectroscopy*, Aspen, p. 301 (1970).
[2] G. Hancock and D. E. Heard, *Adv. Photochem.* **18**, 1 (1993).
[3] T. R. Fletcher and S. R. Leone, *J. Chem. Phys.* **88**, 4720 (1988).
[4] J. J. Sloan and E. J. Kruus, in *Time Resolved Spectroscopy*, ed. R. J. H. Clark and R. E. Hester, John Wiley & Sons, p. 219 (1989).
[5] G. V. Hartland, W. Xie, H. L. Dai, A. Simon, and M. J. Anderson, *Rev. Sci. Instrum.* **63**, 3261 (1992).
[6] P. W. Seakins, in *The Chemical Dynamics and Kinetics of Small Radicals*, ed. K. Liu and A. Wagner, Singapore, p. 250 (1995).
[7] G. E. Hall, J. T. Muckerman, J. M. Preses, R. E. Weston, and G. W. Flynn, *Chem. Phys. Lett.* **193**, 77 (1992).
[8] J. Eberhard, P. S. Yeh, and Y. P. Lee, *J. Chem. Phys.* **107**, 6499 (1997).
[9] K. Holtzhauer, C. Cometta-Morini, and J. F. M. Oth, *J. Phys. Org. Chem.* **3**, 219 (1990).
[10] S. Davis, Ph. D. dissertation, University of Colorado, 624 (2000).
[11] C. C. Hayden, unpublished.
[12] P. A. Arnold and B. K. Carpenter, *Chem. Phys. Lett.* **328**, 90 (2000).
[13] S. W. North, D. A. Blank, J. D. Gezelter, C. A. Longfellow, and Y. T. Lee, *J. Chem. Phys.* **102**, 4447 (1995).
[14] P. D. Lightfoot, S. P. Kirwan, and M. J. Pilling, *J. Phys. Chem.* **92**, 4938 (1988).
[15] E. L. Woodbridge, T. R. Fletcher, and S. R. Leone, *J. Phys. Chem.* **92**, 5387 (1988).
[16] G. E. Hall, H. W. Metzler, J. T. Muckerman, J. M. Preses, and R. E. Weston Jr., *J. Chem. Phys* **102**, 6660 (1995).

The Effect of Large Amplitude Motion on Spectroscopy and Energy Redistribution in Vibrationally Excited Methanol

David S. Perry, Principal Investigator
University of Akron, Akron OH 44325-3601
DPerry@UAkron.edu

This project involves several different spectroscopic approaches to understanding large amplitude vibrational motion in methanol, its role in coupling the vibrational modes, and the resultant energy redistribution. The originally proposed methods proposed are high-resolution spectroscopy in the 3-micron region and the lower overtones, done at the University of Akron, and IRLAPS spectroscopy up to the higher overtones in collaboration with Rizzo's group in Lausanne Switzerland. With the arrival in Akron of a senior postdoctoral fellow, Indranath Muhkopadhyay, we have extended the domain of the experiments to include high resolution FTIR in the far- mid- and near-infrared regions. These spectra were obtained in collaboration with Dr. Horneman at the U. of Oulu, Finland, and with Drs. Klee and Lock at Liebig U. in Giessen Germany.

Torsional Combinations

The coupling of small amplitude vibrations to torsional motion is most directly revealed by accessing combination states involving excitation of both torsional motion and the small amplitude vibration. Because the first excited torsional state $v_{12}=1$ is close to the top of the torsional barrier and $v_{12}=2$ is well above it, these states allow all torsional conformations to be sampled. The most noteworthy discovery of the past year is that such torsional combination states can be observed as direct excitations from the vibrational ground state. These transitions (Figure 1) are orders of

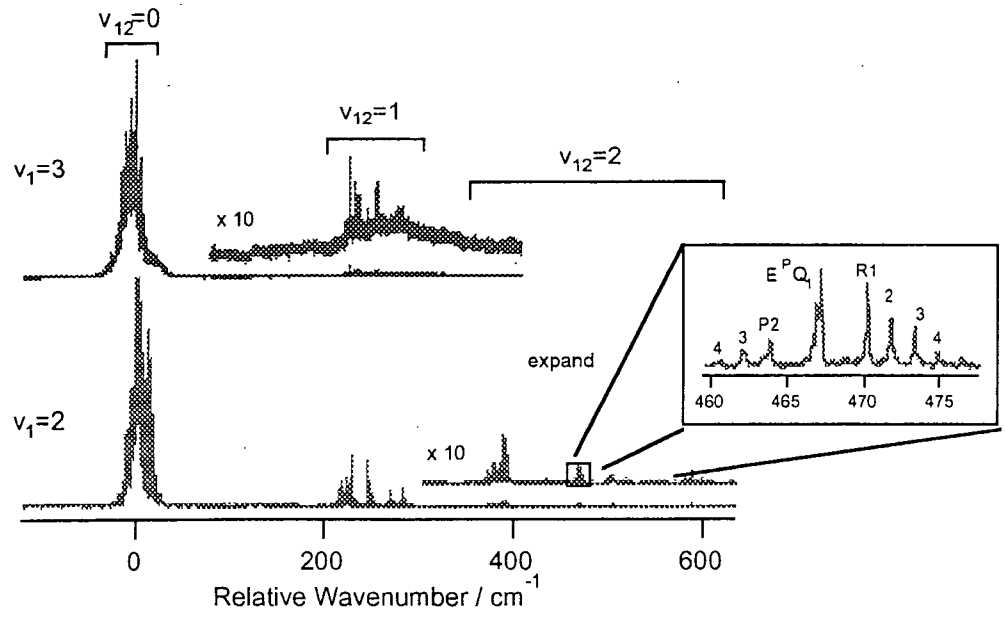

Figure 1. Single resonance IRLAPS spectra of combinations of the OH stretch (v_1) with the torsion (v_{12})

magnitude stronger than had been expected from simple Franck-Condon-like calculations. The fact that the torsional tunneling splitting in these states may be more than 100 cm^{-1} causes the spectra to be spread out over 100's of cm^{-1}. As a result the torsional structure built on the $2\nu_1$ and $3\nu_1$ bands is well resolved and analyzable even in moderately low-resolution single resonance spectra. We have carried out global fits of the torsional manifolds for both $2\nu_1$ and $3\nu_1$ to a torsion-rotation Hamiltonian and obtained unambiguous measures of the torsion-vibration coupling. We have also assigned transitions reaching torsionally excited states built on the C-H stretch vibrations. These transitions are found in the "empty" region between the C-H and O-H stretch fundamentals.

The features in Figure 1 may be used as intermediate states in double resonance IRLAPS spectra which means that it may now be possible to study the IVR dynamics in the whole overtone region as a function of the torsional conformation.

Global Overtone Spectrum

With the IRLAPS technique, we have recorded the complete overtone spectrum from 4900 to 14000 cm^{-1} and specified regions as high as 28000 cm^{-1}. We also have high resolution covering the ranges 0-1200 cm^{-1} and 2700-5000cm^{-1}. In addition to the OH stretch overtones, the overtone region contains the CH overtones and several OH combinations with the COH bend and the CO stretch and the band positions have been fit to an anharmonic Hamiltonian. In the far infrared region, we have assignments for several torsional excited states that have not yet appeared in the literature. Together with published work, the result is an extensive catalog of experimental vibrational energy levels that are the targets needed by the theoretical community.

Infrared CW Cavity Ringdown

Thanks to the arrival of a postdoctoral fellow hired for this purpose, the development of the CW cavity ringdown experiment is now proceeding well. The external cavity diode laser is in place and is being interfaced to computer control. The ringdown cavity has been fabricated and is being tested.

^{13}C-Methanol Results

Because much of the vibrational dynamics of methanol appears to be controlled by the "accidental" resonance of coupled states, spectra of ^{13}C methanol provide a needed check on the validity of the interpretation. Among the concepts tested is the role of a potentially reactive pathway in the coupling of vibrational degrees of freedom. That concept was explained in last year's report. Two papers on ^{13}C-methanol have appeared this year and a third is close to submission.

Inverted Level Structures Resulting from Large-Amplitude Torsional Motion

In 1997 we reported inverted torsional level structure in the CH stretch region (ν_2) and in 1998 reported an additional inverted band (ν_9) and a conceptual framework that accounted for the inversion and predicted its generality for vibrations in methanol whose identities are interchanged by large amplitude internal rotational motion. The generality should apply to other molecules with a three-fold symmetric torsional potential. Since that time Lees and Xu have reported two additional bands with inverted torsional structure (ν_{11} and ν_4) and Hougen has formalized the theoretical underpinnings.

Plans for the Next Year

Development of the ringdown experiment with applications to CH – OH stretch combination bands is continuing. Comprehensive information on the CH stretch-bend coupling has been particularly illusive and these bands provide the best opportunity.

Analysis of CH stretch-torsion combinations that lie in the gap between the CH and OH fundamentals will continue. We currently have high quality FTIR spectra at the Doppler limit throughout this whole region. This analysis will yield the most stringent test of our model of the inverted torsional structure and is likely uncover additional torsion-vibration couplings.

Our work on the torsionally excited states of the $2\nu_1$ and $3\nu_1$ bands leads to the odd situation that more torsional levels have been fit for these high-lying vibrations than for the ground state itself. As a collaboration with Y.-B. Duan (publication 7 below) we plan to apply his more systematic Hamiltonian to torsionally excited states of methanol that could not previously be fit to the desired level of accuracy.

Publications, 1998 - present

[1] X. Wang and D. S. Perry, *An internal coordinate model of coupling between the torsion and C-H stretch vibrations in methanol, J. Chem. Phys.* **109**, 10795-10805 (1998).

[2] O.V. Boyarkin, T.R. Rizzo, and D.S. Perry, *Intramolecular energy transfer in highly vibrationally excited methanol. II. Multiple time scales for energy redistribution, J. Chem. Phys.* **110**, 11359-11367 (1999).

[3] O.V. Boyarkin, T.R. Rizzo, and D.S. Perry, *Intramolecular energy transfer in highly vibrationally excited methanol. III. Rotational and torsional analysis, J. Chem. Phys.* **110**, 11346-11358 (1999).

[4] T. J. Cronin, X. Wang, and D. S. Perry, *High resolution infrared spectra in the C-H region of CH_2F_2: The ν_6 and $2\nu_2$ bands, J. Mol. Spectrosc.* **194**, 236-242 (1999).

[5] A. V. Chirokolava, D. S. Perry, and L.-H. Xu, Sub-Doppler infrared spectra of the O-H stretch fundamental of ^{13}C-methanol, *J. Mol. Spectrosc.* **203**, 320–329 (2000).

[6] A. Chirokolava, D.S. Perry, O.V. Boyarkin, M. Schmidt, and T.R. Rizzo, Intramolecular energy transfer in highly vibrationally excited methanol. IV. Spectroscopy and dynamics of $^{13}CH_3OH$, *J. Chem. Phys.* **113**, 10068-10072 (2000).

[7] L. Wang, Y.-B. Duan, I. Mukhopadhyay, D. S. Perry, and K. Takagi, On the physical interpretation of torsion-rotational parameters for CH_3OD isotopomers, *Chem. Phys.* **263**. 263-279 (2001).

Partially-Premixed Flames in Internal Combustion Engines

Professor Robert W. Pitz, Program Manager and Principal Investigator
Department of Mechanical Engineering, Vanderbilt University, Nashville, TN 37235
robert.w.pitz@vanderbilt.edu
Dr. Michael C. Drake and Dr. Todd D. Fansler, Co-Principal Investigators
General Motors R & D Center, 30500 Mound Road, Warren, MI 48090-9055
michael.c.drake@gm.com, todd.d.fansler@gm.com
Professor Volker Sick, Co-Principal Investigator
Department of Mechanical Engineering, University of Michigan
2023 W. E. Lay Automotive Laboratory, Ann Arbor, MI 48109-2121
vsick@umich.edu

Program scope

The purposes of this joint university-industry research program are: 1) to use advanced laser diagnostics and detailed chemistry models to understand partially-premixed flames in unique laboratory burners, 2) to use advanced laser diagnostics to observe and characterize partially-premixed combustion in optically-accessible direct injection gasoline engines, and 3) to more fully develop laser diagnostic techniques for temperature and flame front imaging in partially-premixed flames and IC engines. The work is being done primarily at Vanderbilt University, General Motors Research and Development Center, and the University of Michigan.

The goals of this research are 1) a better understanding of the effects of strain and curvature on partially-premixed flame structure, 2) better conceptual models of partially-premixed combustion in highly stratified direct injection engines for automotive applications, and 3) improved and more robust laser diagnostic methods for use in university and industrial environments.

Recent progress

At Vanderbilt, a visible laser-based Raman system has been developed to obtain relatively-interference-free Raman signals in hydrocarbon flames (Osborne et al. 2000). This has been applied to opposed jet flames, either flat or curved, burning CH_4 or C_3H_8 (Wehrmeyer et al. 2001a,b; and Mosbacher et al. 2001), with these flames chosen in order to simulate what is expected to occur in a stratified-charge direct injection spark ignition (DISI) engine, where hot products impinge upon a zone of either lean or rich reactants. The C_3H_8 planar flames were modeled using the Oppdif application (part of the CHEMKIN software) with the "M5" mechanism (Haworth et al. 2000). Various combinations of partial premixedness were studied, and in particular several flows involved a very lean C_3H_8-air reactant jet impinging upon hot products produced by a lean H_2-air flame.

Figure 1 shows Raman-derived temperature and gas species concentration measurements for a planar lean (ϕ=0.64) premixed C_3H_8-air flame impinging on the hot products from a lean (ϕ=0.4) H_2-air flame. The lean H_2-air flame was anchored on the jet exit nozzle due to stabilization around the top screen retaining ring, and this leads to the discrepancy among the numerical and experimental data on the right hand side of Fig. 1. However within the lean C_3H_8 flame there is excellent agreement among the experimental and numerical data, especially with the CO_2 profile. This can be viewed as a "positive flame speed" flame, where the lean C_3H_8-air flame exists as a premixed flame on the left hand side of the stagnation plane. However for slightly leaner C_3H_8 flames, at the same strain rate, the propane flame ceases to exist as a self-sustaining premixed flame but only exists as a diffusion flame on the right hand side of the stagnation plane (Wehrmeyer et al. 2001a,c). Only a small fraction of the C_3H_8 diffuses across and hence the measured CO_2 values are at least an order of magnitude smaller than for positive flame speed flames. For the "negative flame speed" flame there is not good agreement among the numerical and experimental CO_2 data, with the experimental CO_2 values about a factor of five higher than numerical. This indicates improvements may need to be made to the C_3H_8 reaction mechanism when it is used to model the hydrocarbon burnout processes for DISI engines.

The effect of curvature on partially premixed flames is assessed both numerically and experimentally. Changes in flame strength, flame structure, and peak flame temperature depend upon the deficient reactant's Lewis number and whether the flame surface is concave or convex toward reactants (Law and Sung 2000). The Oppdif application code was modified for cylindrical opposed jet flame configurations to produce temperature and species profiles as functions of radius. Figure 2 shows two lean H_2-air flames emanating from an inner nozzle that is met by an air flow coming from an outer nozzle. In Fig. 2, the smaller radius (9.5 mm) H_2-air premixed flame is much weaker, having a flame temperature about 100 K lower and a laminar flame speed about 10% lower than the larger

radius (20 mm) flame. These differences are due to the Lewis number effects and this strong temperature change can have dramatic effects on temperature sensitive processes such at NO formation.

At Vanderbilt a unique cylindrical burner has been developed to study cylindrical flames with optical access (Wehrmeyer et al. 2001b,c) and Fig. 3 shows the burner in operation, with a lean CH_4-air flame coming from the inner nozzle and met by an opposing flow of air from the outer nozzle. In Fig. 4, the line Raman spectra of a lean H_2-air flame is shown. The vibrational Raman lines from the major species can be clearly seen. In order to assess curvature effects on these premixed flames, this data is currently being reduced and is included in a recent paper along with numerical calculations (Mosbacher et al. 2001).

At GM R&D (with internal GM funding), partially-premixed flame combustion is being studied in stratified-charge DISI engines. A single cylinder engine, with an extended piston that has optical access through a quartz piston window, is used to obtain high-speed video camera images of the stratified charge combustion processes. Figure 5 shows a schematic of the "glass-piston" engine, along with a field-of-view image of the cylinder. Using narrow-band spectral filters, and a three-ICCD camera system, images of the OH*, CH*, and C_2* emission are obtained. The images show the growth of both the combustion zones and the sooting zones as functions of crank angle. In addition, GM has established a Satellite Research Laboratory at the University of Michigan, which has provided money and equipment to equip an engine test cell with two DISI single-cylinder engines (one all-metal and one with extensive optical access). GM is funding several graduate students at UM as part of the Satellite Laboratory, as well as funding a UM graduate student as a summer intern at GM R&D. Also chemical kinetic mechanisms that were developed at GM were given to Vanderbilt University to be used in the numerical investigation of partially premixed flames.

At the University of Michigan, development of laser diagnostics for DISI engine applications continues. A quantitative measurement of the fuel distribution in dense high-pressure sprays can be obstructed by substantial laser beam and signal attenuation. These processes were characterized experimentally and numerically (Sick and Stojkovic 2001) to allow an improved measurement of the initial phase of the mixture preparation to partially premixed conditions in DISI engines. In addition to the attenuation of the exciting laser beams, measurements under direct-injected conditions can suffer from severe attenuation of the signal light. A method was developed to measure the signal attenuation in two dimensions that perfectly mimics the signal light's spectral composition. Subsequent work was performed on the temporal and spatial history of a spray event to evaluate the penetration, and atomization for engine geometries (Stojkovic and Sick 2001). This work also addressed interference effects on laser-based measurements in direct injected gasoline engines, as they would influence quantitative studies by producing unwanted signal reflections from nearby surfaces.

Measurements in the now completed optical engine have begun. The investigation of partially premixed flames under engine conditions will require accurate measurements of fuel distribution even at very low fuel concentrations, i.e. fuel/air equivalence ratios. The fuel/air equivalence ratio measurements are based on PLIF of toluene that was added to isooctane fuel. The level of unmixedness can be characterized in detail from the PLIF images and comparisons between homogenous and stratified charge conditions are under way. An example of the instantaneous fuel distribution that was measured in the optical engine under very lean conditions in a horizontal plane 5 mm below the injector nozzle is shown in Fig. 6.

The penetration of a turbulent flame front into the unburnt fuel/air mixture is shown in Fig. 7, where a single-shot PLIF image of the fuel visualizes the flame location via the disappearing fuel. As the investigations of partially premixed flames under well-controlled flow conditions in an opposed flow burner (performed at Vanderbilt University as part of the joint research project) show, the complementary fuel and hydroxyl radical distribution as was measured for fully premixed combustion in engines (Arnold et al. 1993) cannot be expected for the partially premixed case. Therefore, the distribution of hydroxyl radicals needs to be measured in the direct injected engine, in particular for highly stratified cases where the partially premixed character of the flames will be most prominent.

Future plans in the current project period

At Vanderbilt, the effect of flame curvature on cylindrical partially premixed flames will be assessed numerically and experimentally. The Raman measurements (e.g., Fig. 4) of hydrogen and methane lean premixed flames will be reduced and compared to numerical predictions. Cylindrical partially premixed flames of H_2 and C_3H_8-air will be measured in the burner and compared to the numerical predictions such as those shown in Fig. 2. A graduate student will spend the summer at GM performing DISI engine research.

At the University of Michigan, fuel/air mixing strategies to produce either homogeneous or stratified fuel distributions at the time of spark will be characterized before studying flame propagation under these conditions in detail. The partially premixed nature of the flames for the stratified charge conditions will be examined and

compared to the findings from the Vanderbilt studies of partially premixed flames under well-controlled flow conditions.

GM R&D will continue a variety of high-speed imaging and other experiments on fuel sprays, mixture formation, and combustion in two optical DISI engines (one shown in Figure 5 and one essentially identical to the optical engine at UM.).

Publications acknowledging DOE support

Mosbacher, D. M., J. A. Wehrmeyer, R. J. Osborne, Z. Cheng, R. W. Pitz, and C. J. Sung, (2001), "Investigation of Partially-Premixed Cylindrical and Axial Opposed Jet Propane-Air Flames," Joint Meeting of the United States Sections of the Combustion Institute, Oakland, CA, March 25-28.

Osborne R. J., J. A. Wehrmeyer, and R. W. Pitz, (2000), "A Comparison of UV Raman and Visible Raman Techniques for Measuring Non-Sooting Partially Premixed Hydrocarbon Flames," AIAA 38th Aerospace Sciences Meeting, Paper No. AIAA-2000-0776, Reno, Nevada, January 10-13.

Sick, V., B. Stojkovic, (2001), "Attenuation Effects on Imaging Diagnostics of Hollow-Cone Sprays," *Applied Optics*, 40, (15) pp. 1-8.

Stojkovic, B., V. Sick, (2001), "Evolution and Impingement of an Automotive Fuel Spray Investigated with Simultaneous Mie/LIF Techniques," *Applied Physics B*, accepted for publication.

Wehrmeyer, J. A., Z. Cheng, D. M. Mosbacher, R. W. Pitz, and R. J. Osborne, (2001a), "Opposed Jet Flames of Near-Limit Premixed Propane-Air Reactants vs. Hot Products," submitted to *Combustion and Flame*.

Wehrmeyer, J. A., R. J. Osborne, D. M. Mosbacher, Z. Cheng, R. W. Pitz, J. Byrd, and C.-J. Sung, (2001b), "Numerical and Experimental Study of Cylindrical Flames," to be submitted to *Combustion, Science and Technology*.

Wehrmeyer, J. A., R. J. Osborne, D. M. Mosbacher, Z. Cheng, R. W. Pitz, and C.-J. Sung, (2001c), "Investigation of Partially Premixed Propane-Air Flames with Flame Curvature," AIAA 39th Aerospace Sciences Meeting, Paper No. AIAA-2001-1083, Reno, Nevada, January 8-11.

Other references cited above

Arnold, A., A. Buschmann, B. Cousyn, M. Decker, V. Sick , F. Vannobel, and J. Wolfrum, (1993), "Simultaneous Imaging of Fuel and Hydroxyl Radicals in an In-Line Four Cylinder SI Engine" *SAE Trans.*, vol. 102, Sec. 4.

Haworth, D. C., R. J. Blint, B. Cuenot, and T. J. Poinsot, (2000), "Numerical Simulation of Turbulent Propane-Air Combustion with Nonhomogenous Reactants," *Combustion and Flame*, 121, pp. 395-417.

Law, C. K., and C. J. Sung, (2000), "Structure, Aerodynamics, and Geometry of Premixed Flamelets," *Progress in Energy and Combustion Science*, vol. 26, pp. 459-505.

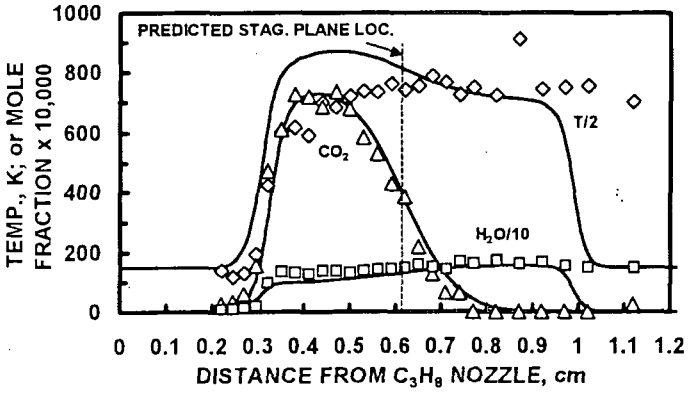

Fig. 1. Raman-derived temperature and product data in a partially-premixed opposed jet flame. C_3H_8-air (ϕ=0.64) vs. H_2-air (ϕ=0.4). a=140 sec^{-1}.

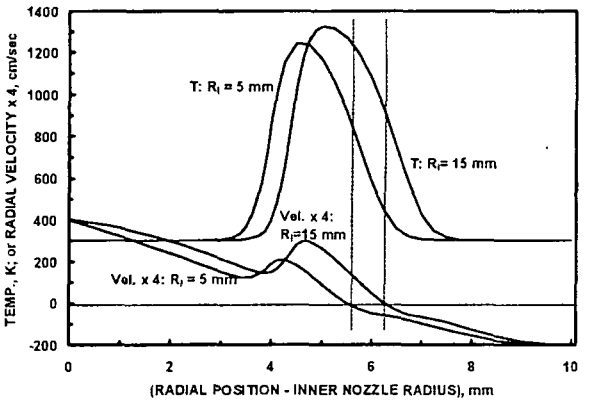

Fig. 2. Temperature and velocity profiles for 2 lean (ϕ = 0.35) H_2-air premixed flames opposed by air. One flame for inner radius of 5mm, one 15mm.

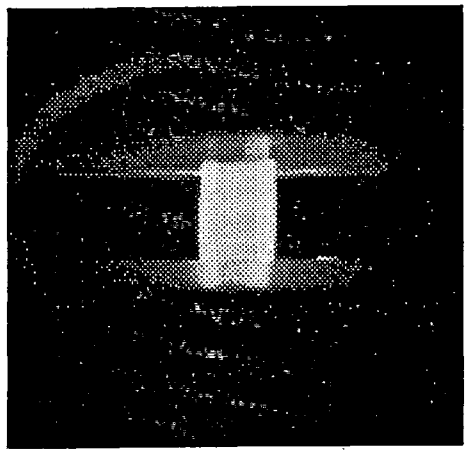

Fig. 3. View through optical access of cylindrical burner port of propane-air cylindrical flame.

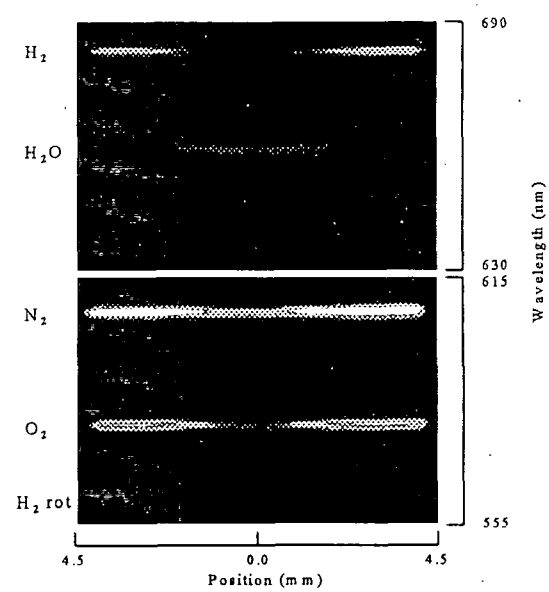

Fig. 4. Raman image of H_2-air (ϕ = 0.18) cylindrical premixed flame.

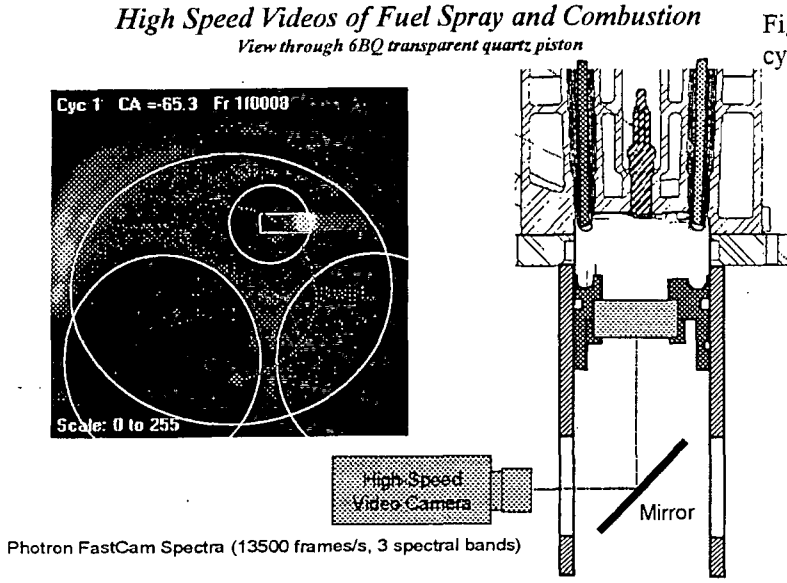

Fig. 5. DISI engine with optical access through the piston.

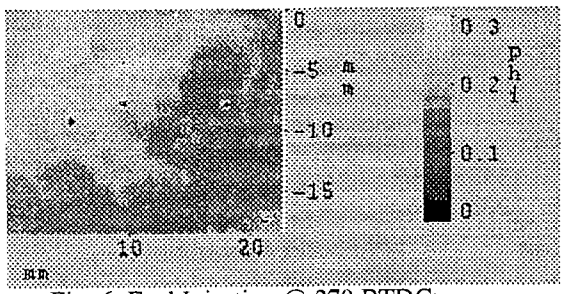

Fig. 6. Fuel Injection @ 270 BTDC; Image @ 180 BTDC; note the presence of droplets.

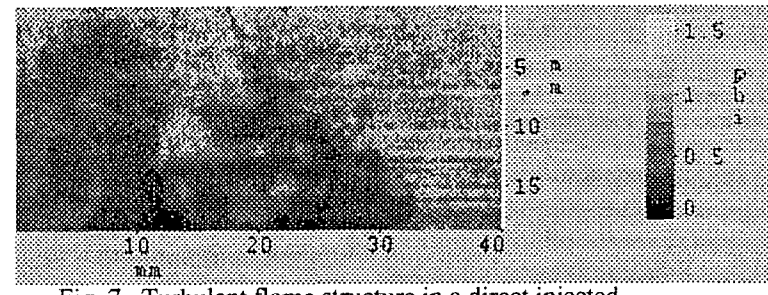

Fig. 7. Turbulent flame structure in a direct injected engine. The image plane is horizontal, 5 mm below the injector. The flame area is marked by the dark areas where the fuel has been burnt.

INVESTIGATION OF NON-PREMIXED TURBULENT COMBUSTION

Grant: DE-FG02-90ER14128

Principal Investigator: Stephen B. Pope
Mechanical & Aerospace Engineering
Cornell University
Ithaca, NY 14853
pope@mae.cornell.edu

Introduction

A major goal of research in combustion is to develop computer models capable of accurately predicting the performance of combustion equipment. Due to the complexity of combustion chemistry and of turbulent and multiphase flows, we are several decades away from achieving this goal. Nevertheless, computer models—though less accurate than desirable—are proving increasingly useful in the design of combustion devices, leading to improved performance and reduced pollutant emissions. The aim of the current research is to apply the best available turbulent combustion models to turbulent flames for which there are reliable experimental data, in order to test (and if necessary improve) the submodels involved.

The turbulent combustion models considered are PDF methods, in which a modelled transport equation is solved for the joint probability density function of velocity, turbulence frequency, and the thermochemical composition of the fluid (species mass fractions and enthalpy). The modelled PDF equation is solved numerically using a particle/mesh method. As described in the subsequent sections, PDF calculations have been performed of bluff-body flames and swirling flames, and considerable effort has been devoted to improving the accuracy and efficiency of the PDF methodology.

Bluff body flames

The parallel work of Xu & Pope (2000) and Tang et al. (2000) has convincingly demonstrated the ability of PDF methods to account accurately, for finite-rate turbulence-chemistry interactions in piloted jet flames. The phenomena included in these flames are local extinction and reignition, and the calculations include radiation and NO formation. The bluff-body flames provide a more challenging flow field for combustion models, including flame stabilization by recirculation.

In the work of Jenny et al. (2001a), three different PDF solution algorithms (to solve the same modelled PDF transport equation) are applied to the non-reacting bluff body flow. The three algorithm are: a stand-alone particle method (Pope 1994); a loosely-coupled hybrid method (Jenny et al. 2001b); and a tightly-coupled hybrid method (Muradoglu et al. 1999).

It is found that, reassuringly, all three methods converge to the same solution, but the hybrid methods are more efficient by two orders of magnitude.

Work on making PDF calculations of the (reacting) bluff-body flames is in progress.

Swirling flames

Turbulent nonpremixed swirl-stabilised flames are common in practical combustors and form the next level of complexity after piloted and bluff-body stabilised flames. Modeling swirling flows remains a challenge especially when the swirl level is high enough to induce vortex breakdown and recirculation. The paper of Masri, Pope & Dally (2000) presents experimental results on the velocity field and the stability characteristics of a new swirl burner which has well-defined boundary conditions. This burner is capable of stabilising turbulent nonpremixed flames which have high swirl numbers and which may have a significant degree of turbulence-chemistry interactions. A Monte Carlo-based Probability Density Function (PDF) method is also used to compute the same turbulent, highly swirling flame using the simplest models for velocity (SLM), turbulent frequency (JPM) and molecular mixing (IEM). A description of these models is provided by Pope (2000). A single flamelet library is used to represent the chemistry. These simple computations reproduce the correct flow structure and compare well with the measured velocity field. Refinements to the computations and more extensive measurements in such flows are in progress.

Consistent hybrid method

PDF methods are based on the numerical solution of a modelled transport equation for the joint PDF of fluid properties. Since the PDF depends, typically, on 20 independent variables, the numerical solution is quite challenging. The stand-alone particle code developed by Pope (1994) has been shown to be accurate, but it is not efficient. In a series of works—Muradoglu et al. (1999, 2001), Jenny et al. (2001a,b)—we have developed much more efficient "hybrid" algorithms.

The hybrid method solves the modelled transport equation for the joint PDF of velocity, turbulence frequency and compositions for turbulent reactive flows. A finite-volume (FV) method is used to solve the mean conservation equations for mass, momentum and energy and the mean equation of state; and a particle method is used to solve the modelled PDF equation. The method is completely consistent at the level of the governing equations solved by the FV and particle algorithms. In the work of Muradoglu et al. (2001), the conditions to be fulfilled for full consistency at the numerical solution level are examined and the independent consistency conditions are identified. Then correction algorithms are developed to enforce these independent consistency conditions to achieve full consistency at the numerical solution level. In addition, a new formulation of the energy equation and the equation of state is developed which is both general and simple. The hybrid method is applied to a non-premixed piloted-jet flame. The numerical results show that the correction algorithms are completely successful in achieving consistency. The convergence of the method is demonstrated; and, in particular, it is shown that the bias error is dramatically reduced (compared to that in previous PDF calculations). In addition, the results are shown to be in a good agreement with some earlier PDF calculations and also with the available experimental data. Because of the substantially reduced numerical error (for given grid size and number of particles), the present hybrid method represents a significant advance in the

computational efficiency of particle/mesh method for the solution of PDF equations.

Future Plans

Topics of current and future work are:

1. incorporating the ISAT algorithm (Pope 1997) into the hybrid code so that PDF calculations can be made with realistic chemistry

2. resolving turbulence-modelling issues in bluff-body flames

3. for the piloted-jet and bluff-body flames, examine the accuracy of different mixing and chemistry sub-models.

References

1. P. Jenny, M. Muradoglu, K. Liu, S.B. Pope, D.A. Caughey (2001) "PDF simulations of a bluff-body stabilized flow," J. Comp. Phys. (to be published).

2. P. Jenny, S.B. Pope, M. Muradoglu and D.A. Caughey (2001) "A hybrid algorithm for the joint PDF equation for turbulent reactive flows," J. Comp. Phys. **166**, 281–252.

3. A.R. Masri, S.B. Pope and B.B. Dally (2000) "PDF computations of a strongly swirling nonpremixed flame stabilised on a new burner," Proceedings of the Combustion Institute, **28**, (to be published).

4. M. Muradoglu, P. Jenny, S.B. Pope and D.A. Caughey (1999). "A Consistent Hybrid Finite-Volume/Particle Method for the PDF Equations of Turbulent Reactive Flows," Journal of Computational Physics **154**, 342–371.

5. M. Muradoglu, S.B. Pope and D.A. Caughey (2000). "The hybrid method for the PDF equations of turbulent reactive flows: consistency conditions and correction algorithms," J. Comp. Phys. (submitted).

6. S.B. Pope (2000) "Turbulent Flows," Cambridge University Press.

7. S.B. Pope (1997) "Computationally Efficient Implementation of Combustion Chemistry using In Situ Adaptive Tabulation," Combustion Theory and Modelling, **1**, 41–63.

8. Q. Tang, J. Xu and S.B. Pope (2000) "PDF calculations of local extinction and NO production in piloted-jet turbulent methane/air flames," Proceedings of the Combustion Institute, **28**, (to be published).

9. J. Xu and S.B. Pope (2000) "PDF calculations of turbulent nonpremixed flames with local extinction," Combust. Flame **123**, 281–307.

Publications from DOE research, 1999–2001

1. P. Jenny, M. Muradoglu, K. Liu, S.B. Pope, D.A. Caughey (2001) "PDF simulations of a bluff-body stabilized flow," J. Comp. Phys. (to be published).

2. P. Jenny, S.B. Pope, M. Muradoglu and D.A. Caughey (2001) "A hybrid algorithm for the joint PDF equation for turbulent reactive flows," J. Comp. Phys. **166**, 281–252.

3. A.R. Masri, S.B. Pope and B.B. Dally (2000) "PDF computations of a strongly swirling nonpremixed flame stabilised on a new burner," Proceedings of the Combustion Institute, **28**, (to be published).

4. M. Muradoglu, P. Jenny, S.B. Pope and D.A. Caughey (1999). "A Consistent Hybrid Finite-Volume/Particle Method for the PDF Equations of Turbulent Reactive Flows," Journal of Computational Physics **154**, 342–371.

5. M. Muradoglu, S.B. Pope and D.A. Caughey (2000). "The hybrid method for the PDF equations of turbulent reactive flows: consistency conditions and correction algorithms," J. Comp. Phys. (submitted).

6. M.R. Overholt and S.B. Pope (1999) "Direct Numerical Simulation of a Statistically Stationary Turbulent Reacting Flow," Combustion Theory and Modelling, **3**, 371–408.

OPTICAL PROBES OF ATOMIC AND MOLECULAR DECAY PROCESSES

S.T. Pratt
Building 200, D-177
Argonne National Laboratory
9700 South Cass Avenue
Argonne, Illinois 60439

Telephone: (630) 252-4199
E-mail: stpratt@anl.gov

PROJECT SCOPE

The study of molecular photoionization and photodissociation dynamics, and, in particular, the study of autoionization and predissociation processes, can provide considerable insight into the mechanisms responsible for the flow of energy and angular momentum among the electronic, vibrational, and rotational degrees of freedom in isolated molecules. This project is aimed understanding these mechanisms and investigating how they determine the decay rates, products, and branching ratios for the decay of highly excited molecules. Much of the current work involves high-resolution photoelectron spectroscopy, and has focused on the vibrational and rotational autoionization of polyatomic molecules. However, the energetics of most molecules are such that, when ionization can occur, dissociation into neutral fragments is also possible. The interplay between these two decay processes can be quite important. Thus, in general, multiple detection techniques are necessary to characterize the decay processes of highly excited states, and a variety of approaches are used, including the detection of neutral fragments by resonance ionization, the determination of excited-state absorption spectra by fluorescence-dip spectroscopy, and the determination of accurate ionization thresholds by zero kinetic energy (ZEKE) photoelectron spectroscopy.

RECENT PROGRESS

The principal emphasis of our work in the past year was on understanding vibrational autoionization in ammonia, in particular, how the autoionization process depends on the normal mode driving the process. As discussed last year, we have used double-resonance excitation via the $\tilde{C}'\ ^1A_1$ (1300) vibrational level to excite ns or nd Rydberg series converging to the $\tilde{X}\ ^2A_2''$(1300) level of NH_3^+. The NH_3^+ ground state and the Rydberg series converging to it are planar, and ν_1 and ν_2 correspond to the symmetric stretch and umbrella bend, respectively. Photoelectron spectroscopy shows that the members of the observed series are approximately 30 times more likely to decay by $\Delta v_2 = -1$ into the (1200) continuum that by $\Delta v_1 = -1$ into the (0300) continuum. We have developed a qualitative model of vibrational autoionization to rationalize this observation. The model is based on the idea that the coupling between the vibrational and electronic degrees of freedom will be strongest for Rydberg orbitals with penetrating character and with corresponding orbital energies that depend strongly on the normal coordinate near the equilibrium geometry of the molecule. In the language of quantum defect theory, this corresponds to Rydberg states whose quantum defects depend strongly on the normal coordinate. Using Walsh-like diagrams for the symmetric stretch and umbrella motion, it is possible to rationalize our observation for the mode dependence of the process. We are currently trying to make these arguments more quantitative and to extend them to other molecules. Interestingly, these arguments suggest that the electron ejected in the $\Delta v_2 = -1$ process will most likely have the character of odd partial waves. This conclusion is consistent

with the rotational structure observed in the high resolution photoelectron spectra of the (1300) Rydberg series.

Double resonance experiments have also been performed using the $\tilde{B}\ ^1E''$ state, rather than the $\tilde{C}'\ ^1A_1$ state, as the intermediate level. The reason for this choice is two-fold. First, the different electronic symmetry allows transitions to Rydberg series that are forbidden from the $\tilde{C}'\ ^1A_1$ state, making it possible to study how vibrational autoionization depends on the electronic symmetry. Second, combination bands involving the umbrella mode and the asymmetric bending mode and the umbrella mode and the asymmetric stretching mode have been observed for the $\tilde{B}\ ^1E''$ state, but not for the $\tilde{C}'\ ^1A_1$. Double resonance studies through such bands will ultimately allow the comparison of the vibrational autoionization rates for all four normal modes of NH_3. Our initial studies have focused on the $\tilde{B}\ ^1E''$ (0200) intermediate state, and the results of these experiments are currently being analyzed. Experiments using the combination bands will begin in the coming year.

Nonresonant two-photon ionization spectra have also been recorded for jet-cooled NH_3 between the ionization threshold and the $NH_3^+\ \tilde{X}\ ^2A_2''(0200)$ limit. The comparison of these spectra with our earlier double-resonance spectra provides new information on the excited states of NH_3. In particular, the selection rules for two-photon processes favor the excitation out of the "p" lone-pair orbital in the ground state of NH_2 into np and nf Rydberg states, while the selection rules for single-photon excitation from the 3p C' state favor the excitation of ns and nd series. Our observations are consistent with this expectation, and serve to answer questions raised several years ago regarding the interpretation of the room temperature, single-photon spectrum of NH_3.

Although all of the experiments discussed above were performed at Argonne using lasers for the light sources, some experiments have been performed recently in collaboration with Professor Cheuk Ng of Iowa State University in which we used synchrotron radiation at the Chemical Dynamics Beamline at the Advanced Light Source (ALS). The goal of these experiments was to record the single-photon ionization spectrum of jet-cooled ammonia in the region near the ionization threshold. In principle, it should be possible to record these spectra with a resolution of ~1 cm^{-1}, which is comparable to that in the laser experiments. The comparison of such a high-resolution single-photon ionization spectrum with our two-photon spectra and double-resonance spectra should prove informative. In our initial experiments on jet-cooled ammonia , the resolution was limited by instrumental factors to ~4 cm^{-1}, and the rotational structure was not sufficiently resolved to allow a detailed comparison between the different spectra. This issue will be addressed in future work at the ALS.

In an ongoing collaboration with Professor Wallace Glab of Texas Tech University and Professor Mark Child of Oxford University, we have continued to study the autoionization of Rydberg states of water. In the past year, double-resonance techniques were used to access linear excited states of water that are based on the first excited electronic state of the ion. These studies complement earlier work on nonlinear Rydberg states of water based on excited vibrational levels of the ground electronic state of the ion. In the earlier studies, the spectra were exceedingly difficult to analyze, and it was thought that this might be a result of interactions with the linear Rydberg states. By using double-resonance excitation via a low-lying linear state, it should be possible to study the higher-lying linear states in a selective manner. In contrast to the nonlinear Rydberg states, which undergo vibrational autoionization, the linear states decay by electronic autoionization. High-resolution photoelectron spectra have been recorded for a number of

these autoionizing levels, and they are currently being analyzed. Additional experiments using vaccum-ultraviolet absorption for the first step in the double-resonance process are currently being planned.

A new collaboration has been developed with Professor Timothy Zwier of Purdue University to use photoelectron spectroscopy to help characterize the photochemistry of low-lying states of diacetylene. It is believed that photoexcitation of the low-lying 1 $^1\Delta_u$ state of diacetylene is followed by rapid intersystem crossing into the triplet manifold, and the Zwier group has shown that the triplet states so produced undergo a number of interesting reactions with ground state diacetylene and with other unsaturated hydrocarbons. The products of these reactions include both long chained hydrocarbons and ring compounds such as benzene. Studies were undertaken at Argonne to use photoelectron spectroscopy to help characterize the vibronic structure in the 1 $^1\Delta_u$ state and the ground state ion, and to characterize the energetics within the triplet manifold relative to the singlet manifold. We have recorded photoelectron spectra following one-photon resonant, two-photon ionization via a number of vibronic bands of the 1 $^1\Delta_u \leftarrow$ X $^1\Sigma_g^+$ transition. Although the photoelectron spectra show evidence for progressions and combination bands in the C-C stretching mode, ν_2, these are accompanied by a number of additional bands, which may be associated with low-frequency vibrations in both the 1 $^1\Delta_u$ and X $^2\Pi_g$ states. These bands are difficult to interpret because a number of the low-frequency vibrations are Renner-Teller active and the form of the Renner-Teller interaction is different in the 1 $^1\Delta_u$ and X $^2\Pi_g$ states. Work on these assignments is still underway. Our approach to study the triplet states is to excite the 1 $^1\Delta_u \leftarrow$ X $^1\Sigma_g^+$ transition in the expansion of the molecular beam and to probe the resulting triplet states downstream by using photoelectron spectroscopy following single-photon, vacuum-ultraviolet photoionization. Although all of the steps for these experiments have been tested individually, to date we have been unsuccessful at obtaining a photoelectron spectrum in the triplet manifold. We are currently testing some modifications to our approach that we hope will improve this situation. If this approach proves successful, it should be possible to apply it to a number of additional systems.

FUTURE PLANS

In the next year, we will continue our efforts to understand the normal-mode and electronic-state dependence of vibrational autoionization in NH_3. In particular, we will work to perform studies on autoionization via the asymmetric bending and stretching modes of the molecule. The excitation of Rydberg states involving these modes is somewhat more difficult that the excitation of the symmetric stretch and umbrella modes, but several schemes will be investigated. These studies will allow us to test our qualitative model for the mode-dependence of vibrational autoionization in significantly greater detail. We will continue to develop this model through the use of quantum chemical calculations, and we will attempt to apply it to vibrational autoionization in other molecules. In particular, thanks to the work of Ed Grant and coworkers, extensive data exist on the relative rates of vibrational autoionization for the different normal modes of NO_2 and HCO. These data should provide considerably greater insight into the general utility of our qualitative model. Additional studies on these molecules using high-resolution photoelectron spectrsocopy are also a possibility.

In the coming year, we will also continue to work toward investigating the predissociation processes that compete with vibrational autoionization in ammonia. In addition, as discussed above, the collaborations on water and diacetylene are expected to continue in FY2002, and additional experiments are planned for the Chemical Dynamics Beamline at the ALS. The latter may include studies of species such as NF_3 or PF_3, which have structures similar to NH_3.

DOE-SPONSORED PUBLICATIONS SINCE 1999

1. C. A. Raptis and S. T. Pratt
Rotational Autoionization in Ammonia
Chem. Phys. Lett., **303**, 281 (1999).

2. J. A. Bacon and S. T. Pratt
Photoelectron Spectroscopy of Rydberg States of the Methyl Radical
Chem. Phys. Lett., **311**, 346 (1999).

3. K. M. Kemner, W. Yun. Z. Cai, B. Lai, H.-R. Lee, D. G. Legnini, W. Rodrigues, J. Jastrow, R. M. Miller, S. T. Pratt, and A. J. M. Smucker
Using Zone Plates for X-Ray Microimaging and Microspectroscopy in Environmental Science
J. Synchrotron Rad., **6**, 639 (1999).

4. S. T. Pratt
Competition Between Autoionization And Predissociation In Molecular Rydberg States
in *Adv. Ser. in Phys. Chem., Vol. 10.: Photoionization and Photodetachment*, edited by C. Y. Ng (World Scientific, Singapore, 2000) p. 1011.

5. C. A. Raptis, J. A. Bacon, and S. T. Pratt
Double-Resonance Spectroscopy of Autoionizing States of Ammonia
J. Chem. Phys., **112**, 2815 (2000).

6. J. A. Bacon, and S. T. Pratt
Photoelectron Spectroscopy of Autoionizing Rydberg States Ammonia
J. Chem. Phys. **112**, 4153 (2000).

7. C. A. Raptis and S. T. Pratt
Vibrational Autoionization in Rydberg States of Ammonia
Phys. Rev. Lett., 84, 5078 (2000).

8. C. A. Raptis and S. T. Pratt
Mode-Dependent Vibrational Autoionization in Aniline
J. Chem. Phys., 113, 4190 (2000).

9. J. A. Bacon and S. T. Pratt
Photoelectron Spectroscopy of Ammonia: Mode Dependent Vibrational Autoionization
J. Chem. Phys.113, 7188 (2000).

STUDIES IN CHEMICAL DYNAMICS

Herschel Rabitz and Tak-San Ho
Department of Chemistry
Princeton University
Princeton, NJ 08544
hrabitz@princeton.edu, tsho@princeton.edu

Program Scope

This program deals with three avenues of research in chemical dynamics: (A) potential energy surface representation from *ab initio* data, (B) time-dependent reaction dynamics, and (C) global mapping between potential energy surfaces and experimental data.

Recent Progress

During the past year, research in category (A) has been pursued along several fronts: An efficient procedure based on the Reproducing Kernel Hilbert Space (RKHS) interpolation method was formulated for constructing intermolecular potential energy surfaces (PES) using not only calculated *ab initio* data but also *a priori* information on long-range interactions. Use of the reciprocal-power reproducing kernel on the semi-infinite interval $[0,\infty)$ yields a set of exact linear relations between dispersion(multipolar) coefficients and PES data points at finite internuclear separations. The construction of multidimensional PESs was facilitated by invoking a new reproducing kernel for the angular coordinates based on the optimally stable and shape-preserving Bernstein basis functions.

In collaboration with Larry Harding and George Schatz, an improved RKHS potential energy surface for the $1A''$ state of H_2O has been obtained by including new high level *ab initio* calculations, in conjunction with the adoption of Bernstein basis functions. Extensive trajectory studies are underway on the new potential surface to shed light on its effect on the $O(^1D) + H_2$ reaction.

Finally, we extended the RKHS method to handle partially filled data calculated over arbitrarily shaped regions, while keeping nearly intact its accuracy and efficiency. The extension permits points or regions to be added or removed from the grid as needed before doing expensive *ab initio* calculations, thus enabling the construction of RKHS PESs from the data distributions that are most likely to occur

in practice. The utility of the new technique was demonstrated using data from the lowest global RKHS PES for the reaction $O(^1D) + H_2$, showing that ignoring the irrelevant regions of the PES does not adversely impact the accuracy of the surfaces.

In category (B), the numerical of quantum fluid dynamics (QFD) technique is being developed for treating multidimensional molecular dynamics. As a part of this effort, a robust function approximation scheme is being developed for handling problems of irregularly distributed sampling points in high(i.e., 3 or more) dimensions. Specifically, we have implemented a construction procedure based on rational approximation, domain decomposition, and moving least squares methods. The technique involves only monomials of no higher than second order and subdivisions of the sampling data points. Numerical tests with up to six dimensional functions show that new procedure is (1) accurate in reproducing function values and derivatives up to fourth order and (2) computationally efficient because of the subdivisions. The method has been implemented in a Lagrangian QFD solver for three- dimensional dynamics problems, and it also will be applied to constructing molecular potential energy surfaces using irregularly distributed *ab initio* data.

In category (C), a global mapping method based on the high-dimensional model representation (HDMR) has been implemented in three cases: (1) constructing functional maps between diatomic potentials and various atom-atom scattering cross sections, (2) extracting potentials from scattering data, and (3) extracting potentials from spectroscopic data. In (1), a procedure is based on selected solutions of the Schrödinger equations to create mappings between large domains of potential energy space and their physical observables. The maps have been demonstrated to be effective in the nonlinear regime with the capability of providing accurate, global observable response information. In (2) and (3), a global nonlinear procedure for directly extracting molecular potentials from observables has been developed and successfully applied to obtain diatomic and triatomic potentials from differential cross sections and rotational-vibrational transition frequencies. The method ultilizes functional maps of the potential $\rightarrow$ observable relationship to facilitate the extraction process, thus, reducing the arduous task of repeatedly solving the Schrödinger equation for each trial potential. The procedure should have broad applicability for the analysis of dynamics phenomena.

Future Plans

In the coming year, we plan to continue research along the following lines:

We plan on using the RKHS PESs for quantitative studies of various chemical reactions of interest to combustion processes. We plan on implementing algorithms for fast generation of PESs and their gradients for future dynamics studies. Finally, we plan on using a newly developed, robust multi-dimensional function approximation scheme for constructing PESs involving four or more atoms. The scheme based on rational approximation, domain decomposition, and moving least squares methods will play an important role in the research on solving the QFD equations in the Lagrangian description.

The QFD formulation for numerical simulation of molecular dynamics can achieve significant time savings by taking into account that (1) the quantum fluid variables, i.e., density and phase, are generally slowly varying spatially and (2) state of the art fluid dynamics methodologies are widely available. Furthermore, the moving grid Lagrangian scheme makes possible the study of high dimensional problems. We plan on using the QFD approach, especially, within the Lagrangian framework, to study reactive dynamics of several tri- and tetra-atomic systems, including $S+H_2$, $O+H_2$, $N+H_2$, and $H+H_2O$.

The HDMR procedure will be further developed to generate efficient global mappings between potential energy surfaces and experimental data. We plan to explore the use of HDMR maps for a large class of triatomic PESs and various observables associated with both non-reactive and reactive dynamics.

Publications of DOE Sponsored Research(1999 - Present)

1. Efficient Input-output Model Representation, H. Rabitz, O. F. Alis, J. A. Shorter, and K. Shim; Computer Phys. Comm., **117**, 11 (1999).

2. An Efficient Chemical Kinetics Solver Using High Dimensional Model Representation, J. A. Shorter, P. C. Ip, and H. Rabitz, J. Phys. Chem., **103**, 7192 (1999).

3. Exploring the Reaction Dynamics of Nitrogen Atoms: A Combined Crossed Beam and Theoretical Study of $N(^2D) + D_2 \rightarrow ND + D$, M. Alagia, N. Balucani, L. Cartechini, P. Casavecchia, G. G. Volpi, L. A. Pederson, G. C. Schatz, G. Lendvay, L. B. Harding, T. Hollebeek, T.-S. Ho, and H. Rabitz; J. Chem. Phys., **110**, 8857 (1999).

4. Constructing Multidimensional Molecular Potential Energy Surfaces from Ab Initio Data, T. Hollebeek, T.-S. Ho, and H. Rabitz; Annu. Rev. Phys. Chem., **50**, 537 (1999).

5. Potential Energy Surface and Quasiclassical Trajectory Studies of the $N(^2D) + H_2$ Reaction, L. A. Pederson, G. C. Schatz, T.-S. Ho, T. Hollebeek, H. Rabitz, L. B. Harding, and G. Lendvay; J. Chem. Phys., **110**, 9091 (1999).

6. Quantum Fluid Dynamics in the Lagrangian Representation and Applications to Photodissociation Problems, F. Sales Mayor, A. Askar, and H. Rabitz, J. Chem. Phys., **111**, 2423 (1999).

7. Potential Energy Surface of the A State of NH_2 and the Role of Excited States in the $N(^2D) + H_2$ Reaction, L. A. Pederson, G. C. Schatz, T. Hollebeek, T. S. Ho, H. Rabitz, and L. B. Harding; J. Phys. Chem., **104**, 2301 (2000).

8. On the Importance of Exchange Effects in Three-Body Interactions: The Lowest Quartet State of Na_3, J. Higgins, T. Hollebeek, J. Reho, T.-S. Ho, K.K. Lehmann, H. Rabitz, G. Scoles, and M. Gutowski; J. Chem. Phys., **112**, 5751 (2000).

9. Reproducing Kernel Technique for Extracting Accurate Potentials from Spectral Data: Potential Curves of the Two-Lowest States $X^1\Sigma_g^+$ and $a^3\Sigma_u^+$ of the Sodium Dimer, T.-S. Ho, H. Rabitz, and G. Scoles; J. Chem. Phys.,**112**, 6218 (2000).

10. Solving the Bound-State Schrödinger Equation by Reproducing Kernel Interpolation, X.-G. Hu, T.-S. Ho, and H. Rabitz; Phys. Rev. E, **61**, 2074 (2000).

11. Solutions to Quantum Fluid Dynamics using Radial Basis Functions, X.-G. Hu, T.-S. Ho, and H. Rabitz; Phys. Rev. E, **61**, 5967 (2000).

12. Proper Construction of *ab initio* Global Potential Surfaces with Accurate Long-range Interactions, T.-S. Ho and H. Rabitz; J. Chem. Phys.,**113**, 3960 (2000).

13. Efficient Potenial Energy Surfaces from Partially Filled *ab initio* Data over Arbitrarily Shaped Regions, T. Hollebeek, T.-S. Ho, and H. Rabitz, J. Chem. Phys.,**114**, 3940 (2001).

14. Construction of Reproducing Kernel Hilbert Space Potential Energy Surfaces for the $1A''$ and $1A'$ States of the Reaction $N(^2D) + H_2$, T. Hollebeek, T.-S. Ho, H. Rabitz, and L. B. Harding, J. Chem. Phys.,**114**, 3945 (2001).

Reactions of Atoms and Radicals in Pulsed Molecular Beams

Hanna Reisler
Department of Chemistry, University of Southern California
Los Angeles, CA 90089-0482
reisler@chem1.usc.edu

Program Scope

We study photoinitiated reactions of molecules and free radicals that involve competitive pathways and/or isomerization by exploiting multiple-resonance excitation schemes, state-selected product detection, and photofragment translational spectroscopy and ion imaging for generation of correlated distributions. Reaction thresholds are reached either via radiationless transitions from electronically excited states, or by overtone excitation in the ground state.

Recent Progress

The hydroxymethyl radical (CH_2OH) and its isomer, the methoxy radical (CH_3O) are important species in fuel combustion and in atmospheric and interstellar chemistry. CH_2OH, being much more reactive than CH_3O, is also of importance in polluted environments. The isomerization $CH_2OH \leftrightarrow CH_3O$ is intriguing because the calculated barrier is comparable to the $H + CH_2O$ dissociation barrier.[1,2] The study of the photodissociation dynamics of CH_2OH is intriguing for several reasons. First, excitation accesses vibronically resolved Rydberg states, and therefore Rydberg-valence interaction must influence the subsequent dynamics. Second, there is more than one pathway that can terminate in D/H photofrag-ments. Third, the role of isomerization to the methoxy radical can be investigated by comparing the H and D signals obtained in the photolysis of CD_2OH and CH_2OD. Fourth, there are additional distinct chemical channels that can be accessed, e.g. $CH_2 + OH$, $H_2 + HCO$ etc. Last, the combination of a structured vibronic spectrum and multiple dissociation pathways opens the possibility of observing mode or bond specificity in the dissociation.

We produce the radical in a molecular beam using the photoinitiated reaction, $Cl + CH_3OH \rightarrow HCl + CH_2OH$. The reaction is carried out in a quartz tube extension to the pulsed valve under conditions that suppress the rapid consecutive reaction $Cl + CH_2OH \rightarrow CH_2O + HCl$. With a production method at hand, we characterized the state observed previously by REMPI.[1] Based on fittings of rotational line contours at 300 K (flow tube) and 10 K (molecular beam), we reassigned it as the $3p_z(^2A'')$ state, i.e. the fourth excited state of the radical, and determined its lifetime at ~ 1 ps. This was an important first step, because it established the surface crossings that may be necessary for dissociation to ground state products.

Last year we reported our first results identifying H(D) as a photodissociation product of $CH_2OH(D)$ following excitation in the origin band of the $^2A''(3p_z) \leftarrow {}^2A''(\pi^*)$ transition. Since other sources in the reactive mixture might give rise to H/D atom signals, it was imperative to first establish a direct correspondence between the absorption features of CH_2OD and the observed D atom signal. For this reason, photofragment yield spectroscopy was carried out in selected regions of the absorption spectrum of CH_2OD. Because of the large H background in our apparatus, the isotopomers CH_2OD and CD_2OH were used.

The initial work has demonstrated that the $D + CH_2O(S_0)$ channel is a major pathway in the dissociation of CH_2OD excited to the origin band of the $^2A''(3p_z)$ Rydberg state. The mechanism involves predissociation, and the dissociation lifetime is on the order of a

picosecond. Because of H ion background in the experimental setup, our first study concerned only the D photofragments from CH_2OD. D atoms appeared as major products from CH_2OD, but the H photofragment signal was not discerned above the background with sufficient signal to noise ratio.

The D photofragment was examined following origin band excitation using the "core sampling" variant of time-of-flight (TOF) spectroscopy. Both the kinetic energy release and the effective recoil anisotropy parameter, β_{eff}, were determined. The product kinetic energy distribution (KED) was broad, indicating that the formaldehyde co-fragment was in the ground electronic state but its internal energy extended to the thermochemical limit. The recoil anisotropy parameter β corresponded to fast (< 1 ps) dissociation. The results were rationalized by a mechanism that involved nonadiabatic transitions from the initially excited Rydberg state terminating in the ground state.

The previous results were affected by our inability to examine directly H photofragments; they were considered preliminary and the conclusions tentative. Therefore, we decided to improve the experimental conditions, in order to eliminate background. An important step was the replacement of the source chamber diffusion pump with a turbomolecular pump. With the system now evacuated only by turbo pumps, we re-examined the H/D signals, and this time we saw H and D signals correlated with REMPI for both CH_2OD and CD_2OH.

As seen in Fig. 1, the KED's corresponding to the H and D fragments are very different for the two isotopomers of CH_2OH. Whereas the D and H signals from CH_2OD and CD_2OH, respectively, are broad and extend to ~ 4 eV, the corresponding H and D signals are much narrower, terminating at 1.5-2.0 eV. Thus, there are at least two different pathways leading to H and D. It is also clear now why we had such difficulty discerning these signals above a large background: the KED of the slow H is very similar to that from the cracking of pump oil. We also note that the KED of H from CH_2OH appears as the sum of the distributions from the other two isotopomers.

With < 244 nm excitation, the possible sources of H(D) atoms originating in C-H(D) fission are: (i) isomerization to methoxy followed by dissociation on the ground electronic state; (ii) direct C-H(D) bond cleavage on an excited electronic state; (iii) 1,2 elimination with formation of H(D)CO, which then dissociates to H(D) + CO. Regarding channel (ii), the KED seems to extend slightly above the energetically allowed value. However, the heat of formation of HCOH is only calculated, not measured, so the energetic limit is an estimate. Also, the possibility that channel (ii) is the major source of C-bound H/D, while only the small fraction extending to higher energies derives from isomerization, cannot be excluded. Thus, the role of isomerization remains unsettled.

In order to further elucidate the pathways responsible for H/D formation from the $3p_Z$ state, accurate measurements of β, the recoil anisotropy parameter, for both H and D fragments are needed, and those are currently in progress. Our preliminary results indicate that β is speed dependent, and if verified this will indicate how many dissociation pathways are important.

We have also started to examine how the dissociation mechanism is affected by exciting peaks other than the origin band of the $3p_Z(A'') \leftarrow \tilde{X}^2A''$ transition. With CH_2OD, we have obtained D photofragment yield spectra and KED's between 245 and 225 nm, and found that

as the energy above the origin band increases, a *slow* component in the D speed distribution starts to grow in, whose relative importance increases with increasing excitation energy. Figure 2 compares the speed distributions of D from CH_2OD in the origin and 6_0^1 band regions (which are separated by 1621 cm^{-1}). Does the slow component correlate with the opening of another channel, or is this merely an energy dependent branching ratio between the previously observed channels? We will get an answer to this question in the next few months, by examining also the H product, and carrying out similar experiments with CD_2OH.

According to *ab initio* calculations, three other Rydberg states lie below the $3p_z$ state ($3p_y$, $3p_x$ and $3s$). All have planar geometries similar to that of ground state CH_2OH^+.[1,3] These states are located at energies lower than the $3p_z$ state by up to 1.2 eV. Because of the proximity of the $3p_z$ state to the other Rydberg states, Franck-Condon considerations would favor initial couplings to one or more of these states, leading to a sequential coupling mechanism finally terminating in a crossing to the ground state. No calculations including both valence and Rydberg states have yet been reported; thus, the issue of the specific nonadiabatic interactions leading to products remains open.

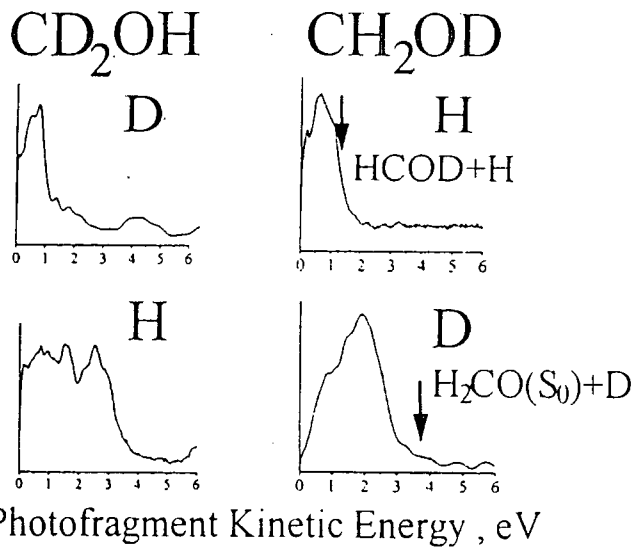

Figure 1: Kinetic energy distributions of H and D from CH_2OD and CD_2OH.

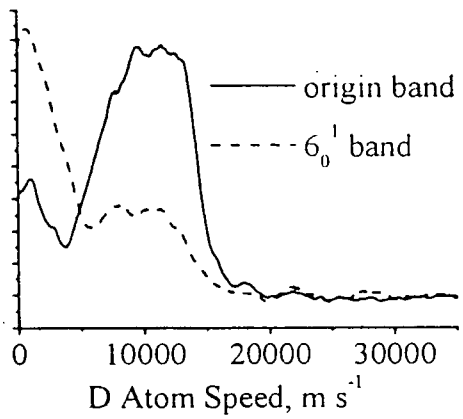

Figure 2: Speed distributions of D atoms from CH_2OD in the origin and 6_0^1 bands of the $3p_z(^2A'') \leftarrow \tilde{X}^2A''$ transition.

Clearly, it is desirable to minimize the number of possible participating potential energy surfaces (PES), and to excite the radical to the lowest electronic state; i.e., the $3s(^2A')$ Rydberg state. In order to carry out the spectroscopic experiments on the excited and ground states of the hydroxymethyl radical, we have recently purchased an OPO system that allows scanning over the region from 1.4 μ (10 mJ) to 223 nm (4 mJ). After some delays, we finally received the laser system at the end of March. The 300 K CH_2OH absorption spectrum has a prominent peak around 285 nm,[3] and we have recently identified by 2+2 REMPI a series of predissociative band in this wavelength region using $CH_2OH(D)$ in a molecular beam. The recent reassignment of the strong REMPI transitions to $3p_z$ calls previous assignments into question, and we are currently in the process of assigning the bands, which are tentatively attributed to excitation of $3s(A')$. It is noteworthy that the vibronic structure of the new

transition is similar to that of the $^2A''(3p_z) \leftarrow {}^2A''(\pi^*)$ transition, indicating the common ion core structure of the two excited Rydberg states.

The collaboration with theory is an important aspect of our program, and we will capitalize on advances in two areas: generation of multidimensional potential energy surfaces, and characterization of surface crossings and conical intersection between electronic surfaces. David Yarkony has initiated a study of the photochemistry of CH_2OH, and has recently identified an intersection between the $3s(A')$ Rydberg state and the ground state.[4] CH_2OH is sufficiently small that with the existence of accurate data to serve as benchmarks, excellent progress can be made.

Future Plans

The experiments on the decomposition of CH_2OH and its isotopomers initiated from the $3p_z(A'')$ surface yielded a wealth of information on the dissociation pathways leading to H and D formation. The relative contributions of isomerization, H_2 elimination, and direct C-H(D) fission will be determined during the next few months. The hydroxymethyl radical can exhibit rich photochemistry both on the ground and the excited potential energy surfaces. We plan to study the photochemistry on the $3s(A')$ Rydberg state, in order to examine the isomerization and dissociation processes. We are also setting up experiments in which the OH or CH vibrational excitation will precede electronic excitation.

1. Johnson, R. D.; Hudgens, J. W. *J. Phys. Chem.* **1996**, *100*, 19874, and references therein.
2. Adams, G. F.; Bartlett, R. J.; Purvis, G. D. *Chem. Phys. Lett.* **1982**, *87*, 311; Saebø, S.; Radom, L.; Schaefer, H. F. *J. Chem. Phys.* **1983**, *78*, 845.
3. Rettrup, S.; Pagsberg, P.; Anastasi, C. *Chem. Phys.* **1988**, *122*, 45.
4. Hoffman B.; Yarkony, D. private communication, 2001.

Publications in 1999-2001:

Symmetry and lifetime of the hydroxymethyl radical in the 3p Rydberg state, V. Aristov, D. Conroy and H. Reisler, Chem. Phys. Lett., **318**, 393 (2000).

HCO rovibrational distributions from the unimolecular decomposition of H_2CO at excess energies 1100-2655 cm^{-1}, L. Valachovic, M.J. Dulligan, M.F. Tuchler, Th. Droz-Georget, M. Zyrianov, A. Kolessov, H. Reisler and C. Wittig, J. Chem. Phys., **112**, 2752 (2000).

The electronic origin and vibrational levels of the first excited singlet state of isocyanic Acid (HNCO), H. Laine Berghout, F. Fleming Crim, Mikhail Zyrianov and Hanna Reisler, J. Chem. Phys., **112**, 6678 (2000).

Photodissociation of the hydroxymethyl radical in the $3p_z$ Rydberg state: formaldehyde + hydrogen atom channel, D. Conroy, V. Aristov, L. Feng and H. Reisler, J. Phys. Chem. A, **104**, 10288 (2000).

Competitive pathways and nonadiabatic transitions in photodissociation, D. Conroy, V. Aristov, L. Feng, A. Sanov, and H. Reisler, Acc. Chem. Res., in press (2001).

Photoionization Studies of Transient and Metastable Species

Branko Ruscic
Chemistry Division, Argonne National Laboratory, 9700 South Cass Avenue, Argonne, IL 60439-4831
ruscic@anl.gov

Program Scope

In most general terms, the fundamental goal of this program is to explore, understand, and utilize the basic processes of interaction of vacuum UV light with atoms and molecules. More specifically, the program uses photoionization mass spectrometry and other related methods to study transient and metastable species that are either intimately connected to energy-producing processes, such as combustion, or play prominent roles in the associated environmental issues. The ephemeral species of interest are produced *in situ* using various suitable techniques, such as sublimation, pyrolysis, microwave discharge, chemical abstraction reactions with H or F atoms, laser photodissociation, on-line synthesis, and others. The desired information is obtained by applying appropriate photoionization techniques, which use both conventional and coherent light sources in the vacuum UV region. The *spiritus movens* of our studies is the need to provide the chemical community with essential information on the species of interest to energy-related processes, such as accurate and reliable thermochemical, spectroscopic and structural data, and thus contribute to the global comprehension of the underlying chemical reactions. The scientific motivation is additionally fueled by the intent to extract, when possible, useful generalities such as bonding patterns within a class of related compounds, or unveil systematic behavior in the ubiquitous autoionization processes and other phenomena occurring during photoionization. In addition, results obtained in this program serve as testing ground for the state-of-the-art electronic structure calculations, and have historically generated a significant impetus for further theoretical developments. The experimental work of this program is coordinated with related experimental and theoretical efforts within the Chemical Dynamics Group to provide a broad perspective on this area of science.

Recent Progress

A New Value for the Bond Dissociation Energy of Water and the Enthalpy of Formation of Hydroxyl

It is quite difficult to identify a significant number of thermochemical quantities that would be generally considered more fundamental than the bond dissociation energy of water:

$H_2O \rightarrow H + OH$ $\quad\quad$ $\Delta H^\circ_{r\,0} \equiv D_0(H\text{-}OH) = \Delta H^\circ_{f0}(OH) + \Delta H^\circ_{f0}(H) - \Delta H^\circ_{f0}(H_2O)$

Its importance arises from its ubiquity, which ranges from relatively simple (though fundamental) reactions in which the water bond is formed and/or destroyed, all the way to complex environments, such as flames or the atmosphere, where the balance between production and consumption of hydroxyl radicals is an important factor shaping the overall chemistry. $D_0(H\text{-}OH)$ – or, equivalently, $\Delta H^\circ_{f0}(OH)$– is one of the essential building blocks of models that describe such systems, where the predictive ability can suffer from inaccuracies in the enthalpies of formation of key intermediate species, such as OH. Furthermore, the significance of OH transcends the systems in which it directly participates as a reactant or product. Namely, the sequential process of building thermochemical tables that follows the "standard" order of elements: O → H → rare gases → halogens → chalcogens → pnicogens → carbon group → etc., requires $\Delta H^\circ_{f0}(OH)$ to be selected (and fixed) very early on, and hence tabulated enthalpies of formation of many other, "less fundamental" species depend directly or indirectly on the selected value for $\Delta H^\circ_{f0}(OH)$.

Two additional thermochemical quantities are tightly related to $D_0(H\text{-}OH)$ and $\Delta H^\circ_{f0}(OH)$: the bond dissociation energy of the hydroxyl radical (i.e. the second bond dissociation energy in water), $D_0(OH)$, and the enthalpy of atomization of water, $\Delta H^\circ_{at\,0}(H_2O)$, a.k.a. $\Sigma D_0(H_2O)$:

$OH \rightarrow H + O$ $\quad\quad$ $\Delta H^\circ_{r\,0} \equiv D_0(OH) = \Delta H^\circ_{f0}(H) + \Delta H^\circ_{f0}(O) - \Delta H^\circ_{f0}(OH)$

$H_2O \rightarrow 2H + O$ $\quad\quad$ $\Delta H^\circ_{r\,0} \equiv \Delta H^\circ_{at\,0}(H_2O) = 2\Delta H^\circ_{f0}(H) + \Delta H^\circ_{f0}(O) - \Delta H^\circ_{f0}(H_2O)$

From generally accepted thermochemistry,[1-3] $\Delta H_{atomiz\,0}^\circ(H_2O)$, which does not involve $\Delta H^\circ_{f0}(OH)$, can be obtained as 219.355 ± 0.024 kcal/mol = 76720.7 ± 8.3 cm^{-1}. Once this quantity is fixed, there is but one degree of freedom among the remaining three quantities: $D_0(H\text{-}OH)$, $D_0(OH)$, and $\Delta H^\circ_{f0}(OH)$, and determining any

one of these is equivalent to determining all three.

The best currently available[4] (and generally accepted) D_0(H-OH) = 118.08 ± 0.05 kcal/mol is based[2] on $\Delta H°_{f0}$(OH) = 9.347 ± 0.048 kcal/mol, which is in turn based on a spectroscopic determination[5] D_0(OH) = 35420 ± 15 cm^{-1}. The widely used JANAF value $\Delta H°_{f0}$(OH) = 9.18±0.29 kcal/mol is a result of a series of unfortunate errors. First of all, JANAF discusses only the older spectroscopic determination of D_0(OH) = 35450 ± 100 cm^{-1}, which, if accepted, should result in $\Delta H°_{f0}$(OH) = 9.26 ± 0.29 kcal/mol (given explicitly in the discussion). However, with no explanation, the actual tables use a different value, apparently arising by inadvertent use of D_0(OH) = 35480 ± 100 cm^{-1}. The OH data in JANAF is also afflicted by additional inaccuracies, the most serious one being an incorrect treatment of the degeneracy and multiplicity of the ground state of OH, resulting in substantial errors in the calculated heat capacity and enthalpy increments.

In contrast to D_0(H-OH) that is based on the spectroscopic value for D_0(OH), the positive ion cycle produces a different value. Using the available appearance energy[6] of OH^+ fragment from H_2O, $AE_0(OH^+/H_2O)$ = 18.115 ± 0.008 eV and the adiabatic ionization energy[7] of OH, IE(OH) = 13.0170 ± 0.0003 eV produces D_0(H-OH) = 117.56 ± 0.18 kcal/mol, which is significantly lower (0.52 kcal/mol or ~180 cm^{-1}). This discrepancy has been known for some time,[4] with the tacit assumption that the positive ion cycle is for some reason in error. However, more recently there were additional hints that the accepted values for D_0(H-OH)/D_0(OH)/$\Delta H°_{f0}$(OH) may not be accurate. For example, we have recently determined $\Delta H°_{f0}(CH_3)$ = 35.86 ± 0.07 kcal/mol, $\Delta H°_{f0}(CH_2)$ = 93.18 ± 0.20 kcal/mol, $D_0(H\text{-}CH_3)$ = 103.42 ± 0.03 kcal/mol, $D_0(H\text{-}CH_2)$ = 108.95 ± 0.20 kcal/mol, and $D_0(H\text{-}CH_2$ to $^1A_1$ $CH_2)$ = 117.97 ± 0.20 kcal/mol. One consequence of these determinations is that the reaction of singlet methylene with water becomes, if anything, slightly endothermic:

$^1CH_2 + H_2O \rightarrow CH_3 + OH$ $\quad \Delta H°_{r\,0} \equiv D_0(H\text{-}OH) - D_0(H\text{-}CH_2$ to $^1A_1$ $CH_2) = 0.11 \pm 0.20$ kcal/mol

while most mechanisms require it to be slightly exothermic. In addition, a recent analysis[9] of the forward and backward rates for $OH + O \rightarrow H + O_2$ appeared to suggest a lower enthalpy for OH. Finally, there was growing clamor among some kineticists that the enthalpy of OH should be revised (although the proposed revision would change the enthalpy in the opposite direction).

A logical analysis of the basic discrepancy between the spectroscopic value for D_0(OH) and the positive ion cycle value for D_0(H-OH) leads to the conclusion that either:

1) The total atomization energy of H_2O is too high
2) The spectroscopic determination of D_0(OH) is too low
3) The positive ion cycle is in error because
   a. The adiabatic ionization energy of OH is too high
   b. The appearance energy of the OH^+ fragment from H_2

While any of the above appear surprising, further scrutiny shows that 1) is extremely unlikely. Hypothesis 2) is possible, since D_0(OH) was obtained by a Birge-Sponer extrapolation (notorious for errors). However, this would mean that an error of 180 cm^{-1} accumulated over a ~270 cm^{-1} extrapolation, which is difficult to believe, on top of the fact that there appears to be further support for the spectroscopic value from observed predissociation. Hypothesis 3a) also appears to be beyond reproach, since the IE has been confirmed in a number of photoelectron and photoionization studies (including our own unpublished data). Hypothesis 3b) is surprising at first glance, since a properly extracted appearance energy is an upper limit, but experimental artifacts such as pressure/field effects or inaccurate energy calibration are possible. Hence, we have extremely carefully re-examined by photoionization the fragmentation threshold of OH^+ from water, mindful of effects that may cause a false early onset, expecting to find some error in the previous determination. However, the result we have obtained, $AE_0(OH^+/H_2O) = 18.116_1 \pm 0.003_5$ eV is only ~1 meV higher than the literature value (the shift needed to reconcile the discrepancy is ~22 meV). Given the importance of the issue, we have sought further confirmation in collaboration with C.-Y. Ng. Indeed, the PFI-PEPICO coincidence experiment produces an upper limit of 18.120±0.005 eV, and the PFI spectrum reveals a step-like structure in the appropriate region. The consensus (weighted average) value of these three photoionization experiments is $AE_0(OH^+/H_2O) = 18.116_5 \pm 0.003_0$ eV. With the known and confirmed IE(OH), this produces D_0(H-OH) = 41130 ± 25 cm^{-1} = 117.60 ± 0.07 kcal/mol, corresponding to D_0(OH) = 35590 ± 25 cm^{-1} = 101.76 ± 0.07 kcal/mol and ΔH_{f0}(OH) = 8.86 ± 0.07 kcal/mol, which are the values that we currently recommend.

Since it appears that the positive ion cycle result is correct, the burden of proof is to show that the spectroscopic $D_0(OH)$ is wrong. In order to demonstrate this, we have intensely collaborated with our theoretical colleagues (A. Wagner and L. Harding, ANL). The potential energy curve of the A state of OH (which was used for the extrapolation) has been calculated using CAS+1+2 with Davidson correction and aug-cc-pV5Z basis set and solved for the vibrational levels. A Birge–Sponer extrapolation using all but the last (unobserved) vibrational level, very closely resembles the experimental one, and clearly underestimates both the position of the unobserved level and the D_0 value, showing that the original Birge-Sponer extrapolation is wrong. Further analysis shows that even the inclusion of the unobserved level does not produce the correct D_0. Other extrapolation methods, that stay away from the Dunham expansion and are based on functions that more appropriately describe the long-range behavior were also tried, but were unable to produce a firm D_0. RKR curves show that the supported vibrational levels (including the last level) simply do not carry sufficient information on the long-range behavior of this potential. In addition, a close scrutiny of the observed predissociation shows that the observed patterns support equally well (or in fact better) the present $D_0(OH)$.

Finally, we have tried to attain further support for the new values from state-of-the-art electronic structure calculations, which in favorable cases start to be just enough accurate to distinguish differences of the order of 0.5 kcal/mol. Our colleagues at PNNL (D. Dixon, D. Feller, K. Paterson) have carried out CCSD(T) calculations extrapolated to CBS with further corrections (core-valence, scalar relat. corr., FCI corr., exp. spin-orbit). When the highest basis set used was of 6-ζ quality, the results started to be accurate enough and began providing support our new values, but were only marginally convincing, since the atomization energy of water was still off by ~0.3 kcal/mol. However, after a heroic effort to compute O, O^+, OH, OH^+, and H_2O using a 7-ζ basis set, the calculated results achieved extraordinary agreement with our experimental values (to within 0.02 kcal/mol!). These are the highest-level ab initio calculations everperformed for any non-atomic system, and the achieved accuracy is very pleasing. However, there are very few systems for which this level of calculation will be possible in the foreseeable future.

There are numerous consequences of the change in $D_0(H\text{-}OH)$. For example, the gas-phase acidity of water becomes $\Delta G°_{acid\,298}(H_2O) = 383.61\pm0.07$ kcal/mol and $\Delta H°_{acid\,0}(H_2O) = 389.04\pm0.07$ kcal/mol. The reaction of singlet methylene with water becomes slightly exothermic, 0.39 ± 0.20 kcal/mol at 0 K. Several proton affinities change, as well as all R-OH dissociation energies of alcohols, all reaction enthalpies of the type $OH + RH \rightarrow H_2O + R$, and, in fact, all reactions involving OH, etc. Finally, it is not presently clear how many other enthalpies of formation are affected directly or indirectly.

Rotational Autoionization in the Ionization Threshold Region of CH_3

Based on medium-resolution spectra, we have recently reported that the ionization threshold region of CH_3 shows indirect evidence of rich rotational autoionization. We have now obtained high-resolution spectra using our VUV laser setup, fully confirming our prior inferences. Methyl has been prepared by a novel approach that utilizes laser photolysis to generate radicals well-equilibrated at a known temperature (which is needed here both to have a known initial population of neutral CH_3 and to control the population of higher J states, for which this phenomenon is more promptly discerned). The detailed analysis of the spectra is still in progress, but so far we seem to see evidence for both even and odd loss of rotational quanta, as well as evidence for weak K-switching during the autoionization process as well as during the direct ionization process.

Other progress

We had a very successful collaboration (L. Butler, U. of C., who reports some of the details) on the characterization of photodissociation products of trimethylamine at the ALS. In our laboratory, we are currently measuring the photoionization spectra of CH_2OCH_3 radical, and attempting to enhance and modernize both our photoionization setups. We are also currently in the process of developing and implementing radical sources for the ALS at Berkeley. We are developing a novel approach to determination of thermodynamical quantities that involves the use of thermochemical networks and will eventually lead to the development of "active" thermochemical tables. Finally, we are involved in an IUPAC Task Force that aims to critically evaluate thermochemical quantities of combustion-related radicals.

Future Plans

Future plans of this program pivot around the continued investigation of radicals and transient species that are intimately related to combustion processes, particularly those that potentially define the initial attack of O_2 on hydrocarbon moieties during combustion, as well as other ephemeral species that are implicated in subsequent atmospheric chemistry. These investigations will continue to be correlated with other ongoing activities in the Chemical Dynamics Group, and will be enhanced by complementing the research carried in our laboratory using classical and laser sources of radiation with measurements taking advantage of the Advanced Light Source at Lawrence Berkeley Laboratory. We also intend to further test and enhance our fitting method for accurate determination of fragment appearance potentials.

This work is supported by the U.S. Department of Energy, Office of Basic Energy Sciences, Division of Chemical Sciences, under Contract W-31-109-ENG-38

References

1. J. D. Cox, D. D. Wagman, V. A. Medvedev, *CODATA Key Values for Thermodynamics*, Hemisphere, New York, 1989.
2. L. V. Gurvich, I. V. Veyts, C. B. Alcock, *Thermodynamic properties of Individual Substances*, Hemisphere, New York 1989.
3. M. W. Chase, Jr., C. A. Davies, J. R. Downey, Jr., D. J. Frurip, R. A. McDonald, A. N. Syverud, *JANAF Thermochemical Tables*, 3rd ed.; *J. Phys. Chem. Ref. Data* **14** (1985) Suppl. 1.
4. J. Berkowitz, G. B. Ellison, D. Gutman, D. *J. Phys. Chem.* **98** (1994) 2744.
5. C. Carlone, F. W. Dalby, *Can. J. Phys.* **47** (1969) 1945.
6. K. E. McCulloh, *Int. J. Mass Spectrom. Ion Phys.* **21** (1976) 333.
7. R. T. Wiedmann, R. G. Tonkyn, M. G. White, *Chem. Phys.* **97** (1992) 768.
8. B. Ruscic, M. Litorja, and R. L. Asher, J. Phys. Chem. A **103** (1999) 8625; M. Litorja and B. Ruscic, J. Chem. Phys. **108** (1998) 6748; M. Litorja and B. Ruscic, *J. Chem. Phys.* **107** (1997) 9852.
9. J. Hessler, unpublished results

Publications Resulting from DOE Sponsored Research (1998-2000)

- *Direct Observation of the Ionization Threshold of Triplet Methylene by Photoionization Mass Spectrometry*, M. Litorja and B. Ruscic, *J. Chem. Phys.* **108**, 6748-6755 (1998)
- *A Photoionization Study of Hydroperoxyl Radical, HO_2, and Hydrogen Peroxide, H_2O_2*, M. Litorja and B. Ruscic, *J. Electron Spectrosc.* **97**, 131-146 (1998)
- *Simultaneous Adjustment of Experimentally Based Enthalpies of Formation of CF_3X, X = nil, H, Cl, Br, I, CF_3, CN, and a Probe of G3 Theory*, B. Ruscic, J. V. Michael, P. C. Redfern, L. A. Curtiss, and K. Raghavachari, *J. Phys. Chem. A* **102**, 10889-10899 (1998)
- *Sum Rules and the Photoabsorption Cross Section of C_{60}*, J. Berkowitz, *J. Chem. Phys.* **111**, 1446-1453 (1999)
- *Ionization Energy of Methylene Revisited: Improved Values for the Enthalpy of Formation of CH_2 and the Bond Dissociation Energy of CH_3 via Simultaneous Solution of the Local Thermochemical Network*, B. Ruscic, M. Litorja, and R. L. Asher, *J. Phys. Chem. A* **103**, 8625-8633 (1999)
- *Photoionization of HOCO Revisited: A New Upper Limit to the Adiabatic Ionization Energy and Lower Limit to the Enthalpy of Formation*, B. Ruscic and M. Litorja, *Chem. Phys. Lett.* **316**, 45-50 (2000)
- *Characterization of Nitrogen-Containing Radical Products from the Photodissociation of Trimethylamine at 193 nm Using Photoionization Detection*, N. R. Forde, L. J. Butler, B. Ruscic, O. Shorkabi, F. Qi, and A. Suits, *J. Chem. Phys.* **113**, 3088-3097 (2000)
- *Photoionization Mass Spectroscopic Studies of Free Radicals in Gas Phase: Why and How*, B. Ruscic, *Res. Adv. Phys. Chem.* **1**, 39-75 (2000)
- *Evidence for a Lower Enthalpy of Formation of Hydroxyl Radical and a Lower Gas-Phase Bond Dissociation Energy of Water*, B. Ruscic, D. Feller, D. A. Dixon, K. A. Peterson, L. B. Harding, R. L. Asher, and A. F. Wagner, *J. Phys. Chem. A.* **105**, 1-4 (2001)

Interlocking Triplet Electronic States of Isocyanic Acid (HNCO): Sources of Nonadiabatic Photofragmentation Dynamics

Henry F. Schaefer III
Center for Computational Quantum Chemistry, University of Georgia
Athens, Georgia 30602-2525
email: hfsiii@arches.uga.edu
(706)542-2067

The triplet electronic states of isocyanic acid have been systematically investigated by means of state-of-the-art electronic structure methods, including various correlation techniques based on the coupled-cluster ansatz [CCSD, EOM-CCSD, CCSD(T), and BD(TQ)], second- through fifth-order Møller-Plesset perturbation theory (MP2-MP5), and the complete active space self-consistent field approach. The one-particle [(C,N,O)/H] basis sets for these studies ranged in quality from [4s2p1d/2s1p] to [7s6p5d4f3g2h1i/6s5p4d3f2g1h]. Vertical excitation energies were determined for the lowest 13 triplet states (5 valence, 8 Rydberg), and potential energy curves for bending to and from linearity were generated for 10 of these states, revealing intricate state interactions and numerous actual and avoided crossings. An extensive mapping was then executed for the interlocking ã $^3A''$ and b̃ $^3A'$ surfaces, which produced geometric structures, relative energies, harmonic vibrational frequencies, and selected large-amplitude vibrational eigenstates, for torsional conformers, inversion barriers, fragmentation barriers, dissociation products, and ionization limits, in addition to identifying intermingled conical intersections. The lowest-energy conformer on the ã $^3A''$ surface is actually a skewed (C_1) structure with a torsion angle of 143°, a barrier to planarity of only 74 cm^{-1}, an adiabatic excitation energy near T_0 = 30 056 cm^{-1}, and an exit barrier for ^{3}NH + CO fragmentation of only about $\Delta E_0^{\ddagger}$ = 3252 cm^{-1}. It is discovered that there are actually no legitimate minima (removed from conical intersections) on the b̃ $^3A'$ surface, because in-plane optimizations bring associated structures below the companion $^3A''$ state and subsequently connect them to the lowest triplet surface via torsional excursions along imaginary-frequency normal modes.

Research Support by the U. S. Department of Energy 1999, 2000, 2001

1. H. F. Bettinger, P. R. Schleyer, and H. F. Schaefer, "Tetradehydrobenzenes-Singlet-Triplet Energy Separations and Vibrational Frequencies," *J. Amer. Chem. Soc.* **121**, 2829 (1999).
2. T. D. Crawford and H. F. Schaefer, "An Introduction to Coupled Cluster Theory for Computational Chemists", *Reviews in Computational Chemistry* **14**, 33 (1999).
3. J. C. Stephens, Y. Yamaguchi, and H. F. Schaefer, "The Adiabatic and Vertical Ionization Potentials of NH_2 to the Three Lowest-Lying States of NH_2^+," *Keiji Morokuma Issue, J. Molecular Structure (Theochem)* **461/462**, 41 (1999).
4. G. Tarczay, A. G. Csaszar, W. Klopper, V. Szalay, W. D. Allen, and H. F. Schaefer, "The Barrier to Linearity of Water", *J. Chem. Phys.* **110**, 11971 (1999).
5. M. Hofmann and H. F. Schaefer, "The $[C_6H_{10}]^{\bullet+}$ Hypersurface: The Parent Radical Cation Diels-Alder Reaction and Alternative Pathways," *J. Amer. Chem. Soc.* **121**, 6719 (1999).
6. N. Takagi, K. Fukuzawa, Y. Osamura, and H. F. Schaefer, "Ion-Molecule Reactions Producing HC_3NH^+ in Intestellar Space: Forbiddenness of the Reaction between Cyclic $C_3H_3^+$ and the N Atom," *Astrophys. J.* **525**, 791 (1999).
7. R. I. Kaiser, I. Hahndorf, L. C. L. Huang, Y. T. Lee, H. F. Bettinger, P. R. Schleyer, H. F. Schaefer, and P. R. Schreiner, "Crossed Beams Reaction of Atomic Carbon, $C(^3P_j)$, with d_6-Benzene, C_6D_6 ($X\ ^1A_{1g}$): Observation of the Per-Deutero-1, 2- Didehydrocycloheptatrienyl Radical, $C_7D_5(X\ ^2B_2)$", *J. Chem. Phys.* **110**, 6091 (1999).
8. Y. Xie, H. F. Schaefer, X.-Y. Fu, and R.-Z. Liu, "The Infrared Spectrum of the NO Dimer Cation: Problems for Density Functional Theory and a Muddled Relationship to Experiment", *J. Chem. Phys.* **111**, 2532 (1999).
9. H. F. Bettinger, J. C. Rienstra-Kiracofe, B. C. Hoffman, H. F. Schaefer, J. E. Baldwin, and P. R. Schleyer, "Structural Isomerization of Cyclopropane: A New Mechanism Through 1–Propylidene", *J. Chem. Soc. Chem. Communications* 1515 (1999).
10. N. Balucani, O. Asvany, A. H. H. Chang, S. H. Lin, Y. T. Lee, R. I. Kaiser, H. F. Bettinger, P. R. Schleyer, and H. F. Schaefer, "Crossed Beam Reaction of Cyano Radicals with Hydrocarbon Molecules I: Dynamics of Cyanobenzene (C_6H_5CN; $X\ ^1A_1$) and Perdeutero Cyanobenzene (C_6D_5CN; $X\ ^1A_1$) Formation from Reaction of $CN(X\ ^2\Sigma^+)$ with Benzene, $C_6H_6(X\ ^1A_{1g})$ and d_6-Benzene, $C_6D_6(X\ ^1A_{1g})$", *J. Chem. Phys.* **111**, 7457 (1999).
11. N. Balucani, O. Asvany, A. H. H. Chang, S. H. Lin, Y. T. Lee, R. I. Kaiser, H. F. Bettinger, P. R. Schleyer, and H. F. Schaefer, "Crossed Beam Reaction of Cyano Radicals with Hydrocarbon Molecules II: Chemical Dynamics of 1,1-Cyanomethylallene ($CNCH_3CCCH_2$: $X\ ^1A'$) Formation from Reaction of $CN(X\ ^2\Sigma^+)$ with Dimethylacetylene, $CH_3CCCH_3(X\ ^1A_1')$", *J. Chem. Phys.* **111**, 7472 (1999).
12. M. Hofmann and H. F. Schaefer, "Pathways for the Reaction of the Butadiene Radical Cation $[C_4H_6]^{\bullet+}$ with Ethylene", *J. Phys. Chem.* A **103**, 8895 (1999).

13. N. A. Richardson, J. C. Rienstra-Kiracofe, and H. F. Schaefer, "Examining Trends in the Tetravalent Character of Group 14 Elements (C, Si, Ge, Sn, Pb) with Acids and Hydroperoxides", *J. Amer. Chem. Soc.* **121**, 10813 (1999).
14. J. C. Rienstra-Kiracofe, G. B. Ellison, B. C. Hoffman and H. F. Schaefer, "The Electron Affinities of C_3O and C_4O," *William A. Goddard Issue, J. Phys. Chem.* A **104**, 2273 (2000).
15. R. A. King, W. D. Allen, and H. F. Schaefer, "On Apparent Quantized Transition-State Thresholds in the Photofragmentation of Acetaldehyde", *J. Chem. Phys.* **112**, 5585 (2000).
16. R. I. Kaiser, O. Asvany, Y. T. Lee, H. F. Bettinger, P. R. Schleyer, and H. F. Schaefer, "Crossed Beam Reaction of Phenyl Radicals with Unsaturated Hydrocarbon Molecules. I. Chemical Dynamics of Phenylmethylacetylene ($C_6H_5CCCH_3$; X $^1A'$) Formation from Reaction of C_6H_5 (X $^2A_1$) with Methylacetylene, CH_3CCH (X^1A_1)", *J. Chem. Phys.* **112**, 4994 (2000).
17. S. T. Brown, Y. Yamaguchi, and H. F. Schaefer, "The $\tilde{X}\ ^3\Sigma^-$ and $\tilde{A}\ ^3\Pi$ Electronic States of Ketenylidene (CCO): Analysis of the Renner-Teller Effect in the Upper State", *Marilyn Jacox Issue, J. Phys. Chem.* A **104**, 3603 (2000).
18. A. G. Csaszar, W. D. Allen, Y. Yamaguchi, and H. F. Schaefer, "*Ab Initio* Determination of Accurate Ground Electronic State Potential Energy Hypersurfaces for Small Molecules", pages 15-68 in *Computational Molecular Spectroscopy*, editors P. R. Bunker and P. Jensen (Wiley, New York, 2000).
19. T. D. Crawford, S. S. Wesolowski, E. F. Valeev, R. A. King, M. L. Leininger, and H. F. Schaefer, "The Past, Present, and Future of Quantum Chemistry", pages 219 - 246 in *Chemistry for the 21st Century*, editors E. Keinan and I. Schechter (Wiley-VCH, Weinheim, Germany, 2001).
20. I. S. Ignatyev, H. F. Schaefer, and P. R. Schleyer, "Triplet States of Carbenium and Silylium Cations", *Chem. Phys. Lett.* **337**, 158 (2001).
21. M. Hofmann and H. F. Schaefer, "Structure and Reactivity of the Vinylcyclopropane Radical Cation", *Alfred Bauder Issue, J. Mol. Structure*
22. Y. Xie and H. F. Schaefer, "The Puzzling Infrared Spectra of the Nitric Oxide Dimer Radical Cation: A Systematic Application of Brueckner Methods", *Molecular Physics* **98**, 955 (2000).
23. J. C. Rienstra-Kiracofe, W. D. Allen, and H. F. Schaefer", The $C_2H_5+O_2$ Reaction Mechanism: High-Level *Ab Initio* Characterizations", *Feature Article, J. Phys. Chem. A* **104**, 9823 (2000).
24. S.-J. Kim and H. F. Schaefer, "Dimethyldioxirane, Carbonyl Oxide, and the Transition State Connecting Them: Electronic Structures, Relative Energies, and Vibrational Frequencies", *J. Phys. Chem. A* **104,** 7892 (2000).
25. H. F. Bettinger, P. R. Schleyer, P. R. Schreiner, H. F. Schaefer, R. I. Kaiser, and Y. T. Lee, "The Reaction of Benzene with Ground State Carbon Atom, $C(^3P_j)$", *J. Chem. Phys.* **113**, 4250 (2000).
26. C. J. Barden and H. F. Schaefer, "The Singlet-Triplet Separation in Dichlorocarbene: A Surprising Difference between Theory and Experiment", *J. Chem. Phys.* **112**, 6515 (2000).

27. H. F. Schaefer, "Quantum Mechanical Computations of Potential Energy Hypersurfaces", a vignette published on pages 882 - 888 of the Second Edition of *Physical Chemistry*, by R. S. Berry, S. A. Rice, and J. Ross (Oxford University Press, New York, 2000).

28. R. I. Kaiser, C. C. Chiong, O. Asvany, Y. T. Lee, F. Stahl, P. R. Schleyer, and H. F. Schaefer, "Chemical Dynamics of d_1-Methyldiacetylene (CH_3CCCCD; X^1A_1') and d_1-Ethynylallene ($H_2CCCH(C_2D)$; $X\ ^1A'$) Formation from Reaction of $C_2D(X\ ^2\Sigma^+)$ with Methylacetylene, CH_3CCH ($X\ ^1A_1'$)", *J. Chem. Phys.* **114**, 3488 (2001).

29. F. Stahl, P. R. Schleyer, H. F. Bettinger, R. I. Kaiser, Y. T. Lee, and H. F. Schaefer, "Reaction of the Ethynyl Radical, C_2H, with Methylacetylene, CH_3CCH, Under Single Collision Conditions: Implications for Astrochemistry", *J. Chem. Phys.* **114**, 3476 (2001).

30. C. J. Barden and H. F. Schaefer, "Quantum Chemistry in the Twenty-First Century", Cover Article, *Pure and Applied Chemistry* **72**, 1405 (2000).

31. E. F. Valeev, A. G. Csaszar, W. D. Allen, and H. F. Schaefer, "MP2 Limit for the Barrier to Linearity of Water", *J. Chem. Phys.* **114**, 2875 (2001).

32. E. F. Valeev, W. D. Allen, H. F. Schaefer, A. G. Csaszar, and A. L. L. East, "Interlocking Triplet Electronic States of Isocyanic Acid: Sources of Nonadiabatic Photofragmentation Dynamics", *William H. Miller Issue, J. Phys. Chem. A* **105**, 2716 (2001).

33. R. I. Kaiser, T. N. Le, T. L. Nguyen, A. M. Mebel, N. Balucar Stahl, P. R. Schleyer, and H. F. Schaefer, "A Combined Crossed and Ab Initio Investigation of Elementary Reactions with Unsatura Hydrocarbons - Pathways to Hydrogen Deficient Radicals in Flames", Faraday Discussions of the Chemical Society

34. F. Stahl, P. R. Schleyer, H. F. Schaefer, and R. I. Kaiser, Unsaturated and Hydrocarbons in Titan's Atmosphere", Planeta Space Sciences

35. B. G. Rocque, J. M. Gonzales, and H. F. Schaefer, "An Ana Conformers of 1,5-Hexadiene", Amer. Chem. Soc.

36. I. Hahndorf, Y. T. Lee, R. I. Kaiser, L. Vereecken, J. Peeters, R. Schreiner, P. R. Schleyer, and H. F. Schaefer, "A Combined C Initio, and RRKM Investigation of the Reaction of Carbon Specie Molecules I: Benzene (X^1A_{1g}) and -Benzene, ($X\ ^1A_{1g}$)", J. Chem. Phys.

GAS PHASE MOLECULAR DYNAMICS-SPECTROSCOPY AND DYNAMICS OF TRANSIENT SPECIES

Trevor J. Sears (SEARS@BNL.GOV)
Department of Chemistry, Brookhaven National Laboratory, Upton, NY 11973-5000

PROGRAM SCOPE

This research is carried out as part of the Gas Phase Molecular Dynamics group program in the Department of Chemistry at Brookhaven National Laboratory. The goal is a fundamental understanding of factors governing the structure, dynamics and reactivity of short-lived intermediates in gas phase reactions. The focus of the present work is on the development and application of sensitive, high-resolution spectroscopic techniques augmented by high-level quantum chemical calculations to investigate molecular free radicals and other transient species.

RECENT PROGRESS

New spectra of methylene, CH_2, in the near infrared have been analyzed to provide information on more than 20 vibronic states in the singlet manifold near the $\tilde{b}$ state minimum. The data provide the first experimental information on most of the levels and can be used to calibrate the accuracy of high-level *ab initio* calculations in this prototypical species. They also provide avenues for future kinetics and dynamical studies of reactions involving the radical. Figure 1 illustrates the vibronic states for which high resolution information is now available.

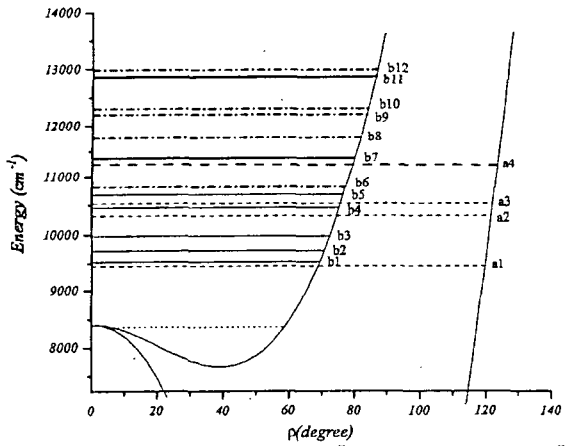

Figure 1: Cuts through the CH_2 $\tilde{a}$ and $\tilde{b}$ state potentials near the $\tilde{b}$ state minimum, along the bending coordinate. The vibronic levels characterized by the experimental measurements are shown. Labels refer to the key in Kobayashi and Sears, Can. J. Phys. 79, 1-12 (2001) and the zero point level of the $\tilde{b}$ state is shown for reference.

Other simple carbenes provide a contrast to CH_2 and can provide insight into the coupling and vibronic level mixing in methylene itself. Experimental and theoretical work has therefore also focussed on bromomethylene and very recently one aspect of the spectrum of chloromethylene. For the former, analysis of spectra obtained at wavelengths close to 1 micron has provided the first detailed picture of the rotational energy levels in the lowest few vibronic levels of the $\tilde{X}$ and $\tilde{A}$ electronic states of the radical. The experimental results strongly suggested that the ν_2 (bending) = 2 level of HCBr in its ground $\tilde{X}^1A'$ state suffers a homogeneous perturbation by the zero point level of the low-lying $\tilde{a}^3A''$ state leading to the observation of a large negative anharmonicity in the bending levels of ground state of the radical. By contrast, the same level of DCBr, lying approximately 600 cm^{-1} lower in energy, is apparently unaffected. With the help of *ab initio* calculations of the $\tilde{X}$, $\tilde{A}$ and $\tilde{a}$ state surfaces of the radical, the experimental results were modeled, resulting in an estimate of the separation between the ground singlet and coupled triplet component of 2028 cm^{-1}. Subsequently, in dispersed laser induced fluorescence spectra obtained in Taiwan, Professor Bor-Chen Chang measured many ground state vibronic level positions close to the calculated energies. Several additional peaks that could be assigned to perturbing triplet state levels were also seen, including one at 2006±8 cm^{-1}, corresponding to the triplet zero point level, thereby confirming our analysis. Hot band absorption spectra obtained at BNL include rotationally resolved transitions involving this perturbing triplet level, but have so far resisted analysis.

In addition to the work on small organic radicals, effort has been directed towards the detection of transition metal-containing radical species using laser absorption based techniques. While many diatomic

and a few triatomic species have been characterized by fluorescence-based spectroscopic techniques, data for more complex molecules is very sparse, probably because fluorescence quantum yields become small due to many competing relaxation pathways opening up as the molecules increase in size. Proof of principle experiments have been carried out resulting in new spectra of the TiO $E^3\Pi - X^3\Delta$ electronic band system. TiO was formed by laser ablation of Ti atoms followed by reaction with an oxidant seeded in low concentration in a supersonic free jet expansion source. The TiO $E - X$ system is poorly characterized in comparison to the much stronger $A - X$ and $B - X$ systems at shorter wavelengths, but dominates the near infrared spectra of certain red (late sequence) stars. Data have been analyzed for both the $v', v'' = 0,0$ and 1,0 bands and effective molecular constants and the equilibrium structure for the TiO E state derived for the first time.

FUTURE PLANS

Building on work on the HOCO radical conducted in our laboratory some years ago, new infrared spectra in the 1810-1830 cm^{-1} range are being recorded in an attempt to detect the C=O stretching vibrational mode of *cis*-HOCO. Calculations in our group suggest this lies just 650 cm^{-1} above the lower *trans*-isomer at equilibrium and may therefore be detectable in our spectrometer. Based on the earlier measurements, the *trans* isomer spectrum in this region can be well modeled and many additional absorption lines belonging to a species with a shorter chemical lifetime have already been detected. In addition, we plan to search for overtone transitions of *trans*-HOCO in the OH stretching vibration (ν_1). Excitation of this vibration lifts the system well above the energy required for dissociation into $H+CO_2$, however a barrier, calculated to be approximately 7800 cm^{-1}, prevents dissociation occurring at the energy of the ν_1 vibrational fundamental, which was also measured some time ago. Excitation of overtones would facilitate tunneling (in the case of $2\nu_1$) or bring the system above the barrier ($3\nu_1$) presumably resulting in line broadening in either case. Detection of the overtone absorption spectrum of the radical should therefore permit a very detailed analysis of the dynamics of the dissociation on a level-by-level basis on the HOCO potential surface.

Double resonance experiments similar in character to stimulated emission pumping, but employing two c.w. near-infrared laser systems will be used in an attempt to simplify the observed spectrum of HCBr in the region where singlet-triplet transitions are thought to lie. The observation of such double resonance signals would enable a measurement of the triplet-singlet spacing in HCBr to better than 10 MHz. The search problem is not severe in this case since the position of the levels are known to within a few wavenumbers and potential transitions have already been identified in hot band spectra, so HCBr should be a good test vehicle for the development of the technique. If experiments are successful, a similar experiment on methylene itself may be possible. Here the singlet-triplet splitting is still only known at the $\pm 5 cm^{-1}$ level despite work in many laboratories. Recent efforts in this laboratory to detect predicted singlet-triplet transitions in the 5 micron region were not completely successful; some absorption lines were detected, but specific transitions could not be assigned.

The singlet-singlet bands of methylene and halomethylenes are examples of type c transitions in which the rotational selection rules allow $\Delta K_a = \pm 1$ changes in the projection quantum number. In the unsymmetrical species one however frequently observes additional sub-bands with $\Delta K_a = 0$ or even ± 2. These appear because of a phenomenon known as axis switching which arises when the two electronic states involved have markedly different equilibrium structures. In this case, the body-fixed axis systems have different orientations and Hougen and Watson developed a theoretical formalism to explain the observed effects in the 1960's. It was therefore surprising to find that the observed effects in spectra of DCBr were some 4× larger than predicted. It appears the discrepancy is also present in spectra of HCCl and DCCl and we have carefully recorded a part of the, previously unobserved, 010-000 band of DCCl in an attempt to quantify the effect and understand the origin of the model's shortcomings.

We plan to begin a search for more complex transition metal-containing radicals now that the TiO results have proven the sensitivity of the technique. Of particular interest is the titanium-carbon system where other workers have characterized particularly stable moieties such as Ti_8C_{12} and $Ti_{14}C_{13}$, and the molybdenum-carbon system, which has shown potential as a replacement for expensive noble metal catalysts. For the titanium-carbon system, TiC and TiC_2 have both been postulated as the predominant building block in the plasma expansion used to create the larger structures. There is very little experimental information available for either of these species. We have computed their electronic structures in the ground and first few excited states and Fockenberg, Muckerman and Preses describe the results in more detail in another abstract. In collaboration with Prof. Philip Johnson (SUNY, Stony Brook) we plan to search for these species first at moderate resolution using threshold ionization techniques, then at high resolution at BNL. Similar methods will be used for the Mo-C system.

ACKNOWLEDGEMENT

Work at Brookhaven National Laboratory was carried out under Contract No. DE-AC02-98CH10886 with the U.S. Department of Energy and is supported by its Division of Chemical Sciences, Office of Science.

PUBLICATIONS SINCE 1999

1 A. J. Marr and T. Sears, J., *Hot Band Spectroscopy of DCBr near 0.96 microns, Molec. Phys.* **97,** 185-193 (1999).

2 C. Fockenberg, H. J. Bernstein, G. E. Hall, J. T. Muckerman, J. M. Preses, T. J. Sears, and R. E. Weston, *Repetitively Sampled Time-of-Flight Mass Spectrometry for Gas Phase Kinetics Studies, Rev. Sci. Instrum.* **70,** 3259-3264 (1999).

3 C. Fockenberg, G. E. Hall, J. M. Preses, T. J. Sears, and J. T. Muckerman, *Kinetics and Product Study of the Reaction of CH_3 Radicals with $O(^3P)$ Atoms using Time Resolved Time-of-Flight Spectrometry., J. Phys. Chem. A* **103,** 5722-5731 (1999).

4 J. Nolte, H. G. Wagner, T. J. Sears, and F. Temps, *The far-Infrared Laser Magnetic Resonance Spectrum of CH_2F., J. Molec. Spectrosc.* **195,** 43-53 (1999).

5 A. J. Marr and T. Sears, J., *Vibronic Reassignment of the A^1A''-X^1A' Band System of Bromomethylene, J. Molec. Spectrosc.* **195,** 367-370 (1999).

6 T. J. Sears, P. M. Johnson, and J. BeeBe-Wang, *Infrared Spectrum of the -CH_2 out-of-Plane Fundamental of C_2H_5, J. Chem. Phys.* **111,** 9213-9221 (1999).

7 P. M. Johnson and T. J. Sears, *Vibrational Effects on the Torsional Motion of Ethyl Radical, J. Chem. Phys.* **111,** 9222-9226 (1999).

8 T. C. Steimle, M. C. Costen, G. E. Hall, and T. J. Sears, *Transient Frequency Modulation Absorption Spectroscopy of Molecules Produced in a Laser Ablation Supersonic Expansion, Chem. Phys. Letts.* **319,** 363-367 (2000).

9 K. Kobayashi, L. D. Pride, and T. J. Sears, *Absorption Spectroscopy of CH_2 near 9500 cm^{-1}, J. Phys. Chem. A* **104,** 10119-10124 (2000).

10 B.-C. Chang, M. C. Costen, A. J. Marr, G. Ritchie, G. E. Hall, and T. J. Sears, *Near Infrared Spectroscopy of Bromomethylene in a Slit Jet Expansion, J. Molec. Spectrosc.* **202,** 131-143 (2000).

11 K. Kobayashi and T. J. Sears, *Absorption Spectroscopy of Singlet CH_2 near 11200 cm^{-1}, Can. J. Phys.* **79,** 1-12 (2001).

12 H.-G. Yu, T. Gonzalez-Lezana, A. J. Marr, J. T. Muckerman, and T. J. Sears, *Experimental and Theoretical Studies of the near-IR Spectrum of Bromomethylene, J. Chem. Phys.* **XXX,** (in press) (2001).

13 K. Kobayashi, G. E. Hall, J. T. Muckerman, T. J. Sears, and A. J. Merer, *The E-X Spectrum of Jet-Cooled TiO Observed in Absorption, J. Chem. Phys.* **XXX,** (submitted) (2001).

Novel Diagnostic Techniques and Strategies: Quantitative Concentration Measurement of Carbon Monoxide by Two-Photon Laser-Induced Fluorescence

T. B. Settersten and R. L. Farrow
Combustion Research Facility, Sandia National Laboratories
P.O. Box 969, MS 9056
Livermore, CA 94509-0969
Telephone: (925) 294-4701, email: tbsette@sandia.gov

Program Scope

The primary objective of this program is the development of novel laser-based techniques for combustion chemistry and reacting flow research. Efforts focus on techniques that demonstrate high specificity, sensitivity, and spatial and temporal resolution. This work includes the development of new laser-induced fluorescence strategies and supporting research, multiphoton ionization and stimulated emission techniques for the sensitive detection of atoms and radicals, and new techniques that exploit advances in coherent Raman or resonant wave-mixing spectroscopies.

Recent Progress

Two-photon LIF of CO. The ultimate goal of this particular project is the development of a comprehensive model for the detection of CO via two-photon laser-induced fluorescence (TP-LIF) using excitation at 230 nm. The model must properly account for the dependencies of excitation dynamics, quenching, and ionization on the laser and environmental parameters as well as for the unintended consequence of photolytically produced CO. We use appropriate experiments to characterize each of these processes individually. Then, the results of the characterizations are incorporated, along with other measured spectroscopic constants, in the LIF simulation code. This model will assists researchers in the quantification of TP-LIF data.

Several experiments, funded by the DOE BES program, have already provided data for several critical pieces of the model. These include measurements of the two-photon cross section,[1] the ionization cross section and ac Stark shift,[2] and the temperature-dependent collisional-broadening and shift coefficients.[3] Research designed to study the remaining pieces of the model, which describe quenching and photolytic effects, is currently underway.

Here, we describe recent measurements of the temperature- and species-dependent quenching of the $B\ ^1\Sigma^+$ (v'=0) state of CO. Although surveys of CO quenching rates in flames have been reported,[4] additional data are needed over wider temperature ranges and for individual quencher species. To this end, the self-quenching cross section and quenching cross sections for collisions with noble gases (He, Ne, Ar, Kr, Xe) and major flame species (H_2, N_2, O_2, CO, H_2O, CO_2, and CH_4) were measured for temperatures ranging from 293 K to 1023 K.

A diagram of the experiment is shown in Fig. 1. The CO $B\,^1\Sigma^+$ (v=0) state was populated via two-photon excitation ($X\,^1\Sigma^+ \rightarrow\rightarrow B\,^1\Sigma^+$) using the frequency-tripled output of a pulse-amplified distributed-feedback dye laser (55-ps pulsewidth). The $B\,^1\Sigma^+ \rightarrow A\,^1\Pi$ fluorescence was collected, spectrally filtered, and detected with a microchannel-plate photomultiplier tube (350-ps falltime). Direct measurement of fluorescence-decay rates of up to 200 MHz was afforded by the use of picosecond excitation and the high-bandwidth detector.

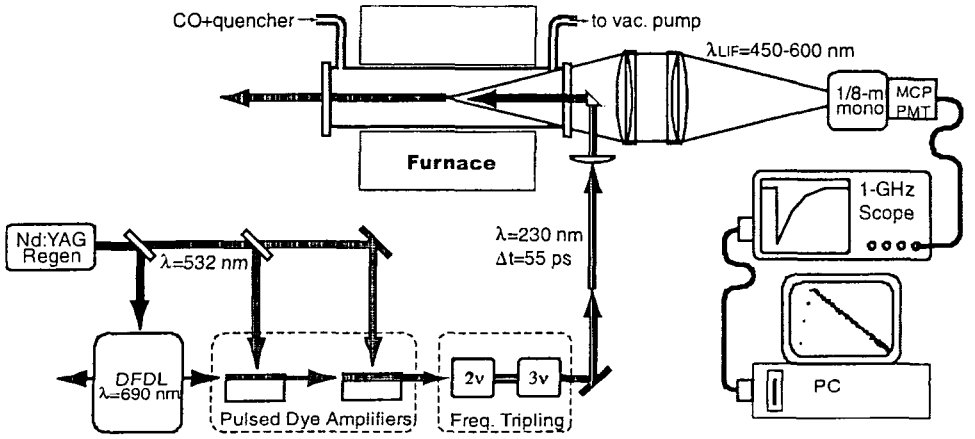

Fig. 1. Experimental setup for time-resolved measurement of TP-LIF of CO. The frequency-tripled pulse-amplified distributed-feedback dye-laser produces 55-ps pulses at 230 nm with over 100 μJ/pulse. The laser is focused to the center of a pressure- and temperature-controlled vacuum cell. Fluorescence from the center of the cell is detected with fast detection electronics, characterized by a Gaussian instrument response with a width of 600 ps (FWHM).

Quenching cross sections were determined from the dependence of the fluorescence-decay rate on quencher-gas pressure. CO and the quencher gas were admitted into a vacuum cell that was placed in a temperature-controlled furnace. LIF decays were collected for gas temperatures of 293 K, 523 K, 773 K, and 1023 K. A summary of the quenching measurements for the major flame species is shown in Fig. 2. Here, we plot the quenching rate coefficient as a function of the gas temperature and use a power-law dependence on temperature to fit the data,

$$q(T) = q_{293}(T/293)^{-x}.$$

The strongest quenchers at room temperature, H_2O, CO_2, CH_4, and O_2, also have the largest negative temperature dependence. Extrapolating the best-fit power-law relationships to 2000 K (shown as dashed lines in the figure), the quenching rate coefficients for these molecules converge to a narrow range between 5 and 7 MHz/Torr.

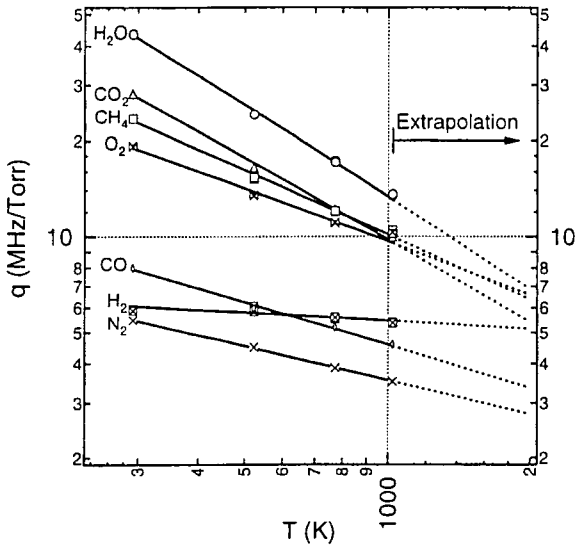

Fig. 2. Measured quenching rate coefficients (symbols) and power-law fits to the data (lines) for several important flame species.

Future Plans

Photolytic interference in the detection of CO by two-photon LIF. Two-photon LIF at 230 nm requires sufficiently high pulse energies that ambient, high-temperature CO_2 may be photolyzed to produce O and CO.[5] With a 5- to 10-ns laser pulse, photolytic CO is produced and detected by the same pulse, limiting the detection sensitivity for native CO. We will study the photolysis of CO_2 as a function of temperature and pulse energy to quantify the interference in TP-LIF measurements at 230 nm. The experiment will photolytically produce CO with one laser, and probe it with TP-LIF using a delayed probe laser. Recently, a second detection scheme involving excitation at 217 nm ($C\ ^1\Sigma^+ \leftarrow\leftarrow X\ ^1\Sigma^+$) has been suggested as an alternative to the commonly used 230-nm excitation of $B\ ^1\Sigma^+ \leftarrow\leftarrow X\ ^1\Sigma^+$.[6] The advantage is a shorter wavelength emission band that has less crosstalk with C_2 Swan lines in flames. However, the 217-nm excitation may suffer from increased photolytic interference because the spin-forbidden dissociation channel $CO_2 \rightarrow CO(X\ ^1\Sigma) + O(^3P)$ has an energy threshold corresponding to a 227.35-nm photon. Therefore, in addition to the measurements at 230 nm, we will also make the measurements with a 217-nm photolysis laser. In doing so, we will determine if the photolysis cross section is significantly different for the two TP LIF schemes

Two-photon-LIF of CO: a comprehensive LIF code. Detection of CO via two-photon excitation of $B \leftarrow\leftarrow X(0,0)$ requires knowledge of the effective lifetime of the $B(v=0)$ state, which depends on collisional quenching, photoionization, and spontaneous emission rates. We are developing an understanding of all of these processes as a result of work in our laboratory. We have measured the rate constants for quenching of CO $B\ ^1\Sigma^+$ ($v=0$) by important combustion species and noble gases between 295 K and 1023 K. Building on modeling approaches pioneered by P. Paul,[7,8] we will use the complete set of quenching measurements to develop a predictive model for the quenching cross-sections in combustion environments. We will incorporate the quenching and photolysis models (see above) and an LIF rate-equation model (based on our measured absorption,

broadening, and photoionization cross-sections) into a comprehensive LIF simulation code, which will be made available to interested users. The code will be designed to allow researchers with limited laser-diagnostics expertise to derive accurate CO concentrations from TP-LIF measurements in combustion environments.

Cited References

1. M. D. Di Rosa and R. L. Farrow, J. Opt. Soc. Am. B **16**, 1988 (1999).
2. M. D. Di Rosa and R. L. Farrow, J. Opt. Soc. Am. B **16**, 861 (1999).
3. M. D. Di Rosa and R. L. Farrow, J. Quant. Spectrosc. Radiat. Transfer **68**, 363 (2001).
4. see, for example, S. Agrup and M. Aldén, Appl. Spectrosc. **48**, 1118 (1994).
5. A. P. Nefedov, V. A. Sinel'shchikov, A. D. Usachev, and A. V. Zobnin, Appl. Opt. **37**, 7729 (1998).
6. S. Linow, A. Dreizler, J. Janicka, E. P. Hassel, Appl. Phys. **B71**, 689 (2000).
7. P.H. Paul, J. L. Durant Jr., J. A. Gray, and M. R. Furlanetto, J. Chem. Phys. **102**, 8378 (1995).
8. P.H. Paul, J. A. Gray, J. L. Durant Jr., and J. W. Thoman Jr., Chem. Phys. Lett. **259**, 508 (1996).

Theoretical Studies of Potential Energy Surfaces and Computational Methods

Ron Shepard
Chemistry Division
Argonne National Laboratory
Argonne, IL 60439
[email: shepard@tcg.anl.gov]

Program Scope: This project involves the development, implementation, and application of theoretical methods for the calculation and characterization of potential energy surfaces (PES) involving molecular species that occur in hydrocarbon combustion. These potential energy surfaces require an accurate and balanced treatment of reactants, intermediates, and products. This difficult challenge is met with general multiconfiguration self-consistent-field (MCSCF) and multireference single- and double-excitation configuration interaction (MRSDCI) methods. In contrast to the more common single-reference electronic structure methods, this approach is capable of describing accurately molecular systems that are highly distorted away from their equilibrium geometries, including reactant, fragment, and transition-state geometries, and of describing regions of the potential surface that are associated with electronic wave functions of widely varying nature. The MCSCF reference wave functions are designed to be sufficiently flexible to describe qualitatively the changes in the electronic structure over the broad range of molecular geometries of interest. The necessary mixing of ionic, covalent, and Rydberg contributions, along with the appropriate treatment of the different electron-spin components (e.g. closed shell, high-spin open-shell, low-spin open shell, radical, diradical, etc.) of the wave functions are treated correctly at this level. Further treatment of electron correlation effects is included using large scale multireference CI wave functions, particularly including the single and double excitations relative to the MCSCF reference space. This leads to the most flexible and accurate large-scale MRSDCI wave functions that have been used to date in global PES studies.

Electronic Structure Code Maintenance and Development: A major component of this project is the development and maintenance of the COLUMBUS Program System. The COLUMBUS Program System is maintained and developed collaboratively with several researchers including Isaiah Shavitt and Russell M. Pitzer (Ohio State University), and Hans Lischka (University of Vienna, Austria). During the past year, the COLUMBUS Program System of electronic structure codes has been maintained on the various machines used for production calculations by the Argonne Theoretical Chemistry Group, including IBM RS6000 workstations, the parallel IBM SP QUAD machine at ANL, the parallel IBM SP at NERSC, and the Theoretical Chemistry Group's IBM SP parallel supercomputer. These computer codes are used in the production-level molecular applications by members and visitors of the Argonne Theoretical Chemistry Group.

In collaboration with Hans Lischka (University of Vienna, Austria) and Robert Harrison (Pacific Northwest National Laboratory), the parallel version of the CI diagonalization program CIUDG has been developed and ported to several large parallel machines. Using the TCGMSG library, this program also runs on networks of workstations, small-scale shared-memory parallel machines (e.g. Alliant and Cray), and small-scale distributed memory machines (e.g. Intel IPSC/i860). The latest version of this parallel code uses the Global Array library. The use of this library eliminates unnecessary synchronization steps from earlier versions of this code, and reduces the overall communications requirements for larger numbers of nodes. Excellent scalability on as many as 320 nodes of the Intel Delta, 256 nodes of the IBM SP, and 512 nodes on the Cray T3D and T3E have been demonstrated. One benchmark calculation by Dachsel, et al [*J.*

Phys. Chem. A, **103**, 152-155 (1999)] using this code employed a 1.3E9 CSF expansion of the wave function, the largest MRSDCI wave function ever reported. This is the first successful attempt to parallelize a production-level MRSDCI code, and this effort represents a major step forward toward using effectively the large-scale parallel supercomputers that are becoming available to scientists. Generalizations of the method are planned that will allow treatment of larger molecular systems. Future effort will be directed also to integrate the parallel version of the code with other parts of the COLUMBUS Program System to allow production-level PES calculations.

Initial applications of the MRSDCI analytic energy gradient code have begun and have included both ground and excited electronic states, and a variety of states including both closed- and open-shell systems and states of mixed valence and Rydberg character. A study of geometry optimizations for several small molecules has been initiated with the current code. This allows direct comparisons with experimental results and with other electronic structure methods. These geometry comparisons demonstrate that even with modest MCSCF reference spaces, the MRSDCI geometries compare very well with the very best single-reference methods currently in use. This is encouraging because the flexible MRSDCI wave functions are expected to be comparably accurate over the entire PES, whereas it is known that the accuracy of single-reference methods is biased toward those regions of the PES that are dominated by the reference determinant (such as near equilibrium conformations). These initial comparisons are for ground-state singlet molecules, and future work will include similar comparisons for high-spin states, radicals, and excited electronic states. Another recent application has been the study of the $1^1B_1(\sigma\text{-}\pi^*)$ and the $2^1A_1(\pi\text{-}\pi^*)$ excited states of formaldehyde. It was found that, with flexible and accurate multireference wave functions, these two states form a conical intersection (see Fig. 1). Optimization of the geometry using analytic energy gradient methods reveals a nonlinear structure, in contrast to the findings of previous theoretical studies of this state. The critical feature of the electronic structure that must be correct in order to describe this conical intersection accurately is the elimination of spurious charge contamination in the C–O bond.

The major computational step involved in MRSDCI analytic energy gradients after the energy calculation is the computation of the CI reduced density matrices. This step typically requires about 10% of the effort of the energy calculation. Very large-scale wave functions can be optimized with the parallel MRSDCI code, reducing the (wall clock) time required for this step considerably. With this reduction in computation time for the energy and wave function optimization step, this leaves the CI density step as the most significant bottleneck in the time-to-solution for PES calculations and geometry optimizations. In the past year, a parallel version of the CI density code has been developed that is based on the same basic methodology that is used in the parallel CI code. This allows the density computation to again take 10% of the time of the energy computation for large-scale MRSDCI wave functions. The first applications have been initiated with this code–the geometry optimization of C_2H_4 with a flexible multireference wave function using three orbital basis sets. The bondlengths are given in Table I for three basis sets for the MCSCF wave function and for two basis sets (the largest basis set calculation is in progress) for the MRSDCI wave function. These bondlengths are extrapolated to the infinite basis set limit in both cases and compared to the spectroscopic experimental values.

Public Distribution of the COLUMBUS Program System: The COLUMBUS Program System is available using the *anonymous ftp* facility of the internet. The codes and online documentation are now also available from the web address http://www.itc.univie.ac.at/~hans/Columbus/columbus.html. The latest code version, 5.7, was released in October, 2000. In addition to the source code, the complete online

documentation, installation scripts, sample calculations, and numerous other utilities are included in the distribution. A partial implementation of an IEEE POSIX 1009.3 library has been developed and is also available from the anonymous ftp server `ftp.tcg.anl.gov`. This library simplifies the porting effort required for the COLUMBUS codes, and also may be used independently for other Fortran programming applications.

Iterative Matrix Diagonalization: A new iterative subspace diagonalization method, called Subspace Projected Approximate Matrix (SPAM), has been developed. In a subspace method, a new trial vector is added to an existing vector subspace each iteration. The choice of expansion vectors determines the convergence rate. The traditional Davidson and Lanczos methods are examples of iterative subspace methods. In the SPAM approach, an approximate matrix is constructed each iteration using a projection operator approach, and the eigenvector of this approximate matrix is used to define the new expansion vector. The convergence rate is improved over the Davidson and Lanczos approaches by choosing an appropriate approximate matrix to define the expansion space. The efficiency of the procedure depends on the relative expense of forming approximate and exact matrix-vector products. In the past year this method has been extended in two different ways. First, it has been extended to simultaneous optimization of several roots. This is achieved by converging all of the roots at the approximate level before contracting and computing the exact matrix-vector products; this minimizes the overall effort required to optimize all of the desired eigenpairs. Second, the method has been extended to allow an arbitrary number of levels of matrix approximations. This results in a multiroot-multilevel SPAM algorithm that has a wide range of possible applications. This matrix diagonalization method has been applied to a wide range of eigenvalue problems, including optimization of the lowest eigenpairs, the highest eigenpairs, and interior eigenpairs using both root-homing and vector-following. Approximations have been generated by neglecting small matrix elements, by tensor-product approximation, by expansion truncation, by neglect of off-diagonal matrix blocks, and by operator approximation. These applications demonstrate the wide range of applicability of the SPAM diagonalization method. Work in progress is directed toward approximation of MRSDCI Hamiltonian matrices based on repulsion integral approximation.

This work was supported by the U.S. Department of Energy, Office of Basic Energy Sciences, Division of Chemical Sciences, under Contract No. W-31-109-ENG-38.

Publications:

"A Systematic *Ab Initio* Investigation on the Open and Cyclic Structures of Ozone," T. Müller, S. S. Xantheas, H. Dachsel, R. J. Harrison, J. Nieplocha, R. Shepard, G. S. Kedziora, and H. Lischka, *Chem. Phys. Letters* **293**, 72-80 (1998).

"High-Performance Computational Chemistry: Hartree-Fock Electronic Structure Calculations on Massively Parallel Processors," J. L. Tilson, M. Minkoff, A. F. Wagner, R. Shepard, P. Sutton, R. J. Harrison, R. A. Kendall, A. T. Wong, *The Int. J. High Performance Computing Applications* **13**, 291-302 (1999).

"Ab Initio Determination of Americium Ionization Potentials," J. L. Tilson, R. Shepard, C. Naleway, A. F. Wagner, and W. C. Ermler, *J. Chem. Phys.* **112**, 2292-2300 (2000).

"High-Level Multireference Methods in the Quantum-Chemistry Program System COLUMBUS: Analytic MR-CISD and MR-AQCC Gradients and MR-AQCC-LRT for Excited States, GUGA Spin-Orbit CI, and Parallel CI," H. Lischka, R. Shepard, R. M. Pitzer, I. Shavitt, M. Dallos, T. Muller, P. G. Szalay, M. Seth, G. S. Kedziora, S. Yabushita, and Z. Zhang, *Phys. Chem. Chem. Phys.* **3**, 664-673 (2001).

"Geometry Optimization of Excited Valence States of Formaldehyde Using Analytical Multireference Configuration Interaction Singles and Doubles and Multireference Averaged Quadratic Coupled-Cluster Gradients, and the Conical Intersection Formed by the $1^1B_1(\sigma\text{-}\pi^*)$ and the $2^1A_1(\pi\text{-}\pi^*)$ States," M. Dallos, T. Muller, H. Lischka, and R. Shepard, *J. Chem. Phys.* **114**, 746-757 (2001).

"The Subspace Projected Approximate Matrix (SPAM) Modification of the Davidson Method," R. Shepard, A. F. Wagner, M. Minkoff, and J. L. Tilson, *J. Comp. Phys.* (*accepted for publication*).

Table I. C_2H_4 Summary

	cc-pVDZ	cc-pVTZ	cc-pVQZ	$\infty Z^\dagger$	Expt.
MCSCF Expansion	3012	3012	3012	3012	
R(C-H)	1.1035	1.0923	1.0918	1.0917	1.081(2)
R(C-C)	1.3553	1.3477	1.3470	1.3470	1.334(2)
MRSDCI Expansion	24,098,072	197,655,128	857,810,264		
R(C-H)	1.0986	1.0834	-	1.0770	1.081(2)
R(C-C)	1.3527	1.3384	-	1.3325	1.334(2)

†The three-point MCSCF basis set extrapolation is based on the exponential model: $R_n=R_\infty+AB^{-n}$. The two-point MRSDCI extrapolation is based on the geometric model: $R_n=R_\infty+An^{-3}$. All bond lengths are in Angstroms.

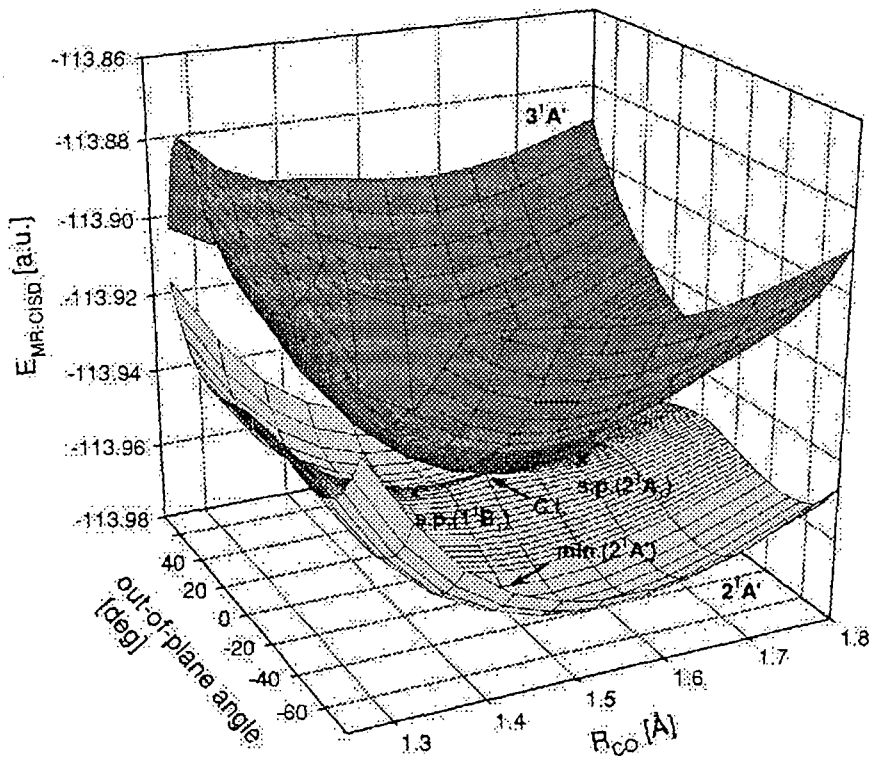

Fig. 1. Conical intersection and minima for the $2^1A'$ and $3^1A'$ states of H_2CO calculated with an accurate MRSDCI wave function.

COMPUTATIONAL AND EXPERIMENTAL STUDY OF LAMINAR FLAMES

M. D. Smooke and M. B. Long
Department of Mechanical Engineering
Yale University
New Haven, CT 06520
mitchell.smooke@yale.edu

Program Scope

Our research has centered on an investigation of the effects of complex chemistry and detailed transport on the structure and extinction of hydrocarbon flames in coflowing axisymmetric configurations. We have pursued both computational and experimental aspects of the research in parallel. The computational work has focused on the application of accurate and efficient numerical methods for the solution of the boundary value problems describing the various reacting systems. Detailed experimental measurements were performed on axisymmetric coflow flames using two-dimensional imaging techniques. Spontaneous Raman scattering and laser-induced fluorescence were used to measure the temperature, major and minor species profiles. Laser-induced incandescence has been used to measure soot volume fractions. Our goal has been to obtain a more fundamental understanding of the important fluid dynamic and chemical interactions in these flames so that this information can be used effectively in combustion modeling.

Recent Progress

The major portion of our work during the past year has focused on a combined computational and experimental study of time varying, axisymmetric, laminar, unconfined, methane-air diffusion flames and on a combined computational and experimental study of the formation of soot in axisymmetric, laminar, unconfined, ethylene-air diffusion flames. The time varying systems can enable the investigator to bridge the gap between laminar and fully turbulent systems. In addition, time varying flames offer a much wider range of interactions between chemistry and fluid dynamics than do steady-state configurations. The sooting flames can enable the investigator to understand the detailed inception, oxidation and surface growth processes by which soot is formed in hydrocarbon flames.

Time-Varying Flames

Atmospheric pressure, overventilated, axisymmetric, coflowing, nonpremixed laminar flames were generated with a burner in which the fuel flows from an uncooled 4.0 mm inner diameter vertical brass tube (wall thickness 0.038 mm) and the oxidizer flows from the annular region between this tube and a 50 mm diameter concentric tube. The oxidizer is air while the fuel is a mixture containing methane and nitrogen 65%/35% by volume, to eliminate soot. The burner includes a small loudspeaker in the plenum of the fuel jet, which allows a periodic perturbation to be imposed on the exit parabolic velocity profile. Perturbations of 30% and 50% of the average velocity have been investigated. Because the flame is slightly lifted, there is no appreciable heat loss to the burner.

Two-dimensional profiles of temperature, mixture fraction, and mole fractions of N_2, CO_2, CH_4, H_2, CO, and H_2O as well as CH* emission have been measured in the time-varying flame. We obtain CH* relative concentration from flame chemiluminescence, and species concentrations and temperature with vibrational Stokes-shifted Raman scattering and Rayleigh scattering using the second harmonic of a Nd:YAG laser. Each measurement is averaged over 1200 laser pulses, with separate data acquisitions for each orthogonal polarization of the scattered light. The signals are integrated over a spectral window large enough to account for spectral broadening due to temperature increases, but small enough

to minimize crosstalk with other species. Measurements are performed at heights above the burner ranging from 2.5 mm to 50 mm, in 0.5 mm increments. These line measurements are then tiled together to form images. Data are acquired for the steady state flame, and for five equally spaced phases of the forced flame over one forcing period.

As a relatively simple experiment, CH* in a flame can be measured from flame chemiluminescence (without a laser). Since CH* occurs in approximately the same location in a flame as CH, and since CH is a good flame front marker, we can easily determine the flame front. Images are obtained for the steady state flame, and for 10 equally spaced phases of the forced flame over one forcing period (five of these phases were identical to the phases for the species and temperature measurements.) Acquisitions are phase-locked and integrated over 200 intensifier gates. An Abel inversion converts the line of sight collection of CH* emission into an in-plane two-dimensional profile.

The modulated flame length increases in time, until the flame begins to pinch off downstream, forming two slightly attached high temperature regions. For the 50% modulation, the two regions break apart, leaving unattached high temperature zones. Eventually the downstream region moves farther downstream, and burns out. The pinch-off phenomenon is more drastic in the 50% modulation than the 30% modulation. For the 50% case, the flame has a larger curvature than for the 30% case. The flame width at the flame anchoring point varies significantly over time, with a larger fluctuation seen for the 50% case. The lift off height stays the same over time, comparable to the steady flame lift off height. There appears to be more soot production for the 50% than for the 30% modulation, and a large increase in soot as compared to the unforced flame. Further investigation into soot production of the forced flame is needed.

Computationally we have generalized the velocity-vorticity model to be able to solve time-dependent problems such as the forced time varying flame. However, preliminary results indicate that, as the velocity perturbation increases, the computations are unable to generate the level of pinching and roll-up as that found experimentally. Enhanced resolution of the flame with mesh refinement techniques improves the comparisons. To remedy the situation while still providing a computationally efficient model, we are developing a high-order spatial version of our model.

Soot Modeling

Soot kinetics are modeled as coalescing, solid carbon spheroids undergoing surface growth in the free molecule limit. The particle mass range of interest is divided into sections and an equation is written for each section including coalescence, surface growth, and oxidation. Sectional analysis makes it possible to obtain the particle size distribution without a-priori assumptions about the form of the distribution. For the smallest section, an inception source term is included. The transport conservation equation for each section includes thermophoresis, an effective bin diffusion rate, and source terms for gas-phase scrubbing. The gas and soot equations are additionally coupled through non-adiabatic radiative loss in the optically-thin approximation. The inception model employed here is based on an estimate of the formation rate of two- and three-ringed aromatic species (naphthalene and phenanthrene), and is a function of local acetylene, benzene, phenyl and molecular hydrogen concentrations. The contributions from the inception processes are incorporated in the first sectional bin, whose lower mass boundary is set equal to the mass of the smallest inception species. In the sectional representation, the sectional mass boundaries vary linearly on a logarithmic scale. The number of sections required for convergence must be examined for each problem and depends on the relative magnitudes of surface growth and inception. Oxidation of soot is by O_2 and OH. The surface growth rate is based upon that of Harris and Weiner [1] with an activation energy as suggested by Hura and Glassman [2].

Gas temperatures were measured with thermocouples and corrected for radiation heat transfer effects using standard techniques. A rapid insertion procedure was used to minimize errors due to soot deposition onto the thermocouple. In soot-free regions, the absolute uncertainty of these measurements is estimated to be ± 50 K and the relative uncertainty to be ± 10 K. Species concentrations were measured by extracting gas samples from the flames with a narrow-tipped quartz microprobe and analyzing these samples with on-line mass spectrometry. Acetylene and ethylene were quantified with an Extrel C50 variable-ionization-energy electron-impact/quadrupole mass spectrometer, and C_3 to C_{12} hydrocarbons with a custom-built photoionization/time-of-flight mass spectrometer. Measurements were directly calibrated and have an absolute uncertainty of 30%. Profiles were generated by moving the burner with translation stages. The axial and radial coordinates, designated z and r, have a relative uncertainty of ± 0.2 mm and an absolute uncertainty of ± 0.5 mm.

Using planar laser imaging, we obtain two-dimensional fields of temperature, fuel concentration, and soot volume fraction in the C_2H_4/N_2 flame. The temperature field is determined using the two scalar approach of Stårner et al. [3] and included the measurement of Rayleigh scattering and the use of the computed fuel concentration. The soot volume fraction field is determined by laser-induced incandescence (LII). At sufficient laser intensities, the LII signal has been shown to be directly proportional to soot volume fraction. Probe measurements of the soot volume fraction are used for calibration.

The chemical kinetic mechanism for ethylene combustion has 52 species and 233 reactions. It was derived from GRIMech 1.2 [4], based upon comparisons to experimental data on ethylene from perfectly stirred and flow reactors and ignition delay data. It includes reactions describing the formation and oxidation of benzene, and related species. Fuel and nitrogen are introduced through the center tube (4mm id) utilizing a parabolic velocity profile and air through the outer coflow with a plug flow profile. Both velocity profiles were those employed in the experiments. Flames containing 40% (60%), 60% (40%) and 80% (20%) mole fractions of ethylene (nitrogen) with a bulk averaged velocity of 35 cm/sec were studied. The coflow air velocity was 35 cm/sec. Reactant temperatures were assumed to be 298 K. All radial velocities were assigned to zero at the flame base. Calculations were performed on an SGI Origin 2000 computer. The computations included 20 soot sections. Starting from a converged solution for an ethylene-air flame without the sectional equations, we typically obtained converged solutions for the complete gas-soot problem in several hours of computer time.

We have found that by placing an upper bound on the size of the soot particles for which surface growth is allowed, we have dramatically improved the comparisons between the predicted soot volume fractions of the model and the experiments, though the magnitude and orientation of some key species still contain significant differences. These results clearly indicate that the ability to make quantitative soot predictions remains limited by some fundamental uncertainties in the soot model (including the lack of aging and aggregate formation effects), by the ability of the chemical kinetic mechanism to predict accurately the concentrations of important species (benzene, propargyl, acetylene and diacetylene) and possibly by the lack of quantitative information concerning the production of translucent particles.

Future Plans

During the next year we hope to expand our research in two main areas. First, we will continue our study of sooting hydrocarbon flames with the goal of understanding the differences in soot distribution between the computational and experimental results. Second, we will continue our study of flickering diffusion flames with the goal of incorporating high order spatial approximations into the model. We will then begin incorporating a detailed soot model into the gas phase system with the goal of predicting soot volume fractions as

a function of time. Laser induced incandescence (LII) will be used to measure soot volume fractions.

References

1. Harris, S.J., and Weiner, A.M., *Combust. Sci. Tech.*, **31**, p. 155, (1983).

2. Hura, H.S. and Glassman, I., *Twenty-Second Symposium (International) on Combustion*, The Combustion Institute, Pittsburgh, 1988, p. 371.

3. Stårner, S., Bilger, R. W., Dibble, R. W., Barlow, R. S., *Combust. Sci. Tech.*, **86**, p. 223, (1992).

4. Bowman, C.T., Hanson, R.K., Davidson, D.F., Gardiner, Jr., W.C. Lissianski, V., Smith, G.P., Golden, D.M., Frenklach, M., Wang, H., and Goldenberg, M., *GRI-Mech version 2.11*, http://www.gri.org (1995).

DOE Sponsored Publications 1999-2000

1. B. A. V. Bennett and M. D. Smooke, "Local Rectangular Refinement with Application to Fluid Flow Problems," **151**, *J. Comp. Phys.*, (1999).

2. B. A. V. Bennett and M. D. Smooke, "A Comparison of the Structures of Lean and Rich Axisymmetric Laminar Diffusion Flames: Application of Local Rectangular Refinement Solution-Adaptive Gridding," *Comb. Theory and Modelling*, **3**, (1999).

3. C. McEnally, L. Pfefferle, R. Mohammed, M. D. Smooke and M. B. Colket, "Mapping of Trace Hydrocarbon Concentrations in Two-Dimensional Flames Using Single-Photon Photoionization Mass Spectrometry, *Anal. Chem*, **71**, (1999).

4. M. D. Smooke, C. S. McEnally, L. D. Pfefferle, R. J. Hall and M. B. Colket, "Computational and Experimental Study of Soot Formation in a Coflow, Laminar Diffusion Flame, *Comb. and Flame*, **117**, (1999).

5. J. Luque, J. B. Jeffries, G. P. Smith, D. R. Crosley, K. T. Walsh, M. B. Long, and M. D. Smooke, "CH(A-X) and OH(A-X) Optical Emisison in an Axisymmetric Laminar Diffusion Flame, *Comb. and Flame*, **122**, (2000).

6. B. A. V. Bennett, C. McEnally, L. Pfefferle, and M. D. Smooke, "Computational and Experimental Study of Axisymmetric Coflow Partially Premixed Methane/Air Flames," *Comb. and Flame*, **123**, (2000).

7. K.T. Walsh, J. Fielding, M.D. Smooke, and M.B. Long, "Experimental and Computational Study of Temperature, Species, and Soot in Buoyant and Nonbuoyant Coflow Laminar Diffusion Flames," *Proceedings of the 28th Combustion Symposium*, 2000.

8. C.S. McEnally, L.D. Pfefferle, A.M. Schaffer, M.B. Long, R.K. Mohammed, M.D. Smooke, and M.B. Colket, "Characterization of a Coflowing Methane Air Nonpremixed Flame with Computer Modelling, Rayleigh-Raman Imaging, and On-Line Mass Spectrometry," *Proceedings of the 28th Combustion Symposium*, 2000.

9. M. D. Smooke and B. V. Bennett, "Modeling Coflow Diffusion Flames with Local mesh Refinement," in Computational Fluid Dynamics in Industrial Combustion, eds. C. E. Baukal, Jr., V. Y. Gershtein, and X. Li, CRC Press, New York, (2000).

Universal/Imaging Studies of Chemical Reaction Dynamics

Arthur G. Suits
Chemistry Department Building 555
Brookhaven National Laboratory
Upton NY 11974
and
Department of Chemistry
SUNY-Stony Brook
Stony Brook, NY 11793
arthur.suits@sunysb.edu

Program Scope

We are interested in the detailed dynamics of systems of relevance to combustion and atmospheric chemistry, with emphasis on primary photodissociation events and the dynamics of bimolecular reactions under crossed-beam conditions. We exploit complementary techniques utilizing UV and VUV lasers or synchrotron radiation in conjunction with velocity map imaging to perform state-resolved and universal product detection. Soft ionization methods provide a probe that is both *universal* and *selective*, affording global insight into reactive processes. Our particular interests are in: reaction dynamics on multiple potential surfaces; the properties and behavior of radicals and other transient species; the detailed reaction dynamics of polyatomic molecules, and in developing new experimental approaches such as the ion pair imaging technique outlined below. We have recently moved our effort from Berkeley to Brookhaven National Laboratory, and we are now obtaining our first results in a newly equipped and refurbished laboratory. Our effort at BNL is strongly coupled with the tightly integrated program in gas phase molecular dynamics already in place there.

Recent Progress

"Second-generation" velocity map imaging

The "velocity mapping" approach introduced by Eppink and Parker in 1997 has had a dramatic impact on the imaging community, and many people have adopted the technique since the appearance of this high-resolution innovation. But one shortcoming of velocity mapping is that, unlike in the original ion imaging method, there is some magnification of the image, and careful calibration is crucial for quantitative velocity measurement. Furthermore, this calibration is extremely sensitive to the ion's birthplace along the flight axis, owing to the large fields typically present there. Using extensive simulations, we have developed and implemented a two-stage variant of the velocity map ion optics to reduce greatly the dependence of the magnification (and the resolution, for large ionization volumes) on the ionization point.

Reactive scattering studied by velocity map imaging

As reported last year, we began a series of investigations of crossed-beam reaction dynamics using velocity map imaging with a single photon ionization probe provided by an F_2 excimer laser at 157nm. This approach affords tremendous sensitivity, making detailed and systematic investigations of polyatomic reaction dynamics quite facile. Our initial studies focused on the crossed beam reaction of ground state Cl ($^2P_{3/2}$) atoms with alcohols (CH_3OH, C_2H_5OH and 2-C_3H_7OH), at collision energies from 5-12 kcal/mol, with probe of the corresponding hydroxyalkyl radical. All of the translational energy distributions peaked at about 6 kcal/mol and on average 30-40% of the available energy was deposited into product translation for all the alcohols studied. We believe all of these results may be rationalized by a direct reaction mechanism that involves a moderately tight, collinear Cl-H-C transition state. More recently, we examined the reaction dynamics of spin-orbit excited chlorine atoms with ethanol at

collision energies comparable to those studied earlier using a pure ground state chlorine atom source. The results of these preliminary studies are shown in Figure 1. At collision energies of 9.7 (Cl) and 8.6 (Cl/Cl*) kcal/mol, we find considerably more energy appearing in translation in the Cl* case. In addition, the angular distributions are on the whole much broader, with considerably more flux appearing at sideways and forward scattering angles. We suspect the reason for this may be that the electronic energy is available in the entrance channel to open up more trajectories to reaction, relaxing the requirement for Cl-H-C collinearity. We plan further studies to probe these issues in depth.

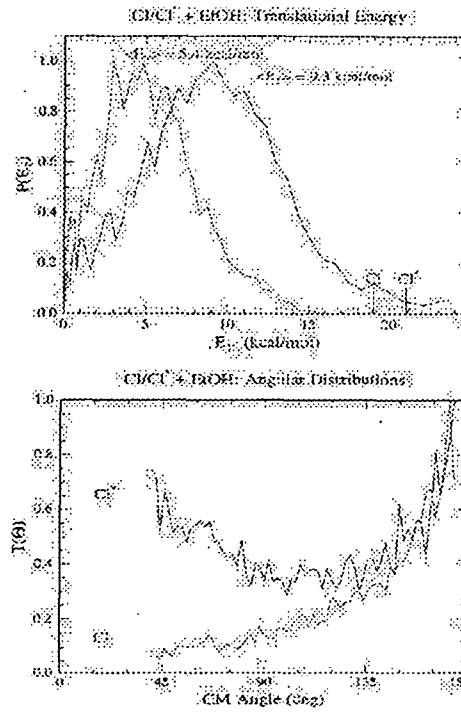

Figure 1. CM translational energy and angular distributions for the indicated reactions.

Ion Pair Imaging Spectroscopy

Photoelectron spectroscopy is a powerful means of probing the energetics and vibrational frequencies of ionic species, and it has long been a principal source of insight into the electronic structure of molecules. Although it is a broadly used and nearly universal tool, there are a great number of systems of considerable importance for which photoelectron spectroscopy is simply not applicable, owing to the absence of suitable neutral molecules as precursors or unfavorable Franck-Condon factors that prevent access to the lowest levels of the ion. Imaging studies of the dissociation of molecules, typically in the vacuum ultraviolet, to give *ion pair* products represents an alternative means of investigating the energy levels and thermochemistry of ionic species as illustrated in Fig. 2. This approach, which we term "Ion Pair Imaging Spectroscopy" (IPIS), is analogous to photoelectron imaging spectroscopy, except the electron is replaced by an atomic anion. This substitution results in both advantages and disadvantages: the process is much slower than photoelectron spectroscopy, so one is not confined to vertical processes, and Franck-Condon considerations are greatly relaxed. Furthermore, starting from stable molecules, one obtains the cation that would result from photoionization of the corresponding radical precursor, eliminating the need to start with radicals that may be difficult to prepare under well-defined conditions. On the other hand, the dissociation may well be accompanied by greater rotational excitation than would be the case for photoelectron spectroscopy, so that an understanding of the ion pair dissociation dynamics may be important to unraveling the spectra.

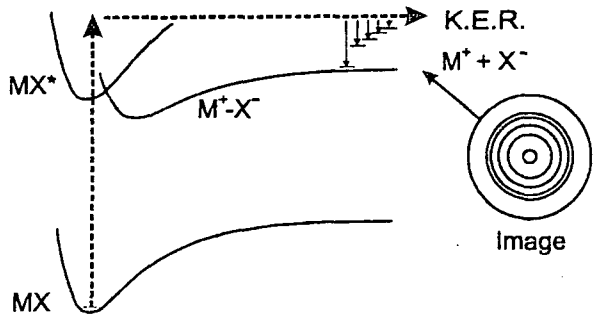

Figure 2. Schematic view of IPIS technique.

We have demonstrated the potential of this method with a preliminary study of ion pair imaging of CH_3Cl. An image of CH_3^+ obtained from the 118 nm ion pair dissociation of methyl chloride is shown in Fig. 3. A series of rings are apparent, representing vibrations in the CH_3^+. The images also show significant anisotropy indicating a prompt dissociation event and a parallel dissociation mechanism. Images for Cl^- give virtually identical results, albeit with lower resolution owing to the kinematics. Analysis of the velocity distribution in the image leads to the translational energy distribution in Fig. 4, shown

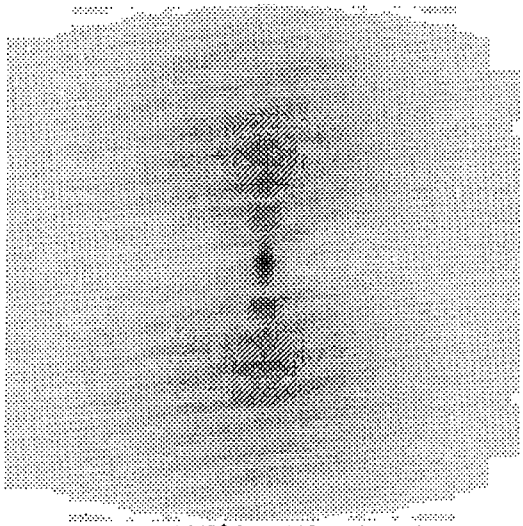

Figure 3. Image of CH_3^+ from 118 nm ion pair dissociation of CH_3Cl.

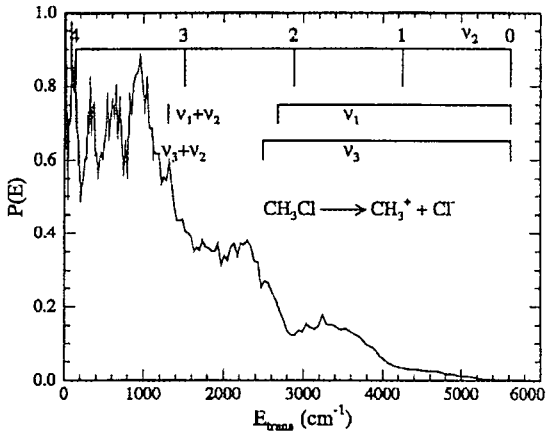

Figure 4. Total translational energy distribution derived from data in Fig. 3.

along with combs indicating calculated (harmonic) vibrational frequencies of CH_3^+. The results are summarized in Table I. Experimental values are known only for the ν_2 (umbrella) and ν_3 (C-H asymmetric stretch) modes, and the uncertainty in the former is considerable. The anticipated dissociation dynamics might lead one to predict considerable umbrella mode excitation in the CH_3^+ as is observed. In addition, peaks likely corresponding to combination bands with one quantum of ν_2 and one each of ν_1 or ν_3 are also seen. As discussed below, we intend to study this system under higher resolution conditions, and with tunable VUV, to explore the role of rotational excitation and attempt to get more accurate measures of these vibrational frequencies.

Table I. Comparison of calculated and experimental vibrational frequencies for CH_3^+ (in cm^{-1}).

Source	ν_1 (a_1')	ν_2 (a_2'')	ν_3 (e')	ν_4 (e')
MP2/aug-cc-pVTZ-*d*(H)-*f*(C)[a]	2912	1357	3108	1377
expt	-	1380(20)[b]	3108.4[c]	-
IPIS	-	1372	3117	-

[a] RV Olkhov, SA Nizkorodov, O Dopfer: J. Chem. Phys. 108 (1998) 10046-60

[b] J Dyke, N Jonathan, E Lee, A Morris: J. Chem. Soc., Faraday Trans. 2 72 (1976) 1385.

[c] MW Crofton, WA Kreiner, MF Jagod, BD Rehfuss, T Oka: J. Chem. Phys. 83 (1985) 3702-03; MW Crofton, MF Jagod, BD Rehfuss, WA Kreiner, T Oka: J. Chem. Phys. 88 (1988) 666-78.

Future plans

Our future plans call for extending the crossed-beam imaging studies to include: high resolution measurements of H atom reactions with hydrocarbons and alcohols; high collision energy studies of the benchmark $O(^1D)+H_2$ system; a systematic investigation of excited state reactivity in Cl/Cl* with alkanes; and finally hydroxyl radical reactions with alkanes. In addition, we plan to extend our investigation of the IPIS technique in the test case methyl chloride, with a careful study of the

wavelength dependence of the process under high resolution conditions. We would then like to extend these measurements to look at ion pair formation in van der Waals systems, where, for example, the HCl in CH_4...HCl may act as a proton donor to produce CH_5^+.

DOE Sponsored Publications 2000-2001

M. Ahmed, D. S. Peterka and A. G. Suits, "Imaging H abstraction dynamics in crossed beams: Cl+ROH reactions," *Phys. Chem. Chem. Phys.*, 2, 861 (2000). LBNL-44340.

M. Ahmed, D. S. Peterka and A. G. Suits, " H abstraction dynamics by crossed-beam velocity map imaging: $Cl+CH_3OH \rightarrow CH_2OH+HCl$, " *Chem. Phys. Lett.*, 317, 264 (2000). LBNL-44126.

W. S. McGivern, O. Sorkhabi, A. Rizvi, A. G. Suits and S. W. North, "Photofragment Translational Spectroscopy with State-Selective 'Universal Detection': the Ultraviolet Photodissociation of CS2," *J. Chem. Phys.*, **112**, 5301 (2000). LBNL-44681.

F. Qi, O. Sorkhabi and A. G. Suits, "Evidence of triplet ethylene produced from photodissociation of ethylene sulfide," *J. Chem. Phys.*, **112**, 10707 (2000). LBNL-45562.

M. Ahmed, D. S. Peterka and A. G. Suits, "New directions in reaction dynamics using velocity map imaging," in **Imaging in Chemical Dynamics**, A. G. Suits and R. E. Continetti, eds., *ACS Symposium Series 770*, (American Chemical Society, Washington DC, 2000). LBNL-45395.

E.R. Wouters, M. Ahmed, D.S. Peterka, A.S. Bracker, A.G. Suits and O.S. Vasyutinskii, "Imaging the Atomic Orientation and Alignment in Photodissociation," ," in **Imaging in Chemical Dynamics**, A. G. Suits and R. E. Continetti, eds., *ACS Symposium Series 770*, (American Chemical Society, Washington DC, 2000). LBNL-45397.

W.S. McGivern, O. Sorkhabi, A.G. Suits, A. Derecskei-Kovaks, and S.W. North, "Primary and Secondary Processes in the Photodissociation of $CHBr_3$," *J. Phys. Chem. A*, **104**, 10085 (2000). LBNL-45435.

N. R. Forde, L. J. Butler, B. Ruscic, O. Sorkhabi, F. Qi and A.G. Suits, "Characterization of nitrogen-containing products from the photodissociation of trimethylamine at 193 nm using photoionization detection," *J. Chem. Phys*, **113**, 3088 (2000). LBNL-45299.

P. Zou, W. S. McGivern, O. Sorkhabi, A. G. Suits and S. W. North, "Quantum yields and energy partitioning in the ultraviolet photodissociation of 1,2 dibromo-tetrafluoroethane (Halon-2402)," *J. Chem. Phys.*, **113**, 7149 (2000).

F. Qi, O. Sorkhabi, A. G. Suits, S.-H. Chien and W.-K. Li, "Photodissociation of ethylene sulfide at 193nm : A photofragment translational spectroscopy study with VUV synchrotron radiation and ab initio calculations," *J. Am. Chem. Soc.*, **123**, 148 (2001).

Julie A. Mueller, Johanna L. Miller, Laurie J. Butler, Fei Qi, Osman Sorkhabi and Arthur G. Suits, "Internal Energy Dependence of the H + Allene / H + Propyne Product Branching from the Unimolecular Dissociation of 2-Propenyl Radicals," *J. Phys. Chem. A* **104,** 48 (2001).

O. Sorkhabi, F. Qi, A.H. Rizvi and A.G. Suits, "The ultraviolet photochemistry of phenylacetylene and the enthalpy of formation of 1,3,5-Hexatriyne," *J. Am. Chem. Soc.*, **123**, 671 (2001).

C. L. Berrie, C. A. Longfellow, A. G. Suits and Y. T. Lee, "Infrared multiphoton dissociation of acetone in a molecular beam," *J. Phys. Chem A*, (in press).

J. A. Mueller, B. F. Parsons, L. J. Butler, F. Qi, O. Sorkhabi and A. G. Suits, "Competing product channels in the 193 nm photolysis of 2-Chloropropene and in the unimolecular dissociation of the 2-propenyl radical," *J. Chem. Phys.* **114**, 4505 (2001).

Elementary Reaction Kinetics of Combustion Species

Craig A. Taatjes
Combustion Research Facility, Mail Stop 9055, Sandia National Laboratories,
Livermore, CA 94551-0969
cataatj@ca.sandia.gov *www.ca.sandia.gov/CRF*

SCOPE OF THE PROGRAM

The scope of this program is to develop new laser-based methods for studying chemical kinetics and to apply these methods to the investigation of fundamental chemistry relevant to combustion science. The central goal is to perform accurate measurements over wide temperature ranges of the rates at which important free radicals react with stable molecules. In the past several years, the program has concentrated on the investigation of CH, C_2H, and Cl + stable molecule reactions, applying the extraordinarily precise techniques of laser photolysis/continuous-wave laser-induced fluorescence (LP/cwLIF) and laser photolysis/continuous-wave infrared long-path absorption (LP/cwIRLPA). The precision of these methods enables kinetic measurements to probe reaction mechanisms, utilizing thermal rate constant and product distribution measurements as indicators of detailed global reaction paths. Another aim has been the investigation and application of new detection methods for precise and accurate kinetics measurements. Absorption-based techniques are emphasized, since many radicals critical to combustion are not amenable to fluorescence detection. As an additional advantage, absorption-based techniques can be straightforwardly applied to determination of absolute concentrations in reacting systems.

RECENT PROGRESS

The efforts of the laboratory center on extending the capabilities of the laser-induced-fluorescence method to new reaction systems, on developing high-sensitivity absorption-based techniques for kinetics measurements, and on applying these techniques to investigate important combustion reactions. Recent work on the LP/cwLIF method to extend the easily usable probe frequency range has been applied to cw LIF detection of HCO in the $B \leftarrow X$ band. Absorption-based techniques for probing reactions, principally in the infrared, are extensively used. In the last year we have continued to concentrate on the application of cw infrared frequency-modulation spectroscopy to measuring product formation in the reaction of alkyl radicals with O_2.

Product Formation in Alkyl + O_2 reactions

We have continued the application of the LP/cwIRLPA method to the reactions of alkyl radicals with O_2. In the past two years a sustained effort has been made to investigate HO_2 production in R + O_2 reactions using the LP/cwIRLPA method. Reactions of alkyl radicals with O_2 are important in understanding autoignition, engine knock, and pre-ignition chemistry. The R + O_2 reactions take place via initial formation of an excited alkylperoxy radical (RO_2), which then can be collisionally stabilized or dissociate to reactants or to products. One possible fate of RO_2 is rearrangement to a hydroperoxyalkyl radical QOOH, which can then decompose to QO + OH or to Q +

HO_2. The QOOH species formed by this isomerization is also an intermediate in many models of hydrocarbon oxidation. Present understanding of these reactions is that HO_2 formation proceeds principally via concerted elimination from RO_2 which competes with the isomerization to form QOOH. This elimination is dominant in the reaction of ethyl + O_2.

Our experiments utilize time-resolved measurements of HO_2 formation in R + O_2 reactions using diode laser absorption in the overtone of the O-H stretch. Alkyl radicals are produced by the reaction of the corresponding alkane with Cl atoms from Cl_2 photolysis at 355 nm. The yield of HO_2 in the reaction is determined by comparison with HO_2 signals from the Cl + CH_3OH + O_2 system, which quantitatively converts Cl atoms to HO_2. Possible formation of OH can be simultaneously monitored by infrared absorption using an F-center laser co-propagating with the diode laser beam. Our recent goal has been to extend the understanding gained from the relatively thoroughly studied ethyl + O_2 reaction to larger alkyl + O_2 systems, where internal isomerizations may begin to compete with the HO_2 elimination channel.

Propyl + O_2. The reaction of Cl with propane produces a mixture of the *i*-propyl and *n*-propyl radicals, which go on to react with O_2. A biexponential time profile of HO_2 is observed above T ~ 575 K, with the production of HO_2 on a slower timescale attributable to propylperoxy radical decomposition. The total HO_2 yield, including the contribution from the slower rise, increases rapidly with temperature from 5% at 500 K to 100% at 683 K. The second slower rise accounts for nearly all the HO_2 formation at these higher temperatures. The phenomenological rate constant for delayed HO_2 production from C_3H_7 + O_2 is slightly larger than for C_2H_5 + O_2 at each temperature. Apparent activation energies, obtained by an Arrhenius plot of the inverse of the time constants for delayed HO_2 production, are very similar for the two systems. Master equation calculations using ab initio calculations of the propyl + O_2 surfaces are in qualitative agreement with the experimental results, and show that concerted HO_2 elimination dominates the reaction.

Butyl + O_2. The time-resolved production of HO_2 in the Cl-initiated oxidation of *i*- and *n*-butane has been measured as a function of temperature between 450 and 698 K. In contrast to reactions of smaller alkyl radicals with O_2, the total HO_2 yield in the butyl radical reactions appears to remain significantly below 1 up to 698 K. The effective rate constants for delayed HO_2 production are slightly different for the two butane isomers, but the apparent activation energy is similar to that measured for smaller alkyl + O_2 reactions, suggesting that the energetics of the HO_2 elimination transition state are similar for a broad range of R + O_2 systems. The non-unity HO_2 yield, however, is suggestive of an increased role for the isomerization to QOOH and the subsequent production of OH. This suggestion is supported by ab initio calculations of the potential energy surfaces for the butyl isomer reactions with O_2 and by OH yield measurements in our laboratory.

Cyclopentyl + O_2. The production of HO_2 from the reaction of *c*-C_5H_9 + O_2 has also been investigated as a function of temperature (296–723 K) using the same laser photolysis / CW infrared frequency modulation spectroscopy technique. The total HO_2 yield, including the contribution from the slower rise attributable to cyclopentyl peroxy radical decomposition, increases dramatically with temperature from ~2 % at 500 K to ~100 % at 683 K. Once again, apparent activation energies, obtained by an Arrhenius plot of the rates of formation for delayed HO_2 formation, are very similar to the C_2H_5 +

O_2, $C_3H_7 + O_2$, and $C_4H_9 + O_2$ reactions. The apparent pre-exponential factor, however, is significantly larger for cyclopentyl + O_2. The reduced internal rotation in the *c*-C_5H_9 radical relative to the other alkyl radicals may result in a smaller entropy loss in reaching the elimination transition state, and hence an increased A-factor, an effect which would be general to cyclic radicals.

Pulsed LIF Detection of OH Formation in R + O_2 Reactions

In order to more thoroughly characterize the reaction of alkyl radicals with O_2, we have undertaken measurements of the time-resolved OH concentration in Cl-initiated oxidation reactions similar to those used in the investigations of HO_2 production. Since measurements employing infrared absorption detection could not deliver the sensitivity necessary to determine the very low yields of OH in the reactions of small alkyl radicals with O_2, LIF detection of the OH product was used. The initiation of the reaction was carried out by photolysis of $CFCl_3$ at 193 nm. The yield of OH in the reaction was normalized by adding NO to the $Cl/CH_3OH/O_2$ reference reaction used in the HO_2 production experiments. The reaction of HO_2 with NO produces 100% OH + NO_2, and modeling of the reaction system was performed to scale the observed signals and obtain relative OH yields. The observed OH is produced promptly. Because of the high reactivity of OH, a kinetic bias favors detection of rapidly produced OH, so contributions from delayed OH make a smaller contribution to the signals. The OH production in the ethyl, propyl, cyclopentyl, and butyl + O_2 reactions have been measured as a function of temperature between 298 K and 750 K. All reactions show a steep activation energy in the OH production, and the yield of OH is larger in the reactions of larger alkyl radicals.

Laser Photolysis/cwLIF Detection of HCO Kinetics

The formyl radical, HCO, is a key intermediate in hydrocarbon combustion, and because of its position as a gateway for oxidation of all hydrocarbons, is an excellent marker for heat release in flames. The reliable detection of HCO by cwLIF through the B state has been a target for years, but production of cw light at 258 nm is a technical challenge. The spectroscopy of the B-X LIF system has been thoroughly investigated, and pulsed LIF on this transition has been used to investigate reactions of vibrationally excited HCO. We have recently found that a ring laser operating with Coumarin 521, previously used as a pulsed laser dye, produces laser light between 505 and 560 nm with remarkable efficiency and stability when pumped by the 457.9 Ar^+ line. Doubling this light allows dependable detection of HCO in concentrations of ~ 10^{10} cm^{-3}, a hundred times better than reported detection of HCO by cavity ring-down in the A-X band. We have begun to apply this technique to the HCO + O_2 reaction, the dominant removal reaction for HCO in flames. Literature measurements have found an inverse deuterium kinetic isotope effect for this reaction, which has been interpreted as evidence for a kinetically significant collision complex. However, unpublished work by Imamura and Washida suggests a normal kinetic isotope effect.

FUTURE DIRECTIONS

In the next two years our characterization of R + O_2 reactions will continue. The current experiments have only begun to probe the rich mechanistic details of these critical reactions. The ability to simultaneously probe various reactants and products will play a

key role in extending these measurements. In future experiments, photolysis of selected alkyl halides will be used to generate individual isomers. The observed HO_2 signals could be scaled using simultaneous detection of the partner fragment, e.g., reactions initiated by 2-bromopropane photolysis could be calibrated by simultaneous infrared absorption detection of HO_2 and Br atom.

Selective deuteration also may make it possible to distinguish among different internal abstraction pathways in R + O_2 reactions. Interpretation of any of these isotopic labeling experiments will require detection of both HO_2 and DO_2 and an understanding of the kinetic isotope effects on the overall reaction. Probing the electronic transition of the HO_2 or DO_2 radical will be accomplished using difference frequency generation of a cw Nd:YAG and a dye laser in $LiNbO_3$, which is presently under construction. This will enable simultaneous detection of HO_2 (in the H-O overtone) and DO_2 (in the A-X band). Detection in the region of the electronic transition is advantageous because of the accessibility of alkylperoxy transitions as well as the HO_2 and DO_2 absorptions in the same region. In the long term, detection of the purported hydroperoxy radical intermediate in the R + O_2 → RO_2 → QOOH → QO + OH mechanism might be possible in the infrared.

Publications acknowledging BES support 1999-2001

Charles D. Pibel, Andrew McIlroy, Craig A. Taatjes, Sterling Alfred, Katina Patrick, and Joshua B. Halpern, "The Vinyl Radical ($\tilde{A}\ ^2A'' \leftarrow X\ ^2A'$) Spectrum between 530 and 415 nm Measured by Cavity Ring-down Spectroscopy," *J. Chem. Phys.* **110,** 1841-1843 (1999).

Craig A. Taatjes, "Infrared Frequency-modulation Measurements of Absolute Rate Coefficients for Cl + HD → HCl (DCl) + D (H) between 295 and 700 K," *Chem. Phys. Lett.* **306,** 33 (1999).

Craig A. Taatjes, Lene K. Christensen, Michael D. Hurley, and Timothy J. Wallington, "Absolute Rate Coefficients and Site-Specific Abstraction Rates for Reactions of Cl with CH_3CH_2OH, CH_3CD_2OH, and CD_3CH_2OH between 295 and 600 K," *J. Phys. Chem. A.*, **103,** 9805-9814 (1999).

Craig A. Taatjes, "Time-Resolved Infrared Absorption Measurements of Product Formation in Cl Atom Reactions with Alkenes and Alkynes," *Int. Rev. Phys. Chem.* **18,** 419-458 (1999).

Eileen P. Clifford, John T. Farrell, John D. DeSain, and Craig A. Taatjes, "Infrared Frequency-Modulation Probing of Product Formation in Alkyl + O_2 Reactions: I. The Reaction of C_2H_5 with O_2 between 295 and 698 K," *J. Phys. Chem. A*, **104,** 11549-11560 (2000).

John D. DeSain, Eileen P. Clifford, and Craig A. Taatjes, "Infrared Frequency-Modulation Probing of Product Formation in Alkyl + O_2 Reactions: II. The Reaction of C_3H_7 with O_2 between 296 and 683 K," *J. Phys. Chem. A,* **105,** 3205–3213 (2001).

Holger Thiesemann, Eileen P. Clifford, Craig A. Taatjes, and Stephen J. Klippenstein, "Temperature Dependence and Deuterium Kinetic Isotope Effects in the CH (CD) + C_2H_4 (C_2D_4) Reaction between 295 and 726 K," *J. Phys. Chem. A.*, in press (2001)

Leonard E. Jusinski and Craig A. Taatjes, "Efficient and Stable Operation of an Ar^+-Pumped CW Ring Laser from 505-560 nm Using a Coumarin Laser Dye," *Rev. Sci. Instrum.*, in press (2001).

Craig A. Taatjes and John F. Hershberger, "Recent Progress in Infrared Absorption Probing of Elementary Reaction Kinetics," *Annu. Rev. Phys. Chem.***52,** 41-70 (2001).

A Scaling Theory for the Assignment of Spectra in the Irregular Region

H. S. Taylor, Principle Investigator
Department of Chemistry, SSC 704
University of Southern California
Los Angeles, CA 90089-0482
E-mail: taylor@chem1.usc.edu
Phone: (213) 740-4112; FAX: (213) 740-3972

The object of this research program is to take the results of measured spectra on the high vibrational levels of polyatomic molecules and to extract from them the various internal motions that when quantized give rise to these spectra. In short we are learning how the atoms in the molecules move and how energy is transferred when specific amounts of energy are put into the molecule. All this can be done if the experimental results can be represented by a spectroscopic Hamiltonian. No potential surfaces or large-scale calculations are needed.

Given this Hamiltonian, if the number of degrees of freedom minus the number of constants of motion are two, we can use the semiclassical limit of the spectroscopic Hamiltonian and canonical transforms to reduce the problem to one of a configuration space of two canonical angles. Then, by comparing the two dimensional density and phase accummulation plots of eigenfunctions, which are trivially obtained from the Hamiltonian, to the tori and organizing periodic orbits projected from the phase space onto the configuration space, we can: (1) classify the eigenstates into several series that are each quantization ladders of similar dynamics; (2) assign meaningful quasiconserved quantum numbers for each state by counting nodes in the density plots if the density is localized in angle space and by counting phase advances in directions where the density is delocalized; (3) relate these series to special organizing structures in phase space which are then transformed back to the full dimension action-angle space and then with appropriate testable assumptions further transformed back into motions in physical space. The result is that we obtain for highly excited spectra various series of levels each based on a definitive type of motion and assignment. These series overlap in energy and when merged yield the spectra which was observed and previously thought to be too complex to be interpretable by previously known methods. Application has been made to C_2H_2[5], CHBrClF[6], DCO and N_2O. Of particular interest are the simplifications in the analysis that we are now testing. It should be realized that the difficult and laborious part of the analysis is to find for each polyad the classical periodic orbits and tori that organize the phase space of the polyad. Moreover the special skills needed to do this are not in the arsenal of skills of most experimentalists and this does not bode well for the methods to be adopted by the large majority of spectroscopists. Happily we have now developed methods that allow almost all (and often all) of the above type of information to be extracted without the necessity of carrying out the phase space mapping part of the classical analysis. From the nature of the localization properties in the density plots of any ladder of states [e.g. density is near $\psi_1=0$ and along ψ_2 etc.] we have figured out a way, using the canonical transform relations to extract the particular frequency and phase locks, that inform us as to the motion in normal, local or displacements coordinates. This then tells us qualitatively the classical internal motions that when quantized give rise to a particular ladder of states. We have applied these new ideas and our full method and simplified methods to N_2O and CHBClF and obtain

essentially similar results as obtained when using our phase space analysis. We are now doing the same test for DCO; the simplified part is already done.

We are also actively working on an extension of the theory to cases where we can only canonically reduce the dimension of the problem to three degrees of freedom. This is needed to treat CDBrClF for which Quack required a four degree of freedom spectroscopic Hamiltonian to fit his results.

Related categories: Non-linear dynamics, Chemical dynamics, and molecular spectroscopy.

Publication associated with the grant and references.

1. All Non-Adiabatic (J = 0) bound States of NO_2, R. Salzgeber, C. Schlier, V. Mandelshtam, and H.S. Taylor, J. Chem. Phys., 110, 3756 (1999).

2. Decimated Signal Diagonalization for Obtaining the Complete Eigenspectra of Large Matrices, D. Belkic, P.A. Dando H.S. Taylor, and J. Main, Chem. Phys. Lett., 315, 135-139 (1999).

3. Decimated Signal Diagonalization for Fourier Transform Spectrometry, D. Belkic, P.A. Dando, J. Main, H.S. Taylor and S.-K. Shin, J. Phys. Chem. A, 104, 11677-11684 (2000).

4. Three Novel High-Resolution Nonlinear Methods for Fast Signal Processing, Dz. Belkic, P. A. Dando, J. Main, and H.S. Taylor, J. Chem. Phys., 113, 6542 (2000)

5. The Acetylene Bending spectrum at ~10,000 cm^{-1}: Quantum Assignment in the Midst of Classical Chaos, C. Jung, M. Jacobson and H.S. Taylor, J. Phys. Chem. A, 105, 681 (2001).

6. Extracting the CH Chromophore Vibrational Dynamics of CHBrClF Directly from Spectra: Unexpected Constants of the Motion and Symmetries, C. Jung, E. Ziemniak and H.S. Taylor, J. Chem. Phys. Submitted, (2001).

VARIATIONAL TRANSITION STATE THEORY

Principal investigator, mailing address, and electronic mail

Donald G. Truhlar
Department of Chemistry, University of Minnesota, 207 Pleasant Street SE, Minneapolis, Minnesota 55455
truhlar@umn.edu

Program scope

This project involves the development and application of variational transition state theory (VTST) and semiclassical transmission coefficients to gas-phase reactions. Our current work is focussed on developing and applying new methods for interfacing reaction-path dynamics calculations with electronic structure theory and new electronic structure methods that are especially well suited for applications in combustion kinetics. The work involves development of the theory, development of practical techniques for applying the theory to various classes of transition states, and applications to specific reactions, with special emphasis on combustion reactions and reactions that provide good test cases for methods needed to study combustion reactions. A theme that runs through our current work is the use of multiple levels of electronic structure and molecular mechanics for a given problem and their creative combination.

Recent progress

We have developed powerful new multi-coefficient correlation methods that allow accurate evaluation of bond energies and reaction energies at relatively low cost compared to previously available methods. These methods are multi-level electronic structure methods in that the predicted energy surface results from extrapolating two or more electronic structure levels to the limit of infinite-order electron correlation (i.e., full CI) and a complete one-electron basis set. Two particularly promising methods of this type are the MC-QCISD and MCG3 methods. The former is especially well suited for economical geometry optimization, and both methods have excellent performance-to-cost ratios, especially when compared to using single-level methods. We have also shown how even greater accuracy can be obtained by using parameters specifically optimized for combustion problems.

We developed a multi-configuration version of molecular mechanics (MCMM) that allows a convenient interface of high-level ab initio calculations with molecular mechanics force fields. Although, strictly speaking, the use of MCMM is not direct dynamics, it accomplishes much the same purpose because it does not require artfulness in surface fitting, and yet it yields a semiglobal potential energy surface that is valid in the whole reaction swath, not just along a one-dimensional path. However, it has the great advantage that it allows the use of high-level electronic methods at minimal cost.

We have developed a new hybrid density functional method parameterized for kinetics, and we have tested this with both the 6-31+G(d,p) and MG3 basis sets. The results have been tested against a 22-reaction database of barrier heights (that we developed specifically for this purpose), and the mean unsigned error in barrier heights is only 1.5 kcal/mol. The new methods have been shown to provide excellent quality for saddle point geometries.

We have made several applications of our methods to calcuate rate constants for specific chemical reactions. Recent applications of this type include $CH_4 + O(^3P)$, $T + H_2$, D_2, and HD, $Cl + CH_4$, $Cl + H_2$ and D_2, $O(^3P) + HCl$, $CH_3 + H_2$, $Cl + HBr$, $OH + CH_4$, $NH_2 + CH_4$, $CH_2F + CH_3Cl$, and $OH + C_3H_8$.

We recently improved the large-curvature tunneling (LCT) method so that it is more robust for anharmonic potential energy surfaces.

We have developed several software packages for applying variational transition state theory with optimized multidimensional tunneling coefficients to chemical reactions. The URL for our software distribution site is http://comp.chem.umn.edu/Truhlar. The number of license requests that we have fulfilled for software packages developed under DOE support are as follows:

	Total	*academic*	*government*	*industry*
POLYRATE	338	276	29	33
MORATE	77	69	3	5
GAUSSRATE	137	111	15	11
ABCRATE	15	14	1	0
AMSOLRATE	21	21	0	0

Future plans

Our objective is to increase the applicability and reliability of variational transition state theory with semiclassical tunneling calculations for combustion reactions. An important part of how we plan to do this is further improvement of the interface with high-level electronic structure calculations. We will continue to develop single-level and dual-level direct dynamics methods as well as multi-configuration molecular mechanics methods for carrying out rate calculations with potential energy surfaces based on high-level electronic structure theory, and we will continue to develop new multi-level electronic structure methods for kinetics. In addition to developing the methods, we are putting them into user-friendly packages that will allow more researchers to carry out calculations conveniently by the new methods.

VTST is being applied to selected reactions of three types: (i) important test cases for the new methods, (ii) reactions of fundamental importance for further development of dynamical theory, and (iii) important combustion reactions, for example, reactions of hydroxyl radicals with unsaturated systems and reactions of hydrogen atoms with alcohols. We are also developing new methods for the calculation of substituent effects.

Publications, 1999-present

Journal articles

1. "A Mapped Interpolation Scheme for Single-Point Energy Corrections in Reaction Rate Calculations and a Critical Evaluation of Dual-Level Reaction-Path Dynamics Methods," Y.-Y. Chuang, J. C. Corchado, and D. G. Truhlar, J. Phys. Chem. A **103**, 1140-1149 (1999).
2. "Optimized Parameters for Scaling Correlation Energy," P. L. Fast, J. Corchado, M. L. Sanchez, and D. G. Truhlar, Journal of Physical Chemistry A **103**, 3139-3143 (1999).
3. "Simple Approximation of Core-Correlation Effects on Binding Energies," P. L. Fast and D. G. Truhlar, Journal of Physical Chemistry A **103**, 3802-3803 (1999).

4. "Multi-Coefficient Correlation Method for Quantum Chemistry," P. L. Fast, J. C. Corchado, M. L. Sánchez, and D. G. Truhlar, Journal of Physical Chemistry A **103**, 5129-5136 (1999).
5. "Multi-Coefficient Gaussian-3 Method for Calculating Potential Energy Surfaces," P. L. Fast, M. L. Sánchez, and D. G. Truhlar, Chemical Physics Letters **306**, 407-410 (1999).
6. "Variational Transition State Theory with Optimized Orientation of the Dividing Surface and Semiclassical Tunneling Calculations for Deuterium and Muonium Kinetic Isotope Effects in the Free Radical Association Reaction H + $C_2H_4 \rightarrow C_2H_5$," J. Villà, J. C. Corchado, A. González-Lafont, J. M. Lluch, and Donald G. Truhlar, Journal of Physical Chemistry A **103**, 5061-5074 (1999).
7. "Direct Dynamics for Free Radical Kinetics in Solution: Solvent Effect on the Rate Constant for the Reaction of Methanol with Atomic Hydrogen," Y.-Y. Chuang, M. L. Radhakrishnan, P. L. Fast, C. J. Cramer, and D. G. Truhlar, Journal of Physical Chemistry **103**, 4893-4909 (1999).
8. "Energetic and Structural Features of the $CH_4 + O(^3P) \rightarrow CH_3 + OH$ Abstraction reaction: Does Perturbation Theory from a Multiconfiguration Reference State (Finally) Provide a Balanced Treatment of Transition States?", O. Roberto-Neto, F. B. C. Machado, and D. G. Truhlar, Journal of Chemical Physics **111**, 10046-10052 (1999); *erratum*: **113**, 3929 (2000).
9. "Statistical Thermodynamics of Bond Torsion Modes," Y.-Y. Chuang and D. G. Truhlar, Journal of Chemical Physics **112**, 1221-1228 (2000).
10. "Multilevel Geometry Optimization," J. M. Rodgers, P. L. Fast, and D. G. Truhlar, Journal of Chemical Physics **112**, 3141-3147 (2000).
11. "Comment on Rate Constants for Reactions of Tritium Atoms with H_2, D_2, and HD," J. Srinivasan and D. G. Truhlar, Journal of Physical Chemistry A **104**, 1965-1967 (2000).
12. "How Should We Calculate Transition State Geometries for Radical Reactions? The Effect of Spin Contamination on the Prediction of Geometries for Open-Shell Saddle Points," Y.-Y. Chuang, E. L. Coitiño, and D. G. Truhlar, Journal of Physical Chemistry A **104**, 446-450 (2000).
13. "Improved Coefficients for the Scaling All Correlation and Multi-Coefficient Correlation Methods," C. M. Tratz, P. L. Fast, and D. G. Truhlar, PhysChemComm **2**, 14:1-10 (1999).
14. "Potential Energy Surface, Thermal and State-Selected Rate Constants, and Kinetic Isotope Effects for $Cl + CH_4 \rightarrow HCl + CH_3$" J. C. Corchado, D. G. Truhlar, and J. Espinosa-Garcia, Journal of Chemical Physics **112**, 9375-9389 (2000).
15. "Multiconfiguration Molecular Mechanics Algorithm for Potential Energy Surfaces of Chemical Reactions" Y. Kim, J. C. Corchado, J. Villà, J. Xing, and D. G. Truhlar, Journal of Chemical Physics **112**, 2718-2735 (2000).
16. "Dynamics of the $Cl+H_2/D_2$ Reaction: A Comparison of Crossed Molecular Beam Experiments with Quasiclassical Trajectory and Quantum Mechanical Calculations," M. Alagia, N. Balucani, L. Cartechini, P. Casavecchia, G. G. Volpi, F. J. Aoiz, L. Bañares, T. C. Allison, S. L. Mielke, and D. G. Truhlar, Physical Chemistry Chemical Physics **2**, 599-612 (2000).
17. "Thermochemical Analysis of Core Correlation and Scalar Relativistic Effects on Molecular Atomization Energies," J. M. L. Martin, A. Sundermann, P. L. Fast, and D. G. Truhlar, Journal of Chemical Physics **113**, 1348-1358 (2000).

18. "MC-QCISD: Multi-Coefficient Correlation Method Based on Quadratic Configuration Interaction with Single and Double Excitations," P. L. Fast and D. G. Truhlar, Journal of Physical Chemistry A **104**, 6111-6116 (2000).
19. "Adiabatic Connection for Kinetics," B. J. Lynch, P. L. Fast, M. Harris, and D. G. Truhlar, Journal of Physical Chemistry A **104**, 4811-4815 (2000).
20. "Improved Algorithm for Corner Cutting Calculations," A. Fernandez-Ramos and D. G. Truhlar, Journal of Chemical Physics **114**, 1491-1496 (2001).
21. "Thermal and State-Selected Rate Coefficients for the $O(^3P)$ + HCl Reaction and New Calculations of the Barrier Height and Width," S. Skokov, S. Zhou, J. M. Bowman, T. C. Allison, D. G. Truhlar, Y. Lin, B. Ramachandran, B. C. Garrett, and B. J. Lynch, Journal of Physical Chemistry A **105**, 2298-2307 (2001).
22. "How Well Can Hybrid Density Functional Methods Predict Transition State Geometries and Barrier Heights?" B. J. Lynch and D. G. Truhlar, Journal of Physical Chemistry A **105**, 2936-2941 (2001).
23. "Multi-Coefficient Correlation Method: Comparison of Specific-Range Reaction Parameters to General Reaction Parameters for $C_nH_xO_y$ Compounds," P. L. Fast, N. Schultz, and D. G. Truhlar, Journal of Physical Chemistry A **105**, 4143-4149 (2001).

Long abstract

1. "Thermochemistry, Solvation, and Dynamics," D. G. Truhlar, Y.-Y. Chuang, E. L. Coitiño, J. C. Corchado, C. J. Cramer, D. Dolney, J. Espinosa-Garcia, P. L. Fast, G. D. Hawkins, Y. Kim, J. Li, B. Lynch, M. L. Radhakrishnan, O. Roberto-Neto, J. M. Rodgers, M. L. Sánchez, J. Villa, P. Winget, and T. Zhu, in *American Chemical Society Division of Fuel Chemistry Preprints of Symposia,* Vol. 44 (American Chemical Society, Washington, 1999), pp. 452-458.

Book chapters

1. "Vignette: Present-Day View of Transition State Theory," in *Physical Chemistry*, 2nd ed., edited by R. S. Berry, S. A. Rice, and J. Ross (Oxford University Press, New York, 2000), Section 30.6.
2. "Molecular Scale Modeling of Reactions and Solvation," D. G. Truhlar, in *Proceedings of FOMMS 2000: Foundations of Molecular Modeling and Simulation*, Keystone, Colorado, July 23-28, 2000, edited by P. T. Cummings and P. R. Westmoreland (American Institute of Chemical Engineers, New York, 2001), to be published.

Computer programs

"POLYRATE-version 8.1," Y.-Y. Chuang, J. C. Corchado, P. L. Fast, J. Villà, W.-P. Hu, Y.-P. Liu, G. C. Lynch, K. A. Nguyen, C. F. Jackels, M. Z. Gu, I. Rossi, E. L. Coitiño, S. Clayton, V. S. Melissas, R. Steckler, B. C. Garrett, A. D. Isaacson, and D. G. Truhlar, University of Minnesota, Minneapolis, May 1999. Version 8.2, Aug. 1999. Version 8.4, Dec. 1999. Version 8.5, Oct. 2000.

"MORATE-version 8.1/P8.1-M5.07," Y.-Y. Chuang, P. L. Fast, W.-P. Hu, G. C. Lynch, Y.-P. Liu, and D. G. Truhlar, July 1999. Version 8.2/P8.2-M5.08, Oct. 1999. Version 8.3/P8.2-M5.09, Oct. 1999. Version 8.4/P8.4-M5.09, Dec. 1999. Version 8.5/P8.5-M5.09, Oct. 2000.

"GAUSSRATE–version 8.4," J. C. Corchado, E. L. Coitiño, Y.-Y. Chuang, and Donald G. Truhlar, Dec. 1999. Version 8.5, Oct. 2000. Version 8.6, Nov. 2000.

"AMSOLRATE-version 8.5," Y.-Y. Chuang, Y.-P. Liu, and Donald G. Truhlar, Jan. 2000.

KINETIC DATABASE FOR COMBUSTION MODELING

Wing Tsang
National Institute of Standards and Technology
Gaithersburg, MD 20899
wing.tsang@nist.gov

Program Scope

The description of combustion phenomenon in terms of fundamental chemical and physical properties has long been an important scientific goal. With the advances in computer technology, the possibilities in simulations promise more practical results. Specifically, simulations can become a powerful tool to complement physical testing for the development of new and the optimization of old technology. The remarkable advances in CFD have now brought renewed attention to the basic chemistry since the combination of fluid dynamics with chemistry means that real devices can be simulated. Such chemistry is represented in the database as the thermodynamic properties and the rate expressions that describe the interactions of molecules. It is the aim of this program to provide the best values through a combination of evaluation of experimental data and predictions based on appropriate theory.

Recent Progress

One of the main impediments to the proper description of combustion chemistry is the treatment of energy transfer effects. In earlier reports we have described our program CHEMRATE that resolves many of the issues. We can now return to our primary mission , the building of kinetic databases for combustion applications. In the following we describe work we have carried out on the ethanol combustion system. They illustrate some of the issues in building such databases.

A. Initial Processes in Ethanol Combustion: Ethanol is an important fuel. Its initial decomposition characterized by three channels. They are:

$$C_2H_5OH \Rightarrow C_2H_4 + H_2O$$
$$C_2H_5OH \Rightarrow CH_3 + CH_2OH$$
$$\Rightarrow C_2H_5 + OH$$

The bond breaking reactions are particularly important since they release radicals into the system. As will be seen below there is sufficient experimental data and from general trends regarding unimolecular reactions to make estimates of the high pressure rate expressions. A particular challenge is the possibility of concerted processes, involving simultaneous bond breaking and formation. The means of estimating such processes on the basis of ab initio theory[6] are now only beginning to appear. Unfortunately there is still considerable uncertainty on the accuracy of such predictions. Hence the constant need for experimental verification

Marinov[1] has recently published a modeling study on the combustion of ethanol. In the course of this work he developed a chemical kinetic database and was able to match a great volume of experimental work. Particularly important is his inclusion of results of sensitivity analysis that indicated that the initial processes are the key reactions influencing the experimental observations on ignition delay. With the lack of fundamental kinetic data on the combustion of

fuels of even moderate complexity, it is clear that increasingly we will have to rely on information of a global nature for fundamental kinetic information. The large volume of data on ignition delays may permit deductions on initial decomposition mechanisms and rates.

Data on the high pressure rate expressions for ethanol decomposition in can be found in Table 1[1,3-6]. The second column contains the recommendations of Marinov in the Arrhenius form. These are based on the implementation of Benson's restricted rotor concept as given in Gilbert and Smith[7]. However it should be noted that Gilbert and Smith has found that a rigorous application of the physical ideas of Benson does not always lead to correct answers. We have used a modified approach where the restricted rotors are described in such a fashion so that correct high pressure rate expressions are obtained. This depends of course on the existence of experimental data either directly or as inferred. Two expressions are given for reactions involving hydroxymethyl this is because Marinov suggested the use of 2.1 kcal/mol as its heat of formation. For our evaluation we have chosen to use a number 4.2 kcal/mol based on the careful analysis of Johnston and Hudgens[2]. Also included are experimental studies at lower temperatures. These are maximum values since no account was taken of the possibility of disproportionation process. We have also included in the second column a semi-empirical estimate we gave many years ago. There is total rate expression for ethanol decomposition at about 2.5 bar or $8.5 \times 10^{13} \exp(-66300/RT)$[8]. It is clear that the estimates of Marinov lead to very large A-factors for the decomposition process and rate constants for the reverse combination process. There is no experimental basis for values as large as the ones that could be deduced from his results. His rate expression for the molecular channel appear to be more reasonable.

Of course at the high temperature environment rate constants are in the fall-off region. Therefore a more direct comparison is offered by a determination of rate constants. Results are summarized in Figure 1. The results of Marinov are based on the Troe expressions presented in his paper. Our results are based on the data presented in Table 1 and using CHEMRATE, with the particular requirement that the total rate constant equal that determined by Herzler et al. It is clear that there remains a large discrepancy between the numbers in Marinov's data base and those derived here. A very serious consequence is that if our recommendations are correct then the agreement with respect to the ignition delay measurements is much poorer. Due to the multichannel nature of the process the rate constants for the three channels are in fact related. Thus if one lowers the rate constant for the molecular channel (the main reaction) then the rate constant for the C-C bond cleavage channel will actually be increased. This inter-relationship is most striking for the highest channel (C-O bond breaking), hence the much smaller rate constant. Indeed, the greater discrepancy with the predictions of Marinov leads us to suspect that he treated each channel on an individual basis. This demonstrates that in the development of kinetic data base, full attention must always be paid to available experimental results.

B: Metathesis Reactions involving Ethanol: There are three types of abstractable hydrogens in ethanol. Standard experimental techniques involving direct determination of the decay of the attacking species leads only to the rate constants for the total reaction. What is needed is the branching ratios for radical attack on ethanol. The sequence of reactions are;

$$R + CH_3CH_2OH \Rightarrow RH + CH_2CH_2OH \Rightarrow CH_2CH_2 + OH$$
$$\Rightarrow RH + CH_3CHOH \Rightarrow CH_3CHO + H$$
$$RH + CH_3CH_2O \Rightarrow CH_2O + CH_3$$

Table 1: Summary of data and results on the unimolecular decomposition of ethanol at limiting high pressures

Reactions		
K ($CH_3 + CH_2OH$)$_{inf}$	**Marinov(1)** $5.8x10^{17}exp(-86670/RT)$ Or exp (-84770/RT)	$5x10^{14}$(1100K)
	Tsang(3) $2.5x10^{16}exp(-84000/RT)$	$3x10^{13}$ (1100 K)
		Pagsberg et al (5) $8.5x10^{13}$
K (CH_3CH_2+OH)$_{inf}$	**Marinov (1)** $4.7x10^{17}exp(-92456/RT)$	**Marinov** $9x10^{14}$
		Fagerstrom (4) $7.7x10^{13}$(200-400K)
K ($C_2H_4 + H_2O$)	**Butkovskaya et al** (calc) (6)) $2.5x10^{14}exp(-69200/RT)$ 1100K	

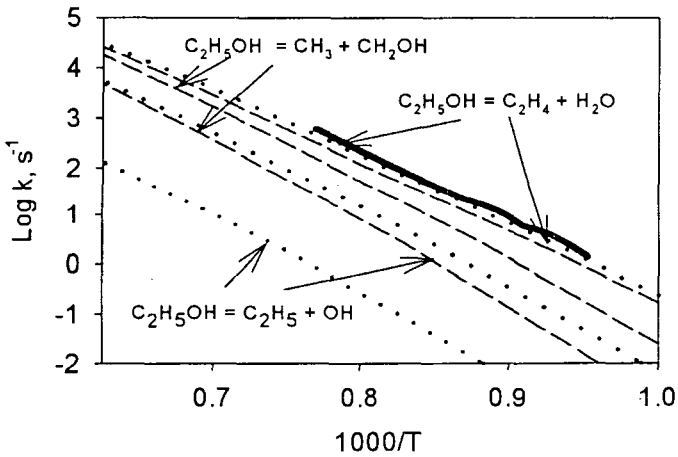

Figure 1: Rate constants as a function of temperature for ethanol decomposition at 2 bar. Dashed lines are the recommendations of Marinov. Dots are from present calculations. Solid line is the experimental results of Hertzler et al. for ethanol disappearance

Obviously the yields of reactive radicals such as OH and H as opposed to a relatively unreactive species such as CH_3 have important consequences in a reactive ethanol system. Dobe et al.[9] have recently determined the branching ratio of OH attack methanol through direct measurment of methoxy and methylhydroxy radicals in the temperature range 300-600 K range. The results are in fair agreement with the correlations developed by Kwok and Atkinson[10] on OH attack on organics. For methyl radicals of Gray and Herod[11] have used deuterium labelling. to determine the branching ratios of CH_3 attack on ethanol. All of these results indicate that the rate constant for the abstraction of a hydrogen from the OH is only slightly smaller than that from a C-H structure. More recent calculational studies by Lendvay et al. [12] for H atom attack on methanol using BAC-MP4 and Gaussian-methods have led to the conclusion that the rate constant for the abstraction of H from OH is much smaller than that of the hydrogen from the methyl group. The actual values being negligible at room temperature and only 10% at 2000 K. The exothermicity of the OH reaction makes the lack of specificity for this reaction not surprising. However when this is coupled with very similar results with methyl, this would seem to make the calculated results with H-atoms extremely surprising. This highlights the problems of using calculational methods for branching ratios. The authors' quoted uncertainty of 2

kcal/mol for each reaction could justify an uncertainty of 4 kcal/mol for the difference in activation energies of the two processes. Furthermore the 2 kcal/mol uncertainty is based on results for ground state molecules. It may well be much larger for transition states. Tentatively we will base our recommendation for H-atom attack on the ratios deduced by Gray and Herod for methyl radical attack on ethanol

Future Plans

For the coming year our attention will be focussed on the reactions of unsaturated radicals that lead to the formation of aromatic rings. This will make full use of our Chemrate program, since the important reactions are the chemical activation processes that lead to the buildup of the larger unsaturated compounds that ultimately lead to soot.

Recent Publications

1. Knyazev, V. D. and Tsang, W., "Incorporation of Non-Steady State Unimolecular and Chemically Activated Kinetics into Complex Kinetic Schemes. 1. Isothermal Kinetics at Constant Pressure", J. Phys. Chem., A103, 3944, 1999,
2. Tsang, W. and Lifshitz, A., "Single Pulse Shock Tube" in Part III "Chemical Reactions in Shock Waves, in Handbook of ShockWaves", Academic Press, New York, in press
3. Tsang, W. and Mokrushin, V. Mechanism and Rate Constants for 1,3-butadiene decomposition, 28th Symo. (Int'l) Comb., The Combustion Institute, Pittsburg, PA, (in press)
4. Knyazev, V. and Tsang, W. Chemically and Thermally Decomposition of Secondary Butyl Radical, J. Phys. Chem., A 104, 10747, 2000
5. Tsang, W., A Pre-processor for the Generation of Chemical Kinetic Data for Simulations **AIAA** Paper **#20001-0359,** Proceedings of the 39th Aerospace Sciences Meeting, Reno, Nevada, 2001

References

1 Marinov, N. M., Int. J. Chem. Kin., 31, 183, 1999
2 . Johnston, R. and Hudgens,J. J. Phys. Chem.,
3 Tsang, W., Int. J. Chem. Kin., 8, 173, 192
4 Pagsberg, P., Munke, J., Sillesen, A and Anastasi, C., Chem. Phys, Lett., 1988, 146, 34.
5 Fagerstrom K., Lund, A., Mahmoud, G., Jodkowski, J, T., and Ratajaczak, E., Chem. Phys. Lett., 1993, 208,321
6 Butkovskaya, N. L., Zhao, Y. and Setser, J. Phys. Chem., 1994, 98. 10779375
7. Gilbert, R. and Smith, S. C. "Theory of Unimolecular and Combination Reactions" Blackwell Scientific Publications, Oxford, 1990
8. Herzler, J., Tsang, W. and Manion, J. A., J. Phys. Chem., 101, 5500, 1997
9 . Dobe, S., Berces, T.,. Temps, F., Wagner, H, Gg., and Ziemer, 25th Symp. (int'l) on Combustion 1994; 775
10 Kwok, E. C. S. and Atkinson, R., Atm. Env. 195, 29, 1685
11. Gray, P., and Herod, Trans. Farad.Soc., 64, 1568, 1968
12. Lendvay, G., Berces, T., and Marta, F., J. Phys. Chem., 1997, 101, 1588

SINGLE-COLLISION STUDIES OF ENERGY TRANSFER AND CHEMICAL REACTION

James J. Valentini
Department of Chemistry
Columbia University
3000 Broadway, MC 3120
New York, NY 10027
jjv1@chem.columbia.edu

PROGRAM SCOPE

This research program aims to develop an understanding of the dynamics of reactions that are actually important in combustion media, those that are prototypes of such reactions, and those that illustrate fundamental dynamical principles that underlie combustion reactions. Study of reaction dynamics means asking many different questions. The one that we pose in our current work is how "many body" effects influence bimolecular reactions. By many-body effects we mean almost anything that results from having a reaction with a potential energy surface of more than three dimensions. These are polyatomic reactions, that is, reactions in which one or both the reactants and one or both of the products are triatomic or larger molecules. Our major current interest is in reactions for which the reactants offer multiple, identical reaction sites. Our aim is not to provide a complete description of any one molecular system, but rather to develop a general understanding of how the factors of energetics, kinematics, and reactant/product structure control the dynamics in a series of analogous systems. In a newer effort we are interested in many-body effects in simple reactions studied in molecular clusters.

Our experiments are measurements of quantum-state-resolved partial cross sections under single-collision conditions. We use pulsed uv lasers to produce reactive radical species and thereby initiate chemical reactions. The reaction products are detected and characterized by Doppler-resolved resonant multi-photon ionization and time-of-flight mass spectroscopy.

RECENT PROGRESS

State-to-State Dynamics of H + RH → H_2 + R (RH = alkane)

We have studied a homologous series of reactions, H + RH → H_2 + R reactions, where RH is an alkane. H atoms are prepared by laser photolysis; H_2 is state-selectively detected under single-collision conditions by pulsed laser REMPI. The rovibrational state distributions of the H_2 product are measured. Doppler profiles of the REMPI transitions for each rovibrational state reveal the translational energy disposal. We have now completed such experiments for CD_4, $CDCl_3$, the linear alkanes ethane, propane, n-pentane, n-hexane, and the cyclic alkanes cyclobutane, cyclopentane, and cyclohexane. All the reactions have the same light + light-heavy → light-light + heavy kinematics. All have nearly the same thermochemistry. They are

differentiated by their structure, specifically by the stereochemisty of neighboring C-H reaction sites, and by their moments of inertia.

We have developed a model to describe these reactions, which we call the local reaction model. It builds on the model we developed and confirmed in our previous experimental and theoretical studies of the energetically and kinematically similar H + HX → H_2 + X (HX = HCl, HBr, HI) reactions. The local reaction model invokes two aspects of the structure of the RH reactant and R product as influencing the dynamics. The first is the proximity and stereochemistry of multiple, identical, competing C-H sites in RH. The second is the small rotational constants of the alkyl radical.

Multiple, competing reaction sites reduce the H_2 product rotational angular momentum through truncation of the local opacity function, an opacity function expressed in terms of a local impact parameter, the distance from the relative velocity vector to a line parallel to it passing through the abstracted H atom. This local impact parameter was shown to be the source of the rotational angular momentum of the H_2 product of the H + HX reactions. The truncation of the opacity function comes from the overlap of cones of acceptance on adjacent C-H reaction sites.

The small rotational constants of the alkyl radical product exert a counterbalancing effect, facilitating rotational excitation of the H_2 by relaxing the otherwise very strong coupling between conservation of total angular momentum and total energy. The rotational constants are so small that the energy "cost" of R rotational angular momentum is essentially zero on the energy scale of these reactions. At zero energy "cost" R rotation serves as a very effective sink for angular momentum, opening up larger H_2 rotational angular momentum at a particular total angular momentum.

Our model shows how these two opposing effects work differentially on H_2 in v′=0 and v′=1, leading to higher rotational excitation in v′=1 than in v′=0, the feature that is observed to be common to all H + RH reactions. It can also explain the differentiation of the reactions in terms of their energy disposal, accounting for the changes in energy disposal between classes and within classes of RH.

Kinematic Constraints on Product Energy Disposal

Stemming from our work on the H + RH reactions we have developed a kinematic model to describe a very interesting, and apparently universal, feature of energy disposal in bimolecular reactions at suprathreshold energies. Reviewing extensive work from our own lab as well as a large body of work from many other labs in which quantum state distributions of the products of bimolecular reactions have been determined, we found a startling result: only a fraction of the energetically and dynamically accessible quantum states are actually being populated. The set of data on which this conclusion rests is very large, spanning reactions that take place on a variety of different potential energy surfaces, so it must be a dynamical effect that is not connected with the specific features of one, or even one class of, reactions.

We have shown that the organizing principle, the physical phenomenon responsible for this behavior, is a kinematic constraint. Briefly, at suprathreshold collision energies we posit that reaction takes place by a

trajectory reflecting off the inner corner of the potential energy surface. Using that concept alone we show that the trajectory will lead to products only if the product translational energy is greater than a minimum value, given by $E_{rel} \sin^2\beta$ where β is the skew angle and E_{rel} is the relative energy of the reactants. This minimum translational energy implies a maximum internal energy, which is $E_{rel} \cos^2 \beta - \Delta H$, where ΔH is the reaction enthalpy. We computed this maximum energy for all the reactions for which state-to-state measurements were available, and we found that in all cases the highest energy populated quantum states were those with this maximum energy.

Reactions in Clusters

A future direction of our work is to investigate many-body effects in reactions in clusters. The clusters provide an environment in which three-body effects, like those that govern termolecular processes such as recombination, can be readily explored. We will be looking at reactions/energy transfer in HX (HX = HCl, HBr, HI) dimers in which one of the two H-X bonds is broken by uv photolysis and the whole range of possible chemical processes—energy transfer, abstraction reaction, exchange reaction, recombination—are examined and characterized:

$$\begin{aligned} H'X' \bullet HX \rightarrow [H' + X' + HX] &\rightarrow H' + X' + HX^{\dagger} \\ &\rightarrow H'X^{\dagger} + X' + H \\ &\rightarrow H'X'^{\dagger} + HX^{\dagger} \\ &\rightarrow H'H^{\dagger} + X' + X. \end{aligned}$$

Here the dagger indicates rovibrational excitation. To begin that effort we have quite thoroughly characterized a molecular beam source of HCl dimer, establishing conditions for which the dimer is the only abundant cluster species. We have studied the vibrational predisscíation of $(HCl)_2$, and have: measured very accurately the dimer bond energy, determined predissociation lifetimes for several different dimer vibrational states, characterized the excitation-mode-dependence of the HCl product state distributions, and established the correlation between the rotational states of the two HCl products. We have also studied the uv photodissociation dynamics of the dimer, measuring the rovibrational state distribution of the HCl product (all channels). One surprising result of these two measurements is that the HCl product of the vibrational predissociation is very much "hotter" rotationally than the HCl product of the uv (193 nm) photodissociation. Further, the uv photolysis yields no detectable v'=1 HCl, despite the fact that the 193 nm photolysis makes states up to v'= 5 energetically accessible.

FUTURE PLANS

In the next year we expect to bring to a conclusion our studies of H + RH $\rightarrow H_2$ + R reactions. Measurements of the H_2 product rovibrational state distributions for RH = cyclopropane, isobutane, and neopentane will be completed. These will further test the local reaction model we have developed to describe the dynamics of these reactions. We also expect to

begin detailed measurements of the product branching and energy disposal in photoinduced reactions in $(HCl)_2$. We plan to measure both rovibrational state distributions as well as angle-speed distributions of as many products as are detectable.

PUBLICATIONS

1. H. Ni, J. Serafin, and J.J. Valentini, "Dynamics of the Vibrational Predissociation of HCl Dimer," J. Chem. Phys. 113, 3055-3066 (2000).

2. C.A. Picconatto, A. Srivastava, and J.J. Valentini, "Reactions at Suprathreshold Energy: Evidence of a Kinematic Limit to the Internal Energy of the Products," J. Chem. Phys. 114, 1663-1671 (2001).

3. C.A. Picconatto, A. Srivastava, and J.J. Valentini, "The H + n-C_5H_{12}/n-C_6H_{14} → $H_2(v', j')$ + C_5H_{11}/C_6H_{13} Reactions: State-to-State Dynamics and Models of Energy Disposal," J. Chem. Phys. 114, 4837-4845 (2001).

4. C.A. Picconatto, H. Ni, A. Srivastava, and J.J. Valentini, "Quantum State Distribution of HCl from the uv Photodissociation of HCl Dimer," J. Chem. Phys. 114, xxxx (2001).

5. C.A. Picconatto, A. Srivastava, and J.J. Valentini, "State-to-State Dynamics of the H + $CD_3(CH_2)_4CD_3$ → H_2 + $CD_3((CH_2)_3CH)CD_3$ Reaction: Dynamics of Abstraction of Secondary H in Linear Alkanes," Chem. Phys. Lett. 138 xxx (2001).

6. J.J. Valentini, "State-to-State Chemical Reaction Dynamics in Polyatomic Systems: Case Studies," Ann. Rev. Phys. Chem. 52, 15-39 (2001).

Theoretical Studies of the Dynamics of Chemical Reactions

Albert F. Wagner

Gas Phase Chemical Dynamics Group
Chemistry Division
Argonne National Laboratory
Argonne, IL 60439
wagner@tcg.anl.gov

Program Scope

The goal of this program is to apply and extend dynamics and kinetics theories to elementary reactions of interest in combustion. Typically, the potential energy surfaces used in these applications are determined from ab initio electronic structure calculations, usually by other members of the group. Generally the calculated kinetics or dynamics is compared to experimental results, often generated by other members of the group.

Recent Progress

Studies of the OH+CO van der Waals Molecules. In collaboration with M. Lester (U. of Pennsylvania) and L. Harding and S. Gray in our group, we have been studying both experimentally and theoretically the van der Waals molecules of OH and CO that precede the transition state for entering the HOCO well:

$$\mathrm{OH + CO \leftrightarrow (OH)\text{-}(CO) \leftrightarrow [HOCO]^* \rightarrow H + CO_2}$$

$$\downarrow \mathrm{M}$$

$$\mathrm{HOCO}$$

In the experiments of Lester, OH-CO complexes are formed in a molecular beam and then studied with infrared action spectroscopy using the vibrational overtone of OH. Vibrational levels of several bound states appear. Harding's electronic structure calculations of the potential energy surface in the vicinity of van der Waals region confirm that two minima exist and that both are connected to the reaction path that leads to the barrier at the entrance of the HOCO well. The minima have the linear geometry OHCO and OHOC. This means that excitations of the bending vibrational levels of these van der Waals molecules can push the system along the reaction path, resulting in either reactive chemistry ($H+CO_2$) or extended exploration of the HOCO well. Both these outcomes can be in principle experimentally detected. Such detection in a spectroscopic experiment would give a refined characterization to the HOCO transition state which has so far only been characterized via kinetics experiments. To understand the present measurements, the Renner-Teller effect comes into play because bending off of linear OHCO or OHOC produces A' and A" electronic states. On a reduced three dimensional surface for both the A' and A" states, Gray has carried out quantum dynamics calculations for the first twenty or so bound states. Using these levels, perturbation theory for the Renner-Teller coupling, and the asymptotic spin-orbit splitting of the OH, an initial theoretical estimate of the van der Waals spectra can be made. While rough, this estimate does reproduce the ordering and approximate location of the observed states. Further calculations using higher dimensional surfaces are in progress.

Electrostatic Effects in the Stabilization of HO_2*. In collaboration with J. Michael in our group, we are investigating the buffer gas dependence of the low pressure limit of the recombination of H with O_2.

$$H + O_2 \leftrightarrow [HO_2]^* \rightarrow HO + O$$

$$\downarrow M$$

$$HO_2$$

Recent experiments by Michael confirm the observations of others that when M is H_2O, the recombination rate constant to form HO_2 is more than a factor of 10 higher than when M is a rare gas or N_2. As the major chain branching reaction in flames, it is important to understand this pressure dependence. The stabilization ability of M is controlled by two factors: the number of collisions between M and $[HO_2]^*$ and the average energy transfer that results from each collision. To explore the M dependence of the first factor, the collision number can be estimated by the thermal rate constant to recombine M and HO_2 as if they both were thermalized reactants colliding under the influence of long-range electrostatic forces. This is not to say that M-HO_2 form a collision complex that last long enough to influence chemistry but rather that the closeness of approach required by complex formation is a good measure of the kind of collisions that de-activate chemically activated molecules. This approximation is similar to the work of others (e.g., I. Smith at Birmingham) in estimating the high pressure limit of A+BC by measuring the deactivation of A+BC(v=1). We have calculated the dipole and quadrupole moments of HO_2 and found them comparable to those of water. The average polarizability of HO_2 and numerous other gases have been tabulated by others. By replacing the moments by compact point charge distributions rigidly attached to the molecular frame, the code VARIFLEX can be used to systematically study M+HO_2 "recombination" in the high pressure limit. For M=H_2O, this amounts to an electrostatic long range potential energy surface with R^{-3}, R^{-4}, R^{-5}, and R^{-6} terms. For M=Ar, only the R^{-6} induction term is present. The resulting collision numbers vary by about a factor of five between H_2O and Ar with H_2O being higher. The dissociation energy hydrogen-bonded complex HO_2-H_2O has been calculated by several others. It is bound by about 9.4 kcal/mole. The electrostatic model produces a similar energy at a similar separation between the HO_2 and H_2O center of mass. However, the geometry in the electrostatic model is planar where as that for the hydrogen-bonded system is highly non-planar. Further studies in progress will see if these calculations clarify the M dependence of the H+O_2 recombination.

Cyclopentadienyl Entropy. In collaboration with H. Wang (U. of Delaware) and J. Kiefer (UIC), we have determined the entropy of the cyclopentadienyl radical C_5H_5 including its Jahn-Teller coupling. The C_5H_5 molecule is implicated in several routes to the formation of the first aromatic rings in the sooting chemistry of aliphatic fuels. However, several key reactions, in particular,

$$C_3H_3 + C_2H_2 \rightarrow c\text{-}C_5H_5$$

have been studied only in the reverse direction, requiring an accurate equilibrium constant and thus entropy to obtain the rate in the direction needed. C_5H_5 is distorted from D_{5h} symmetry by the Jahn-Teller effect. The result is a peudorotation of all the atoms in the molecule about each atom's D_{5h} position. The $^2A_2$ and $^2B_1$ electronic states are each visited alternately five times in a complete pseudorotational period. The $^2A_2$ electronic state provides an equilibrium C_{2v} structure and the $^2B_1$ electronic state provides a transition state only a few wavenumbers higher in energy than the equilibrium energy. We carried out CASSCF/cc-PVDZ calculations of both potential surfaces involved in C_5H_5 along all normal coordinates that can be affected by Jahn-

Teller distortion. Both the E'_2 in-plane bend and stretch modes are found to be involved, but the bend contribution is very small and its contribution to the entropy is negligible. The in-plane stretch modes strongly dominate, affording a maximum stabilization energy of 4.73 kcal/mol (i.e., the difference between the conical intersection at D_{5h} geometry and the $^2A_2$ equilibrium geometry. Harmonic frequencies are calculated for the other modes in the D_{5h} configuration, and these are scaled in accordance with a comparison of experimental frequencies with similar calculations on cyclopentadiene. Energy levels for nuclear motion in the Jahn-Teller modes are then determined using the calculated surface, and these are combined with the scaled harmonic frequencies to obtain complete thermodynamic functions for the radical. The computed results allow us to compare the Jahn-Teller thermochemistry with two other simpler but approximate models. One model ignores the Jahn-Teller coupling altogether and derives from the potential energy surfaces what the frequencies would have been if the conical intersection were removed. The second model uses the frequencies for the $^2A_2$ equilibrium geometry, eventhough the lowest frequencies is hindered-rotor like as it corresponds to motion along the direction of the pseudorotation. The Jahn-Teller entropy splits the difference between these two models, being about 1 cal/mole-degree higher than that for the model that ignores the Jahn-Teller and about 2 to 3 cal/mole-degree lower than that for the model that uses the $^2A_2$ equilibrium frequencies.

Other work. In collaboration with J. Michael in our group and T. Truong (U. of Utah), experimental and theoretical studies of the reactions:

$$H_2CO + O_2 \rightarrow HO_2 + HCO.$$
$$H+NO_2 \rightarrow HO+NO$$

have been completed and are being written up. In collaboration with D. Truhlar (U. of Minnesota) and R. Duchovic (Purdue U. Indiana U. at Fort Wayne), we have constructed a potential energy surface subroutine library called POTLIB, the description of which has recently been submitted for publication. Because of an a common interface, any code that uses potential energy surfaces can check out any subroutine from the library and, via a single interface routine, compile, link, and execute with that subroutine. The library contains five example interface routines for ABCRATE and POLYRATE (Truhlar et al.), VENUS (Hase et al.), VARIFLEX (Klippenstein et al.), and DYNASOLVE (Zhang et al.). With M. Minkoff (ANL Math. and Comp. Sci. Division), we are developing a parallelized code for the direct calculation of the cumulative reaction probability (CRP) in a time independent manner using formalism originally developed by Miller et al. (Berkeley). Up to seven degree of freedom model problems have been examined on up to 128 processors at the NERSC SP with relatively good parallelization and a time to solution per eigenvalue of under eight minutes for the largest problem. The SPAM technique (see R. Shepard's abstract) may result in an effective preconditioner for this problem. This and other preconditioners will be explored.

Future Plans

Several of the studies discussed above are in progress and these will be continued. In a new direction, we plan to become more active in theoretical support for our emerging experimental program to study soot morphology (see J. Hessler) at the Advanced Photon Source at ANL. This support could be expressed in reaction rate calculations of soot precursors under experimental study elsewhere (e.g., A. Fahr at NIST). It could also be expressed in simulations with coupled kinetics models (e.g., those of M. Frencklach, Berkeley) aimed directly at morphology. It could also be expressed in terms of Monte Carlo simulations of soot structures and their consequent small angle Xray scattering (SAXS) signal. Soot particles can be extracted from flames and analyzed for their major aromatic components. In principle these components can be assembled with Monte Carlo techniques into 3D structures whose synthetic signal can then be compared to SAXS measurements.

Publications from DOE Sponsored Work from 1998-2001.

The Subspace Projected Approximate Matrix (SPAM) Modification of the Davidson Method
R. Shepard, A. F. Wagner, M. Minkoff, and J. L. Tilson, J. Comp. Phys. (in press).

Mapping the OH+CO → HOCO reaction pathway through infrared spectroscopy of the OH-CO reactant complex
M. I. Lester, B. V. Pond, M.D. Marshall, D. T. Anderson, L. B. Harding, A. F. Wagner, *Faraday Discussions*, **118** (in press)

Evidence of a Lower Enthalpy of Formation of Hydroxyl Radical and a Lower Gas-Phase Bond Dissociation Energy of Water
B. Ruscic, D. Feller, D.A. Dixon, K.A. Peterson, L.B. Harding, R. L. Asher, and A. F. Wagner, J. Phys. Chem. A. **105**, 1-4 (2001).

Initiation in H2/O2: Rate Constants for H_2+O_2 -> $H+HO_2$ at High Temperature
J. V. Michael, J. W. Sutherland, L. B. Harding, and A. F. Wagner, 28th Symposium (International) on Combustion, (in press)

Exploring the OH+CO Reaction Coordinate via Infrared Spectroscopy of OH-CO Reactant Complexes
M. I. Lester, B. V. Pond, D. T. Anderson, L. B. Harding, A. F. Wagner, *J. Chem. Phys.* **113**, 9889-9892 (2000)

High-Performance Computational Chemistry: Hartree-Fock Electronic Structure Calculations on Massively Parallel Processors
J. L. Tilson, M. Minkoff, A. F. Wagner, R. Shepard, P. Sutton, R. J. Harrison, R. A. Kendall, and A. T. Wong, Int. J. High Performance Computing Applications **13**, 291-302 (1999).

Chemical Kinetic Modeling of Combustion

C. K. Westbrook and W. J. Pitz, Principal Investigators
Lawrence Livermore National Laboratory, P. O. Box 808, Livermore, CA 94550

This program involves the use of chemical kinetic modeling to study fundamental combustion processes, primarily involving hydrocarbon fuels. Modeling work is closely coordinated with experimental and theoretical studies at other institutions. In addition, kinetic modeling is used to analyze combustion studies in practical combustion systems, particularly internal combustion engines.

Experimental studies of hydrocarbon ignition in rapid compression machines were used to develop and refine kinetic models of low and intermediate temperature hydrocarbon ignition. In particular, ignition of isomers of pentane provided an interesting study of the influence of molecular structure on low temperature ignition [2]. This work confirmed earlier indications that the overall rate of ignition depends on the types of C – H bonds in the fuel and the size of the fuel molecule. A parallel study [3, 10] used exactly the same kinetic reaction mechanisms and models to study ignition in diesel engines and the variation in sooting tendencies for different fuels, especially those with oxygen included in the fuel. Other modeling studies [6,9] examined the ignition of hydrocarbon fuels in a new class of internal combustion engines, using Homogeneous Charge Compression Ignition (HCCI) technology.

All of this work has focused on the kinetics of low and intermediate temperature hydrocarbon oxidation. This is the same kinetic regime that is responsible for engine knock in spark-ignition engines, ignition in diesel engines, sooting tendencies in diesel engines, ignition in rapid compression machines, and HCCI combustion, and a review of these similarities and interconnections was published [6]. In one important sense, this work places the processes of ignition in practical combustion devices into a new, coherent framework for the first time.

A particularly interesting feature of this work has been the demonstration of the role that oxygen content of diesel fuel plays in soot production. Experimental data from various oxygenated fuels (e.g., methanol, ethanol, dimethyl ether, etc.) in diesel combustion has demonstrated that the soot emissions with these fuels is reduced, compared to conventional diesel fuels, and the amount of soot reduction is proportional to the amount of oxygen in the fuel. Kinetic modeling studies showed that oxygen enrichment reduces the concentrations of selected hydrocarbon species during diesel ignition, and since these are the species that lead to soot production, the oxygen enrichment leads to reduced soot production. Several kinetic modeling studies [3,10] have confirmed this view.

Another kinetic modeling study examined the variation in adiabatic flame temperature with pressure for hydrocarbon flames. Previous studies had examined this effect for stoichiometric fuel-air mixtures at atmospheric pressure. However, in internal combustion engines, most combustion occurs at elevated pressures of 50-100 bars. Our kinetic

modeling work [1] examined the effect of fuel-air equivalence ratio and pressure on flammability limits. This kinetic modeling work showed that the limit to flammability can be related to competition between the main chain branching reaction between atomic hydrogen and molecular oxygen that produces O and OH radicals, and the corresponding reaction with the same reactants to produce hydroperoxy radicals. This balance shifts to richer equivalence ratios at the lean limit of flammability. The implication of this modeling study is that practical engine combustion, occurring at elevated pressures, cannot proceed unless the adiabatic flame temperatures are high enough to make the production of oxides of nitrogen (NOx) inevitable. This result has considerable implications with respect to practical engine combustion studies and could influence regulatory decisions with respect to emissions regulations.

Further kinetic modeling studies consisted of refinements in the basic kinetic data in the models, based on detailed flame studies [5] and rapid compression machine studies [2]. Current work is directed towards refinements of the influence of factors of fuel size and molecular structure on ignition rates. We have also continued to develop the kinetic models for soot chemistry [8], in collaboration with Prof. A. Burcat, an expert in the kinetics of aromatic species chemistry.

An interesting extension of our current hydrocarbon kinetics development has been our work on chemical kinetic modeling of the reaction of chemical warfare nerve agents and their less toxic surrogate compounds that are used frequently in experimental studies. Since many of these compounds are very similar to common hydrocarbon species, it has been possible to extend hydrocarbon mechanisms by including the new groups of chemical species and chemical bonds from the nerve agents and their surrogates. We have published some of this work [4,7], and experimental workers around the world have asked us to participate in their kinetic studies of agent consumption, including the group at Novosibirsk, Russia. This work provides considerable verification of current hydrocarbon models, and it requires only a modest amount of model extension.

The most interesting application of our kinetic modeling work has been to provide a theoretical and modeling understanding of the process of homogeneous charge compression ignition (HCCI) combustion. In this engine, a generally lean fuel-air mixture is ignited by compression in an engine. The mixture is sufficiently lean that the adiabatic flame temperature of the mixture is so low that negligible production of NOx is observed. Our kinetic models have demonstrated that we can predict ignition behaviour in these engines and can confirm the low NOx emissions levels. However, the modeling also shows that these engines will produce substantial unburned hydrocarbon emissions, an observation confirmed by experiments. These calculations, which involve homogeneous ignition in the presence of a thermal boundary layer, show that the low NOx emissions are the result of low combustion temperatures. However, the high hydrocarbon and CO emissions also result from the low temperatures and the extended thermal boundary layers at the engine chamber walls. We will continue to work on this problem and try to develop strategies to make this engine productive.

Our work continues to relate basic chemical kinetics to practical combustion systems. The chemical models are evaluated and verified by comparison between computed results and experimental results in a wide range of conditions, so comparison between experimental and computed results is a very important part of our program. We expect to continue the development of new kinetic models for important hydrocarbons with practical applications in spark-ignition, diesel, and HCCI engines. We also expect to extend models for practical CW agents to increasingly complex nerve agent kinetics. We also expect to continue to develop fundamental data to improve our kinetic models of hydrocarbon combustion, primarily in collaboration with other experimental studies.

Recent Publications

1. Flynn, P. F., Hunter, G. L., Farrell, L. A., Durrett, R. P., Akinyemi, O. C., zur Loye, A. O., Westbrook, C. K., and Pitz, W. J., "The Inevitability of Engine-Out NOx Emissions from Spark-Ignition and Diesel Engines", **Proc. Combust. Inst. 28:** (2001).

2. Ribaucour, M., Minetti, R., Sochet, L.R., Curran, H.J., Pitz, W.J.,and Westbrook, C.K., "Ignition of Isomers of Pentane: An Experimental and Kinetic Modeling Study", **Proc. Combust. Inst. 28:** (2000).

3. Fisher, E. M., Pitz, W. J., Curran, H. J., and Westbrook, C. K., "Detailed Chemical Kinetic Mechanisms for Combustion of Oxygenated Fuels", **Proc. Combust. Inst. 28:** (2000).

4. Glaude, P.-A., Curran, H. J., Pitz, W. J., and Westbrook, C. K., "Kinetic Study of the Combustion of Organophosphorus Compounds", **Proc. Combust. Inst. 28:** (2000).

5. Kaiser, E. W., Wallington, T. J., Hurley, M. D., Platz, J., Curran, H. J., Pitz, W. J., and Westbrook, C. K., "Experimental and Modeling Study of Premixed Atmospheric-Pressure Dimethyl Ether-Air Flames", **Journal of Physical Chemistry A 104**, No. 35, 8194-8206 (2000).

6. Westbrook, C. K., (invited), "Chemical Kinetics of Hydrocarbon Ignition in Practical Combustion Systems", **Proc. Combust. Inst. 28:** (2000).

7. Glaude, P. A., Curran, H. J., W. J. Pitz, and C. K. Westbrook, "A Thermochemical and Kinetic Study of Combustion of Organophosphate Compounds," Annual Meeting of the Gas Phase Kinetic and Photochemical Association, Paris, France, June 6, 2000.

8. Curran, H.J., Wu, C., Marinov, N.M., Pitz, W.J., Westbrook, C.K., and Burcat, A., "The Ideal Gas Thermodynamics of Diesel Fuel Ingredients: I. Naphthalene Derivatives and Their Radicals", **J. Phys. Chem. Ref. Data 29**, 463-517 (2000).

9. Aceves, S. M., Flowers, D. L., Martinez-Frias, J., Smith, J. R., Westbrook, C. K., Pitz, W. J., Dibble, R., Wright, J. F., Akinyemi, W. C., and Hessel, R. P., "A Sequential Fluid-Mechanic Chemical-Kinetic Model of Propane HCCI Combustion," Society of Automotive Engineers paper SAE-2001-01-1027 (2001).

10. Curran, H. J., Fisher, E. M., Glaude, P.-A., Marinov, N. M., Pitz, W. J., Westbrook, C. K., Layton, D. W., Flynn, P. F., Durrett, R. P., zur Loye, A. O., Akinyemi, O. C., and Dryer, F. L., "Detailed Chemical Kinetic Modeling of Diesel Combustion with Oxygenated Fuels," Society of Automotive Engineers paper SAE-2001-01-0653 (2001).

PROBING FLAME CHEMISTRY WITH MBMS, THEORY, AND MODELING

Phillip R. Westmoreland
Department of Chemical Engineering
University of Massachusetts Amherst
159 Goessmann Laboratory, P. O. Box 33110
Amherst, Massachusetts 01003-3110
Phone 413-545-1750
FAX 413-545-1647
westm@ecs.umass.edu
http://www.ecs.umass.edu/che/westmoreland.html

Program Scope

The program's objective is to establish kinetics of combustion and molecular-weight growth in hydrocarbon flames as part of an ongoing study of flame chemistry. Our approach combines molecular-beam mass spectrometry (MBMS) experiments on low-pressure flat flames; *ab initio* thermochemistry and transition-state structures; rate constants predicted by transition-state and collision-mediated reaction theories; and whole-flame modeling using mechanisms of elementary reactions. The MBMS technique is powerful because it can be used to measure a wide range of species quantitatively, including radicals, with high sensitivity and low probe perturbation. Ethylene and allene-doped ethylene flames are presently being studied.

Recent Progress

Summary. In the past year, we have:

- Upgraded our MBMS apparatus to obtain higher sensitivity and more species;
- Begun mapping a fuel-lean allene-doped ethylene flame, including radial profiles;
- Collaborated to develop a photoionization-MBMS flame apparatus at the LBNL ALS;
- Collaborated in mechanism development for a wide range of pressures using low-pressure flame data and high-pressure flow-reactor data from Princeton;
- Developed approaches for flat-flame modeling with accurate energy balances;
- Added data sets to our Web site of flame-profile data.

Upgrade of MBMS and system components. In our flame-sampling MBMS apparatus, we have installed and are shaking down key new experimental components. These include an x-y burner positioner, a McKenna burner, a syringe pump for metering liquids (then vaporized) for feed and calibration, and a new quadrupole mass spectrometer system. The last (from ABB Extrel) is giving higher mass resolution, higher signal sensitivity, negative- as well as positive-ion capability, and more stable operation. Electron-impact ionization is being used in the transverse-mounted MS with both analog and pulse-counting detection modes. Mass ranges are 1-50 amu (ultra-high resolution for separation of O atom from CH_4), 1-500, and 4-2000. The equipment has been delivered and installed. Full use has so far been held back by several returns of the manufacturer's electronics due to problems we discovered. However, initial experiments bear out the new capabilities.

Flame mapping. Our focus is presently on an allene-doped version of a fuel-lean ethylene flame studied earlier in this project by Bhargava.[1] This flame has proved intriguing because of difficulties in modeling the undoped flame by our group, Wang, and Lindstedt, in contrast to more successful modeling of our fuel-rich ethylene flame.[2] We have made a number of consistency checks within the data and data analyses with only modest uncertainties found. Likewise, we have considered uncertainties in the reaction set, experimental temperatures, burner-surface reactions, and probe perturbations. Only modeling with a drastically modified

[1] A. Bhargava and P. R. Westmoreland, *Combustion and Flame* **115**, 456-467 (1998).
[2] A. Bhargava and P. R. Westmoreland, *Combustion and Flame* **113**, 333-347 (1998).

temperature profile made sufficient difference, but the needed alteration is hard to justify and some previous agreement with the data was worsened.

In parallel to mapping the allene-doped flame, we are re-mapping the lean flame using a McKenna burner. This is not the identical flame, even though both are flat flames of the same mixture of feed gases. Like the burner used in our previous studies, this is a sintered-bronze, internally cooled burner. However, its diameter is 6.03 cm compared to 9.91 cm previously. The 40% decrease in diameter corresponds to 63% decrease in flow cross-section and a smaller radius of curvature, which makes experimental edge effects more significant. Consequently, it proved impossible to stabilize the flame at the mixture and linear velocity of the previous study. By reducing the velocity, it is possible to create a flame of the same standoff distance and thus with comparable mole fraction profiles.

New studies of two-dimensional effects are possible because of the added radial-mapping capability. These effects include the approach to ideal flatness, edge effects, and data for examining the mixed fluid-mechanics, heat-transfer, and mass-transfer radial boundary conditions of the flame. Burner uniformity has been a concern even with sintered burners because of Zabielski's observation of apparent jetting in a UTRC MBMS apparatus. Mapping stable species and OH, the present measurements demonstrate good uniformity as close as 2 mm. The edge profiles promise to make it possible to test two-dimensional models of burner-stabilized flames.

Photoionization MBMS using the LBL ALS. A flame-sampling MBMS apparatus is under construction at the LBL Advanced Light Source in collaboration with Tom Baer, Terry Cool, and Andy McIlroy (http://www.chemicaldynamics.lbl.gov/es3/es3set.htm). With the intensity of finely tuned photons from the Chemical Dynamics Beamline, we should be able to discriminate many isomeric species by their photoionization thresholds. This is difficult with tunable laser photoionization because of intensity / resolution limits, and it is worse with electron-impact ionization because of thermal spread in electron energies. Photoionization MS will be carried out with a time-of-flight apparatus, and the beam will also pass through the electron-impact ionization region of a quadrupole MS.

Limited access time on the beamline precludes complete mapping of flames with this apparatus, but the burner arrangement has been designed so the McIlroy and Westmoreland configurations match it. Although extensive measurements of composition, temperature, and streamlines cannot be pursued on the ALS MBMS, they can on the other two systems, which each of which has special capabilities. The key capability of the ALS system is that it can be used to probe questions that have arisen in the other two systems about isomeric species. Specific examples are C_3H_4 (propadiene, propyne, and cyclopropene), C_3H_2, C_4H_3, C_4H_4, C_4H_5, C_5H_5, and C_6H_6 isomers which are important in questions about aromatics formation. The ALS apparatus will also give useful data on photoionization cross-sections.

Modeling combustion over a wide range of pressure and temperature. In collaboration with Fred Dryer's DOE-funded group at Princeton, we have developed a mechanism for use from 30 Torr to 10 atm in C_1 and C_2 hydrocarbon combustion [DOE Publ. 4]. The experimental systems are ethylene combustion in the Bhargava fuel-rich flat flame[1], operated at 20 Torr and a fuel-equivalence ratio of 1.9, and in the Princeton Flow Reactor, operated at lower temperature (850-950 K) and higher pressure (5-10 atm).

The reaction set predicted species profiles with reasonable accuracy in both cases, allowing us to contrast the reaction pathways. The contrasting high-temperature / low-density and high-density / lower-temperature cases share some important reactions, but abstraction chemistry dominates the first while addition dominates the second. Other reaction sets from the literature were tested, but each showed serious errors in at least one of the cases.

In the low-pressure flame, C_2H_4 is mainly consumed by H abstraction, while in the high-pressure system OH abstraction competes with addition of H, making C_2H_5. In both cases, C_2H_3 then proceeds to HCO and CH_2O and eventually to CO and CO_2. However, sensitivity analysis reveals that predictions are not sensitive to the same reactions in both cases. HO_2 chemistry is emphasized in the flow reactor, particularly through the reaction $CH_2O+HO_2 = HCO+H_2O_2$. The model comparisons support a lower value of the rate constant for this reaction, consistent with that recommended by Hochgreb and Dryer [1.5E13 exp(-15200 cal/mol /RT)].

Another improvement is the kinetics for $C_2H_4+HO_2$, which is assigned in a number of mechanisms to the product channel $CH_3CHO+OH$ kinetics. The flow reactor data do not show formation of CH_3CHO. Theoretical considerations indicate that the product should instead be ethylene oxide (oxirane) +OH. The same rate constant is reasonable with only a change of product. Because neither reverse reaction would be important, the change in product has no effect on the rate of C_2H_4 destruction.

In the low-pressure flame, $C_2H_3+O_2$ kinetics determines how much CH_2O and HCO were formed relative to C_2H_2 from C_2H_3 decomposition. Surprisingly, the formation of C_2H_2 from C_2H_3 was slow despite the predicted high level of C_2H_3, the low pressure slowing down the conversion by third-body effects. Formation of C_2H_3OO was negligible in the low-pressure flame, but in the high-pressure system, it was expected to be formed more effectively because of third-body enhancement. However, it was not. When the predictions were made, little C_2H_3 was formed, so little C_2H_3OO was formed. In contrast, C_2H_5 was formed effectively in the flow reactor, yet the net formation of C_2H_5OO was low because its formation and destruction rates were both high. Also, using a recent theoretical rate constant for $C_2H_3+O_2$ -> C_2H_3O+O from Mebel et al.[3] (corrected for a typographical error in the paper) had little effect in the flame but ruins agreement with the flow-reactor data.

Other modeling has focused on data from our recent allene-doped, fuel-rich ethylene flame, re-examining key reactions of C_3 hydrocarbons with literature and theoretical kinetics.

Developing a new flame modeling method. Work has continued toward developing a solution method for solving the nonadiabatic energy equation in a flat flame [DOE Publ. 3]. This work was originally motivated by finding that the use of a temperature profile for modeling could account for failures by us and by others to successfully model our slightly lean ethylene flame.

We have developed modifications to the Chemkin II version of the Sandia Premix code that explicitly incorporate radiative losses and burner losses into the energy equation and boundary conditions. An empirical heat loss to the burner (which we have developed techniques to measure) may be used for a given flame on a given burner or the burner temperature may be used.

We adapted RADCAL, a subroutine written at NIST to model gas-phase radiation of CO_2, H_2O, CH_4, CO, O_2, and N_2 in addition to the soot contribution. Upon implementation of this code, the predicted temperature for the fuel-rich flame was slightly too high and did not accurately represent the experimentally observed decrease in the post-flame zone. One of the assumptions initially made was that this rich flame was non-sooting because no yellow soot luminosity was detected. Non-black-body radiation by heavy hydrocarbons would decrease the maximum and the post-flame temperatures.

Modeling the fuel-lean flame indicates problems in the modeling that seem most likely due to the kinetics. At the experimental flame condition, the maximum temperature was only predicted to be about 1550 K, lower than was measured directly in the post-flame gases by a

[3] A.M. Mebel, E.W.G. Diau, M.C. Lin, and K. Morokuma, *J. Am. Chem. Soc.* **118**, 9759 (1996).

radiation-compensated, Y_2O_3-BeO glass-coated thermocouple. The true temperature must be higher than this, but radiative loss is relatively small. The problem then is lack of sufficient heat generation, most likely a fault of the kinetic mechanism. Such a result illustrates how solving the coupled nonadiabatic energy equation can be a more exacting test of kinetics than using the experimental profile. We are continuing to examine other flames for tests of the radiation model.

We have also examined surface-catalyzed reactions that could affect the flame modeling [DOE Publ. 1]. A reactive burner boundary condition was tested using the surface reaction H+H = H_2, recognizing that of the various radicals, H should reach the burner most easily because of his high diffusivity. However, even when the rate constant was increased to unit collision efficiency, the H profile only changed near the burner and did not impact the rest of the flame.

Web repository of flame-profile data. We have continued to build a Web repository of flame-profile data, http://www.ecs.umass.edu/MBMS/, emphasizing the comprehensive sets available from MBMS experiments.

Future Plans

The UMass MBMS experiments during the next year will be focused on the fuel-lean ethylene flame doped with propadiene, at the same time re-mapping the undoped flame on the new burner at the same conditions. This study will emphasize C_3H_4 and C_3H_3 oxidation kinetics, exploiting the higher sensitivity of the new mass spectrometer. We will emphasize traditional axial mapping of the flat flame, but we will gather data for a first full two-dimensional map. Temperature measurements are in progress while the manufacturer is correcting problems in the new MS electronics. In parallel, the ALS MBMS will be tested using three well-characterized flames, possibly fuel-rich methane,[4,5] acetylene,[6] and ethylene.[6] Also, modeling of the low-pressure / high-pressure conditions will be expanded to other fuels, and the nonadiabatic energy equation solutions will be used to probe causes of low heat release in the fuel-lean flame. Using ab initio methods, we will also generate C3 oxidation rate constants as indicated by modeling of the allene-doped ethylene flame.

Publications of DOE-sponsored Research, 1999-2001

1. P.-A. Bui, D.G. Vlachos, and P.R. Westmoreland, "On the local stability of multiple solutions and oscillatory dynamics of spatially distributed flames," *Combustion and Flame* **117**, 307-322 (1999).
2. T. Carriére and P.R. Westmoreland, "Improving Kinetic Models for Ethylene Flat Flames," *Chem. Phys. Prop. Combustion*, 125-128 (1999).
3. T. Carriére and P.R. Westmoreland, "Temperature Profiles, Energy Balances, and the Modeling of MBMS Flame Data," *28th International Symposium on Combustion,* P5-D18 (2000).
4. T. Carriére, P.R. Westmoreland, A. Kazakov, Y.S. Stein, and F.L. Dryer, "Modeling Ethylene Combustion from Low to High Pressure," *2nd Joint Meeting of the US Sections of the Combustion Institute*, Oakland CA, March 25-28, 2001, paper 89.

---

[4] C.J. Langley and A.R. Burgess, *Proc. Royal Soc. Lond. A* **421**, 259 (1989).

[5] L. I. Yeh and F. Luo, *4th International Conference on Chemical Kinetics*, NIST, July 14-18, 1997, paper F8.

[6] P.R. Westmoreland, J.B. Howard, and J.P. Longwell, *Proc. of the Combustion Institute* **21**, 773 (1986).

Reactions of Small Molecular Systems

Curt Wittig
Department of Chemistry
University of Southern California
Los Angeles, CA 90089-0482
wittig@chem1.usc.edu

Program Scope

The focus of our program is reaction and energy transfer mechanisms that are relevant to combustion. One of our goals has been to examine long-range interactions, which is a frontier area for theory and experiment. For radical-radical and radical-molecule systems, long-range interactions contain contributions from several PES's which become degenerate at large separation. The van der Waals well depths are comparable to spin-orbit energies, both of which are comparable to collision energies, and the role of anisotropy is subtle.

In principle, it is possible to probe long range interactions by using weakly bound precursors. We used this strategy previously to examine a unique form of hot hydrogen atom chemistry, but progress was limited by higher-than-binary clusters. We recently extended the technique to the regime of chemical systems that are sensitive to the long range part of the potential. The idea is to probe the long-range region of Cl-HCl. There are three PES's due to the Cl spin-orbit levels in combination with the anistropic electrostatic interaction. The main experimental diagnostic has been the high-*n* Rydberg time-of-flight method, including double resonance (DR), probing H atom products. To implement DR, a laser source was stabilized at the transitions of species that are present in low concentrations and are not chemically stable. This problem exists when carrying out DR studies of radicals, clusters, excited states, etc. Such experiments and their extensions may result in a new era of detailed studies. A summary of this work is given and our current studies are then described.

Results

The HCl dimer is excited to first overtone levels of the free HCl, and 193 nm radiation dissociates the tagged bond. The vibrationally excited dimers also undergo predissociation, resulting in correlated product state distributions of the monomer pairs. This is expected to occur with low (acceptor) and high (donor) rotational excitation. The predissociation lifetime is estimated to be ≥ 3 ns, based on linewidth. Both tagged dimers and internally excited monomers produced via predissociation can be photolyzed by the 193 nm radiation, and by varying the IR-UV delay, it is possible to separate these contributions. A cavity ring-down spectrometer was integrated into the setup to locate dimer transitions, and jet-cooled dimers were generated in a pulsed expansion. Tunable IR radiation (20 mJ at 1.77 μm) was produced in an OPO capable of long-term locking to a single mode. Two laser beams (121.6 and 366 nm) excited H atoms to high-*n* Rydberg states. For double resonance, data were collected with the IR alternately on and off.

Signals at long IR-UV delays arise mainly from predissociated monomer pairs, while the short delay data contain contributions from both direct and predissociation channels. We do not know the predissociation lifetime (τ_{PD}) of the dimer at the first overtone of free HCl. However, on the basis of studies of the vibrational dependence of the predissociation life-

time in $(HF)_2$ and the predissociation of $(HCl)_2$ at the free fundamental ($\tau_{PD} \geq 100$ ns), we assume that $\tau_{PD} < 100$ ns. Peaks in the signals lie at energies that correspond to highly rotationally excited HCl. For example, the two highest-energy peaks differ by the energy difference between J = 20 and 21 of HCl(v=0). In the present case, two quanta in the free HCl are transferred to internal excitation of one of the recoiling monomers (presumably the donor) upon predissociation.

Signals from $(HCl)_2^{\dagger} + h\nu_{UV} \rightarrow H + Cl\text{-}HCl$ can be obtained from differences between DR spectra taken at short and long delays. The departing H atom carries information about Cl-HCl. This complex does not undergo significant decomposition on the rapid timescale characteristic of H-atom removal. At low resolution, one can expect to see the Cl atom spin-orbit levels, whereas with better resolution, the PES's of the Cl-HCl system are reflected. Rapid H-atom removal creates a coherent superposition of electronic and vibrational levels of the Cl-HCl complex. At higher resolution, it may be possible to resolve vibrational structure and widths arising from Cl-HCl decomposition. Despite modest S/N, the data reflect the PES's of Cl-HCl. The main features are associated with the Cl spin-orbit levels; they are broader than those associated with photodissociation of unclustered HCl. We believe this broadening is due to Cl-HCl vibrational and electronic excitations; it is present at all levels of signal averaging. All of these results have been published.[1]

Current Work

Following the above studies of the HCl dimer, we have initiated a study of the intramolecular dynamics and unimolecular decomposition of water on the ground PES. In parallel, we are working on a theoretical explanation of the highly selective V∅R energy transfer in HCl dimer. This is being carried out in collaboration with Professor Pavel Jungwirth from Prague, who is spending a sabbatical at USC. He will be here until the end of the summer; thus, this study will be completed by the end of the summer. This work involves Jungwirth and Wittig; the students and postdoc are working full time on the water project.

The experimental strategy for the water studies uses two complementary methods. One is to use overtone-combination band excitation to promote the system to the region from just below to just above D_0. The water system is amenable to a high level of theory and can serve as a benchmark against which calculations can be judged. As a warm-up, the OPO system was tuned to the (011) ← (000) combination band and the excited molecules were photodissociated at 193 nm. The S/N was good, showing the distribution of OH rotational levels, and theory matches experiment (A. McCoy, unpublished). Next, we will use 4←0 or 5←0 local mode excitation and then move to higher energies by pumping 10←4, 11←5 and other high overtones (and combination bands). It is expected that the S/N will be good for 4←0 and 5←0, in fact better than (011) ←(000). Major challenges will arise in trying to reach energies near D_0. Following a few experimental disasters that consumed several months (*e.g.*, the Lambda Physik excimer laser cavity filling with water from a broken cooling line), we are back in business and starting experiments again.

In addition, a system is being built for recording absorption spectra with high sensitivity by using cavity enhancement. Though cavity-enhanced absorption methods have been available for decades,[2,3] only recently have they emerged as practical tools for studies of molecular spectroscopy, reaction dynamics, and the detection of minority species.[4-6] In our earlier work, we have used the simplest version of cavity ringdown absorption spectroscopy (CRAS) to detect absorptions of less than one part per million.[7] In this form, pulsed radiation enters the cavity and rattles around for a long time (10 – 20 μs) before exiting. This sensitivity is an order of magnitude lower than the state-of-the-art when using broadband

pulsed lasers. However, it is about *five* orders of magnitude below the theoretical (shot noise) limit of cavity enhanced methods.[8] Clearly, there is much to be gained.

Recently, He and Orr used a cw diode laser to carry out CRAS measurements.[9] The narrow-linewidth diode laser radiation (~1 MHz) is brought into and out of resonance with a mode of an external (ringdown) cavity by modulating the cavity length with a PZT. Their sensitivity is an order of magnitude higher than what we have reported. More important is that their paper gives recommendations for increasing sensitivity. Straightforward improvements and a simple implementation of heterodyne detection improve this by an additional order of magnitude. We have been fortunate to have Professor Brian Orr at USC as a Provost's Visiting Scholar for a week in February. His group has developed this technique and he has indicated that he will collaborate with us. With the high sensitivity provided by cavity enhancement, it should be straightforward ot observe $\Delta v = 7$ transitions. The goal is to use this technique to record spectra at energies that lie above a reaction barrier or at energies where the intramolecular dynamics can provide important information.

An interesting combination can be achieved by using excitation of an overtone such as $4 \leftarrow 0$ in combination with cavity enhanced spectroscopy. The $4 \leftarrow 0$ absorption cross section is large and high excitation efficiencies can be achieved with the photoexcitation beam collinear with the molecular beam. Cavity enhanced spectroscopy can then be applied to the $v = 4$ levels, which will stand out from ground state molecules because of their relatively large absorption cross sections, which also enable $\Delta v \geq 7$ transitions to be recorded.

References

1. K. Liu, A. Kolessov, J. Partin, I. Bezel, C. Wittig, Chem. Phys. Lett. 299, 374 (1999).
2. J. M. Herbelin, J. A. McKay, M. A. Kwok, R. H. Ueunten, D. S. Urevig, D. J. Spencer, D. J. Benard, Appl. Opt. 19, 144 (1980).
3. D. Z. Anderson, J. C. Frisch, C. S. Masser, Appl. Opt., 1238 (1984).
4. 21st Annual DOE Combustion Research Conference, May 2000, paper by M. C. Lin.
5. 21st Annual DOE Combustion Research Conference, May 2000, paper by R. Bersohn.
6. J. W. Thoman Jr., A. McIlroy, J. Phys. Chem. A 104, 4953 (2000).
7. K. Liu, M. Dulligan, I. Bezel, A. Kolessov, C. Wittig, J. Chem. Phys. 108, 9614 (1998).
8. M. D. Levenson, B. A. Paldus, T. G. Spence, C. C. Harb, J. S. Harris Jr., R. N. Zare, Chem. Phys. Lett. 290, 335 (1998).
9. Y. He, B.J. Orr, Chem. Phys. Lett. 319, 131 (2000).

DOE Publications: 1998 – Present

1. Quenching of interconversion tunneling: Free HCl stretch first overtone of $(HCl)_2$, K. Liu, M. Dulligan, I. Bezel, S. Kolessov, C. Wittig, J. Chem. Phys. 108, 9614 (1998).
2. Probing the Cl-HCl Complex via Bond-Specific Photodissociation of $(HCl)_2$, K. Liu, A. Kolessov, J.W. Partin, I. Bezel and C. Wittig, Chem. Phys. Lett. 299, 374 (1999).
3. Photoinitiated H_2CO unimolecular decomposition: accessing H + HCO products via S_0 and T_1 pathways, L.R. Valachovic, M.F. Tuchler, M. Dulligan, Th. Droz-Georget, M. Zyrianov, A. Kolessov, H. Reisler and C. Wittig, J. Chem. Phys. 112, 2752 (2000).
4. Highly Specific Rotational Excitations in the Vibrational Predissociation of HCl Dimer, P. Jungwirth and C. Wittig, unpublished.

Theoretical Studies of the Reactions and Spectroscopy of Radical Species Relevant to Combustion Reactions and Diagnostics

David R. Yarkony
Department of Chemistry, Johns Hopkins University, Baltimore, MD 21218
yarkony@jhuvms.hcf.jhu.edu

Our research employs computational techniques to study spin-nonconserving and spin-conserving electronically non adiabatic processes involving radical species that are relevant to combustion reactions and combustion diagnostics.

Characterizing Conical Intersections using continuity constrained parameters[1,2]

The existence of conical intersections can, depending on the local topography, significantly enhance the probability of a nonadiabatic transition. For this reason techniques to efficiently characterize the topography of conical intersections along the seam, a subspace of dimension $N-2$, are quite important. Conical intersections can be characterized in terms a set of four conical parameters, s_x, s_y, g and h, derived from three characteristic vectors, $\mathbf{s}^{II}$, $\mathbf{g}^{II}$, $\mathbf{h}^{II}$, with $s_x = \mathbf{s}^{II} \cdot \mathbf{g}^{II}/g$, $s_y = \mathbf{s}^{II} \cdot \mathbf{h}^{II}/h$, $g = \|\mathbf{g}^{II}\|$, $h = \|\mathbf{h}^{II}\|$.[3] Continuity of these parameters along the seam is not guaranteed. It is achieved by choosing the linear combinations of the degenerate wave functions so that the vectors defining the g-h or branching space, $\mathbf{g}^{II}$ and $\mathbf{h}^{II}$ are orthogonal.[4] The dissociation of photoexcited HNCO:

$$HNCO(S_0={}^1A')+h\nu \rightarrow HNCO(S_1={}^1A'') \quad \rightarrow H+NCO(X^2\Pi) \text{ or } HN(a^1\Delta)+CO$$

has been the object of many DoE BES supported experimental studies[1-3] and theoretical studies.[4-7] In HNCO photodissociation a large barrier precludes directed dissociation on S_1 to produce H + NCO.[8,9] This channel is accessed via an $S_1 \rightarrow S_0$ internal conversion facilitated by a seam of conical intersection. Following photoexcitation R(C–N) increases as the system evolves toward the stable *trans* isomer on S_1.[10] For this reason we determined, and characterized using continuous conical parameters, energy minimized cross sections of the seam as a function of R(C–N) with emphasis on *trans* structures. Conical intersections for both *trans* planar (a symmetry-allowed seam) and *trans* nonplanar (a same symmetry seam) configurations were found that are above the H + NCO asymptote but accessible with the energies commonly used in photodissociation experiments. These sections of the conical intersection seam provide the pathways for internal conversion

Unexpected conical intersection topographies[2]

Perhaps the most interesting feature of the HNCO symmetry-allowed seam is the existence of confluences or intersecting seams.[1] By altering the topography at the intersection, a confluence can significantly alter nuclear dynamics near a conical. In fact at a confluence, the topography is NOT that of a double cone. We showed[2,5] using perturbation theory that in a tetra-atomic molecule a subspace of confluences of dimension up to $N^{int}-3 = N^{seam}-1$, where N^{seam} is the dimension of the seam,

may be embedded in a symmetry-allowed seam of conical intersection. These confluences satisfy τ = (x=0, y=0, $z_i = \zeta_i e_i$) with $(h + b_2^{(z_i)}\zeta_i) / b_3^{(\rho)} = 0$, $\sum_{i=1}^{N^{intern}} e_i = 1$ where τ the nuclear geometry is expressed in intersection adapted coordinates,[6] , and h, $b_i^{(zi)}$, $b_j^{(\rho)}$ are parameters from an expansion of the energy difference between the two states near a conical intersection. The following Table[2] reports a portion of that subspace of confluences in *trans* HNCO

Confluences on 1^1A - 2^1A seam of conical intersection in HNCO[a]

R(H-N)	R(C-N)	R(C-O)	∠HNC	∠ NCO	h	E	ΔE	ζ_i|i
1.946	**3.146**	**2.242**	**104.0**	**101.3**	**.881(-3)**	**9623.**	**0.92**	τ^{x1}
1.916	*3.146*	*2.246*	*99.7*	*101.2*	*.491(-4)*	*9813*	*32.*	0.111|1
2.436	*3.153*	*2.243*	*96.3*	*101.4*	*.195(-3)*	*16745*	*107.*	0.383|2
1.953	*3.154*	*2.230*	*103.9*	*101.7*	*-.498(-4)*	*10009*	*4.5*	0.018|4
2.024	*3.150*	*2.235*	*101.4*	*100.9*	*.244(-4)*	*10156*	*8.8*	**A**

[a] All structures are *trans*. Energies in cm^{-1} relative to ,$E_{1_{A''}}(\tau^{eq\text{-}trans})$ = -168.103374a.u. for **A** **e** = (0.26, 0.17, 0.0, 0.57). Origin of perturbation expansion in **bold** type face, confluences in *italic* type face.

The confluence labeled **A** serves to confirm the multi dimensional (here 2 see Ref. [2]) character of the confluence. The subspace of confluences represents a slice through the symmetry allowed seam near R(C-N) = 3.15 a_0. These confluences are only on the order of 1500 cm^{-1} above the lowest energy *trans* intersections at R(C-N) = 3.15 a_0. They are above the $NCO(X^2\Pi)$ + H asymptote, which is at 38370 cm^{-1}, based on the experimental data in Ref. [1]. Therefore for R(C-O) ≅ 2.24 a_0 (similar to its value at the equilibrium structure in the ground state and in the *trans* excited state[1]) as R(C-N) reaches 3.15 a_0 conical intersections on these confluences can be accessed by the dissociating HNCO.

Photodissociation of the hydroxymethyl radical CH_2OH

The hydroxymethyl radical plays an important role in atmospheric, combustion, CO/H_2 surface and interstellar chemistry and is known to be a major link in the alkene photochemistry of polluted atmospheres. At the wave lengths currently used for photoexcitation, the low-lying Rydberg states corresponding to a hydroxymethyl cation core and a carbon Rydberg electron (H_2COH^+)-C(3s or 3p), are accessed. Sufficient energy is available to break the OH or CO bonds or permit isomerization to CH_3O, with OH bond breaking, that is the H_2CO + H channel, being preferred. To date we have focussed on the reaction of the lowest excited state

$$H_2COH(D_0) + h\nu \rightarrow H_2COH(D_1) \rightarrow H_2COH(D_0) \rightarrow H_2CO + H$$

which is necessarily non adiabatic involving a Rydberg-valence transition. The table below summarizes our most significant results to date, obtained using flexible multireference configuration interaction wave functions comprised of over 3.5 million CSFs:

State	Energy (cm^{-1})	C-O	O-H	C-H C-H	∠H-C-H	∠C-O-H	∠H-C-H-O	∠H-O-C-H
D_0 gs	0.00	2.5981	1.8060	2.0570 2.0491	120.3	110.31	147.0	33.08
x1	39349	2.6375	3.1000	2.0575 2.0638	116.34	106.90	137.72	27.95
x2	307410	2.5004	2.8000	2.0534 2.0553	121.87	108.10	177.32	1.722
D_1 3S	318830	2.3277	1.9351	2.0758 2.0612	122.6	113.0	180	180.0

The equilibrium structures for the ground and first excited states $\mathbf{R}_e(D_i)$, i =0,1 have been determined, as have points $\mathbf{R}^{xi}$ i =1, 2 (more will be determined) on seam of conical intersection using R(O-H) as a parameter. Both $\mathbf{R}^{xi}$ and $\mathbf{R}_e(D_1)$ are energetically accessible following vertical excitation. To characterize the propensity for a nonadiabatic transition, the (linear) conical parameters at $\mathbf{R}^{x2}$ were determined and found to be g = 0.023850, h = 0.196812, s_x =0.0004, s_y= 0.0013. Since s_x and s_y are small the cone is vertical and given the size of g and h it is expected to efficiently funnel excited state products to the ground state potential energy surface. However, we found that starting from the Franck-Condon region on D_1 paths obtained by following the gradient of the electronic energy lead to $\mathbf{R}_e(D_1)$ (which is similar to the situation in both H_2CCO and HNCO reported previously).[1,7] Thus, dynamics on the upper surface are expected to play a significant role in determining the rate of internal conversion.

In the coming months this analysis will be expanded using a somewhat more compact CSF expansion. The existing seam of conical intersection will be extended and characterized in terms of conical parameters through second order. These results will form the basis for a future determination of a reduced dimensionality representation of the relevant potential energy surfaces, and their couplings, as is currently being done for ketene. See below.

Photodissociation of Ketene

The energy dependence of the photo-fragmentation rate constant or the reaction

$H_2CCO(S_0=X^1A_1) + h\nu \rightarrow H_2CCO(S_1) \rightarrow H_2CCO(S_0) \rightarrow H_2CCO(T_1) \rightarrow {}^3CH_2 + CO(X^1\Sigma^+)$

revealed the existence of a step-like structure[8] that has to date defied theoretical interpretation. It has been suggested the entire multi electronic state non adiabatic process must be analyzed if agreement with experiment is to be obtained.[9] To this end we are currently determining, three parameter, reduced dimensionality potential energy surfaces for the S_0, S_1, and T_1 states together with the requisite intersections and coupling matrix elements. Based on our previous calculations[7] the CH_2 moiety(*Me)* and the C-O distance are treated as spectators while R(*Me*-C) and ∠*Me*-C-O, two C_s symmetry preserving coordinates, are treated explicitly. The remaining parameter, a single out of plane coordinate, must provide the out of plane interstate coupling. It will be determined once the

reduced dimensionality conical intersection seam has been fully constructed.

References

(1) D. R. Yarkony, *J. Chem. Phys.* **114,** 2614 (2001).

(2) D. R. Yarkony, *Molec. Phys.* , accepted for publication (2001).

(3) D. R. Yarkony, *Acc. Chem. Res.* **31,** 511-518 (1998).

(4) D. R. Yarkony, *J. Chem. Phys.* **112,** 2111-2120 (2000).

(5) D. R. Yarkony, *J. Phys. Chem. A* (2001).

(6) G. J. Atchity, S. S. Xantheas, and K. Ruedenberg, *J. Chem. Phys.* **95,** 1862 (1991).

(7) D. R. Yarkony, *J. Phys. Chem. A* **103,** 6658-6668 (1999).

(8) S. K. Kim, E. R. Lovejoy, and C. B. Moore, *Science* **256,** 1541 (1992).

(9) J. D. Gezelter and W. H. Miller, *J. Chem. Phys.* **104,** 3546 (1996).

PUBLICATIONS SUPPORTED BY DE-FG02-91ER14189: 1999 - present

[1] Perspective on:*Some Recent Developments in the Theory of Molecular Energy Levels*: by H. C. Longuet-Higgins[Advances in Spectroscopy 2, 429-472 (1961)]. The geometric phase effect.
David R. Yarkony, *Theoretical Chemistry Accts*, New century issue, *103*, 242-246 **(2000).**

[2] *Conical intersections: The New Conventional Wisdom* – Feature Article,
D. R. Yarkony, J. Phys. Chem., accepted for publication

[3] *A theoretical analysis of the state-specific decomposition of OH($A^2\Sigma^+$, v', N', F_1 / F_2) levels, including the effects of spin-orbit and Coriolis interactions*
Gérard Parlant and David R. Yarkony, *J. Chem. Phys.* **110,** 363-376 (**1999**).

[4] *On the S_1 - S_0 Internal Conversion in Ketene:I.The Role of Conical Intersections*
David R. Yarkony , J. Phys. Chem. A. **103,** 6658-6668 (**1999**).

[5] *Substituent effects and the noncrossing rule: The importance of reduced symmetry subspaces. I. The quenching of OH($A^2\Sigma^+$) by H_2*
David R. Yarkony , J. Chem. Phys. ***111,*** 6661-6664, (**1999**).

[6] *The Role of Conical Intersections in the Non-adiabatic Quenching of OH ($A^2\Sigma^+$) by H_2*
Brian C. Hoffman and David R. Yarkony, J.Chem. Phys., **113**,10091(**2000**)

[7] *Characterizing the Local Topology of Conical Intersections Using Orthogonality Constrained Parameters: Application to the internal conversion $S_1 \rightarrow S_0$*
David R. Yarkony, J. Chem..Phys. **114**, 2614 (**2001**)

[8] *Intersecting Conical Intersection Seams in Tetra atomic Molecules : The S_1 - S_0 Internal Conversion in HNCO*
David R. Yarkony, *Molec Phys.* accepted for publication

Laser Studies of the Chemistry and Spectroscopy Of Excited State Hydrocarbons

Timothy S. Zwier
Department of Chemistry, Purdue University, West Lafayette, IN 47907-1393
zwier@purdue.edu

Program Definition/Scope

The objectives of this research program are to identify and spectroscopically characterize the primary products of reactions of electronically excited molecules with the hydrocarbons present in abundance in sooting flames. The molecules of current interest include diacetylene, vinylacetylene, butadiene, and various aromatic derivatives. The unusual soot-forming ability of these molecules when they are doped into flames [4] suggests that they may contribute to the molecular chemistry important in moderate-temperature, sooting flames. We seek to determine the structures, energies, and lifetimes of the triplet states of these molecules.[1] Furthermore, the rich chemistry of the triplet states of diacetylene (C_4H_2*) and vinylacetylene (C_4H_4*) with other hydrocarbons also leads to products with unusual structures and unexplored spectroscopy, which we seek to characterize.[2,3]

Recent Progress

Our studies of C_4H_2* chemistry utilize one tunable ultraviolet laser pulse to resonantly excite diacetylene to a singlet state from which intersystem crossing to the triplet manifold produces the metastable state responsible for the ultraviolet photochemistry. The high reactivity of C_4H_2* toward polymerization necessitates the use of a small reaction tube that limits reactive collisions to the first 20 microseconds following laser excitation. Reaction is initiated by the first UV laser pulse, but is quenched as the gas mixture expands from the tube into vacuum. VUV photoionization, resonant two-photon ionization (R2PI)/time-of-flight mass spectroscopy, and resonant ion-dip infrared spectroscopy (RIDIRS) are being used to detect, mass-analyze, and spectroscopically characterize the reaction products.

Building on our recent study of the C_4H_2* reactions with benzene and toluene,[3] we are nearing completion of a study of the reaction of C_4H_2* with styrene and phenylacetylene. These mixtures have been particularly difficult to study due to the lower vapor pressure and UV absorptions of the aromatic reactants. A motivation for this work is to explore whether these reactions provide a route to formation of the fused ring product naphthalene, analogous to the reaction of C_4H_2* +1,3-butadiene, which formed benzene. An array of products are formed in the reaction of C_4H_2* with styrene, including $C_{10}H_8$, $C_{11}H_8$, and $C_{12}H_8$:

$$C_4H_2^* + C_6H_5CH{=}CH_2 \rightarrow C_{10}H_8 \ (+ C_2H_2) \quad (1a)$$
$$\rightarrow C_{11}H_8 \ (+ CH_2) \quad (1b)$$
$$\rightarrow C_{12}H_8 \ (+ H_2, 2H). \quad (1c)$$

The R2PI spectrum of the $C_{10}H_8$ product shows no evidence of naphthalene formation, but transitions due to several aromatic derivatives are observed. UV-UV hole-burning spectroscopy has been used to dissect the R2PI spectrum into spectra due to $C_{10}H_8$ isomers. We are currently comparing the photochemical product R2PI spectrum to R2PI spectra of synthesized samples of the following $C_{10}H_8$ isomers.

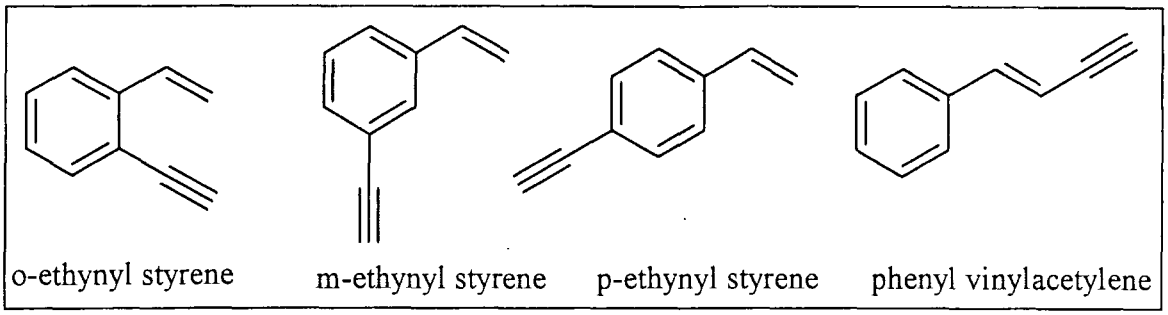

The mass 140 product also has an R2PI spectrum characteristic of an aromatic. The assignment of this spectrum is not yet in hand, but an indene derivative is one of the possibilities being explored.

Finally, we have taken two routes toward better characterization of the excited states of C_4H_2, vinylacetylene, and 1,3-butadiene. First, we have recorded the gas-phase optical spectrum of the lowest singlet-triplet transition of 1,3-butadiene, over the 430-490 nm region, using cavity ring-down spectroscopy. The transition is extremely weak ($\sigma_{abs}(0^0_0)=$ cm^2), with Rayleigh scattering of the same size as the absorptions. The triplet state vibronic levels are clearly due to a planar structure, despite the calculated presence of a twisted minimum at slightly lower energy. Second, we are collaborating with Dr. Stephen Pratt to record photoelectron spectra of C_4H_2 following R2PI through various intermediate vibronic levels of the $^1\Delta_u$ state.

Future Plans

We will finish our study of the reaction of C_4H_2* with styrene and phenylacetylene. R2PI and RIDIR spectroscopy will be used to record the ultraviolet and infrared spectra of synthesized samples of the suspected photochemical products, including those shown above, which are proposed intermediates on the way toward formation of the second aromatic ring in flames. The photochemistry of these substituted aromatics molecules will also be interesting in their own right. We will begin to explore this photochemistry with synthesized samples of these molecules. Finally, we will search for the photoelectron spectrum and infrared spectrum of the triplet state of C_4H_2.

Publications acknowledging DOE support, 1999-present

1. F.C. Hagemeister, C.A. Arrington, B.J. Giles, B. Quimpo, L. Zhang, and T.S. Zwier, "Cavity ringdown methods for studying intramolecular and intermolecular dynamics", chapter in "Cavity ring-down spectroscopy – An Ultratrace-Absorption Measurement Technique", ed. K.S. Busch and M.A. Busch, ACS Symposium Series 720, Chap. 14, pp. 210-232 (1999).

2. C.A. Arrington, C. Ramos, A.D. Robinson, and T.S. Zwier, "The ultraviolet photochemistry of diacetylene with alkynes and alkenes: Spectroscopic characterization of the products", J. Phys. Chem. **103**, 1294-1299 (1999).

3. Allison G. Robinson, Paul R. Winter, Christopher Ramos, and Timothy S. Zwier, "Ultraviolet Photochemistry of Diacetylene: Reactions with Benzene and Toluene", *J. Phys. Chem. A* **104**, 10312-10320 (2000).

4. Charles S. McEnally, Allison G. Robinson, Lisa D. Pfefferle, and Timothy S. Zwier, "Aromatic Hydrocarbon Formation in Nonpremixed Flames Doped with Diacetylene, Vinylacetylene, and Other Hydrocarbons: Evidence for Pathways Involving C4 Species", Combustion and Flame **123**, 344-357 (2000).

Participants

Dr. William T. Ashurst
Combustion Research Facility
MS9051
Sandia National Laboratories
Livermore, California 94551-0969
Phone: 925.294.2274
ashurs@ca.sandia.gov

Prof. Tomas Baer
Department of Chemistry
University of North Carolina
Chapel Hill, North Carolina 27599-3290
Phone: 919.962.1580
baer@unc.edu

Dr. Robert S. Barlow
Combustion Research Facility
MS9051
Sandia National Laboratories
Livermore, California 94551-0969
Phone: 925.294.2688
barlow@ca.sandia.gov

Dr. John B. Bell
Center for Computational Sciences & Eng.
MS 50D
Lawrence Berkeley National Laboratory
1 Cyclotron Road
Berkeley, California 94720
Phone: 510.486.5391
JBBell@lbl.gov

Prof. Richard Bersohn
Department of Chemistry
Columbia University
116th Street and Broadway
New York, New York 10027
Phone: (212)854-2192
rb18@columbia.edu

Prof. Joel M. Bowman
Department of Chemistry
Emory University
1515 Pierce Drive
Atlanta, Georgia 30322
Phone: (404)727-6590
bowman@euch4e.chem.emory.edu

Prof. C. Thomas Bowman
Department of Mechanical Engineering
Stanford University
Stanford, California 94305
Phone: 650.723.1745
bowman@navier.stanford.edu

Professor Kenneth Brezinsky
Chemical Engineering Dept.
810 S. Clinton
The University of Illinois at Chicago
Chicago, Illinois 60607-7022
Phone: (312)996-9430
kenbrez@uic.edu

Dr. Nancy Brown
Environmental Technologies Division
Lawrence Berkeley Laboratory MS 70-108B
One Cyclotron Road
Berkeley, California 94720
Phone: (510)486-4241
njbrown@lbl.gov

Prof. Laurie J. Butler
The James Franck Institute
The University of Chicago
5640 S. Ellis Avenue
Chicago, Illinois 60637
Phone: 773.702.7206
ljb4@midway.uchicago.edu

Prof. Barry K. Carpenter
Department of Chemistry
Cornell University
Ithaca, NY 14853-1301
Phone: (607)255-3826
bkc1@cornell.edu

Dr. David W. Chandler
Combustion Research Facility
MS 9055
Sandia National Laboratories
Livermore, California 94551-0969
Phone: 925.294.2091
chandler@ca.sandia.gov

Dr. Jacqueline H. Chen
Combustion Research Facility
MS9051
Sandia National Laboratories
Livermore, California 94551-0969
Phone: 925.294.2586
jhchen@sandia.gov

Dr. Robert K. Cheng
Energy and Environment Division
Lawrence Berkeley Laboratory
One Cyclotron Road
Berkeley, California 94720
Phone: 510.486.5438
rkcheng@lbl.gov

Prof. Jerzy Cioslowski
Supercomputer Comp. Res. Inst.
406 Science Center Library
Florida State University
Tallahassee, Florida 32306-4052
Phone: 850.644.8274
jerzy@scri.fsu.edu

Dr. Meredith B. Colket, III
MS 29
United Technologies Research Center
411 Silver Lane
East Hartford, CT 06108
Phone: 860.610.7481
colket@utrc.utc.com

Prof. Robert E. Continetti
Department of Chemistry, 0340
University of California, San Diego
9500 Gilman Drive
La Jolla, CA 92093-0340
Phone: 858.534.5559
rcontinetti@ucsd.edu

Prof. F. Fleming Crim
Department of Chemistry
University of Wisconsin
1101 University Avenue
Madison, Wisconsin 53706
Phone: (608)263-7364
fcrim@chem.wisc.edu

Prof. Robert F. Curl, Jr.
Department of Chemistry
Rice University
P.O. Box 1892
Houston, Texas 77251
Phone: (713)527-4816
rfcurl@rice.edu

Prof. Hai-Lung Dai
Department of Chemistry
University of Pennsylvania
Philadelphia, Pennsylvania 19104-6323
Phone: 215.898.5077
dai@sas.upenn.edu

Dr. Michael Davis
Chemistry Division
Argonne National Laboratory
9700 South Cass Avenue
Argonne, Illinois 60439
Phone: 630.252.4802
davis@tcg.anl.gov

Prof. H. Floyd Davis
Department of Chemistry
Baker Laboratory
Cornell University
Ithaca, New York 14853-1301
Phone: 607-255-0014
hfd1@cornell.edu

Dr. Anthony M. Dean
Department of Chemical Engineering and
Petroleum Refining
Colorado School of Mines.
Golden, Colorado 80401
Phone: 303.273.3643
amdean@mines.edu

Dr. Michael C. Drake
Physical Chemistry Department
General Motors R&D Center
30500 Mound Road
Warren, Michigan 48090-9055
Phone: 810.986.1320
michael.c.drake@gm.com

Prof. Frederick L. Dryer
Department of Mechanical & Aerospace
Engineering
Princeton University
Princeton, New Jersey 08544
Phone: (609)258-5206
fldryer@princeton.edu

Prof. G. Barney Ellison
Department of Chemistry
University of Colorado
Boulder, Colorado 80309
Phone: 303.492.8603
barney@jila.Colorado.EDU

Prof. Kent M. Ervin
Department of Chemistry/216
College of Arts and Sciences
University of Nevada, Reno
Reno, Nevada 89557-0020
Phone: 775.784.6676
ervin@chem.unr.edu

Prof. James M. Farrar
Department of Chemistry
University of Rochester
Rochester, New York 14627
Phone: 716.275.5834
farrar@chem.rochester.edu

Dr. Roger Farrow
Combustion Research Facility
MS 9055
Sandia National Laboratories
Livermore, California 94551-0969
Phone: 925.294.3259
farrow@sandia.gov

Prof. Peter M. Felker
Department of Chemistry and Biochemistry
University of California at Los Angeles
Los Angeles, CA 90024-1406
Phone: 310.206.6924
felker@chem.ucla.edu

Prof. Robert W. Field
Department of Chemistry
Massachusetts Institute of Technology
18-390 Massachusetts Ave.
Cambridge, Massachusetts 02139
Phone: 617.253.1489
rwfield@mit.edu

Prof. George Flynn
Department of Chemistry
Mail Stop 3109
Columbia University
3000 Broadway
New York, New York 10027
Phone: (212)854-4162
flynn@chem.columbia.edu

Dr. Christopher Fockenberg
Chemistry Department
Brookhaven National Laboratory
Upton, NY 11973-5000
Phone: 631.344.4372
fknberg@bnl.gov

Dr. Jonathan H. Frank
Combustion Research Facility
MS 9051
Sandia National Laboratories
Livermore, California 94551
jhfrank@ca.sandia.gov

Prof. Michael Frenklach
Department of Mechanical Engineering
Lawrence Berkeley Laboratory
University of California at Berkeley
Berkeley, California 94720-1740
Phone: (510)643-1676
myf@me.berkeley.edu

Dr. Robert J. Gallagher
Combustion Research Facility
Sandia National Laboratories MS 9056
Livermore, California 94551-0969
Phone: 925.294.3117
rjgalla@sandia.gov

Prof. Graham P. Glass
Department of Chemistry
Rice University
P.O. Box 1892
Houston, Texas 77251
Phone: 713.737.5683
gglass@rice.edu

Dr. John Goldsmith
Combustion Research Facility
Sandia National Laboratories
Livermore, California 94551-0969
Phone: (925)294-2432
jgold@sandia.gov

Prof. Edward R. Grant
Department of Chemistry
Purdue University
West Lafayette, Indiana 47907
Phone: (765)494-9006
egrant@chem.purdue.edu

Dr. Stephen K. Gray
Chemistry Division
Argonne National Laboratory
9700 South Cass Ave.
Argonne, Illinois 60439
Phone: 630.252.3594
gray@tcg.anl.gov

Prof. William H. Green, Jr.
Department of Chemical Engineering
66-448
Massachusetts Institute of Technology
77 Massachusetts Ave.
Cambridge, Massachusetts 02139
Phone: 617.253.4580
whgreen@mit.edu

Dr. Gregory E. Hall
Chemistry Department
Brookhaven National Laboratory
Upton, New York 11973
Phone: 631.344.4376
g_hall@bnl.gov

Prof. Ronald K. Hanson
Department of Mechanical Engineering
Stanford University
Stanford, California 94305
Phone: 650.723.4023
hanson@cdr.stanford.edu

Dr. Lawrence Harding
Chemistry Division
Argonne National Laboratory
9700 South Cass Avenue
Argonne, Illinois 60439
Phone: (630)252-3591
harding@tcg.anl.gov

Dr. Carl C. Hayden
Combustion Research Facility
Sandia National Laboratories MS 9055
Livermore, California 94551-0969
Phone: 925.294.2298
cchayde@sandia.gov

Prof. Martin Head-Gordon
Department of Chemistry
University of California at Berkeley
Berkeley, California 94720
Phone: 510.642.5957
mhg@bastille.cchem.berkeley.edu

Prof. John Hershberger
Department of Chemistry
North Dakota State University
Fargo, ND 58105-5516
Phone: (701)231-8225
John_Hershberger@ndsu.nodak.edu

Dr. Jan P. Hessler
Chemistry Division
Argonne National Laboratory
9700 South Cass Avenue
Argonne, Illinois 60439
Phone: (630)252-3717
hessler@anl.gov

Prof. Paul L. Houston
Department of Chemistry
122 Baker Laboratory
Cornell University
Ithaca, New York 14853-1301
Phone: 607.255.4303
plh2@cornell.edu

Prof. Jack B. Howard
Department of Chemical Engineering
Massachusetts Institute of Technology
Cambridge, Massachusetts 02139
Phone: (617)253-4574
jbhoward@mit.edu

Dr. Jan Hrbek
Department of Chemistry
Brookhaven National Laboratory
Upton, New York 11973
Phone: 631.344.4344
hrbek@bnl.gov

Prof. Philip M. Johnson
Department of Chemistry
State University of New York
at Stony Brook
Stony Brook, New York 11794
Phone: (631)632-7912
Philip.Johnson@sunysb.edu

Prof. Michael E. Kellman
Department of Chemistry
University of Oregon
Eugene, Oregon 97403
Phone: 541.346.4196
kellman@oregon.uoregon.edu

Dr. Alan R. Kerstein
Combustion Research Facility
MS9051
Sandia National Laboratories
Livermore, California 94551-0969
Phone: 925.294.2390
arkerst@sandia.gov

Prof. John Kiefer
Department of Chemical Engineering
University of Illinois at Chicago
Chicago, Illinois 60607
Phone: (312) 996-571
john.h.kiefer@uic.edu

Dr. William H. Kirchhoff
Office of Basic Energy Sciences SC-141
U.S. Department of Energy
19901 Germantown Road
Germantown MD 20874-1290
Phone: (301)903-5809
william.kirchhoff@science.doe.gov

Dr. Stephen J. Klippenstein
Combustion Research Facility
Sandia National Laboratories MS 9055
Livermore, California 94551-0969
Phone: (925)294-2289
SJKLIPP@sandia.gov

Dr. Allan H. Laufer
Office of Basic Energy Sciences SC-141
U.S. Department of Energy
19901 Germantown Road
Germantown MD 20874-1290
Phone: 301.903.4417
allan.laufer@oer.doe.gov

Prof. C. K. Law
Department of Mechanical & Aerospace Engineering
Princeton University
Princeton, New Jersey 08544
Phone: 609-258-5271
cklaw@pucc.princeton.edu

Prof. Stephen R. Leone
Department of Chemistry
University of Colorado
Campus Box 215
Boulder, Colorado 80309
Phone: 303.492.5128
srl@jila.colorado.edu

Prof. Marsha I. Lester
Department of Chemistry
University of Pennsylvania
231 South 34th Street
Philadelphia, Pennsylvania 19104-6323
Phone: (215)898-4640
milester@sas.upenn.edu

Prof. William A. Lester, Jr.
Department of Chemistry
University of California at Berkeley
Berkeley, California 94720
Phone: 510.643.9590
walester@lbl.gov

Prof. John C. Light
The James Franck Institute
The University of Chicago
5640 S. Ellis Avenue
Chicago, Illinois 60637
Phone: 773.702.7197
light@pclight.uchicago.edu

Prof. Ming-Chang Lin
Department of Chemistry
Emory University
1515 Pierce Drive
Atlanta, Georgia 30322
Phone: (404)727-2825
chemmcl@emory.edu

Prof. Marshall B. Long
Department of Mechanical Engineering
Yale University
P.O. Box 208284
New Haven, Connecticut 06520-8284
Phone: 203.432.4229
long-marshall@yale.edu

Prof. Robert P. Lucht
Department of Mechanical Engineering
315 Engineering/Physics Building
Texas A&M University
College Station, TX 77843-3123
Phone: 979.862.2623
rlucht@mengr.tamu.edu

Dr. R. Glen Macdonald
Chemistry Division
Argonne National Laboratory
9700 South Cass Avenue
Argonne, Illinois 60439
Phone: (630)252-7742
macdonald@anlchm.chm.anl.gov

Dr. Andrew McIlroy
Combustion Research Facility
Sandia National Laboratories MS 9055
Livermore, California 94551-0969
Phone: 925.294.3054
amcilr@sandia.gov

Dr. William J. McLean, Director
Center for Combustion and Materials Research and Technology
Sandia National Laboratories MS9054
Livermore, California 94551-0969
Phone: (925)294-2687
wjmclea@sandia.gov

Dr. Joe V. Michael
Chemistry Division
Argonne National Laboratory
9700 South Cass Avenue
Argonne, Illinois 60439
Phone: (630)252-3171
michael@anlchm.chm.anl.gov

Prof. William H. Miller
Department of Chemistry
University of California at Berkeley
Berkeley, California 94720
Phone: (510)642-0653
miller@neon.cchem.berkeley.edu

Dr. James A. Miller
Combustion Research Facility
MS-9055
Sandia National Laboratories
Livermore, California 94551-0969
Phone: 925.294.2759
jamille@sandia.gov

Dr. Darren J. Mollot
Office of Fossil Energy FE-26
U.S. Department of Energy
1000 Independence Ave., S.W.
Washington D.C. 20585
Phone: 202.586.0429
darren.j.mollot@hq.doe.gov

Dr. David Moncrieff
Supercomputer Comp. Res. Inst.
496 Science Center Library
Florida State University
Tallahassee, Florida 32306-4130
Phone: 850.644.4885
moncrieff@csit.fsu.edu

Dr. James Muckerman
Chemistry Department
Brookhaven National Laboratory
Upton, NY 11973
Phone: 631.344.4368
muckerma@bnl.gov

Dr. Habib Najm
Combustion Research Facility
Sandia National Laboratories MS9051
Livermore, California 94551-0969
Phone: 925.294.2054
hnnajm@ca.sandia.gov

Prof. Daniel M. Neumark
Department of Chemistry
University of California at Berkeley
Berkeley, California 94720
Phone: 510.642.3502
neumark@cchem.berkeley.edu

Prof. Cheuk-Yiu Ng
Department of Chemistry
Iowa State University
Ames, Iowa 50011
Phone: (515)294-4225
cyng@ameslab.gov

Dr. David L. Osborn
Combustion Research Facility
MS 9055
Sandia National Laboratories
Livermore, California 94551-0969
Phone: 925-294-4622
dlosbor@sandia.gov

Prof. David S. Perry
Department of Chemistry
University of Akron
Akron, Ohio 44325
Phone: 330.972.6825
dperry@uakron.edu

Prof. Robert W. Pitz
Department of Mechanical Engineering
Vanderbilt University
Box 1592, Station B
Nashville, Tennessee 37235
Phone: 615.322.2950
pitzrw@vuse.vanderbilt.edu

Dr. William J. Pitz
Lawrence Livermore National Laboratory
P. O. Box 808, L-092
Livermore, California 94550
Phone: 925.422.7730
pitz1@llnl.gov

Prof. Stephen B. Pope
Department of Mechanical and Aerospace Engineering
Cornell University
106 Upson Hall
Ithaca, New York 14853
Phone: (607)255-4314
pope@mae.cornell.edu

Dr. Stephen Pratt
Chemistry Division
Argonne National Laboratory
9700 South Cass Avenue
Argonne, Illinois 60439
Phone: 630.252.4199
stpratt@anl.gov

Dr. Jack M. Preses
Chemistry Department
Brookhaven National Laboratory
Upton, New York 11973
Phone: 631.344.4371
preses@bnl.gov

Prof. Herschel A. Rabitz
Department of Chemistry
Princeton University
Princeton, New Jersey 08544
Phone: (609)258-3917
hrabitz@chemvax.princeton.edu

Dr. Larry A. Rahn
Combustion Research Facility
Sandia National Laboratories MS 9056
Livermore, California 94551-0969
Phone: 925.294.2091
rahn@sandia.gov

Prof. Hanna Reisler
Department of Chemistry
University of Southern California
Los Angeles, California 90089-0482
Phone: (213)740-7071
reisler@chem1.usc.edu

Dr. Gabriel D. Roy
Mechanics and Energy Conservation S&T
Office of Naval Research ONR 333
800 N. Quincy St., Ballston Tower One
Arlington, VA 22217-5660
Phone: 703.696.4406
royg@onr.navy.mil

Prof. Klaus Ruedenberg
Department of Chemistry
Iowa State University of Science and Technology
Ames, Iowa 50011
Phone: (515)294-5253
ruedenberg@iastate.edu

Dr. Branko Ruscic
Chemistry Division
Argonne National Laboratory
9700 South Cass Avenue
Argonne, Illinois 60439
Phone: 630.252.4079
ruscic@anl.gov

Prof. Henry Frederick Schaefer III
Department of Chemistry
University of Georgia
Athens, Georgia 30602
Phone: (706)542-2067
hfsiii@uga.cc.uga.edu

Dr. Trevor Sears
Chemistry Department
Brookhaven National Laboratory
Upton, New York 11973
Phone: 631.344.4374
sears@bnl.gov

Dr. Thomas B. Settersten
Combustion Research Facility
Sandia National Laboratories MS 9056
Livermore, California 94551-0969
Phone: 925.294.4701
tbsette@sandia.gov

Dr. Ron Shepard
Chemistry Division
Argonne National Laboratory
9700 South Cass Avenue
Argonne, Illinois 60439
Phone: 708.252.3584
shepard@tcg.anl.gov

Prof. Volker Sick
2023 Automotive Laboratory
Department of Mechanical Engineering
University of Michigan
1231 Beall Avenue
Ann Arbor, Michigan 48109-2121
Phone: 734.647.9607
vsick@umich.edu

Prof. Irene Slagle
Department of Chemistry
The Catholic University of America
Michigan Avenue at 7th Street, N.E.
Washington, D.C. 20064
Phone: (202)319-5384
slagle@cua.edu

Prof. Mitchell Smooke
Department of Mechanical Engineering
Yale University
P.O. Box 208284
New Haven, Connecticut 06520-8284
Phone: (203)432-4344
mitchell.smooke@yale.edu

Dr. Walter J. Stevens
Office of Basic Energy Sciences, SC-141
U.S. Department of Energy
19901 Germantown Road
Germantown, Maryland 20874-1290
Phone: 301.903.2046
Walter.Stevens@science.doe.gov

Prof. Arthur G. Suits
Department of Chemistry
State University of New York at Stony Brook
Stony Brook, NY 11794
Phone: 631.632.1702
arthur.suits@sunysb.edu

Dr. Craig Taatjes
Combustion Research Facility MS 9055
Sandia National Laboratories
Livermore, California 94551-0969
Phone: 925.294.2764
cataatj@california.sandia.gov

Ms. Karen Talamini
Office of Basic Energy Sciences SC-14
U.S. Department of Energy
19901 Germantown Road
Germantown MD 20874-1290
Phone: 301.903.4563
Karen.Talamini@science.doe.gov

Prof. Lawrence Talbot
Department of Mechanical Engineering
6173 Etcheverry Hall
University of California, Berkeley
Berkeley, California 94720-1740
Phone: 510.642.6780
talbot@me.berkeley.edu

Prof. Howard S. Taylor
Department of Chemistry
University of Southern California
Los Angeles, California
Phone: 213.740.4112
taylor@chem1.usc.edu

Prof. Donald G. Truhlar
Department of Chemistry
139 Smith Hall
University of Minnesota
207 Pleasant St. SE
Minneapolis, Minnesota 55455
Phone: (612)624-7555
truhlar@chem.umn.edu

Dr. Wing Tsang
Chemical Kinetics Division
Center for Chemical Technology
Natl. Inst. of Standards and Technology
Gaithersburg, Maryland 20899
Phone: (301)975-2507
wtsang@enh.nist.gov

Dr. Frank P. Tully
Combustion Research Facility
Sandia National Laboratories
Livermore, California 94551-0969
Phone: 925.294.2316
tully@sandia.gov

Prof. James J. Valentini
Department of Chemistry
Columbia University
3000 Broadway, MC 3120
New York, New York 10027
Phone: (212)854-7590
jjv1@chem.columbia.edu

Dr. Albert F. Wagner
Chemistry Division
Argonne National Laboratory
9700 South Cass Avenue
Argonne, Illinois 60439
Phone: (630)252-3597
wagner@tcg.anl.gov

Dr. Charles K. Westbrook
Division of Computational Physics
Lawrence Livermore National Laboratory
P. O. Box 808, L-091
Livermore, California 94550
Phone: 925.422.4108
westbrook1@llnl.gov

Prof. Phillip R. Westmoreland
Department of Chemical Engineering
University of Massachusetts
Amherst, Massachusetts 01003
Phone: (413)545-1750
westm@ecs.umass.edu

Dr. Randall E. Winans
Chemistry Division
Argonne National Laboratory
9700 South Cass Avenue
Argonne, Illinois 60439
Phone: 630.252.7479
rewinans@anl.gov

Prof. Curt Wittig
Department of Chemistry
University of Southern California
Los Angeles, California 90089-0484
Phone: (213)740-7368
wittig@chem1.usc.edu

Prof. David R. Yarkony
Department of Chemistry
Johns Hopkins University
Charles and 34th Streets
Baltimore, Maryland 21218
Phone: 410.516.4663
yarkony@jhuvms.hcf.jhu.edu

Prof. Timothy S. Zwier
Department of Chemistry
Purdue University
West Lafayette, Indiana 47907
Phone: (765)494-5278
zwier@chem.purdue.edu

Author Index